STEREOSELECTIVE TRANSFORMATIONS OF

IMINIUM IONS VIA COPPER CATALYSIS

by

Samantha O. Santana

A dissertation submitted to the Faculty of the University of Delaware in partial
fulfillment of the requirements for the degree of Doctor of Philosophy in Chemistry
and Biochemistry

Summer 2022

STEREOSELECTIVE TRANSFORMATIONS OF

IMINIUM IONS VIA COPPER CATALYSIS

by

Samantha O. Santana

Approved: _____
Brian J. Bahnson, Ph.D.
Chair of the Department of Chemistry and Biochemistry

Approved: _____
John A. Pelesko, Ph.D.
Dean of the College of Arts and Sciences

Approved: _____
Louis F. Rossi, Ph.D.
Vice Provost for Graduate and Professional Education and
Dean of the Graduate College

I certify that I have read this dissertation and that in my opinion it meets the academic and professional standard required by the University as a dissertation for the degree of Doctor of Philosophy.

Signed: _____

Mary P. Watson, Ph.D.
Professor in charge of dissertation

I certify that I have read this dissertation and that in my opinion it meets the academic and professional standard required by the University as a dissertation for the degree of Doctor of Philosophy.

Signed: _____

Joseph M. Fox, Ph.D.
Member of dissertation committee

I certify that I have read this dissertation and that in my opinion it meets the academic and professional standard required by the University as a dissertation for the degree of Doctor of Philosophy.

Signed: _____

Catherine L. Grimes, Ph.D.
Member of dissertation committee

I certify that I have read this dissertation and that in my opinion it meets the academic and professional standard required by the University as a dissertation for the degree of Doctor of Philosophy.

Signed: _____

Stephen A. Habay, Ph.D.
Member of dissertation committee

ACKNOWLEDGMENTS

To the MPW Group: our dynamic as a group has grown substantially and it was so easy to come and talk to anyone with problems I had, or just to talk about random topics. To my lab partner Weiye: it has always been a pleasure working with you; I look forward to the possibility of working together again in the future. To Yun: you were someone with whom I felt comfortable being around even in complete silence, and I cherish every time we went for coffee and talked about life. To Cameron, Diana, Bria, Rebecca, Windsor: it was never a dull moment talking to you! I have no doubt that you will become greater chemists than you already are, and I look forward to seeing where you go in the future. To my mentee Alex: I am happy to have been your mentor during my time at UD. I have confidence in your capabilities as a scientist and I look forward to seeing you progress through your Ph.D.

To the friends I made at UD: Marina, Claire, Brendan, John T., John M., A.J., Ryan, Olivia, Carly, Raphael, Linh, Tim: I will never forget our first moments when we arrived here. We have grown so much and have all become amazing chemists. To my best friend, Matt Von Bargen: Thank you for keeping me level-headed, focused, and determined. Thank you for validating my feelings and keeping me sane. We will always be friends, no matter where we go in the future.

To my partner James: thank you for being by my side for so many years. You have seen me at my best and at my worst, and despite whatever chaos ensues you always welcome me with big open arms. I will never forget the things you have done for me, and I look forward to when my journey becomes our journey. Thank you for everything, I love you!

DEDICATION

This work is dedicated to my mom, the late great Anna Marie Santana, who passed away at the time of writing of this thesis. My mom has always been my biggest cheerleader and advocate since day one. When she was told that I would never be able to speak or socialize, she wouldn't accept that as my fate. Whenever I told her about the things I couldn't do, or the things that seemed too difficult, she asked me, "Why can't you do those things? Who says you can't?". Despite my doubts in myself, or the doubts that others had of me, she believed that I could achieve anything I wanted to do. She put so much effort into giving me a better life and she worked every day to provide for me and the rest of our family. She was an inspiration, and I wish that one day I could be a fraction of a fighter that she had always been. My only regret in life is not finishing my doctorate work within the time she had been alive. Even if she is not physically here in the sense that we know, I know she is just as proud of me as when she was alive. I have been given this opportunity because of my mom and she deserves to be recognized. To my mom: to say that I miss you is an understatement, and there hasn't yet been a day where I don't wish you were here. I know at some point somewhere we will meet again, and I'll have so many things to tell you. I love you, mom. I'll see you when I see you.

TABLE OF CONTENTS

LIST OF TABLES

LIST OF FIGURES

LIST OF SCHEMES

ABSTRACT

This dissertation focuses on stereoselective transformations of iminium ions, which are mediated via copper(I) catalysts. Chapters 1–3 focus on developing stereoselective alkynylations to yield saturated, substituted N-heterocycles from commercial or easily-synthesized precursors. Chapter 4 describes discovery and examination of a novel kinetic resolution of benzoisoxazolines.

Chapter 1 describes an enantioselective alkynylation of unstabilized cyclic iminium ions, formed *in situ* from cyclic α-methoxyaminals. This method utilizes a copper(I)/PyBOX catalyst to generate chiral copper(I) acetylides, which undergo an addition to the iminium ion to yield enantioenriched, substituted cyclic amines. Broad scope is demonstrated in both alkynyl partners and aminal identity under mild conditions and with high enantioselectivities. This research finds its utility in medicinal chemistry and total synthesis to synthesize saturated heterocycles with highly predictable stereochemical outcomes.

Chapter 2 describes a diastereoselective alkynylation of β-bromoiminium ions, which are formed *in situ* from α,β-methoxy-bromoaminals. This method uses a Lewis acid to cleave a C–O bond and form the iminium ion, which is stabilized and stereo-controlled by the bromide moiety. These factors result in a diastereoselective alkynylation using a copper(I) acetylide to yield β-bromo-alkynylated cyclic amines.

This method offers broad scope under mild conditions, demonstrating stereoselective heterocyclic synthesis and facile derivatization of potentially bioactive compounds.

Chapter 3 describes my efforts towards an enantioselective and diastereoselective halogenation-alkynylation of cyclic enecarbamates. I envisioned a dynamic kinetic resolution wherein the enecarbamate could react with a halide source via reversible halogenation. These intermediates could then interconvert between both enantiomers of the halo-iminium ion, where one of the intermediates could be preferentially attacked by a chiral copper(I) acetylide. Alternatively, I hypothesized a pathway in which the halogenation could be achieved via a chiral halogenating reagent, which would provide a single enantiomer of the halo-iminium ion. This reaction could then be followed by a diastereoselective alkynylation to yield enantioenriched halo-alkynylated piperidines.

Chapter 4 describes a kinetic resolution of benzoisoxazolines, which employs a chiral copper(I)/PHOX catalyst to differentiate between two enantiomers of starting material. One enantiomer of starting material reacts to form a benzoxazepine while the other enantiomer remains untouched and enantioenriched. This method requires 1.) a stoichiometric amount of terminal alkyne and base and 2.) specific properties for the terminal alkyne for the overall reaction to be successful. Cleavage of the N-O bond may also lead to enantioenriched α-tetrasubstituted amines, allowing for further derivatization and pathways for bioactive synthesis.

Chapter 1

ENANTIOSELECTIVE ALKYNYLATIONS OF CYCLIC IMINIUM IONS VIA COPPER(I) CATALYSIS

Work described here has been published (Guan, W.; Santana, S. O.; Liao, J.; Henninger, K.; Watson, M. P.; *ACS Catal*. **2020**, *10*, *23*, 13820–13824). It is reprinted in this chapter with permission from *ACS Catalysis* (Copyright © 2020, American Chemical Society).

1.1   Introduction

α-Chiral cyclic amines are crucial and invaluable motifs in organic chemistry.[1-9] Molecules containing these structures include a variety of pharmaceuticals and natural products due to their tendency to have a wide range of bioactivities (**Figure 1.1**). For example, saxagliptin (Onglyza) is a medication used to treat and manage type-2 diabetes, and anisomycin is a compound produced in the bacterium *Streptomyces griseolus* that has been used as an antibiotic.[10, 11] Natural products have also been harnessed for their therapeutic properties for millennia, including nicotine for its highly addictive tendencies and lupinine for its several different bioactivities.[12-15] A commonality among these compounds is that they all contain an α-chiral cyclic

amine moiety, making it evident that developing methods to synthesize such compounds efficiently is of immense interest and importance.

Figure 1.1 – Pharmaceuticals and Natural Products with α-Chiral Cyclic Amines

Anisomycin (from *Streptomyces griseolus*)
(antibiotic)

Saxagliptin (*Onglyza*)
(hypoglycemic)

Clindamycin
(antibiotic)

Lupinine
(natural product)

Nicotine
(natural product)

Coniine
(natural product)
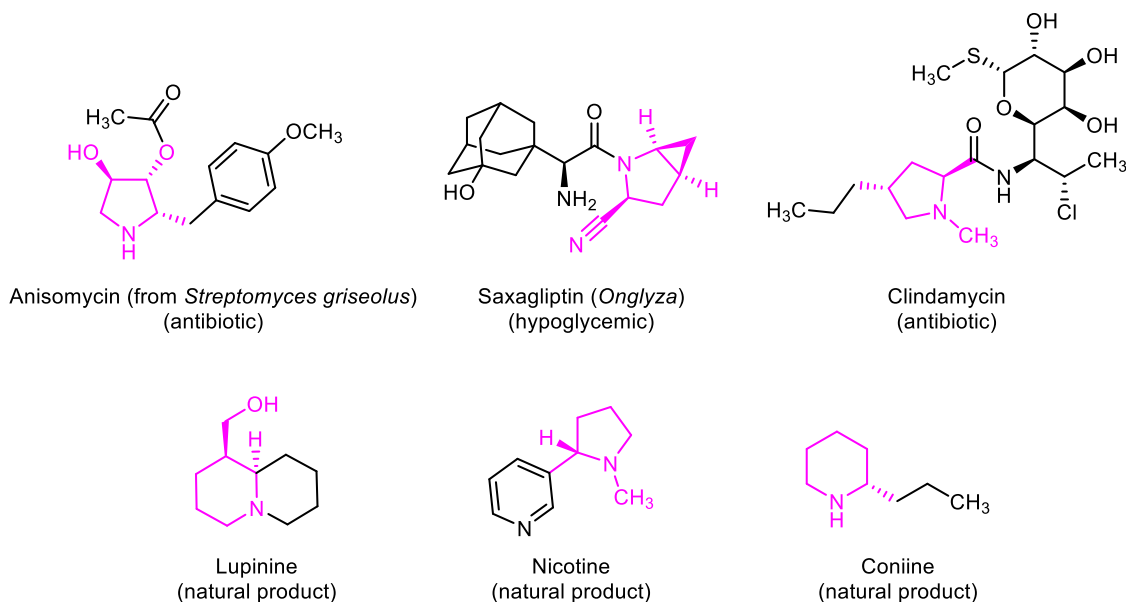
The most common method of synthesizing α-chiral cyclic amines is through cyclization of a pre-functionalized acyclic amine (**Scheme 1.1**). In this approach, the stereocenters are set through an acyclic precursor. A typical synthetic approach would be a substitution or alkylation reaction wherein a primary or secondary amine attacks a carbon containing a leaving group.

2

Scheme 1.1 – Common Method to Saturated Heterocycles with Stereochemistry
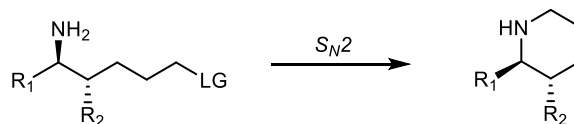
Other conventional methods include but are not limited to Prins cyclizations, aza-Michael reactions, ring-closing metatheses, and hydrogenations (**Scheme 1.2**).[6, 16-29] While these methods are prevalent and reliable for cyclic amine synthesis, a more efficient method would rely on less synthetic steps while maintaining the predictability of the stereochemical outcome. One way to circumvent this issue would be to directly functionalize a cyclic amine stereoselectively, wherein no prior functionalization of an acyclic amine would be required.

Scheme 1.2 – Other Methods to Synthesize Saturated Cyclic Amines

Prins

MeAlCl$_2$
CHCl$_3$
60 °C, overnight

88%, 99:1 dr

Aza-Michael

2M HCl in Et$_2$O
MeOH
-78 °C to rt, 2 hr

+

89%, 3:1 dr

Ring-closing Metathesis

1.) HCl conc. in Et$_2$O, 30 min
2.) Grubbs 2nd Gen. Cat., 5 mol %
CH$_2$Cl$_2$, reflux, 1 hr

98% ee

70%, 98% ee

Hydrogenation

H$_2$
1-3 mol % Titanocene
80 psig
65 °C, 7 hr

84%, 99% ee
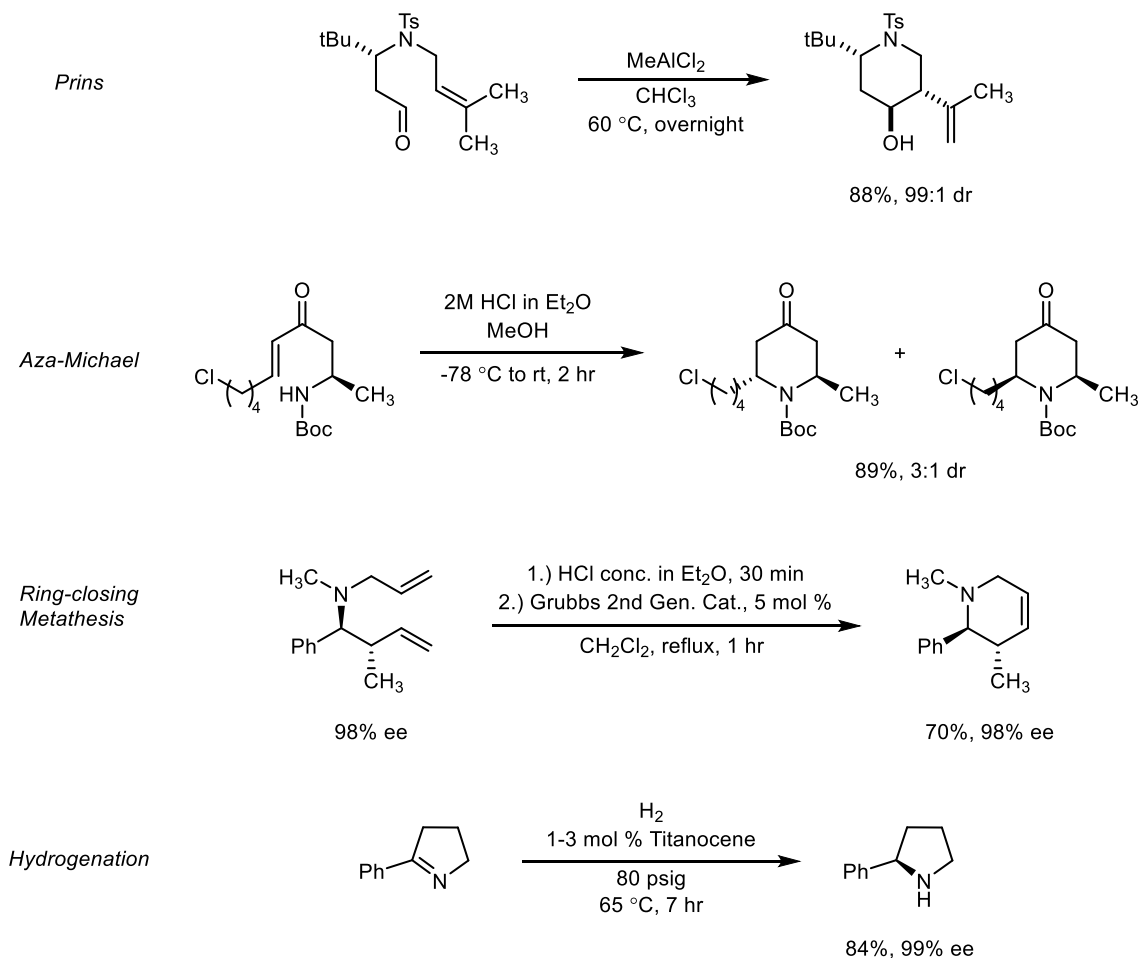
Direct functionalization can be achieved via activation of the α-carbon adjacent to the nitrogen, in which the carbon atom could subsequently become either nucleophilic or electrophilic (**Scheme 1.3**). Both approaches have been proven successful in recent years, and there has been a growing interest in developing methods with highly predictable stereochemistry to yield enantioenriched products.

4

Scheme 1.3 – Direct Functionalization of Cyclic Amines via Carbon Activation
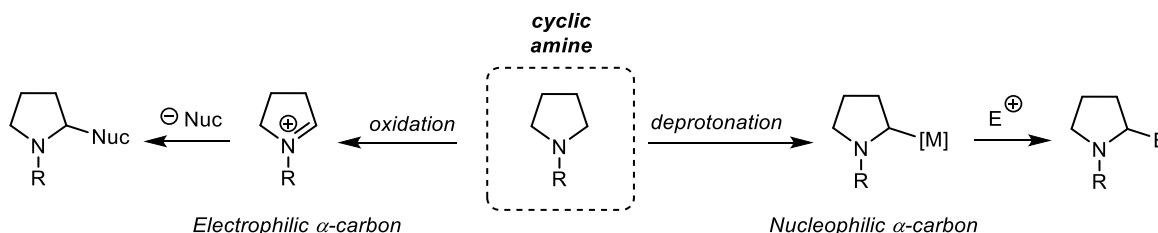
It has been shown previously that a nucleophilic α-carbon approach can be successful in installing substitution onto cyclic amines, using *sec*-butyllithium to deprotonate the α-carbon and a carbamate protecting group to assist in directing the stereochemistry.[30, 31] For example, Coldham and Leonari have demonstrated a successful enantioselective addition using this nucleophilic α-carbon approach (**Scheme 1.4**), wherein they are able to selectively deprotonate the α-carbon of N-Boc-pyrrolidine using *sec*-butyllithium and (-)-sparteine as a chiral ligand.[31] This mixture is then charged with zinc(II) chloride copper(I) cyanide di(lithium chloride) complex solution, and allyl bromide to yield allylated pyrrolidine in 81% yield and 95:5 enantiomeric ratio (er). This product was then pushed forward to generate enantioenriched (+)-coniceine, a poisonous indolizidine alkaloid.[32] This method is one of many that have been developed using the nucleophilic α-carbon approach.

Scheme 1.4 – Coldham and Leonari's Approach to Cyclic Amines
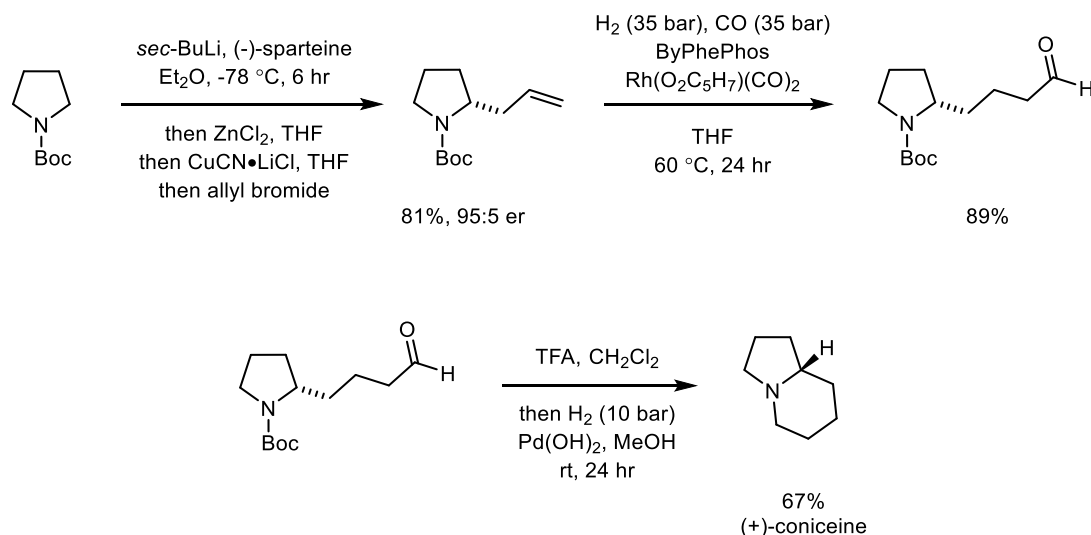
Conversely, an electrophilic α-carbon approach is also possible, wherein an oxidation would result in an electrophilic carbon atom that can be attacked by a nucleophile.[30] This carbon can be further stabilized by the nitrogen atom through resonance, formally known as the iminium ion (**Scheme 1.5**). For example, Santos and coworkers have demonstrated this pathway through a diastereoselective cyanation and a "cation-pool" method.[33] Cation-pool refers to an oxidation method in which the iminium ion was generated through low-temperature electrolysis, a type of anodic oxidation. A chiral auxiliary, 8-phenylmenthyl, was used as a protecting group on the nitrogen atom to better control diastereoselectivity. Cyanation was achieved with TMSCN and β-cyclodextrin (β-CD), an oligosaccharide, as a co-catalyst, which resulted in cyanated piperidine in 35% yield and 90% ee. This substrate was then pushed forward to yield various enantioenriched anesthetic pharmaceuticals such as mepivacaine, levobupivacaine, and ropivacaine.

Scheme 1.5 – Santos' Electrophilic Carbon Approach to Cyclic Amines

R = 8-phenylmenthyl

35%, 90% ee

R = Me; mepivacaine
R = Bu; levobupivacaine
R = Prop; ropivacaine
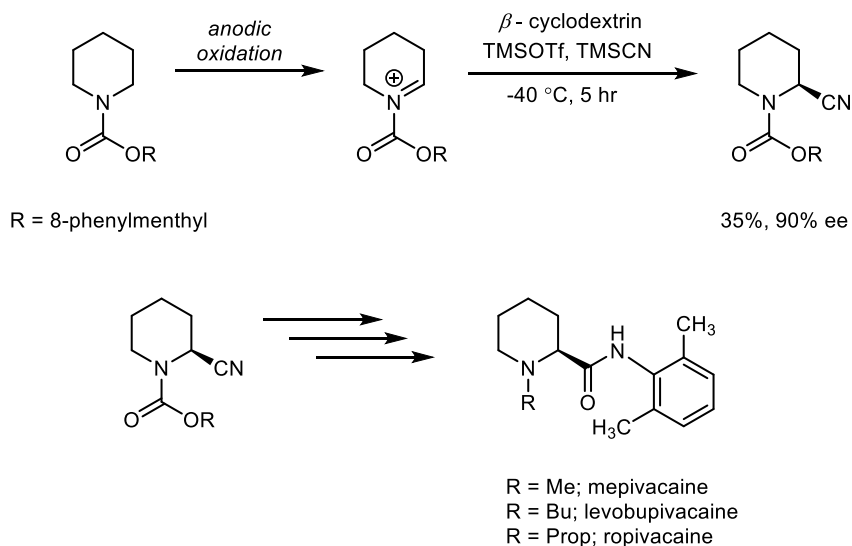
I decided to focus on the electrophilic α-carbon approach, as there is a greater potential for functional group tolerance without the use of harsh conditions or reagents as seen in the nucleophilic α-carbon approach.[30] It is important to recognize the work that has been previously published in relation to oxocarbenium ion chemistry to better understand the scope of iminium ion chemistry. Oxocarbenium and iminium ion intermediates have similar properties and reactivities, wherein the heteroatom can provide stability to the electropositive carbon via resonance (**Scheme 1.6**). Additionally, these oxocarbenium and iminium ions can be readily formed *in situ*, generating a reactive and prochiral intermediate that is prone to highly predictable stereochemical outcomes.

Scheme 1.6 – Oxocarbenium and Iminium Ion Intermediates

prochiral intermediates
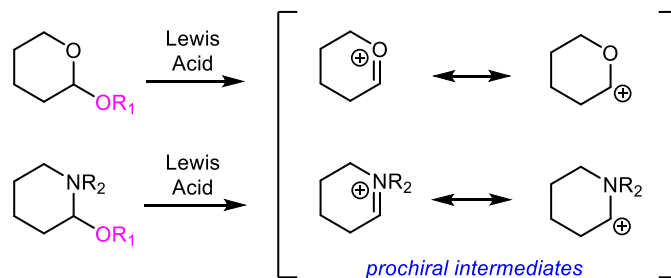
This research area has been investigated particularly with deprotonated terminal alkynes (acetylides) as nucleophilic partners, among other nucleophiles.[34-36] Alkynes are a privileged functional group that can be transformed into other functional groups through various syntheses such as reductions, additions, oxidations, and cycloadditions (**Scheme 1.7**).[37]

Scheme 1.7 – Versatility of the Alkyne Functional Group

8

The versatility of the alkyne has sparked interest in enantioselective alkynylation methods by many research groups.[34] Alkynylations to oxocarbenium ions were initially inspired by the success of enantioselective alkynylations to aldehydes. Mukaiyama and Carreira pioneered this field (**Scheme 1.8**),[38-40] which was further influential in the synthesis of drug molecules such as efavirenz (Sustiva) (**Scheme 1.9**).[41]

Scheme 1.8 – Mukaiyama and Carreira's Alkynylations to Aldehydes
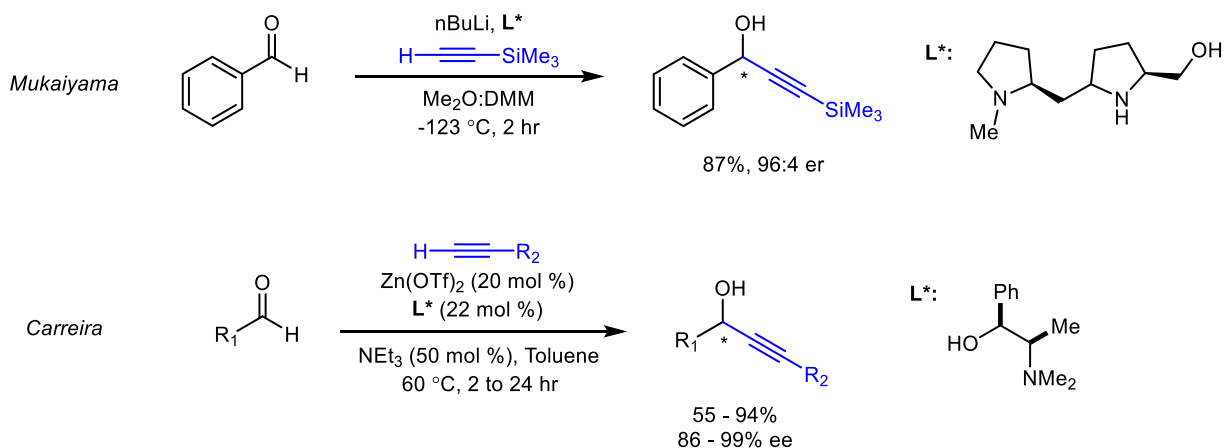
Scheme 1.9 – Enantioselective Alkynylation to the HIV Drug Efavirenz
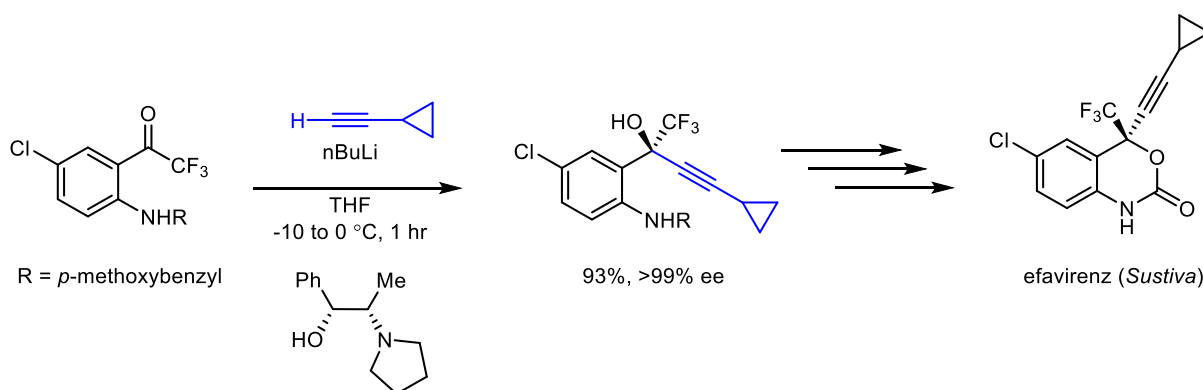
Much like the analogous work with oxocarbenium ions, many research groups have focused on harnessing iminium ions as electrophiles in alkynylation reactions.[34] The Li and Knochel groups have developed both racemic and enantioselective alkynylations to acyclic iminium ions.[42-46] Li and coworkers found that by treating imines with catalytic Cu(OTf)/PhPyBOX and stoichiometric phenylacetylene in toluene (**Scheme 1.10a**), they were able to obtain enantioenriched alkynylated amines ranging from 48–93% yield and 78–96% ee.[42] Interestingly, this method was also able to be conducted in water, albeit a slight detriment in enantioselectivity. Knochel and co-workers also developed an enantioselective alkynylation to acyclic iminium ions with a different approach in starting material.[44, 45] The iminium ion was generated *in situ* from an acyclic enamine, which acted as a base to deprotonate the coordinated alkyne (**Scheme 1.10b**).

Scheme 1.10 – First Reports of Enantioselective Alkynylations to Iminium Ions
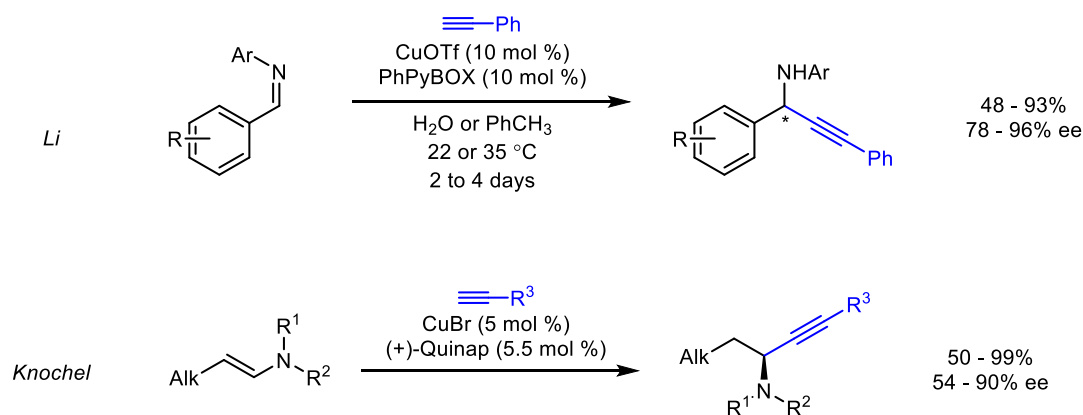
Following these reports of acyclic iminium alkynylations, the Li group then reported the first successful example of an enantioselective alkynylation to cyclic iminium ions via copper catalysis.[47] The iminium ion was generated through a peroxide-mediated oxidation, and the enantioselectivity was achieved using PhPyBOX as the ligand for the copper(I) acetylide, resulting in yields ranging from 11–72% and enantioselectivities from 5–74% (**Scheme 1.11**). This work would then be improved upon as demonstrated in their subsequent 2006 publication.[48] It was noted that improved yields and enantioselectivities could be achieved by introducing the iminium bromide salt of the substrate rather than performing the oxidation *in situ*.

Scheme 1.11 – Li's Enantioselective Alkynylation with Cyclic Iminium Ions
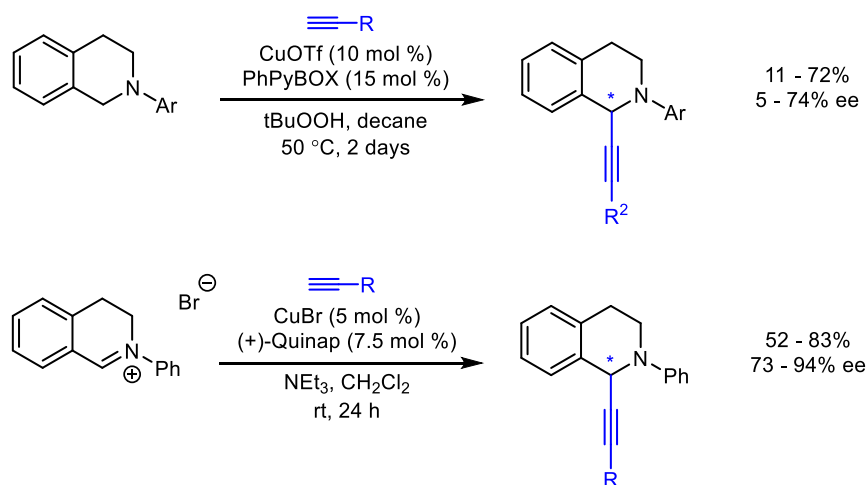
Since the initial work by Li and Knochel, other research groups have developed successful stereoselective alkynylation methods to various cyclic iminium ions such as isoquinoliums, tetrahydroisoquinoliums (THIQs), quinolium ions, and pyridinium ions (**Scheme 1.12**).[47-56]

Scheme 1.12 – Examples of Alkynylations to Cyclic Iminium Ions

Taylor/Schreiber

$\equiv$—R^2
CuBr (5 mol %)
(+)-Quinap (5.5 mol %)

NEt$_3$, CH$_2$Cl$_2$
-55 °C, 48 h

67 - 95%
70 - 99% ee

Aponick

$\equiv$—R
ClCO$_2$Et
CuBr (5.5 mol %)
(S)-StackPhos (5.5 mol %)

i-Pr$_2$NEt, CH$_2$Cl$_2$
-20 °C, 22 h

45 - 86%
90 - 98% ee

Ma

$\equiv$—CO$_2$R
CuI (10 mol %)
IndaBOX (10 mol %)

i-Pr$_2$NPr-n, CH$_2$Cl$_2$
-78 °C, 15 h

65 - 81%
86 - 98% ee

Arndtsen

$\equiv$—R
CuCl (5 mol %)
Pinap Ligand (5.5 mol %)

i-Pr$_2$NEt, CH$_2$Cl$_2$/MeCN
-78 °C, 14 h

33 - 92%
62 - 84% ee

(+)-Quinap

(S)-StackPhos

indaBOX

Pinap Ligand
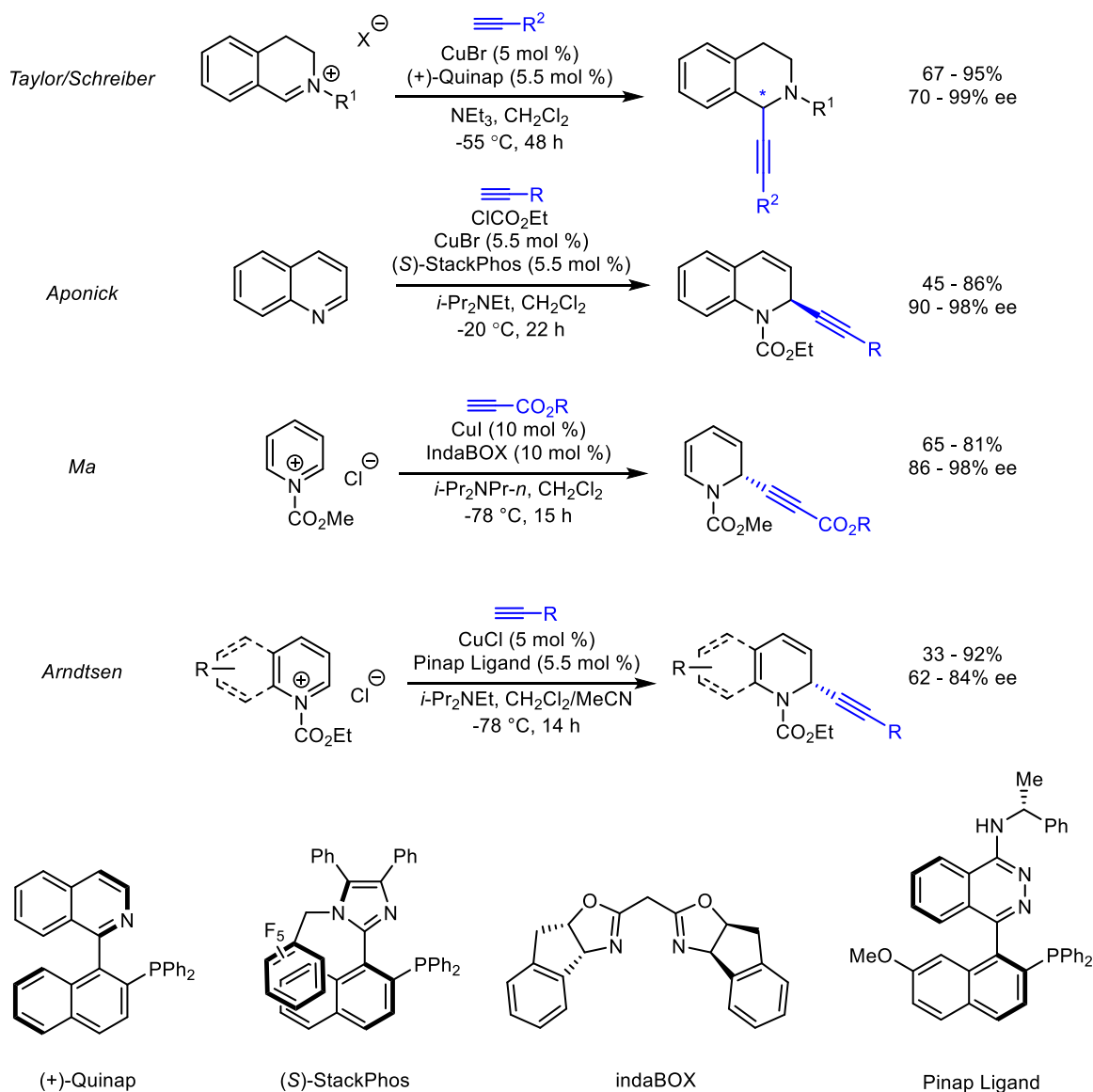
Although there has been a lot of work towards enantioselective alkynylations of various iminium ions, stereoselective alkynylations of cyclic, saturated iminium ions are still largely unknown. These iminium ions in particular have been shown to be difficult substrates due to their lack of stabilization through resonance or aromaticity;

without additional stabilization, they are more susceptible to decomposition such as E1 elimination and polymerization (**Scheme 1.13**).[57]

Scheme 1.13 – Challenges of Unstabilized Cyclic Amines

Polymerization

Elimination
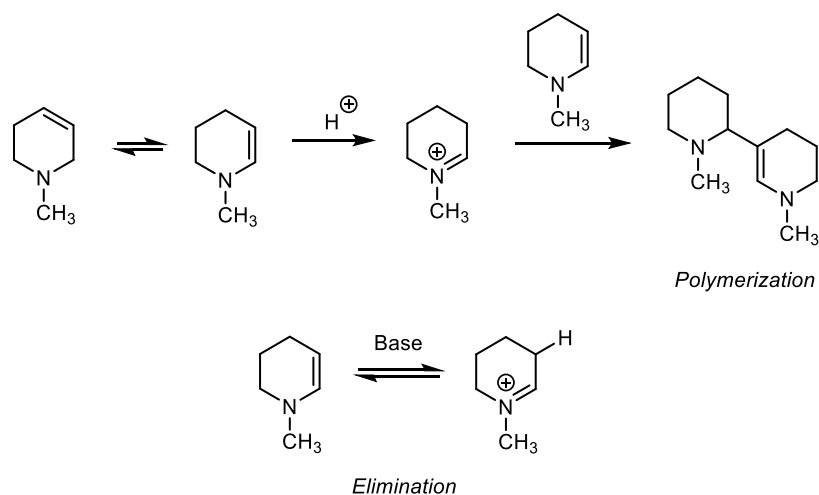
Despite the challenges, there have been efforts in developing stereoselective alkynylations of unstabilized cyclic iminium ions (**Scheme 1.14**). As mentioned previously, Knochel and co-workers developed an enantioselective alkynylation to acyclic iminium ions from benzyl-protected enamines.[44] While investigating a racemic pathway, they explored a single example of a cyclic benzyl-protected enamine that resulted in a yield of 86% (**Scheme 1.14a**). However, this cyclic example was not reported in the scope using chiral catalyst even though it was successful in the non-asymmetric variation.

Scheme 1.14 – Alkynylations to Unstabilized Cyclic Iminium Ions
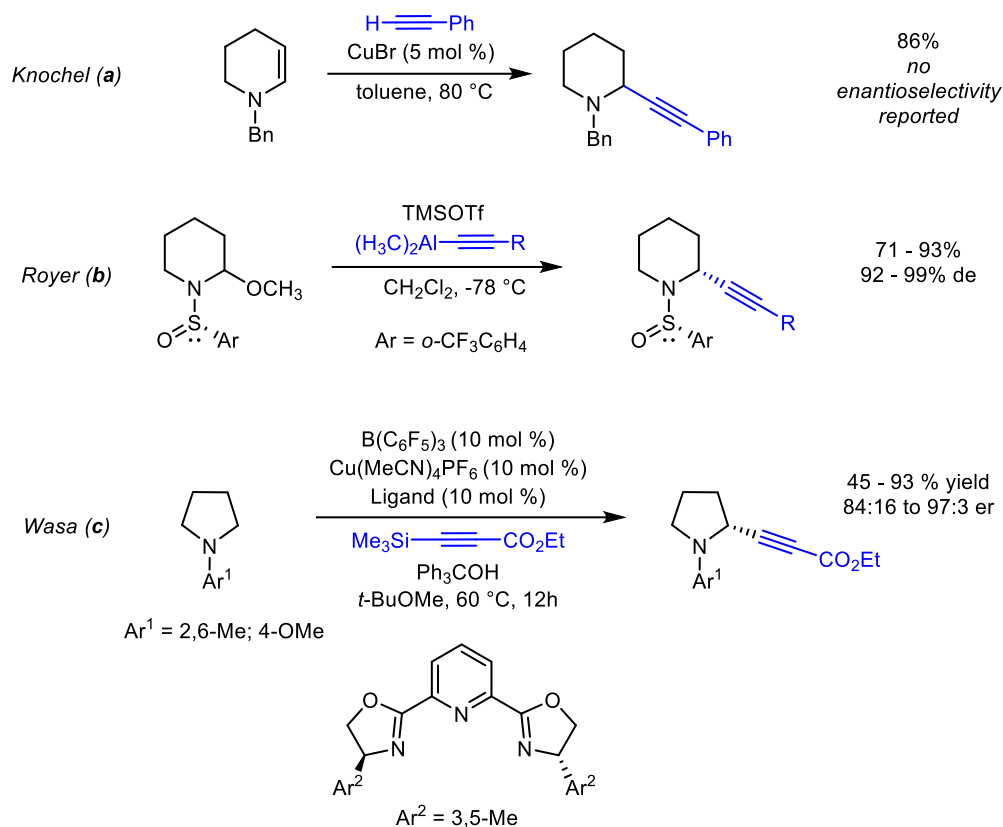
The Royer group explored a diastereoselective alkynylation of saturated cyclic amines with aluminum acetylides (**Scheme 1.14b**);[58] they were able to utilize a chiral sulfonyl auxiliary on the nitrogen atom, which enabled 91 – 99% de. This method yielded alkynylated piperidines with great diastereoselectivities, and upon cleavage of the auxiliary would reveal enantioenriched piperidines. There were numerous drawbacks to this method despite achieving enantioenriched cyclic amines; addition and cleavage of the auxiliary may be cumbersome, and the stoichiometric addition of aluminum acetylide poses a challenge on functional group tolerance.

While we were developing the method discussed below, Wasa and co-workers reported an alkynylation method using chiral copper(I)/PhPyBOX acetylides that were generated *in situ* from silyl propionates (**Scheme 1.14c**).[59] This was an important example of an enantioselective alkynylation to unstabilized cyclic iminium ions, however this method still had its detriments. The silyl propionates must be activated *in situ* using an additional trityl alcohol substrate. Furthermore, the scope of this method is limited in both alkynyl substrate and specific aryl groups attached to the nitrogen atom.

Weiye Guan, a member of the Mary P. Watson group at the University of Delaware, discovered and optimized conditions for a successful enantioselective alkynylation of unstabilized cyclic iminium ions, which utilized a copper(I)/PhPyBOX catalyst (**Scheme 1.15**).

Scheme 1.15 – Watson's Alkynylation of Unstabilized Iminium Ions
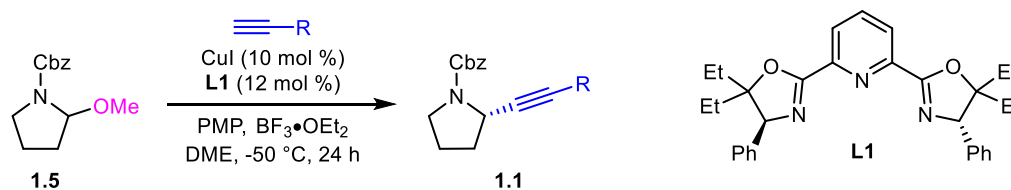

She identified and synthesized the optimal ligand for this reaction according to the literature precedent;[60] a tetra-(ethyl) PhPyBOX ligand (**L1**) was crucial for both the reactivity and enantioselectivity. After she finished the method optimization, she recruited me to assist in the investigation of the substrate scope.

1.2 Results and Discussion

Weiye optimized the alkynylation using benzyl-2-methoxypyrrolidine-1-carboxylate (**1.5**) and identified the following optimized conditions:[61] 10 mol % copper(I) iodide, 12 mol % chiral ligand **L1** (synthesized according to the literature procedure),[60] 1.2 equivalents of alkyne, 1.5 equivalents of pentamethylpiperidine (PMP), 1.1 equivalents of boron trifluoride etherate (BF$_3$•OEt$_2$), and DME (0.05M) at –50 °C for 24 hours. I assisted my colleagues Weiye and Kelci with exploration of substrate scope, synthesis of starting materials, and characterization of compounds.

Scheme 1.16 – Preparation of α-Methoxyaminals
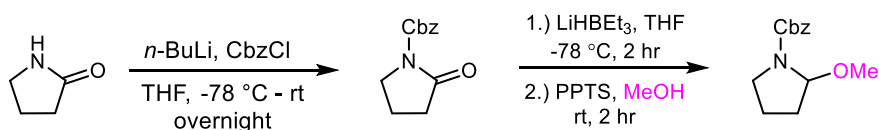
The *α*-Methoxyaminal (**1.5**) can be easily synthesized from pyrrolidone in two steps (**Scheme 1.16**).[62, 63] I investigated three compounds (**1.2, 1.3, 1.4**) of the substrate scope in total, which provided good yields in the alkynylation, however it was noted that electron-donating groups on the para position of the aryl ring (**1.4**) gave lower enantioselectivities (**Scheme 1.17**). Indeed, a Hammett correlation was observed, in which the log of the enantiomeric ratio was dependent on the electronic character of the acetylene (**Figure 1.2**). Copper acetylides with electron-withdrawing groups provided higher enantioselectivities, which we hypothesized was due to their later transition states during the C–C bond formation.

16

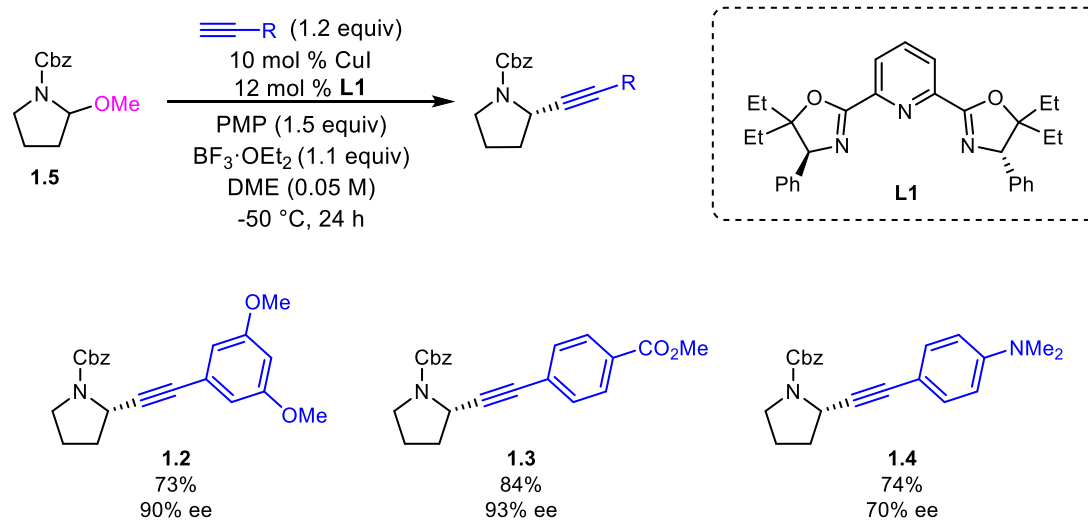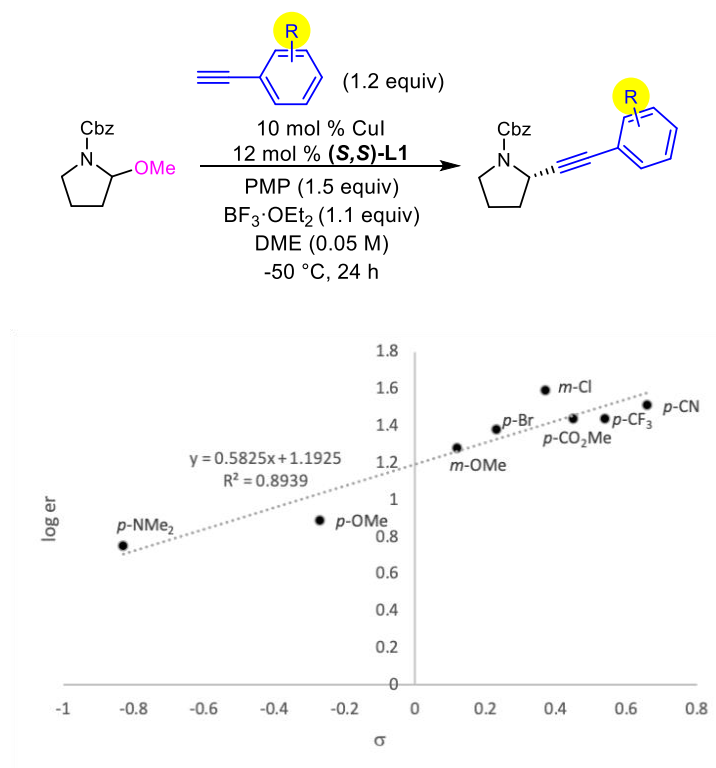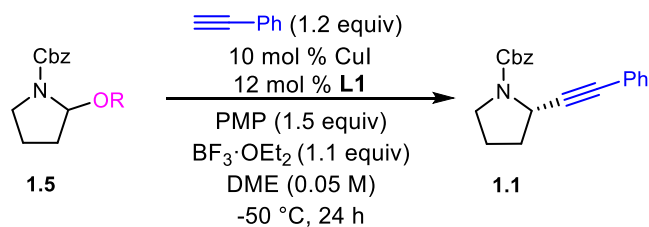## Scheme 1.17 – Investigation of Substrate Scope

1.2
73%
90% ee

1.3
84%
93% ee

1.4
74%
70% ee

Figure 1.2 – Hammett Correlation

$y = 0.5825x + 1.1925$
$R^2 = 0.8939$

Overall, we were able to demonstrate a wide substrate scope in both acetylide and aminal partners. Varying steric and electronic effects on the aryl ring of the acetylide were successful in the reaction, providing good yields and enantioselectivities. Aminals bearing a Boc-protecting group as opposed to a Cbz-protecting group were also successful. In addition, 5 and 6-membered rings also reacted favorably under the reaction conditions. Finally, substitution on the aminal ring was not detrimental to the reaction, including spirocyclic and di-(methyl) aminal ethers.

Upon submission of this alkynylation method to *ACS Catalysis*, reviewers questioned the possibility of using other aminal ethers in the reaction, as our method had only demonstrated α-methoxyaminals. Alternative aminal substrates were then synthesized according to literature precedent and subjected to the reaction conditions (**Scheme 1.18**).[64-66] Although other alkyl ethers (entries 1–3) provided similar yields, their enantioselectivities decreased with more steric hindrance. Surprisingly, the acetate aminal ether (entry 4) provided lower yield and high enantioselectivity, which may be explained by the labile nature of the acetate leaving group. Elimination and polymerization byproducts were more likely to form since the acetate is much more favorable as a leaving group, particularly in the presence of excess base. Indeed, these byproducts were seen in the NMR spectrum of the crude reaction mixture. Unsurprisingly, the free alcohol aminal substrate (entry 5) was not successful under the reaction conditions, providing only decomposition byproducts.

Scheme 1.18 – Investigation of Hemiaminal Ethers

entry	aminal (OR)	yield(%)^a	ee (%)^b
1	OMe	89	91
2	OEt	92	89
3	OiPr	83	86
4	OAc	27	93
5	OH	trace	nd^c

^{a}Determined by ^{1}H NMR with 1,3,5-trimethoxybenzene as internal standard.^{b}Determined by HPLC using a chiral stationary phase. ^{c}nd = not determined.

1.3 Conclusion

Our group has developed an enantioselective alkynylation of saturated cyclic iminium ions via copper(I) catalysis.[61] This work demonstrates a wide substrate scope of alkynes and aminals under mild conditions with labile nitrogen protecting groups, which showcases potential in the preparation of valuable, bioactive cyclic amines. This work was published in *ACS Catalysis* in 2020 and has been highlighted in

Synfacts in 2021.[67] Investigation of other nucleophilic partners and examination of the mechanism of this reaction are ongoing in our lab.

1.4   Experimental

General Information

All reactions were performed in a nitrogen-atmosphere glovebox in oven-dried 1-dram vials with Teflon-lined caps, or in oven-dried round-bottomed flasks fitted with rubber septa under a positive pressure of nitrogen. Stainless steel syringes were used to transfer air and moisture sensitive liquids. Flash chromatography was performed on silica gel 60 (40 – 63 µm, 60 Å). Thin layer chromatography (TLC) was conducted on glass plates coated with silica gel 60 (40 – 63 µm, 60 Å). Commercial reagents were purchased from Sigma Aldrich, Acros, Fisher Scientific, Strem, TCI Chemicals, Combi-Blocks, Alfa Aesar, AK Scientific, Cambridge Isotopes Laboratories, Ambeed, or Oakwood Chemicals and used as received except for the following: bases such as diisopropylethylamine were dried, distilled, and degassed via freeze-pump-thaw method. Solvents such as THF, CH_2Cl_2, and toluene were dried by passing through drying columns, then degassed by sparging with nitrogen. Nuclear magnetic resonance (NMR) for both proton (^1H NMR) and carbon (^{13}C NMR) spectra were recorded on 400 MHz and 600 MHz spectrometers. Chemical shifts for proton spectra are reported in parts per million downfield from tetramethylsilane and are referenced to the NMR solvent ($CHCl_3 = \delta$ 7.26). Chemical shifts for carbon spectra are reported in parts per million downfield from tetramethylsilane and are referenced

to the NMR solvent (CHCl₃ = δ 77.16). Data is represented as follows: chemical shift, multiplicity (br = broad, s = singlet, d = doublet, t = triplet, q = quartet, p = pentet, m = multiplet, dd = doublet of doublets, h = heptet), coupling constants in Hertz (Hz), and integration. Infrared spectra (IR) were obtained by loading material onto a KBr plate and recording via FTIR spectrophotometer. The mass spectral data were obtained at the University of Delaware facilities using a Q-Exactive Orbitrap Mass Spectrometer (Thermo Scientific) for ESI and a GCT Premier (Waters) for LIFDI. Melting points were taken on a Thomas-Hoover Uni-Melt Capillary Melting Point Apparatus. X-Ray Crystallography was performed by Dr. Glenn P. A. Yap at the University of Delaware. Preparative chiral SFC was performed by Lotus Separations, Inc.

General Procedure A: Enantioselective Alkynylation of *α*-Methoxyaminals
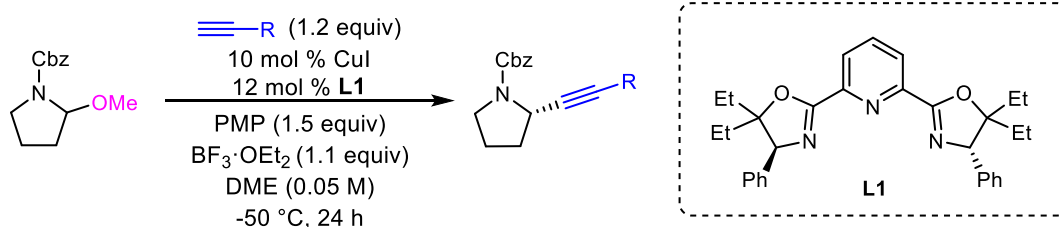
In a N₂-filled glovebox, CuI (5.7 mg, 0.030 mmol, 10 mol %), **L1** (17.3 mg, 0.036 mmol, 12 mol %), and dimethoxyethane (DME, 1.5 mL) were added to a 2-dram vial. The vial was capped with a septum-lined pierceable cap and the mixture was stirred for 30 min at room temperature. Then alkyne (0.36 mmol, 1.2 equiv), 1,2,2,6,6- pentamethylpiperidine (PMP, 0.45 mmol, 1.5 equiv), *α*-methoxyaminal **1.5**

(0.30 mmol, 1.0 equiv), and DME (4.5 mL, 0.05 M) were added to the vial. The vial was again sealed with a septum-lined pierceable cap, removed from the glovebox, and cooled to –50 °C. After 10 min, BF$_3$·OEt$_2$ (48% in Et$_2$O, 0.33 mmol, 1.1 equiv) was slowly added over 5 minutes via microsyringe, and the mixture was stirred for 24 hours at -50 °C. The reaction mixture was then diluted with Et$_2$O (2 mL) and filtered through a plug of silica gel, which was then washed with more Et$_2$O (20 mL). The filtrate was concentrated and purified by silica gel chromatography.
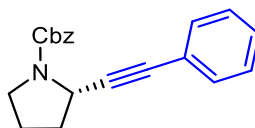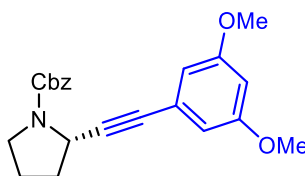

Benzyl (*S*)-2-(phenylethynyl)pyrrolidine-1-carboxylate (1.1). Prepared via General Procedure A on a 0.3-mmol scale. Crude material was purified by silica gel chromatography (8–16% EtOAc:Hexanes) to give compound 3 (run 1: 271 mg, 89%; run 2: 280 mg, 92%) as light-yellow oil. The enantiomeric excess was determined to be 92% (run 1: 92% ee; run 2: 91% ee) by chiral HPLC analysis (CHIRALPAK IB, 1 mL/min, 10% *i*-PrOH/hexane, l = 254 nm); t$_R$(major) = 6.38 min, t$_R$(minor) = 5.55 min. [a]D 22 = –55.2 (c 1.25, CHCl$_3$).

^{1}H NMR (600 MHz, CDCl$_3$, mixture of rotamers) δ 7.43 – 7.26 (m, 10H), 5.34 – 5.11 (m, 2H), 4.84 – 4.77 (m, 1H), 3.62 – 3.44 (m, 2H), 2.18 – 2.14 (m, 3H), 1.98 – 1.95 (m, 1H).

^{13}C NMR (101 MHz, CDCl$_3$, mixture of rotamers) δ 154.7, 137.1, 132.0, 131.8, 128.5, 128.3, 128.2, 128.1, 127.8, 127.7, 123.1, 89.6, 82.4, 67.0, 49.3, 48.9, 46.4, 46.0, 34.1, 33.4, 24.7, 23.9.

The spectral data matches that reported in the literature.[68]

Benzyl (*S*)-2-((3,5-dimethoxyphenyl)ethynyl)pyrrolidine-1-carboxylate (1.2). Prepared via General Procedure A on a 0.3 mmol scale. Crude material was purified by silica gel chromatography (30% EtOAc:Hexanes) to give compound 13 (run 1: 69 mg, 63%; run 2: 89 mg, 82%) as colorless oil. The enantiomeric excess was determined to be 90% (run 1: 91% ee; run 2: 88% ee) by chiral HPLC analysis (CHIRALPAK IB, 0.5 mL/min, 10% *i*-PrOH/hexane, l = 254 nm); t$_R$(major) = 22.34 min, t$_R$(minor) = 17.54 min. [a]D 22 = –102.9 (c 1.35, CHCl$_3$).

^{1}H NMR (400 MHz, CDCl$_3$, mixture of rotamers) δ 7.53 – 7.18 (m, 5H), 6.65 – 6.38 (m, 3H), 5.36 – 5.08 (m, 2H), 4.88 - 4.71 (m, 1H), 3.75 (s, 6H), 3.66 – 3.52 (m, 1H), 3.51 – 3.36 (m, 1H), 2.27 – 2.06 (m, 3H), 2.03 – 1.90 (m, 1H).

^{13}C NMR (101 MHz, CDCl$_3$, mixture of rotamers) δ 160.5, 160.4, 154.6, 137.0, 136.9, 128.6, 128.5, 128.0, 127.8, 127.6, 127.5, 127.0, 124.4, 124.3, 109.6, 109.5, 101.8,

101.7, 89.1, 88.7, 82.3, 82.2, 66.9, 66.8, 55.5, 49.2, 48.7, 46.3, 45.9, 34.0, 33.3, 29.8, 24.6, 23.8.

FTIR (neat) 2954, 1704, 1589, 1417, 1205, 1156 cm^{-1}.

HRMS (ESI+) [M+H]$^{+}$ calculated for $C_{22}H_{24}NO_4$: 366.1705, found 366.1695.
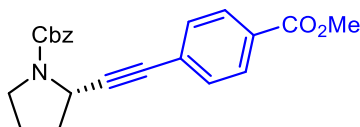
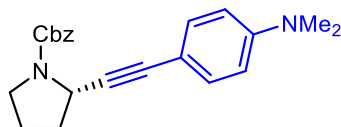**Benzyl (S)-2-((4-(methoxycarbonyl)phenyl)ethynyl)pyrrolidine-1-carboxylate (1.3).** Prepared via General Procedure A on a 0.3 mmol scale. Crude material was purified by silica gel chromatography (30% EtOAc:Hexanes) to give compound 17 (run 1: 81 mg, 74%; run 2: 102 mg, 94%) as colorless oil. The enantiomeric excess was determined to be 93% (run 1: 92% ee; run 2: 94% ee) by chiral HPLC analysis (CHIRALPAK IA, 1 mL/min, 5% i-PrOH/hexane, l = 254 nm); t_R(major) = 16.10 min, t_R(minor) = 13.23 min. [a]D 22 = −110.8 (c 1.6, CHCl$_3$).

^{1}H NMR (600 MHz, CDCl$_3$, mixture of rotamers) δ 7.95 (d, *J = 8.2 Hz*, 2H), 7.55 – 7.18 (m, 7H), 5.42 – 5.00 (m, 2H), 4.90 – 4.69 (m, 1H), 3.90 (s, 3H), 3.69 – 3.53 (m, 1H), 3.53 – 3.34 (m, 1H), 2.25 – 1.91 (m, 4H).

^{13}C NMR (151 MHz, CDCl$_3$, mixture of rotamers) δ 166.6, 154.5, 137.0, 131.7, 129.6, 129.4, 128.5, 128.0, 127.9, 127.7, 92.7, 92.4, 81.7, 67.0, 52.2, 49.3, 48.8, 46.3, 45.9, 33.9, 33.2, 24.6, 23.9.

FTIR (neat) 2951, 1706, 1409, 1356, 1276, 1111, 769 cm^{-1}.

HRMS (ESI+) [M+H]$^+$ calculated for $C_{22}H_{22}NO_4$: 364.1549, found 364.1540.

Benzyl (*S*)-2-((4-(dimethylamino)phenyl)ethynyl)pyrrolidine-1-carboxylate (1.4).

Prepared via General Procedure A on a 0.3 mmol scale. Crude material was purified by silica gel chromatography (12–24% EtOAc:Hexanes) to give compound 19 (run 1: 74.7 mg, 70%; run 2: 74.5 mg, 78%) as yellow oil. The enantiomeric excess was determined to be 70% (run 1: 72% ee; run 2: 68% ee) by chiral HPLC analysis (CHIRALPAK IB, 1 mL/min, 5% iPrOH/hexane, l = 254 nm); t_R(major) = 19.04 min, t_R(minor) = 12.88 min. [a]D 22 = –101.2 (c 1.75, CHCl$_3$).

^{1}H NMR (600 MHz, CDCl$_3$, mixture of rotamers) δ 7.59 – 7.11 (m, 7H), 6.60 (d, *J = 8.2 Hz*, 2H), 5.37 – 5.07 (m, 2H), 4.87 – 4.72 (m, 1H), 3.67 – 3.34 (m, 2H), 2.97 (s, 6H), 2.28 – 1.87 (m, 4H).

^{13}C NMR (151 MHz, CDCl$_3$, mixture of rotamers) δ 154.8, 150.2, 137.3, 132.9, 128.5, 128.0, 127.8, 127.7, 111.9, 87.2, 83.2, 66.9, 49.5, 49.1, 46.3, 45.9, 40.4, 34.3, 33.6, 24.6, 23.9.

FTIR (neat) 2949, 2222, 1703, 1608, 1521, 1411, 1355 cm^{-1}.

HRMS (ESI+) [M+H]$^+$ calculated for $C_{22}H_{25}N_2O_2$: 349.1916, found 349.1910.

Preparation of α-Methoxyaminals
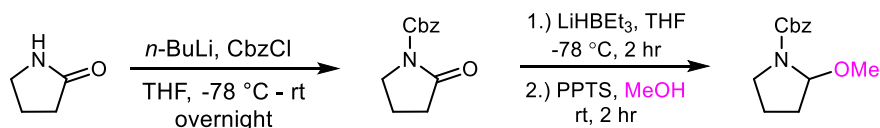
The Cbz-protected lactam was synthesized according to the literature precedent.[63] The preparation of α-methoxyaminals was adapted from a literature procedure.[64] A solution of lithium triethylborohydride (SuperHydride®) (1.0 M in THF, 1.2 equiv) was added dropwise to a solution of carbamate (1.0 equiv) in anhydrous THF (0.18 M) at -78 °C under N_2. After stirring at -78 °C for 1 hour, the reaction mixture was allowed to warm to 0 °C and treated with saturated aqueous $NaHCO_3$ (10 mL), and 1 drop of H_2O_2. The mixture was stirred for an additional 10 minutes. The organic and aqueous layers were separated, and the aqueous layer was extracted with Et_2O. The combined organic layers were washed with H_2O (1 x 20 mL) and sat. NaCl solution (1 x 20 mL). The organics were dried with $MgSO_4$, filtered through a cotton plug, and concentrated in vacuo to provide the crude hemiaminal as an oil. It was then dissolved in anhydrous MeOH (0.77 M) and treated with trimethylorthoformate (5.0 equiv) and PPTS (pyridinium p-toluenesulfonate, 15 mol %). After stirring at room temperature overnight, Et_3N (0.40 equiv) was added to the flask. The solvent was evaporated and the crude α-methoxyaminal was purified by silica gel chromatography.
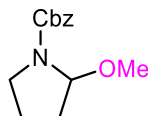
Benzyl-2-methoxypyrrolidine-1-carboxylate (1.5). Prepared on a 10-mmol scale with benzyl 2-oxopyrrolidine-1-carboxylate. Crude material was purified by silica gel chromatography (8–16% EtOAc:Hexanes) to give **5** (1.83 g, 78%) as a colorless oil:

^{1}H NMR (400 MHz, CDCl$_3$, mixture of rotamers) δ 7.44 – 7.27 (m, 5H), 5.27 – 5.09 (m, 3H), 3.57 – 3.48 (m, 1H), 3.47 - 3.23 (m, 4H), 2.14 – 1.99 (m, 1H), 1.99 – 1.84 (m, 2H), 1.83 – 1.69 (m, 1H).

^{13}C NMR (151 MHz, CDCl$_3$, mixture of rotamers) δ 155.9, 155.1, 136.8, 128.6, 128.2, 128.0, 89.3, 88.7, 67.3, 67.0, 56.1, 55.5, 46.1, 45.9, 32.7, 32.1, 22.8, 21.9.

The spectral data matches that reported in the literature.[69]

Investigation of Hemiaminal Ethers

α-ethoxyaminal and α-isopropoxyaminal ethers (entries 2 and 3) were prepared using the same procedure as for the α-methoxyaminal but with their respective orthoformate and alcohol reagents. The acetate ether (entry 4) was prepared according to literature procedure.[64-66]

Table 1.1 – Investigation of Hemiaminal Ethers
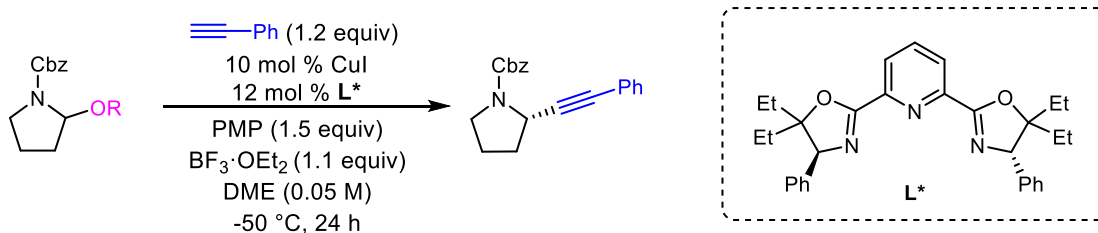
Entry	Aminal (OR)	Yield(%)[a]	ee (%)[b]
1	OMe	89	91
2	OEt	92	89
3	OiPr	83	86
4	OAc	27	93
5	OH	trace	nd[c]

[a]Determined by ^{1}H NMR with 1,3,5-trimethoxybenzene as internal standard. [b]Determined by HPLC using a chiral stationary phase. [c]nd = not determined.

1.5   References

1.   Daly, J. W., Ernest Guenther Award in Chemistry of Natural Products. Amphibian Skin: A Remarkable Source of Biologically Active Arthropod Alkaloids. *J. Med. Chem.* **2003,** *46* (4), 445-452.
2.   Edwards, J. R.; Turner, P. J.; Wannop, C.; Withnell, E. S.; Grindey, A. J.; Nairn, K., In Vitro Antibacterial Activity of SM-7338, a Carbapenem Antibiotic with Stability to Dehydropeptidase I. *Antimicrob. Agents Chemother.* **1989,** *33* (2), 215-222.
3.   Kongkiatpaiboon, S.; Schinnerl, J.; Felsinger, S.; Keeratinijakal, V.; Vajrodaya, S.; Gritsanapan, W.; Brecker, L.; Greger, H., Structural relationships of stemona alkaloids: assessment of species-specific accumulation trends for exploiting their biological activities. *J. Nat. Prod.* **2011,** *74* (9), 1931-8.
4.   Martin, G.; Angyal, P.; Egyed, O.; Varga, S.; Soos, T., Total Syntheses of Dihydroindole Aspidosperma Alkaloids: Reductive Interrupted Fischer Indolization Followed by Redox Diversification. *Org. Lett.* **2020,** *22* (12), 4675-4679.

5.   Schinnerl, J.; Brem, B.; But, P. P.; Vajrodaya, S.; Hofer, O.; Greger, H., Pyrrolo- and pyridoazepine alkaloids as chemical markers in Stemona species. *Phytochemistry.* **2007,** *68* (10), 1417-27.

6.   Secor, H. V. S., J. I., The Preparation of "Elongated" Nicotine Analogues. *Heterocycles* **1986,** *24* (6), 1687-1698.

7.   Taylor, R. D.; MacCoss, M.; Lawson, A. D. G., Rings in Drugs. *J. Med. Chem.* **2014,** *57* (14), 5845-5859.

8.   Wierzejska, J.; Motogoe, S.; Makino, Y.; Sengoku, T.; Takahashi, M.; Yoda, H., A new approach toward the total synthesis of (+)-batzellaside B. *Beilstein J. Org. Chem.* **2012,** *8*, 1831-8.

9.   Vitaku, E.; Smith, D. T.; Njardarson, J. T., Analysis of the Structural Diversity, Substitution Patterns, and Frequency of Nitrogen Heterocycles among U.S. FDA Approved Pharmaceuticals. *J. Med. Chem.* **2014,** *57* (24), 10257-10274.

10.   Ali, S.; Fonseca, V., Saxagliptin overview: special focus on safety and adverse effects. *Expert Opin. Drug. Saf.* **2013,** *12* (1), 103-109.

11.   Butler, K., Anisomycin. II.1 Biosynthesis of Anisomycin. *J. Org. Chem.* **1966,** *31*, 317-320.

12.   Saha, S. P.; Bhalla, D. K.; Whayne, T. F., Jr.; Gairola, C., Cigarette smoke and adverse health effects: An overview of research trends and future needs. *Int. J. Angiol.* **2007,** *16* (3), 77-83.

13.   Chang, M.-Y.; Tai, H.-M.; Lin, C.-H.; Chang, N.-C., Synthesis of Lupinine. *Heterocycles* **2005,** *65* (2), 395-402.

14.   Davies, S. G.; Fletcher, A. M.; Foster, E. M.; Houlsby, I. T.; Roberts, P. M.; Schofield, T. M.; Thomson, J. E., An efficient asymmetric synthesis of (-)-lupinine. *Chem. Commun.* **2014,** *50* (61), 8309-11.

15.   Santos, L.; Mirabal-Gallardo, Y.; Shankaraiah, N.; Simirgiotis, M., Short Total Synthesis of (-)-Lupinine and (-)-Epiquinamide by Double Mitsunobu Reaction. *Synthesis.* **2010,** *2011* (01), 51-56.

16.   Willoughby, C. A.; Buchwald, S. L., Synthesis of highly enantiomerically enriched cyclic amines by the catalytic asymmetric hydrogenation of cyclic imines. *J. Org. Chem.* **1993,** *58* (27), 7627-7629.

17.   Han, J.; Xu, B.; Hammond, G. B., Highly Efficient Cu(I)-Catalyzed Synthesis of N-Heterocycles through a Cyclization-Triggered Addition of Alkynes. *J. Am. Chem. Soc.* **2010,** *132* (3), 916.

18.   Bell, J. D.; Harkiss, A. H.; Wellaway, C. R.; Sutherland, A., Stereoselective synthesis of 2,6-trans-4-oxopiperidines using an acid-mediated 6-endo-trig cyclisation. *Org. Biomol. Chem.* **2018,** *16* (35), 6410-6422.

19.   Cariou, C. A.; Kariuki, B. M.; Snaith, J. S., Stereoselective synthesis of 2,4,5-trisubstituted piperidines by carbonyl ene and Prins cyclisations. *Org. Biomol. Chem.* **2008,** *6* (18), 3337-48.

20.   Guerola, M.; Escolano, M.; Alzuet-Pina, G.; Gomez-Bengoa, E.; Ramirez de Arellano, C.; Sanchez-Rosello, M.; Del Pozo, C., Synthesis of substituted piperidines

by enantioselective desymmetrizing intramolecular aza-Michael reactions. *Org. Biomol. Chem.* **2018,** *16* (25), 4650-4658.

21.　　Iza, A.; Uria, U.; Reyes, E.; Carrillo, L.; Vicario, J. L., A general approach for the asymmetric synthesis of densely substituted piperidines and fully substituted piperidinones employing the asymmetric Mannich reaction as key step. *RSC Adv.* **2013,** *3* (48), 25800-25811.

22.　　Li, P.; Huang, Y.; Hu, X.; Dong, X. Q.; Zhang, X., Access to Chiral Seven-Member Cyclic Amines via Rh-Catalyzed Asymmetric Hydrogenation. *Org. Lett.* **2017,** *19* (14), 3855-3858.

23.　　Reddy, A. G. K.; Satyanarayana, G., A simple efficient sequential one-pot intermolecular aza-Michael addition and intramolecular Buchwald–Hartwig α-arylation of amines: synthesis of functionalized tetrahydroisoquinolines. *Tetrahedron* **2012,** *68* (38), 8003-8010.

24.　　Tripathi, S.; Ambule, M. D.; Srivastava, A. K., Construction of Highly Functionalized Piperazinones via Post-Ugi Cyclization and Diastereoselective Nucleophilic Addition. *J. Org. Chem.* **2020,** *85* (11), 6910-6923.

25.　　Van Beek, W. E.; Van Stappen, J.; Franck, P.; Abbaspour Tehrani, K., Copper(I)-Catalyzed Ketone, Amine, and Alkyne Coupling for the Synthesis of 2-Alkynylpyrrolidines and -piperidines. *Org. Lett.* **2016,** *18* (19), 4782-4785.

26.　　Wdowik, T.; Galster, S. L.; Carmo, R. L. L.; Chemler, S. R., Enantioselective, Aerobic Copper-Catalyzed Intramolecular Carboamination and Carboetherification of Unactivated Alkenes. *ACS. Catal.* **2020,** *10* (15), 8535-8541.

27.　　Wilde, J. H.; Dickie, D. A.; Harman, W. D., A Highly Divergent Synthesis of 3-Aminotetrahydropyridines. *J. Org. Chem.* **2020,** *85* (12), 8245-8252.

28.　　Xie, L.-H.; Cheng, J.; Luo, Z.-W.; Lu, G., Mannich Reaction of Indole with Cyclic Imines in Water. *Tet. Lett.* **2018,** *59* (5), 457-461.

29.　　Zhang, Y.; Kong, D.; Wang, R.; Hou, G., Synthesis of chiral cyclic amines via Ir-catalyzed enantioselective hydrogenation of cyclic imines. *Org. Biomol. Chem.* **2017,** *15* (14), 3006-3012.

30.　　Mitchell, E. A.; Peschiulli, A.; Lefevre, N.; Meerpoel, L.; Maes, B. U., Direct alpha-functionalization of saturated cyclic amines. *Chem. Eur. J.* **2012,** *18* (33), 10092-10142.

31.　　Coldham, I.; Leonori, D., Regioselective and stereoselective copper(I)-promoted allylation and conjugate addition of N-Boc-2-lithiopyrrolidine and N-Boc-2-lithiopiperidine. *J. Org. Chem.* **2010,** *75* (12), 4069-77.

32.　　Park, S. H.; Kang, H. J.; Ko, S.; Park, S.; Chang, S., A short and concise synthetic route to (−)-coniceine. *Tetrahedron Asymmetry.* **2001,** *12* (18), 2621-2624.

33.　　Shankaraiah, N.; Pilli, R. A.; Santos, L. S., Enantioselective total syntheses of ropivacaine and its analogues. *Tet. Lett.* **2008,** *49* (34), 5098-5100.

34.　　Liu, J. X.; Dasgupta, S.; Watson, M. P., Enantioselective additions of copper acetylides to cyclic iminium and oxocarbenium ions. *Beilstein J. Org. Chem.* **2015,** *11*, 2696-2706.

35.   Maity, P.; Srinivas, H. D.; Watson, M. P., Copper-Catalyzed Enantioselective Additions to Oxocarbenium Ions: Alkynylation of Isochroman Acetals. *J. Am. Chem. Soc.* **2011,** *133* (43), 17142-17145.

36.   Dasgupta, S.; Rivas, T.; Watson, M. P., Enantioselective Copper(I)-Catalyzed Alkynylation of Oxocarbenium Ions to Set Diaryl Tetrasubstituted Stereocenters. *Angew. Chem. Int. Ed.* **2015,** *54* (47), 14154-14158.

37.   Cozzi, Pier G.; Hilgraf, R.; Zimmermann, N., Acetylenes in Catalysis: Enantioselective Additions to Carbonyl Groups and Imines and Applications Beyond. *Eur. J. Org. Chem.* **2004,** *2004* (20), 4095-4105.

38.   Mukaiyama, T.; Suzuki, K.; Soai, K.; Sato, T., Enantioselective Addition of Acetylene to Aldehyde. Preparation of Optically Active Alkynyl Alcohols. *Chem. Lett.* **1979,** *8* (5), 447-448.

39.   Frantz, D. E.; Fässler, R.; Carreira, E. M., Facile Enantioselective Synthesis of Propargylic Alcohols by Direct Addition of Terminal Alkynes to Aldehydes. *J. Am. Chem. Soc.* **2000,** *122* (8), 1806-1807.

40.   Anand, N. K.; Carreira, E. M., A Simple, Mild, Catalytic, Enantioselective Addition of Terminal Acetylenes to Aldehydes. *J. Am. Chem. Soc.* **2001,** *123* (39), 9687-9688.

41.   Pierce, M. E.; Parsons, R. L.; Radesca, L. A.; Lo, Y. S.; Silverman, S.; Moore, J. R.; Islam, Q.; Choudhury, A.; Fortunak, J. M. D.; Nguyen, D.; Luo, C.; Morgan, S. J.; Davis, W. P.; Confalone, P. N.; Chen, C.-y.; Tillyer, R. D.; Frey, L.; Tan, L.; Xu, F.; Zhao, D.; Thompson, A. S.; Corley, E. G.; Grabowski, E. J. J.; Reamer, R.; Reider, P. J., Practical Asymmetric Synthesis of Efavirenz (DMP 266), an HIV-1 Reverse Transcriptase Inhibitor. *J. Org. Chem.* **1998,** *63* (23), 8536-8543.

42.   Wei, C.; Li, C.-J., Enantioselective Direct-Addition of Terminal Alkynes to Imines Catalyzed by Copper(I)pybox Complex in Water and in Toluene. *J. Am. Chem. Soc.* **2002,** *124* (20), 5638-5639.

43.   Wei, C.; Mague, J. T.; Li, C.-J., Cu(I)-catalyzed direct addition and asymmetric addition of terminal alkynes to imines. *Proc. Natl. Acad. Sci. U. S. A.* **2004,** *101* (16), 5749.

44.   Koradin, C.; Polborn, K.; Knochel, P., Enantioselective Synthesis of Propargylamines by Copper-Catalyzed Addition of Alkynes to Enamines†. *Angew. Chem. Int. Ed.* **2002,** *41* (14), 2535-2538.

45.   Koradin, C.; Gommermann, N.; Polborn, K.; Knochel, P., Synthesis of Enantiomerically Enriched Propargylamines by Copper-Catalyzed Addition of Alkynes to Enamines. *Chem. Eur. J.* **2003,** *9* (12), 2797-2811.

46.   Gommermann, N.; Koradin, C.; Polborn, K.; Knochel, P., Enantioselective, Copper(I)-Catalyzed Three-Component Reaction for the Preparation of Propargylamines. *Angew. Chem. Int. Ed.* **2003,** *42* (46), 5763-5766.

47.   Li, Z.; Li, C.-J., Catalytic Enantioselective Alkynylation of Prochiral sp3 C−H Bonds Adjacent to a Nitrogen Atom. *Org. Lett.* **2004,** *2* (26), 4997.

48.   Li, Z.; MacLeod, P. D.; Li, C.-J., Studies on Cu-catalyzed asymmetric alkynylation of tetrahydroisoquinoline derivatives. *Tetrahedron Asymmetry.* **2006,** *17* (4), 590-597.

49.   Li, Z.; Li, C.-J., CuBr-Catalyzed Efficient Alkynylation of sp3 C−H Bonds Adjacent to a Nitrogen Atom. *J. Am. Chem. Soc.* **2004,** *126* (38), 11810.

50.   Taylor, A., M. ; Schreiber, S. L., Enantioselective Addition of Terminal Alkynes to Isolated Isoquinoline Iminiums. *Org. Lett.* **2006,** *8* (1), 143.

51.   Dasgupta, S.; Liu, J.; Shoffler, C. A.; Yap, G. P. A.; Watson, M. P., Enantioselective, Copper-Catalyzed Alkynylation of Ketimines To Deliver Isoquinolines with alpha-Diaryl Tetrasubstituted Stereocenters. *Org. Lett.* **2016,** *18* (23), 6006-6009.

52.   Black, D. A.; Beveridge, R., E.; Arndtsen, B. A., Copper-Catalyzed Coupling of Pyridines and Quinolines with Alkynes: A One-Step, Asymmetric Route to Functionalized Heterocycles. *J. Org. Chem.* **2007,** *73* (5), 1906.

53.   Hashimoto, T.; Omote, M.; Maruoka, K., Catalytic Asymmetric Alkynylation of C1-Substituted C,N-Cyclic Azomethine Imines by CuI/Chiral Brønsted Acid Co-Catalyst. *Angew. Chem. Int. Ed.* **2011,** *50* (38), 8952-8955.

54.   Sun, S.; Li, C.; Floreancig, P. E.; Lou, H.; Liu, L., Highly Enantioselective Catalytic Cross-Dehydrogenative Coupling of N-Carbamoyl Tetrahydroisoquinolines and Terminal Alkynes. *Org. Lett.* **2015,** *17* (7), 1684-1687.

55.   Pappoppula, M.; Cardoso, F. S.; Garrett, B. O.; Aponick, A., Enantioselective Copper-Catalyzed Quinoline Alkynylation. *Angew. Chem. Int. Ed.* **2015,** *54* (50), 15202-6.

56.   Sun, Z.; Yu, S.; Ding, Z.; Ma, D., Enantioselective Addition of Activated Terminal Alkynes to 1-Acylpyridinium Salts Catalyzed by Cu−Bis(oxazoline) Complexes. *J. Am. Chem. Soc.* **2007,** *129* (30), 9300-9301.

57.   Beekan, P.; Fowler, F. F., N-Methyl-1,2,3,4-tetrahydropyridine. *J. Org. Chem.* **1980,** *45*, 1336-1338.

58.   Turcaud, S.; Sierecki, E.; Martens, T.; Royer, J., Asymmetric α-Alkynylation of Piperidine via N-Sulfinyliminium Salts. *J. Org. Chem.* **2007,** *72* (13), 4882-4885.

59.   Chan, J. Z.; Yesilcimen, A.; Cao, M.; Zhang, Y.; Zhang, B.; Wasa, M., Direct Conversion of N-Alkylamines to N-Propargylamines through C–H Activation Promoted by Lewis Acid/Organocopper Catalysis: Application to Late-Stage Functionalization of Bioactive Molecules. *J. Am. Chem. Soc.* **2020,** *142* (38), 16493-16505.

60.   Tse, M. K.; Bhor, S.; Klawonn, M.; Anilkumar, G.; Jiao, H.; Döbler, C.; Spannenberg, A.; Mägerlein, W.; Hugl, H.; Beller, M., Ruthenium-Catalyzed Asymmetric Epoxidation of Olefins Using H2O2, Part I: Synthesis of New Chiral N,N,N-Tridentate Pybox and Pyboxazine Ligands and Their Ruthenium Complexes. *Chem. Eur. J.* **2006,** *12* (7), 1855-1874.

61.   Guan, W. Y.; Santana, S. O.; Liao, J. N.; Henninger, K.; Watson, M. P., Enantioselective Alkynylation of Unstabilized Cyclic Iminium Ions. *ACS. Catal.* **2020,** *10* (23), 13820-13824.

62.   Louwrier, S.; Tuynman, A.; Hiemstra, H., Synthesis of bicyclic guanidines from pyrrolidin-2-one. *Tetrahedron* **1996,** *52* (7), 2629-2646.

63.   Liu, X.-K.; Ye, J.-L.; Ruan, Y.-P.; Li, Y.-X.; Huang, P.-Q., Total Synthesis of (−)-Sessilifoliamide J. *J. Org. Chem.* **2013,** *78* (1), 35-41.

64.   Steffan, T.; Renukappa-Gutke, T.; Höfner, G.; Wanner, K. T., Design, synthesis and SAR studies of GABA uptake inhibitors derived from 2-substituted pyrrolidine-2-yl-acetic acids. *Bioorg. Med. Chem.* **2015,** *23* (6), 1284-1306.

65.   Nicolaou, K. C.; Patron, A. P.; Ajito, K.; Richter, P. K.; Khatuya, H.; Bertinato, P.; Miller, R. A.; Tomaszewski, M. J., Total Synthesis of Swinholide A, Preswinholide A, and Hemiswinholide A. *Chem. Eur. J.* **1996,** *2* (7), 847-868.

66.   Fonseca, T. d. S.; Silva, M. R. d.; de Oliveira, M. d. C. F.; Lemos, T. L. G. d.; Marques, R. d. A.; de Mattos, M. C., Chemoenzymatic synthesis of rasagiline mesylate using lipases. *Appl. Catal. A: Gen.* **2015,** *492*, 76-82.

67.   Lautens, M.; Marchese, A. D., Copper-Catalyzed Enantioselective Alkynylation of Unstabilized Cyclic Iminium Ions. *Synfacts* **2021,** *17* (2), 170.

68.   Le Vaillant, F.; Courant, T.; Waser, J., Room-Temperature Decarboxylative Alkynylation of Carboxylic Acids Using Photoredox Catalysis and EBX Reagents. *Angew. Chem. Int. Ed.* **2015,** *54* (38), 11200-11204.

69.   Kabeshov, M. A.; Musio, B.; Murray, P. R. D.; Browne, D. L.; Ley, S. V., Expedient Preparation of Nazlinine and a Small Library of Indole Alkaloids Using Flow Electrochemistry as an Enabling Technology. *Org. Lett.* **2014,** *16* (17), 4618-4621.

Chapter 2

DIASTEREOSELECTIVE ALKYNYLATIONS OF *β*-BROMOIMINIUM IONS VIA COPPER(I) CATALYSIS

Work described here will be published in Organic Letters (Santana, S. O.; Guan, W.; Yap, G. P. A.; Watson, M. P.).

2.1 Introduction

As mentioned in Chapter 1.1, α-chiral cyclic amines are a highly valued moiety in organic chemistry.[1-9] α,β-Difunctionalized cyclic amines are also important and relevant compounds yet are even more difficult to directly synthesize from cyclic amines. Saxagliptin, anisomycin, and lupinine were previously discussed in Chapter 1.1 (**Figure 1.1, Figure 2.1**) Aprepitant (Emend) is a difunctionalized amine that is used to alleviate the emetic effects (nausea) of chemotherapy (**Figure 2.1**).[10, 11] Febrifugine is a natural product found in the hydrangea plant, and has been shown to exhibit anti-malarial, anti-protozoal, and other bioactivities.[12-15] Much like α-chiral cyclic amines, α, β-difunctionalized cyclic amines are commonly synthesized via cyclization of pre-functionalized acyclic amines (**Scheme 1.2**).[6, 16-29] Rather than a multi-step functionalization/cyclization of an acyclic amine, it would be more efficient to functionalize a cyclic amine with fewer steps and less reliance on inherent substrate bias.

Figure 2.1 – Bioactive Difunctionalized Amines

anisomycin
antibiotic

saxagliptin (Onglyza®)
hypoglycemic

lupinine
natural product

febrifugine
antimalarial and antiprotozoal

aprepitant (Emend®)
anti-nausea medication
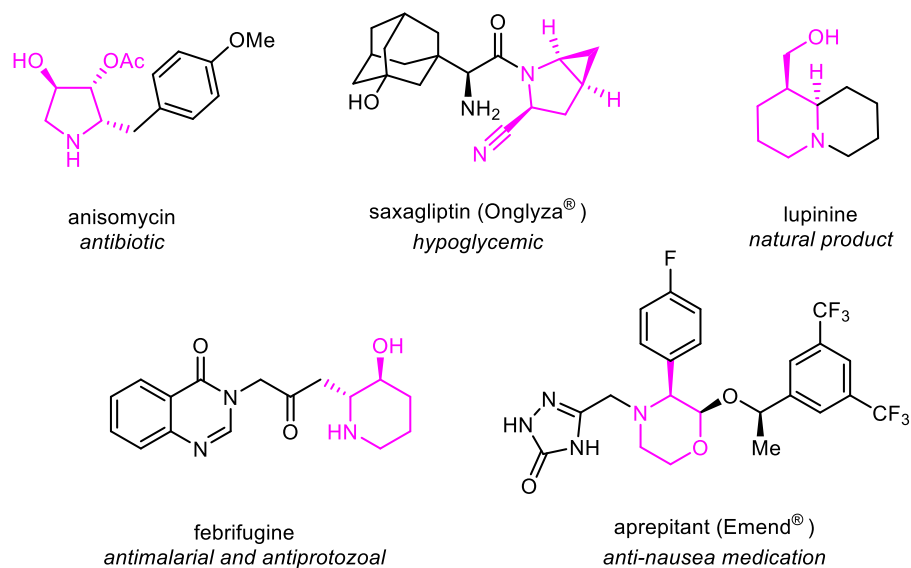
There are few examples of stereoselective difunctionalization of cyclic amines. Our group has previously developed a diastereoselective difunctionalization of cyclic oxocarbenium ions with zinc acetylides; this two-step method yields *anti-α,β*-substituted tetrahydropyrans from *β*-(halo)-acetals in good yields and high diastereoselectivities (**Scheme 2.1**).[30] The alkynylation step is proposed to proceed via a *β*-bromo-oxocarbenium ion, where the bromide substituent forces alkynylation from the opposite π-face. Although this method does not describe the use of iminium ions as electrophiles, it has been discussed in Chapter 1.1 that oxocarbenium and iminium ions have similar chemical properties and thus similar reactivities.

Scheme 2.1 – Watson's Difunctionalization Method of Oxocarbenium Ions
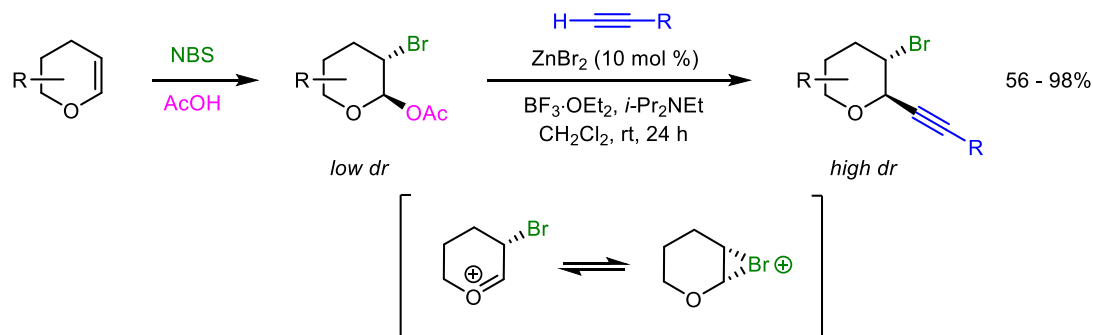
Onomura and co-workers have developed a method to yield *syn-α*, *β*-substituted piperidines using aryl boronic acids.[31, 32] This method provides good yields and great diastereoselectivities. The diastereoselectivity is controlled via coordination of the boron to the *β*-hydroxy substituent (**Scheme 2.2**). Additionally, they have demonstrated a vinylation method with halide substituents at the *β*-position of the piperidine ring to yield *anti-α*, *β*-substituted piperidines.

Scheme 2.2 – Onomura's Difunctionalization Using Boronic Acids
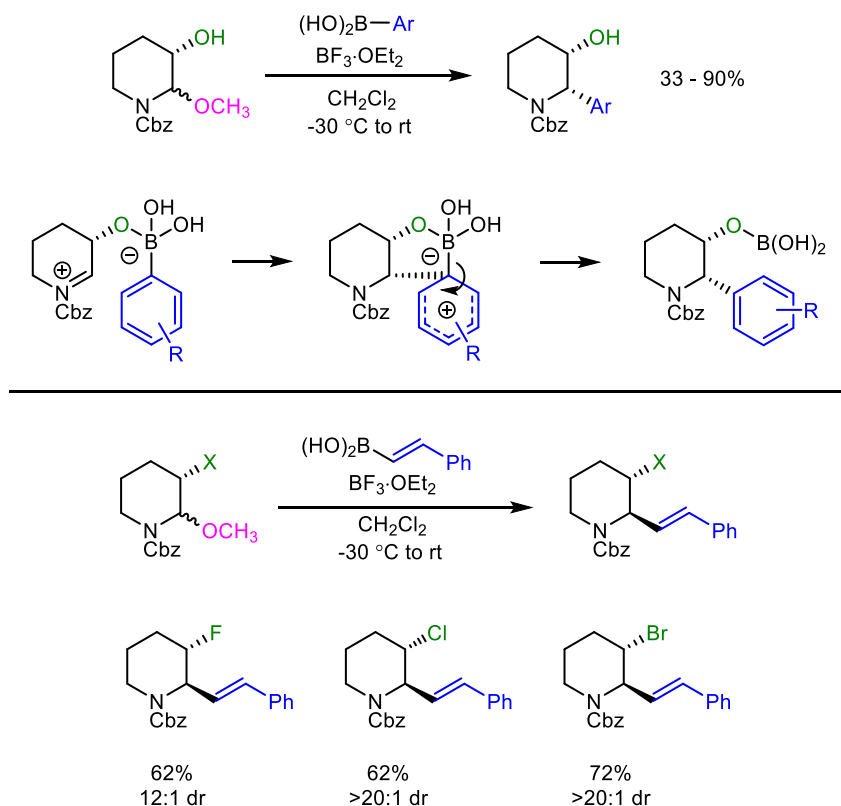
In this case, the diastereoselectivity is controlled by the halide, which is preferentially positioned axial in the half-chair conformation of the iminium ion transition state (**Figure 2.2**). When chloride or bromide are present on the ring, Onomura suggests a steric repulsion effect that forces the nucleophile to approach the iminium ion from the opposite face, resulting in an *anti*-selectivity (**2.2**). If fluoride is present, Onomura suggests a dipole-dipole electrostatic effect (**2.1**). The position of the fluoride stabilizes the orbitals of the electropositive carbon atom, so long as the fluoride is positioned axial in the half-chair conformation.

Figure 2.2 – Onomura's Stereochemical Rationale

| Dipole-Dipole Electrostatic Effect | Steric Repulsion Effect |
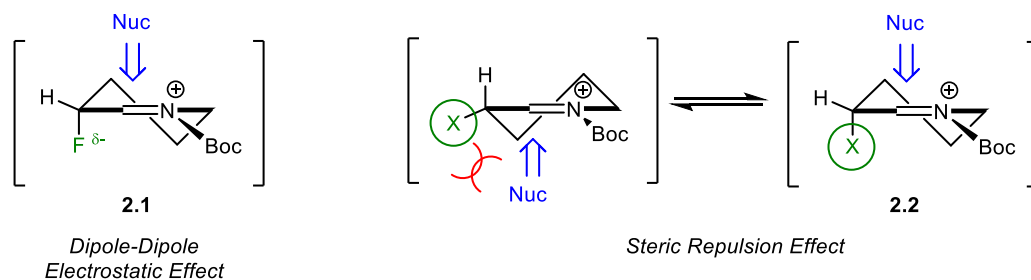
Beyond Watson's alkynylation work with oxocarbenium ions and Onomura's vinylation work with iminium ions, stereoselective difunctionalization of cyclic iminium ions with other nucleophiles remains largely unknown to date. Given the versatility of an alkyne substituent and the importance of nitrogen heterocycles in bioactive molecules, we were interested in developing a halogenation/alkynylation sequence to provide α,β-difunctionalized nitrogen heterocycles with high diastereoselectivity.

2.2   Results and Discussion

I envisioned a pathway to synthesize the iminium ion *in situ* similar to our previous work with oxocarbenium and iminium ions, wherein the iminium ion could be formed via ionization of the C–O bond assisted by Lewis acid. The halide and methoxide substitution could be installed simultaneously from an enamine (**2.3**) using *N*-bromosuccinimide (NBS) in methanol (**Scheme 2.3**).[30, 33, 34]

Scheme 2.3 – Our Goal for Difunctionalization of Cyclic Iminium Ions
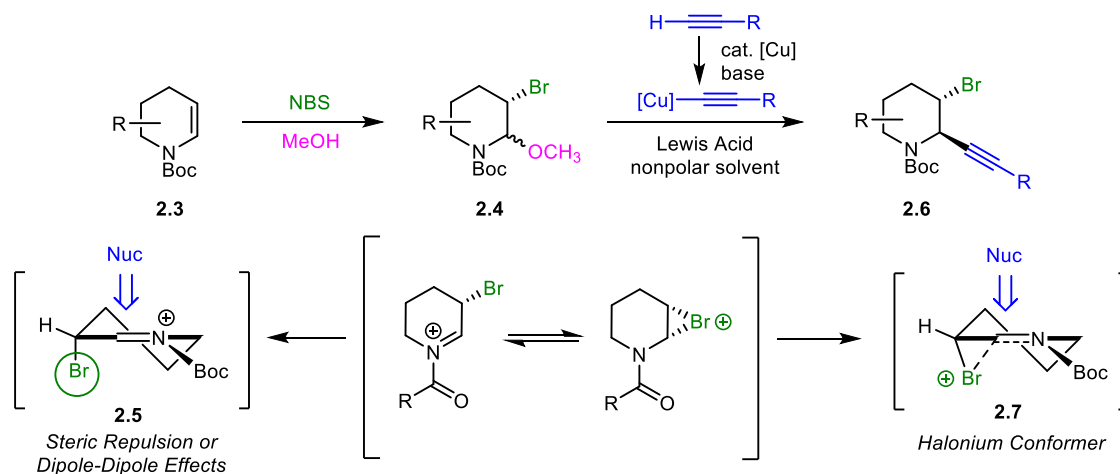
This reaction was known to provide poor stereoselectivity,[33, 34] however cleavage of the methoxide would generate the iminium ion and the bromide could assist in stabilization, either through Onomura's steric repulsion theory (**2.5**) or through a resonance-stabilized bromonium ion traditionally seen in halogenation reactions (**2.7**).[30, 31] In either scenario, the bromide would control the stereoselectivity such that a nucleophile, in this case an acetylide, would preferentially attack the opposite face of the iminium ion, yielding an *anti*-substituted piperidine. Noting that the bromination step was run in methanol, we hypothesized that the use of a less polar solvent in the alkynylation step might lead to higher diastereoselectivity because the iminium ion would be more reliant on bromonium stabilization in the absence of strong solvent dipoles. Indeed, Onomura observes high diastereoselectivity when using dichloromethane as a fairly nonpolar solvent.[31, 32]

I chose to protect the nitrogen atom with a Boc group, as it is a labile protecting group that can be easily deprotected via trifluoroacetic acid in dichloromethane. The general route to the enamine precursors is shown in **Scheme 2.4**. Boc-protected enamine was synthesized from commercially available 1-Boc-2-piperidone via reduction-elimination (**Scheme 2.4**);[35] in some cases, the use of LiHBEt$_3$ was more successful in synthesizing the enamine precursors.[36]

Scheme 2.4 – Reduction of Piperidones to Enecarbamates
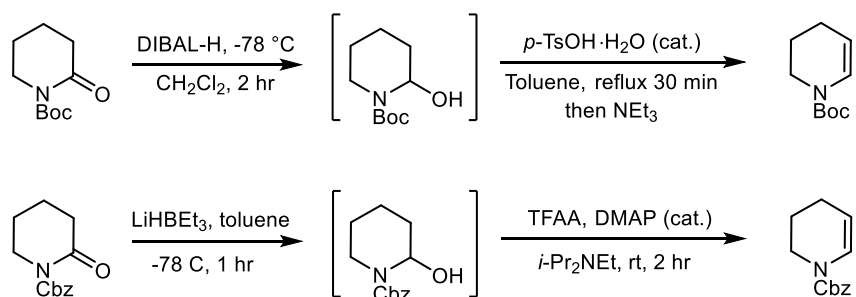
The bromination was then performed using freshly recrystallized NBS in anhydrous methanol at ambient temperature, as shown in **Scheme 2.5** for the synthesis of *tert*-butyl-3-bromo-2-methoxypiperidine-1-carboxylate (**2.4**).[30, 33] It is imperative that NBS is freshly recrystallized as significantly lower yields were observed upon skipping this step. Another crucial detail is that an aqueous sodium thiosulfate solution must be introduced during work-up to quench any remaining bromine or NBS in the organic layer. Neglecting this wash affected the subsequent alkynylation reaction detrimentally and may also degrade the starting material over time. The pure aminal (**2.4**) was not prone to spontaneous decomposition and was stable to air, moisture, and

silica gel chromatography. The compound was a pale-yellow to clear oil and exhibited rotamers and diastereomers in the NMR spectra under numerous deuterated solvents. Variable-temperature NMR (VT-NMR) in DMSO-d_6 was used to confirm the presence of diastereomers, and the diastereomeric ratio (dr) was determined to be 2.3:1. As shown in **Scheme 2.7** below, this procedure was effective for a range of enamine substrates, delivering the hemiaminal ethers in an average yield of 69%.
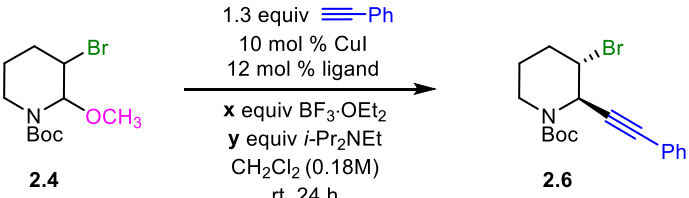
Scheme 2.5 – Bromination of Enecarbamates to β-(bromo)Hemiaminal Ethers

2.3 → **2.4**, NBS, MeOH, 0 °C, to r.t., 16 h, 75%, 2.3:1 dr
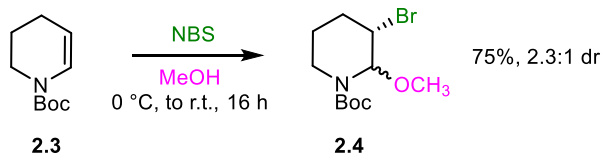
The alkynylation of hemiaminal ether with phenyl acetylene was used as the model reaction for optimization. Copper(I) iodide, ligand (synthesized according to the literature precedent),[37] and base (diisopropyl-*N*-ethylamine, DIPEA) were used to form the copper acetylide *in situ.* Boron trifluoride etherate (BF$_3$•OEt$_2$, 48%) was selected as the Lewis acid to ionize the aminal and give the iminium ion intermediate. The first parameter to be investigated was ligand (**Table 2.1**), which was theorized to increase the solubility of copper iodide as well as increase the reactivity of the copper acetylide. The use of PhPyBOX provided a promising yield of 21%, but an achiral ligand was desired as a less expensive and reasonable additive in lieu of the enantioenriched ligand. Bispyrazolpyridine (1-bpp) was determined to be a reliable substitute for the ligand, and so I continued the optimization using this ligand. It is of

note that introducing any chiral ligand under these conditions did not provide any enantioenriched product.

Table 2.1 – Investigation of Ligands

entry	ligand	equiv base/Lewis acid	yield (%)[b]
1	PhPyBOX	1.5 : 3.0	21
2	terpy	1.5 : 3.0	15
3	1-bpp	1.5 : 3.0	18
4	1-bpp	1.5 : 1.0	65
5	Phen	1.5 : 1.0	40
6	bipy	1.5 : 1.0	40
7	terpy	1.5 : 1.0	0
8	PhPyBOX	1.5 : 1.0	62
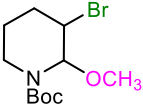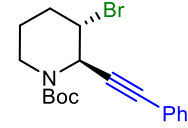
[a]Conditions: aminal (0.1 mmol, 1.0 equiv), CuI (0.010 mmol, 10 mol %), ligand, (0.012 mmol, 12 mol %) alkyne (0.13 mmol, 1.3 equiv), BF$_3$·OEt$_2$ (0.1 mmol, 1.0 equiv), i-Pr$_2$NEt (0.2 mmol, 2.0 equiv), CH$_2$Cl$_2$ (0.18M). [b]Determined by ^{1}H NMR analysis with 1,3,5-trimethoxybenzene as an internal standard.
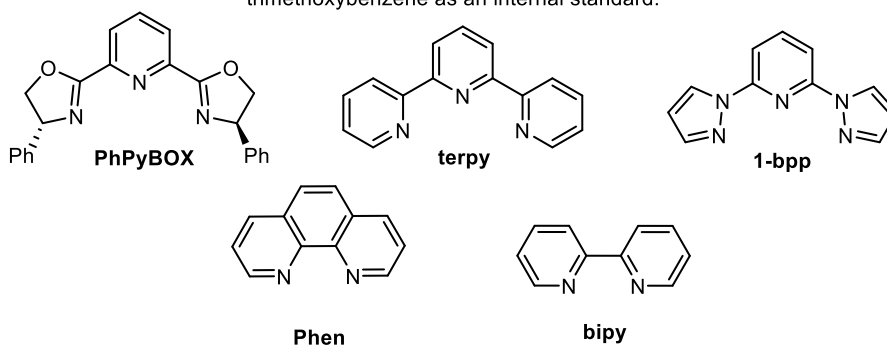
A variety of solvents were investigated for this reaction (**Table 2.2**). Dichloromethane (entry 1) was effective and gave 21% product, but chloroform (entry

2) was not as successful in the reaction. Ethereal solvents such as dioxane (entry 4), ether (entry 5), and MTBE (entry 7) did not lead to product formation. Polar solvents like DMA (entry 3) and NMP (entry 9) showed some product formation. Tetrahydrofuran (THF) yielded 47% of product (entry 6), but concern was raised when 2-methyl tetrahydrofuran (2-MeTHF) resulted in trace amount of product (entry 8). It was theorized that THF may be coordinating with $BF_3 \cdot OEt_2$, and thus reduced the reactivity of the Lewis acid and preventing decomposition of the iminium ion intermediates or other undesired side reactions.[38] Binding BF_3 would not be as favorable with 2-MeTHF as the additional methyl group would disfavor coordination via steric interaction. This lack of coordination would cause excess Lewis acid to decompose the starting material over time. To rectify this issue, the equivalents of $BF_3 \cdot OEt_2$ were decreased from 3.0 to 1.0, with the expectation that similar yield would then be observed for both THF and 2-MeTHF. This hypothesis seemed plausible, as yields in THF and 2-MeTHF were 66% and 52%, respectively, when less Lewis acid was used. Additionally, varying equivalents of base and Lewis acid were investigated (**Table 2.3**). This data shows that base must be in excess of Lewis acid, which further suggests that excess Lewis acid leads to decomposition of the starting material. Therefore, further optimization was continued using THF as the solvent and 1.0 equivalent of $BF_3 \cdot OEt_2$.

Table 2.2 – Investigation of Solvents

entry	solvent	solubility	equiv. Lewis acid	yield (%)[b]
1	CH_2Cl_2	heterogenous	3.0	18
2	$CHCl_3$	heterogenous	3.0	0
3	DMA	heterogenous	3.0	18
4	dioxane	heterogenous	3.0	0
5	Et_2O	heterogenous	3.0	0
6	THF	homogenous	3.0	47
7	MTBE	homogenous	3.0	trace
8	2-MeTHF	homogenous	3.0	trace
9	NMP	heterogenous	3.0	16
10	MeCN	homogenous	3.0	4
11	THF	homogenous	1.0	66
12	2-MeTHF	homogenous	1.0	52

[a]Conditions: aminal (0.1 mmol, 1.0 equiv), CuI (0.010 mmol, 10 mol %), 1-bpp (0.012 mmol, 12 mol %), alkyne (0.13 mmol, 1.3 equiv), $BF_3 \cdot OEt_2$ (0.1 mmol, 1.0 equiv), i-Pr_2NEt (0.2 mmol, 2.0 equiv), solvent (0.18M). [b]Determined by ^{1}H NMR analysis with 1,3,5-trimethoxybenzene as an internal standard.

Other bases were investigated to improve the yield of product; however, commonly used bases in alkynylations did not improve product yield (**Table 2.4**). The equivalents of base did, however, result in an increase of the yield from 66% to 87% (**Table 2.3**, entries 1 and 7)

Table 2.3 – Investigation of Lewis acid Equivalents
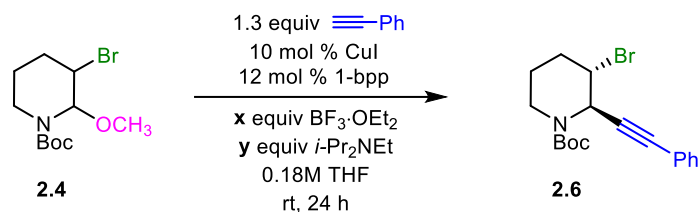
entry	equiv base/Lewis acid	yield (%)[b]
1	1.5 : 1.0	66
2	1.5 : 1.1	60
3	1.5 : 1.3	55
4	1.5 : 1.5	30
5	1.5 : 1.7	39
6	1.5 : 2.0	15
7	2.0 : 1.0	87

[a]Conditions: aminal (0.1 mmol, 1.0 equiv), CuI (0.010 mmol, 10 mol %), 1-bpp (0.012 mmol, 12 mol %)alkyne (0.13 mmol, 1.3 equiv), BF$_3$·OEt$_2$ (0.1 mmol, 1.0 equiv), i-Pr$_2$NEt (0.2 mmol, 2.0 equiv), solvent (0.18M). [b]Determined by ^{1}H NMR analysis with 1,3,5-trimethoxybenzene as an internal standard.

Table 2.4 – Investigation of Bases
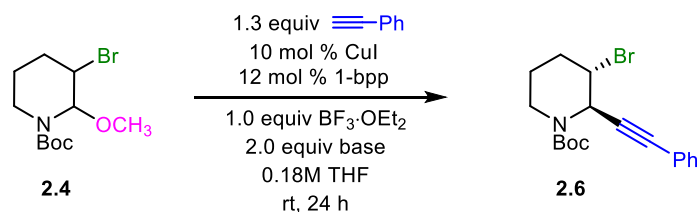
entry	base	yield (%)[b]	RSM
1	i-Pr$_2$NEt	87	0
2	Cy$_2$NEt	68	0
3	NEt$_3$	5	95
4	PMP	91	0

[a]Conditions: aminal (0.1 mmol, 1.0 equiv), CuI (0.010 mmol, 10 mol %), 1-bpp (0.012 mmol, 12 mol %), alkyne (0.13 mmol, 1.3 equiv), BF$_3$·OEt$_2$ (0.1 mmol, 1.0 equiv), i-Pr$_2$NEt (0.2 mmol, 2.0 equiv), solvent (0.18M). [b]Determined by ^{1}H NMR analysis with 1,3,5-trimethoxybenzene as an internal standard.

Investigation of other copper sources provided interesting results. Other copper(I) halides gave similar product yields (**Table 2.5**, entries 1–3), and copper(II) triflate gave a lower yield with a noticeable increase in homocoupled alkyne byproduct (entry 4). Surprisingly, copper(I) thiocyanate provided 98% product yield. Unfortunately, however, the results with copper(I) thiocyanate and phenylacetylene were not analogous to reactions with different alkynyl partners, which provided significantly lower and inconsistent yields. Therefore, copper(I) iodide was chosen as the copper source for this reaction.

Table 2.5 – Investigation of Copper Sources
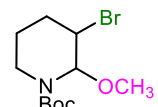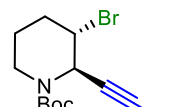
entry	[Cu]	yield (%)^b
1	CuI	83
2	CuBr	88
3	CuCl	78
4	Cu(OTf)$_2$	41^c
5	CuSCN	98
6	Cu(MeCN)$_4$BF$_4$	60

^{a}Conditions: aminal (0.1 mmol, 1.0 equiv), CuI (0.010 mmol, 10 mol %), 1-bpp (0.012 mmol, 12 mol %) alkyne (0.13 mmol, 1.3 equiv), BF$_3$·OEt$_2$ (0.1 mmol, 1.0 equiv), i-Pr$_2$NEt (0.2 mmol, 2.0 equiv), solvent (0.18M). ^{b}Determined by ^{1}H NMR analysis with 1,3,5-trimethoxybenzene as an internal standard. ^{c}46% dimer.

Control experiments were also conducted to verify the necessity of each component of the reaction (**Table 2.6**). It was discovered that all components except for ligand were necessary for the reaction to be successful, and it was also found that no pre-stir ligation of the copper and ligand was necessary (entry 6). When 1-bpp ligand was omitted from the reaction, a comparable yield of 81% was observed (entry 3). As a result, ligand was ultimately omitted from the final alkynylation conditions, providing copper(I) iodide as the sole catalyst for the reaction.

Table 2.6 – Control Experiments

entry	perturbation	yield (%)[b]
1	no change	83
2	no copper	0
3	no ligand	81
4	no base	0
5	no Lewis acid	0
6	no pre-stir	88

[a]Conditions: aminal (0.1 mmol, 1.0 equiv), CuI (0.010 mmol, 10 mol %), alkyne (0.13 mmol, 1.3 equiv), BF$_3$·OEt$_2$ (0.1 mmol, 1.0 equiv), i-Pr$_2$NEt (0.2 mmol, 2.0 equiv), solvent (0.18M). [b]Determined by ^{1}H NMR analysis with 1,3,5-trimethoxybenzene as an internal standard.

With these optimized conditions in hand, broad substrate scope of this alkynylation was demonstrated by myself and my colleague, Weiye Guan. The final conditions for the difunctionalization were as follows: 10 mol % copper iodide, 1.2

equivalents of terminal alkyne, 2.0 equivalents of DIPEA, 1.0 equivalents of BF$_3$•OEt$_2$, and THF (0.18M) under nitrogen at ambient temperature for 24 hours. A wide variety of terminal alkynes could be employed in this reaction (**Scheme 2.6**). Particularly, aryl acetylenes with substitutions on the *ortho* (**8**), *meta* (**12**), and *para* (9–11) positions were well-tolerated in the reaction (compounds **2.8, 2.9, 2.12**). Electron-donating groups on the aryl ring of the alkyne were also successful (compounds **2.9, 2.10**), providing a single diastereomer of product. For these specific compounds, using 5% copper iodide and 6% 1-bpp ligand led to an increase in yield, suggesting that 1-bpp as an additive could be beneficial to the reaction in some, but not all cases.

Scheme 2.6 – Investigation of Acetylenes
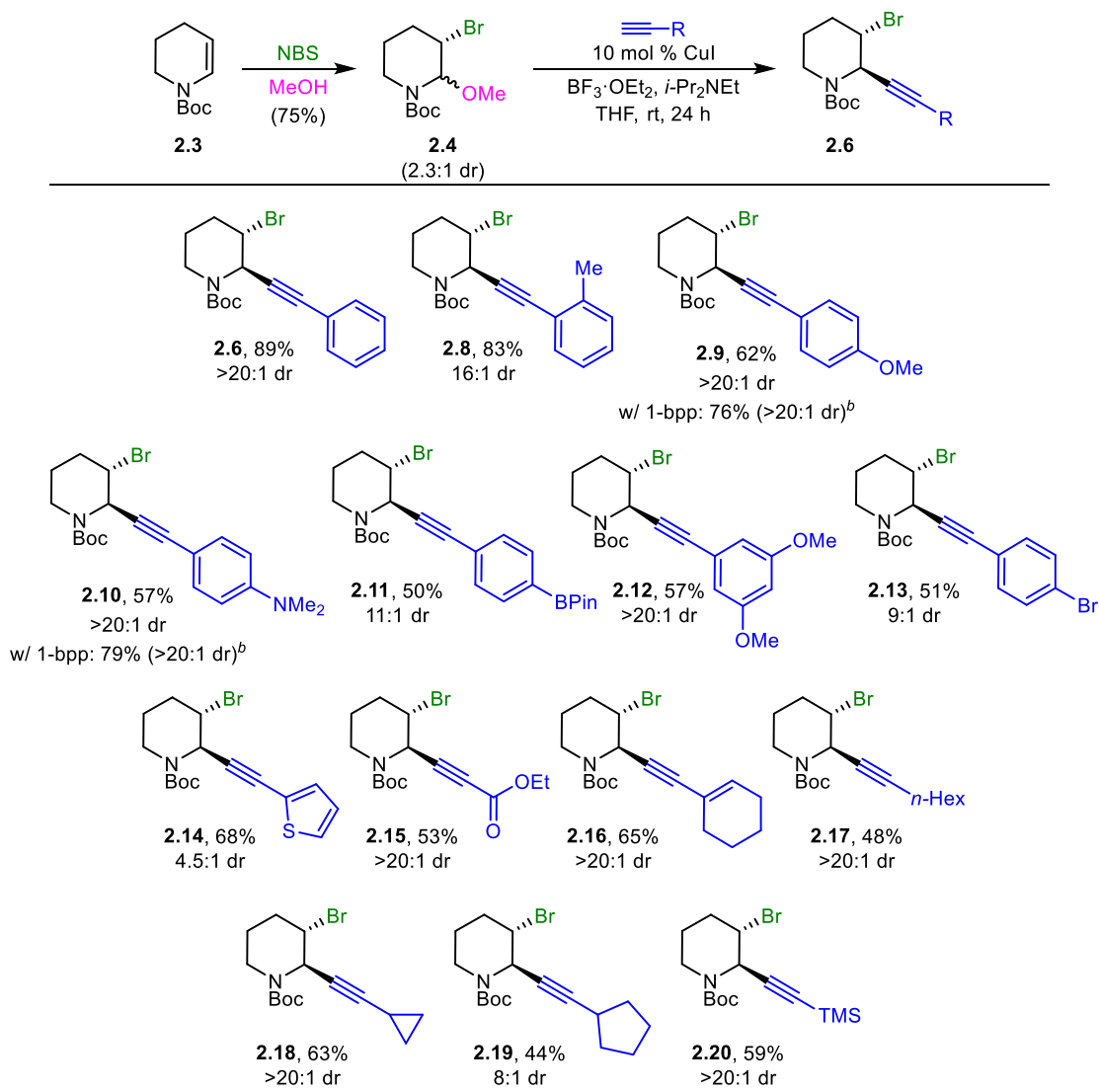
However, aryl acetylenes with electron-withdrawing groups were not successful in the reaction, possibly due to the low reactivity of the copper acetylides and susceptibility

of the starting material to undergo rapid E1 elimination (see **2.4 Experimental**). Other acetylides were successful in the reaction, specifically alkynes with sp²-hybridized carbon substituents such as the ethyl propiolate (**2.15**), as well as the cyclohexenyl (**2.16**), and thiophenyl (**2.14**) acetylides (**Scheme 2.6**). The thiophene provided lower dr, which is hypothesized to avoid steric interactions with the bromide tether, thus resulting in the *syn*-addition product as the minor diastereomer in a 4.5:1 ratio. Aliphatic alkynes are also well-tolerated under the reaction conditions, such as the hexyl (**2.17**), cyclopropyl (**2.18**), and cyclopentyl (**2.19**) substituted alkynes. Trimethylsilylacetylene (**2.20**) can also be incorporated, which can be further elaborated upon in subsequent syntheses.

Additionally, broad scope was observed in the aminal substrate (**Scheme 2.7**). Various ring sizes were successful in the reaction, such as the 5-membered (**2.21**) and 7-membered (**2.22**) cyclic enecarbamates. Azepine (**2.22**) was formed in lower dr, which may be due to the increased flexibility of the ring, which is not characteristic of the rigid structures seen in the 5 and 6-membered rings.

Scheme 2.7 – Investigation of Aminal Substrates

Step 1: Halogenation

Step 2: Alkynylation

2.21
Step 1: 85% (2.6:1 dr)
Step 2: 87% (12:1 dr)

2.22
Step 1: 65% (1.6:1 dr)
Step 2: 83% (4.5:1 dr)[b,c]

2.23
Step 1: 87% (1.3:1 dr)
Step 2: 30% (>20:1 dr)[b]

2.24
Step 1: 63% (2.2:1 dr)
Step 2: 94% (13.7:1 dr)[b,c]

2.25
Step 1: 77% (2.2:1 dr)
Step 2: 74% (>20:1 dr)

2.26
Step 1: 81% (2.5:1 dr)
Step 2: 80% (>20:1 dr)

2.27
Step 1: 22% (1.1:1 dr)
Step 2: 57% (>20:1 dr)[b,c]

2.28
Step 1: 75% (1.1:1 dr)
Step 2: 89% (1.1:1 dr)
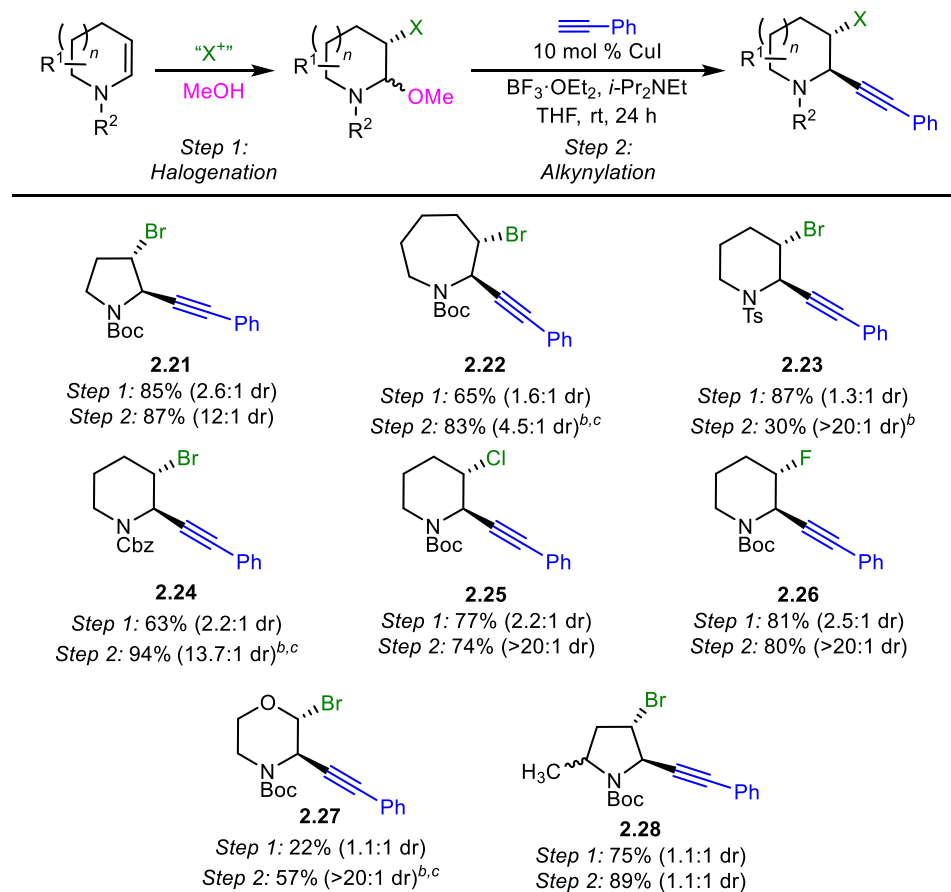
[a]Conditions: aminal (1.0 mmol, 1.0 equiv), CuI (0.10 mmol, 10 mol %), alkyne (1.3 mmol, 1.3 equiv), BF$_3$·OEt$_2$ (1.0 mmol, 1.0 equiv), i-Pr$_2$NEt (2.0 mmol, 2.0 equiv), solvent (0.18M). [b]Run for 72 h.

Excitingly, other halides are also successful. Both β-chloro- and β-fluoro-hemiaminal ethers provided single diastereomers of product (**2.25**, **2.26**). This exceptional selectivity can be explained using the rationale described by Onomura, as mentioned in the introduction of this chapter.[31] The chloride, like the bromide, can block one face of the iminium via steric interactions or through a chloronium ion intermediate (see **Figure 2.2** above). The fluoride can stabilize the orbitals of the electropositive carbon so long as it remains axial in the half-chair conformation, and the nucleophile then

adds to the opposite face to balance opposing dipoles. Other nitrogen protecting groups can also be used, such as carboxybenzyl (**2.24**) and tosyl (Ts, **2.23**), albeit with a longer reaction time but consistent diastereoselectivity. Other substitutions on the ring are also possible, as illustrated by morpholine (**2.28**) and α-methyl pyrrolidine (**2.29**). Although the morpholine substrate provided a single diastereomer of product, the α-methyl pyrrolidine substrate resulted in a 1.2:1 diastereomeric ratio of products. These diastereomers arise by poor diastereoselectivity in the formation of the bromonium relative to the α-methyl stereocenter. High diastereoselectivity is still observed in the alkynylation, with the alkyne adding *anti* to the bromine (see **2.4 Experimental).**

Although NMR spectroscopy was used to determined dr, I also grew X-ray quality crystals to further validate the *anti*-relationship between the alkyne and the halide. Compounds **2.9** and **2.25** were recrystallized and submitted to Dr. Glenn Yap, an X-ray crystallographer from the University of Delaware, who solved the crystal structures for these compounds and illustrated the *anti*-relationship of the substituents (**Figures 2.3 and 2.4**).
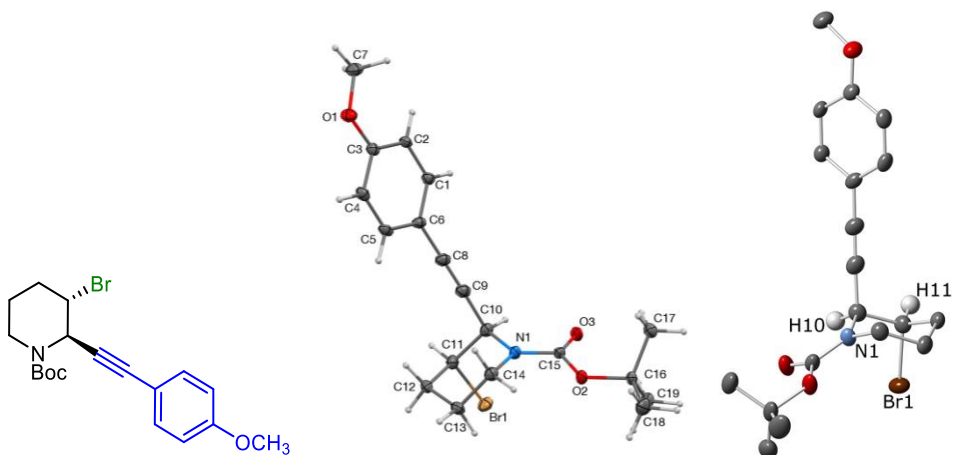
Figure 2.3 – Crystal Structure of Compound 2.9 with ellipsoids at 50% probability. Most H-atoms omitted for clarity. Depicted H-atoms are with arbitrary radius
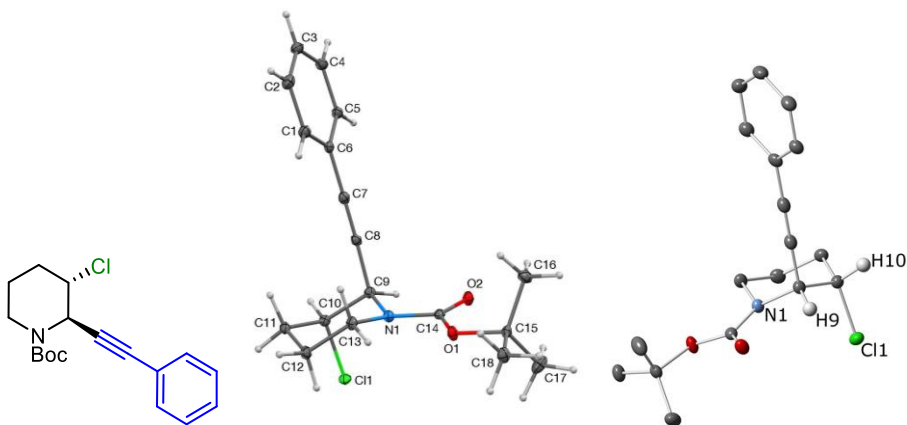
Figure 2.4 – Crystal Structure of Compound 2.25 with ellipsoids at 50% probability. Most H-atoms omitted for clarity. Depicted H-atoms are with arbitrary radius

The utility of this method was demonstrated in elaborations of the resulting alkynylated products. Facile deprotection of the Boc-protecing group was explored for

some of the compounds and provided the free difunctionalized amines (**Scheme 2.8a**). The deprotection was crucial in determining the identity of the diastereomers for the *α*-methyl pyrrolidine substrate (**2.33**, see **2.4 Experimental**). Furthermore, pyrrolidine **2.21** was reduced with palladium on carbon in the presence of hydrogen to give alkylated amine **2.34 (Scheme 2.8b)**. This amine was then deprotected and subjected to reductive amination conditions to give methylated amine **2.35**.

Scheme 2.8 – Product Elaborations
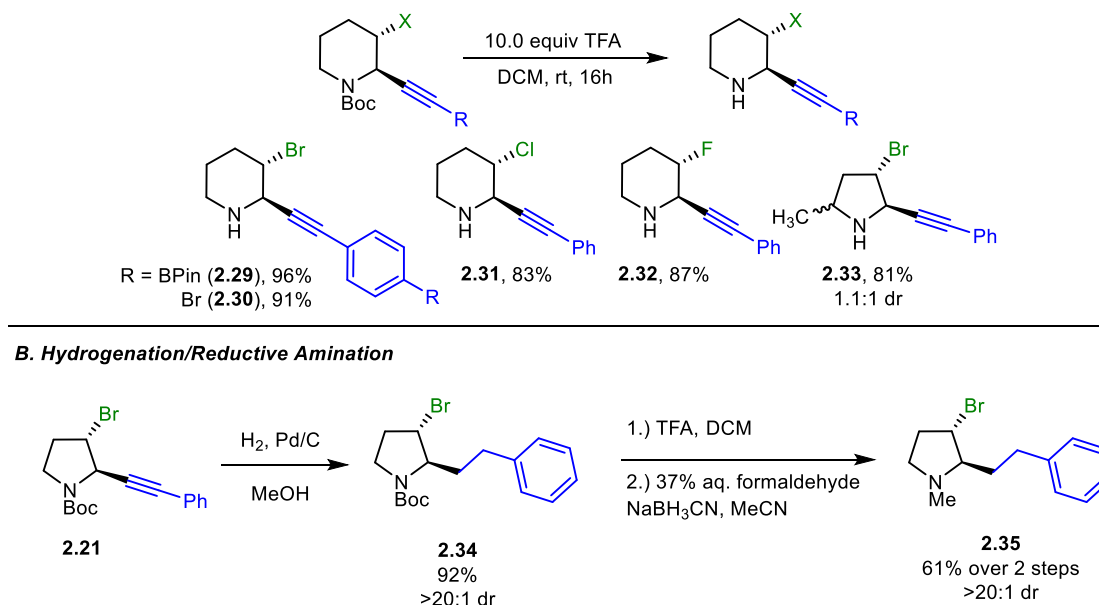
2.3 Conclusion

I developed a diastereoselective difunctionalization of cyclic enamides via copper(I) catalysis. My colleague Weiye and I investigated the substrate scope of the reaction, which included broad tolerance for different acetylides and *β*-halo-

hemiaminal ether substrates. The utility of the products has also been shown, via facile deprotection of the protecting groups and further elaborations.

2.4 Experimental

General Procedure A: Optimization Procedure
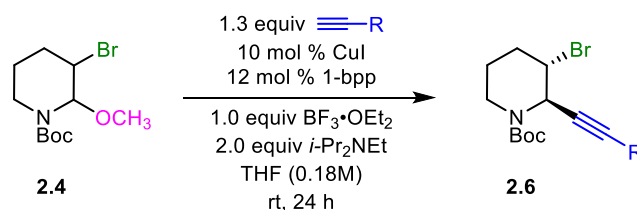
In a N$_2$-filled glovebox, Cu(I) salt (0.010 mmol, 1.9 mg) and ligand (0.012 mmol, 2.5 mg) were weighed out into a 1-dram vial equipped with a stir bar. Solvent (0.18 M) was added, and the solution was stirred for 35 minutes. β-Halo-aminal (0.10 mmol, 29.4 mg), alkyne (0.13 mmol, 14.3 µL) base (0.2 mmol, 35 µL), and Lewis acid (0.10 mmol, 26 µL) were then added to the vial. The vial was fitted with a Teflon-lined cap and removed from the glovebox. The vial was further sealed with electrical tape and the mixture was stirred for 24 h at room temperature. The reaction mixture was diluted with EtOAc (1 mL) and filtered through a plug of silica gel, which was further rinsed with EtOAc (4 x 2 mL). After the filtrate was concentrated 1,3,5-trimethoxybenzene (TMB) was added as an internal standard and the yield was quantified via ¹H NMR spectroscopic analysis.

Brief Investigation of Zinc Catalysis
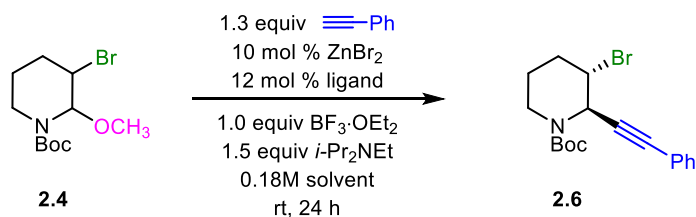
entry	ligand	yield (CH$_2$Cl$_2$)[b]	yield (CHCl$_3$)[b]
1	none	trace	0
2	(-)-pseudoephedrine	trace	0
3	(S)-BINOL	trace	0
4	1-bpp	trace	0
5	PhPyBOX	trace	-
6	(+)-indanol	-	0

[a]Conditions: aminal (0.1 mmol, 1.0 equiv), ZnBr$_2$ (0.010 mmol, 10 mol %), ligand (0.012 mmol, 12 mol %), alkyne (0.13 mmol, 1.3 equiv), BF$_3$·OEt$_2$ (0.1 mmol, 1.0 equiv), i-Pr$_2$NEt (0.2 mmol, 2.0 equiv), solvent (0.18M). [b]Determined by ^{1}H NMR analysis with 1,3,5-trimethoxybenzene as an internal standard.

(-)-pseudoephedrine   (S)-BINOL   1-bpp

PhPyBOX   (+)-aminoindanol

56
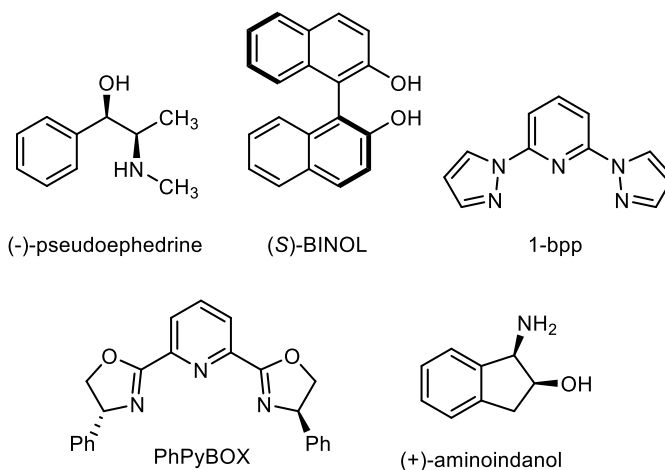
Representative Limitations

The following alkynes and aminals were not compatible with the reaction conditions. In most cases, elimination side reactions and/or inactivity of the starting materials were observed.

11%
(RSM and elimination byproducts observed)

1%
(RSM and elimination byproducts observed)

25%
(RSM and elimination byproducts observed)

0%
(elimination byproduct observed)

0%
(RSM observed)

0%
(RSM observed)
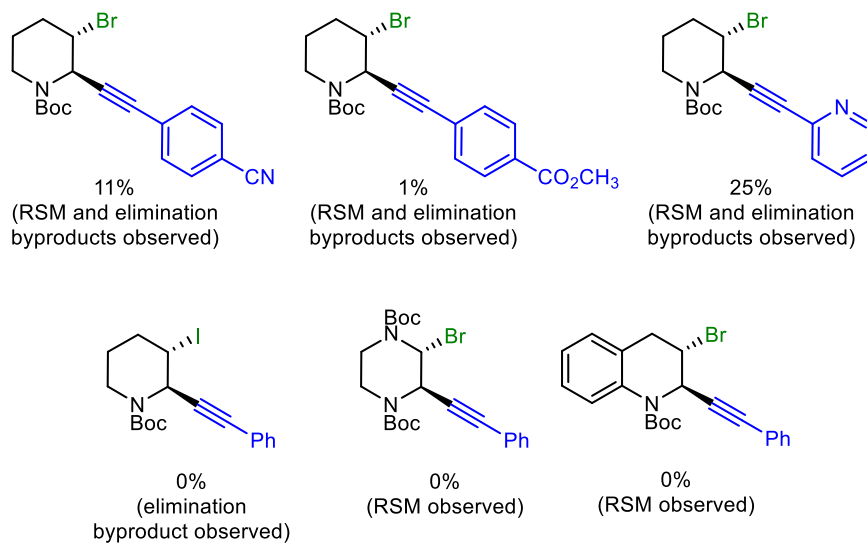
Experiments were done on a 0.1 mmol scale and prepared in a N_2-filled glovebox. Yields were determined via ^{1}H NMR analysis using 1,3,5-trimethoxybenzene as an internal standard.

General Procedure B: Alkynylation
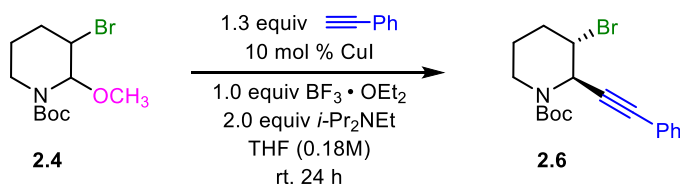
In a N$_2$-filled glovebox, CuI (0.10 mmol, 19.0 mg) was weighed out into an oven-dried round-bottomed flask equipped with a stir bar. After addition of THF (0.18 M), β-halo-aminal (1.0 mmol, 294 mg), alkyne (1.3 mmol, 0.143 mL), diisopropyl-N-ethylamine (2.0 mmol, 0.348 mL), and 48% boron trifluoride etherate (1.0 mmol, 0.259 mL), the flask was fitted with a rubber septum and removed from the glovebox. The reaction was then stirred for 24 – 72 h at room temperature under a positive pressure of nitrogen. The reaction mixture was diluted with Et$_2$O (5 mL) and filtered through a pad of silica gel, rinsed with Et$_2$O (4 x 10 mL). The solution was concentrated under reduced pressure and the crude material was then purified via silica gel chromatography.
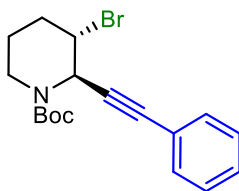
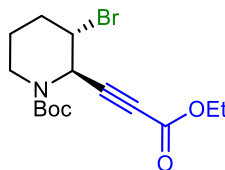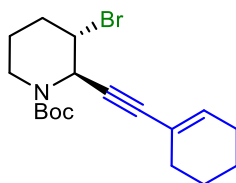***Tert*-butyl-trans-3-bromo-2-(phenylethynyl)piperidine-1-carboxylate (2.6).** Prepared via General Procedure B on a 1.0 mmol scale for 24 hours. The crude mixture was purified by silica gel chromatography (5–10% Et$_2$O:Hexanes) to give **2.6** (323 mg, 89%, >20:1 dr) as a white solid (mp: 101 – 103 °C).

¹H NMR (400 MHz, MeOD) δ 7.37 – 7.31 (m, 2H), 7.30 – 7.19 (m, 3H), 5.32 (s, 1H), 4.56 – 4.49 (m, 1H), 4.00 – 3.89 (m, 1H), 3.15 – 2.96 (m, 1H), 2.40 – 2.27 (m, 1H), 1.97 – 1.84 (m, 2H), 1.48 – 1.42 (m, 1H), 1.38 (s, 9H).

¹³C NMR (101 MHz, MeOD) δ 153.1, 129.7, 127.0, 126.6, 120.3, 84.6, 81.9, 79.0, 52.8, 49.6, 37.5, 26.6, 25.6, 17.8.

FTIR (thin film, cm⁻¹): 2975, 1698, 1411, 1167, 1141, 1113, 757.

HRMS (ESI) m/z, calcd for $[C_{18}H_{22}BrNO_2]^+$: 364.2830; found 364.0903.
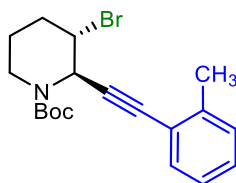
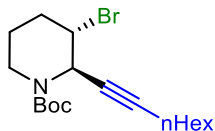***Tert*-butyl-trans-3-bromo-2-((2-methylphenyl)ethynyl)piperidine-1-carboxylate (2.8).** Prepared via General Procedure B on a 1.0 mmol scale for 24 hours. The crude mixture was purified by silica gel chromatography (5–15% Et₂O:Hexanes) to give **2.8** (315 mg, 83%, 16:1 dr) as a white solid (mp: 68 – 70 °C).

¹H NMR (400 MHz, MeOD) δ 7.28 (d, *J* = 7.7 Hz, 1H), 7.18 – 7.09 (m, 2H), 7.09 – 7.01 (m, 1H), 5.36 (s, 1H), 4.57 – 4.49 (m, 1H), 4.00 – 3.90 (m, 1H), 3.14 – 2.99 (m, 1H) ,2.40 – 2.31 (m, 1H), 2.30 (s, 3H), 1.95 – 1.86 (m, 2H), 1.48 – 1.42 (m, 1H), 1.39 (s, 9H).

¹³C NMR (151 MHz, MeOD) δ 154.8, 140.0, 131.6, 129.2, 128.6, 125.4, 121.5, 87.7, 85.1, 80.7, 51.2, 50.5, 39.2, 28.2, 27.3, 19.6, 19.4.

FTIR (thin film, cm⁻¹) 2975, 1697, 1411, 1365, 1168, 1140, 1112, 757.

HRMS (ESI) m/z, calcd for $[C_{19}H_{24}BrNO_2]^+$: 378.3100; found 378.1062.
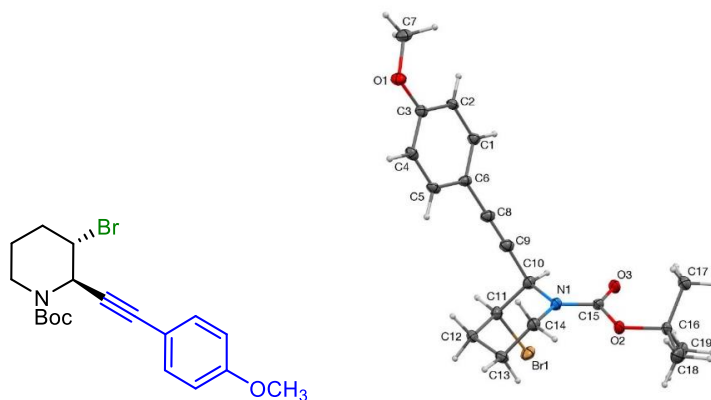
***Tert*-butyl-trans-3-bromo-2-((4-methoxyphenyl)ethynyl)piperidine-1-carboxylate**

(2.9). Prepared via General Procedure B on a 1.0 mmol scale for 24 hours. The crude mixture was purified by silica gel chromatography (10% EtOAc:Hexanes) to give **2.9** (233 mg, 62%, >20:1 dr) as a white solid (mp: 100 – 102 °C).

Product **9** was also prepared via General Procedure B on a 1.0 mmol scale for 24 hours, except that 1-bpp (12.7 mg, 0.06 mmol, 6 mol %) was added. The crude mixture was purified by silica gel chromatography (10% EtOAc:Hexanes) to give **2.9** (298 mg, 76%, >20:1 dr) as a white solid.

^{1}H NMR (400 MHz, MeOD) δ 7.27 (d, J = 8.8 Hz, 2H), 6.78 (d, J = 8.8 Hz, 2H), 5.29 (s, 1H), 4.54 – 4.44 (m, 1H), 3.99 – 3.85 (m, 1H), 3.69 (s, 3H), 3.13 – 2.97 (m, 1H), 2.40 – 2.26 (m, 1H), 1.98 – 1.78 (m, 2H), 1.47 – 1.40 (m, 1H), 1.38 (s, 9H).

^{13}C NMR (151 MHz, MeOD) δ 160.2, 154.8, 132.8, 113.8, 113.7, 86.4, 82.0, 80.6, 54.4, 51.4, 50.5, 38.8, 28.1, 27.2, 19.4.

FTIR (thin film, cm^{-1}) 2974, 2215, 1695, 1510, 1412, 1249, 1169, 1140, 832.

HRMS (ESI) m/z, calcd for $[C_{19}H_{24}BrNO_3]^+$: 394.3090; Found 394.1006.
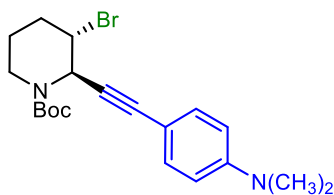
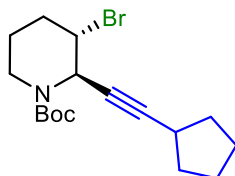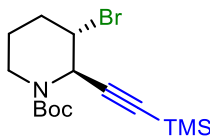***Tert*-butyl-trans-3-bromo-2-((4-dimethylamino-phenyl)ethynyl)piperidine-1-carboxylate (2.10).** Prepared via General Procedure B on a 1.0 mmol scale for 24 hours. The crude mixture was purified by silica gel chromatography (10% Et₂O:Hexanes) to give **2.10** (239 mg, 57%, >20:1 dr) as a white solid (mp: 114 – 117 °C).

Product **2.10** was also prepared via General Procedure B on a 1.0 mmol scale for 24 hours, except that 1-bpp (12.7 mg, 0.06 mmol, 6 mol %) was added. The crude mixture was purified by silica gel chromatography (10% Et₂O:Hexanes) to give **2.10** (323 mg, 79%, >20:1 dr) as a white solid.

¹H NMR (600 MHz, MeOD) δ 7.21 (d, *J* = 9.1 Hz, 2H), 6.61 (d, *J* = 8.8 Hz, 2H), 5.32 (s, 1H), 4.53 – 4.50 (m, 1H), 4.00 – 3.93 (m, 1H), 3.18 – 3.04 (m, 1H), 2.89 (s, 6H), 2.44 – 2.36 (m, 1H), 1.97 – 1.90 (m, 2H), 1.50 – 1.46 (m, 1H), 1.44 (s, 9H).

¹³C NMR (151 MHz, MeOD) δ 154.8, 150.6, 132.3, 111.5, 108.5, 87.6, 81.0, 80.4, 51.8, 39.0, 38.9, 28.1, 27.2, 19.5.

FTIR (thin film, cm⁻¹) 2929, 2213, 1694, 1608, 1522, 1411, 1364, 1167.

HRMS (ESI) m/z, calcd for [C₂₀H₂₇BrN₂O₂]⁺: 407.3520; Found 407.1330.
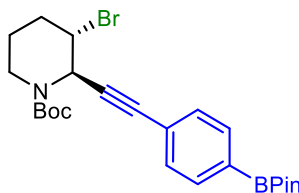
***Tert*-butyl-trans-3-bromo-2-((4-phenylboronic acid pinacol ester))ethynyl)piperidine-1-carboxylate (2.11).** Prepared via General Procedure B on a 1.0 mmol scale for 24 hours. The crude mixture was purified by silica gel chromatography (10% EtOAc:Hexanes) to give **2.11** (245 mg, 50%, 11:1 dr) as a white solid (mp: 42 – 47 °C).

¹H NMR (600 MHz, MeOD) δ 7.66 (d, *J* = 8.2 Hz, 2H), 7.39 (d, *J* = 8.6 Hz 2H), 5.39 (s, 1H), 4.64 – 4.53 (m, 1H), 4.05 – 3.93 (m, 1H), 3.18 – 3.02 (m, 1H), 2.45 – 2.29 (m, 1H), 2.02 – 1.89 (m, 2H), 1.53 – 1.47 (m, 1H), 1.44 (s, 9H), 1.28 (s, 12H).

¹³C NMR (151 MHz, MeOD) δ 154.7, 134.2, 130.5, 124.6, 86.2, 85.0, 83.9, 80.6, 74.4, 51.1, 39.0, 28.2, 27.2, 23.7, 23.7, 19.4.

FTIR (thin film, cm⁻¹) 2977, 1698, 1399, 1359, 1167, 1142.

HRMS (ESI) m/z, calcd for $[C_{24}H_{34}BBrNO_4]^+$: 490.2450; Found 490.1760.
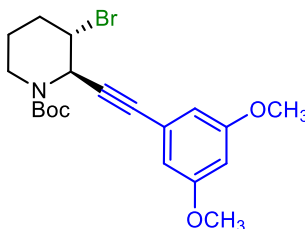
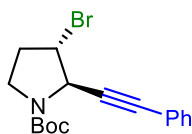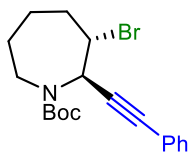***Tert*-butyl-trans-3-bromo-2-((3,5-dimethoxyphenyl)ethynyl)piperidine-1-carboxylate (2.12).** Prepared via General Procedure B on a 1.0 mmol scale for 24 hours. The crude mixture was purified by silica gel chromatography (10% Et₂O:Hexanes) to give **2.12** (243 mg, 57%, >20:1 dr) as a colorless oil.

¹H NMR (400 MHz, MeOD) δ 6.48 (d, *J* = 2.3 Hz, 2H), 6.38 (t, *J* = 2.3 Hz, 1H), 5.31 (s, 1H), 4.55 – 4.44 (m, 1H), 3.99 – 3.87 (m, 1H), 3.64 (s, 6H), 3.12 – 2.96 (m, 1H), 2.39 – 2.22 (m, 1H), 1.96 – 1.83 (m, 2H), 1.45 – 1.41 (m, 1H), 1.38 (m, 9H).

¹³C NMR (151 MHz, MeOD) δ 160.8, 154.6, 123.1, 109.2, 101.4, 86.3, 83.1, 80.6, 54.5, 51.2, 50.4, 39.1, 28.2, 27.2, 19.4.

FTIR (thin film, cm⁻¹) 2972, 1696, 1589, 1413, 1205, 1157, 1140, 1063.

HRMS (ESI) m/z, calcd for $[C_{20}H_{26}BrNO_4]^+$: 424.3350; Found 424.1114.
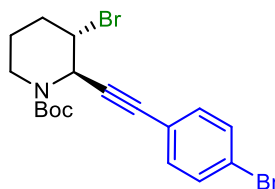
***Tert*-butyl-trans-3-bromo-2-((4-bromo-phenyl)ethynyl)piperidine-1-carboxylate**
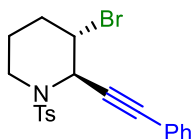
(2.13). Prepared via General Procedure B on a 1.0 mmol scale for 24 hours. The crude mixture was purified by silica gel chromatography (15% EtOAc:Hexanes) to give **2.13** (226 mg, 51%, 9:1 dr) as a white solid (mp: 128 – 130 °C).

¹H NMR (400 MHz, MeOD, major diastereomer) δ 7.41 (d, *J* = 8.5 Hz, 2H), 7.26 (d, *J* = 8.5 Hz, 2H), 5.31 (s, 1H), 4.56 – 4.47 (m, 1H), 4.01 – 3.88 (m, 1H), 3.10 – 2.94 (m, 1H), 2.35 – 2.27 (m, 1H), 1.93 – 1.85 (m, 2H), 1.48 – 1.40 (m, 1H), 1.38 (s, 9H).

¹³C NMR (151 MHz, MeOD, major diastereomer) δ 154.8, 133.0, 131.4, 122.7, 120.9, 84.8, 80.7, 54.4, 50.9, 40.0, 28.2, 27.2, 27.0, 19.4.

FTIR (thin film, cm⁻¹) 2974, 1695, 1485, 1411, 1365, 1253, 1166, 1140, 1010.

HRMS (ESI) m/z, calcd for $[C_{18}H_{21}Br_2NO_2]^+$: 443.1790; Found 443.9986.
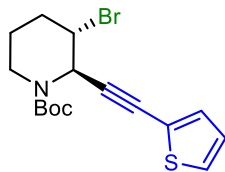
***Tert*-butyl-trans-3-bromo-2-(ethynyl-thiophene)piperidine-1-carboxylate** **(2.14).**
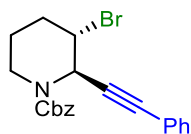Prepared via General Procedure B on a 1.0 mmol scale for 24 hours. The crude
mixture was purified by silica gel chromatography (10% EtOAc:Hexanes) to give **2.14**
(251 mg, 68%, 4.5:1 dr) as a yellow solid (62 – 64 °C).

^{1}H NMR (400 MHz, MeOD, major diastereomer) δ 7.32 (d, J = 5.1 Hz, 1H), 7.17 (d, J
= 3.6 Hz, 1H), 6.93 (t, J = 8.6, 4.8 Hz, 1H), 5.33 (s, 1H), 4.55 – 4.45 (m, 1H), 3.97 –
3.91 (m, 1H), 3.11 – 2.92 (m, 1H), 2.36 – 2.18 (m, 1H), 1.93 – 1.86 (m, 2H), 1.47 –
1.41 (m, 1H), 1.38 (s, 9H).

^{13}C NMR (101 MHz, MeOD, major and minor diastereomers) δ 154.6, 132.5, 127.7,
126.8, 121.3, 87.3, 84.7, 83.5, 80.7, 80.5, 79.4, 54.4, 50.9, 37.4, 36.0, 29.5, 28.2, 27.2,
27.1, 26.4, 26.1, 19.4.

FTIR (thin film, cm^{-1}) 2975, 1696, 1409, 1365, 1167, 1140, 1113, 976, 701.

HRMS (ESI) m/z, calcd for [C$_{16}$H$_{20}$BrNO$_2$S]$^+$: 370.3050; Found 370.0470.

***Tert*-butyl-trans-3-bromo-2-(ethynyl-ethylcarboxylate)piperidine-1-carboxylate**
(2.15). Prepared via General Procedure B on a 1.0 mmol scale for 24 hours. The crude
mixture was purified by silica gel chromatography (10% EtOAc:Hexanes) to give **2.15**
(run 1: 179 mg, 50%, >20:1 dr; run 2: 202 mg, 56%, >20:1 dr) as a colorless oil.

¹H NMR (400 MHz, MeOD) δ 5.28 (s, 1H), 4.56 – 4.44 (m, 1H), 4.12 (q, 2H), 4.01 – 3.88 (m, 1H), 3.01 – 2.82 (m, 1H), 2.22 – 2.06 (m, 1H), 1.97 – 1.77 (m, 2H), 1.51 – 1.40 (m, 1H), 1.38 (s, 9H), 1.18 (t, J = 7.1 Hz, 3H).

¹³C NMR (101 MHz, MeOD) δ 154.3, 152.6, 81.0, 80.9, 77.3, 62.0, 50.4, 49.4, 39.2, 28.3, 27.1, 19.1, 12.8.

FTIR (thin film, cm⁻¹) 2978, 2233, 1700, 1409, 1366, 1245, 1167, 1141.

HRMS (ESI) m/z, calcd for $[C_{15}H_{22}BrNO_4]^+$: 360.2480; Found 360.0802.

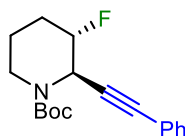***Tert*-butyl-trans-3-bromo-2-(ethynyl-cyclohexene)piperidine-1-carboxylate (2.16).**

Prepared via General Procedure B on a 1.0 mmol scale for 24 hours. The crude mixture was purified by silica gel chromatography (5% Et₂O:Hexanes) to give **2.16** (240 mg, 65%, >20:1 dr) as a white solid (mp: 71 – 75 °C).

¹H NMR (400 MHz, MeOD) δ 6.05 – 5.94 (m, 1H), 5.17 (s, 1H), 4.45 – 4.31 (m, 1H), 3.94 – 3.81 (m, 1H), 3.06 – 2.85 (m, 1H), 2.33 – 2.15 (m, 1H), 2.02 – 1.96 (m, 4H), 1.92 – 1.79 (m, 2H), 1.57 – 1.46 (m, 4H), 1.44 – 1.38 (m, 1H), 1.37 (s, 9H).

¹³C NMR (151 MHz, MeOD) δ 154.7, 135.4, 119.6, 88.2, 80.8, 80.5, 51.5, 50.4, 38.7, 28.7, 28.0, 27.2, 25.1, 21.9, 21.1, 19.4.

FTIR (thin film, cm⁻¹) 2974, 2930, 2859, 2218, 1698, 1412, 1365, 1168, 1140.

HRMS (ESI) m/z, calcd for $[C_{18}H_{26}BrNO_2]^+$: 368.3150; Found 368.1218.

***Tert*-butyl-trans-3-bromo-2-(octyne)piperidine-1-carboxylate (2.17).** Prepared via General Procedure B on a 1.0 mmol scale for 48 hours. The crude mixture was purified by silica gel chromatography (0-1% Et₂O:Toluene) to give **2.17** (177 mg, 48%, >20:1 dr) as a colorless oil.

¹H NMR (400 MHz, MeOD) δ 5.04 (s, 1H), 4.38 – 4.31 (m, 1H), 3.90 – 3.81 (m, 1H), 3.05 – 2.85 (m, 1H), 2.29 – 2.19 (m, 1H), 2.12 (td, *J* = 6.9, 2.2 Hz, 2H), 1.90 – 1.78 (m, 2H), 1.41 – 1.37 (m, 2H), 1.35 (s, 9H), 1.32 – 1.27 (m, 2H), 1.24 – 1.15 (m, 5H), 0.79 (t, *J* = 6.8 Hz, 3H).

¹³C NMR (101 MHz, MeOD) δ 153.2, 85.5, 78.8, 73.2, 50.1, 36.9, 29.4, 27.8, 26.6, 26.5, 26.3, 25.6, 20.6, 17.8, 16.2, 11.4.

FTIR (thin film, cm⁻¹) 2974, 2933, 1701, 1401, 1366, 1176, 1151, 1079.

HRMS (ESI) m/z, calcd for $[C_{18}H_{30}BrNO_2]^+$: 372.3470; Found 372.1534.
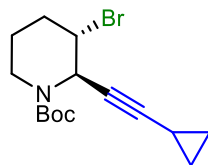
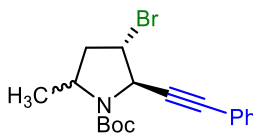***Tert*-butyl-trans-3-bromo-2-(ethynyl-cyclopropane)piperidine-1-carboxylate (2.18).** Prepared via General Procedure B on a 1.0 mmol scale for 24 hours. The crude mixture was purified by silica gel chromatography (5% Et₂O:Hexanes) to give **2.18** (208 mg, 63%, >20:1 dr) as a colorless oil.

¹H NMR (400 MHz, MeOD) δ 5.03 (s, 1H), 4.39 – 4.30 (m, 1H), 3.92 – 3.79 (m, 1H), 3.04 – 2.84 (m, 1H), 2.30 – 2.15 (m, 1H), 1.90 – 1.77 (m, 2H), 1.42 – 1.38 (m, 1H), 1.37 (s, 9H), 1.24 – 1.17 (m, 1H), 0.75 – 0.65 (m, 2H), 0.59 – 0.48 (m, 2H).

^{13}C NMR (101 MHz, MeOD) δ 153.1, 88.8, 78.8, 68.1, 50.2, 48.7, 37.5, 26.4, 25.7, 17.9, 5.8, -2.9.

FTIR (thin film, cm^{-1}) 2975, 2245, 1697, 1413, 1365, 1168, 1140.

HRMS (ESI) m/z, calcd for [C$_{15}$H$_{22}$BrNO$_2$]$^+$: 328.2500; Found 328.0905.

Tert-butyl-trans-3-bromo-2-(ethynyl-cyclopentane)piperidine-1-carboxylate

(2.19). Prepared via General Procedure B on a 1.0 mmol scale for 48 hours. The crude mixture was purified by silica gel chromatography (0-1% Et$_2$O:Toluene) to give **2.19** (158 mg, 44%, 8:1 dr) as a colorless oil.

^{1}H NMR (600 MHz, MeOD) δ 5.12 (s, 1H), 4.46 – 4.38 (m, 1H), 3.97 – 3.88 (m, 1H), 3.10 – 2.96 (m, 1H), 2.71 – 2.60 (m, 1H), 2.36 – 2.26 (m, 1H), 1.97 – 1.85 (m, 4H), 1.74 – 1.64 (m, 2H), 1.59 – 1.51 (m, 4H), 1.48 – 1.44 (m, 1H), 1.43 (s, 9H).

^{13}C NMR (151 MHz, MeOD) δ 154.7, 91.5, 80.3, 74.4, 51.8, 50.7, 39.2, 33.4, 29.8, 27.9, 27.2, 24.4, 19.4.

FTIR (thin film, cm^{-1}) 2961, 2869, 2228, 1699, 1413, 1365, 1168, 1139.

HRMS (ESI) m/z, calcd for [C$_{17}$H$_{26}$BrNO$_2$]$^+$: 356.3040; Found 356.1220.

Tert-butyl-trans-3-bromo-2-(ethynyl-trimethylsilyl)piperidine-1-carboxylate

(2.20). Prepared via General Procedure B on a 1.0 mmol scale for 24 hours. The crude

mixture was purified by silica gel chromatography (10% EtOAc:Hexanes with 1% NEt₃) to give **2.20** (213 mg, 59%, >20:1 dr) as a colorless oil.

¹H NMR (600 MHz, MeOD) δ 5.16 (s, 1H), 4.49 – 4.46 (m, 1H), 3.99 – 3.95 (m, 1H), 3.10 – 2.97 (m, 1H), 2.35 – 2.29 (m, 1H), 1.97 – 1.91 (m, 2H), 1.51 – 1.48 (m, 1H), 1.45 (s, 9H), 0.16 (s, 9H).

¹³C NMR (151 MHz, MeOD) δ 154.6, 100.1, 91.3, 80.6, 51.6, 51.0, 38.7, 29.3, 28.0, 27.3, 19.4, -1.4.

FTIR (thin film, cm⁻¹) 2959, 2931, 2171, 1701, 1411, 1365, 1251, 1168, 845.

HRMS (ESI) m/z, calcd for $[C_{15}H_{26}BrNO_2Si]^+$: 360.3670; Found 360.0989.

***Tert*-butyl-trans-3-bromo-2-(phenylethynyl)pyrrolidine-1-carboxylate (2.21).**
Prepared via General Procedure B on a 1.0 mmol scale for 24 hours. The crude mixture was purified by silica gel chromatography (15% Et₂O:Hexanes) to give **2.21** (305 mg, 87%, 12:1 dr) as a white solid (mp: 65 – 67 °C).

¹H NMR (400 MHz, MeOD) δ 7.33 – 7.26 (m, 2H), 7.26 – 7.18 (m, 3H), 4.82 – 4.74 (m, 1H, overlaps with MeOD), 4.60 – 4.51 (m, 1H), 3.62 – 3.44 (m, 2H), 2.73 – 2.52 (m, 1H), 2.25 – 2.09 (m, 1H), 1.38 (s, 9H).

¹³C NMR (101 MHz, MeOD, rotamers) δ [154.6,154.4], [131.3, 131.1],128.4, [128.1, 128.0], 122.0, [85.5, 85.3], [84.2, 84.1], 80.5, [58.7, 58.3], [52.0, 51.5], [43.8, 43.3], [34.2, 33.4], 27.2.

FTIR (thin film, cm⁻¹) 2975, 1700, 1390, 1366, 1164, 1113, 756, 691.

HRMS (ESI) m/z, calcd for $[C_{17}H_{20}BrNO_2]^+$: 349.0677; Found 349.1831.

Tert-butyl-trans-3-bromo-2-(phenylethynyl)azepane-1-carboxylate **(2.22).**

Prepared via General Procedure B on a 1.0 mmol scale for 72 hours. The crude mixture was purified by silica gel chromatography (5% EtOAc:Hexanes) to give **2.22** (313 mg, 83%, 4.5:1 dr) as a colorless oil.

^{1}H NMR (400 MHz, DMSO-d_6 at 350K, major diastereomer) δ 7.48 – 7.30 (m, 5H), 4.96 – 4.81 (m, 1H), 4.76 – 4.66 (m, 1H), 4.14 – 3.95 (m, 1H), 3.04 (s, 1H), 2.45 – 2.34 (m, 0.5H), 2.14 – 2.05 (m 0.5H), 1.50 (s, 1H), 1.49 (s, 1H) 1.46 (s, 9H), 1.45 (s, 1H), 1.36 (d, J = 6.2 Hz, 1H), 1.26 (d, J = 6.2 Hz, 1H).

^{13}C NMR (101 MHz, DMSO-d_6, mix of diastereomers) δ 154.6, 153.7, 132.0, 131.8, 129.3, 129.19, 129.15, 122.1, 122.0, 87.6, 87.2, 84.2, 83.7, 80.4, 80.3, 57.1, 56.7, 55.6, 54.6, 44.1, 35.9, 35.7, 28.4, 27.4, 27.2, 26.2.

FTIR (thin film, cm^{-1}) 2974, 2931, 1695, 1403, 1365, 1154, 756.

HRMS (ESI) m/z, calcd for [C$_{19}$H$_{24}$BrNO$_2$]$^+$: 378.3100; Found 378.1063.

Toluenesulfonyl-trans-3-bromo-2-(phenylethynyl)piperidine-1-carboxylate (2.23).

Prepared via General Procedure B on a 1.0 mmol scale for 72 hours. The crude mixture was purified by silica gel chromatography (15% EtOAc:Hexanes) to give **2.23** (120 mg, 30%, >20:1 dr) as a yellow oil.

^{1}H NMR (600 MHz, CDCl$_3$) δ 7.73 (d, *J* = 8.9 Hz, 2H), 7.31 – 7.27 (m, 1H), 7.23 (t, *J* = 14.3, 7.3, 2H), 7.20 (d, *J* = 8.1 Hz, 2H), 7.02 (d, *J* = 7.6 Hz, 2H), 5.14 (s, 1H), 4.49 – 4.44 (m, 1H), 3.79 – 3.73 (m, 1H), 2.92 (td, *J* = 12.2, 2.8 Hz, 1H), 2.27 (s, 3H), 2.20 – 2.15 (m, 1H), 1.98 – 1.93 (m, 1H), 1.61 – 1.57 (m, 1H).

^{13}C NMR (151 MHz, CDCl$_3$) δ 142.7, 142.5, 136.6, 134.0, 130.4, 128.8, 128.3, 127.7, 127.1, 126.9, 125.8, 120.4, 87.6, 84.7, 80.7, 64.8, 55.7, 51.6, 48.5, 48.2, 40.7, 37.8, 28.6, 28.2, 26.7, 25.4, 20.5, 20.3, 19.0, 14.2.

FTIR (thin film, cm^{-1}) 2952, 1353, 1164, 1096, 923, 676, 552.

HRMS (ESI) m/z, calcd for [C$_{20}$H$_{20}$BrNO$_2$S]$^+$: 418.3490, found 418.0476.

Benzyl-trans-3-chloro-2-(phenylethynyl)piperidine-1-carboxylate (2.24). Prepared via General Procedure B on a 1.0 mmol scale for 72 hours. The crude mixture was purified by silica gel chromatography (15% EtOAc:Hexanes) to give **2.24** (375 mg, 94%, 13.7:1 dr) as a colorless oil.

^{1}H NMR (400 MHz, MeOD) δ 7.34 – 7.30 (m, 2H), 7.29 – 7.19 (m, 8H), 5.39 (s, 1H), 5.06 (s, 2H), 4.58 – 4.49 (m, 1H), 4.07 – 3.93 (m, 1H), 3.18 – 3.03 (m, 1H), 2.41 – 2.25 (m, 1H), 1.98 – 1.86 (m, 2H), 1.51 – 1.42 (m, 1H).

^{13}C NMR (101 MHz, MeOD) δ 155.5, 136.4, 131.4, 128.6, 128.2, 128.1, 127.7, 127.4, 121.7, 86.5, 83.3, 67.3, 51.2, 50.8, 39.8, 28.0, 19.4.

FTIR (thin film, cm^{-1}) 2951, 2361, 1702, 1422, 1254, 1110, 757, 692.

HRMS (ESI) m/z, calcd for [C$_{21}$H$_{20}$BrNO$_2$]$^+$: 398.3000; Found 398.0755.
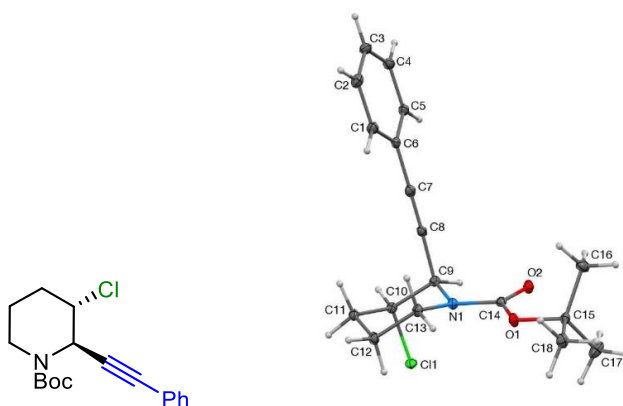
***Tert*-butyl-trans-3-chloro-2-(phenylethynyl)piperidine-1-carboxylate** **(2.25).**

Prepared via General Procedure B on a 1.0 mmol scale for 24 hours. The crude mixture was purified by silica gel chromatography (15% Et$_2$O:Hexanes) to give **2.25** (238 mg, 74%, >20:1 dr) as a white solid (mp: 105 – 107 °C).

^{1}H NMR (400 MHz, MeOD) δ 7.36 – 7.32 (m, 2H), 7.26 – 7.21 (m, 3H), 5.27 (s, 1H), 4.45 – 4.31 (m, 1H), 4.01 – 3.85 (m, 1H), 3.13 – 2.93 (m, 1H), 2.39 – 2.18 (m, 1H), 1.97 – 1.76 (m, 2H), 1.46 – 1.40 (m, 1H), 1.38 (s, 9H).

13C NMR (101 MHz, MeOD) δ 153.3, 129.7, 127.0, 126.6, 120.2, 84.6, 81.9, 79.1, 56.8, 49.6, 37.9, 26.0, 25.6, 16.9.

FTIR (thin film, cm^{-1}) 2974, 1696, 1411, 1168, 1140, 756.

HRMS (ESI) m/z, calcd for [C$_{18}$H$_{22}$ClNO$_2$]$^+$: 319.8290; Found 320.140.

***Tert*-butyl-trans-3-fluoro-2-(phenylethynyl)pyrrolidine-1-carboxylate** **(2.26).**

Prepared via General Procedure B on a 1.0 mmol scale for 24 hours. The crude mixture was purified by silica gel chromatography (5% EtOAc:Hexanes) to give **2.26**

(run 1: 236 mg, 78%, >20:1 dr; run 2: 244 mg, 81%, >20:1 dr) as a tan solid (mp: 103 – 106 °C).

^{1}H NMR (600 MHz, MeOD) δ 7.39 – 7.36 (m, 2H), 7.32 – 7.26 (m, 3H), 5.33 (bs, 1H), 5.39 – 5.27 (m, 1H, overlaps with MeOD), 3.99 – 3.93 (m, 1H), 3.18 – 3.02 (m, 1H), 2.08 – 1.93 (m, 2H), 1.79 – 1.69 (m, 1H), 1.51 – 1.46 (m, 1H), 1.43 (s, 9H).

^{13}C NMR (151 MHz, MeOD) δ 155.1, 131.3, 128.5, 128.1, 121.9, 88.3, 87.1, 86.1, 82.5, 82.4, 80.5, 38.9, 27.2, 24.9, 24.8, 18.8.

^{19}F NMR (376 MHz, MeOD) δ -184.67 (d, $J = 168.8$ Hz).

FTIR (thin film, cm^{-1}) 2951, 1697, 1412, 1366, 1172, 1146, 758.

HRMS (ESI) m/z, calcd for $[C_{18}H_{22}FNO_2]^+$: 303.3774; Found 304.1705.
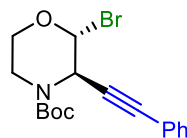
***Tert*-butyl-trans-3-bromo-2-(phenylethynyl)morpholin-1-carboxylate (2.27).**
Prepared via General Procedure B on a 1.0 mmol scale for 72 hours. The crude mixture was purified by silica gel chromatography (10–15% EtOAc:Hexanes) to give **2.27** (210 mg, 57%, >20:1 dr) as a pale yellow solid (55 – 57 °C).

^{1}H NMR (600 MHz, MeOD) δ 7.41 – 7.37 (m, 2H), 7.32 – 7.27 (m, 3H), 4.92 (s, 1H), 4.70 (s, 1H), 3.89 – 3.82 (m, 1H), 3.75 – 3.71 (m, 1H), 3.57 – 3.50 (m, 1H), 1.44 (s, 10H).

^{13}C NMR (151 MHz, MeOD) δ 154.9, 131.3, 128.3, 128.1, 122.2, 97.6, 84.42, 83.6, 80.7, 57.8, 53.6, 38.7, 27.1.

FTIR (thin film, cm^{-1}) 2975, 2930, 1698, 1472, 1409, 1390, 1167, 1121, 1068, 758.

HRMS (ESI) m/z, calcd for $[C_{18}H_{23}NO_4]^+$: 317.1627, found 317.2463 (displacement of bromide) .

***Tert*-butyl-trans-3-bromo-2-(phenylethynyl)-5-methylpyrrolidine-1-carboxylate (2.28).** Prepared via General Procedure B on a 1.0 mmol scale for 24 hours. The crude mixture was purified by silica gel chromatography (2% Et₂O/Hexanes) to give **2.28** (run 1: 312 mg, 86%, 1.1:1 dr; run 2: 325 mg, 89%, 1.1:1 dr) as a white solid (mp: 63 – 65 °C).

¹H NMR (400 MHz, MeOD, mix of diastereomers) δ 7.34 – 7.25 (m, 4H), 7.25 – 7.15 (m, 6H), 4.91 – 4.79 (m, 2H), 4.54 – 4.47 (m, 2H), 4.10 – 3.94 (m, 2H), 3.05 – 2.89 (m, 1H), 2.50 – 5.23 (m, 2H), 2.12 – 1.93 (m, 1H), 1.45 – 1.39 (m, 3H), 1.39 (s, 9H), 1.38 (s, 9H), 1.29 (d, *J* = 6.2 Hz, 3H).

¹³C NMR (101 MHz, MeOD, mix of diastereomers) δ 153.0, 129.6, 126.9, 126.6, 126.6, 120.5, 120.5, 84.4, 84.2, 83.7, 82.6, 82.3, 79.0, 78.9, 78.7, 58.8, 51.5, 49.5, 48.1, 47.4, 39.4, 38.6, 25.8, 25.8, 19.7, 18.7.

FTIR (thin film, cm⁻¹) 2975, 2930, 1699, 1380, 1351, 1168, 756, 690.

HRMS (ESI) m/z, calcd for $[C_{18}H_{22}BrNO_2]^+$: 364.2830, found 364.0904.

Product Elaborations – Deprotection
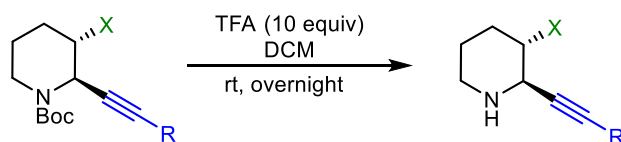
Alkynylated amine (0.1 mmol) was weighed out into a 1-dram vial equipped with a stir bar, then diluted with dry dichloromethane (1.0 mL). TFA (10 equiv, 77 µL) was added dropwise to the vial and the solution was stirred at room temperature overnight. The solution was then added to a separatory funnel containing saturated sodium bicarbonate solution. The organic layer was washed with saturated sodium bicarbonate solution (2 x 10 mL) and with brine (1 x 10 mL). The organic layers were dried over MgSO₄ and the solution was filtered through cotton plug. The solution was then concentrated to give the free amine products.
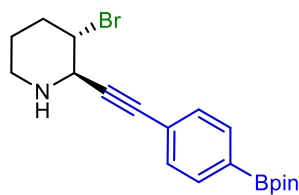
***Trans*-3-bromo-2-((4-phenylboronic acid pinacol ester))ethynyl)piperidine (2.29).**
Prepared on a 0.10 mmol scale to give **2.29** (37.4 mg, 96%, >20:1 dr) as a white solid.
¹H NMR (600 MHz, CDCl₃) δ 7.73 (d, *J* = 8.2 Hz, 2H), 7.43 (d, *J* = 8.2 Hz, 2H), 4.24 – 4.13 (m, 1H), 4.01 – 3.90 (m, 1H), 3.18 – 3.09 (m, 1H), 2.82 – 2.72 (m, 1H), 2.50 – 2.42 (m, 1H), 1.97 – 1.90 (m, 1H), 1.86 – 1.79 (m, 1H), 1.58 – 1.51 (m, 1H), 1.33 (s, 12H).

^{13}C NMR (151 MHz, CDCl$_3$) δ 134.5, 131.6, 130.9, 125.2, 89.1, 84.9, 83.9, 55.3, 53.2, 43.9, 33.5, 25.6, 24.8.

FTIR (thin film, cm^{-1}) 3444.4, 2977.5, 1606.5, 1471.9, 1398.2, 1359.6, 1143.7, 1089.0, 733.7, 654.1.

HRMS (ESI) m/z, calcd for [C$_{19}$H$_{25}$BBrNO$_2$]$^+$: 390.1280, found 390.1227.
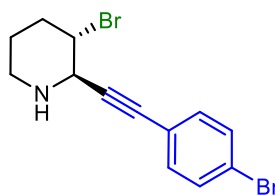
***Trans*-3-bromo-2-((4-bromo-phenyl)ethynyl)piperidine (2.30).** Prepared on a 0.112 mmol scale to give **2.30** (34.8 mg, 91%, 20:1 dr) as a yellow oil.

^{1}H NMR (600 MHz, CDCl$_3$) δ 7.43 (d, *J* = 8.5 Hz, 2H), 7.29 (d, *J* = 8.5 Hz, 2H), 4.16 (bs, 1H), 3.93 (d, *J* = 7.3 Hz, 1H), 3.15 – 3.09 (m, 1H), 2.81 – 2.75 (m, 1H), 2.48 – 2.41 (m, 1H), 1.97 – 1.91 (m, 1H), 1.85 – 1.79 (m, 1H), 1.60 – 1.53 (m, 1H), 1.27 – 1.22 (m, 1H).

^{13}C NMR (151 MHz, CDCl$_3$) δ 133.2, 131.5, 122.7, 121.5, 88.8, 83.8, 55.3, 52.8, 44.3, 33.8, 25.7.

FTIR (thin film, cm^{-1}) 3442.3, 2949.8, 1641.3, 1485.1, 823.7, 730.4.

HRMS (ESI) m/z, calcd for [C$_{13}$H$_{13}$Br$_2$N]$^+$: 343.0620, found 343.9462.
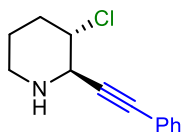
***Trans*-3-chloro-2-(phenylethynyl)piperidine (2.31).** Prepared on a 0.156 mmol scale to give **2.31** (28.5 mg, 83%, >20:1 dr) as a white solid.

¹H NMR (600 MHz, CDCl₃) δ 7.47 – 7.41 (m, 2H), 7.35 – 7.27 (m, 3H), 4.10 – 3.97 (m, 1H), 3.88 (d, J = 6.8 Hz, 1H), 3.15 – 3.06 (m, 1H), 2.80 – 2.72, (m, 1H), 2.44 – 2.34 (m, 1H), 2.00 (s, 1H), 1.86 – 1.77 (m, 2H), 1.58 – 1.49 (m, 1H).

¹³C (151 MHz, CDCl₃) δ 131.7, 128.3, 128.2, 122.6, 87.5, 84.7, 60.2, 55.1, 43.8, 32.7, 24.5.

FTIR (thin film, cm⁻¹) 3444.4, 1635.9, 757.0, 691.6, 530.1.

HRMS (ESI) [M+H]+ m/z, calcd for $[C_{13}H_{14}ClN]^+$: 220.7120, found 220.09.
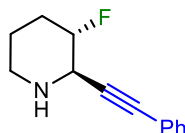
***Trans*-3-fluoro-2-((phenyl)ethynyl)piperidine (2.32).** Prepared on a 0.165 mmol scale to give **2.32** (29.0 mg, 87%, >20:1 dr) as a pale-yellow solid.

¹H NMR (600 MHz, CDCl₃) δ 7.47 – 7.40 (m, 2H), 7.34 – 7.28 (m, 3H), 4.67 – 4.50 (m, 1H), 3.95 (t, J = 7.6, 5.6 Hz, 1H), 3.16 – 3.04 (m, 1H), 2.79 – 2.69 (m, 1H), 2.23 – 2.08 (m, 1H), 1.94 – 1.87 (m, 1H), 1.84 – 1.75 (m, 2H) 1.55 – 1.48 (m, 1H).

¹³C NMR (151 MHz, CDCl₃) δ 131.7, 128.3, 128.2, 122.6, 90.2, 89.0, [86.6, 86.5], 85.1, [51.8, 51.6], 42.9, [28.1, 27.9], 22.6.

¹⁹F NMR (376 MHz, CDCl₃) δ -179.63.

FTIR (thin film, cm⁻¹) 3442.2, 1636.3, 757.4, 691.8, 541.5.

HRMS (ESI) [M+H]+ m/z, calcd for $[C_{13}H_{14}FN]^+$: 204.2604, found 204.1183.
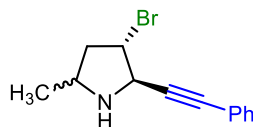
***Trans*-3-bromo-2-((phenyl)ethynyl)-5-methylpyrrolidinepiperidine** **(2.33).**

Prepared on a 0.137 mmol scale to give **2.33** (29.4 mg, 81%, 1.1:1 dr) as a brown oil.

^{1}H NMR (400 MHz, CDCl$_3$, mix of diastereomers) δ 7.43 – 7.30 (m, 4H), 7.31 – 7.29 (m, 6H), 4.42 – 4.37 (m, 2H), 4.35 (t, *J* = 3.2 Hz, 1H), 4.28 (d, *J* = 4.5 Hz, 1H), 3.63 – 3.55 (m, 2H), 2.83 – 2.76 (m, 1H), 2.39 – 2.31 (m, 1H), 2.18 – 2.09 (m, 1H), 1.95 (bs, 2H), 1.92 – 1.83 (m, 2H), 1.32 (d, *J* = 6.3 Hz, 3H), 1.29 (d, *J* = 6.3 Hz, 3H).

^{13}C NMR (101 MHz, CDCl$_3$, mix of diastereomers) δ 131.7, 131.6, 128.4, 128.4, 128.2, 122.5, 122.5, 87.8, 87.4, 84.6, 84.5, 60.2, 59.8, 53.7, 53.3, 53.0, 52.8, 44.4, 44.0, 21.9, 21.4.

FTIR (thin film, cm^{-1}) 3438.5, 2973.3, 2928.2, 1577.5, 1443.0, 1256.7, 759.7, 728.8, 692.3.

HRMS (ESI) m/z, calcd for [C$_{13}$H$_{14}$BrN]$^+$: 264.1660, found 264.0384.

Product Elaborations – Hydrogenation/Deprotection/Methylation
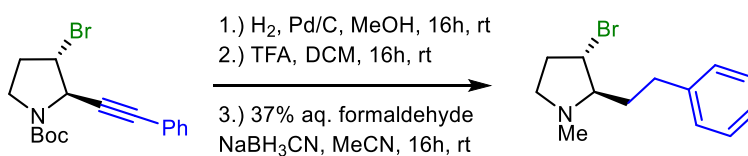
Alkyne **2.21** (512 mg) was added to an oven-dried round-bottom flask equipped with a stir bar, and subsequently dissolved with anhydrous MeOH (14.6 mL). Pd/C (31.1 mg) was then added to the flask and sealed with a rubber septum. The flask was flushed under a positive pressure of H$_2$ and allowed to stir at room

temperature overnight. The reaction mixture was diluted with dichloromethane and filtered through a pad of celite. The solution was concentrated to give **2.35**, which was used without further purification.

The subsequent amine was added to an oven-dried round-bottomed flask equipped with a stir bar. Dry DCM (1.43 mL) was added, and the solution was cooled to 0 °C. TFA (1.10 mL) was then added dropwise to the flask, and the solution was allowed to stir overnight at ambient temperature. The solution was diluted with water and basified with 10% aqueous NaOH solution. The solution was then added to a separatory funnel containing saturated sodium bicarbonate solution and extracted 3 times with DCM. The organic layers were washed with saturated sodium bicarbonate solution (1x), brine (1x), and dried over $MgSO_4$. The solution was filtered through a cotton plug and concentrated to yield the free amine, which was immediately subjected to the next step without further purification.

Methylation conditions were adapted from a known procedure.[6] Crude amine (505 mg) was added to an oven-dried round-bottom flask equipped with a stir bar and diluted with dry acetonitrile (4.77 mL). The solution was then cooled to 0 °C and 37% aqueous formaldehyde (0.532 mL) was added to the flask. Sodium cyanoborohydride (100 mg) was added portion-wise to the flask and the reaction was warmed to room temperature, then allowed to stir overnight. The reaction was basified with 10% sodium hydroxide solution and was then extracted with dichloromethane (3 x 15 mL). The organic layers were washed with 2M HCl solution (1 x 15 mL), saturated $NaHCO_3$ solution (1 x 15 mL), and brine (1 x 15 mL). The solution was then dried with magnesium sulfate and filtered through a fritted funnel. The solution was concentrated to yield the methylated amine.
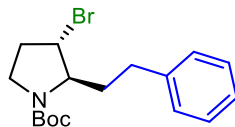
Tert-butyl-3-Bromo-2-ethylphenyl-1-methyl-pyrrolidine-1-carboxylate **(2.34).**

Prepared on a 0.96 mmol scale to give **2.34** (310 mg, 92%, >20:1 dr) as a yellow oil

and was used without any further purification.

^{1}H NMR (600 MHz, MeOD, rotamers) δ 7.23 – 7.18 (m, 2H), 7.17 – 7.06 (m, 3H),

4.49 – 4.36 (m, 1H), 4.09 – 3.95 (m, 1H), 3.59 – 3.52 (m, 1H), 3.43 – 3.34 (m, 1H),

2.70 – 2.54 (m, 2H), 2.50 – 2.41 (m, 1H), 2.17 – 2.08 (m, 1H), 1.92 – 1.80 (m, 1H),

1.66 – 1.53 (m, 1H), 1.43 – 1.33 (s, 9H).

^{13}C NMR (151 MHz, MeOD, rotamers) δ 155.1, 141.3, 141.0, 128.1, 128.0, 127.9,

125.7, 125.6, [80.0, 79.7], [68.0, 67.8], [51.7, 51.3], [44.0, 43.5], [35.8, 35.6], 33.4,

32.6, 32.3, 27.3.

FTIR (thin film, cm^{-1}) 3443.0, 2976.2, 1694.5, 1694.5, 1652.7, 1394.0, 1170.8,

1114.5, 699.8.

HRMS (ESI) m/z, calcd for $[C_{17}H_{24}BrNO_2]^+$: 354.2880, found 354.1057.
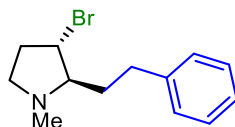
3-Bromo-2-ethylphenyl-1-methyl-pyrrolidine (2.35). Prepared on a 1.43 mmol scale

to give **2.35** (236 mg, 61%, >20:1 dr) as a colorless oil and was used without any

further purification.

^{1}H NMR (400 MHz, CDCl$_3$) δ 7.32 – 7.27 (m, 2H), 7.24 – 7.16 (m, 3H), 4.15 – 4.10

(m, 1H), 3.11 – 3.02 (m, 1H), 2.82 – 2.57 (m, 4H), 2.52 – 2.42 (m, 1H), 2.40 (s, 3H),

2.16 – 2.08 (m, 1H), 2.03 – 1.93 (m, 1H), 1.80 – 1.68 (m, 1H).

13C NMR (151 MHz, CDCl₃) δ 142.0, 128.4, 128.3, 125.8, 75.1, 54.9, 51.6, 40.9, 35.1, 33.8, 31.4.

FTIR (thin film, cm⁻¹) 3443.0, 2923.6, 1635.7, 1454.0, 1219.9, 1030.0, 698.9.

HRMS (ESI) m/z, calcd for [C₁₃H₁₈BrN]⁺: 268.1980, found 268.0695.

General Procedure C: Synthesis of β-Halo-Aminals
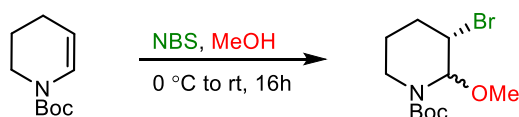
Synthesis of β-Halo-aminals was adapted from the literature.[30, 33, 34] Freshly recrystallized N-Bromosuccinimide (NBS) (21.8 mmol, 2.14 g) was added to an oven-dried round-bottomed flask equipped with a stir bar. The round bottomed flask was fitted with a rubber septum and put under a positive pressure of nitrogen. Anhydrous MeOH (198 mmol, 50 mL) was added, and the mixture was stirred at room temperature until the NBS fully dissolved. The solution was then cooled to 0 °C and enamine (19.8 mmol, 2.00 mL) was added dropwise. The solution was maintained at 0 °C for 1 h, after which it was warmed to room temperature and allowed to stir for 16 h. The mixture was diluted with Et₂O (25 mL) and the organic layer was washed with H₂O (3 x 25 mL), NaHCO₃ (2 x 25 mL), 10 % sodium thiosulfate solution (1 x 25 mL), and saturated NaCl solution (1 x 25 mL). The organic layer was dried over MgSO₄, filtered, concentrated, and purified via silica gel chromatography to give the halogenated aminal. For chlorinated and fluorinated substrates, NBS was replaced with N-Chlorosuccinimide (NCS) or SelectFluor®, respectfully.
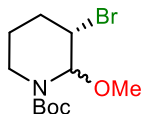
***Tert*-butyl-3-bromo-2-methoxypiperidine-1-carboxylate (2.4).** Prepared via General Procedure C on a 16 mmol scale. The crude mixture was purified by silica gel chromatography (15% EtOAc:Hexanes) to give **2.4** (4.75 g, 75%, 2.3:1 dr) as a colorless oil. The spectral data matches that which was previously reported in the literature.[39]

^{1}H NMR (400 MHz, MeOD, mix of diastereomers) δ 5.38 – 5.29 (m, 1H), 4.39 – 4.25 (m, 1H), 3.91 – 3.72 (m, 1H), 3.21 (s, 3H), 2.96 – 2.76 (m, 1H), 2.29 – 2.17 (m, 1H), 1.89 (dt, J = 13.1, 4.2 Hz, 1H), 1.85 – 1.78 (m, 1H), 1.65 – 1.52 (m, 1H), 1.43 (s, 9H).
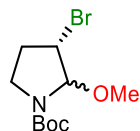
***Tert*-butyl-3-bromo-2-methoxypyrrolidine-1-carboxylate (2.36).** Prepared via General Procedure C on a 8.87 mmol scale to give **2.36** (2.12 g, 85%, 1.1:1 dr) as a colorless oil, and was used without further purification.

^{1}H NMR (400 MHz, CDCl$_3$, mix of diastereomers) δ 5.25 (s, 1H), 5.12 (s, 1H), 4.22 – 4.20 (m, 2H), 3.67 – 3.57 (m, 2H), 3.48 – 3.45 (m, 2H), 3.40 (s, 3H), 3.36 (s, 3H), 2.60 – 2.51 (m, 2H), 2.19 – 2.11 (m, 2H), 1.49 (s, 18H).

^{13}C NMR (101 MHz, CDCl$_3$, mix of diastereomers) δ 155.1, 154.4, 94.7, 94.5, 80.6, 80.3, 56.3, 56.0, 50.9, 50.0, 44.2, 43.7, 32.4, 31.6, 28.3.

FTIR (thin film, cm^{-1}) 2977, 2933, 1705, 1387, 1164, 1117, 1079.

HRMS (LIFDI) m/z calcd for C$_{10}$H$_{18}$BrNO$_3$: 279.0470; Found 279.045.
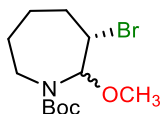
***Tert*-butyl-3-bromo-2-methoxyazepane-1-carboxylate (2.37).** Prepared via General Procedure C on a 8.06 mmol scale. The crude mixture was purified by silica gel chromatography (5% Et$_2$O:Hexanes) to give **2.37** (1.61 g, 65%, 1.2:1 dr) as a colorless oil.

^{1}H NMR (400 MHz, MeOD, mix of diastereomers) δ 5.47 (d, *J* = 7.0 Hz, 1H), 5.37 (d, *J* = 6.7 Hz, 1H), 3.95 (dddd, *J* = 18.0, 11.0, 6.8, 1.4 Hz, 2H), 3.61 – 3.45 (m, 2H), 3.33 – 3.26 (m, 1H), 3.24 (s, 2H), 3.21 (s, 3H), 2.84 – 2.76 (m, 2H), 2.21 – 2.10 (m, 2H), 1.92 – 1.72 (m, 4H), 1.60 – 1.51 (m, 4H), 1.47 (s, 18H).

^{13}C NMR (101 MHz, MeOD, mix of diastereomers) δ 155.9, 154.8, 92.0, 91.0, 80.9, 80.4, 54.6, 54.5, 54.2, 54.1, 41.1, 40.4, 35.3, 35.1, 28.0, 27.6, 27.2, 27.2, 26.8, 26.1.

FTIR (thin film, cm[-1]) 2975, 2932, 1699, 1405, 1154, 1086, 945.

HRMS (LIFDI) m/z, calcd for [C$_{12}$H$_{22}$BrNO$_3$]$^+$: 307.0783; Found 307.0785.
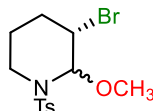
***Tert*-butyl-3-bromo-2-methoxypiperidine-1-tosyl (2.38).** Prepared via General Procedure C on a 3.47 mmol scale to give **2.38** (1.20 g, 87%, 1.2:1 dr) as a white solid (82 – 85 °C) and was used without further purification. The spectral data matches that of the literature.[40]

^{1}H NMR (400 MHz, DMSO-d$_6$, mix of diastereomers) δ 7.81 – 7.73 (m, 3H), 7.45 – 7.38 (m, 4H), 5.09 (dd, *J* = 7.2, 2.7 Hz, 2H), 4.62 (q, *J* = 2.9 Hz, 1H), 4.12 (ddd, *J* = 12.5, 4.6, 3.1 Hz, 1H), 3.34 (s, 6H), 3.25 (d, *J* = 5.2 Hz, 5H), 2.92 (td, J = 13.3, 2.9 Hz,

1H), 2.84 (td, J = 12.7, 3.0 Hz, 1H), 2.53 – 2.46 (m, 2H), 2.45 – 2.35 (m, 5H), 2.14 – 1.88 (m, 2H), 1.81 – 1.40 (m, 4H), 1.40 – 1.17 (m, 1H), 1.09 (t, J = 7.0 Hz, 1H).
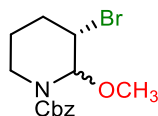
Benzyl-3-bromo-2-methoxypiperidine-1-carboxylate (2.39). Prepared via General Procedure C on a 8.38 mmol scale. The crude mixture was purified by silica gel chromatography (15% EtOAc:Hexanes) to give **2.39** (2.75 g, 62%, 2.2:1 dr) as a pale yellow oil. The spectral data matches that of the literature.[33]

^{1}H NMR (400 MHz, DMSO-d_6, mix of diastereomers) δ 7.44 – 7.25 (m, 7H), 5.46 – 5.00 (m, 4H), 4.50 (s, 1H), 3.90 (d, J = 4.2 Hz, 1H), 3.28 – 3.07 (m, 4H), 3.07 – 2.74 (m, 2H), 2.25 – 2.02 (m, 1H), 1.90 – 1.71 (m, 2H), 1.70 – 1.54 (m, 1H), 1.54 – 1.37 (m, 1H).
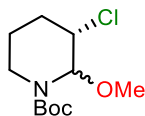
***Tert*-butyl-3-chloro-2-methoxypiperidine-1-carboxylate (2.40).** Prepared via General Procedure C on a 5.40 mmol scale, with NCS instead of NBS. The crude mixture was purified by silica gel chromatography (10% Et$_2$O:Hexanes) to give **2.40** (0.960 g, 71%, 2.2:1 dr) as a clear oil.

^{1}H NMR (400 MHz, MeOD, major diastereomer) δ 5.34 – 5.15 (m, 1H), 4.17 (s, 1H), 3.91 – 3.83 (m, 1H), 3.21 (s, 3H), 2.98 – 2.70 (m, 1H), 2.23 – 2.08 (m, 1H), 1.92 – 1.79 (m, 1H), 1.79 – 1.72 (m, 1H), 1.61 – 1.48 (m, 1H), 1.42 (s, 9H).

^{13}C NMR (151 MHz, MeOD, mix of diastereomers) δ 155.7, 155.3, 154.9, 154.3, 85.3, 84.7, 84.0, 83.9, 83.5, 80.8, 80.5, 80.4, 57.67, 57.61, 56.4, 56.1, 54.6, 54.1, 48.6, 38.4, 37.5, 36.9, 36.1, 28.6, 27.4, 27.3, 27.2, 26.2, 25.4, 25.1, 24.8, 18.4, 18.3, 18.1.

FTIR (thin film, cm^{-1}) 2976, 1701, 1637, 1153, 1078, 768.

HRMS (LIFDI) m/z, calcd for [C$_{11}$H$_{20}$ClNO$_3$]$^+$: 249.1132; Found 249.1136.
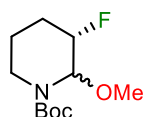
Tert-butyl-3-fluoro-2-methoxypiperidine-1-carboxylate (**2.41**). Prepared via General Procedure C on a 4.29 mmol scale, with SelectFluor® instead of NBS. The crude mixture was purified by silica gel chromatography (10% EtOAc:Hexanes) to give **2.41** (810 mg, 81%, 2.5:1 dr) as a yellow oil. The spectral data matches that of the literature.[41]

^{1}H NMR (400 MHz, MeOD, mix of diastereomers) δ 5.39 – 5.14 (m, 1H), 4.61 – 4.22 (m, 1H), 3.87 – 3.73 (m, 1H), 3.18 (s, 3H), 2.94 – 2.59 (m, 1H), 1.90 – 1.71 (m, 2H), 1.71 – 1.55 (m, 1H), 1.38 (s, 10H).
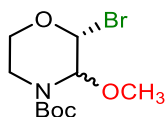
Tert-butyl-3-bromo-2-methoxymorpholine-1-carboxylate (**2.42**). Prepared via General Procedure C to give **2.42** (344 mg, 22%, 1:1 dr) as a pale-yellow oil and was used without further purification.

^{1}H NMR (400 MHz, CDCl$_3$, mix of diastereomers and rotamers) δ 5.11 – 4.88 (m, 1H), 4.60 – 4.48 (m, 1H), 3.92 – 3.84 (m, 1H), 3.79 – 3.57 (m, 1H), 3.56 – 3.45 (m, 1H), 3.37 (s, 3H), 3.30 (s, 3H), 3.27 – 3.09 (m, 1H), 1.47 (s, 10H).

^{13}C NMR (101 MHz, CDCl$_3$, mix of diastereomers) δ 155.1, 155.0, 97.0, 96.6, 81.9, 80.7, 80.6, 80.5, 57.9, 57.8, 55.0, 54.8, 54.7, 54.6, 38.5, 36.9, 28.3.

FTIR (thin film, cm^{-1}) 2976, 2933, 2832, 1702, 1415, 1367, 1326, 1170, 1102, 1061, 938.

HRMS (LIFDI) m/z, calcd for [C$_{11}$H$_{21}$BrNO$_5$]$^+$: 247.1420, found 247.1178 (displacement of bromide).
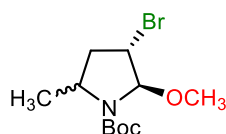
***Tert*-butyl-3-bromo-2-methoxy-5-methylpyrrolidine-1-carboxylate** **(2.43).**

Prepared via General Procedure C on a 7.75 mmol scale to give **2.43** (1.60 g, 70%, 1.2:1 dr) as a colorless oil, and was used without further purification.

^{1}H NMR (400 MHz, DMSO-d$_6$, mix of diastereomers) δ 5.18 – 5.08 (m, 1H), 4.54 – 4.43 (m, 1H), 4.27 (ddd, *J* = 11.9, 7.3, 4.3 Hz, 1H), 3.98 – 3.90 (m, 1H), 3.72 (h, *J* = 6.9 Hz, 1H), 3.31 (s, 3H), 3.26 (s, 3H), 2.41 – 2.34 (m, 1H), 2.23 – 2.12 (m, 1H), 1.91 – 1.76 (m, 1H), 1.45 – 1.39 (m, 18H), 1.28 – 1.17 (m, 6H).

^{13}C NMR (101 MHz, DMSO-d$_6$, mix of diastereomers) δ 155.0, 154.1, 153.7, 153.3, 96.6, 96.4, 95.5, 95.3, 88.4, 88.3, 88.0, 80.0, 79.8, 56.5, 55.7, 55.2, 52.9, 52.8, 52.7, 52.5, 52.3, 51.7, 51.0, 49.5, 49.4, 49.0, 48.5, 46.1, 45.7, 41.2, 40.9, 38.3, 29.7, 29.5, 28., 28.3, 22.7, 22.6, 21.95, 21.90, 21.15, 21.10.

FTIR (thin film, cm^{-1}) 2976, 2933, 1702, 1378, 1318, 1166, 1081.

HRMS (LIFDI) m/z, calcd for [C$_{11}$H$_{20}$BrNO$_3$]$^+$: 293.0627, found 293.0628.

General Procedure D: Synthesis of Enecarbamates (DIBAL-H)
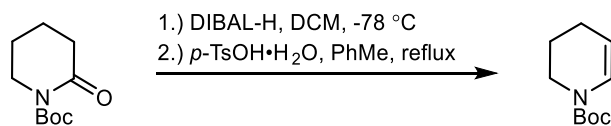
Boc-protected enamine was synthesized from commercially available 1-Boc-2-piperidone using DIBAL-H according to the literature precedent;[42] some enamines were also synthesized using this procedure. To an oven-dried round-bottomed flask equipped with a stir bar was added piperidone (12.5 mmol, 2.50 g). The flask was fitted with a rubber septum and purged with nitrogen. Dry dichloromethane (25 mL) was added to dissolve the piperidone and the solution was cooled to – 78 °C. DIBAL-H (1.0 M in hexanes, 15.1 mmol, 15.1 mL) was added dropwise to the flask and the solution was allowed to stir for 2 hours at -78 °C. The flask was opened to air and H_2O was slowly added. The flask was warmed to room temperature and ~10 mL of 4 M HCl was added. The mixture was extracted with dichloromethane, after which the organic layers were washed with H_2O (2 x 25 mL) and brine (1 x 25 mL). The organic layers were dried with magnesium sulfate, filtered through a fritted funnel, then concentrated. The crude material was used in the next step without further purification.

Boc-protected aminal was dissolved in toluene (15 mL) in an oven-dried round-bottomed flask equipped with a stir bar. Catalytic amount of para-tosylic acid monohydrate (0.15 mmol, 15 mg) was added and the reaction was brought to reflux, stirring for 30 minutes. The reaction was then cooled and quenched with triethylamine (0.4 mL). The mixture was concentrated to remove toluene and the crude residue was

dissolved in diethyl ether. The mixture was washed with H_2O (2 x 25 mL) and brine (1 x 25 mL) and dried with sodium sulfate. The solution was filtered through a fritted funnel, concentrated, and subjected to column chromatography.
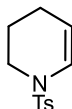
1-(toluene-4-sulfonyl)-1,2,3,4-tetrahydropyridine (2.44). Prepared via General Procedure D on a 13.8 mmol scale. The crude mixture was purified via silica gel chromatography (10% EtOAc:Hexanes) to give **2.44** (0.820 g, 88%) as a white solid. The spectral data matches that of the literature.[40, 43, 44]

^{1}H NMR (600 MHz, CDCl$_3$) δ 7.66 (d, *J* = 8.39 Hz, 2H); 7.30 (d, *J* = 7.81 Hz, 2H); 6.63 (d, *J* = 8.39 Hz, 1H); 5.00 – 4.92 (m, 1H); 3.40 – 3.31 (m, 2H); 2.42 (s, 3H) 1.93 – 1.85 (m, 2H); 1.66 – 1.60 (m, 2H).

General Procedure E: Synthesis of Enecarbamates (Super-Hydride®)
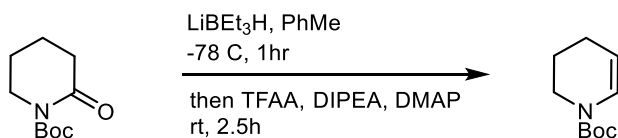
Boc-protected enamine was synthesized from commercially available 1-Boc-2-piperidone using Super Hydride® according to the literature precedent;[36] some enamines were also synthesized using this procedure. To an oven-dried round-bottomed flask equipped with a stir bar was added piperidone (8.92 mmol, 2.08 g). The flask was fitted with a rubber septum and purged with nitrogen. Dry toluene (12.1

mL) was added to dissolve the piperidone and the solution was cooled to − 78 °C. Super Hydride® (1 M in THF) was added dropwise to the flask and the solution was stirred for 1 hour at -78 °C. Then DMAP (0.09 mmol, 11 mg), DIPEA (50.84 mmol, 8.86 mL), and trifluoroacetic anhydride (10.70 mmol, 1.51 mL) was added to the flask, which was warmed to room temperature and allowed to stir for an additional 2.5 hours. The mixture was quenched with H_2O at 0 °C and further washed with H_2O (1 x 25 mL) and brine (1 x 25 mL). The organic layers were dried with magnesium sulfate, filtered through a fritted funnel, then concentrated. The crude material was then subjected to column chromatography.
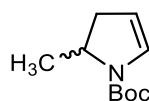
Tert-**butyl 2-methyl-2,3-dihydropyrrole-1-carboxylate (2.45).** Prepared via General Procedure E on a 7.68 mmol scale. The crude mixture was purified via silica gel chromatography (5% EtOAc:Hexanes, 1% NEt_3) to give **2.45** (1.00 g, 71%) as a pale yellow oil.

^{1}H NMR (400 MHz, CDCl$_3$, rotamers) δ 6.52 – 6.28 (m, 1H), 4.91 – 4.75 (m, 1H), 4.24 – 4.01 (m, 1H), 2.93 – 2.74 (m, 1H), 2.17 – 2.00 (m, 1H), 1.42 (9H), 1.21 – 1.14 (m, 3H).

^{13}C NMR (101 MHz, CDCl$_3$, rotamers) δ [152.1, 151.3], 128.8, [105.7, 105.6], 79.7, [52.8, 52.7], [38.1, 37.2], 28.3, [21.0, 20.5].

FTIR (thin film, cm^{-1}) 2967, 2872, 1701, 1382, 1174, 1075, 1009.

HRMS (ESI) m/z, calcd for [C$_{10}$H$_{17}$NO$_2$]$^+$: 183.2510, found 184.1334.

Enecarbamates that were not commercially available were prepared from their corresponding amide according to the literature precedent.[33, 36, 42, 45-47]
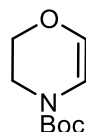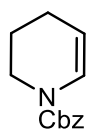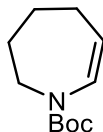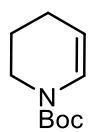
Synthesis of Amides

Amides that were not commercially available were prepared from their corresponding amine according to the literature precedent.[42-45, 48-50]
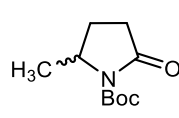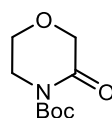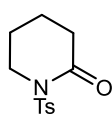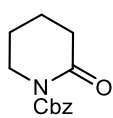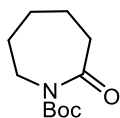
X-Ray Crystallographic Data
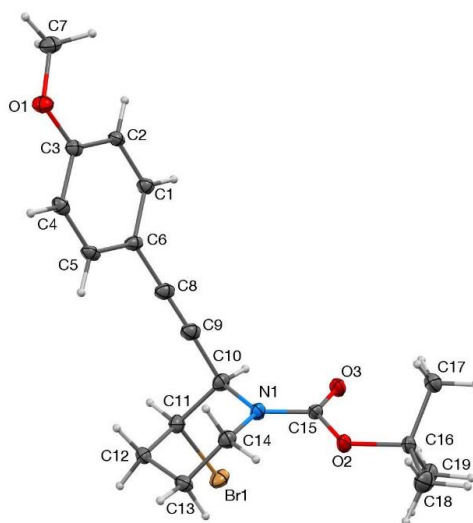
Experimental

Single crystals of $C_{19}H_{24}BrNO_3$ [**tert-butyl-trans-3-bromo-2-((4-methoxyphenyl)ethynyl)piperidine-1-carboxylate (2.9)**] were obtained from slow evaporation from 5% Et_2O in hexanes. A suitable crystal was selected and placed on a Bruker APEX-II CCD diffractometer. The crystal was kept at 100.0 K during data collection. Using Olex2 [1], the structure was solved with the SHELXT [2] structure solution program using Intrinsic Phasing and refined with the XL [3] refinement package using Least Squares minimisation.

1. Dolomanov, O.V., Bourhis, L.J., Gildea, R.J, Howard, J.A.K. & Puschmann, H.; *J. Appl. Cryst.* **2009**, *42*, 339-341.

2. Sheldrick, G.M.; *Acta Cryst.* **2015**. *A71*, 3-8.

3. Sheldrick, G.M.; *Acta Cryst*. **2008**. *A64*, 112-122.

Crystal structure determination of 9.

Crystal Data for $C_{19}H_{24}BrNO_3$ (M = 394.30 g/mol): triclinic, space group P-1 (no. 2), a = 6.6726(13) Å, b = 8.8939(17) Å, c = 16.433(3) Å, α = 102.052(6)°, β = 95.156(6)°, γ = 95.355(6)°, V = 943.6(3) Å3, Z = 2, T = 100.0 K, μ(CuKα) = 3.096 mm-1, Dcalc = 1.388 g/cm3, 24273 reflections measured (5.534° ≤ 2Θ ≤ 151.566°), 3719 unique (Rint = 0.0657, Rsigma = 0.0366) which were used in all calculations. The final R1 was 0.0592 (I > 2σ(I)) and wR2 was 0.1422 (all data).

Table S1. Crystal data and structure refinement for mary042.

Identification code   mary042

Empirical formula   C19H24BrNO3

Formula weight   394.30

Temperature/K   100.0

Crystal system   triclinic

Space group   P-1

a/Å   6.6726(13)

b/Å   8.8939(17)

c/Å   16.433(3)

α/°   102.052(6)

β/°   95.156(6)

γ/°   95.355(6)

Volume/Å3   943.6(3)

Z   2

ρcalcg/cm3   1.388

μ/mm-1   3.096

F(000) 408.0

Crystal size/mm3   0.138 × 0.114 × 0.073

Radiation   CuKα (λ = 1.54178)

2Θ range for data collection/° 5.534 to 151.566

Index ranges   -8 ≤ h ≤ 8, -10 ≤ k ≤ 11, -20 ≤ l ≤ 19

Reflections collected 24273

Independent reflections   3719 [Rint = 0.0657, Rsigma = 0.0366]

Data/restraints/parameters   3719/0/221

Goodness-of-fit on F2 1.123

Final R indexes [I>=2σ (I)]   R1 = 0.0592, wR2 = 0.1413

Final R indexes [all data]   R1 = 0.0608, wR2 = 0.1422

Largest diff. peak/hole / e Å-3   0.94/-0.91

Table S2. Fractional Atomic Coordinates (×104) and Equivalent Isotropic
Displacement

Parameters (Å2×103) for mary042. Ueq is defined as 1/3 of of the trace of the
orthogonalised UIJ tensor.

Atom	x	y	z	U(eq)
Br1	-478.4(7)	3361.6(5)	2497.3(3)	36.01(18)
O1	12972(4)	9304(3)	6414.6(18)	32.4(6)
O2	2420(5)	6782(3)	1134.5(17)	36.6(7)
O3	661(5)	7534(3)	2246.2(18)	39.0(7)
N1	3086(5)	5930(4)	2300.6(19)	27.4(7)

C1	7673(6)	8895(4)	5495(2)	26.1(8)
C2	9411(6)	9505(4)	6033(2)	24.5(8)
C3	11173(6)	8792(4)	5940(2)	25.3(8)
C4	11162(6)	7455(4)	5320(2)	28.2(8)
C5	9427(6)	6851(4)	4792(2)	27.7(8)
C6	7642(6)	7566(4)	4865(2)	25.7(8)
C7	13016(7)	10569(5)	7114(3)	38.4(10)
C8	5872(7)	6954(5)	4287(2)	31.0(9)
C9	4467(7)	6446(5)	3773(2)	32.6(9)
C10	2710(6)	5773(5)	3142(2)	29.6(8)
C11	2233(6)	4062(5)	3152(2)	30.1(8)
C12	3791(6)	3080(4)	2780(2)	28.7(8)
C13	4194(7)	3368(4)	1917(3)	30.5(8)
C14	4695(7)	5080(5)	1949(3)	31.4(9)
C15	1942(7)	6815(4)	1920(2)	30.1(9)
C16	1436(8)	7784(5)	643(3)	40.7(11)
C17	1940(10)	9476(5)	1097(3)	52.1(14)
C18	2513(11)	7476(6)	-155(3)	55.9(15)
C19	-799(9)	7303(6)	458(3)	51.4(13)

Table S3. Anisotropic Displacement Parameters (Å2×103) for mary042.
The Anisotropic displacement factor exponent takes the form: -
2π2[h2a*2U11+2hka*b*U12+…].

Atom	U11	U22	U33	U23	U13	U12
Br1	32.2(3)	40.3(3)	32.9(3)	10.39(18)	-3.88(17)	-7.58(18)
O1	27.6(14)	31.9(15)	34.1(15)	1.2(12)	2.3(11)	-0.5(12)
O2	67(2)	26.9(14)	19.6(13)	10.2(11)	5.2(13)	13.4(14)
O3	58(2)	33.3(16)	27.7(14)	4.5(12)	2.5(14)	23.9(15)
N1	38.8(19)	27.5(16)	18.9(15)	8.3(12)	6.4(13)	9.2(14)
C1	31(2)	23.7(18)	23.6(18)	3.9(14)	5.9(15)	4.3(15)
C2	32(2)	17.8(16)	22.6(17)	1.1(13)	4.8(15)	1.8(14)
C3	30(2)	22.6(18)	23.0(18)	5.8(14)	5.5(15)	-1.7(15)
C4	33(2)	24.9(18)	29.0(19)	5.8(15)	11.2(16)	7.4(16)
C5	40(2)	20.5(17)	21.9(17)	0.5(14)	10.6(16)	2.6(16)
C6	34(2)	23.3(18)	18.1(17)	3.4(14)	4.7(15)	-4.3(15)
C7	39(2)	34(2)	35(2)	-0.5(18)	-2.3(18)	-5.2(19)
C8	39(2)	31(2)	21.3(18)	2.6(15)	6.1(16)	-0.9(17)
C9	43(2)	30(2)	24.3(19)	3.7(16)	8.2(17)	1.2(18)
C10	35(2)	33(2)	23.3(18)	8.4(15)	6.9(16)	5.2(17)
C11	36(2)	29(2)	26.8(19)	10.8(16)	4.0(16)	1.9(17)
C12	37(2)	20.3(18)	28.4(19)	6.5(15)	-0.1(16)	1.7(16)
C13	36(2)	23.5(19)	30(2)	1.6(15)	6.7(16)	5.3(16)
C14	36(2)	32(2)	27.0(19)	7.5(16)	6.4(16)	6.7(17)
C15	50(3)	21.3(18)	18.2(17)	4.4(14)	0.3(16)	5.3(17)
C16	77(3)	21.8(19)	24(2)	9.0(16)	-6(2)	7(2)
C17	92(4)	25(2)	37(2)	8.7(19)	-9(3)	5(2)
C18	101(5)	44(3)	25(2)	15(2)	4(2)	4(3)

C19   74(4)   37(2)   40(3)   12(2)   -17(2)   6(2)

Table S4. Bond Lengths for mary042.

Atom	Atom	Length/Å	Atom	Atom	Length/Å
Br1	C11	1.995(4)	C4	C5	1.375(6)
O1	C3	1.356(5)	C5	C6	1.404(6)
O1	C7	1.427(5)	C6	C8	1.434(6)
O2	C15	1.352(5)	C8	C9	1.190(6)
O2	C16	1.480(5)	C9	C10	1.483(6)
O3	C15	1.212(5)	C10	C11	1.528(6)
N1	C10	1.461(5)	C11	C12	1.509(6)
N1	C14	1.462(5)	C12	C13	1.535(6)
N1	C15	1.351(5)	C13	C14	1.517(6)
C1	C2	1.385(5)	C16	C17	1.525(6)
C1	C6	1.396(5)	C16	C18	1.538(7)
C2	C3	1.392(5)	C16	C19	1.499(8)
C3	C4	1.394(5)			

Table S5. Bond Angles for mary042.

Atom	Atom	Atom	Angle/°	Atom	Atom	Atom	Angle/°
C3	O1	C7	117.7(3)	N1	C10	C11	109.8(3)
C15	O2	C16	118.7(3)	C9	C10	C11	108.8(3)
C10	N1	C14	115.3(3)	C10	C11	Br1	106.5(3)
C15	N1	C10	118.5(3)	C12	C11	Br1	110.2(3)

C15	N1	C14	126.3(3)	
C2	C1	C6	121.4(4)	
C1	C2	C3	119.5(3)	
O1	C3	C2	124.8(3)	
O1	C3	C4	115.4(3)	
C2	C3	C4	119.9(4)	
C5	C4	C3	120.3(4)	
C4	C5	C6	120.8(3)	
C1	C6	C5	118.2(4)	
C1	C6	C8	121.8(4)	
C5	C6	C8	120.0(3)	
C9	C8	C6	176.4(4)	
C8	C9	C10	178.3(4)	
N1	C10	C9	112.3(3)	

C12	C11	C10	113.0(3)
C11	C12	C13	111.3(3)
C14	C13	C12	111.4(3)
N1	C14	C13	109.7(3)
O3	C15	O2	125.2(4)
O3	C15	N1	123.9(4)
N1	C15	O2	110.9(3)
O2	C16	C17	109.8(3)
O2	C16	C18	101.1(4)
O2	C16	C19	111.1(4)
C17	C16	C18	109.8(4)
C19	C16	C17	112.6(5)
C19	C16	C18	111.8(4)

Table S6. Torsion Angles for mary042.

A	B	C	D	Angle/°	A	B	C	D	Angle/°
Br1	C11	C12	C13	68.3(4)	C10	N1	C15	O2	-177.2(3)
O1	C3	C4	C5	-178.8(3)	C10	N1	C15	O3	2.6(6)
N1	C10	C11	Br1	-69.6(4)	C10	C11	C12	C13	-50.7(4)
N1	C10	C11	C12	51.5(4)	C11	C12	C13	C14	52.1(5)
C1	C2	C3	O1	178.4(3)	C12	C13	C14	N1	-54.5(5)
C1	C2	C3	C4	-1.5(5)	C14	N1	C10	C9	64.7(4)

96

C2	C1	C6	C5	0.3(5)	C14	N1	C10	C11	-56.4(5)
C2	C1	C6	C8	-177.9(4)	C14	N1	C15	O2	2.3(6)
C2	C3	C4	C5	1.1(6)	C14	N1	C15	O3	-177.9(4)
C3	C4	C5	C6	0.1(6)	C15	O2	C16	C17	60.0(6)
C4	C5	C6	C1	-0.8(5)	C15	O2	C16	C18	176.0(4)
C4	C5	C6	C8	177.5(4)	C15	O2	C16	C19	-65.3(5)
C6	C1	C2	C3	0.8(6)	C15	N1	C10	C9	-115.7(4)
C7	O1	C3	C2	6.7(5)	C15	N1	C10	C11	123.2(4)
C7	O1	C3	C4	-173.4(4)	C15	N1	C14	C13	-120.9(4)
C9	C10	C11	Br1	167.2(3)	C16	O2	C15	O3	5.0(6)
C9	C10	C11	C12	-71.7(4)	C16	O2	C15	N	-175.2(4)
C10	N1	C14	C13	58.6(4)					

Table S7. Hydrogen Atom Coordinates (Å×104) and Isotropic Displacement
Parameters (Å2×103) for mary042.

Atom	x	y	z	U(eq)
H1	6477.56	9390.74	5555.84	31
H2	9400.23	10402.31	6462.86	29
H4	12357.86	6958.9	5261.9	34
H5	9435.1	5937.7	4372.25	33
H7A	12582.62	11468.75	6919.23	58
H7B	14397.29	10827.23	7399.96	58
H7C	12098.54	10279.58	7503.55	58
H10	1511.86	6318.67	3301.36	36

H11	2152.31	3958.95	3742.85	36
H12A	3305.31	1973.45	2725.23	34
H12B	5070.56	3322.75	3160.91	34
H13A	5336.67	2809.07	1721.23	37
H13B	2981.33	2955.05	1510.98	37
H14A	5999.97	5470.33	2298.73	38
H14B	4830.92	5240.85	1377.13	38
H17A	3412.61	9722.39	1222.88	78
H17B	1311.6	9652.39	1620.3	78
H17C	1420.16	10140.49	740.12	78
H18A	2260.16	6372.63	-423.29	84
H18B	3973.52	7771.42	-7.2	84
H18C	1992.42	8086.11	-541.98	84
H19A	-1389.11	7908.17	81.92	77
H19B	-1426.56	7486.27	981.05	77
H19C	-1044.51	6200	188.74	77
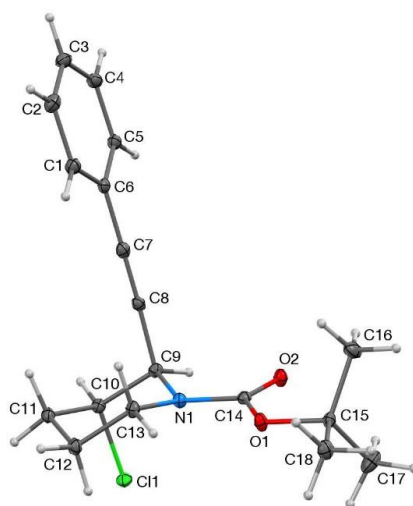
Experimental

Single crystals of $C_{18}H_{22}ClNO_2$ [**tert-butyl-trans-3-chloro-2-(phenylethynyl)piperidine-1-carboxylate (2.25)**] were obtained from slow evaporation from 5% Et_2O in hexanes. A suitable crystal was selected and placed on a Bruker APEX-II CCD diffractometer. The crystal was kept at 100.0 K during data collection. Using Olex2 [1], the structure was solved with the SHELXT [2] structure solution program using Intrinsic Phasing and refined with the XL [3] refinement package using Least Squares minimisation.

1.   Dolomanov, O.V., Bourhis, L.J., Gildea, R.J, Howard, J.A.K. & Puschmann, H.; *J. Appl. Cryst*. **2009**, *42*, 339-341.

2.   Sheldrick, G.M.; *Acta Cryst.* **2015**. *A71*, 3-8.

3.   Sheldrick, G.M.; *Acta Cryst.* **2008**. *A64*, 112-122.

Crystal structure determination of 25.

Crystal Data for $C_{18}H_{22}ClNO_2$ (M = 319.81 g/mol): monoclinic, space group P21/n (no. 14), a = 6.1462(4) Å, b = 29.3034(16) Å, c = 9.2678(5) Å, β = 98.6320(10)°, V = 1650.27(17) Å3, Z = 4, T = 100.0 K, μ(CuKα) = 2.098 mm-1, Dcalc = 1.287 g/cm3, 12404 reflections measured (6.032° ≤ 2Θ ≤ 151.508°), 3262 unique (Rint = 0.0444, Rsigma = 0.0438) which were used in all calculations. The final R1 was 0.0458 (I > 2σ(I)) and wR2 was 0.1266 (all data).

Table S1. Crystal data and structure refinement for mary041.

Identification code   mary041

Empirical formula   C18H22ClNO2

Formula weight   319.81

Temperature/K   100.0

Crystal system monoclinic

Space group   P21/n

a/Å   6.1462(4)

b/Å   29.3034(16)

c/Å   9.2678(5)

α/°   90

β/°   98.6320(10)

γ/°   90

Volume/Å3   1650.27(17)

Z   4

ρcalcg/cm3   1.287

μ/mm-1   2.098

F(000) 680.0

Crystal size/mm3   0.224 × 0.204 × 0.104

Radiation   CuKα (λ = 1.54178)

2Θ range for data collection/° 6.032 to 151.508

Index ranges   -7 ≤ h ≤ 5, -36 ≤ k ≤ 35, -11 ≤ l ≤ 10

Reflections collected   12404

Independent reflections   3262 [Rint = 0.0444, Rsigma = 0.0438]

Data/restraints/parameters   3262/0/202

Goodness-of-fit on F2 1.101

Final R indexes [I>=2σ (I)]   R1 = 0.0458, wR2 = 0.1265

Final R indexes [all data]   R1 = 0.0459, wR2 = 0.1266

Largest diff. peak/hole / e Å-3   0.26/-0.42

Table S2. Fractional Atomic Coordinates (×104) and Equivalent Isotropic
Displacement Parameters (Å2×103) for mary041.

Ueq is defined as 1/3 of of the trace of the orthogonalised UIJ tensor.

Atom	x	y	z	U(eq)
Cl1	3609.4(6)	5085.3(2)	8076.3(4)	18.64(15)
O1	3393(2)	5980.7(4)	3562.5(12)	18.0(3)
O2	1667.7(19)	6279.3(4)	5363.7(13)	18.6(3)
N1	4778(2)	5848.6(5)	5895.5(14)	14.5(3)
C1	10919(3)	7071.9(6)	8201.6(19)	20.5(4)
C2	12359(3)	7424.0(6)	8675(2)	22.8(4)
C3	11867(3)	7733.2(6)	9722(2)	22.7(4)
C4	9909(3)	7688.5(6)	10291.3(19)	20.3(4)
C5	8458(3)	7336.9(6)	9829.7(18)	18.1(3)
C6	8954(3)	7024.3(5)	8784.1(18)	16.9(3)
C7	7488(3)	6652.2(6)	8321.9(18)	17.7(3)

C8	6283(3)	6339.8(5)	7931.5(17)	15.9(3)
C9	4854(3)	5944.8(5)	7455.8(17)	15.1(3)
C10	5704(3)	5524.3(5)	8360.1(18)	15.3(3)
C11	7860(3)	5346.6(6)	7953.8(18)	17.0(3)
C12	7674(3)	5262.2(6)	6312.7(19)	18.6(4)
C13	6844(3)	5685.5(6)	5450.1(18)	16.5(3)
C14	3149(3)	6058.8(5)	4962.4(17)	14.3(3)
C15	1934(3)	6200.3(6)	2351.3(17)	15.8(3)
C16	2125(3)	6713.1(6)	2478(2)	26.7(4)
C17	-408(3)	6032.3(8)	2291(2)	28.5(4)
C18	2899(3)	6036.0(6)	1022.6(18)	21.0(4)

Table S3. Anisotropic Displacement Parameters ($Å^2 \times 10^3$) for mary041.

The Anisotropic displacement factor exponent takes the form: -$2\pi^2[h^2a^{*2}U11+2hka^*b^*U12+\ldots]$.

Atom	U11	U22	U33	U23	U13	U12
Cl1	16.5(2)	17.8(2)	21.5(2)	1.97(13)	2.27(16)	-3.18(13)
O1	21.9(6)	21.1(6)	10.8(6)	1.5(4)	2.1(5)	7.4(5)
O2	16.7(6)	23.4(6)	15.9(6)	-1.0(4)	2.7(4)	5.5(5)
N1	14.5(6)	16.7(6)	12.5(7)	-0.4(5)	2.9(5)	2.0(5)
C1	19.5(8)	22.3(8)	18.7(8)	-1.0(7)	-0.2(7)	0.5(6)
C2	18.3(8)	28.0(9)	21.6(9)	0.6(7)	1.6(7)	-2.7(7)
C3	25.0(9)	20.1(8)	20.7(9)	1.0(7)	-3.6(7)	-5.5(7)
C4	25.0(9)	16.4(8)	18.3(8)	-2.0(6)	-0.9(7)	0.8(7)
C5	18.9(8)	17.9(8)	16.4(8)	0.0(6)	-0.5(6)	1.9(6)
C6	17.7(8)	15.1(8)	16.1(8)	1.6(6)	-3.1(6)	1.4(6)
C7	20.8(8)	18.0(8)	14.2(8)	0.1(6)	2.1(6)	3.0(6)
C8	19.5(8)	14.5(7)	13.6(8)	-0.1(6)	2.1(6)	2.6(6)
C9	15.7(7)	16.6(8)	13.1(8)	-0.9(6)	2.6(6)	0.4(6)
C10	14.7(7)	16.8(8)	14.6(7)	1.2(6)	2.5(6)	-0.7(6)
C11	13.7(8)	18.3(8)	18.5(8)	2.5(6)	0.7(6)	0.9(6)
C12	14.3(8)	20.9(8)	20.7(8)	-1.1(6)	2.9(6)	4.3(6)
C13	13.8(7)	21.0(8)	15.1(8)	-0.1(6)	4.0(6)	2.2(6)
C14	16.2(7)	12.9(7)	13.8(8)	0.3(6)	1.5(6)	-1.9(6)
C15	16.3(8)	17.2(8)	12.9(7)	2.2(6)	-0.9(6)	1.6(6)
C16	40.0(11)	17.3(9)	20.7(9)	1.8(7)	-2.3(8)	1.1(7)
C17	19.6(9)	45.0(12)	20.2(9)	-1.4(8)	0.6(7)	-8.1(8)
C18	24.6(9)	24.7(9)	13.7(8)	1.5(6)	3.3(7)	4.1(7)

Table S4. Bond Lengths for mary041.

Atom	Atom	Length/Å	Atom	Atom	Length/Å
Cl1	C10	1.8109(17)	C5	C6	1.400(2)
O1	C14	1.348(2)	C6	C7	1.438(2)
O1	C15	1.4753(18)	C7	C8	1.199(2)
O2	C14	1.219(2)	C8	C9	1.480(2)
N1	C9	1.467(2)	C9	C10	1.537(2)
N1	C13	1.473(2)	C10	C11	1.523(2)
N1	C14	1.367(2)	C11	C12	1.528(2)
C1	C2	1.387(2)	C12	C13	1.522(2)
C1	C6	1.402(2)	C15	C16	1.511(2)
C2	C3	1.393(3)	C15	C17	1.514(2)
C3	C4	1.391(3)	C15	C18	1.523(2)
C4	C5	1.388(2)			

Table S5. Bond Angles for mary041.

Atom	Atom	Atom	Angle/°	Atom	Atom	Atom	Angle/°
C14	O1	C15	121.03(12)	C8	C9	C10	109.06(13)
C9	N1	C13	115.92(13)	C9	C10	Cl1	108.32(11)
C14	N1	C9	116.68(13)	C11	C10	Cl1	110.32(11)
C14	N1	C13	123.31(13)	C11	C10	C9	112.11(13)
C2	C1	C6	119.86(16)	C10	C11	C12	111.30(13)
C1	C2	C3	120.59(17)	C13	C12	C11	111.11(14)
C4	C3	C2	119.59(16)	N1	C13	C12	110.63(13)
C5	C4	C3	120.35(16)	O1	C14	N1	110.83(13)
C4	C5	C6	120.17(16)	O2	C14	O1	125.44(15)
C1	C6	C7	119.88(15)	O2	C14	N1	123.72(15)
C5	C6	C1	119.43(16)	O1	C15	C16	110.09(13)
C5	C6	C7	120.69(16)	O1	C15	C17	110.63(14)
C8	C7	C6	179.33(19)	O1	C15	C18	102.19(12)
C7	C8	C9	178.28(17)	C16	C15	C17	112.87(16)
N1	C9	C8	111.95(13)	C16	C15	C18	110.02(15)
N1	C9	C10	109.96(13)	C17	C15	C18	110.52(14)

Table S6. Torsion Angles for mary041.

A	B	C	D	Angle/°	A	B	C	D	Angle/°

Cl1	C10	C11	C12	67.71(15)	C9	C10	C11	C12	-53.10(18)
N1	C9	C10	Cl1	-70.09(14)	C10	C11	C12	C13	53.67(18)
N1	C9	C10	C11	51.88(17)	C11	C12	C13	N1	-53.51(18)
C1	C2	C3	C4	-0.2(3)	C13	N1	C9	C8	67.11(17)
C2	C1	C6	C5	0.6(3)	C13	N1	C9	C10	-54.29(17)
C2	C1	C6	C7	-178.35(16)	C13	N1	C14	O1	17.4(2)
C2	C3	C4	C5	0.4(3)	C13	N1	C14	O2	-163.79(15)
C3	C4	C5	C6	-0.1(3)	C14	O1	C15	C16	60.00(19)
C4	C5	C6	C1	-0.4(2)	C14	O1	C15	C17	-65.44(19)
C4	C5	C6	C7	178.55(15)	C14	O1	C15	C18	176.87(14)
C6	C1	C2	C3	-0.3(3)	C14	N1	C9	C8	-90.97(16)
C8	C9	C10	Cl1	166.80(11)	C14	N1	C9	C10	147.64(14)
C8	C9	C10	C11	-71.23(17)	C14	N1	C13	C12	-147.79(15)
C9	N1	C13	C12	55.74(18)	C15	O1	C14	O2	5.8(2)
C9	N1	C14	O1	173.66(13)	C15	O1	C14	N1	-175.35(13)
C9	N1	C14	O2	-7.5(2)					

Table S7. Hydrogen Atom Coordinates (Å×104) and Isotropic Displacement

Parameters (Å2×103) for mary041.

Atom	x	y	z	U(eq)
H1	11263.9	6863.45	7484.11	25
H2	13693.47	7454.67	8282.19	27
H3	12862.56	7972.96	10044.3	27
H4	9562.55	7899.97	11000.1	24
H5	7124.54	7308.12	10224.4	22
H9	3328.67	6014.36	7644.06	18
H10	5947.73	5610.35	9416.18	18
H11A	8264.17	5058.31	8483.99	20
H11B	9042.94	5571.52	8255.99	20
H12A	9133.27	5175.83	6069.82	22
H12B	6648.81	5005.53	6034.03	22
H13A	7970.47	5929.01	5617.51	20
H13B	6594.8	5613.03	4394.85	20
H16A	1468.48	6816.55	3321.89	40
H16B	1349.14	6854.71	1589.24	40
H16C	3680.51	6800.88	2606.24	40
H17A	-410.57	5698.72	2366.5	43
H17B	-1278.96	6125.16	1363.79	43
H17C	-1050.32	6164.24	3102.35	43
H18A	4435.1	6135.3	1101.82	31
H18B	2051.45	6164.9	136.29	31

H18C   2832.01   5702.13   974.79   31

2.5   References

1.   Daly, J. W., Ernest Guenther Award in Chemistry of Natural Products. Amphibian Skin: A Remarkable Source of Biologically Active Arthropod Alkaloids. *J. Med. Chem.* **2003,** *46* (4), 445-452.

2.   Edwards, J. R.; Turner, P. J.; Wannop, C.; Withnell, E. S.; Grindey, A. J.; Nairn, K., In Vitro Antibacterial Activity of SM-7338, a Carbapenem Antibiotic with Stability to Dehydropeptidase I. *Antimicrob. Agents Chemother.* **1989,** *33* (2), 215-222.

3.   Kongkiatpaiboon, S.; Schinnerl, J.; Felsinger, S.; Keeratinijakal, V.; Vajrodaya, S.; Gritsanapan, W.; Brecker, L.; Greger, H., Structural relationships of stemona alkaloids: assessment of species-specific accumulation trends for exploiting their biological activities. *J. Nat. Prod.* **2011,** *74* (9), 1931-8.

4.   Martin, G.; Angyal, P.; Egyed, O.; Varga, S.; Soos, T., Total Syntheses of Dihydroindole Aspidosperma Alkaloids: Reductive Interrupted Fischer Indolization Followed by Redox Diversification. *Org. Lett.* **2020,** *22* (12), 4675-4679.

5.   Schinnerl, J.; Brem, B.; But, P. P.; Vajrodaya, S.; Hofer, O.; Greger, H., Pyrrolo- and pyridoazepine alkaloids as chemical markers in Stemona species. *Phytochemistry.* **2007,** *68* (10), 1417-27.

6.   Secor, H. V. S., J. I., The Preparation of "Elongated" Nicotine Analogues. *Heterocycles* **1986,** *24* (6), 1687-1698.

7.   Taylor, R. D.; MacCoss, M.; Lawson, A. D. G., Rings in Drugs. *J. Med. Chem.* **2014,** *57* (14), 5845-5859.

8.   Wierzejska, J.; Motogoe, S.; Makino, Y.; Sengoku, T.; Takahashi, M.; Yoda, H., A new approach toward the total synthesis of (+)-batzellaside B. *Beilstein J. Org. Chem.* **2012,** *8*, 1831-8.

9.   Vitaku, E.; Smith, D. T.; Njardarson, J. T., Analysis of the Structural Diversity, Substitution Patterns, and Frequency of Nitrogen Heterocycles among U.S. FDA Approved Pharmaceuticals. *J. Med. Chem.* **2014,** *57* (24), 10257-10274.

10.   Brands, K. M. J.; Payack, J. F.; Rosen, J. D.; Nelson, T. D.; Candelario, A.; Huffman, M. A.; Zhao, M. M.; Li, J.; Craig, B.; Song, Z. J.; Tschaen, D. M.; Hansen, K.; Devine, P. N.; Pye, P. J.; Rossen, K.; Dormer, P. G.; Reamer, R. A.; Welch, C. J.; Mathre, D. J.; Tsou, N. N.; McNamara, J. M.; Reider, P. J., Efficient Synthesis of NK1 Receptor Antagonist Aprepitant Using a Crystallization-Induced Diastereoselective Transformation. *J. Am. Chem. Soc.* **2003,** *125* (8), 2129-2135.

11.   Zhao, M. M.; McNamara, J. M.; Ho, G.-J.; Emerson, K. M.; Song, Z. J.; Tschaen, D. M.; Brands, K. M. J.; Dolling, U.-H.; Grabowski, E. J. J.; Reider, P. J.; Cottrell, I. F.; Ashwood, M. S.; Bishop, B. C., Practical Asymmetric Synthesis of

Aprepitant, a Potent Human NK-1 Receptor Antagonist, via a Stereoselective Lewis Acid-Catalyzed Trans Acetalization Reaction. *J. Org. Chem.* **2002,** *67* (19), 6743-6747.

12.   Cossy, J.; Sieng, B.; Ventura, O.; Bellosta, V., A Convergent Total Synthesis of (+)-Febrifugine. *Synlett* **2008,** *2008* (8), 1216-1218.

13.   Keller, T. L.; Zocco, D.; Sundrud, M. S.; Hendrick, M.; Edenius, M.; Yum, J.; Kim, Y. J.; Lee, H. K.; Cortese, J. F.; Wirth, D. F.; Dignam, J. D.; Rao, A.; Yeo, C. Y.; Mazitschek, R.; Whitman, M., Halofuginone and other febrifugine derivatives inhibit prolyl-tRNA synthetase. *Nat. Chem. Biol.* **2012,** *8* (3), 311-7.

14.   Pansare, S.; Paul, E., Synthesis of (+)-Febrifugine and a Formal Synthesis of (+)-Halofuginone Employing an Organocatalytic Direct Vinylogous Aldol Reaction. *Synthesis.* **2013,** *45* (13), 1863-1869.

15.   Smullen, S.; Evans, P., An asymmetric synthesis of febrifugine, halofuginone and their hemiketal isomers. *Tetrahedron* **2017,** *73* (37), 5493-5499.

16.   Willoughby, C. A.; Buchwald, S. L., Synthesis of highly enantiomerically enriched cyclic amines by the catalytic asymmetric hydrogenation of cyclic imines. *J. Org. Chem.* **1993,** *58* (27), 7627-7629.

17.   Han, P.; Mao, Z. Y.; Si, C. M.; Zhou, Z.; Wei, B. G.; Lin, G. Q., Stereoselective Synthesis of Pyrido- and Pyrrolo[1,2- c][1,3]oxazin-1-ones via a Nucleophilic Addition-Cyclization Process of N, O-Acetal with Ynamides. *J. Org. Chem.* **2019,** *84* (2), 914-923.

18.   Bell, J. D.; Harkiss, A. H.; Wellaway, C. R.; Sutherland, A., Stereoselective synthesis of 2,6-trans-4-oxopiperidines using an acid-mediated 6-endo-trig cyclisation. *Org. Biomol. Chem.* **2018,** *16* (35), 6410-6422.

19.   Cariou, C. A.; Kariuki, B. M.; Snaith, J. S., Stereoselective synthesis of 2,4,5-trisubstituted piperidines by carbonyl ene and Prins cyclisations. *Org. Biomol. Chem.* **2008,** *6* (18), 3337-48.

20.   Guerola, M.; Escolano, M.; Alzuet-Pina, G.; Gomez-Bengoa, E.; Ramirez de Arellano, C.; Sanchez-Rosello, M.; Del Pozo, C., Synthesis of substituted piperidines by enantioselective desymmetrizing intramolecular aza-Michael reactions. *Org. Biomol. Chem.* **2018,** *16* (25), 4650-4658.

21.   Iza, A.; Uria, U.; Reyes, E.; Carrillo, L.; Vicario, J. L., A general approach for the asymmetric synthesis of densely substituted piperidines and fully substituted piperidinones employing the asymmetric Mannich reaction as key step. *RSC Adv.* **2013,** *3* (48), 25800-25811.

22.   Li, P.; Huang, Y.; Hu, X.; Dong, X. Q.; Zhang, X., Access to Chiral Seven-Member Cyclic Amines via Rh-Catalyzed Asymmetric Hydrogenation. *Org. Lett.* **2017,** *19* (14), 3855-3858.

23.   Reddy, A. G. K.; Satyanarayana, G., A simple efficient sequential one-pot intermolecular aza-Michael addition and intramolecular Buchwald–Hartwig α-arylation of amines: synthesis of functionalized tetrahydroisoquinolines. *Tetrahedron* **2012,** *68* (38), 8003-8010.

24.   Tripathi, S.; Ambule, M. D.; Srivastava, A. K., Construction of Highly Functionalized Piperazinones via Post-Ugi Cyclization and Diastereoselective Nucleophilic Addition. *J. Org. Chem.* **2020,** *85* (11), 6910-6923.

25.   Van Beek, W. E.; Van Stappen, J.; Franck, P.; Abbaspour Tehrani, K., Copper(I)-Catalyzed Ketone, Amine, and Alkyne Coupling for the Synthesis of 2-Alkynylpyrrolidines and -piperidines. *Org. Lett.* **2016,** *18* (19), 4782-4785.

26.   Wdowik, T.; Galster, S. L.; Carmo, R. L. L.; Chemler, S. R., Enantioselective, Aerobic Copper-Catalyzed Intramolecular Carboamination and Carboetherification of Unactivated Alkenes. *ACS. Catal.* **2020,** *10* (15), 8535-8541.

27.   Wilde, J. H.; Dickie, D. A.; Harman, W. D., A Highly Divergent Synthesis of 3-Aminotetrahydropyridines. *J. Org. Chem.* **2020,** *85* (12), 8245-8252.

28.   Xie, L.-H.; Cheng, J.; Luo, Z.-W.; Lu, G., Mannich Reaction of Indole with Cyclic Imines in Water. *Tet. Lett.* **2018,** *59* (5), 457-461.

29.   Zhang, Y.; Kong, D.; Wang, R.; Hou, G., Synthesis of chiral cyclic amines via Ir-catalyzed enantioselective hydrogenation of cyclic imines. *Org. Biomol. Chem.* **2017,** *15* (14), 3006-3012.

30.   Haidzinskaya, T.; Kerchner, H. A.; Liu, J. X.; Watson, M. P., Diastereoselective, Zinc-Catalyzed Alkynylation of alpha-Bromo Oxocarbenium Ions. *Org. Lett.* **2015,** *17* (15), 3857-3859.

31.   Mizuta, S.; Onomura, O., Diastereoselective addition to N-acyliminium ions with aryl- and alkenyl boronic acids via a Petasis-type reaction. *RSC Adv.* **2012,** *2* (6), 2266-2269.

32.   Onomura, O.; N. Gichuhi, P.; Kuriyama, M., Diastereoselective Synthesis of 3-Fluoro-2-substituted Piperidines and Pyrrolidines. *Heterocycles* **2014,** *88* (1), 331-346.

33.   Rouchaud, A.; Braekman, J.-C., A New and Efficient Synthesis of Derivatives of Octahydro-4H-pyrrolo[1,2-c]pyrido[1′,2′-a]imidazole. *Eur. J. Org. Chem.* **2011,** *2011* (12), 2346-2353.

34.   Kiewel, K.; Luo, Z.; Sulikowski, G. A., Stereocontrolled Synthesis of the DE Ring System of the Marine Alkaloid Upenamide. *Org. Lett.* **2005,** *7* (23), 5163-5165.

35.   Wilkinson, T. J.; Stehle, N. W.; Beak, P., Enantioselective Syntheses of 2-Alkyl- and 2,6-Dialkylpiperidine Alkaloids: Preparations of the Hydrochlorides of (−)-Coniine, (−)-Solenopsin A, and (−)-Dihydropinidine. *Org. Lett.* **2000,** *2* (2), 155-158.

36.   Jurong Yu, V. T., Peter Riebel, Elizabeth Hierl, and Boguslaw Mudryk, One-pot Conversion of Lactam Carbamates to Cyclic Enecarbamates: Preparation of 1-tert-butoxycarbonyl-2,3-dihydropyrrole. *Org. Synth.* **2008,** *85* (64).

37.   Liu, S.; Zeng, X.; Xu, B., CuII-catalyzed regioselective borylation of alkynes and alkenes. *Tet. Lett.* **2016,** *57* (33), 3706-3710.

38.   Evans, A. B.; Knight, D. W., Boron trifluoride–tetrahydrofuran complex: a superior trigger for the Yamaguchi–Hirao alkylation of lithio-acetylides by epoxides. *Tet. Lett.* **2001,** *42* (39), 6947-6948.

39.   Tatsuya, S.; Yoshihiro, M.; Masaru, O.; Osamu, O., A New Method for Introducing Some Active Methylene or Methine Groups to the 3-Position of Pyrrolidine or Piperidine Skeleton, and Its Application to Preparation of a Key Intermediate for (±)-Eburnamonine Synthesis. *Chem. Lett.* **1987,** *16* (7), 1447-1450.

40.   Harrison, T. J.; Dake, G. R., Pt(II) or Ag(I) Salt Catalyzed Cycloisomerizations and Tandem Cycloadditions Forming Functionalized Azacyclic Arrays. *Org. Lett.* **2004,** *6* (26), 5023-5026.

41.   Fischer, P.; Morris, M.; Müller-Bunz, H.; Evans, P., Synthesis and Structural Elucidation of 1,2-Disubstituted 3-Fluoropiperidines. *Eur. J. Org. Chem.* **2020,** *2020* (9), 1165-1176.

42.   Wilkinson, T. J.; Stehle, N. W.; Beak, P., Enantioselective syntheses of 2-alkyl- and 2,6-dialkylpiperidine alkaloids: preparations of the hydrochlorides of (-)-coniine, (-)-solenopsin A, and (-)-dihydropinidine. *Org. Lett.* **2000,** *2* (2), 155-8.

43.   Liu, G.; Zheng, L.; Shao, M.; Zhang, H.; Qiao, W.; Wang, X.; Liu, B.; Zhao, H.; Wang, J., A six-coordinated cationic ruthenium carbyne complex with liable pyridine ligands: synthesis, structure, catalytic investigation, and DFT study on initiation mechanism. *Tetrahedron* **2014,** *70* (32), 4718-4725.

44.   Åhman, J.; Somfai, P., Carbon☐carbon bond formation via N-tosyliminium ions. *Tetrahedron* **1992,** *48* (43), 9537-9544.

45.   De Simone, F.; Saget, T.; Benfatti, F.; Almeida, S.; Waser, J., Formal Homo-Nazarov and Other Cyclization Reactions of Activated Cyclopropanes. *Chem. Eur. J.* **2011,** *17* (51), 14527-14538.

46.   Li, G.; Kates, P. A.; Dilger, A. K.; Cheng, P. T.; Ewing, W. R.; Groves, J. T., Manganese-Catalyzed Desaturation of N-Acyl Amines and Ethers. *ACS. Catal.* **2019,** *9* (10), 9513-9517.

47.   Tereshchenko, O. D.; Perebiynis, M. Y.; Knysh, I. V.; Vasylets, O. V.; Sorochenko, A. A.; Slobodyanyuk, E. Y.; Rusanov, E. B.; Borysov, O. V.; Kolotilov, S. V.; Ryabukhin, S. V.; Volochnyuk, D. M., Electrochemical Scaled-up Synthesis of Cyclic Enecarbamates as Starting Materials for Medicinal Chemistry Relevant Building Bocks. *Adv. Synth. Catal.* **2020,** *362* (15), 3229-3242.

48.   Yang, T.; Yin, Q.; Gu, G.; Zhang, X., A one-pot process for the enantioselective synthesis of tetrahydroquinolines and tetrahydroisoquinolines via asymmetric reductive amination (ARA). *Chem. Commun.* **2018,** *54* (52), 7247-7250.

49.   Dake, G. R.; Fenster, M. D. B.; Hurley, P. B.; Patrick, B. O., Synthesis of Functionalized 1-Azaspirocyclic Cyclopentanones Using Bronsted Acid or N-Bromosuccinimide Promoted Ring Expansions. *J. Org. Chem.* **2004,** *69* (17), 5668-5675.

50.   Cossy, J.; de Filippis, A.; Pardo, D. G., Palladium-Catalyzed Intermolecular α-Arylation of N-Protected 2-Piperidinones. *Org. Lett.* **2003,** *5* (17), 3037-3039.

Chapter 3

PROGRESS TOWARDS AN ENANTIOSELECTIVE DIFUNCTIONALIZATION OF CYCLIC ENAMIDES VIA A BROMINATION/ALKYNYLATION CASCADE

3.1 Introduction

As mentioned in Chapter 2.1, diastereoselective difunctionalization of enamines was underdeveloped. Enantioselective additions to saturated cyclic iminium ions were also uncommon, as shown in Chapter 1.1. Because our stereoselective alkynylation of saturated cyclic iminium ions have been successful, I sought to develop an enantioselective and diastereoselective difunctionalization, in which we could harness the reversibility of the formation of a β-(bromo)iminium ion and achieve a high level of control over enantioselectivity and diastereoselectivity.

In terms of prior art in the enantioselective difunctionalization of enamines, the best example was reported by the Masson group. Masson has demonstrated enantioselective halogenations of acyclic enecarbamates.[1-4] Succinimide-based halide sources were used to achieve halogenation and subsequent addition of succinimide to the iminium ion intermediate. The enantioselectivity was achieved by the use of a chiral phosphoric acid catalyst (**Scheme 3.1**). Substrate scope has been demonstrated at the R_1 and carboxylate positions, with moderate to great yields and

enantioselectivities. However, only acyclic enecarbamates were reported, and succinimide was the only nucleophile that was introduced.

Scheme 3.1 – Masson's α-Halogenation of Enecarbamates
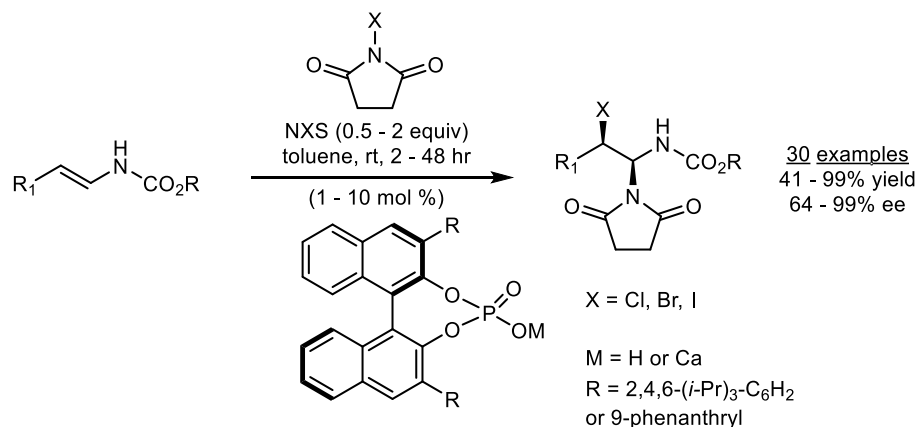
Given our group's interest in using chiral copper(I) catalysts to control enantioselective alkynylations,[5-7] I was interested in developing a different strategy to achieve highly enantioselective difunctionalizations of cyclic enamines. Our overall concept for this process would be to generate the bromo-iminium ion *in situ* from enamine starting material **3.1**, which would provide two enantiomers of the intermediate (*S*)-**3.2** and (*R*)-**3.2** (**Scheme 3.2**). We envisioned that this bromination could be reversible under specific conditions, after which a chiral copper acetylide could then preferentially react with one enantiomer of intermediate **3.2** over the other. This event would favor a single enantiomer of product **3.3** and thus coax the equilibrium between (*S*)-**3.2** and (*R*)-**3.2** towards the intermediate being more quickly consumed. This general approach for a dynamic kinetic resolution has been theorized

previously by Denmark and Burk specifically centered around intramolecular halolactonization.[8] The reversibility of the bromination of alkenes has also been studied previously.[9] Challenges with taking this approach include potential polymerization of the enamine starting material with the iminium ion intermediates, or elimination reactions of the intermediates[10]. Both phenomena are challenges we have seen in previous method development as discussed in Chapters 1 and 2.

Scheme 3.2 – Our Approach for a Dynamic Kinetic Resolution
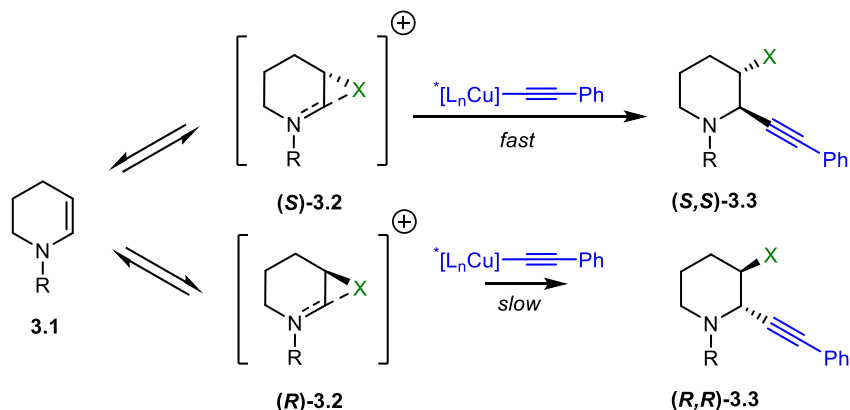
We conceptualized an enantioselective halogenation which would form only one enantiomer of the bromo-iminium intermediate (**Scheme 3.2**). This iminium ion could then act as the electrophile in a stereospecific copper-catalyzed alkynylation, which I had developed and described in Chapter 2.

3.2   Results and Discussion

I initially focused on the dynamic kinetic resolution using *tert*-butyl 1,2,3,4-tetrahydro-1-pyridinecarboxylate (**3.1**). I started with the conditions, similar to the combined reagents for the stepwise bromination/alkynylation sequence in Chapter 2, except that MeOH was not added: 10 mol % copper(I) iodide, 1.2 equivalents of phenylacetylene, 1.5 equivalents of di-isopropyl-N-ethylamine, 1.1 equivalents of halogenating reagent, and THF (0.18M) at ambient temperature for 24 hours.

I first investigated halogen sources, particularly *N*-halo-succinimides as they have been successful in the synthesis of the β–(bromo)hemiaminal ethers starting materials discussed in Chapter 2 (**Table 3.1**). Introduction of NBS, NCS, NIS, and SelectFluor did not provide the desired alkynylated product (entries 1, 3–5), and instead led to either recovered starting materials (with NCS and SelectFluor) or the succinimide adduct (**3.4**) (with NBS and NIS). The succinimide adduct byproduct was a result of the succinimide anion acting as the nucleophile to the β-(bromo)-iminium ion rather than the copper(I) acetylide, similar to what was seen in Masson's work (see **Scheme 3.1** above).[1-4]

Table 3.1 – Preliminary Investigation of Halogen Source

entry	halogen source	3.1 (%)[b]	3.3 (%)[b]	3.4 (%)[b]	3.5 (%)[b]
1	NBS	5	0	53	18
2	NBS[c]	20	2	trace	18
3	NCS	60	0	10	13
4	NIS	0	0	78	0
5	SelectFluor	80	0	0	0
6	DBDMH	30	6	0	64
7	DBDMH[d]	0	12	22	35

[a]Conditions: **3.1** (0.1 mmol, 1.0 equiv), CuI (0.010 mmol, 10 mol %), alkyne (0.12 mmol, 1.2 equiv), i-Pr$_2$NEt (0.15 mmol, 1.5 equiv), halide source (0.11 mmol, 1.1 equiv), THF (0.18M). [b]Determined by ^{1}H NMR analysis with 1,3,5-trimethoxybenzene as an internal standard. [c]Sm(OTf)$_3$ was added (0.010 mmol, 10 mol %). [d]NEt$_3$ as base.
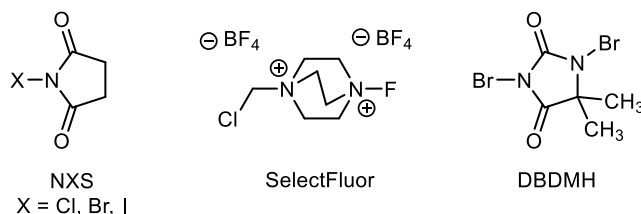
According to Masson's research,[1] it is possible that the succinimide anion can coordinate with a Lewis acid such as Sm(OTf)$_3$, which would lower its nucleophilicity towards the iminium ion. I decided to add Sm(OTf)$_3$ to the reaction mixture to prevent the formation of the adduct. Indeed, less adduct formation was observed when Sm(OTf)$_3$ was introduced into the reaction, albeit with an increase of the vinyl halide elimination byproduct (**3.5**) (entry 2). However, elimination to the vinyl halide can occur in the presence of base after the iminium ion forms *in situ*, as previously discussed in Chapter 1. Elimination to the vinyl halide **3.5** was the main product when

Sm(OTf)$_3$ was added, but 2% of desired product **3.3** was also observed. Succinimide adduct (**3.4**) and vinyl halide (**3.5**) were the main competing byproducts for this method, and the yields of these byproducts were monitored in each screen moving forward. In contract to NBS, 1,3-dibromo-5,5-dimethylhydantoin (DBDMH) showed reactivity towards the enamine with a significant decrease in adduct formation and without the influence of samarium (entry 6). However, an increase of elimination byproduct **3.5** was also observed.

Because base is required for the elimination, other organic and inorganic bases were investigated (**Table 3.2**). Bulky bases similar to i-Pr$_2$NEt provided analogous results (entries 1–6), although triethylamine resulted in a significant increase in product yield (entry 4). Interestingly, inorganic bases such as cesium carbonate and potassium phosphate led solely to adduct formation, which may be of interest in future research (entries 7–9).

Table 3.2 – DBDMH and Bases

1.1 equiv DBDMH
1.2 equiv ≡—Ph
10 mol % CuI

1.5 equiv base
THF (0.18M)
rt, 24 h

3.1   3.3   3.4   3.5

entry	base	3.1 (%)^b	3.3 (%)^b	3.4 (%)^b	3.5 (%)^b
1	i-Pr$_2$NEt	30	6	0	64
2	PMP	0	0	0	62
3	Cy$_2$NEt	30	0	0	83
4	NEt$_3$	0	12	24	35
5	DBU	0	0	0	0
6	MTBD	0	0	58	0
7	Cs$_2$CO$_3$	0	0	91	0
8	K$_3$PO$_4$	0	0	137	0
9	NaOTMS	0	0	53	0

[a]Conditions: **3.1** (0.1 mmol, 1.0 equiv), CuI (0.010 mmol, 10 mol %), alkyne (0.12 mmol, 1.2 equiv), base (0.15 mmol, 1.5 equiv), halide source (0.11 mmol, 1.1 equiv), THF (0.18M).
[b]Determined by ^{1}H NMR analysis with 1,3,5-trimethoxybenzene as an internal standard.

Various temperatures ranging from 80 to -80 °C were explored, as well as a range of solvents. At room temperature (entries 1–6) dioxane gave the highest yield of 20% (entry 1) while 2-MeTHF gave the lowest yields of side reaction products (entry 2). Increasing the temperature to 50 °C helped to increase the yield of **3.3** in the case of DME (entry 8), however byproducts **3.4** and **3.5** were also seen in all solvents. Further increasing the temperature to 80 °C did not increase product yield, and instead led to more byproduct formation (entries 10–13). When decreasing the temperature to -50 °C (entries 14–16), DME and THF gave the best yield of product **3.3** at 22% and 25%, respectfully (**Table 3.3**). Further decreasing the temperature to -80 °C did not increase product yield, and also led to more byproduct formation (entries 17–20).

Table 3.3 – Investigation of Temperature and Solvent

entry	solvent	temp (°C)	3.1 (%)^b	3.3 (%)^b	3.4 (%)^b	3.5 (%)^b
1	THF	rt	0	12	22	35
2	2-MeTHF	rt	42	12	11	11
3	DME	rt	1	9	33	41
4	dioxane	rt	3	20	26	33
5	toluene	rt	31	12	25	31
6	CPME	rt	21	16	27	16
7	THF	50	30	10	16	11
8	DME	50	12	22	23	28
9	2-MeTHF	50	30	10	16	11
10	2-MeTHF	80	trace	17	24	24
11	toluene	80	35	13	24	13
12	dioxane	80	4	14	23	26
13	DME	80	15	9	26	44
14	THF	-50	6	25	29	37
15	DME	-50	7	22	37	36
16	2-MeTHF	-50	24	11	14	11
17	THF	-80	3	3	22	39
18	DME	-80	6	9	25	30
19	toluene	-80	16	10	26	12
20	CPME	-80	trace	12	28	14

^{a}Conditions: **3.1** (0.1 mmol, 1.0 equiv), CuI (0.010 mmol, 10 mol %), alkyne (0.12 mmol, 1.2 equiv), NEt$_3$ (0.20 mmol, 2.0 equiv), DBDMH (0.11 mmol, 1.1 equiv), solvent (0.18M).
^{b}Determined by ^{1}H NMR analysis with 1,3,5-trimethoxybenzene as an internal standard.

A variety of chiral ligands was investigated alongside these experiments (**Table 3.4**). When commercially available PyBOX ligands were introduced to the reaction, comparable product yield was seen but the enantioselectivity varied. PhPyBOX (**L1**) gave little to no yield of product (entry 1). Excitingly, *i*-PrPyBOX (**L2,** entry 2) and *t*-BuPyBOX (**L3,** entry 3) gave enantioselectivities of -37% ee and -29% ee, respectfully. These results could indicate that more sterically encumbering groups on the oxazoline ring may improve enantioselectivity, as these ligands would be better

able to squeeze the chiral pocket as seen in the enantioselective alkynylation described in Chapter 1.[7] In order to investigate this theory further, non-commercial ligands **L4 – L10** were synthesized according to the literature precedent and used as the ligand under the optimization parameters.[11] Ligands **L4**, **L5,** and **L6** improved the yield and ee more than the PyBOX ligands without additional substitution on the oxazoline ring. Interestingly, **L6** in particular resulted in product **3.3** in 19% yield and 53% ee, which was also determined to be the optimal chiral ligand in the previously discussed enantioselective alkynylation.[7] Other PyBOX ligands with tetra-ethyl substitution on the oxazoline ring (**L7 – L10**) were also synthesized, however these ligands were not successful in increasing the yield or enantioselectivity. The decrease in enantioselectivity with more sterically encumbering groups suggests a limit to the ligand's steric bulk that could be beneficial to the reaction.

Table 3.4 – Preliminary Investigation of Ligand
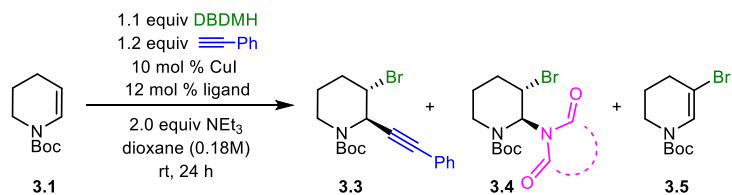
entry	ligand	3.1 (%)[b]	3.3 (%)[b]	ee of 3.3 (%)[c]	3.4 (%)[b]	3.5 (%)[b]
1	L1	13	3	nd	34	27
2	L2	15	20	-37	34	27
3	L3	29	24	-29	18	11
4	L4	0	26	31	28	28
5	L5	8	20	-33	20	27
6	L6	11	19	53	25	35
7	L7	20	9	36	18	24
8	L8	4	27	1	23	33
9	L9	16	5	nd	18	20
10	L10	33	22	5	16	14
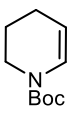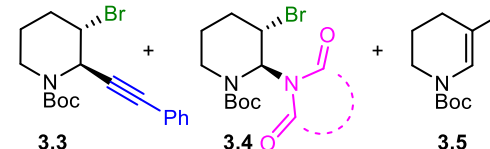
[a]Conditions: 3.1 (0.1 mmol, 1.0 equiv), CuI (0.010 mmol, 10 mol %), ligand (12 mol %), alkyne (0.12 mmol, 1.2 equiv), NEt$_3$ (0.20 mmol, 2.0 equiv), DBDMH (0.11 mmol, 1.1 equiv), THF (0.18M). [b]Determined by ^{1}H NMR analysis with 1,3,5-trimethoxybenzene as an internal standard. [c]Determined by HPLC analysis using a chiral stationary phase. Negative sign indicates the opposite enantiomer.
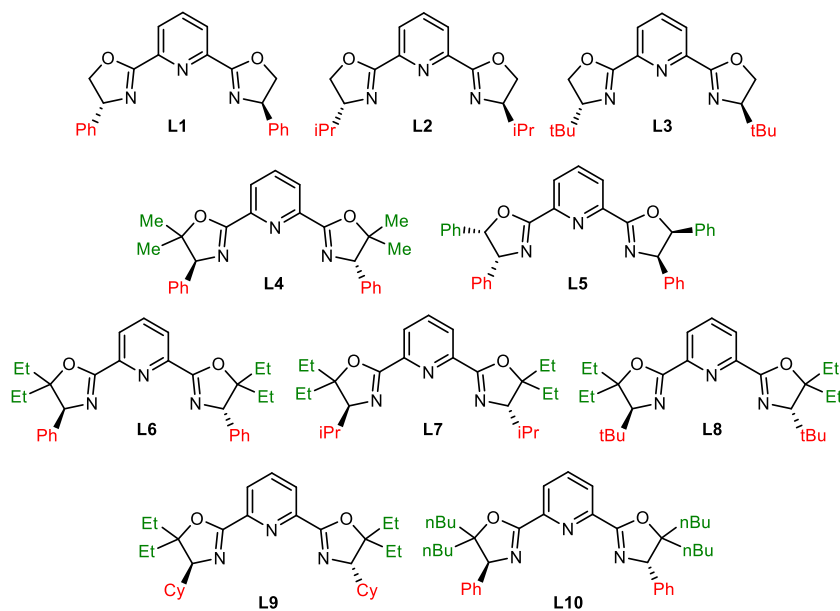
To investigate the ligands at a lower temperature, it was necessary to switch from dioxane to a similar ethereal solvent due to its low freezing point. Decreasing the

temperature to -20 °C with DME as the solvent resulted in 19% yield and 60% ee (entry 2, **Table 3.5**). When further decreasing the temperature to -50 °C, THF provided 25% product yield with 65% ee, which was the best result to date. Decreasing the temperature to -80 °C led primarily to adduct byproduct **3.4** and elimination byproduct **3.5** in all solvents.

Table 3.5 – Investigation of Ligand at -50 °C

entry	solvent	**3.1** (%)^b	**3.3** (%)^b	ee of **3.3** (%)^c	**3.4** (%)^b	**3.5** (%)^b
1	DME^d	6	19	60	32	31
2	THF	6	25	65	29	37
3	DME	7	22	63	37	36
4	2-MeTHF	24	11	51	14	11

^{a}Conditions: **3.1** (0.1 mmol, 1.0 equiv), CuI (0.010 mmol, 10 mol %), **L6** (12 mol %), alkyne (0.12 mmol, 1.2 equiv), NEt$_3$ (0.20 mmol, 2.0 equiv), DBDMH (0.11 mmol, 1.1 equiv), solvent (0.18M). ^{b}Determined by ^{1}H NMR analysis with 1,3,5-trimethoxybenzene as an internal standard. ^{c}Determined by HPLC analysis using a chiral stationary phase. ^{d}Run at -20 °C

Silver catalysis and silver acetylides were briefly explored, though unsuccessful in yielding the alkynylated product (**Table 3.6**). Silver acetylide was used in lieu of copper acetylide to circumvent the formation of the elimination byproduct, which is formed via base (entry 1). It was hypothesized that the elimination would not occur without base unless the acetylide is more basic than nucleophilic. This observation was not the case when silver acetylide was introduced into the

reaction, omitting copper(I) iodide, phenylacetylene, and triethylamine. These changes

led to the elimination byproduct regardless of the presence of copper or base (entry 1).

This observation could be attributed to the basicity of the silver acetylide, which could

also lead to elimination byproduct. It is also known that silver acetylides can be

formed *in situ* without base. However, when silver catalysts were introduced using

previously reported silver alkynylation conditions (entries 2 and 3), only adduct

formation was observed with no alkynylated product.[12, 13]

Table 3.6 – Investigation of Silver Catalysis

entry	conditions	3.1 (%)[b]	3.3 (%)[b]	ee of 3.3 (%)[c]	3.4 (%)[b]	3.5 (%)[b]
1	1.2 equiv Ag———Ph in THF	34	trace	nd	18	33
2	AgOTf (10 mol %) (R)-BINAP (5 mol %) in THF	0	0	nd	47	0
3	AgOAc (5 mol %) (R)-TRIP (10 mol %) in dioxane	0	0	nd	39	0

[a]Conditions: **3.1** (0.1 mmol, 1.0 equiv), [Ag] (0.010 mmol, 10 mol %), ligand (12 mol %), alkyne (0.12 mmol, 1.2 equiv), NEt$_3$ (0.20 mmol, 2.0 equiv), DBDMH (0.11 mmol, 1.1 equiv), solvent (0.18M). [b]Determined by ^{1}H NMR analysis with 1,3,5-trimethoxybenzene as an internal standard. [c]Determined by HPLC analysis using a chiral stationary phase.

Because enantioselectivity had only been observed at low yield, a time screen

was conducted to better understand whether this reaction was a dynamic kinetic

resolution or a kinetic resolution. In a dynamic kinetic resolution, the two enantiomers of the β-(bromo)-iminium intermediate would be able to interconvert. If the chiral catalyst differentiated between these enantiomeric intermediates well, all starting material could be funneled to product in high yield and high enantioselectivity (**Scheme 3.3**). In contrast, a kinetic resolution would result if the iminium enantiomers could not interconvert. In this case, the maximum ee and yield would depend on the selectivity factor (*s*) for the chiral cooper acetylide to react with one iminium enantiomer over the other. For high selectivity, the best result would be >99% ee at 50% yield. These two possibilities can theoretically be differentiated by whether the ee of product changes with increasing yield.

Scheme 3.3 – Kinetic Resolution versus Dynamic Kinetic Resolution
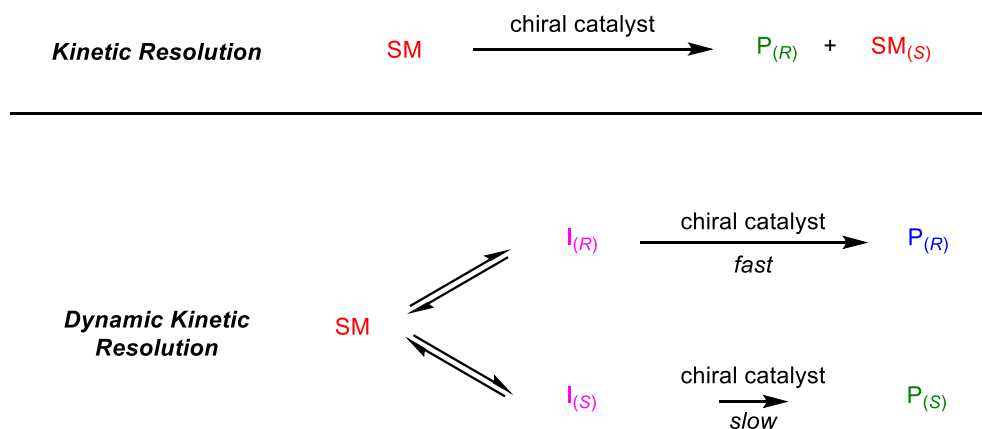
Identical reactions were set up and quenched at various time points (**Table 3.6**). It was to be expected that the yield of the product would increase, allowing us to see if ee changed with yield. However, this was not observed. The yield (and

121

enantioselectivity) was consistent regardless of reaction time. it is also of note that elimination and adduct formation were still seen. Although the conversion is low, the consistency in enantioselectivity suggests that this process is not likely to be a kinetic resolution. In an effort to achieve higher yield, the copper iodide and **L6** were used stoichiometrically, but this did not improve the product yield, and actually decreased the conversion of starting material.

Table 3.7 – Investigation of Reaction Time

entry	time (h)	3.1 (%)^b	3.3 (%)^b	ee of 3.3 (%)^c	3.4 (%)^b	3.5 (%)^b
1	2	52	11	65	18	14
2	4	44	8	64	19	21
3	6	53	13	57	20	16
4	22	27	17	64	16	33

^{a}Conditions: **3.1** (0.1 mmol, 1.0 equiv), CuI (0.010 mmol, 10 mol %), **L6** (12 mol %), alkyne (0.12 mmol, 1.2 equiv), NEt$_3$ (0.20 mmol, 2.0 equiv), DBDMH (0.11 mmol, 1.1 equiv), THF (0.18M). ^{b}Determined by ^{1}H NMR analysis with 1,3,5-trimethoxybenzene as an internal standard. ^{c}Determined by HPLC analysis using a chiral stationary phase.

Interestingly, it was noted that when preparing the reaction setup, a pre-stir of the reagents prior to cooling to -50 °C led to an increase of elimination and adduct formation without changing product yield or enantioselectivity. This observation suggested that side reactions would inevitably occur once DBDMH was added to the

mixture. Thus, I hypothesized that a solution of DBDMH in THF should be added dropwise to the reaction mixture once the vials have been removed from the glovebox and cooled to -50 °C. Indeed, this change in reaction setup led to 15% yield and 61% ee with 31% conversion, and trace amounts of elimination and adduct byproducts (entry 1, **Table 3.7**). Other halogenating reagents were investigated via this new reaction setup, wherein the halogen sources were dissolved in THF and added to the reaction mixture dropwise at -50 °C. Ultimately, other halide sources were not successful in improving the yield or ee (entries 2–5). It was noted that pyridinium tribromide (PTB) provided a yield of 10% with 17% ee (entry 2); if pyridine were to be generated judging from the relative pKa's of pyridine (5.25) and triethylamine (10.8) respectfully, then it is possible that pyridine could be coordinating with the copper catalyst in lieu of, or displacing, **L6**, which would substantially affect the ee.

Table 3.8 – Investigation of Halogen Sources and Order of Addition
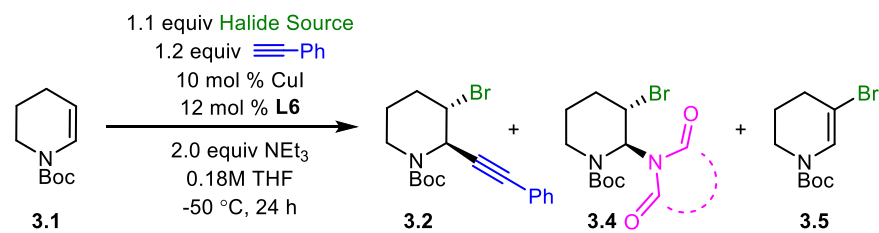
entry	halide source	RSM (%)^b	yield (%)^b	ee (%)^c	adduct (%)^b	VB (%)^b
1	DBDMH	69	15	61	8	trace
2	PTB	32	10	17	0	0
3	DEDBM	79	3	nd	0	0
4	NIS	61	5	nd	0	0
5	NBB	57	0	nd	0	0

^{a}Conditions: enecarbamate (0.1 mmol, 1.0 equiv), CuI (0.010 mmol, 10 mol %), **L6** (12 mol %), alkyne (0.12 mmol, 1.2 equiv), NEt$_3$ (0.20 mmol, 2.0 equiv), halide source (0.11 mmol, 1.1 equiv), THF (0.18M). ^{b}Determined by ^{1}H NMR analysis with 1,3,5-trimethoxybenzene as an internal standard. ^{c}Determined by chiral HPLC analysis.
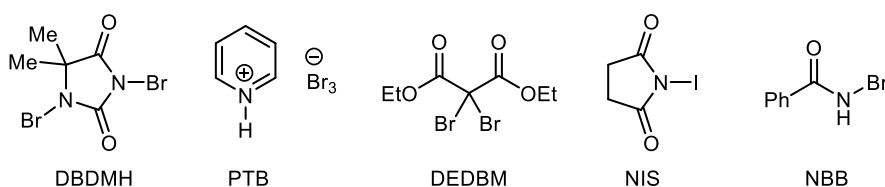
3.3 Conclusion

This chapter describes our efforts towards developing a novel method for enantio- and diastereoselective enamide difunctionalization. The best results to date involve copper(I) iodide in conjunction with PhPyBOX ligand, **L6**, which provides *tert*-butyl-trans-3-bromo-2-(phenylethynyl)piperidine-1-carboxylate (**3.3**) in 25% yield with 65% ee. Although it is still unclear whether this reaction proceeds through a dynamic kinetic resolution or a kinetic resolution, the discovery of the slow addition of a DBDMH solution after cooling the reaction mixture is a promising improvement

for minimizing the elimination and adduct products. Increasing conversion of starting material to alkynylation product is paramount. It is possible that other potential copper(I) catalysts could be helpful in improving the yield, as this parameter had not been investigated at the time of writing this thesis. It may also be of interest to explore alkene-alkene transfer reagents to potentially facilitate the halide reversibility.[14-16] Further studies are needed to improve the yield and enantioselectivity further. Ongoing studies towards this method are currently underway in the Mary Watson research lab.

3.4 Experimental

General Information

The enamide material **3.1** was synthesized according to the literature precedent.[17] The PyBOX ligand **L6**, and well as ligands **L1–L10** were synthesized according to the literature precedent using their corresponding amino alcohols.[7, 11] *N*-Bromobenzamide was synthesized according to the literature precedent.[18]

Enantioselective Difunctionalization of Enecarbamates
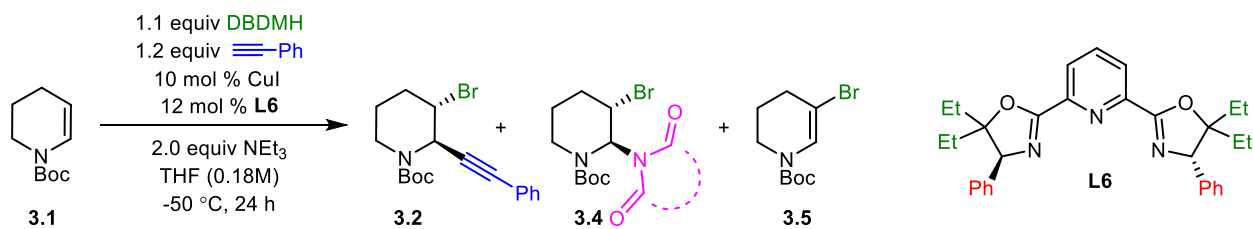
In a N$_2$-filled glovebox, CuI (0.010 mmol, 10 mol %) and **L6** (0.012 mmol, 12 mol %) were added to a 1-dram vial equipped with a micro stir bar. THF (200 µL) was added to the vial and the solution was stirred at room temperature for 30 minutes. In a second 1-dram vial, DBDMH was added and diluted with THF (356 µL). Phenylacetylene (0.13 mmol, 1.3 equiv) and triethylamine (0.20 mmol, 2.0 equiv) were added to the first vial and allowed to stir for 5 minutes. Enecarbamate **3.1** (0.10 mmol, 1.0 equiv) was then added to the first vial, which was capped with a Teflon-lined cap. Both vials were removed from the glovebox and the first vial was cooled to -50 °C for 5 minutes. The contents from the second vial were added dropwise to the first vial at -50 °C, which continued to stir at this temperature for 24 hours. The vial was then allowed to warm to room temperature and was diluted with Et$_2$O (2 mL). The solution was filtered through a pad of silica gel and washed with Et$_2$O (5 mL), then subsequently concentrated. 1-3-5-Trimethoxybenzene (TMB) was added to the vial as an internal standard to quantify the yield via ^{1}H NMR spectroscopy. The yield of **3.3** was determined to be 25% and the enantioselectivity (ee) was determined to be 65% ee. The sample was prepared via preparatory TLC plate and subjected to high-

throughput liquid chromatography (HPLC) using a chiral stationary phase column to obtain enantiomeric excess.

tert-Butyl-trans-3-bromo-2-(phenylethynyl)piperidine-1-carboxylate (3.3) was isolated via silica gel column chromatography to give **3.3** as a white solid. The spectral data matched those from compound **2.6**, which was discussed in Chapter 2. The enantiomeric excess was confirmed to be 65% ee (CHIRALPAK IE, 1 mL/min, 3% *i*-PrOH/hexane, l = 254 nm); t_R(major) = 11.78 min, t_R(minor) = 13.32 min).

tert-Butyl-2-(1,3-dibromo-5,5-dimethylhydantoin)-3-bromopiperidine-1-carboxylate (3.4) was also isolated via silica gel column chromatography to give **3.3** as a yellow oil:

^{1}H NMR (400 MHz, CDCl$_3$) δ 5.92 (d, *J* = 7.5 Hz, 1H), 5.65 (s, 1H), 4.72 – 4.63 (m, 1H), 4.02 (dd, *J* = 13.6, 7.2 Hz, 1H), 3.56 (ddd, *J* = 14.0, 12.2, 5.6 Hz, 1H), 2.37 – 2.27 (m, 1H), 2.08 – 1.90 (m, 2H), 1.80 – 1.72 (m, 1H), 1.43 (s, 15H).

[13]C (101 MHz, CDCl$_3$) δ 176.0, 155.0, 154.2, 81.2, 66.4, 58.4, 46.3, 38.6, 28.8, 28.3, 25.1, 21.3.

tert-Butyl 5-bromo-3,4-dihydropyridine-1(2H)-carboxylate (3.5) was also isolated via silica gel column chromatography to give **3.4.** The spectral data matched that which was previously reported in the literature.[19]

3.5 References

1.   Alix, A.; Lalli, C.; Retailleau, P.; Masson, G., Highly Enantioselective Electrophilic α-Bromination of Enecarbamates: Chiral Phosphoric Acid and Calcium Phosphate Salt Catalysts. *J. Am. Chem. Soc.* **2012,** *134* (25), 10389-10392.
2.   Dumoulin, A.; Lalli, C.; Retailleau, P.; Masson, G., Catalytic, highly enantioselective, direct amination of enecarbamates. *Chem. Commun.* **2015,** *51* (25), 5383-5386.
3.   Lebée, C.; Blanchard, F.; Masson, G., Highly Enantioselective Intermolecular Iodo- and Chloroamination of Enecarbamates Catalyzed by Chiral Phosphoric Acids or Calcium Phosphate Salts. *Synlett* **2016,** *27* (4), 559-563.
4.   Dumoulin, A.; Bernadat, G.; Masson, G., Enantioselective Three-Component Amination of Enecarbamates Enables the Synthesis of Structurally Complex Small Molecules. *J. Org. Chem.* **2017,** *82* (3), 1775-1789.
5.   Liu, J. X.; Dasgupta, S.; Watson, M. P., Enantioselective additions of copper acetylides to cyclic iminium and oxocarbenium ions. *Beilstein J. Org. Chem.* **2015,** *11*, 2696-2706.
6.   Dasgupta, S.; Liu, J.; Shoffler, C. A.; Yap, G. P. A.; Watson, M. P., Enantioselective, Copper-Catalyzed Alkynylation of Ketimines To Deliver Isoquinolines with alpha-Diaryl Tetrasubstituted Stereocenters. *Org. Lett.* **2016,** *18* (23), 6006-6009.
7.   Guan, W. Y.; Santana, S. O.; Liao, J. N.; Henninger, K.; Watson, M. P., Enantioselective Alkynylation of Unstabilized Cyclic Iminium Ions. *ACS. Catal.* **2020,** *10* (23), 13820-13824.
8.   Denmark Scott, E.; Burk Matthew, T., Lewis base catalysis of bromo- and iodolactonization, and cycloetherification. *Proc. Natl. Acad. Sci. U.S.A.* **2010,** *107* (48), 20655-20660.
9.   Brown, R. S.; Nagorski, R. W.; Bennet, A. J.; McClung, R. E. D.; Aarts, G. H. M.; Klobukowski, M.; McDonald, R.; Santarsiero, B. D., Stable Bromonium and Iodonium Ions of the Hindered Olefins Adamantylideneadamantane and Bicyclo[3.3.1]nonylidenebicyclo[3.3.1]nonane. X-Ray Structure, Transfer of Positive Halogens to Acceptor Olefins, and ab Initio Studies. *J. Am. Chem. Soc.* **1994,** *116* (6), 2448-2456.
10.   Beekan, P.; Fowler, F. F., N-Methyl-1,2,3,4-tetrahydropyridine. *J. Org. Chem.* **1980,** *45*, 1336-1338.
11.   Tse, M. K.; Bhor, S.; Klawonn, M.; Anilkumar, G.; Jiao, H.; Döbler, C.; Spannenberg, A.; Mägerlein, W.; Hugl, H.; Beller, M., Ruthenium-Catalyzed Asymmetric Epoxidation of Olefins Using H2O2, Part I: Synthesis of New Chiral N,N,N-Tridentate Pybox and Pyboxazine Ligands and Their Ruthenium Complexes. *Chem. Eur. J.* **2006,** *12* (7), 1855-1874.
12.   Su, Y.; Lu, M.; Dong, B.; Chen, H.; Shi, X., Silver-Catalyzed Alkyne Activation: The Surprising Ligand Effect. *Adv. Synth. Catal.* **2014,** *356* (4), 692-696.

13.   Ren, Y.-Y.; Wang, Y.-Q.; Liu, S., Asymmetric Alkynylation of Seven-Membered Cyclic Imines by Combining Chiral Phosphoric Acids and Ag(I) Catalysts: Synthesis of 11-Substituted-10,11-dihydrodibenzo[b,f][1,4]oxazepine Derivatives. *J. Org. Chem.* **2014,** *79* (23), 11759-11767.

14.   Denmark, S. E.; Kuester, W. E.; Burk, M. T., Catalytic, Asymmetric Halofunctionalization of Alkenes—A Critical Perspective. *Angew. Chem. Int. Ed.* **2012,** *51* (44), 10938-10953.

15.   Bock, J.; Daniliuc, C. G.; Hennecke, U., Stable Bromiranium Ion Salts as Reagents for Biomimetic Indole Terpenoid Cyclizations. *Org. Lett.* **2019,** *21* (6), 1704-1707.

16.   Neverov, A. A.; Brown, R. S., Br+ Transfer to reactive alkenes from the bromonium ion of adamantylideneadamantane. *Canadian Journal of Chemistry* **1994,** *72* (12), 2540-2543.

17.   Jurong Yu, V. T., Peter Riebel, Elizabeth Hierl, and Boguslaw Mudryk, One-pot Conversion of Lactam Carbamates to Cyclic Enecarbamates: Preparation of 1-tert-butoxycarbonyl-2,3-dihydropyrrole. *Org. Synth.* **2008,** *85* (64).

18.   Fujisaki, S.; Hamura, S.; Eguchi, H.; Nishida, A., Organic Synthesis Using Sodium Bromate. II. A Facile Synthesis of N-Bromo Imides and Amides Using Sodium Bromate and Hydrobromic Acid (or Sodium Bromide) in the Presence of Sulfuric Acid. *Bull. Chem. Soc. Jap.* **1993,** *66* (8), 2426-2428.

19.   Tereshchenko, O. D.; Perebiynis, M. Y.; Knysh, I. V.; Vasylets, O. V.; Sorochenko, A. A.; Slobodyanyuk, E. Y.; Rusanov, E. B.; Borysov, O. V.; Kolotilov, S. V.; Ryabukhin, S. V.; Volochnyuk, D. M., Electrochemical Scaled-up Synthesis of Cyclic Enecarbamates as Starting Materials for Medicinal Chemistry Relevant Building Bocks. *Adv. Synth. Catal.* **2020,** *362* (15), 3229-3242.

Chapter 4

KINETIC RESOLUTION OF BENZOISOXAZOLINES

4.1 Introduction

Alkynylations of various iminium ions have been developed; acyclic, unsaturated cyclic, and saturated cyclic substrates have all been successful under copper-catalyzed alkynylation conditions (**Figure 4.1**).[1-4] However, the majority of these methods rely on aldiminium ions, resulting in tertiary stereocenters. Only two reports disclose methods for ketiminium ions, resulting in formation of tetrasubstituted stereocenters. Maruoka reported an alkynylation to azomethine iminium ions using a copper(I) catalyst and Brønsted acid co-catalyst (**Scheme 4.1**, top).[5] Additionally, the Watson group developed an alkynylation to form tetrasubstituted stereocenters on isoquinoline and tetrahydroisoquinoline (THIQ) products (**Scheme 4.1**, bottom).[6]

Figure 4.1 – Alkynylations to Iminium and Ketiminium Ions

acyclic iminiums	tetrahydroisoquinoliums (THIQ)	quinoliums	pyridiniums	cyclic iminiums	ketiminiums
Li Knochel	Li Taylor/Schreiber Maruoka, Su Ma, Liu Watson	Arndtsen Aponick	Ma Arndtsen	Knochel Royer Wasa Watson	Maruoka Watson
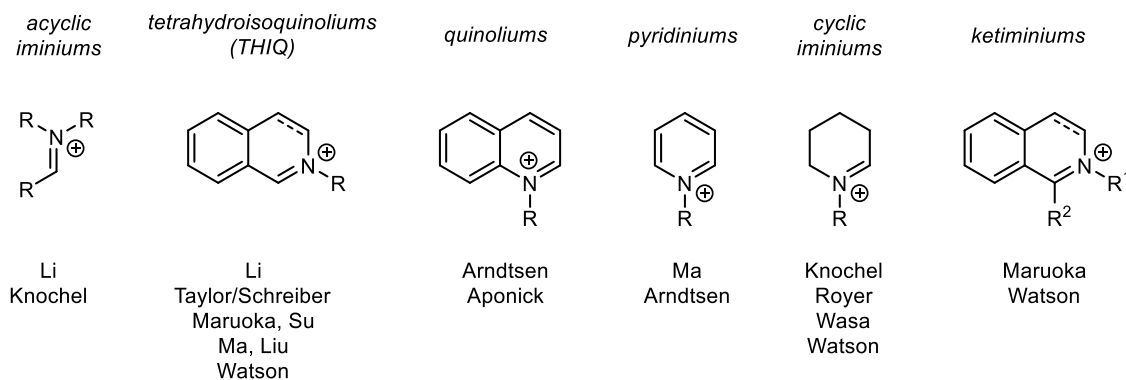
Scheme 4.1 – Maruoka's and Watson's Alkynylations to Ketiminium Ions

Maruoka

$\equiv\!-R^2$
CuOAc (5 mol %)
(R,R)-PhPyBOX (5.5 mol %)
(R)-**1** (6 mol %)

CH_2Cl_2, 0 °C, 48 hr

82 - 99% yield
43 - 96% ee

(R)-**1**

Watson

1.) $ClCO_2Me$
2.) $\equiv\!-R^1$
CuI (10 mol %)
PhPyBOX (12 mol %)

i-Pr_2NEt, $CHCl_3$
4 °C, 48 hr

38 - 93% yield
4 - 98% ee
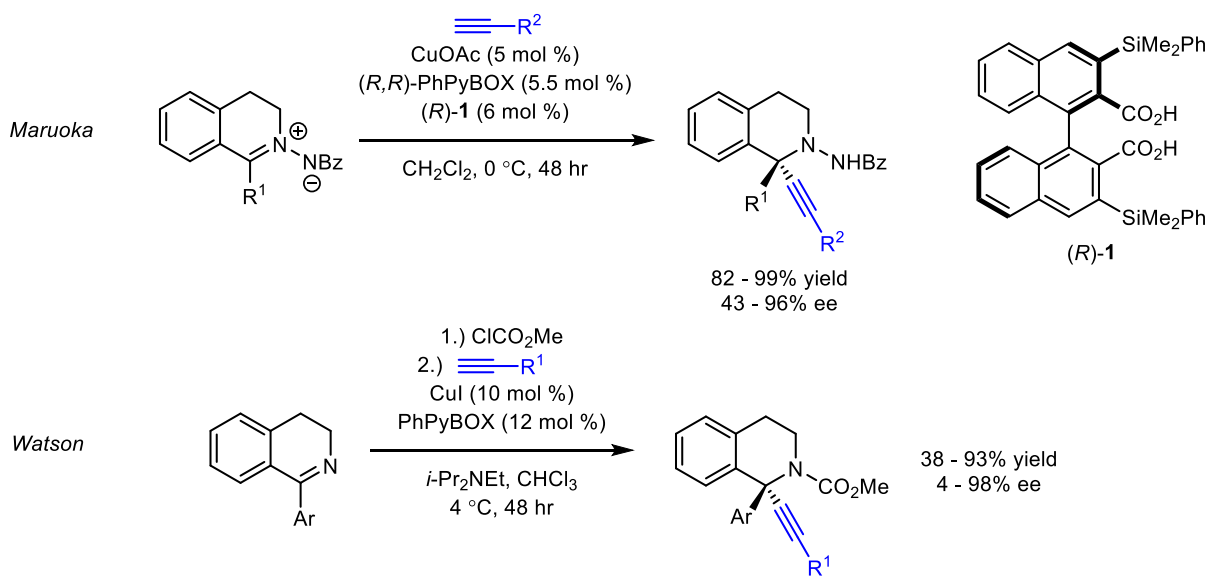
Our group sought to further push the boundaries of what is possible via alkynylations of iminium ions. We envisioned replacing the all-carbon bridge of the THIQ substrates with a removeable tether that could be cleaved after the alkynylation (**Figure 4.2**). This approach would result in an acyclic amine with an α,α-diaryl

tetrasubstituted stereocenter, which are challenging to synthesize in high enantiomeric purity by other methods.

Figure 4.2 – Pushing the Boundaries of Alkynylations to Ketiminium Ions

α,α–diaryl-
tetrasubstituted
amines
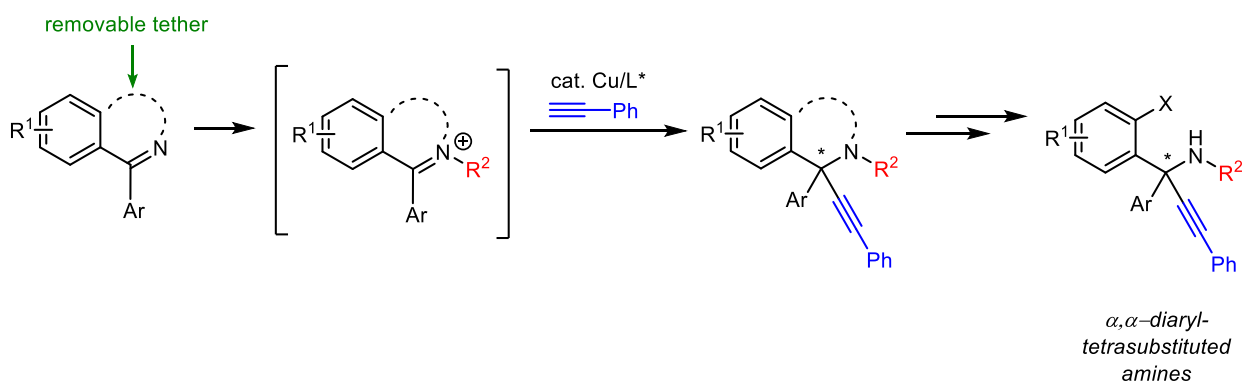
This method would be impactful, because amines with $α,α$-diaryl tetrasubstituted stereocenters are prevalent in pharmaceuticals and bear a varying range of bioactivities (**Figure 4.3**).[7] Our method would create a facile pathway towards these complicated molecules.

Figure 4.3 – Bioactive Amines with α,α-Diaryl Tetrasubstituted Stereocenters

BMS-795311 (BMS)
*Cholesteryl ester transfer
protein inhibitor*

Dizocilpine (Merck)
anticonvulsant/anesthetic

Nicotinamide Derivative (Pfizer)
allergy/respiratory treatment
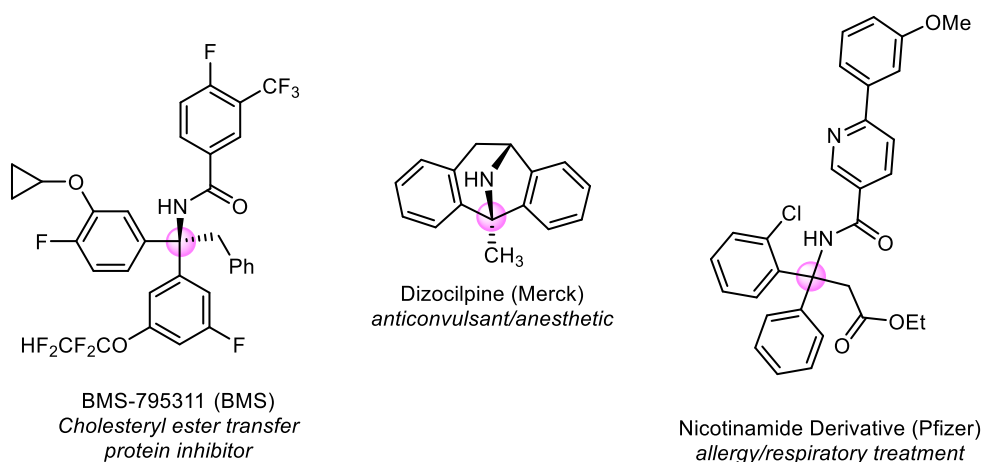
A previous lab member, Jennie Liao, discovered promising enantioselectivities with a benzoisoxazolium salt (**4.2**) and a copper(I)/PHOX catalyst, albeit with low yield. Because she only observed low yields, she explored the possibility that product **4.3** decomposes under the reaction conditions. To test this possibility, she synthesized the racemic product and subjected it to her best conditions to date (**Scheme 4.2**, top). She discovered that not only did the racemic product indeed decompose, but that the recovered starting material was highly enantioenriched (**Scheme 4.2**, bottom). This serendipitous result was indicative of a kinetic resolution process and was at the point where I started investigating this reaction.

Scheme 4.2 – Discovery of Kinetic Resolution through Alkynylation
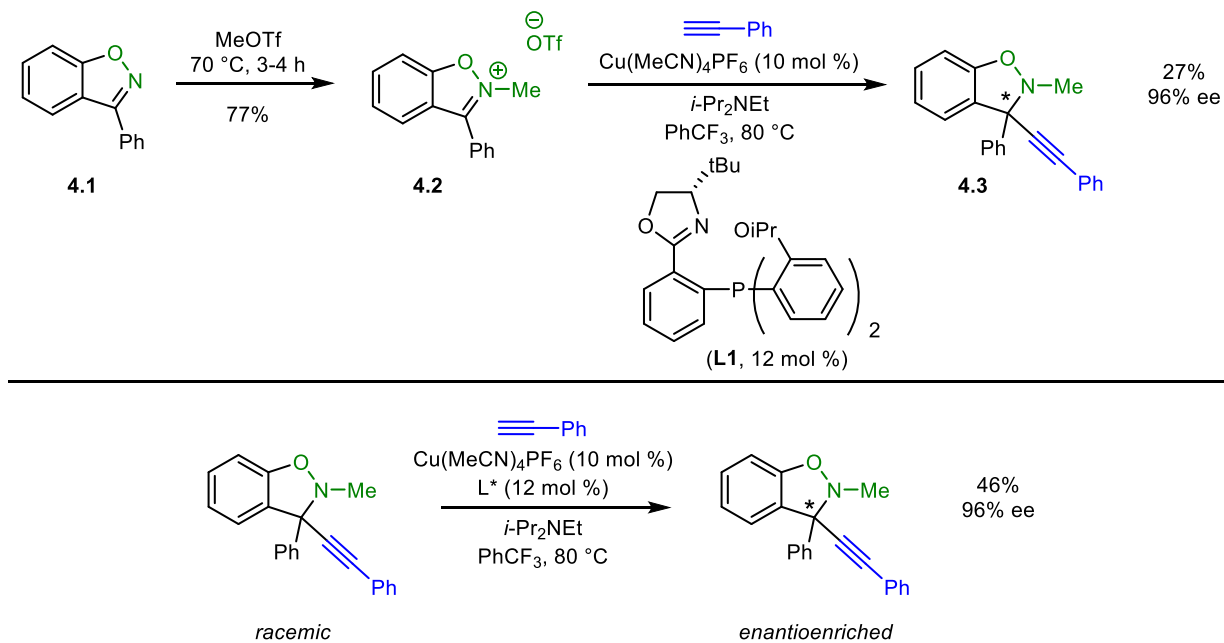
4.2   Results and Discussion

I first sought to determine if all the reaction components were necessary for the kinetic resolution to take place, because Jennie was initially investigating conditions to develop an alkynylation of benzisoxazolium triflate salts. Jennie's conditions for the kinetic resolution were as follows: 10 mol % tetrakisacetonitrilecopper(I) pentafluorophosphate, 12 mol % (*S*)-2-(2-(bis(2-isopropoxyphenyl)phosphaneyl)phenyl)-4-(*tert*-butyl)-4,5-dihydrooxazole **L1,** 1.2 equivalents of phenylacetylene, 1.5 equivalents of diisopropyl-N-ethyl amine, 1.0 equivalent of benzoisoxazoline (**4.3**), and trifluorotoluene (1.0M) at 80 °C for 24

hours. On a 0.1 mmol scale, I omitted each reagent of the model reaction to ascertain the impact of each reagent (**Table 4.1**).

Table 4.1 – Control Experiments for Required Reagents[a]

entry	perturbation	yield (%)[b]	ee (%)[c]
1	no change	46	96
2	no Cu	98	0
3	no ligand	quant.	0
4	no alkyne	<5	nd
5	no base	<5	nd
6	cat. base and alkyne	<5	nd

[a]Conditions: benzisoxazoline **4.3** (0.1 mmol, 1.0 equiv), Cu(MeCN)$_4$PF$_6$ (0.010 mmol, 10 mol %), **L1** (0.012 mmol, 12 mol %), alkyne (0.12 mmol, 1.2 equiv), *i*-Pr$_2$NEt (0.15 mmol, 1.5 equiv), trifluorotoluene (0.1M). [b]Determined by ^{1}H NMR analysis with 1,3,5-trimethoxybenzene as an internal standard. [c]Determined by HPLC analysis using a chiral stationary phase.

When the copper catalyst or PHOX ligand **L1** were excluded from the reaction, conversion was low and only racemic starting material (**4.3**) was recovered, i.e. no reaction had taken place. Interestingly, complete starting material decomposition was observed when alkyne or base were excluded from the reaction and led to an unidentifiable mixture. Initially the purpose of the alkyne and base was to synthesize a chiral copper(I) acetylide that would attack a benzisoxazolium salt. However, the starting material for this kinetic resolution process is a benzoisoxazoline substrate. It is

also of note that catalytic amounts of alkyne and base also led to decomposition of unidentifiable material, indicating that a stoichiometric amount of these reagents is necessary.

Because phenylacetylene was required for a successful kinetic resolution, I hypothesized that the acetylene identity might impact the yield and ee of recovered **4.3**. I explored a variety of acetylenes in lieu of phenylacetylene **4.4** and noticed a stark difference among the alkynes (**Scheme 4.3**). Phenylacetylenes with electron-donating groups, such 4-methoxyphenylacetylene (**4.5**) and napthyl-methoxyl (**4.7**) provided poor enantioselectivities compared to the model reaction. Phenylacetylenes with electron-withdrawing groups, such as 3,5-dimethoxyphenylacetylene (**4.9**) and 4-trifluoromethylphenylacetylene (**4.10**), provided comparable yields to phenylacetylene, but slightly lower enantioselectivities.

Scheme 4.3 – Alkyne as a Possible Optimization Handle[a]
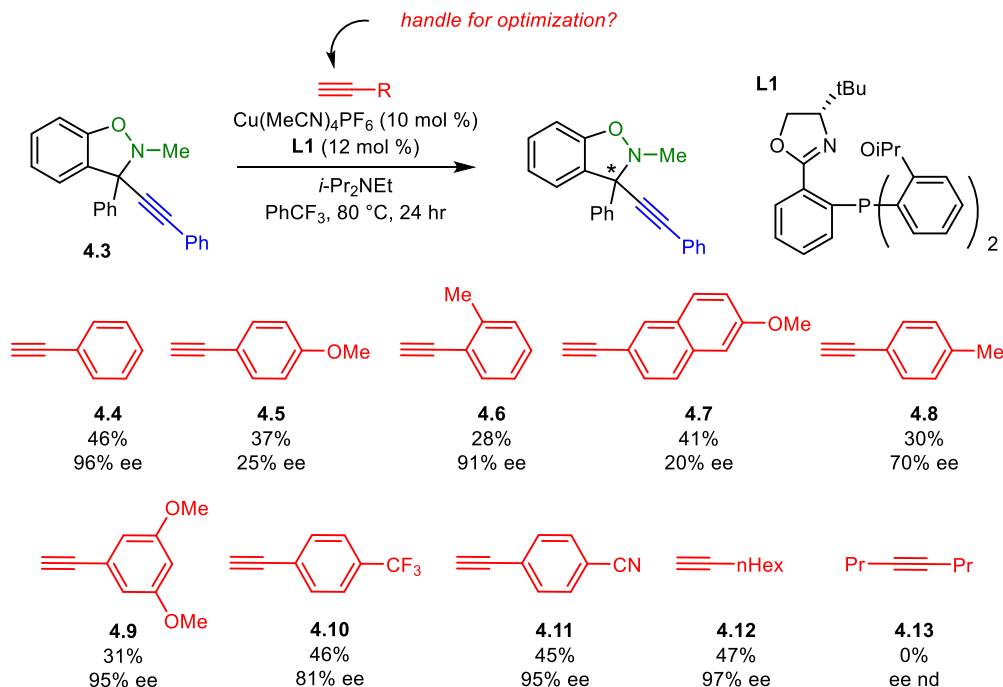
[a]Conditions: benzisoxazoline **4.3** (0.1 mmol, 1.0 equiv), Cu(MeCN)$_4$PF$_6$ (0.010 mmol, 10 mol %), **L1** (0.012 mmol, 12 mol %), alkyne (0.12 mmol, 1.2 equiv), i-Pr$_2$NEt (0.15 mmol, 1.5 equiv), trifluorotoluene (0.1M). Yields determined by ^{1}H NMR analysis with 1,3,5-trimethoxybenzene as an internal standard. ee's determined by HPLC analysis using a chiral stationary phase.

Inexplicably, 4-cyanophenylacetylene (**4.11**) and 1-octyne (**4.12**) provided both similar yield and enantioselectivity as phenylacetylene **4.4**, suggesting that very specific electronics for the alkyne substrate are required for this reaction to be successful. It is also of note that the use of internal alkyne, 4-octyne (**4.13**), resulted in complete decomposition of **4.3**, similar to when alkyne and base were omitted from the reaction (**Table 4.1**, entries 4–6). This finding suggests that a terminal alkyne is required.

The necessity of the alkyne and the specific electronics required for the alkyne have also brought into the question the mechanism of the reaction. Because this

process is a kinetic resolution, it is assumed that one enantiomer of the starting material reacts with the chiral catalyst much faster than the other enantiomer, but it was unclear what the other product was. Yao and coworkers reported that once benzoisoxazoline **4.14** was generated under their reaction conditions, increasing the temperature would induce a thermal rearrangement to benzoxazoline **4.15**, with the N–O bond cleaving in either a two-electron or radical-mediated process (**Scheme 4.4a**).[8]

Scheme 4.4 – Yao's Synthesis of Benzoisoxazolines from Oximes
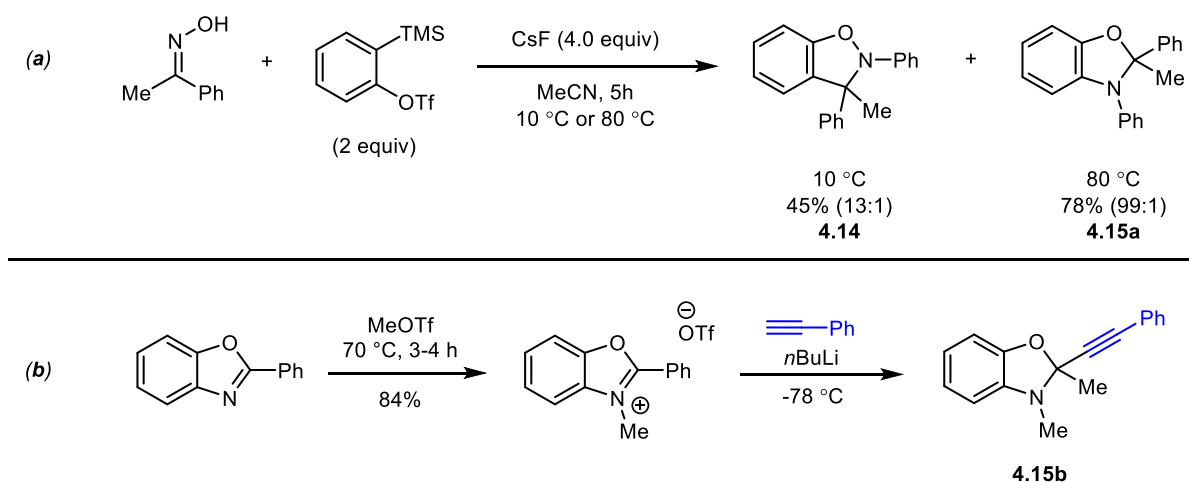
Although their conditions were different, I initially hypothesized that our copper(I) catalyst might induce an analogous N–O bond cleavage via single electron transfer step, leading to a similar benzoxazoline product (**4.15b**). To support this theory, I attempted to synthesize the proposed benzoxazoline from commercially available 2-phenylbenzoxazole. I first formed the benzoxazolium triflate salt and subjected the salt to alkynylation conditions using *n*-butyllithium and phenylacetylene (**Scheme 4.4b**). By ^{1}H NMR analysis of the crude reaction mixture, there appeared to

be desired product **4.15b**. However, no product was isolated after silica gel chromatography. A second attempt at the synthesis and purification was done, wherein a 2D TLC plate analysis of the crude reaction mixture suggested decomposition on silica gel. Synthesis and isolation of the resulting benzoxazoline product was ultimately unsuccessful, as the product rapidly decomposed under exposure to silica gel purification. Deactivation of the silica gel with triethylamine also led to rapid decomposition. The sensitivity and instability of the compound on silica gel led me to believe that it was unlikely to be the byproduct of the kinetic resolution, since the kinetic resolution work-up requires filtering of the crude mixture through a pad of silica gel, and the ^{1}H NMR spectrum of the mixture still shows byproduct peaks. It is also of note that the benzoxazoline formation would not help to rationalize the necessity of the additional alkyne and base. These key observations led me to hypothesize another pathway towards a different product. My second hypothesis was that alkyne substrate becomes incorporated into the byproduct through a copper-mediated N–O bond activation to form a benzoxazepine as shown in the scheme below (**Scheme 4.5**). Indeed, the peaks associated with the byproduct in both the NMR and LC/MS of the crude reaction mixtures are consistent with the structure of **4.16**. In addition, the byproduct was isolated from the reaction and characterization by ^{1}H NMR confirms this structure.

Based on the identity of the byproduct, I proposed a mechanism by which this byproduct is formed in the kinetic resolution (**Scheme 4.5**). Copper catalyst and PHOX ligand **L1** are pre-stirred and copper(I) acetylide is formed from

phenylacetylene and base. Benzoisoxazoline **4.3** is introduced, and one enantiomer undergoes a single electron transfer with the copper(I) acetylide to yield intermediate **Int-1** and copper(II). Oxidative addition occurs to give intermediate **Int-2**, and the anionic nitrogen atom attacks the alkyne to form **Int-3**. The step from **Int-2** to **Int-3** is likely to be the most probable factor in determining which enantiomer is decomposed. The vinylogous electrons are protonated, presumably from the conjugate acid of *i*-Pr$_2$NEt, to form **Int-4**, which undergoes reductive elimination to yield byproduct **4.16** and reform copper(I).

Scheme 4.5 – Plausible Byproduct for Kinetic Resolution of Benzoisoxazolines
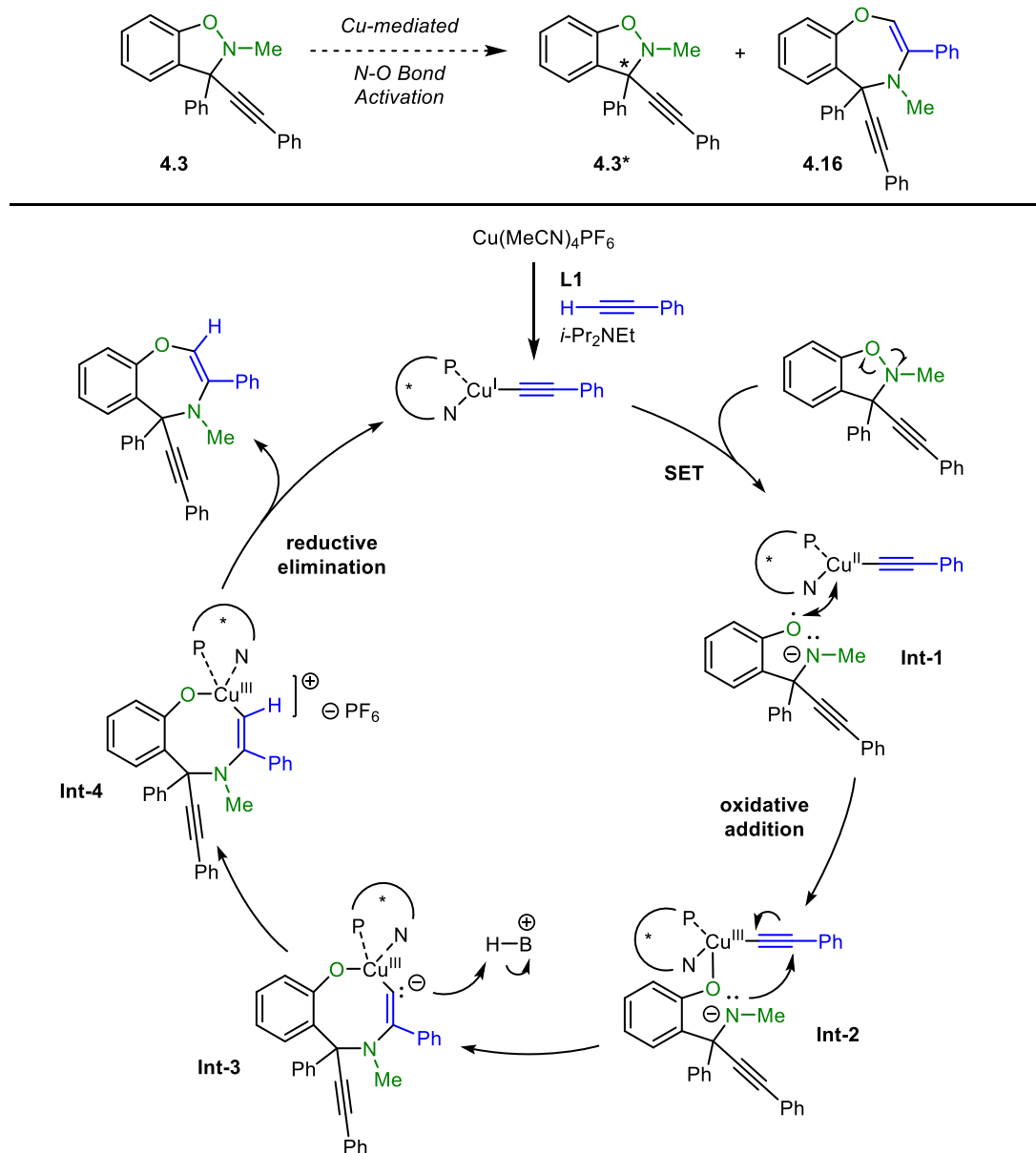
To investigate the efficacy of the kinetic resolution, I synthesized two benzoisoxazoline derivatives differing on the alkynyl portion and subjected them to

the reaction conditions (**Scheme 4.6**). I was pleased to see that both derivatives were successful in the reaction, providing high enantioselectivities and reasonable yield.

Scheme 4.6 – Preliminary Scope for the Kinetic Resolution[a]
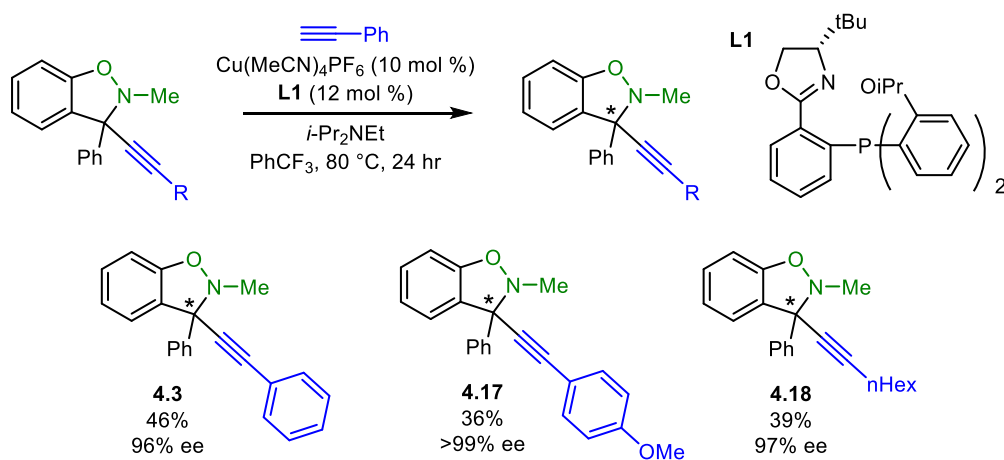
This observation led me to consider other derivatives of the model substrate with varying substitution on the benzisoxazole ring. Along with an incoming graduate student Alex, I synthesized a library of substrates. The most common method in which we synthesized these benzoisoxazolines is described in (**Scheme 4.7**); following a Grignard addition to 2-chlorobenzaldehydes, we performed an oxidation to yield the respective ketone. The oxime was then formed, and a cyclization via S$_N$Ar was induced to yield the benzisoxazole. We then ionized the nitrogen atom using methyl triflate to give the benzisoxazolium salt; to date, other substitutions on the nitrogen

142

atom have been unsuccessful, but this is an avenue that we wish to examine further once we establish our substrate scope and methodology. Finally, we can perform another addition reaction with a nucleophile (i.e. metal acetylide) to achieve the racemic benzoisoxazoline substrates.

Scheme 4.7 – General Procedure for Synthesizing Benzisoxazoline Substrates
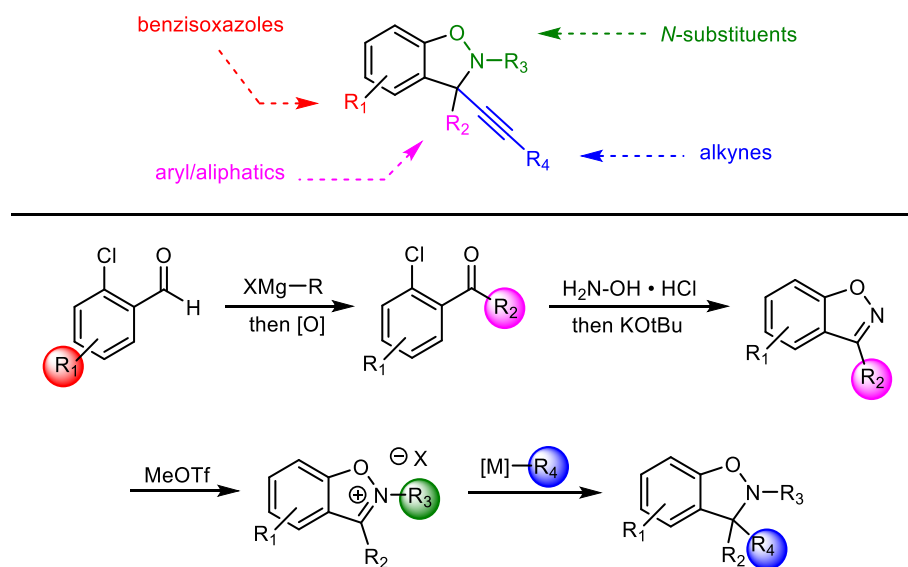
With benzoisoxazolines in hand, Alex and I investigated the efficacy of the kinetic resolution with varying substrate moieties. The first parameter we investigated was the alkyne substitution (**Scheme 4.8**). To date, the kinetic resolution of aryl alkynes with electron-neutral (**4.3, 4.8, 4.14**) and electron-donating groups (**4.7, 4.9**) proceed smoothly with high enantioselectivities and 28–55% yields. Substrates with electron-withdrawing groups (**4.10, 4.11**) exhibit significantly lower enantioselectivities. Replacing the alkyne with other functionalities provided unusual

143

results (**Scheme 4.9**). Introducing a cyanide (**4.16**) or an alkyl chain (**4.17**) at the stereocenter proved to be unsuccessful in inducing a kinetic resolution.

Scheme 4.8 – Investigation of Benzoisoxazolines (Aryl Alkynes)[a]

Scheme 4.9 – Investigation of Benzoisoxazolines (Non-Aryl Alkynes)[a]
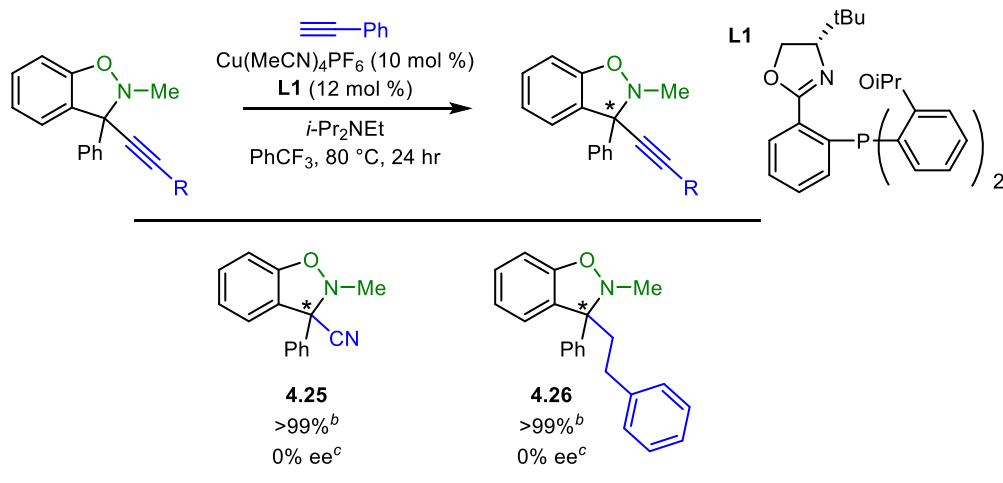
We also investigated functional groups at the tertiary stereocenter in lieu of the phenyl ring (**Scheme 4.10**). Interestingly, introducing an electron-withdrawing group on the phenyl ring, like a trifluoromethyl group (**4.27**) results in a substantial decrease in stereoselectivity, but it should be noted that 60% yield of **4.27** was recovered, indicating a slower resolution. Higher ee may be observed at higher conversion. Aliphatic rings (**4.28, 4.29**) also result in poor outcomes, via lack of reactivity and/or low enantioselectivities. It is noteworthy to mention that a cyclopropyl appendage results in 54% yield with 95% ee (**4.30**). This observation suggests that a carbon with π-character is more likely to provide better ee. The effects of substitution on the benzisoxazole ring are to be investigated in future scope studies.

145

Scheme 4.10 – Investigation of Benzoisoxazolines (Stereocenter Substitution)[a]
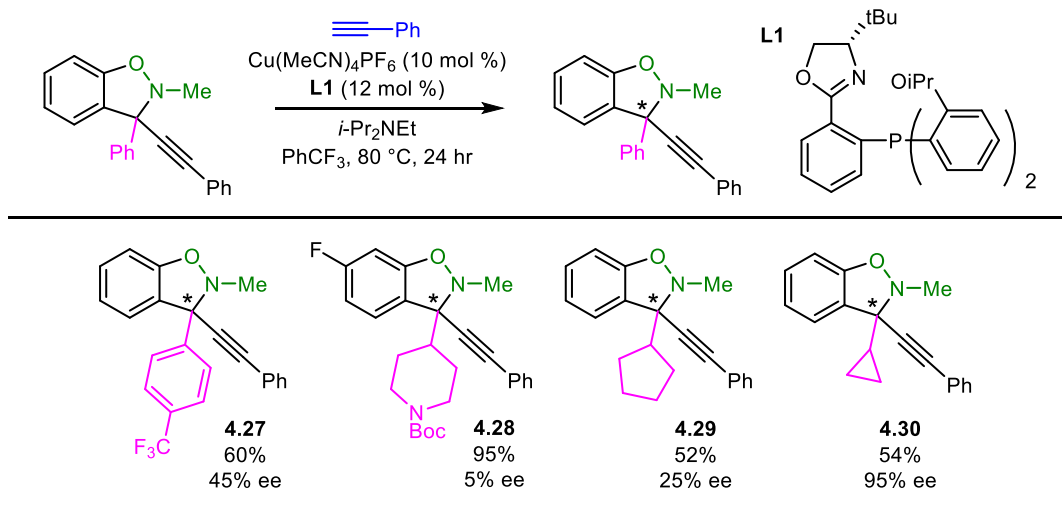
4.3 Conclusion

We have discovered a kinetic resolution of benzoisoxazolines utilizing a chiral copper(I) catalyst under mild conditions. We theorize that a copper-catalyzed N–O bond activation occurs preferentially with one enantiomer of benzoisoxazoline to provide a benzoxazepine (**4.16**), and the other enantiomer of starting material can then be recovered in high enantioselectivity. Notably, both products are useful, highlighting the utility of this method. Further investigations are needed to fully develop this reaction, including determining whether benzoxazepine **4.16** is enantioenriched, further studies of substrate scope, and mechanistic studies. Since 5-membered benzoisoxazolines and 7-membered benzoxazepines are an interesting and overlooked class of bioactive molecules, a novel enantioselective pathway towards these

substrates would be highly valuable, as there are no methods to our knowledge that accomplishes synthesis towards these classes of substrates.

4.4   Experimental

General Information

The non-commercial PHOX ligand **L1** was synthesized according to the previously reported literature precedent.[9]
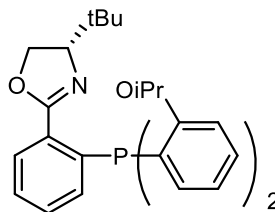
(*S*)-2-(2-(Bis(2-isopropoxyphenyl)phosphaneyl)phenyl)-4-(*tert*-butyl)-4,5-dihydrooxazole (L1).

^{1}H NMR (400 MHz, CDCl$_3$) δ 7.88 (ddd, *J* = 7.7, 3.7, 1.4 Hz, 1H), 7.33 (td, *J* = 7.5, 1.4 Hz, 1H), 7.25 – 7.19 (m, 3H), 7.06 (ddd, *J* = 7.8, 3.4, 1.3 Hz, 1H), 6.85 – 6.75 (m, 6H), 4.46 (dp, *J* = 12.2, 6.1 Hz, 2H), 4.15 – 4.02 (m, 2H), 3.95 (dd, *J* = 10.2, 7.7 Hz, 1H), 1.61 – 1.54 (m, 1H), 1.14 – 1.05 (m, 9H), 1.00 – 0.90 (m, 3H), 0.75 (s, 9H).

^{13}C NMR (101 MHz, CDCl$_3$) δ 159.5, 159.4, 134.7, 134.3, 129.7, 129.3, 129.28, 129.24, 129.1, 127.5, 120.2, 120.0, 111.3, 70.1, 69.6, 68.4, 33.8, 25.8, 21.86, 21.83, 21.5.

^{31}P NMR (162 MHz, CDCl$_3$) δ –24.43.

General Procedure A: Kinetic Resolution of Benzoisoxazolines
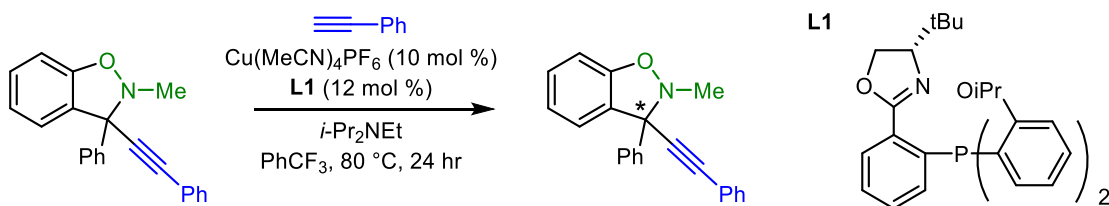
In a N$_2$-filled glovebox, tetrakis(acetonitrile)copper(I) hexafluorophosphate (0.010 mmol, 10 mol %) and ligand (0.012 mmol, 12 mol %) were added to a 1-dram vial equipped with a micro stir bar. Trifluorotoluene (200 µL) was added to the vial and the solution was stirred at room temperature for an hour. The solution was further diluted with trifluorotoluene (800 µL) and alkyne (0.12 mmol, 1.2 equiv), diisopropyl-N-ethylamine (0.15 mmol, 1.5 equiv), and benzoisoxazoline (0.10 mmol, 1.0 equiv) were added to the vial. The vial was then sealed with a Telfon-lined cap and removed from the glovebox. The vial was placed on a heating block at 80 °C the solution was stirred at this temperature for 24 hours. The vial was cooled to room temperature and diluted with Et$_2$O (1 x 2 mL), then filtered through a pad of silica gel which was rinsed with Et$_2$O (1 x 5 mL). The solution was concentrated in vacuo and 1-3-5-trimethoxybenzene (TMB) was added as an internal standard. The yield was determined via ^{1}H NMR analysis. The enantioselectivity (ee) was determined via high-pressure liquid chromatography (HPLC) using a chiral stationary phase column.
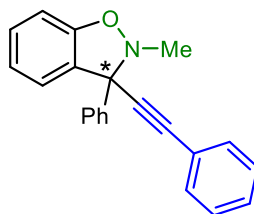
2-Methyl-3-phenyl-3-(phenylethynyl)-2,3-dihydrobenzo[*d*]isoxazoline (4.3).
Prepared via General Procedure A on a 0.1 mmol scale to give **4.3** (46%, 96% ee). The enantiomeric excess was determined by chiral HPLC analysis (CHIRALPAK IC, 0.5 mL/min, 0.3% *i*-PrOH/hexane, l = 254 nm); t_R(major) = 19.49 min, t_R(minor) = 22.04 min).
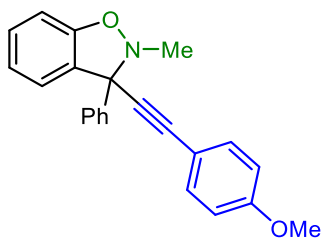
2-Methyl-3-phenyl-3-(4-methoxyphenylethynyl)-2,3-dihydrobenzo[*d*]isoxazoline (4.17). Prepared via General Procedure A on a 0.1 mmol scale to give **4.17** (36%, >99% ee). The enantiomeric excess was determined by chiral SFC analysis (CHIRALCEL OJ-3, 2.5 mL/min, 5% MeOH); t_R(major) = 3.60 min, t_R(minor) = 3.87 min).
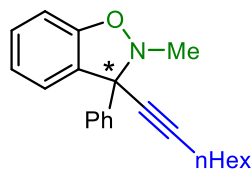
2-Methyl-3-phenyl-3-(octynyl)-2,3-dihydrobenzo[*d*]isoxazoline (4.18). Prepared via General Procedure A on a 0.1 mmol scale to give **4.18** (39%, 97% ee). The enantiomeric excess was determined by chiral HPLC analysis (CHIRALCEL OJ-H, 0.2 mL/min, 5% *i*-PrOH/hexane, l = 254 nm); t_R(major) = 23.24 min, t_R(minor) = 25.38 min).
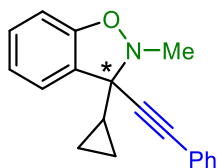
Methyl-3-cyclopropyl-3-(phenylethynyl)-2,3-dihydrobenzo[*d*]isoxazoline (4.30). Prepared via General Procedure A on a 0.1 mmol scale to give **4.30** (54%, 95% ee). The enantiomeric excess was determined by chiral SFC analysis (CHIRALCEL OJ-3, 2.5 mL/min, 5% MeOH); t_R(major) = 4.70 min, t_R(minor) = 7.41 min).

General Procedure B: Alkynylation of Benzisoxazolium Salts
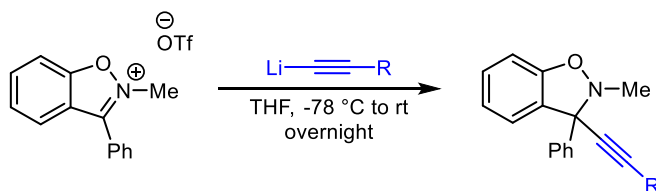
Terminal alkyne (1.5 equiv) was added to an oven-dried round-bottomed flask and diluted with anhydrous THF (0.3 M), then cooled to -78 C. nBuLi (2.5 M in hexanes, 1.7 equiv) was added dropwise to the flask and the solution stirred at this temperature to 1 hour. Benzisoxazolium salt (1.0 equiv) was added to another oven-dried round-bottomed flask and dissolved in anhydrous THF (0.3 M), then cooled to -78 °C. The solution of lithium acetylide was added dropwise to the second flask, which was allowed to warm to room temperature and stir overnight. The reaction was quenched with H_2O and added to a separatory funnel. The aqueous layer was extracted with CH_2Cl_2 (3 x 20 mL), and the organic layers were washed with brine and dried over $MgSO_4$. The solution was filtered through a cotton plug and concentrated in vacuo. The crude reside was purified via silica gel chromatography to yield racemic benzoisoxazoline.
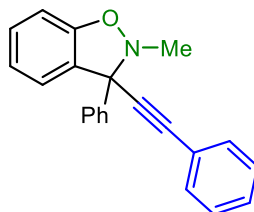
2-Methyl-3-phenyl-3-(phenylethynyl)-2,3-dihydrobenzo[*d*]isoxazoline (4.3).
Prepared via General Procedure B on a 0.662 mmol scale to give **4.3** (170 mg, 83%) as an off-white solid. The enantiomeric excess was determined by chiral HPLC analysis (CHIRALPAK IC, 0.5 mL/min, 0.3% *i*-PrOH/hexane, l = 254 nm); t_R(major) = 19.49 min, t_R(minor) = 22.04 min).

¹H (400 MHz, CDCl₃) δ 7.82 – 7.74 (m, 2H), 7.51 – 7.48 (m, 2H), 7.43 – 7.31 (m, 6H), 7.23 (td, J = 7.8, 1.4 Hz, 1H), 7.03 (d, J = 7.6, 1.3 Hz, 1H), 6.93 (t, J = 7.5 Hz, 1H), 6.87 (d, J = 8.0 Hz, 1H), 3.04 (s, 3H).

¹³C (101 MHz, CDCl₃) δ 155.9, 139.7, 132.7, 132.1, 131.7, 129.0, 128.7, 128.4, 128.3, 128.1, 123.6, 122.3, 121.8, 108.0, 93.3, 84.3, 73.3, 39.8.
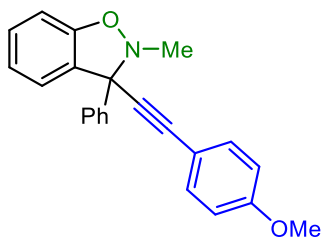
2-Methyl-3-phenyl-3-(4-methoxyphenylethynyl)-2,3-dihydrobenzo[*d*]isoxazoline (4.17). Prepared via General Procedure B on a 1.46 mmol scale to give **4.17** (353 mg, 70%) as a yellow oil: The enantiomeric excess was determined by chiral SFC analysis (CHIRALCEL OJ-3, 2.5 mL/min, 5% MeOH); t_R(major) = 3.60 min, t_R(minor) = 3.87 min).

¹H (400 MHz, CDCl₃) δ 7.81 – 7.74 (m, 2H), 7.44 – 7.35 (m, 5H), 7.22 (td, J = 8.1, 7.4, 1.4 Hz, 1H), 7.02 (d, J = 7.5, 1.4 Hz, 1H), 6.93 (td, J = 7.5, 1.0 Hz, 1H), 6.88 – 6.83 (m, 3H), 3.81 (s, 3H), 3.02 (s, 3H).

¹³C (101 MHz, CDCl₃) δ 159.8, 155.9, 139.9, 133.2, 132.8, 128.9, 128.4, 128.2, 128.1, 123.6, 121.7, 114.4, 113.9, 108.0, 82.9, 73.4, 55.3, 39.8.
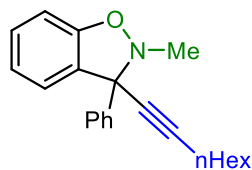
2-Methyl-3-phenyl-3-(octynyl)-2,3-dihydrobenzo[*d*]isoxazoline (4.18). Prepared via General Procedure B on a 1.56 mmol scale to give **4.18** (431 mg, 86%) as a yellow oil: The enantiomeric excess was determined by chiral HPLC analysis (CHIRALCEL OJ-H, 0.2 mL/min, 5% *i*-PrOH/hexane, l = 254 nm); t_R(major) = 23.24 min, t_R(minor) = 25.38 min).

^{1}H (400 MHz, CDCl$_3$) δ 7.73 – 7.66 (m, 2H), 7.38 – 7.31 (m, 3H), 7.22 – 7.17 (m, 1H), 6.98 – 6.93 (m, 1H), 6.90 (td, *J* = 7.4, 1.0 Hz, 1H), 6.83 (d, *J* = 8.0, 0.8 Hz, 1H), 2.93 (s, 3H), 2.34 (t, *J* = 7.1 Hz, 2H), 1.60 – 1.53 (m, 2H), 1.44 – 1.37 (m, 2H), 1.31 – 1.26 (m, 4H), 0.90 – 0.84 (m, 3H).

^{13}C (101 MHz, CDCl$_3$) δ 155.8, 133.3, 129.0, 128.7, 128.2, 128.1, 128.0, 123.4, 121.6, 107.9, 73.0, 39.7, 31.2, 28.6, 28.5, 22.5, 19.0, 14.1, 14.0.
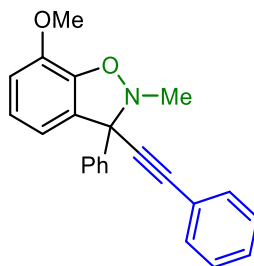
2-Methyl-3-phenyl-3-(phenylethynyl)-8-methoxy-2,3-dihydrobenzo[*d*]isoxazoline (4.31). Prepared via General Procedure B on a 2.05 mmol scale to give **4.31** (713 mg, quantitative) as an orange oil:

^{1}H (400 MHz, CDCl$_3$) δ 7.83 – 7.76 (m, 2H), 7.51 – 7.48 (m, 2H), 7.43 – 7.30 (m, 7H), 6.91 – 6.85 (m, 1H), 6.84 – 6.79 (m, 1H), 6.62 (d, *J* = 7.5, 1.2 Hz, 1H), 3.93 (s, 3H), 3.07 (s, 3H).

^{13}C (101 MHz, CDCl$_3$) δ 144.7, 143.2, 133.8, 132.1, 131.7, 128.8, 128.7, 128.5, 128.32, 128.30, 128.1, 122.5, 122.3, 115.5, 111.9, 83.6, 73.8, 56.1, 39.8.
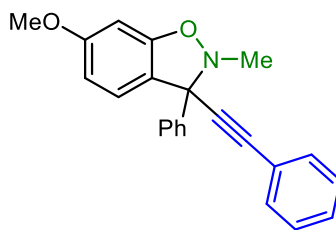
2-Methyl-3-phenyl-3-(phenylethynyl)-7-methoxy-2,3-dihydrobenzo[*d*]isoxazoline (4.32). Prepared via General Procedure B on a 0.96 mmol scale to give **4.32** (329 mg, quantitative) as a yellow oil:

154

^{1}H (400 MHz, CDCl$_3$) δ 7.81 – 7.73 (m, 2H), 7.51 – 7.48 (m, 2H), 7.41 – 7.32 (m, 6H), 6.90 (d, *J* = 8.3 Hz, 1H), 6.48 (dd, *J* = 8.3, 2.3 Hz, 1H), 6.44 (d, *J* = 2.2 Hz, 1H), 3.79 (s, 3H), 3.02 (s, 3H).

^{13}C (101 MHz, CDCl$_3$) δ 161.0, 157.2, 132.5, 132.1, 131.7, 128.8, 128.6, 128.4, 128.3, 128.0, 124.9, 123.9, 122.4, 122.0, 107.6, 94.3, 83.6, 73.1, 40.0.i
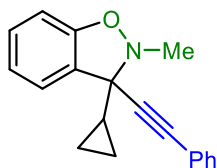
2-Methyl-3-cyclopropyl-3-(phenylethynyl)-2,3-dihydrobenzo[*d*]isoxazoline (4.30).

Prepared via General Procedure B on a 2.17 mmol scale to give **4.30** (559 mg, 93%) as a yellow oil. (CHIRALCEL OJ-3, 2.5 mL/min, 5% MeOH); t$_R$(major) = 4.70 min, t$_R$(minor) = 7.41 min).

^{1}H (400 MHz, CDCl$_3$) δ 7.36 – 7.14 (m, 7H), 6.93 (t, *J* = 7.4 Hz, 1H), 6.77 (d, *J* = 8.0 Hz, 1H), 3.03 (s, 3H), 1.46 – 1.32 (m, 1H), 0.77 – 0.48 (m, 4H).

^{13}C (101 MHz, CDCl$_3$) δ 155.6, 131.7, 131.5, 128.9, 128.6, 128.2, 123.1, 122.1, 121.4, 108.1, 82.5, 71.7, 65.8, 41.5, 17.9, 0.78.

General Procedure C: Methylation of Benzisoxazoles
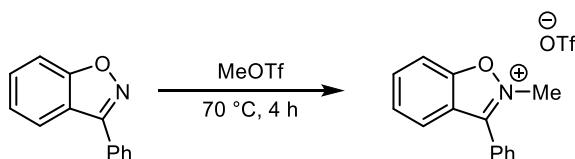
Methylation was adapted from the previously reported literature precedent[10].

Benzisoxazole (1.0 equiv) was added to an oven-dried round-bottomed flask and dissolved in anhydrous CH_2Cl_2 (10.0 M). Methyl triflate (1.5 equiv) was added dropwise to the flask and the solution was left to stir at room temperature for up to 24 hours. The solution was diluted with Et_2O upon which a precipitate formed. This solution was stirred for 5 minutes and filtered through a fritted funnel. The solid precipitate was dried over vacuum for 10 minutes to yield benzisoxazolium salt.
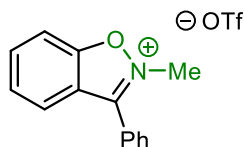
2-Methyl-3-phenylbenzo[*d*]isoxazol-2-ium   trifluoromethanesulfonate   (4.2). Prepared via General Procedure C on a 2.56 mmol scale to give **4.2** (850 mg, 92%) as a white powder:

^{1}H (600 MHz, DMSO-d$_6$) δ 8.26 – 8.22 (m, 2H), 8.20 (d, J = 0.4 Hz, 1H), 8.04 – 7.99 (m, 2H), 7.94 – 7.88 (m, 1H), 7.87 – 7.80 (m, 3H), 4.52 (s, 3H).
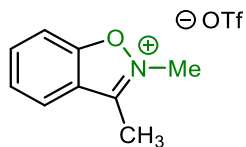
2-Methyl-3-methylbenzo[*d*]isoxazol-2-ium   trifluoromethanesulfonate   (4.33).
Prepared via General Procedure C on a 6.01 mmol scale to give **4.33** (1.64 g, 92%) as
a brown solid:

^{1}H (400 MHz, DMSO-d$_6$) δ 7.68 – 7.62 (m, 1H), 7.59 – 7.50 (m, 3H), 3.46 (s, 3H),
2.32 (d, *J* = 1.6 Hz, 3H).
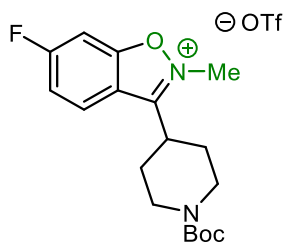
2-Methyl-3-(tert-butyl-piperidine   carboxylate)-7-fluoro-benzo[*d*]isoxazol-2-ium
trifluoromethanesulfonate (4.34). Prepared via General Procedure C on a 0.30 mmol
scale to give **4.34** (137 mg, 94%) as a white power:

^{1}H (400 MHz, DMSO-d$_6$) δ 7.14 – 6.81 (m, 3H), 3.12 (s, 3H), 2.19 (s, 9H), 1.68 – 1.52
(m, 2H), 1.15 – 1.08 (m, 4H), 0.92 – 0.79 (m, 3H).
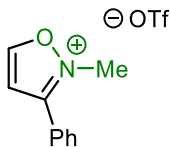
2-methyl-3-phenylisoxazolium trifluoromethanesulfonate (4.35). Prepared via General Procedure C on a 4.85 mmol scale to give **4.35** (1.32 g, 88%) as an off-white powder. The spectral data matched that which was previously reported in the literature.[11]

General Procedure D: Synthesis of Benzisoxazoles from Ketones
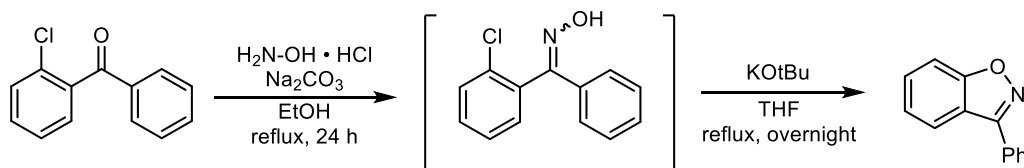
This synthetic route was previously reported in the literature.[12] To an oven-dried round-bottomed flask was added 2-chlorobenzophenone (1.0 equiv), hydroxylamine hydrochloride (3.0 equiv), and sodium carbonate (3.0 equiv). The solids were dissolved in ethanol (0.4M) and heated to reflux (90 °C), which was vigorously stirred for 24 hours. The solution was cooled to room temperature and H_2O was added. The solution was added to a separatory funnel and the aqueous layer was extracted with EtOAc (3 x 20 mL). The organic layers were washed with brine and dried over Na_2SO_4. The solution was filtered through a cotton plug and concentrated in vacuo. The crude oxime was added to a new oven-dried round-bottomed flask along

with KOtBu (2.0 equiv). The solids were dissolved in anhydrous THF (0.15 M) and heated to reflux (66 °C), which stirred overnight. The solution was cooled to room temperature and H_2O was added to the flask. The solution was added to a separatory funnel and the aqueous layer was extracted with EtOAc (3 x 30 mL). The organic layers were washed with brine and dried over Na_2SO_4. The solution was filtered through a cotton plug and concentrated in vacuo to give a crude red oil. The residue was purified via silica gel column chromatography to yield benzisoxazole.
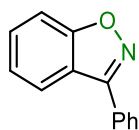
3-Phenylbenzo[*d*]isoxazole (4.1). Prepared via General Procedure D on a 9.23 mmol scale to give **4.1** (1.19 g, 66%) as a pale-yellow solid. The spectral data matched that which was reported in the literature.[12]
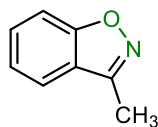
3-Methylbenzo[*d*]isoxazole (4.36). Prepared via General Procedure D on a 15.02 mmol scale to give **4.36** (1.50 g, 75%) as a white powder. The spectral data matched that which was reported in the literature.[13, 14]

^{1}H (600 MHz, CDCl$_3$) δ 7.34 – 7.32 (m, 1H), 7.26 – 7.19 (m, 3H), 2.20 (s, 3H).

General Procedure E: Synthesis of Alcohols with Aryl Grignard Reagents
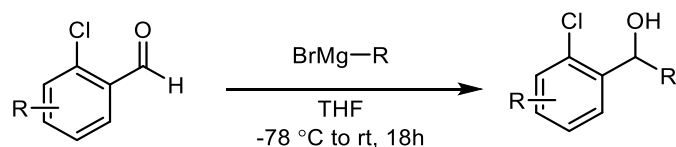
This synthesis was adapted from a previously reported literature precedent[15]. To an oven-dried round-bottomed flask was added 2-chlorobenzaldehyde (1.0 equiv) and diluted with anhydrous THF (0.3 M). The flask was cooled to 0 °C with an ice water bath. Aryl Grignard (1.5 equiv) was added dropwise to the flask, which was then allowed to warm to room temperature. The reaction was left to stir at this temperature for up to 2 hours, after which 2 M aqueous HCl solution was added to quench the reaction. The solution was added to a separatory funnel and the aqueous layers were extracted with EtOAc (3 x 20 mL). The organic layers were washed with 1 M HCl solution (1 x 20 mL) and brine, then dried over MgSO$_4$. The solution was filtered through a cotton plug and concentrated in vacuo to give the crude alcohol, which was used without further purification.
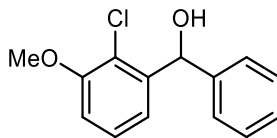
(2-chloro-3-methoxyphenyl)(phenyl)methanol   (4.37).   Prepared   via   General
Procedure E on an 8.0 mmol scale to give **4.37** (1.87 g, 94%) as an orange oil. The
spectral data matched that which was previously reported in the literature.[15]
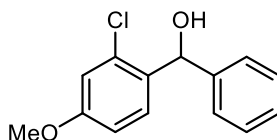
(2-chloro-4-methoxyphenyl)(phenyl)methanol   (4.38).   Prepared   via   General
Procedure E on an 8.0 mmol scale to give **4.38** (2.10 g, quantitative) as an orange oil.
The spectral data matches that which was previously reported in the literature.[15]
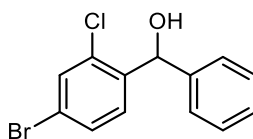
(2-chloro-4-bromophenyl)(phenyl)methanol (4.39). Prepared via General Procedure
E on a 6.72 mmol scale to give **4.39** (2.15 g, quantitative) as an orange oil:

[1]H (600 MHz, CDCl$_3$) δ 7.53 (d, J = 8.3 Hz, 1H), 7.51 (d, J = 2.0 Hz, 1H), 7.44 (dd, J
= 8.4, 2.0 Hz, 1H), 7.37 – 7.32 (m, 4H), 7.31 – 7.27 (m, 1H), 6.15 (s, 1H), 2.22 (bs,
1H).
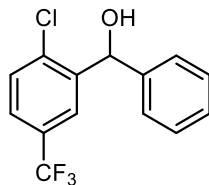
(2-chloro-5-trifluoromethylphenyl)(phenyl)methanol (4.40). Prepared via General

Procedure E on a 6.98 mmol scale to give **4.40** (2.14 g, quantitative) as an orange oil.

^{1}H (600 MHz, CDCl$_3$) δ 8.03 (d, 1H), 7.50 – 7.48 (m, 1H), 7.46 – 7.44 (m, 1H), 7.38 –

7.34 (m, 4H), 7.32 – 7.28 (m, 1H), 6.21 (s, 1H), 2.29 (s, 1H).
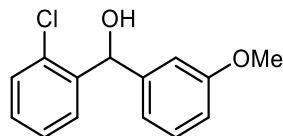
(2-chlorophenyl)(3-methoxyphenyl)methanol (4.41). Prepared via General

Procedure E on a 20.1 mmol scale to give **4.41** (5.52 g, quantitative) as a yellow oil.

The spectral data matches that which was reported in the literature.[16]

General Procedure F: Synthesis of Alcohols with Isopropyl Magnesium Chloride
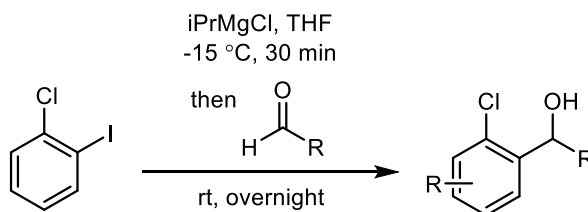
This synthesis was adapted from a previously reported literature precedent[17]. 2-Chloroiodobenzene (1.0 equiv) was added to an oven-dried round-bottomed flask and diluted with anhydrous THF (2.0 M). The flask was cooled to -15 °C with NaCl and an ice bath. Isopropylmagnesium chloride (2.0 M in THF, 1.2 equiv) was added dropwise to the flask and the solution was stirred at this temperature for 30 minutes. Aldehyde (0.83 equiv) was added dropwise to the flask and the solution was allowed to warm to room temperature and stir overnight. The reaction was quenched with saturated ammonium chloride solution in H_2O and added to a separatory funnel. The aqueous layer was extracted with EtOAc (3 x 10 mL). The organic layers were washed with brine and dried over Na2SO4. The solution was filtered through a cotton plug and concentrated in vacuo to yield the alcohol, which was used in the next step without further purification.
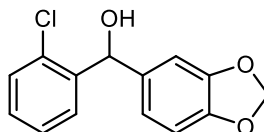
(2-chlorophenyl)(3,4-phenyldioxolane)methanol (4.42). Prepared via General Procedure F on a 7.61 mmol scale to give **4.42** (1.80 g, 90%) as a yellow oil. The spectral data matched that which was previously reported in the literature.[18]

[1]H (600 MHz, CDCl3) δ 7.63 (d, J = 7.8, 1.7 Hz, 1H), 7.34 – 7.30 (m, 2H), 7.22 (td, J = 7.7, 1.7 Hz, 1H), 6.89 – 6.85 (m, 2H), 6.76 (d, J = 7.9 Hz, 1H), 6.12 (s, 1H), 5.93 – 5.92 (m, 2H), 2.36 (bs, 1H).

^{13}C (151 MHz, CDCl$_3$) δ 147.7, 147.1, 140.9, 136.3, 132.3, 129.5, 128.7, 127.7, 127.1, 120.6, 108.1, 107.5, 101.0, 72.5.
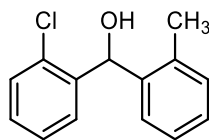
(2-chlorophenyl)(2-methylphenyl)methanol (4.43). Prepared via General Procedure F on an 8.59 mmol scale to give **4.43** (1.17 g, 59%) as a white solid. The spectral data matched that which was previously reported in the literature.[16]

^{1}H (600 MHz, CDCl$_3$) δ 7.40 – 7.36 (m, 2H), 7.34 – 7.31 (m, 1H), 7.26 – 7.23 (m, 2H), 7.23 – 7.20 (m, 2H), 7.20 – 7.17 (m, 1H), 6.36 (s, 1H), 2.35 (s, 1H), 2.31 (s, 3H).

^{13}C (151 MHz, CDCl$_3$) δ 140.3, 139.9, 135.9, 133.2, 130.5, 129.5, 128.9, 128.5, 127.8, 127.0, 126.3, 126.1, 69.8, 19.1.

Protections of Benzisoxazoles
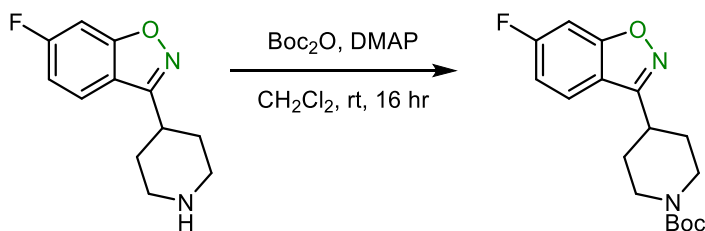
This synthesis was adapted from a known procedure that was previously reported[13]. Amine (3.12 mmol, 1.0 equiv) was added to an oven-dried round-bottomed

flask equipped with a stir bar and dissolved in anhydrous CH$_2$Cl$_2$ (0.2 M, 16 mL). DMAP (0.31 mmol, 10 mol %) and BOC$_2$O (3.43 mmol, 1.1 equiv) were added to the flask, which was stirred at room temperature for 16 hours. The solvent was removed in vacuo and the residue was subjected to silica gel column chromatography (20% EtOAc:Hexanes) to give the protected amine (947 mg, 95%) as a white solid. The spectral data matched that which was previously reported in the literature.[13]

Benzoxazepine – Probable Byproduct of Kinetic Resolution
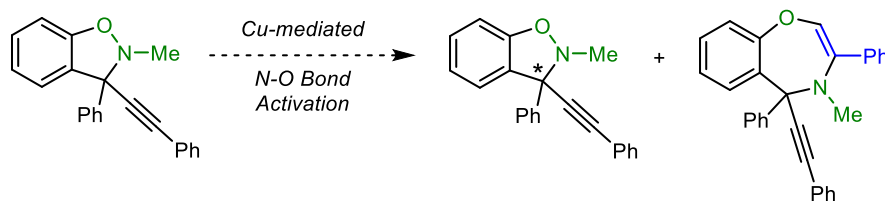
To elucidate the structure of the byproduct **4.16**, the reaction was performed in duplicate on a 0.1 mmol scale according to General Procedure A. After 24 hours, the mixtures were cooled to room temperature and filtered through a plug of silica gel into the same vial. The vial was concentrated *in vacuo* and the crude material was subjected to column chromatography to yield byproduct **4.44** (88%) as a dark red solid.
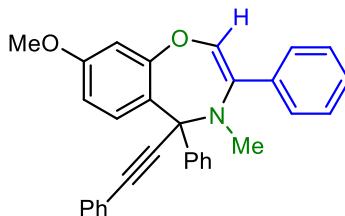
3-phenyl-4-methyl-5-phenyl-5-phenylacetylen-9-methoxy--1,4-benzoxazepine (4.44).

^{1}H NMR (400 MHz, CDCl$_3$) δ 7.90 (d, *J* = 7.32 Hz, 2H), 7.72 (d, *J* = 7.32 Hz, 2H), 7.47 – 7.31 (m, 12H), 7.12 (d, *J* = 8.9 Hz, 1H), 6.91 (d, *J* = 2.9 Hz, 1H), 6.75 (d, *J* = 8.8 Hz, 1H), 5.42 (s, 1H), 3.83 (s, 3H), 2.61 (s, 3H).

^{13}C NMR (101 MHz, CDCl$_3$) δ 155.8, 154.7, 149.4, 142.4, 136.1, 136.0, 131.8, 128.64, 128.61, 128.39, 128.31, 128.2, 128.0, 127.6, 125.8, 123.3, 122.8, 110.8, 110.1, 106.2, 88.1, 86.8, 67.7, 55.6, 37.5.

4.5   References

1.   Liu, J. X.; Dasgupta, S.; Watson, M. P., Enantioselective additions of copper acetylides to cyclic iminium and oxocarbenium ions. *Beilstein J. Org. Chem.* **2015,** *11*, 2696-2706.
2.   Guan, W. Y.; Santana, S. O.; Liao, J. N.; Henninger, K.; Watson, M. P., Enantioselective Alkynylation of Unstabilized Cyclic Iminium Ions. *ACS. Catal.* **2020,** *10* (23), 13820-13824.
3.   Koradin, C.; Polborn, K.; Knochel, P., Enantioselective Synthesis of Propargylamines by Copper-Catalyzed Addition of Alkynes to Enamines†. *Angew. Chem. Int. Ed.* **2002,** *41* (14), 2535-2538.
4.   Turcaud, S.; Sierecki, E.; Martens, T.; Royer, J., Asymmetric α-Alkynylation of Piperidine via N-Sulfinyliminium Salts. *J. Org. Chem.* **2007,** *72* (13), 4882-4885.
5.   Hashimoto, T.; Omote, M.; Maruoka, K., Catalytic Asymmetric Alkynylation of C1-Substituted C,N-Cyclic Azomethine Imines by CuI/Chiral Brønsted Acid Co-Catalyst. *Angew. Chem. Int. Ed.* **2011,** *50* (38), 8952-8955.
6.   Dasgupta, S.; Liu, J.; Shoffler, C. A.; Yap, G. P. A.; Watson, M. P., Enantioselective, Copper-Catalyzed Alkynylation of Ketimines To Deliver

Isoquinolines with alpha-Diaryl Tetrasubstituted Stereocenters. *Org. Lett.* **2016,** *18* (23), 6006-6009.

7.   Kovacic, P.; Somanathan, R., Clinical Physiology and Mechanism of Dizocilpine (MK-801): Electron Transfer, Radicals, Redox Metabolites and Bioactivity. *Oxidative Medicine and Cellular Longevity* **2010,** *3*, 530859.

8.   Yao, T.; Ren, B.; Wang, B.; Zhao, Y., Highly Selective Synthesis of Dihydrobenzo[d]isoxazoles and Dihydrobenzo[d]oxazoles from Oximes and Arynes via in Situ Generation of Nitrones. *Org. Lett.* **2017,** *19* (12), 3135-3138.

9.   Tani, K.; Behenna, D. C.; McFadden, R. M.; Stoltz, B. M., A Facile and Modular Synthesis of Phosphinooxazoline Ligands. *Org. Lett.* **2007,** *9* (13), 2529-2531.

10.   Bennasar, M. L.; Jiménez, J.-M.; Vidal, B.; Sufi, B. A.; Bosch, J., Nucleophilic Addition of 1-Acetylindole Enolates to Pyridinium Salts. Stereoselective Formal Synthesis of (±)-Geissoschizine and (±)-Akagerine via 1,4-Dihydropyridines. *J. Org. Chem.* **1999,** *64* (26), 9605-9612.

11.   Ikeda, R.; Kuwano, R., Asymmetric Hydrogenation of Isoxazolium Triflates with a Chiral Iridium Catalyst. *Chem. Eur. J.* **2016,** *22* (25), 8610-8618.

12.   Shan, G.; Huang, G.-Y.; Rao, Y.; Zhang, H., Palladium-catalyzed ortho-selective CH bond chlorination of aromatic ketones. *Chin. Chem. Lett.* **2015,** *26* (10), 1236-1240.

13.   Taylor, N. J.; Emer, E.; Preshlock, S.; Schedler, M.; Tredwell, M.; Verhoog, S.; Mercier, J.; Genicot, C.; Gouverneur, V., Derisking the Cu-Mediated 18F-Fluorination of Heterocyclic Positron Emission Tomography Radioligands. *J. Am. Chem. Soc.* **2017,** *139* (24), 8267-8276.

14.   Udd, S.; Jokela, R.; Franzén, R.; Tois, J., Copper-catalyzed cyclization of Z-oximes into 3-methyl-1,2-benzisoxazoles. *Tet. Lett.* **2010,** *51* (7), 1030-1033.

15.   Regier, J.; Maillet, R.; Bolshan, Y., A Direct Brønsted Acid-Catalyzed Azidation of Benzhydrols and Carbohydrates. *Eur. J. Org. Chem.* **2019,** *2019* (13), 2390-2396.

16.   Sui, Y.-Z.; Zhang, X.-C.; Wu, J.-W.; Li, S.; Zhou, J.-N.; Li, M.; Fang, W.; Chan, A. S. C.; Wu, J., CuII-Catalyzed Asymmetric Hydrosilylation of Diaryl- and Aryl Heteroaryl Ketones: Application in the Enantioselective Synthesis of Orphenadrine and Neobenodine. *Chem. Eur. J.* **2012,** *18* (24), 7486-7492.

17.   Co., B.-M. S. Substituted Bicyclic Heteroaryl Compounds. WO2013/49263, 2013.

18.   Liu, W.; Guo, J.; Xing, S.; Lu, Z., Highly Enantioselective Cobalt-Catalyzed Hydroboration of Diaryl Ketones. *Org. Lett.* **2020,** *22* (7), 2532-2536.

Appendix

A. SPECTRAL & CHROMATOGRAPHY DATA FOR CHAPTER 1
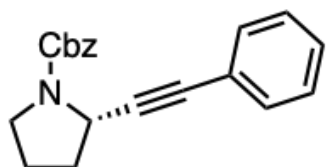
Compound 1.1
^{1}H NMR (600 MHz, CDCl$_3$)

7.43
7.35
7.34
7.29
7.28
7.27
7.26 CDCl3

5.34
5.31
5.13
5.11
4.84
4.78
4.77

3.62
3.62
3.60
3.47
3.46
3.45
3.44

2.18
2.17
2.16
2.14
1.97

9.28

2.09

1.00

1.05
1.14

2.95
1.07
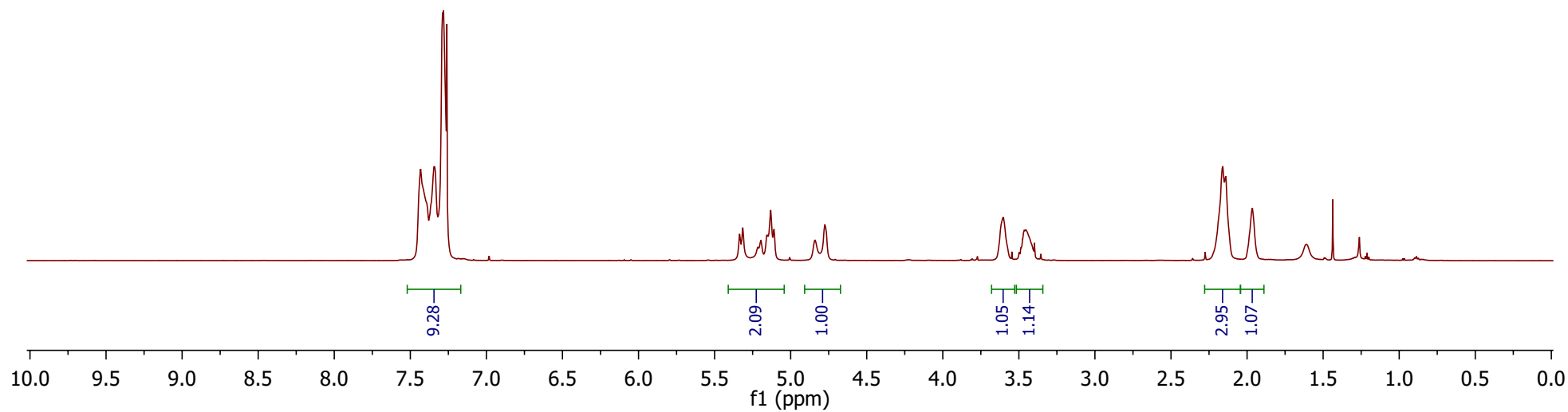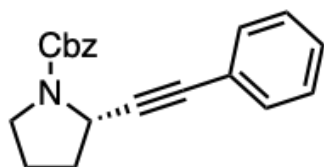
Compound 1.1
^{13}C NMR (101 MHz, CDCl$_3$)

154.67

137.13
131.97
131.82
128.53
128.33
128.26
128.06
127.84
127.72
123.11

89.60
82.41
77.37 CDCl3
77.16 CDCl3
76.95 CDCl3
66.97

49.33
48.86
46.36
45.95

34.14
33.41

24.67
23.90
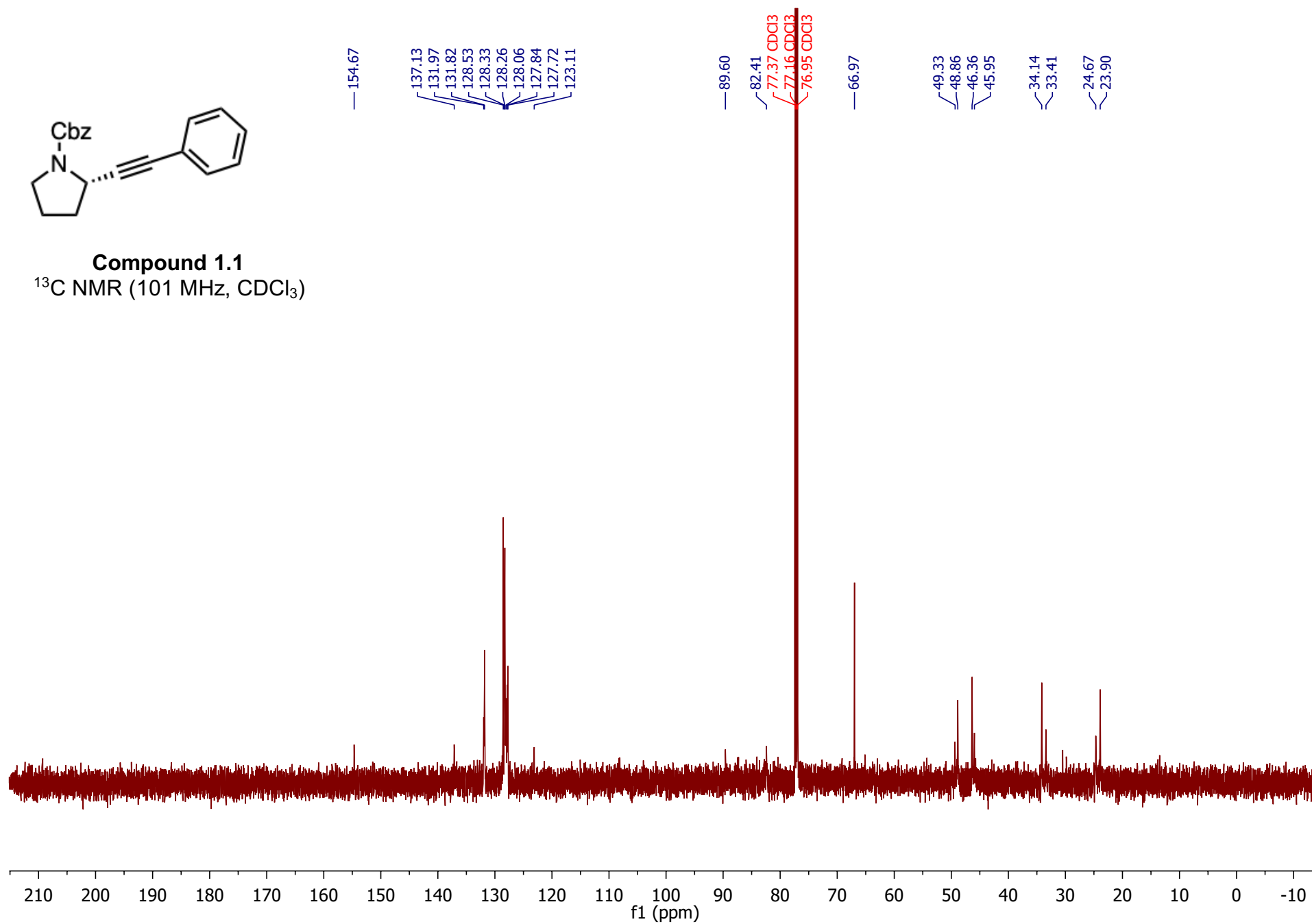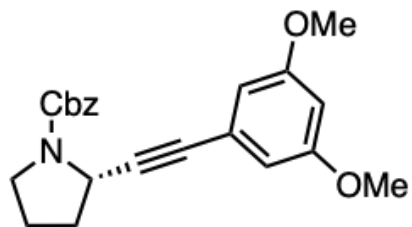
Compound 1.2
¹H NMR (400 MHz, CDCl₃)
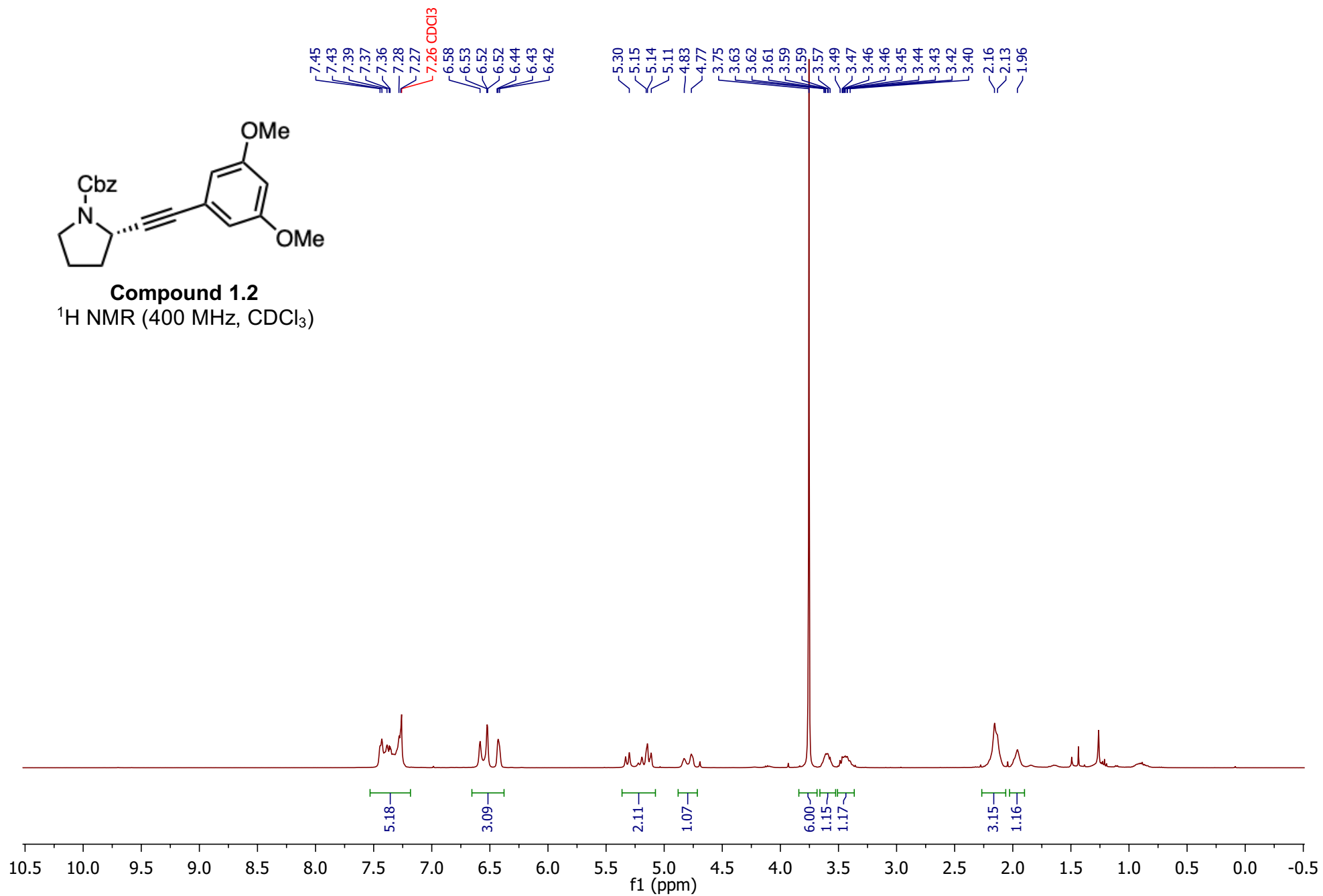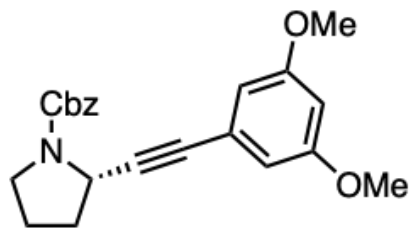
Compound 1.2
^{13}C NMR (101 MHz, CDCl$_3$)

160.49
160.42
154.57
137.00
136.89
128.56
128.50
128.46
128.03
127.76
127.58
127.53
127.01
124.35
124.27
109.59
109.47
101.80
101.73
89.10
88.74
82.29
82.15
77.48 CDCl3
77.16 CDCl3
76.84 CDCl3
66.94
66.87
55.46
49.19
48.73
46.30
45.89
34.01
33.30
29.78
24.62
23.84
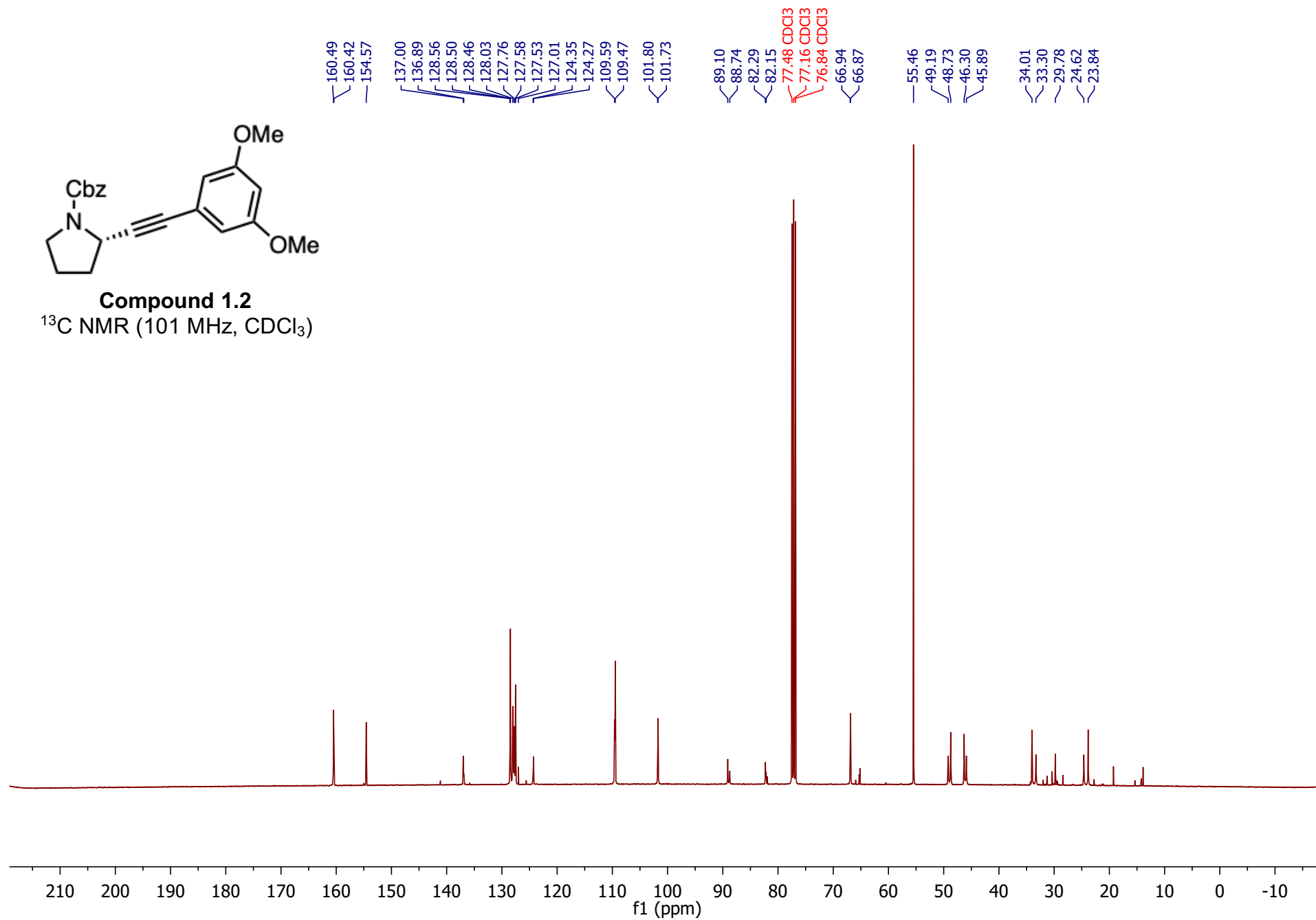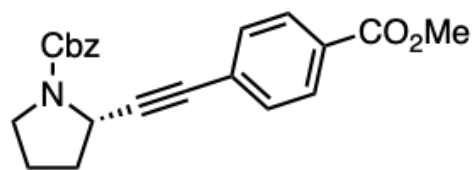
Compound 1.3
^{1}H NMR (600 MHz, CDCl$_3$)
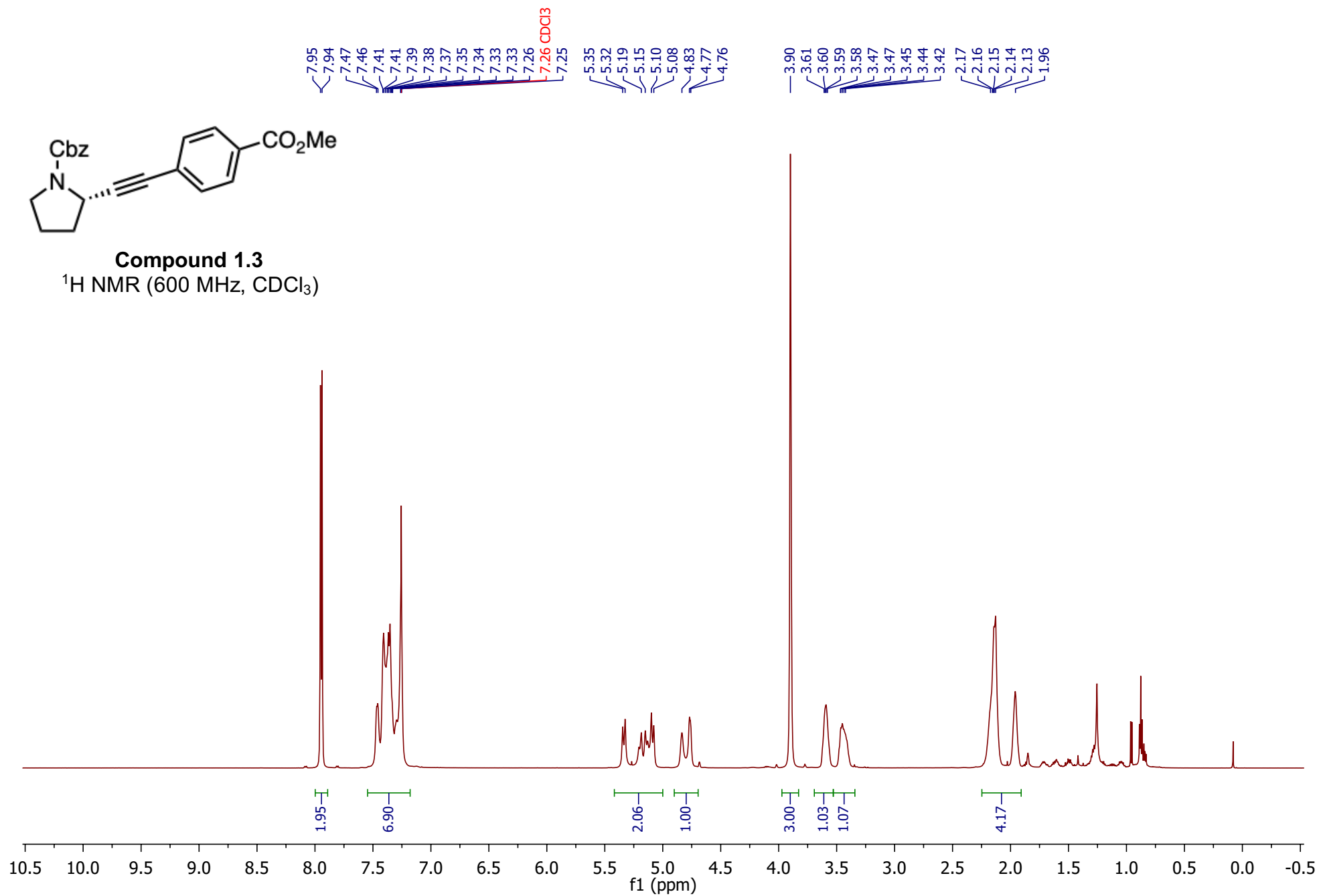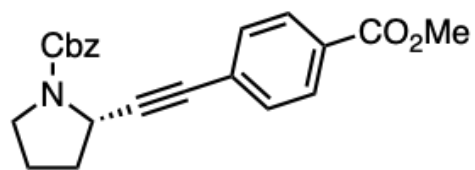
Compound 1.3
^{13}C NMR (151 MHz, CDCl$_3$)
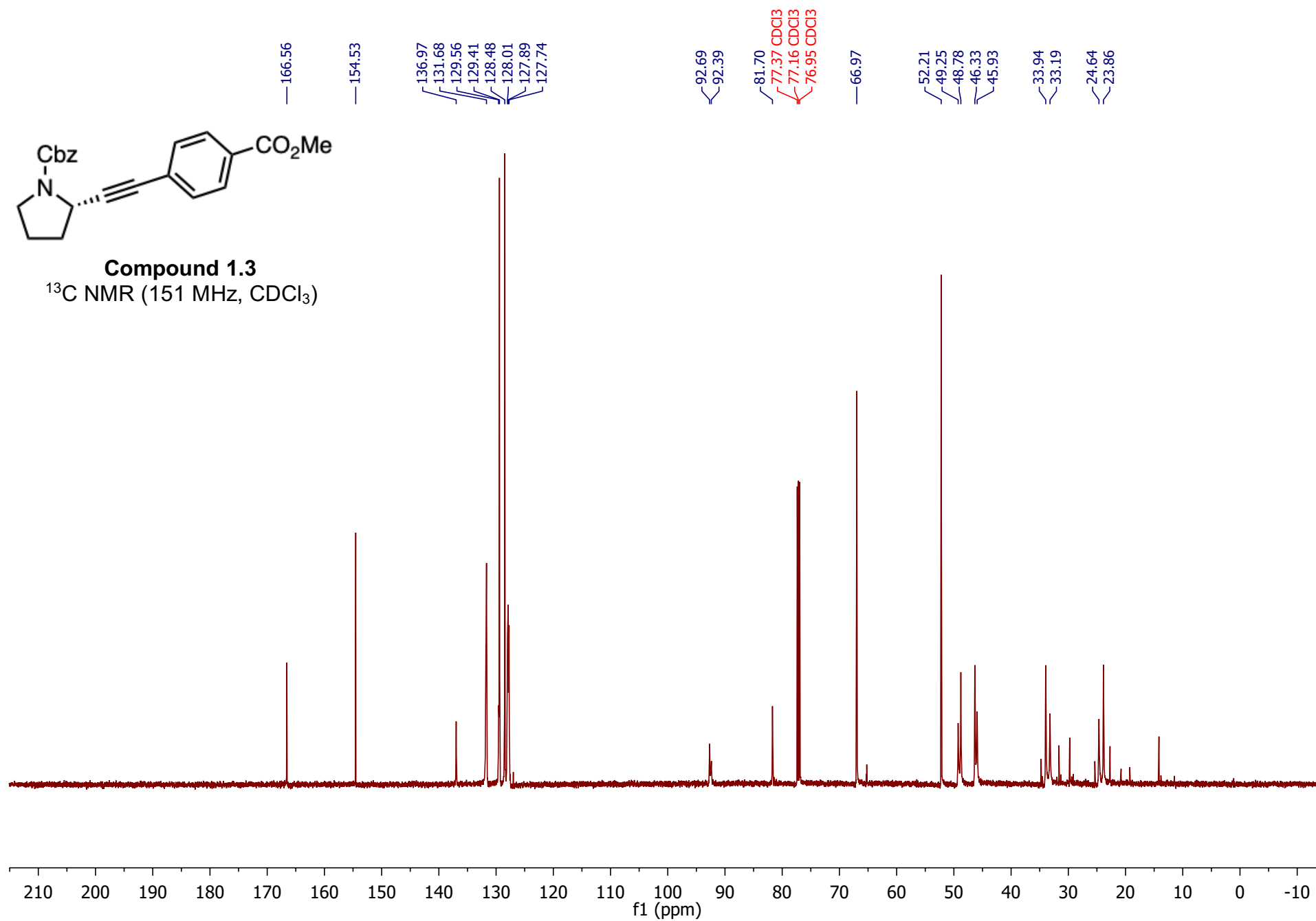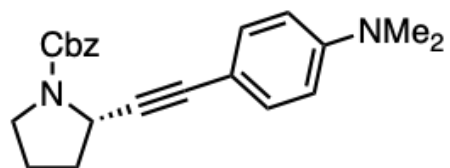
Compound 1.4
^{1}H NMR (600 MHz, CDCl$_3$)
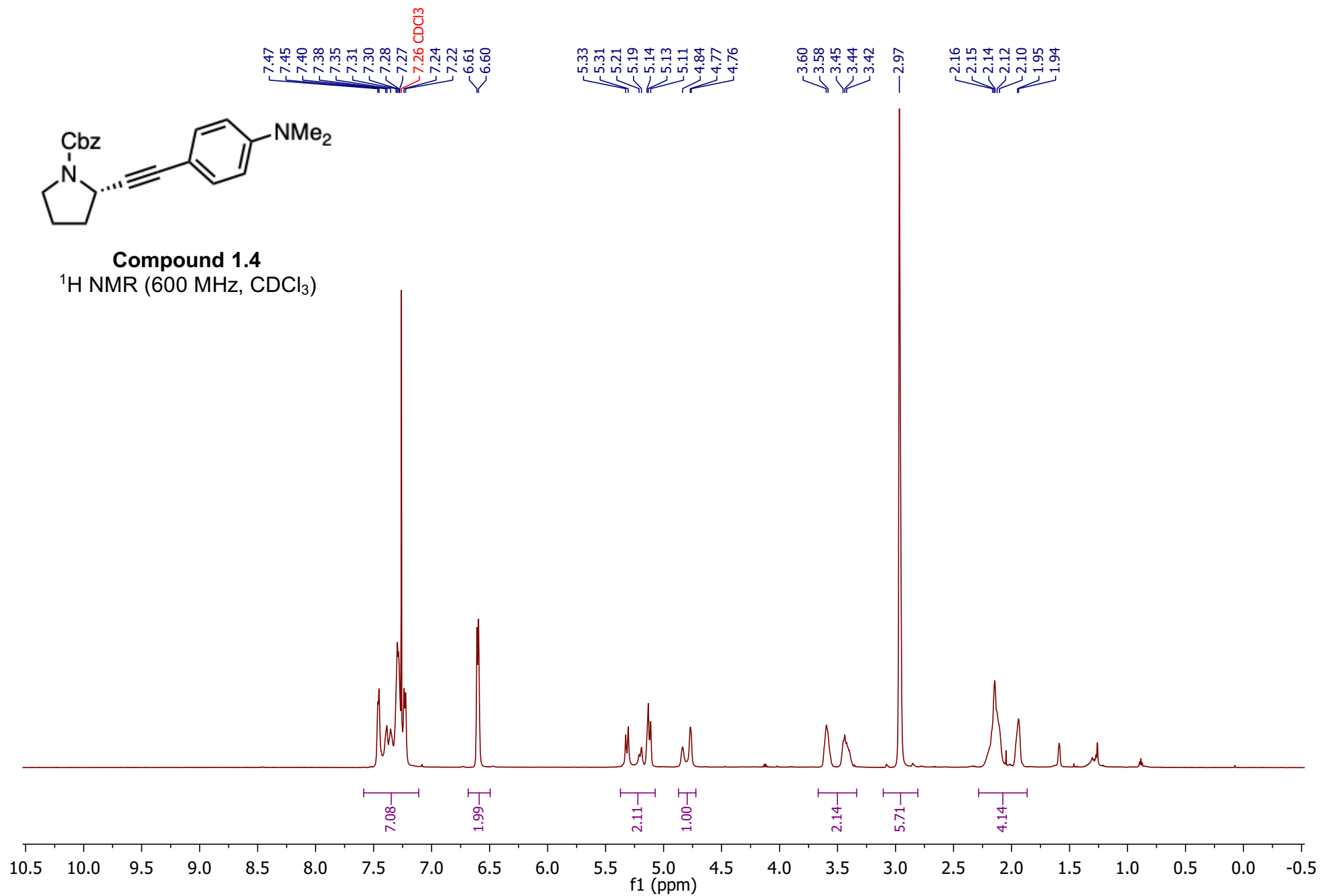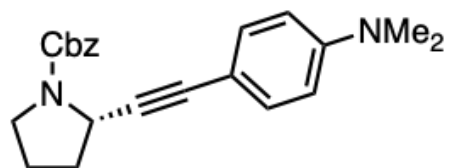
Compound 1.4
^{13}C NMR (151 MHz, CDCl$_3$)

154.78
150.20
137.28
132.88
128.52
128.02
127.75
127.65
111.92
87.21
83.19
77.37 CDCl3
77.16 CDCl3
76.95 CDCl3
66.88
49.54
49.09
46.31
45.89
40.38
34.34
33.64
24.64
23.88
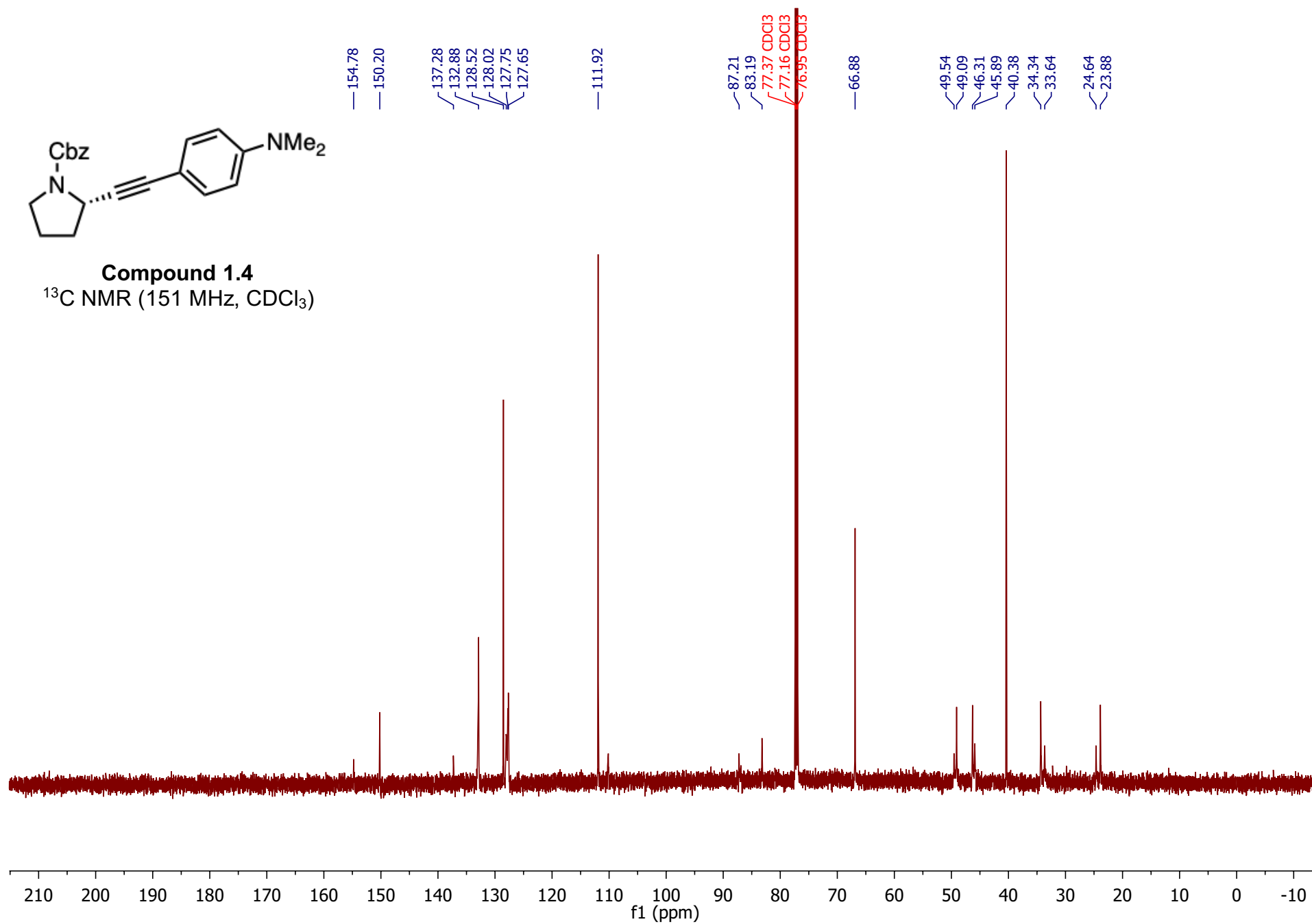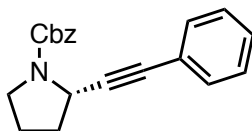
Compound 1.1, racemic
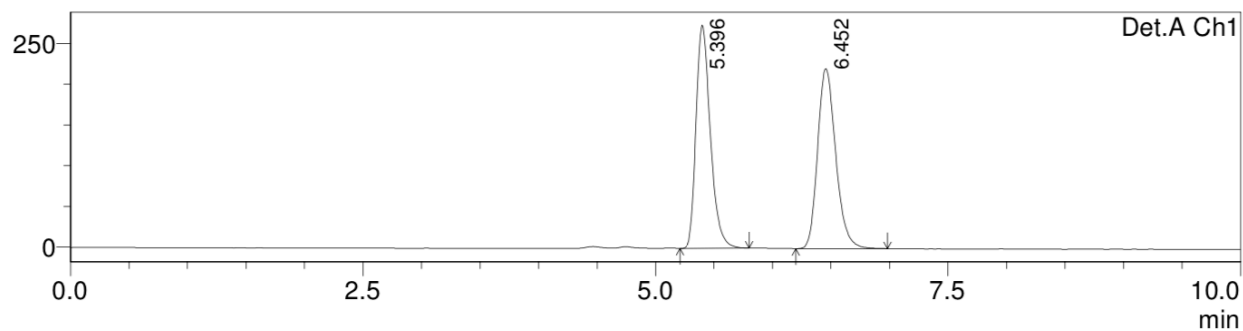
Detector A Ch1 254nm

Peak#	Ret. Time	Area	Height	Area %	Height %
1	5.396	2329814	274018	49.488	55.374
2	6.452	2378006	220832	50.512	44.626
Total		4707820	494850	100.000	100.000

Compound 1.1, 92% ee
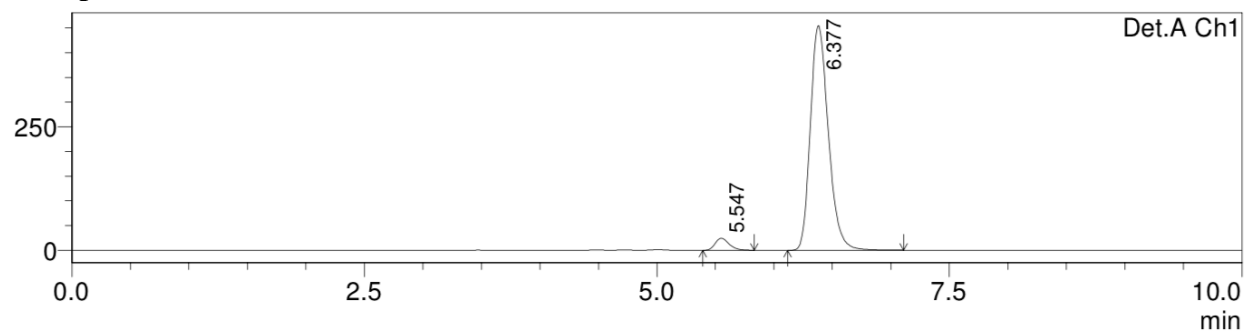
Detector A Ch1 254nm

Peak#	Ret. Time	Area	Height	Area %	Height %
1	5.547	204730	24599	4.034	5.129
2	6.377	4870670	455048	95.966	94.871
Total		5075399	479646	100.000	100.000
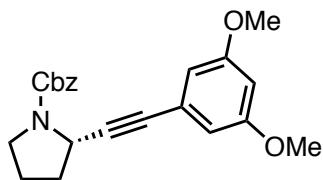
Compound 1.2, racemic
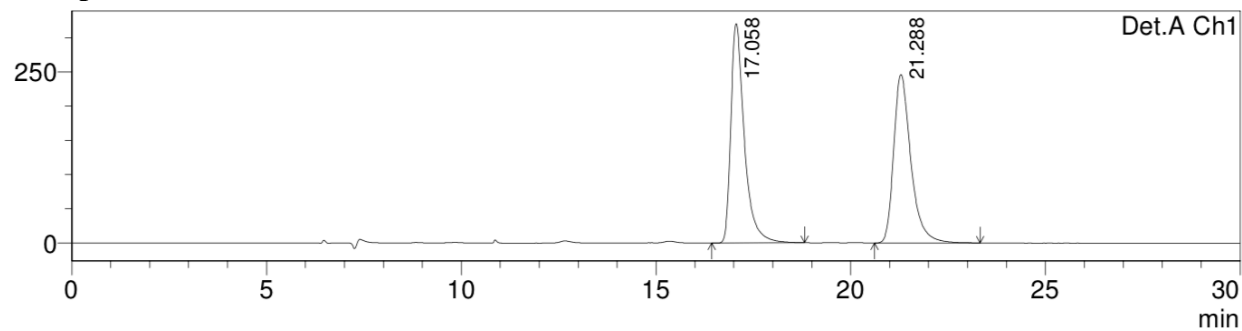
Detector A Ch1 254nm

Peak#	Ret. Time	Area	Height	Area %	Height %
1	17.058	7734991	320742	50.545	56.570
2	21.288	7568085	246244	49.455	43.430
Total		15303076	566986	100.000	100.000

Compound 1.2, 91% ee
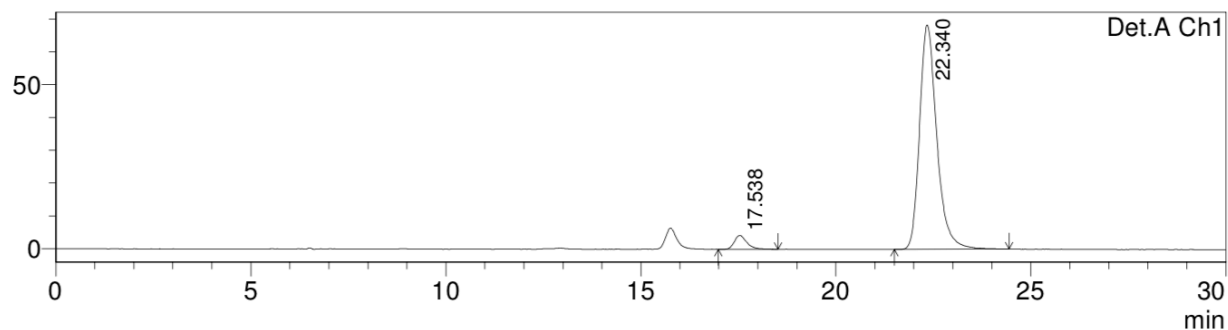
Detector A Ch1 254nm

Peak#	Ret. Time	Area	Height	Area %	Height %
1	17.538	93112	4202	4.255	5.786
2	22.340	2094949	68420	95.745	94.214
Total		2188061	72621	100.000	100.000
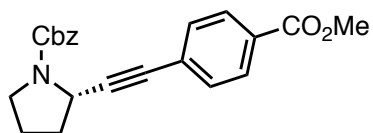
Compound 1.3, racemic
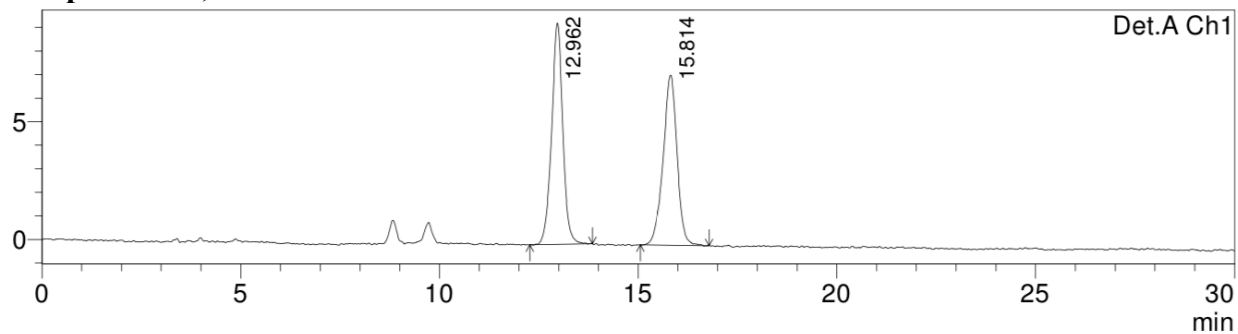
Detector A Ch1 254nm

Peak#	Ret. Time	Area	Height	Area %	Height %
1	12.962	183623	9397	50.989	56.534
2	15.814	176499	7225	49.011	43.466
Total		360122	16622	100.000	100.000

Compound 1.3, 94% ee
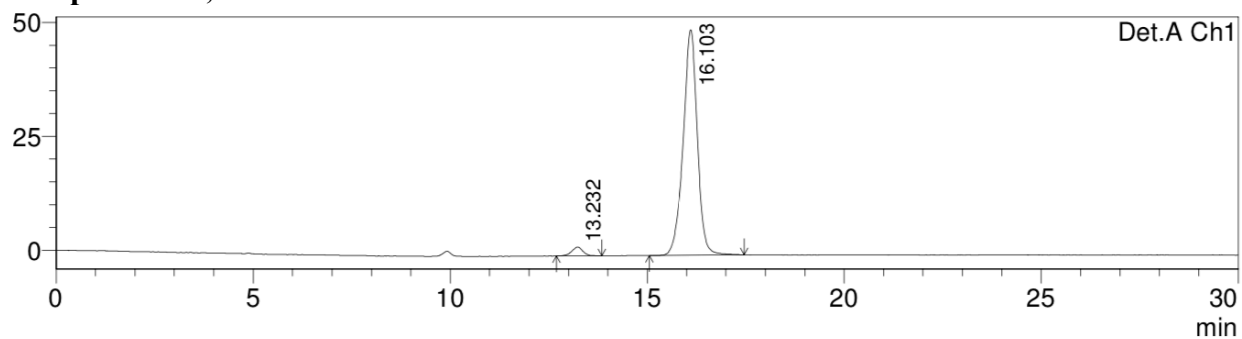
Detector A Ch1 254nm

Peak#	Ret. Time	Area	Height	Area %	Height %
1	13.232	38921	1937	3.043	3.764
2	16.103	1240182	49511	96.957	96.236
Total		1279103	51448	100.000	100.000
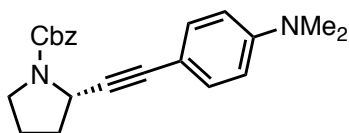
Compound 1.4, racemic
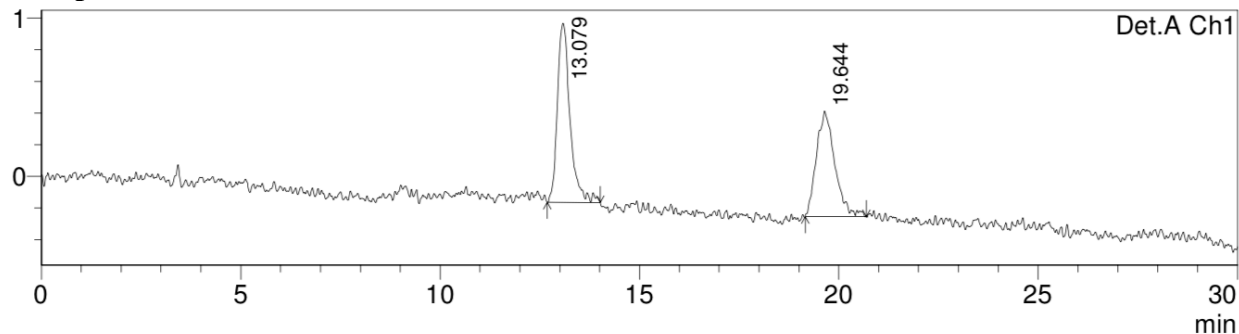
Detector A Ch1 254nm

Peak#	Ret. Time	Area	Height	Area %	Height %
1	13.079	24940	1131	53.814	62.910
2	19.644	21405	667	46.186	37.090
Total		46345	1798	100.000	100.000

Compound 1.4, 72% ee
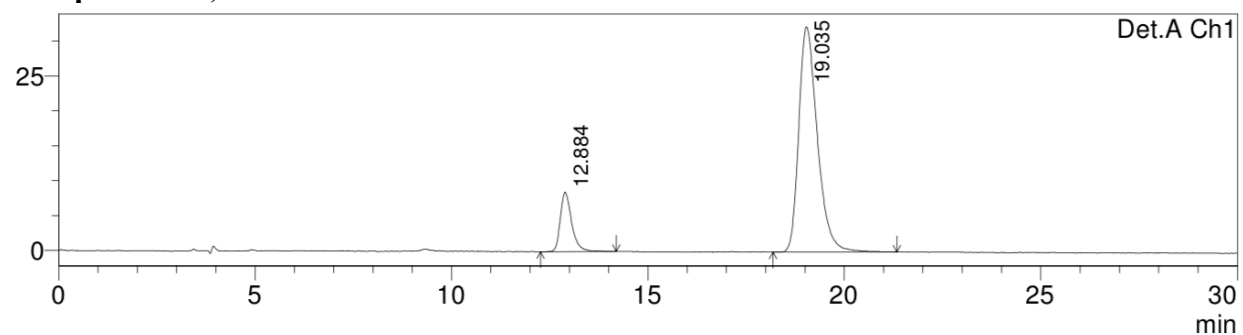
Detector A Ch1 254nm

Peak#	Ret. Time	Area	Height	Area %	Height %
1	12.884	169673	8509	13.790	20.859
2	19.035	1060746	32284	86.210	79.141
Total		1230419	40793	100.000	100.000

B. SPECTRAL & CHROMATOGRAPHY DATA FOR CHAPTER 2
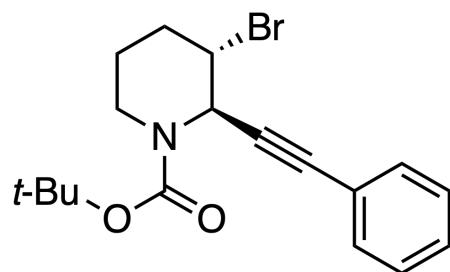
Compound 2.6
>20:1 dr
^{1}H NMR (400 MHz, CD$_3$OD)
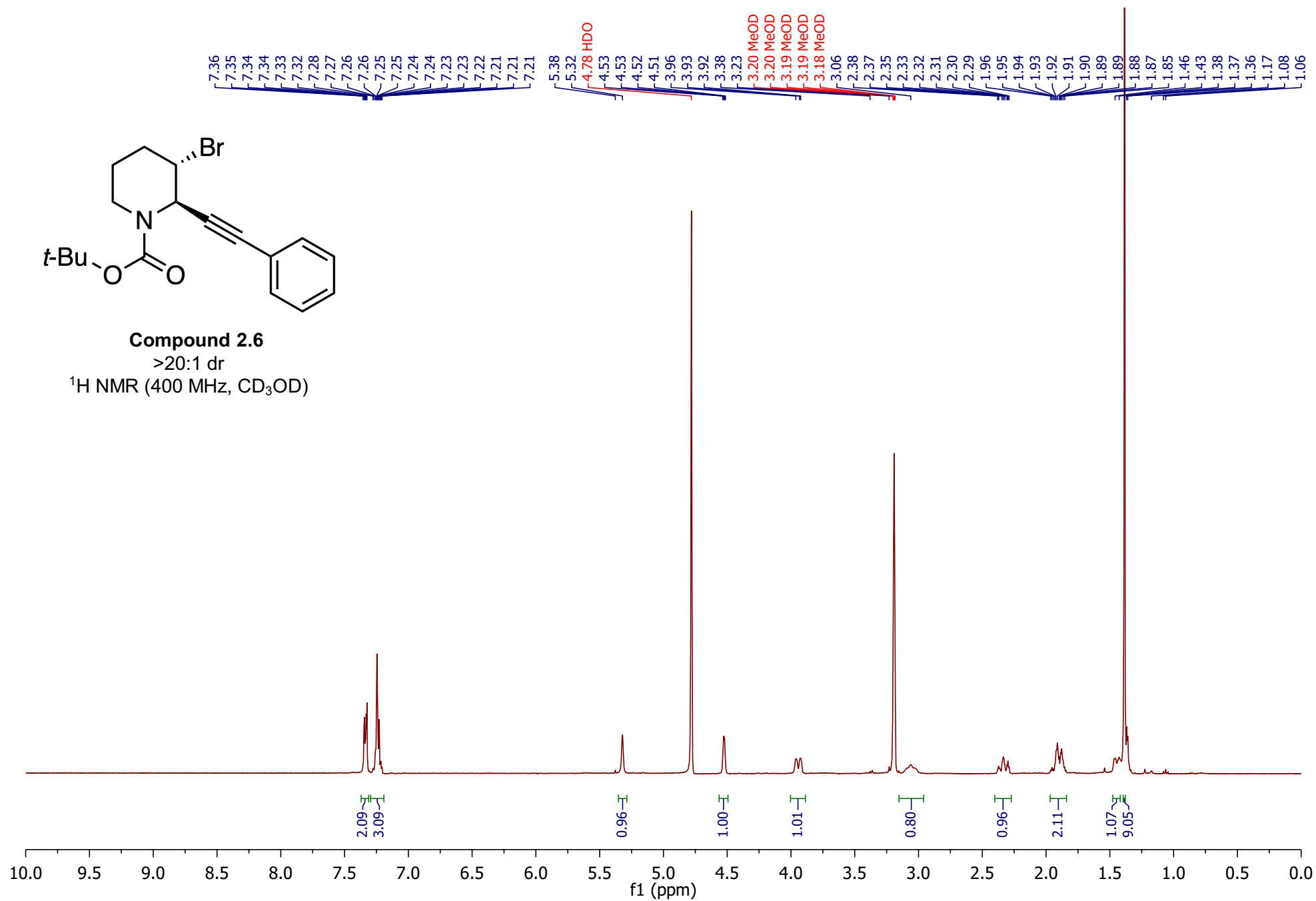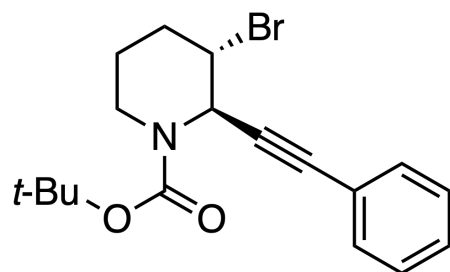
Compound 2.6
>20:1 dr
^{13}C NMR (101 MHz, CD$_3$OD)

153.15
129.76
127.01
126.61
120.30
84.68
81.95
79.05
52.87
49.69
37.51
26.64
25.64
17.87
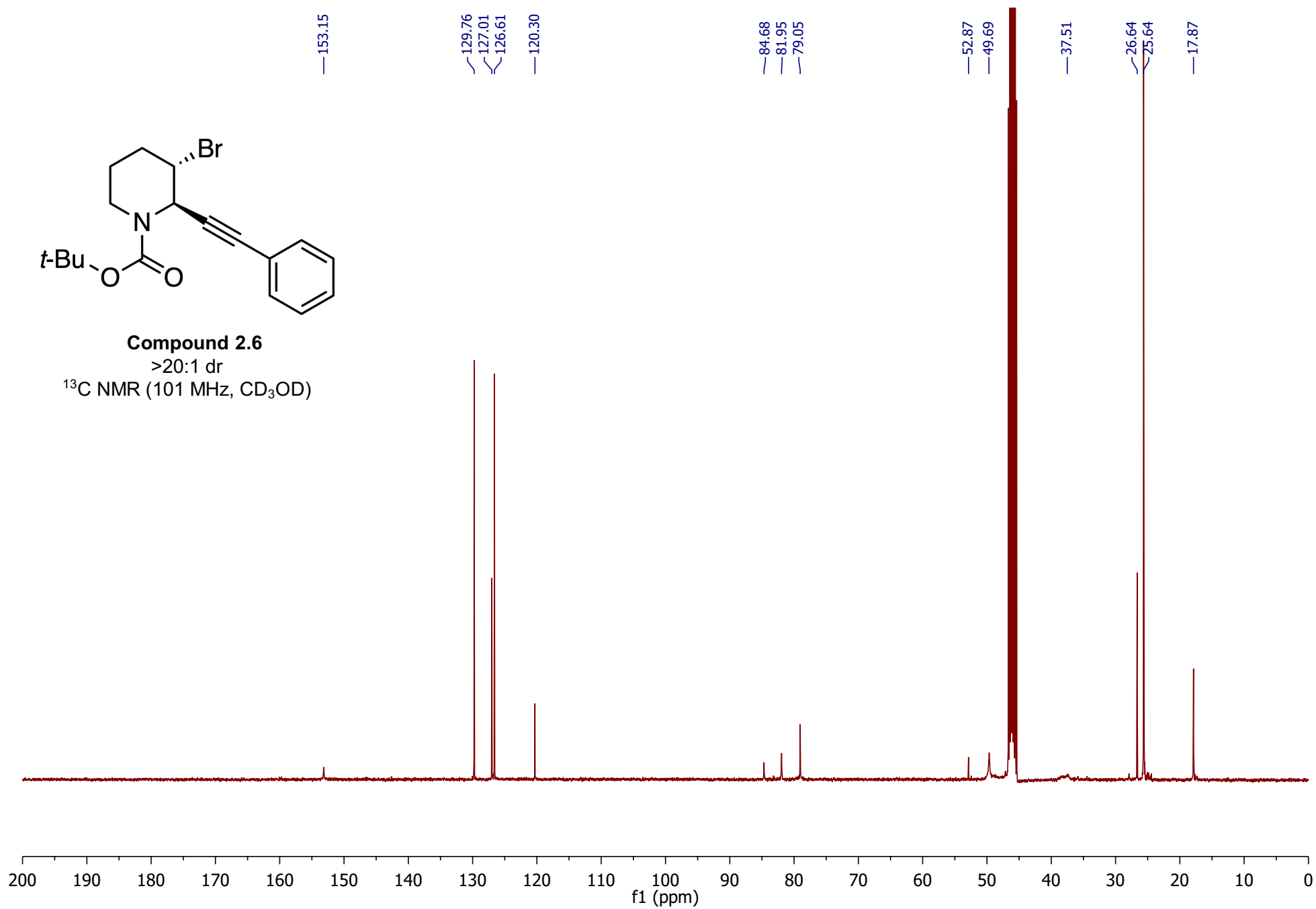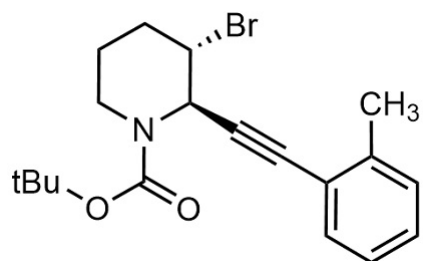
Compound 2.8
>20:1 dr
^{1}H NMR (400 MHz, CD$_3$OD)
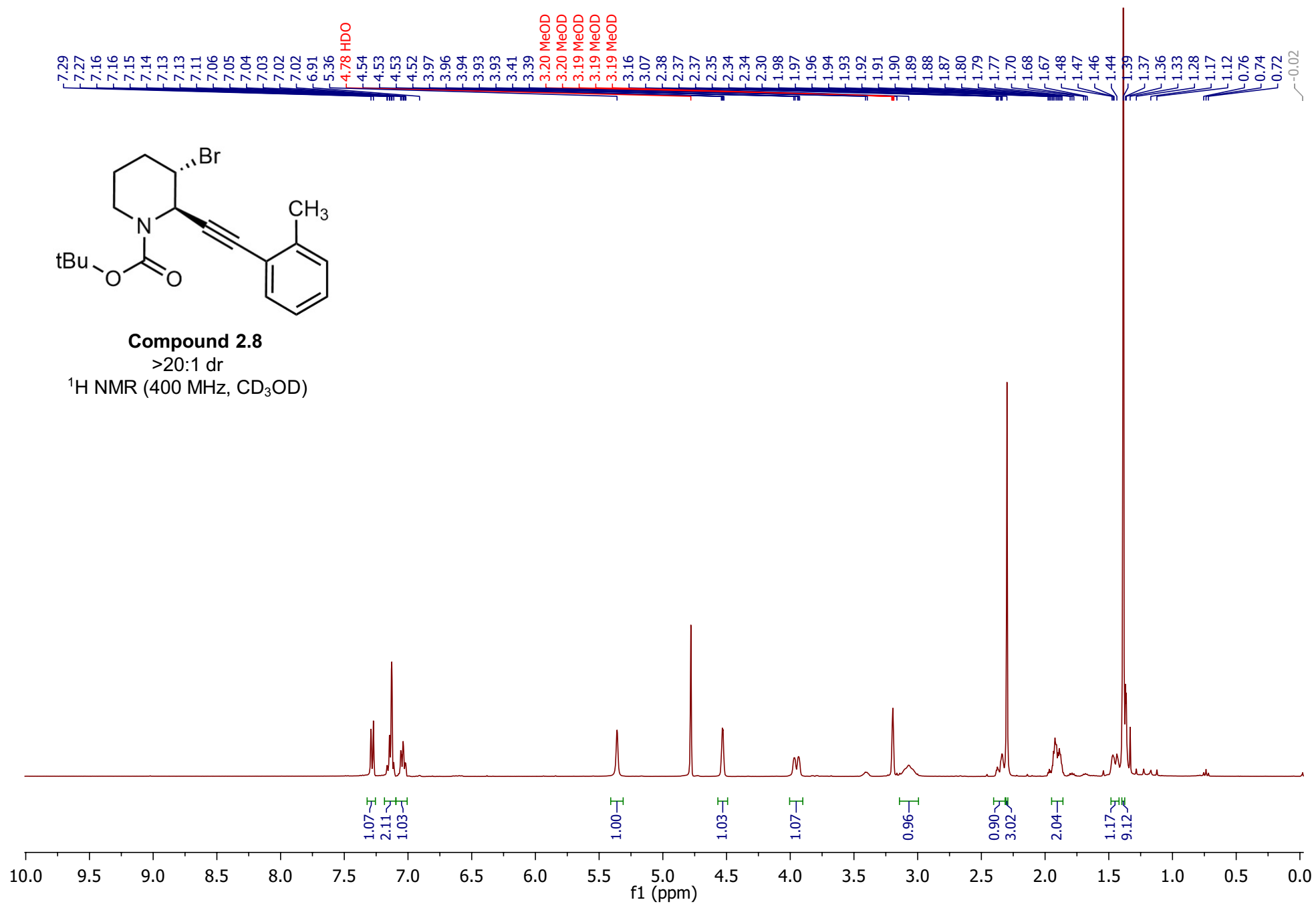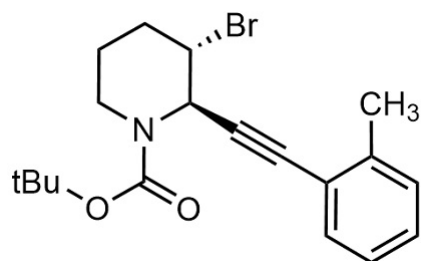
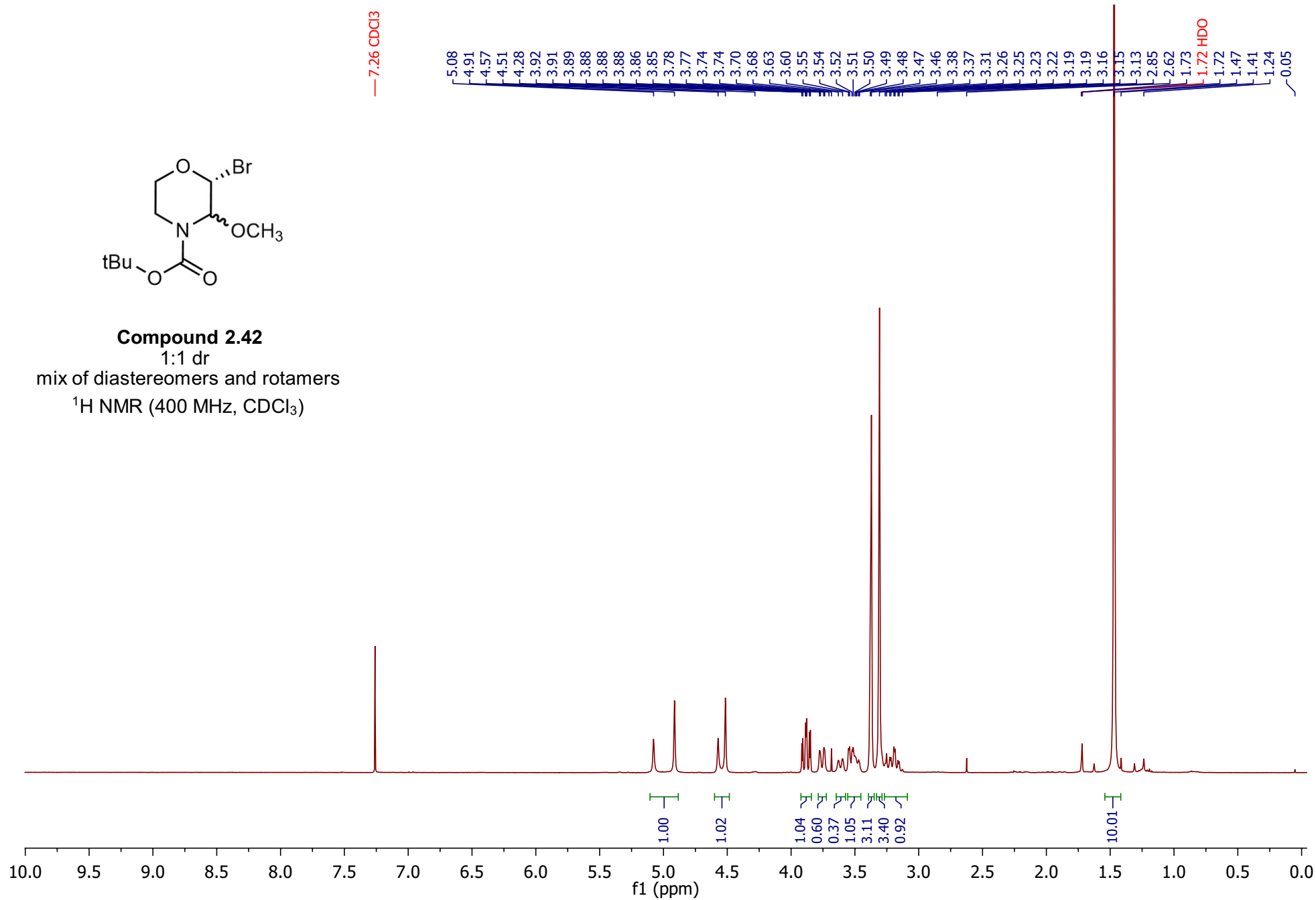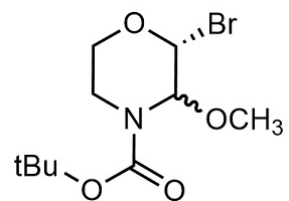**Compound 2.8**
>20:1 dr
^{13}C NMR (151 MHz, CD$_3$OD)

Peak labels (left to right): 154.84, 140.00, 131.69, 129.24, 128.69, 125.48, 121.56, 87.74, 85.19, 80.70, 51.23, 50.56, 39.20, 28.27, 27.33, 19.67, 19.49

f1 (ppm)
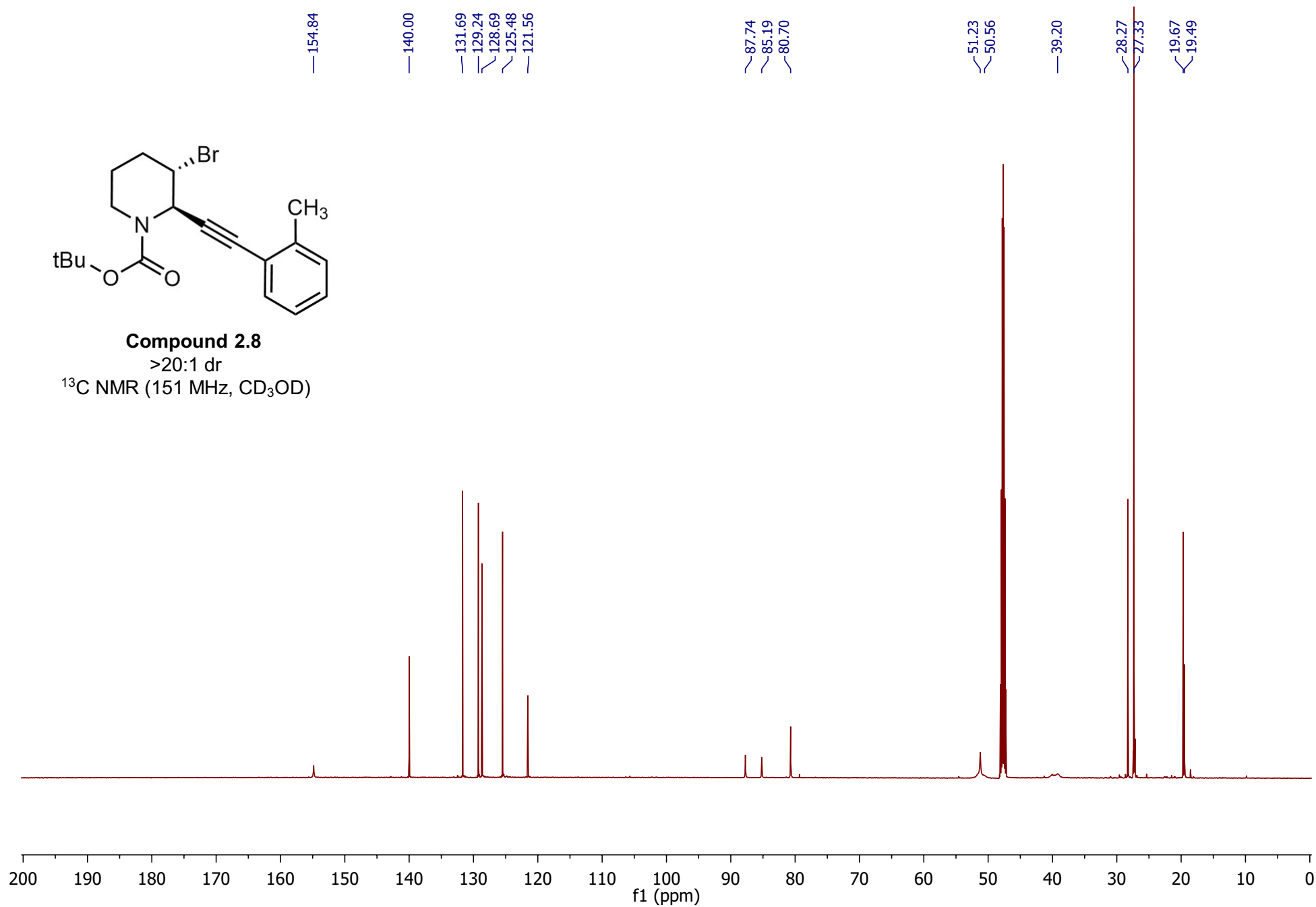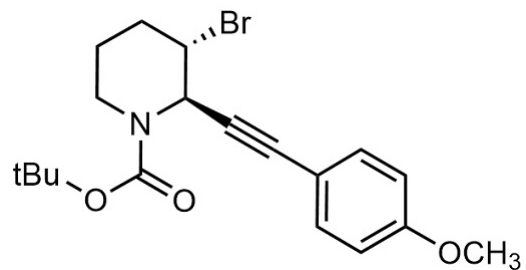
Compound 2.9
>20:1 dr
^{1}H NMR (400 MHz, CD$_3$OD)

Compound 2.9
>20:1 dr
^{13}C NMR (151 MHz, CD$_3$OD)

160.24
154.80
132.85
113.81
113.77
86.40
82.05
80.63
54.44
51.45
50.56
38.81
28.18
27.26
19.48
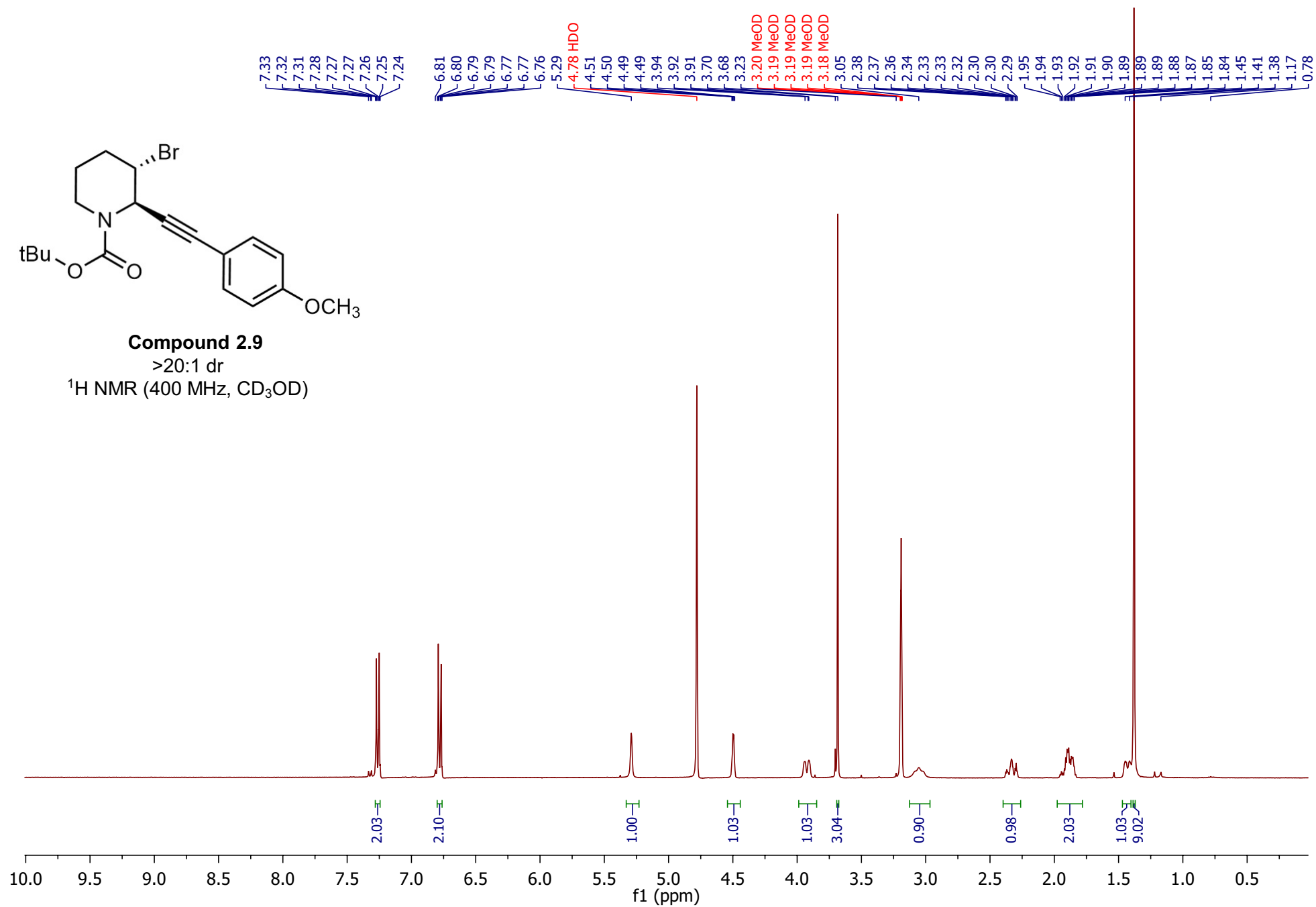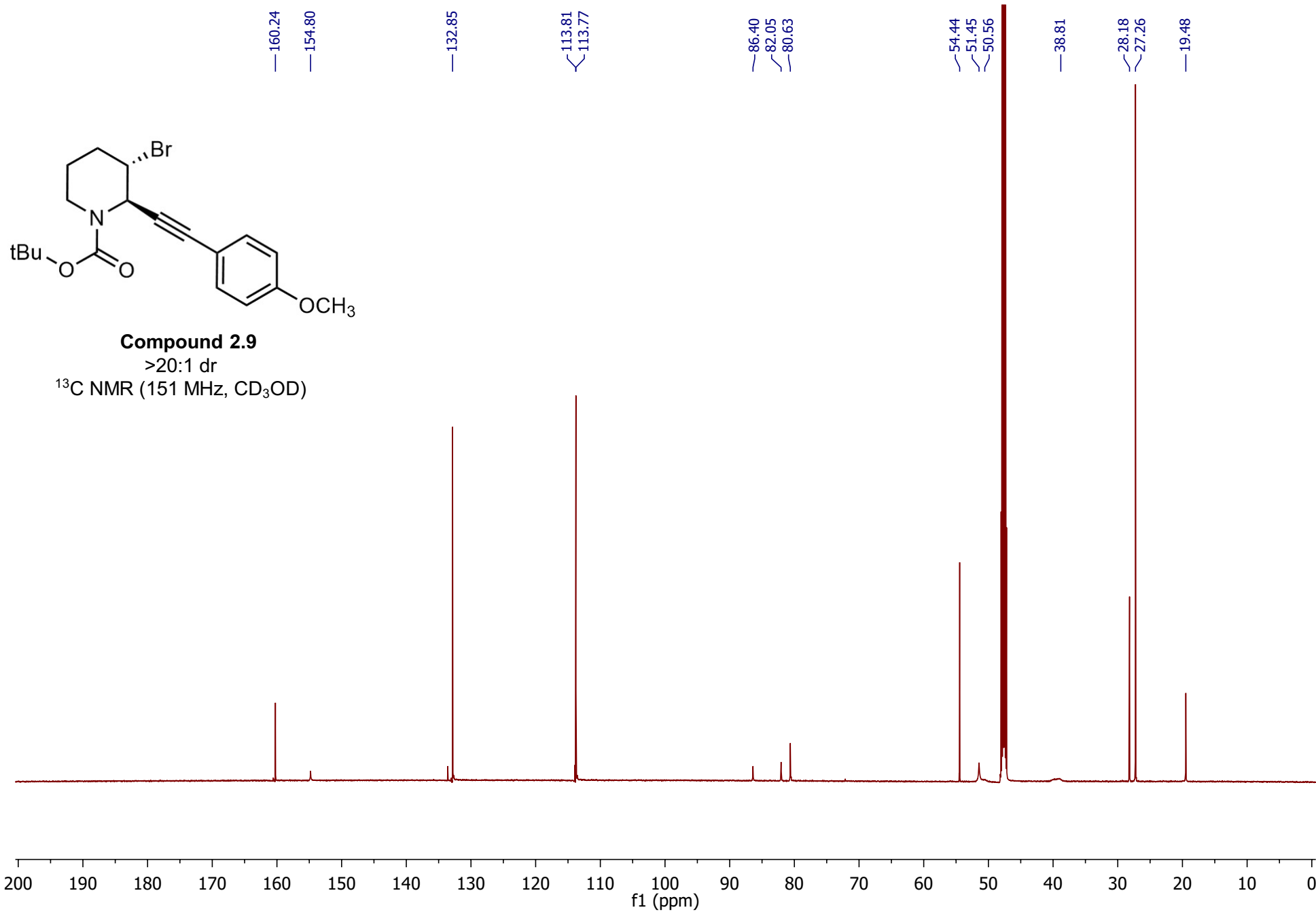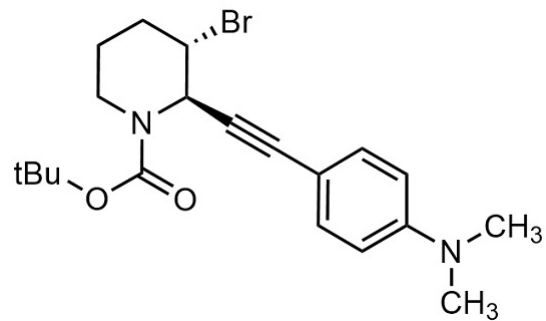
Compound 2.10
>20:1 dr
^{1}H NMR (600 MHz, CD$_3$OD)
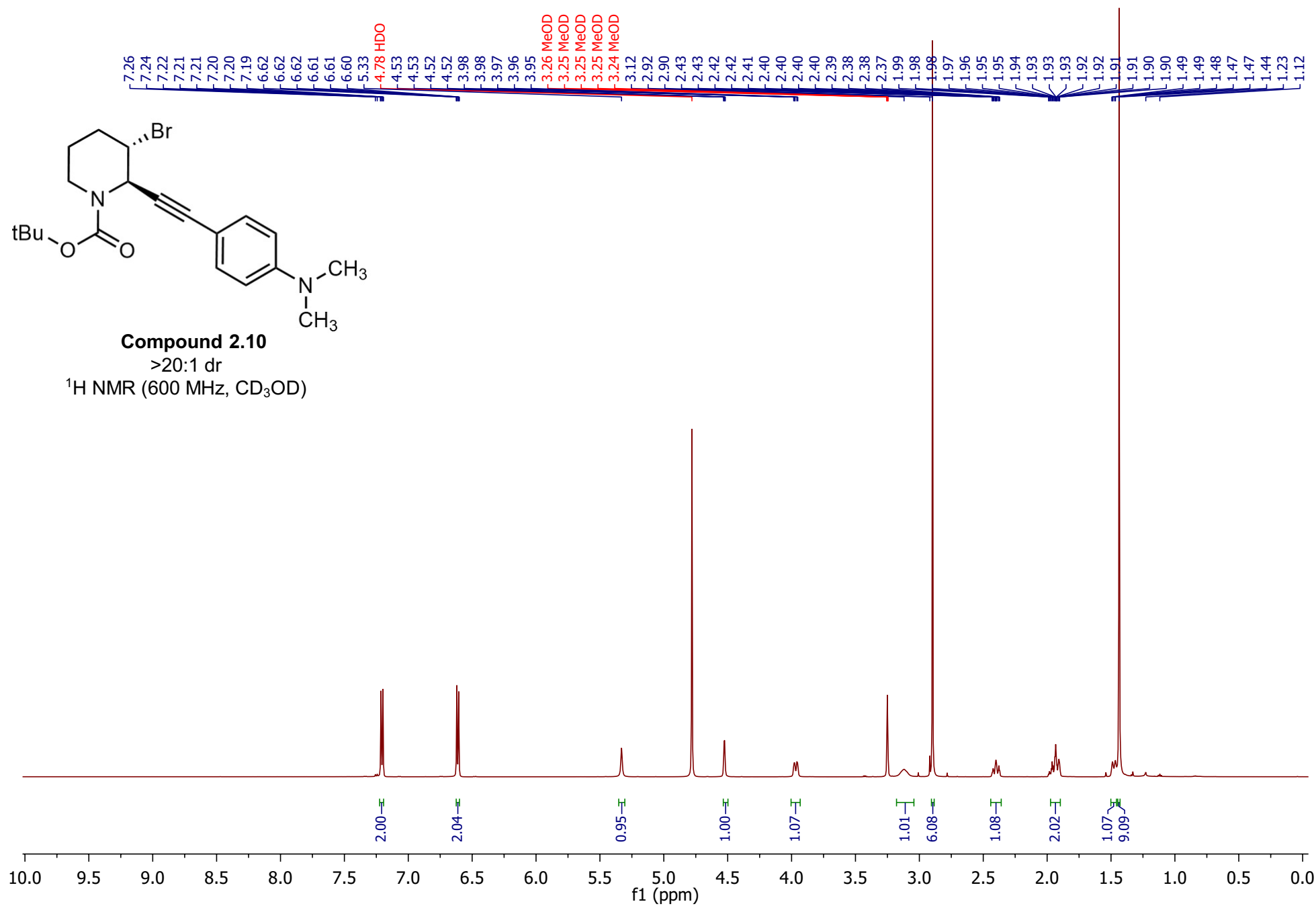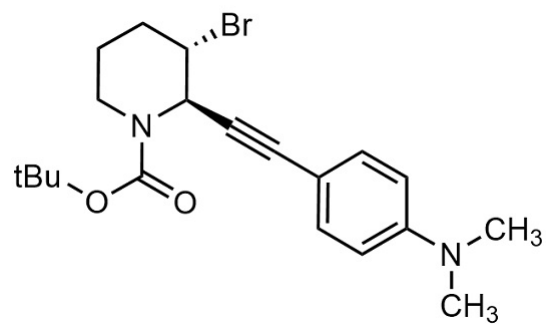
Compound 2.10
>20:1 dr
^{13}C NMR (151 MHz, CD$_3$OD)

154.82
150.69
132.35
111.57
108.51
87.65
81.03
80.49
51.80
39.06
38.94
28.14
27.25
19.52
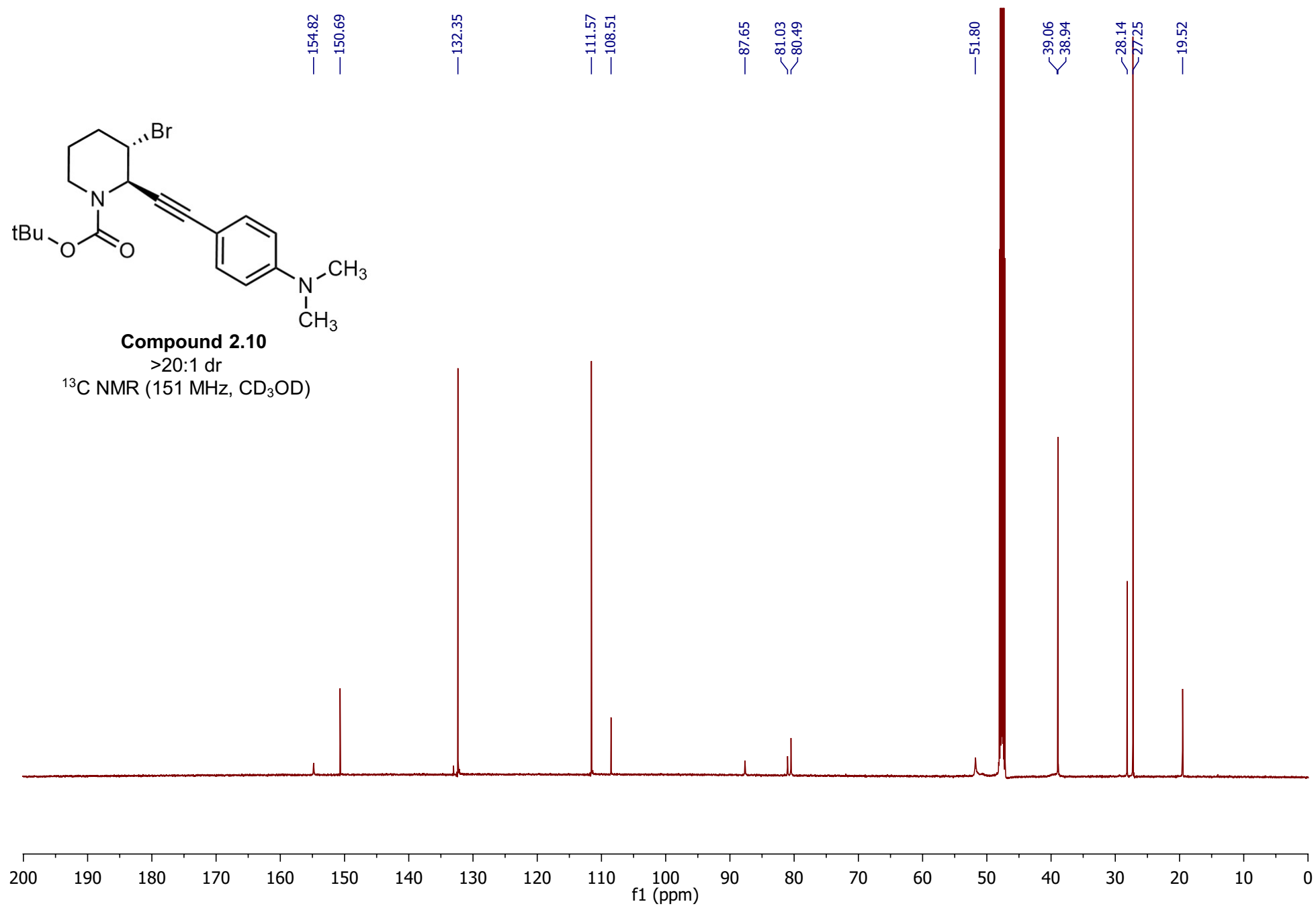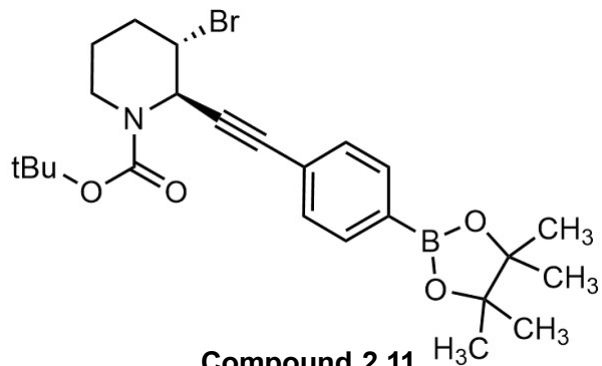
Compound 2.11
>20:1 dr
^{1}H NMR (600 MHz, CD$_3$OD)
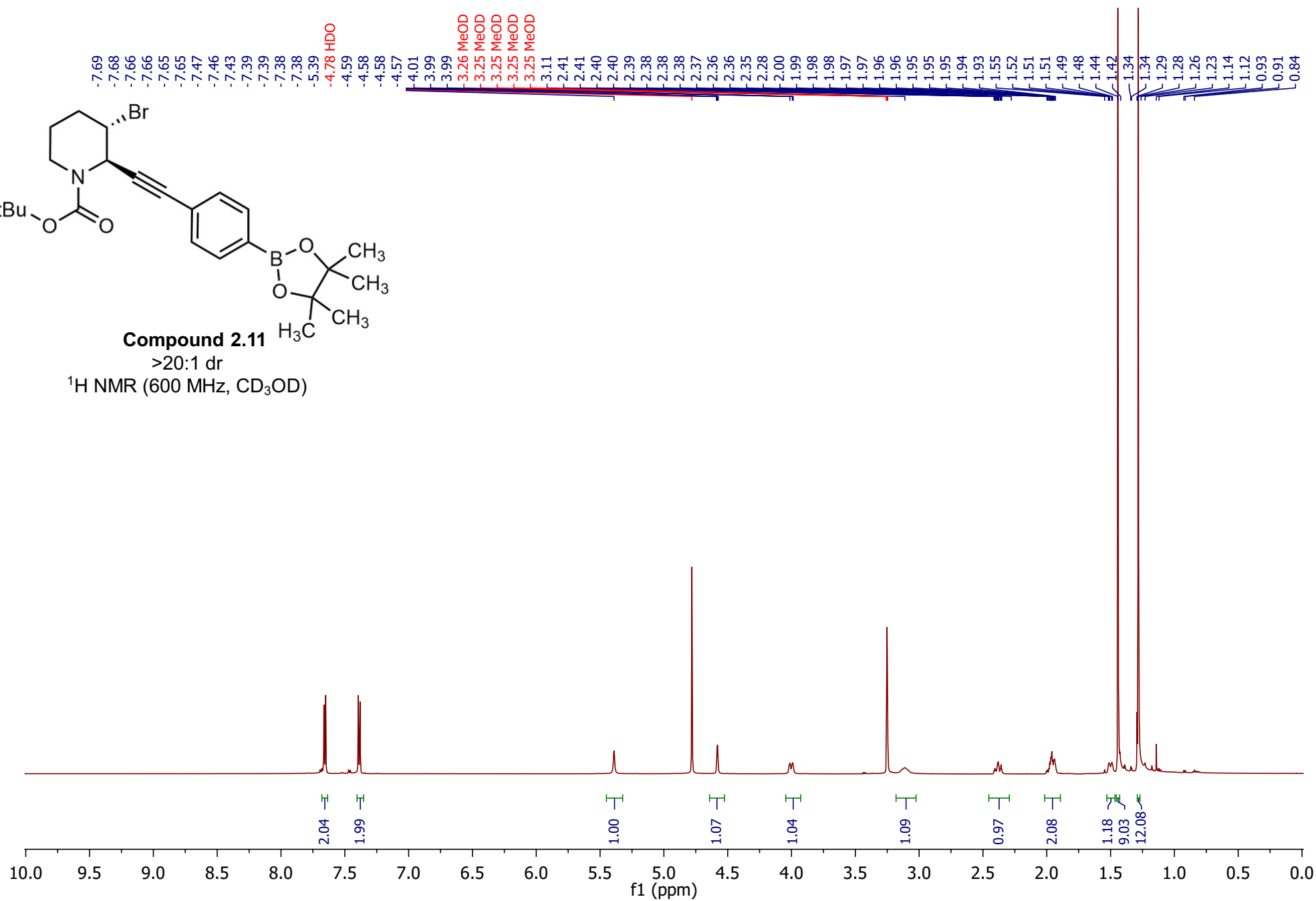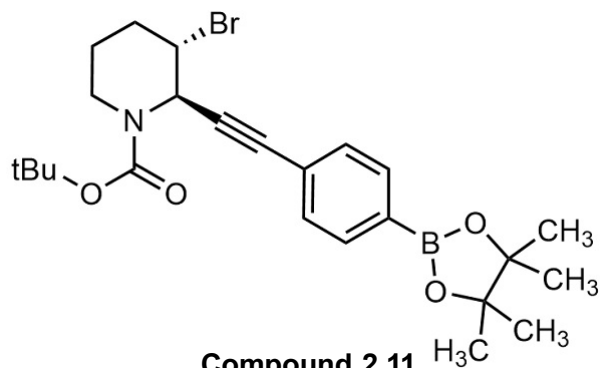
Compound 2.11
>20:1 dr
^{13}C NMR (151 MHz, CD$_3$OD)

154.74

134.25
130.54

124.64

86.22
85.01
83.95
80.67

74.43

51.11

39.00

28.25
27.23
23.79
23.63
19.44

200 190 180 170 160 150 140 130 120 110 100 90 80 70 60 50 40 30 20 10 0
f1 (ppm)
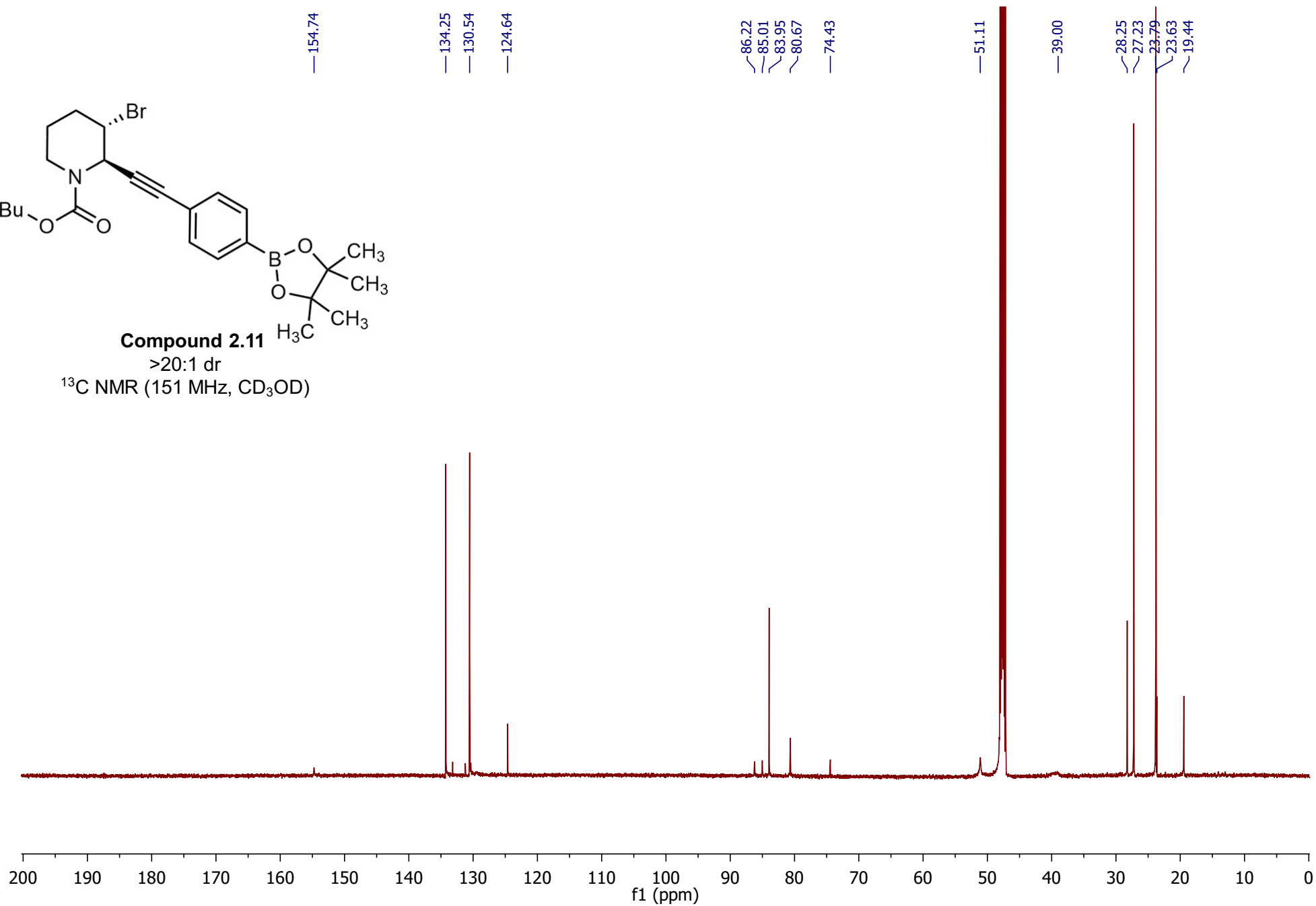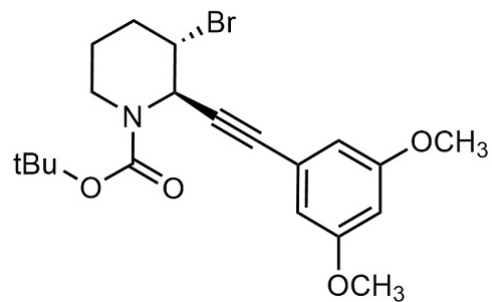
Compound 2.12
>20:1 dr
^{1}H NMR (400 MHz, CD$_3$OD)

6.58
6.48
6.48
6.39
6.38
6.38
5.31
4.78
4.51
4.51
4.50
4.49
3.95
3.92
3.92
3.66
3.64
3.20
3.20
3.19
3.19
3.18
3.04
2.36
2.35
2.32
2.31
2.29
2.28
2.27
1.94
1.91
1.90
1.88
1.87
1.87 HDO
1.85
1.84
1.45
1.44
1.41
1.38
1.28

1.99
0.99
1.00
1.05
1.00
6.00
0.96
1.00
2.10
1.01
9.08
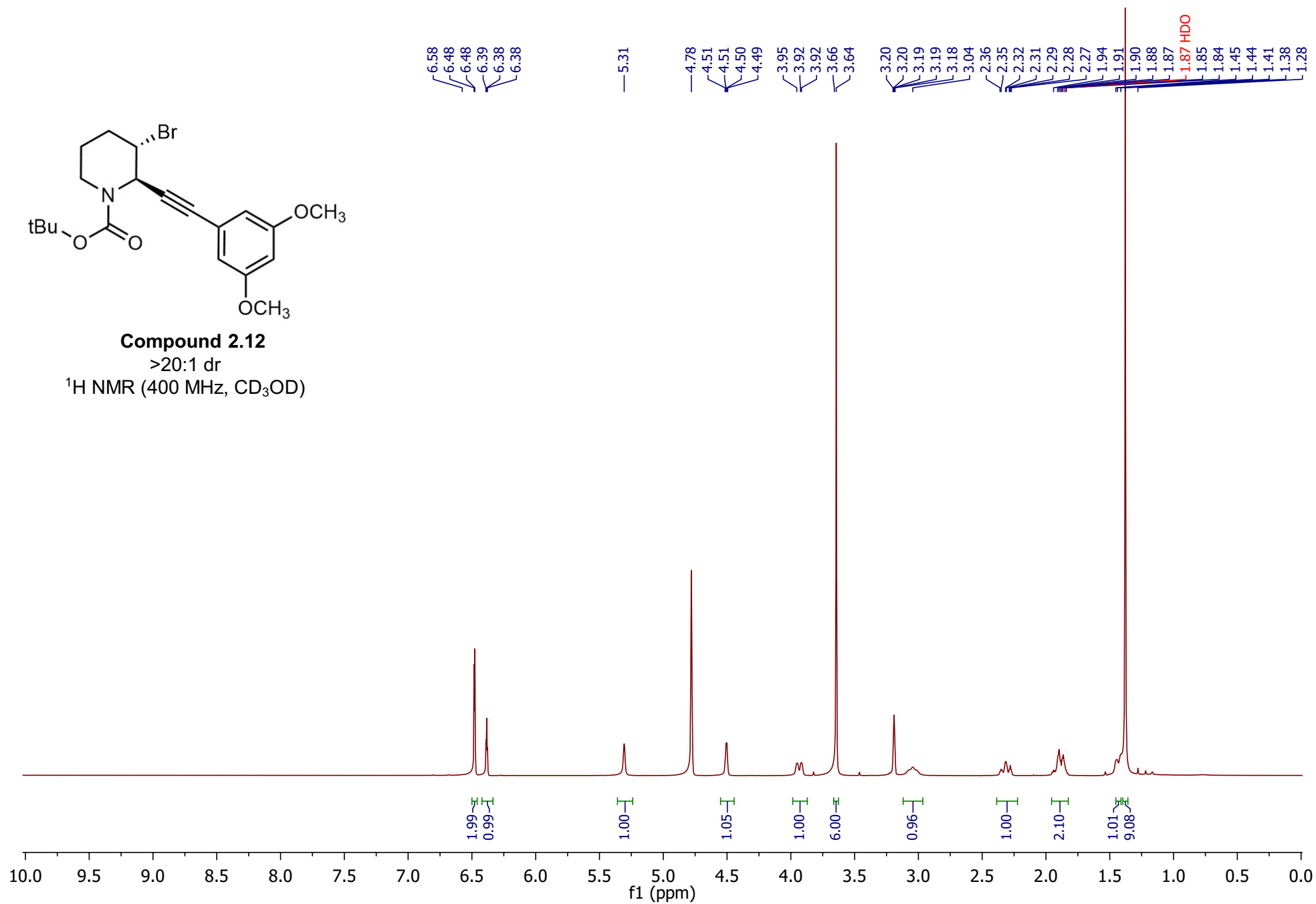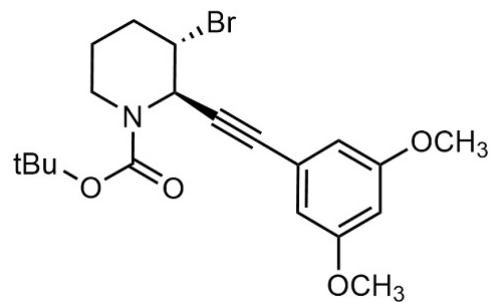
Compound 2.12
>20:1 dr
^{13}C NMR (151 MHz, CD$_3$OD)

160.81
154.68
123.15
109.21
101.48
86.33
83.10
80.63
54.56
51.25
50.40
39.11
28.29
27.29
19.48
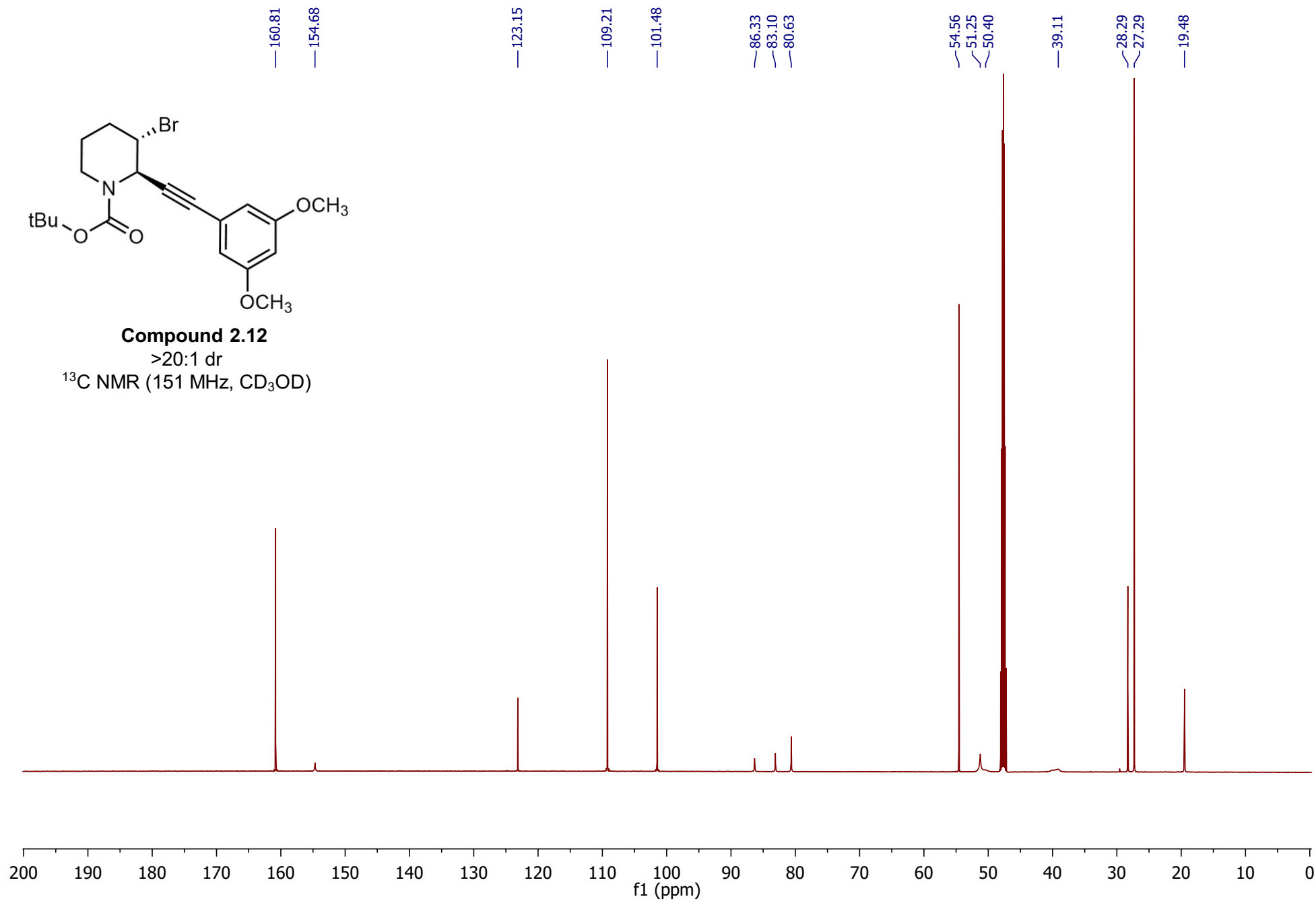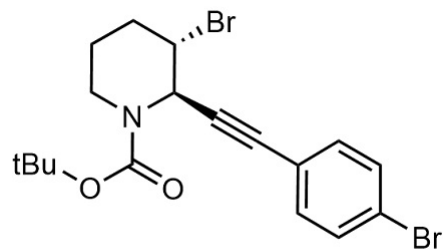
Compound 2.13
9:1 dr
^{1}H NMR (400 MHz, CD$_3$OD)
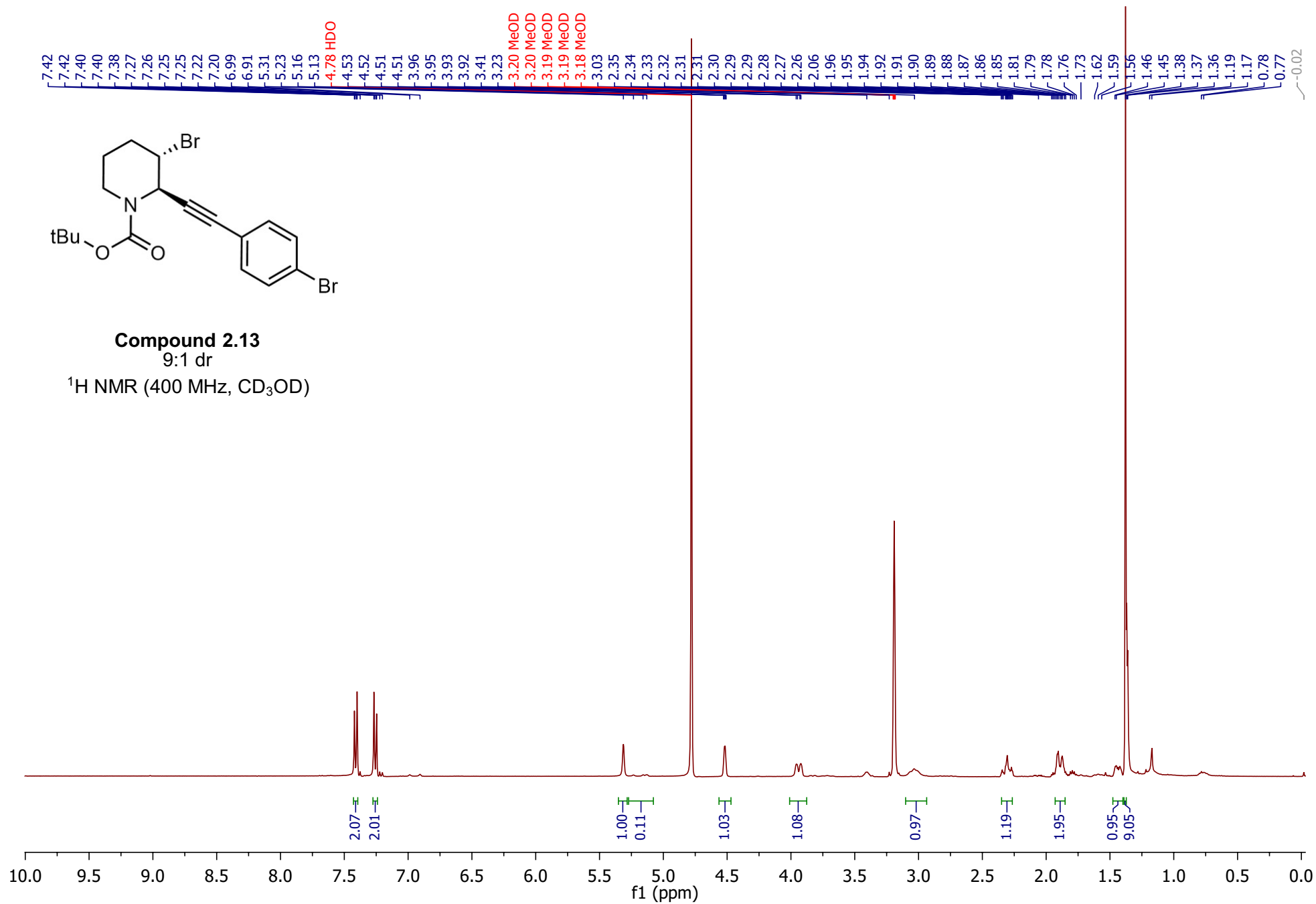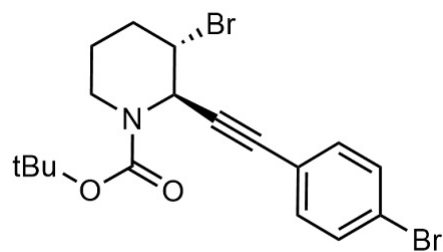
Compound 2.13
9:1 dr
^{13}C NMR (151 MHz, CD$_3$OD)
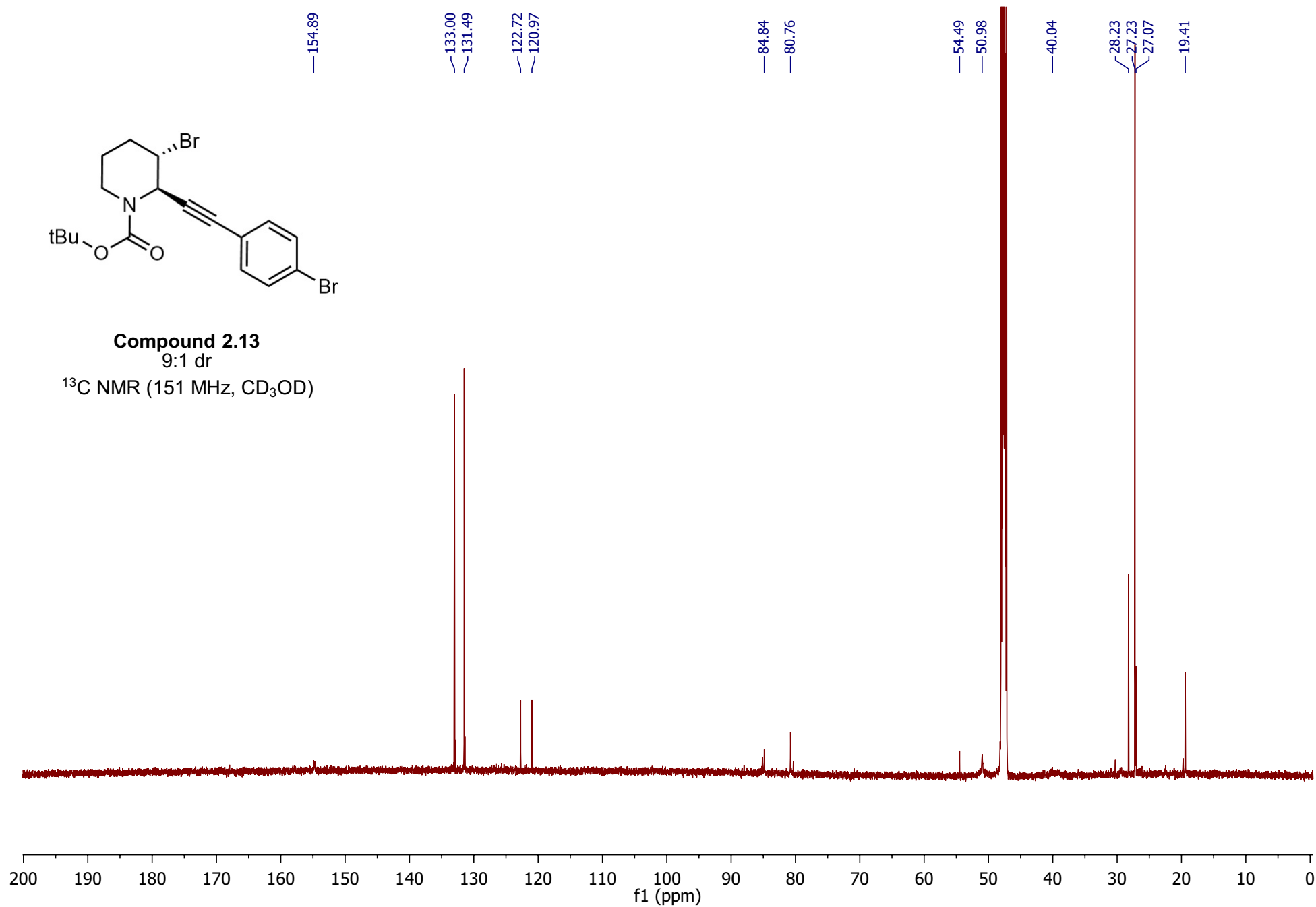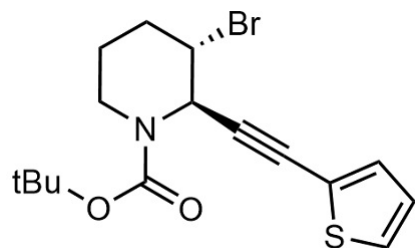
Compound 2.14

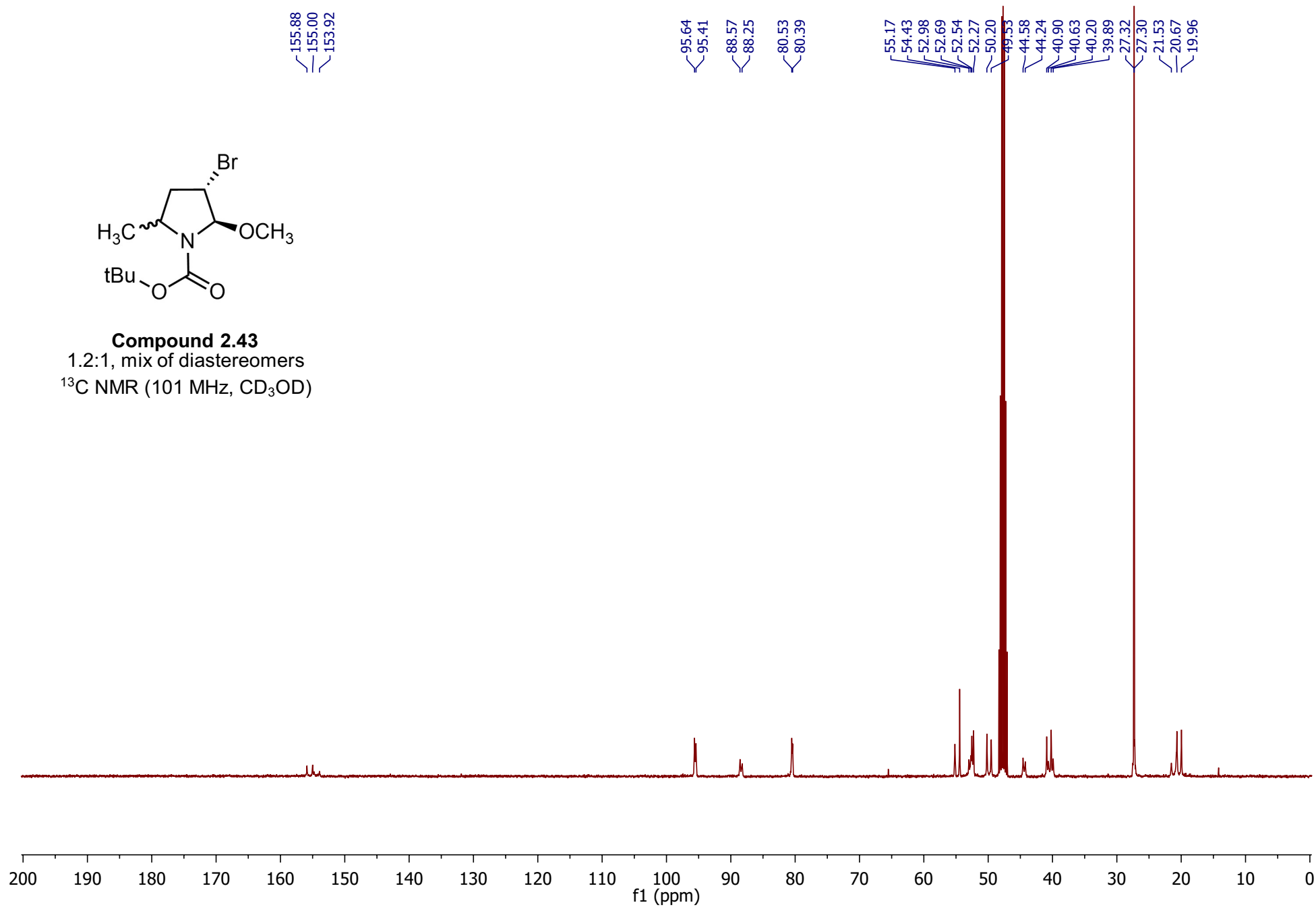4.5:1 dr, mix of diastereomers

^{1}H NMR (400 MHz, CD$_{3}$OD)

Compound 2.14
4.5:1 dr, mix of diastereomers
^{13}C NMR (101 MHz, CD$_3$OD)

154.68

132.55
127.75
126.88

121.36

87.37
84.78
83.59
80.70
80.51
79.49

54.47
50.94
48.70

37.43
36.01
29.51
28.28
27.24
27.16
26.49
26.16

19.43

200 190 180 170 160 150 140 130 120 110 100 90 80 70 60 50 40 30 20 10 0
f1 (ppm)
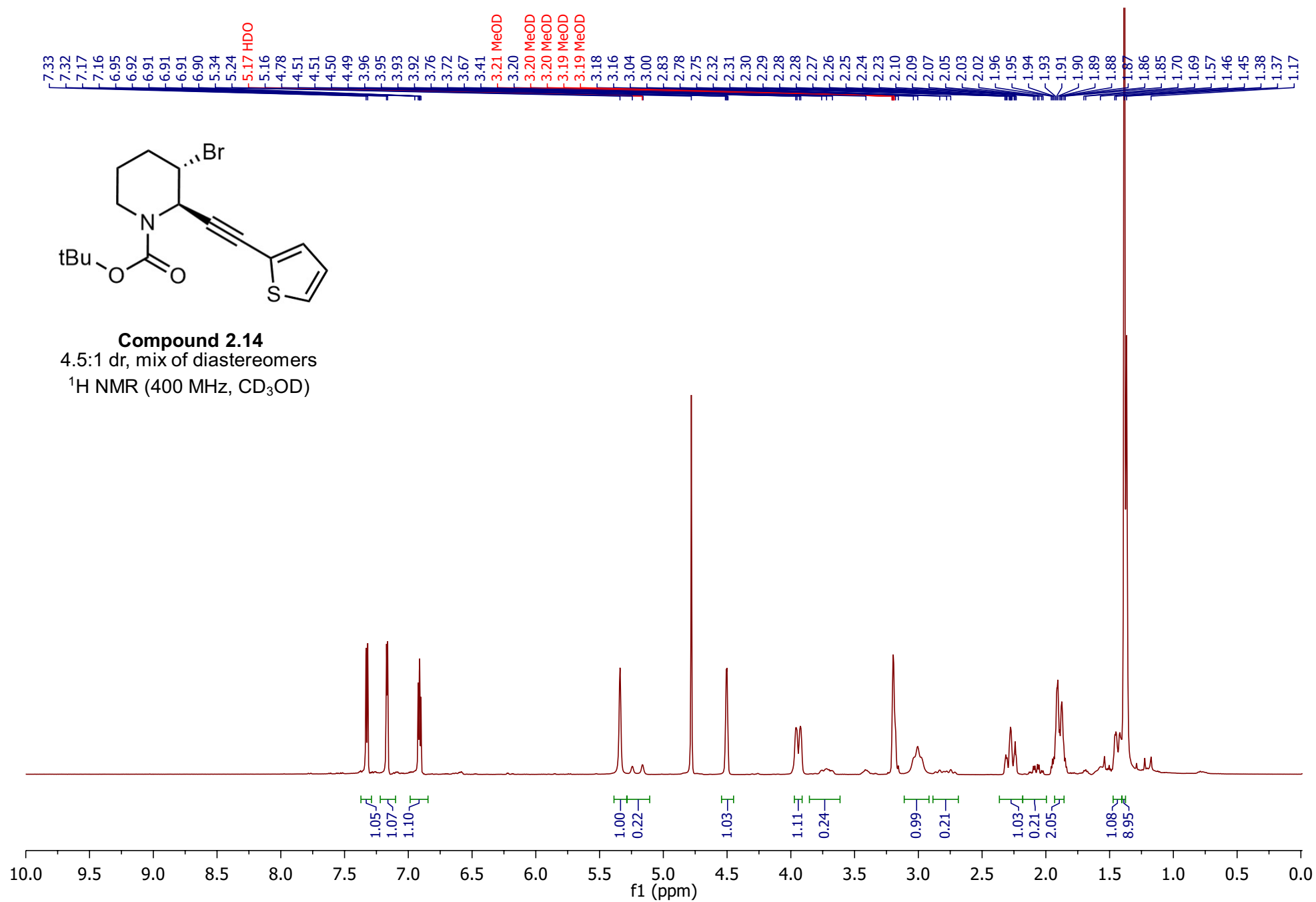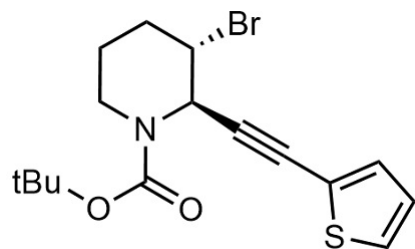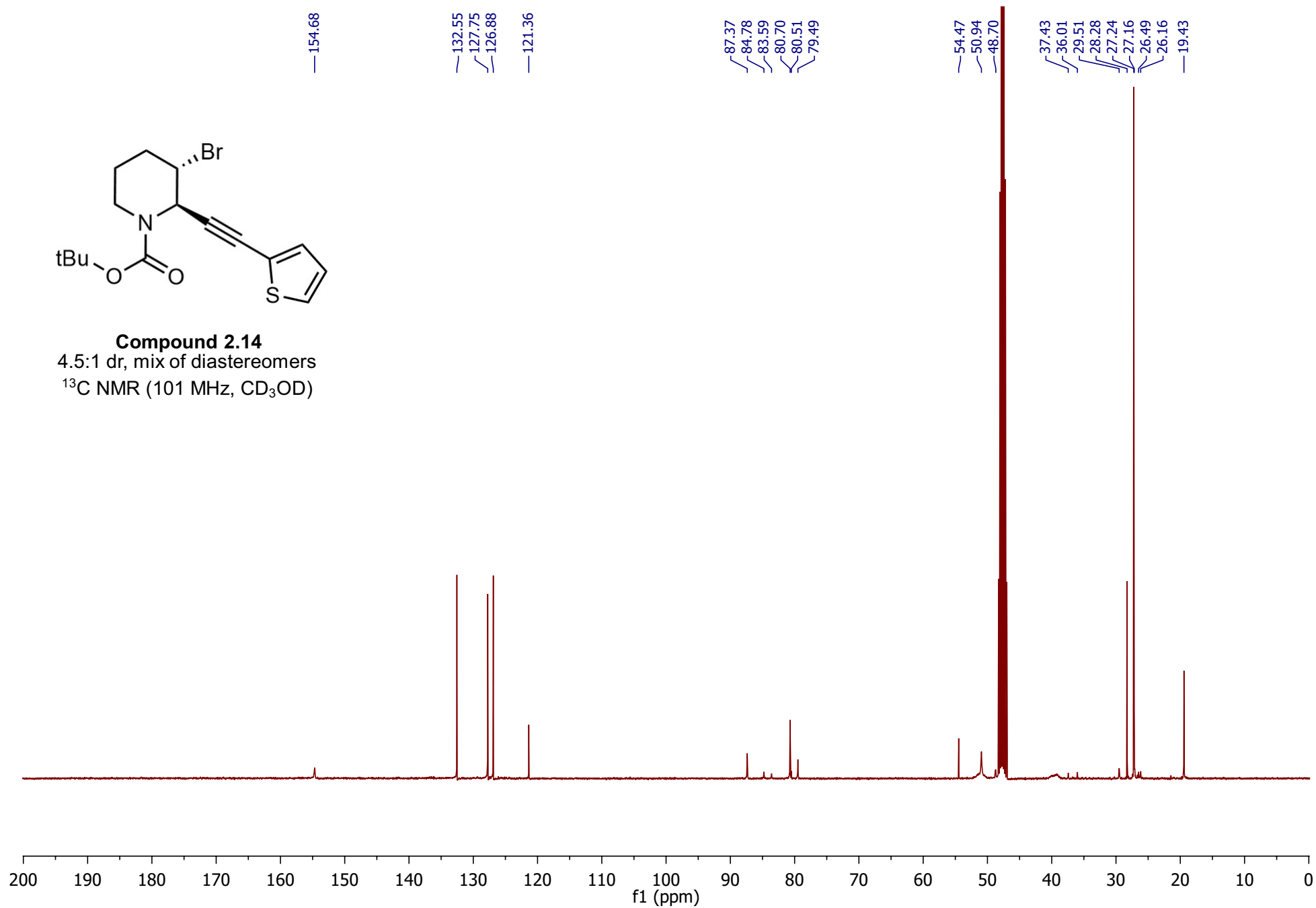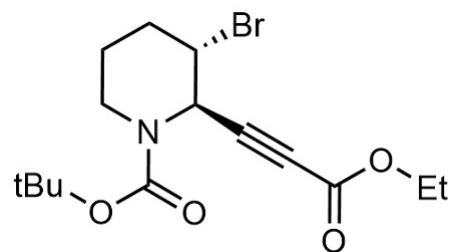
Compound 2.15
>20:1 dr
^{1}H NMR (400 MHz, CD$_3$OD)
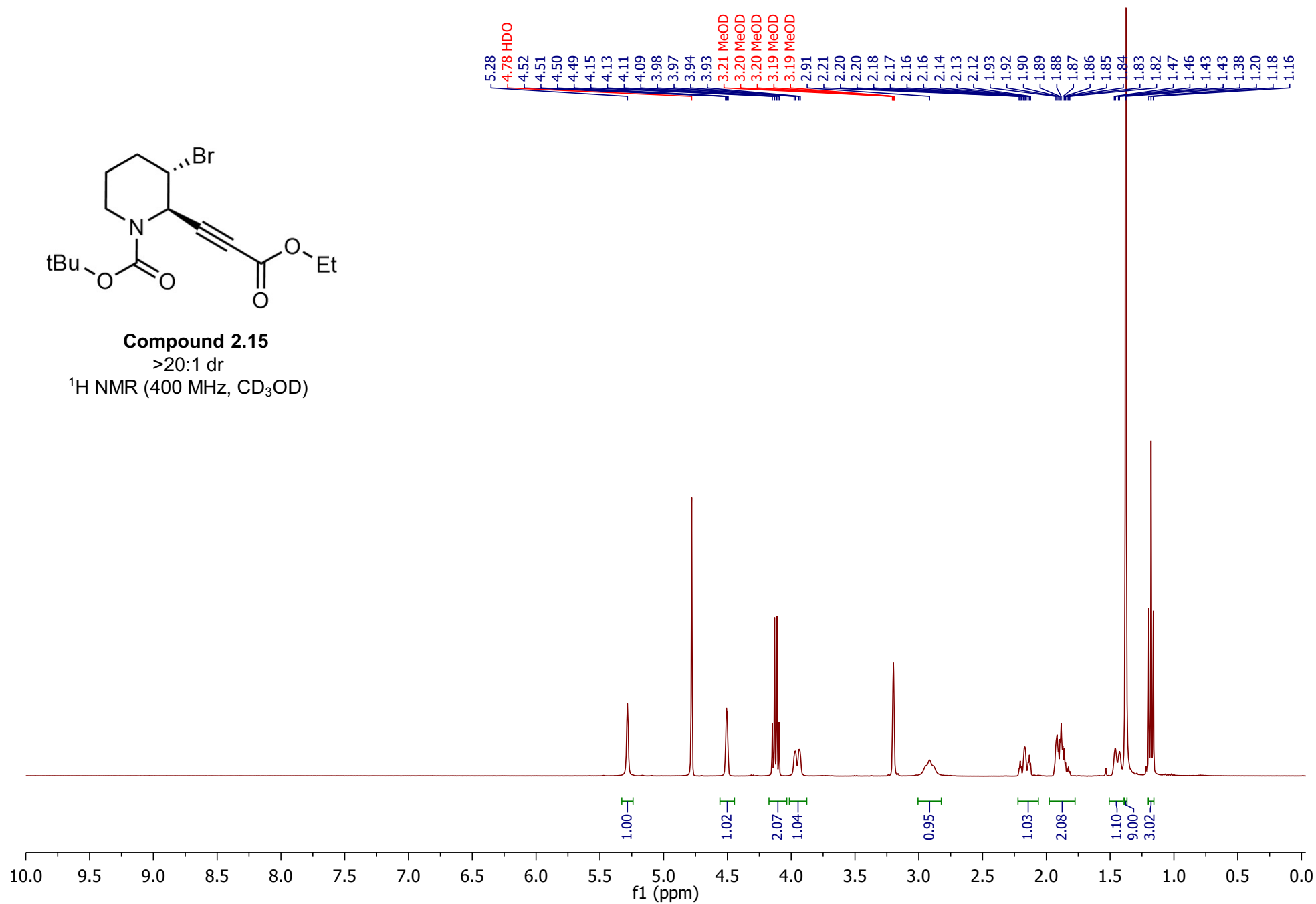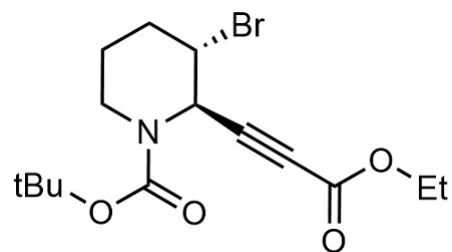
Compound 2.15
>20:1 dr
^{13}C NMR (101 MHz, CD$_3$OD)
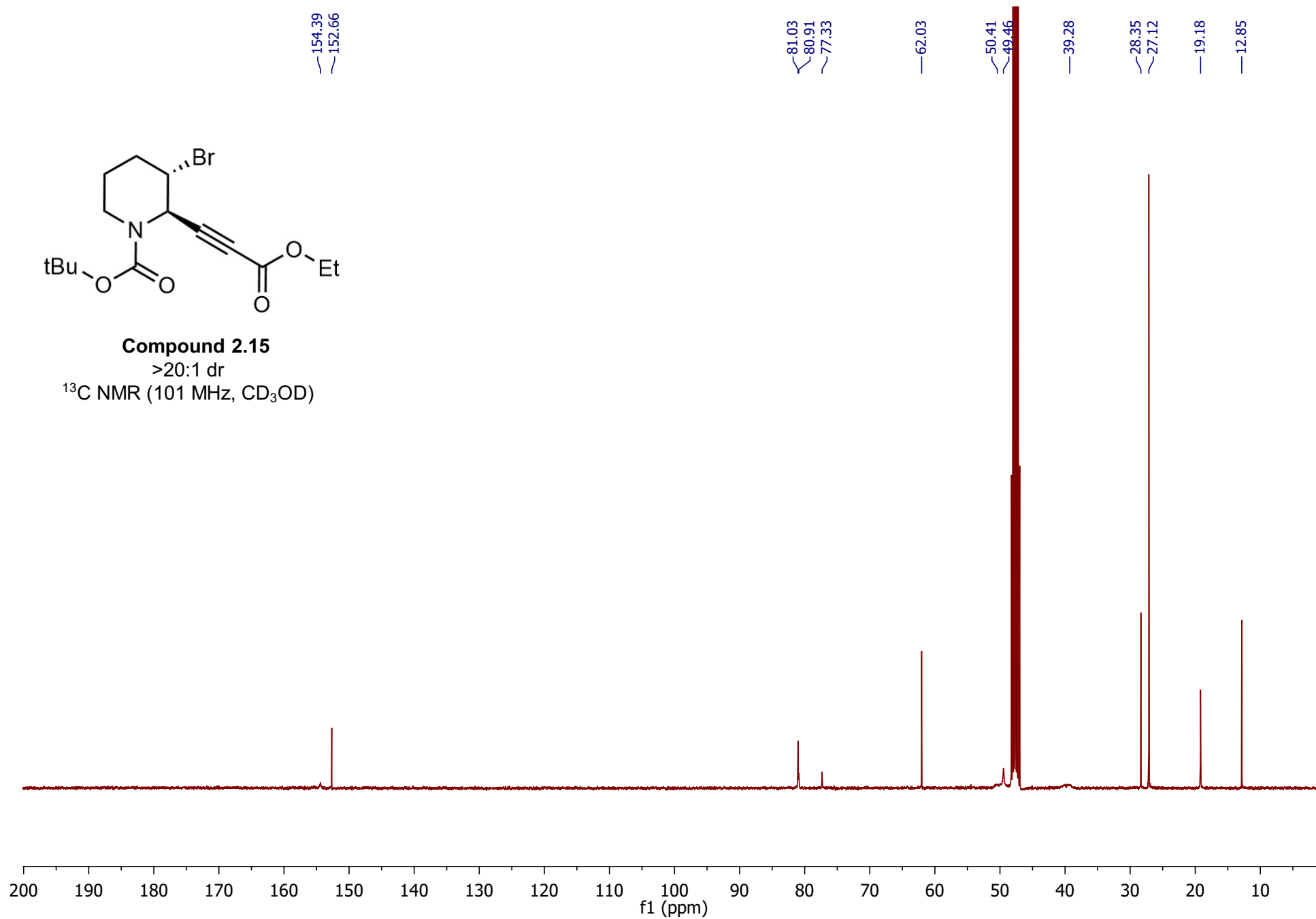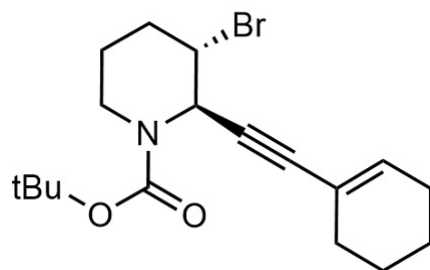
Compound 2.16
>20:1 dr
^{1}H NMR (400 MHz, CD$_3$OD)
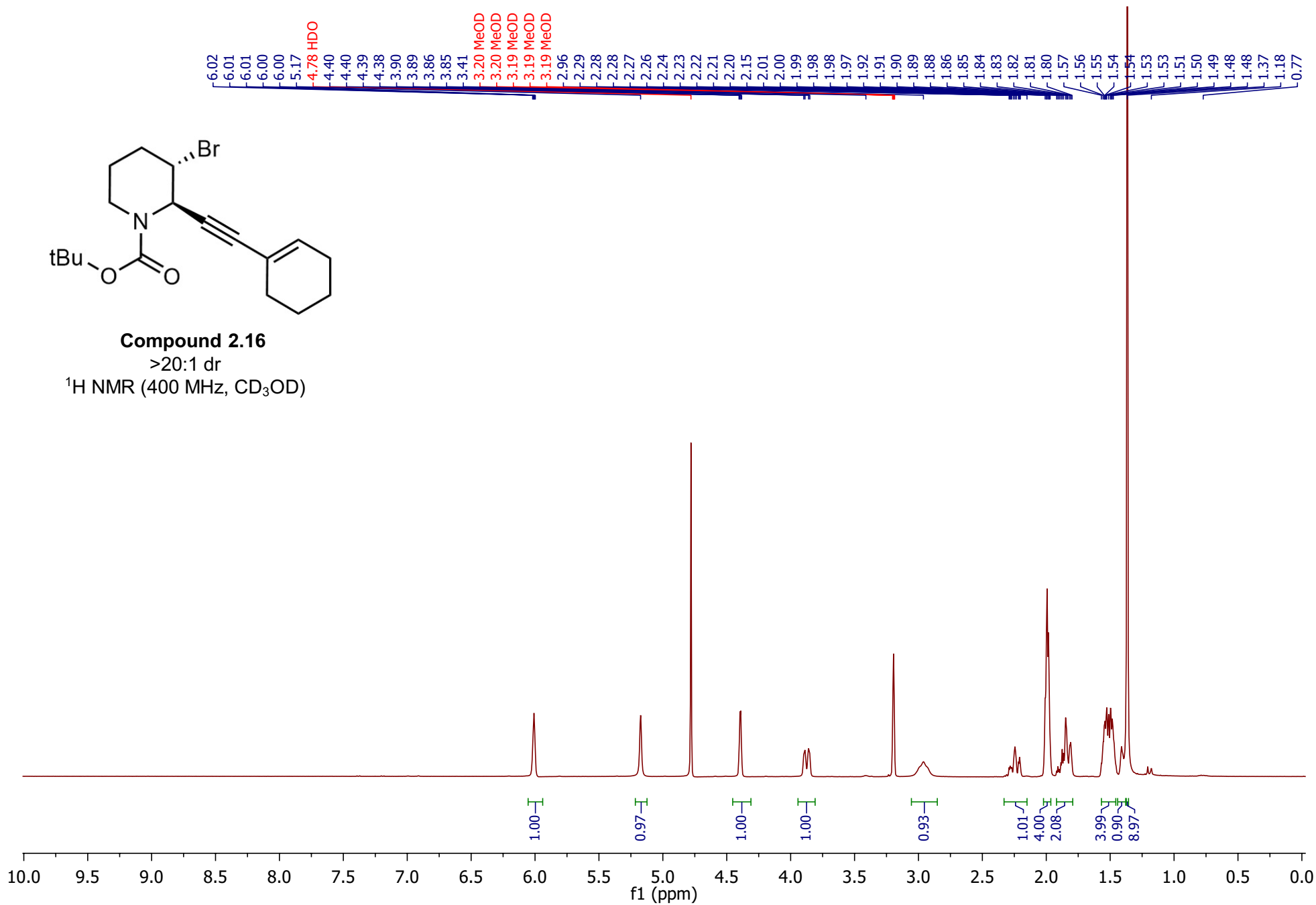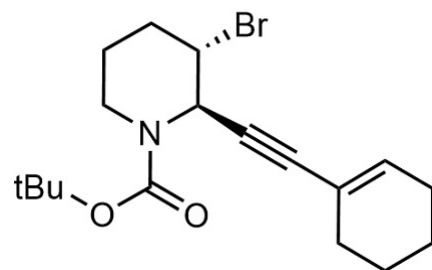
Compound 2.16
>20:1 dr
^{13}C NMR (151 MHz, CD$_3$OD)

154.76

135.47

119.66

88.23

80.87
80.56

51.54
50.46

38.76

28.75
28.07
27.28
25.18
21.94
21.14
19.46
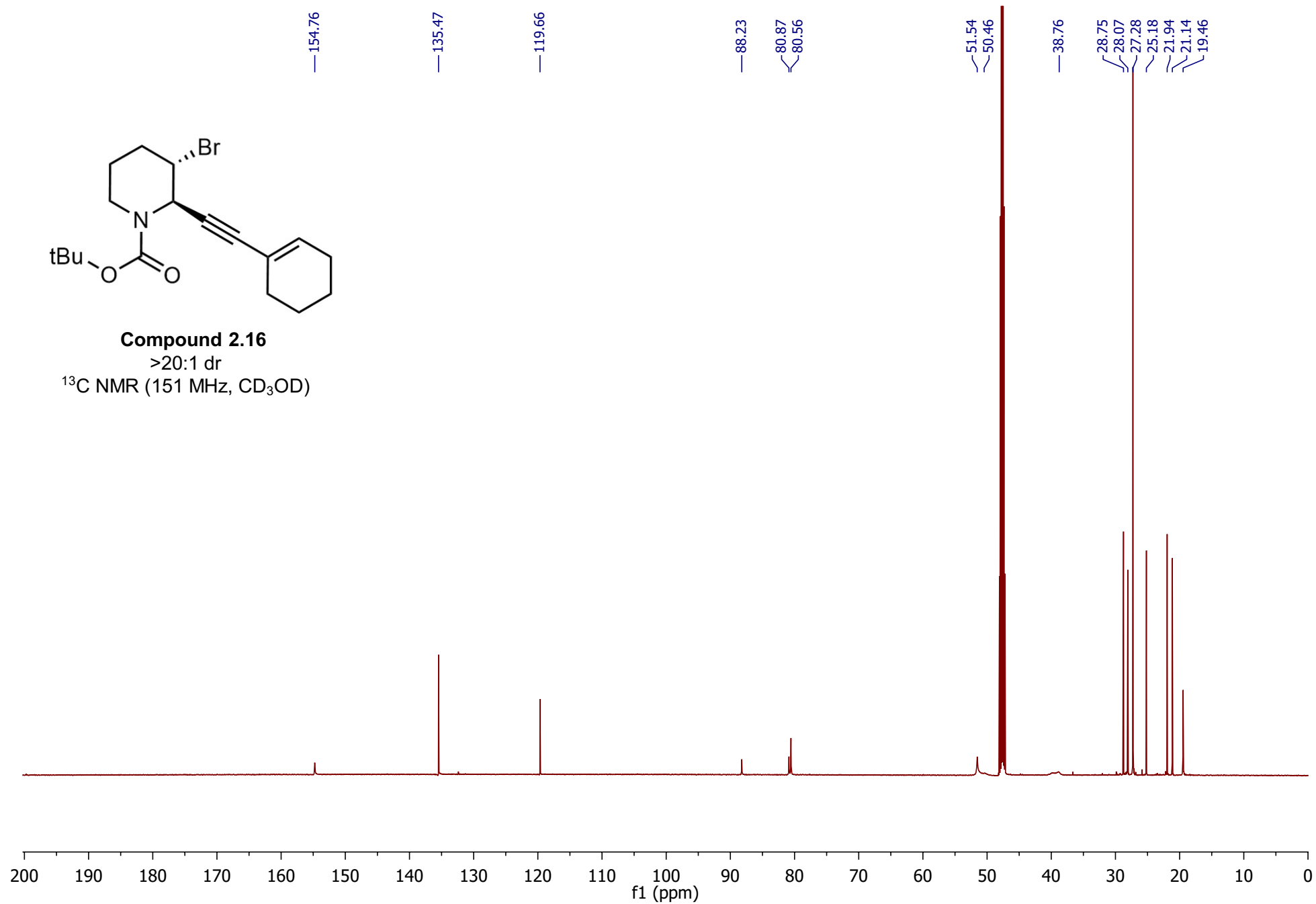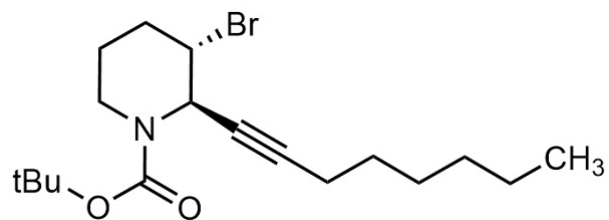
Compound 2.17
>20:1 dr
^{1}H NMR (400 MHz, CD$_3$OD)
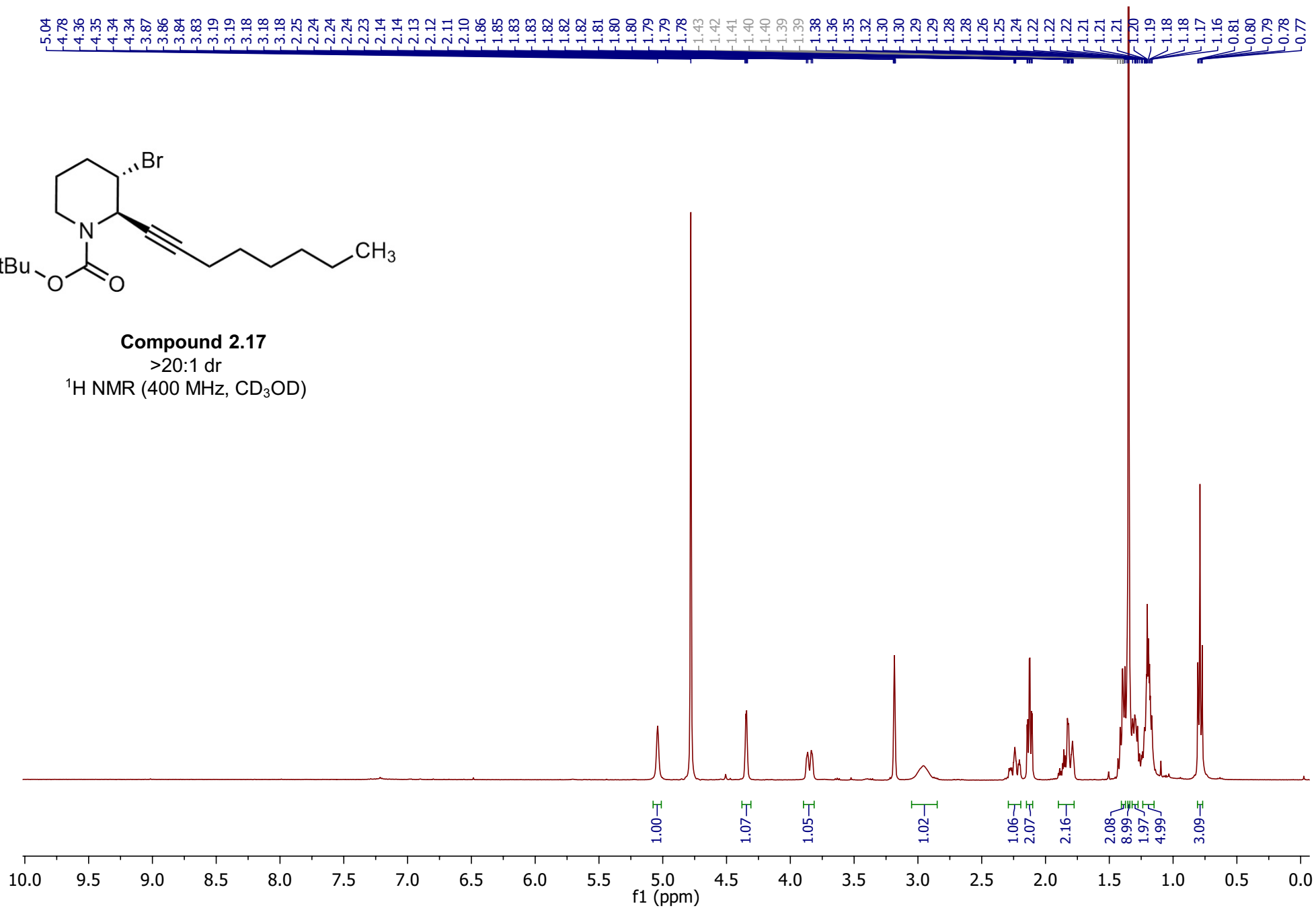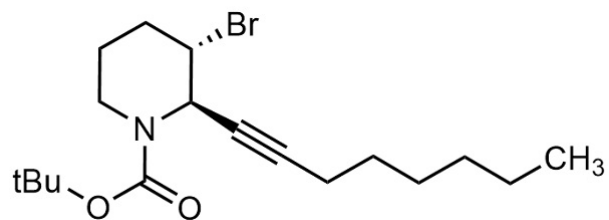
Compound 2.17
>20:1 dr
^{13}C NMR (101 MHz, CD$_3$OD)
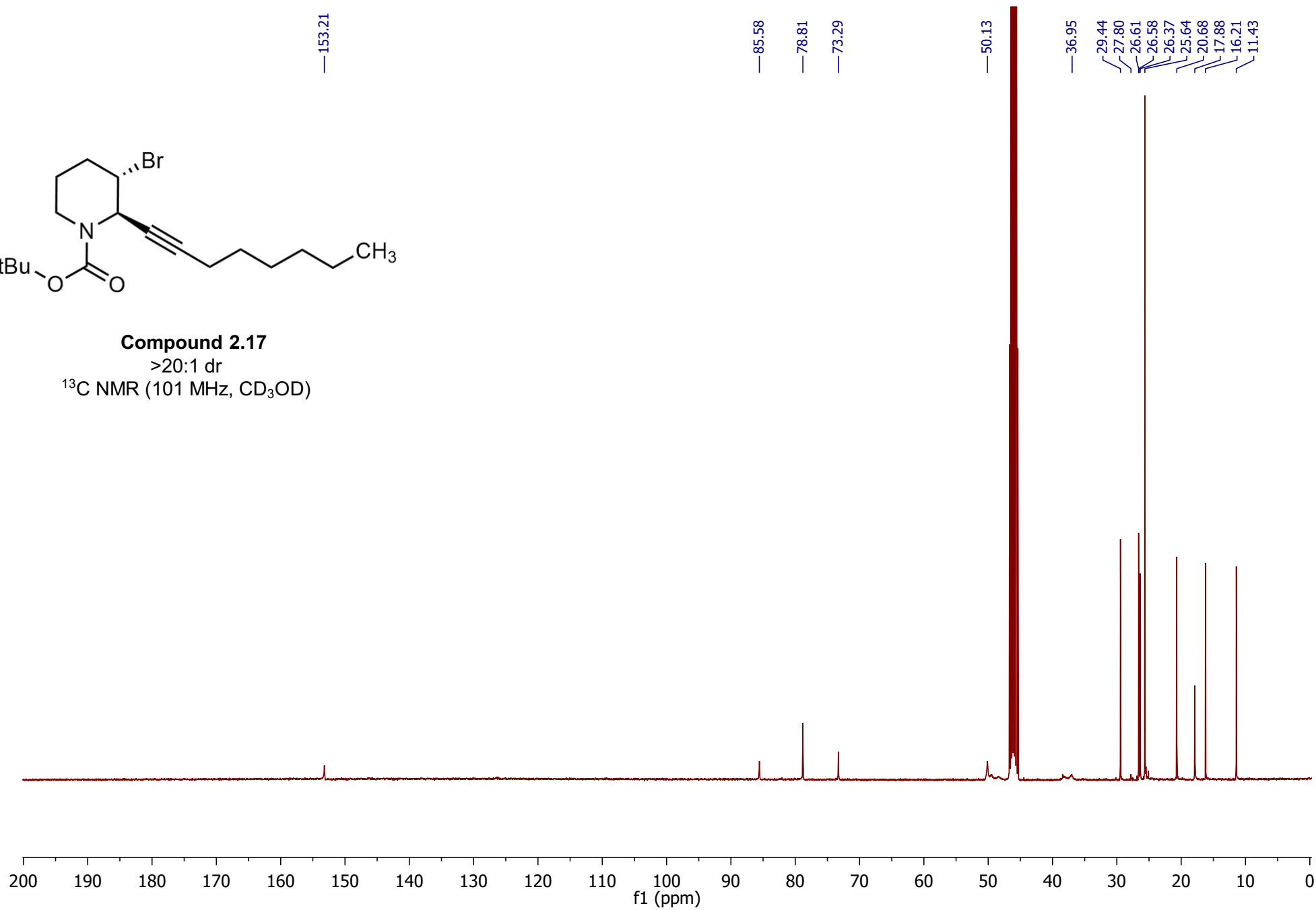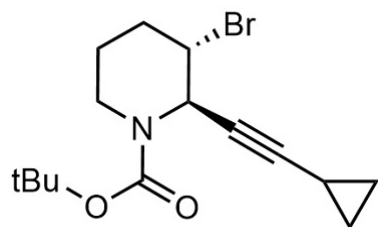
Compound 2.18
>20:1 dr
^{1}H NMR (400 MHz, CD$_3$OD)
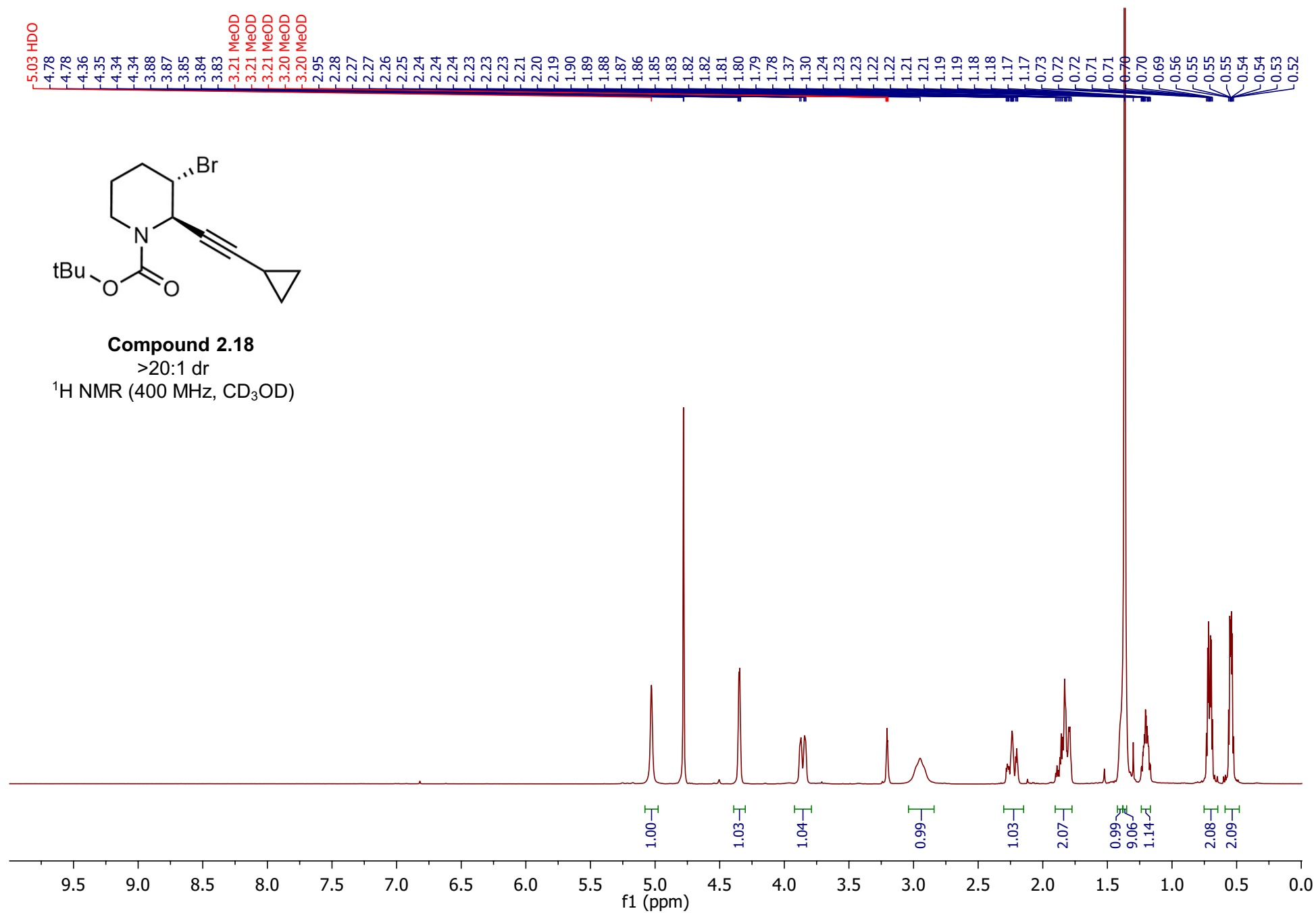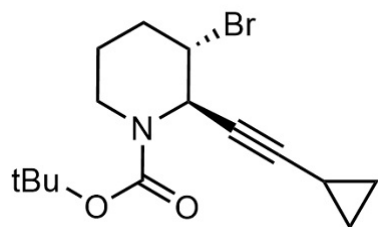
Compound 2.18
>20:1 dr
^{13}C NMR (101 MHz, CD$_3$OD)
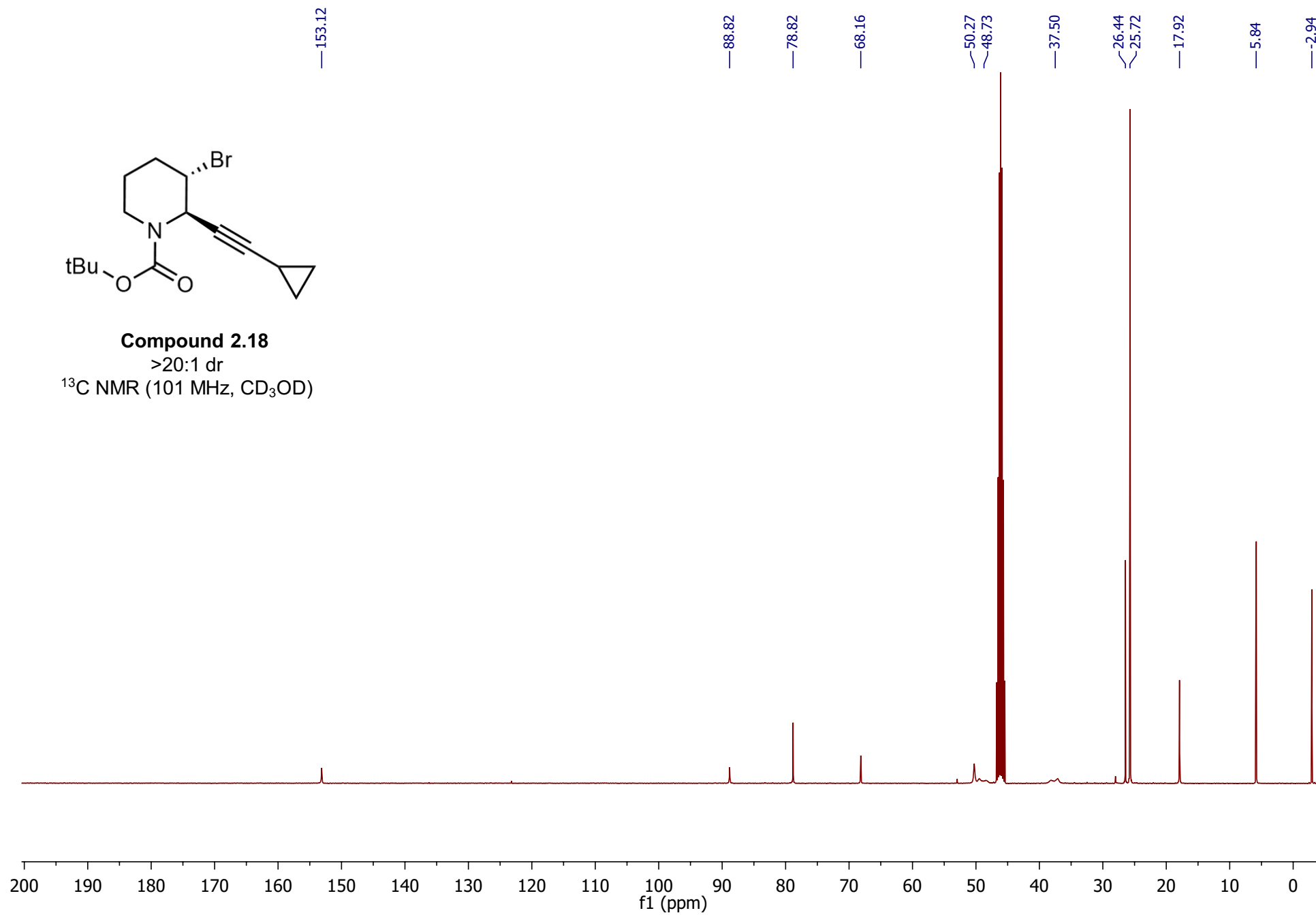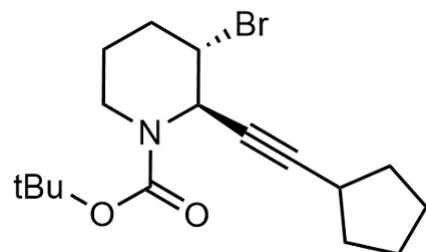
Compound 2.19
>20:1 dr
^{1}H NMR (600 MHz, CD$_3$OD)
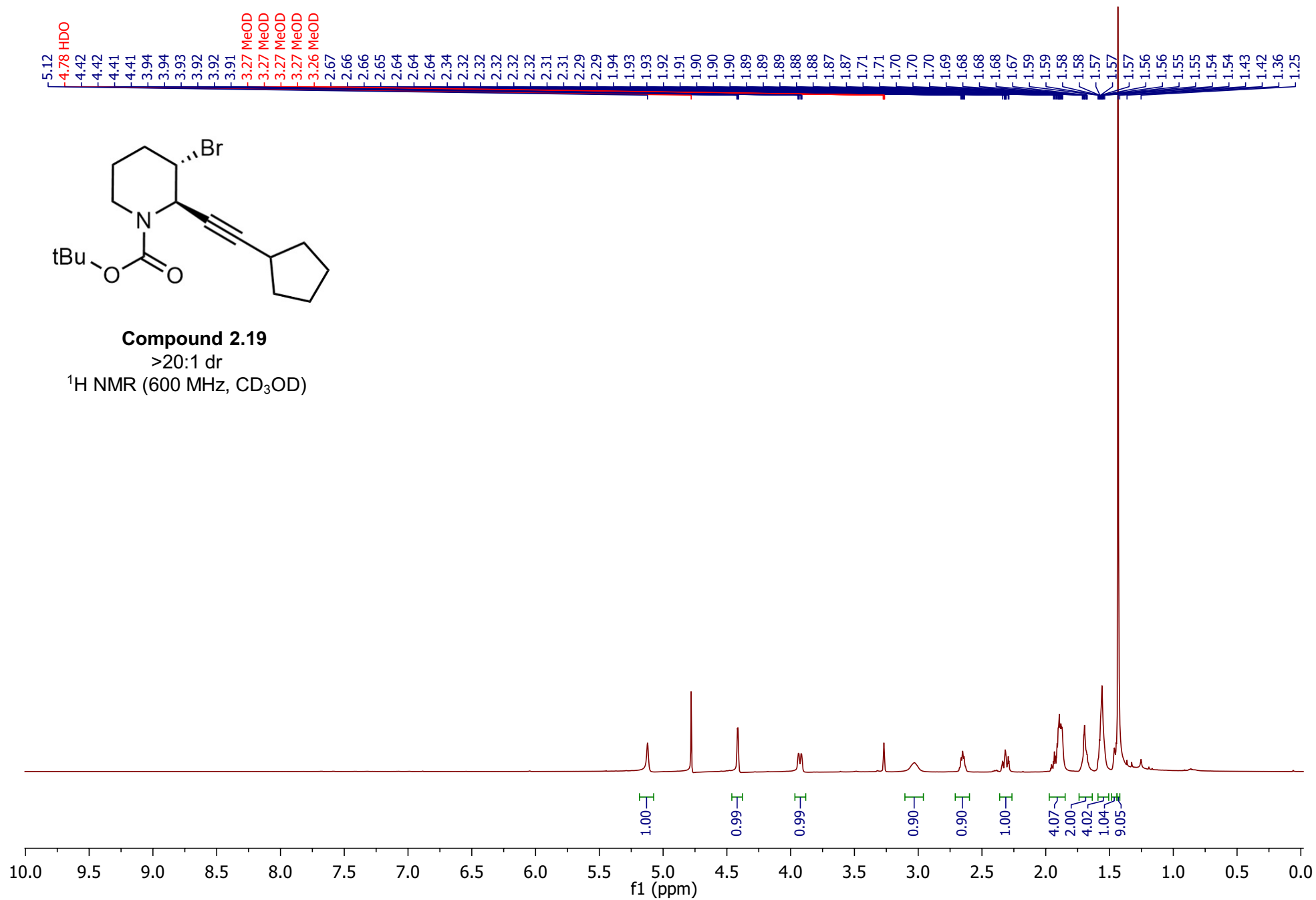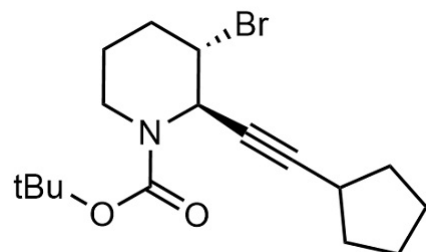
Compound 2.19
>20:1 dr
^{13}C NMR (151 MHz, CD$_3$OD)

154.78

91.54

80.37

74.44

51.80
50.78

39.29

33.45
29.84
27.98
27.27
24.43
19.48
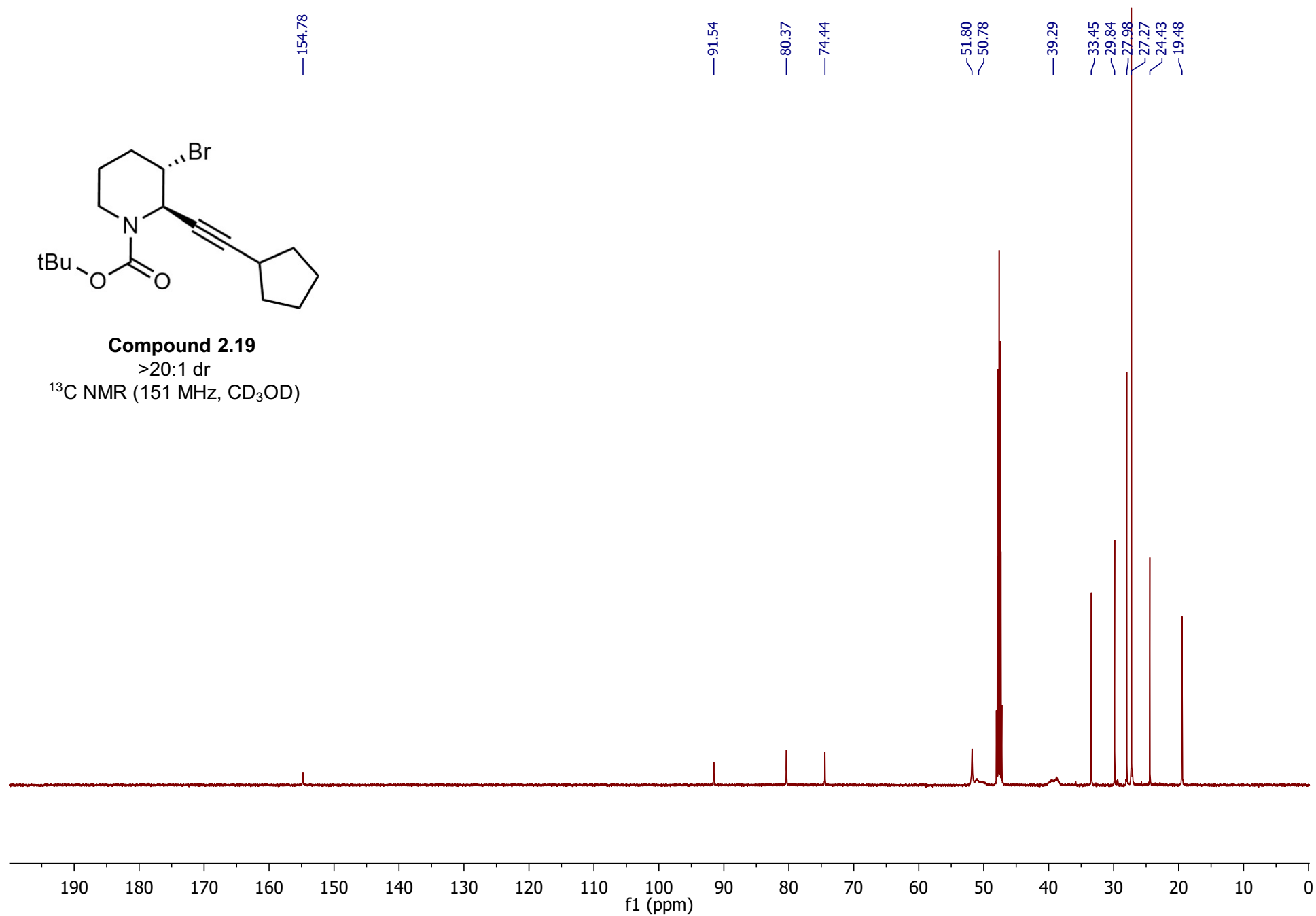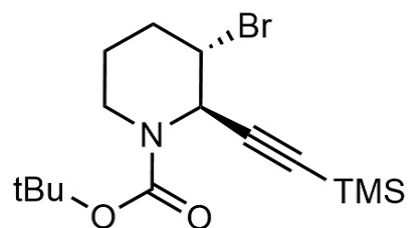
Compound 2.20
>20:1 dr
^{1}H NMR (600 MHz, CD$_3$OD)
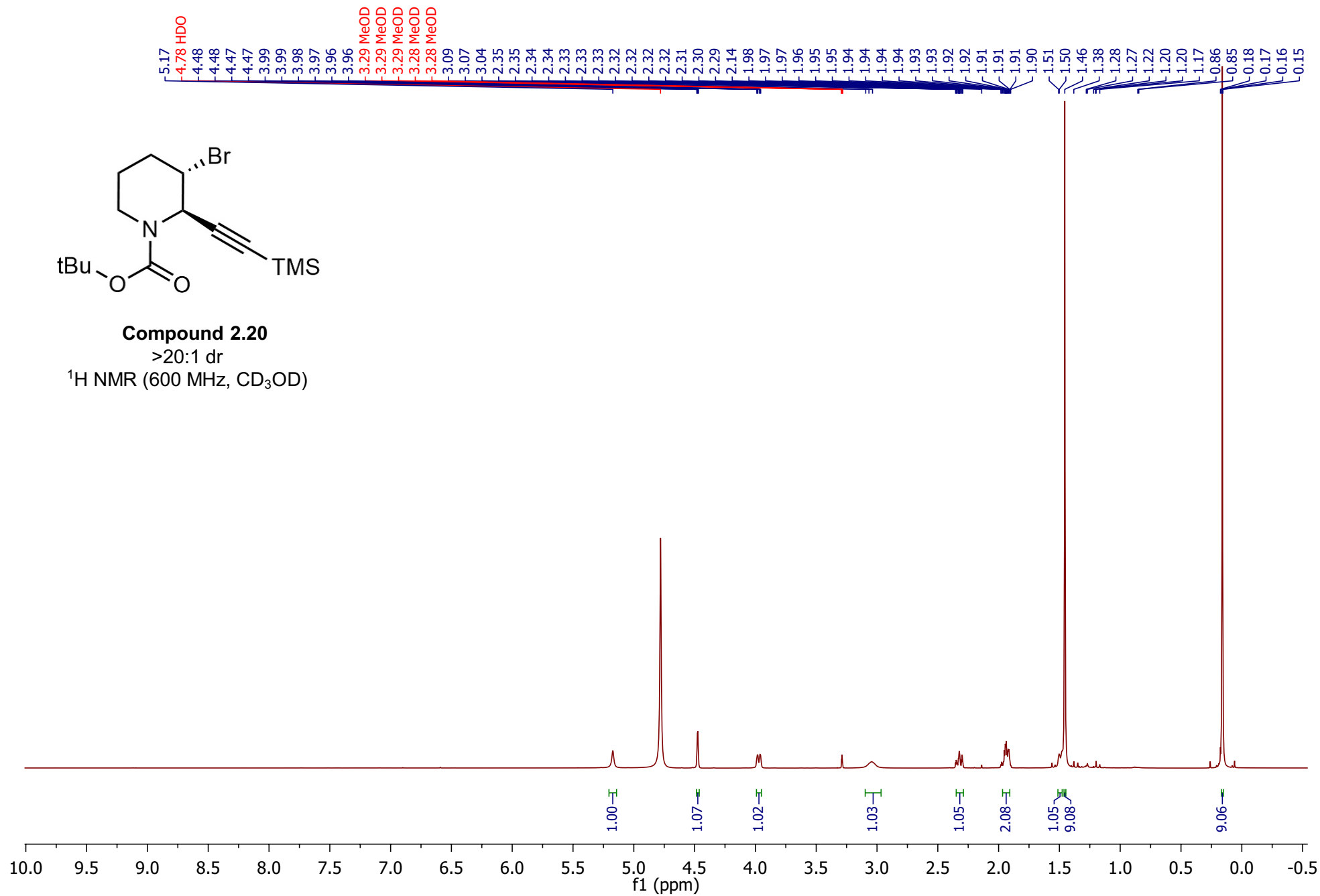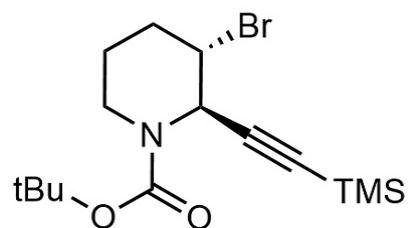
Compound 2.20
>20:1 dr
^{13}C NMR (151 MHz, CD$_3$OD)
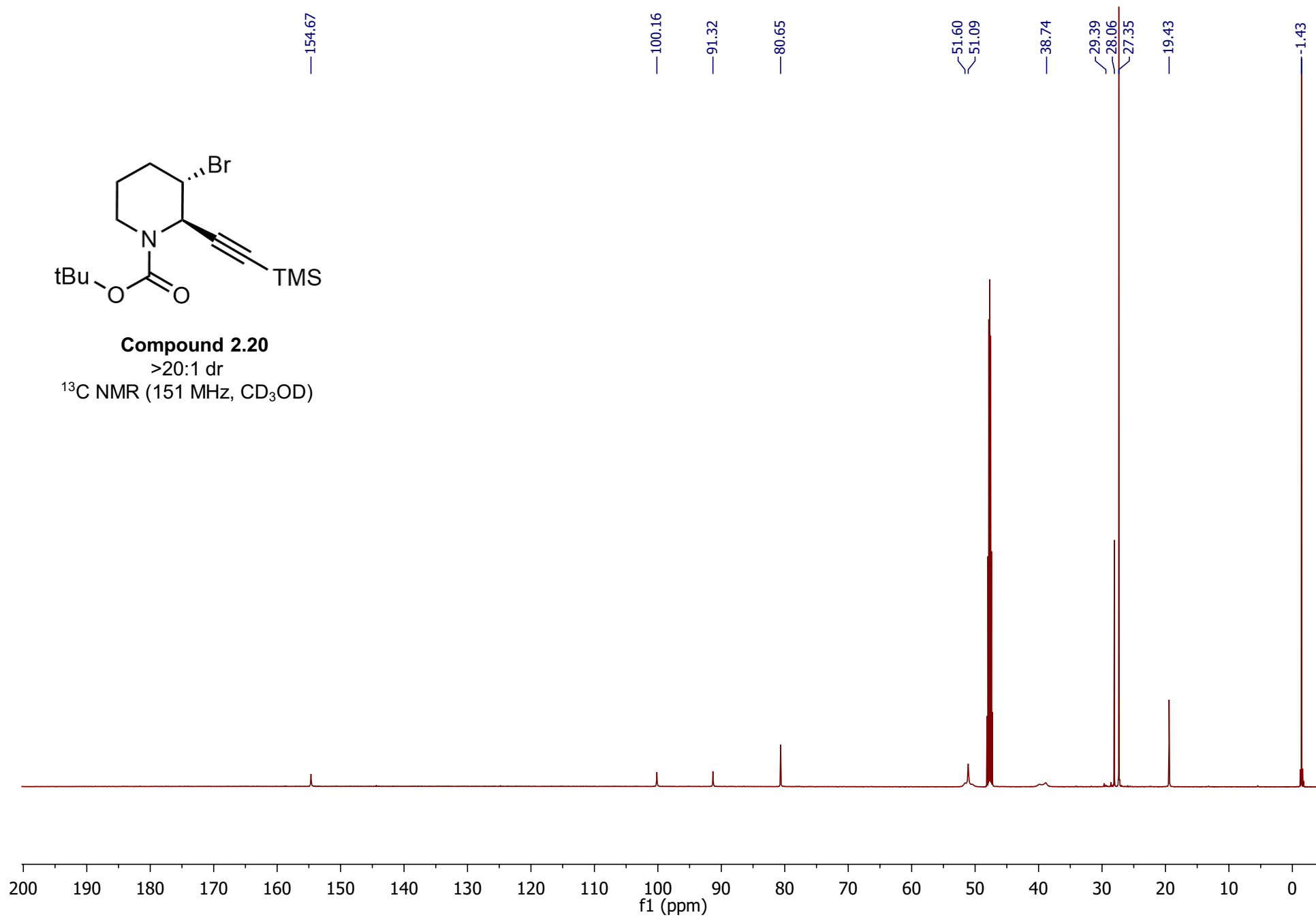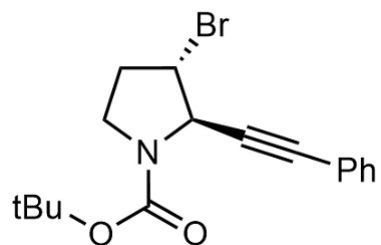
Compound 2.21
>20:1 dr
^{1}H NMR (400 MHz, CD$_3$OD)
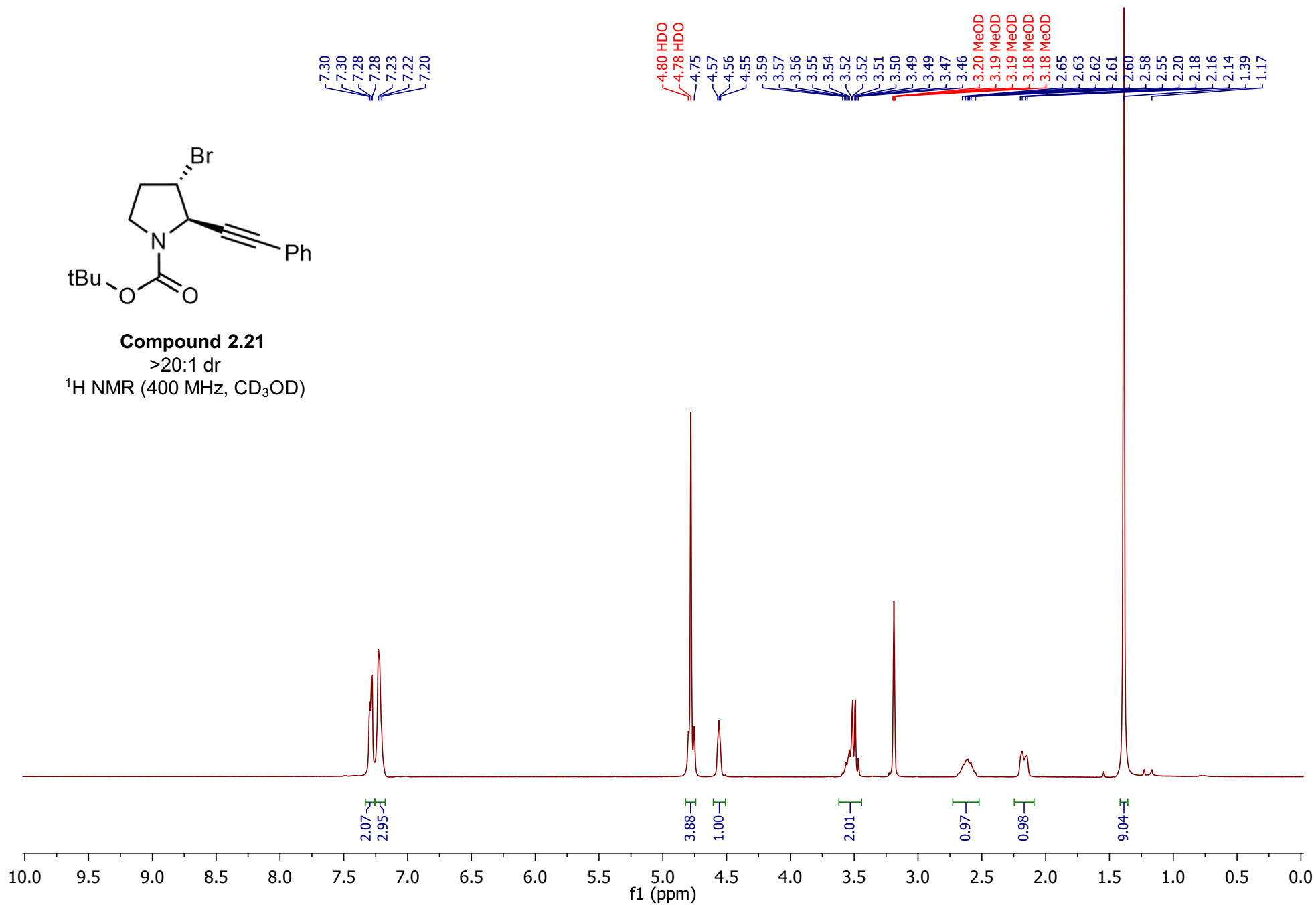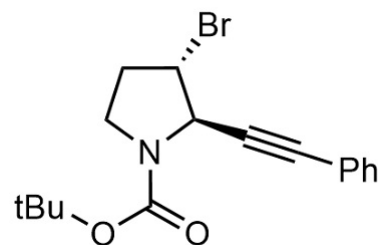
Compound 2.21
>20:1 dr, rotamers
^{13}C NMR (101 MHz, CD$_3$OD)

154.62
154.48
131.30
131.19
128.48
128.18
128.09
122.07
85.53
85.34
84.29
84.12
80.57
58.72
58.31
52.08
51.59
43.80
43.35
34.20
33.45
27.29
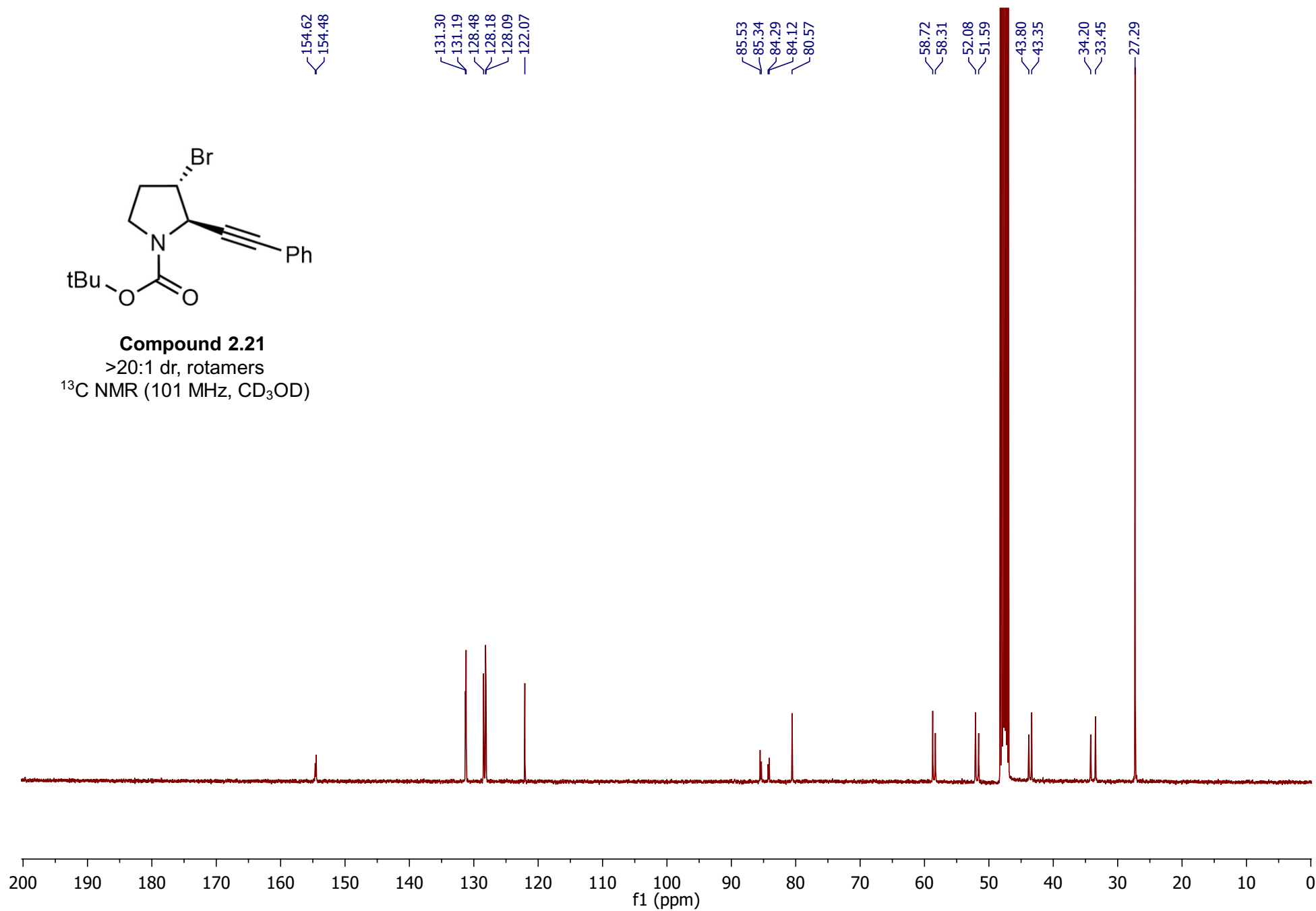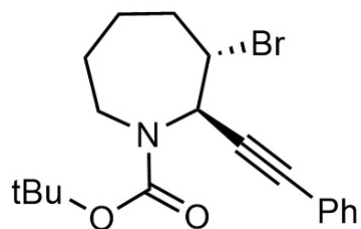
Compound 2.22

4.5:1 dr

mix of diastereomers and rotamers

^{1}H NMR (400 MHz, DMSO, 298K)
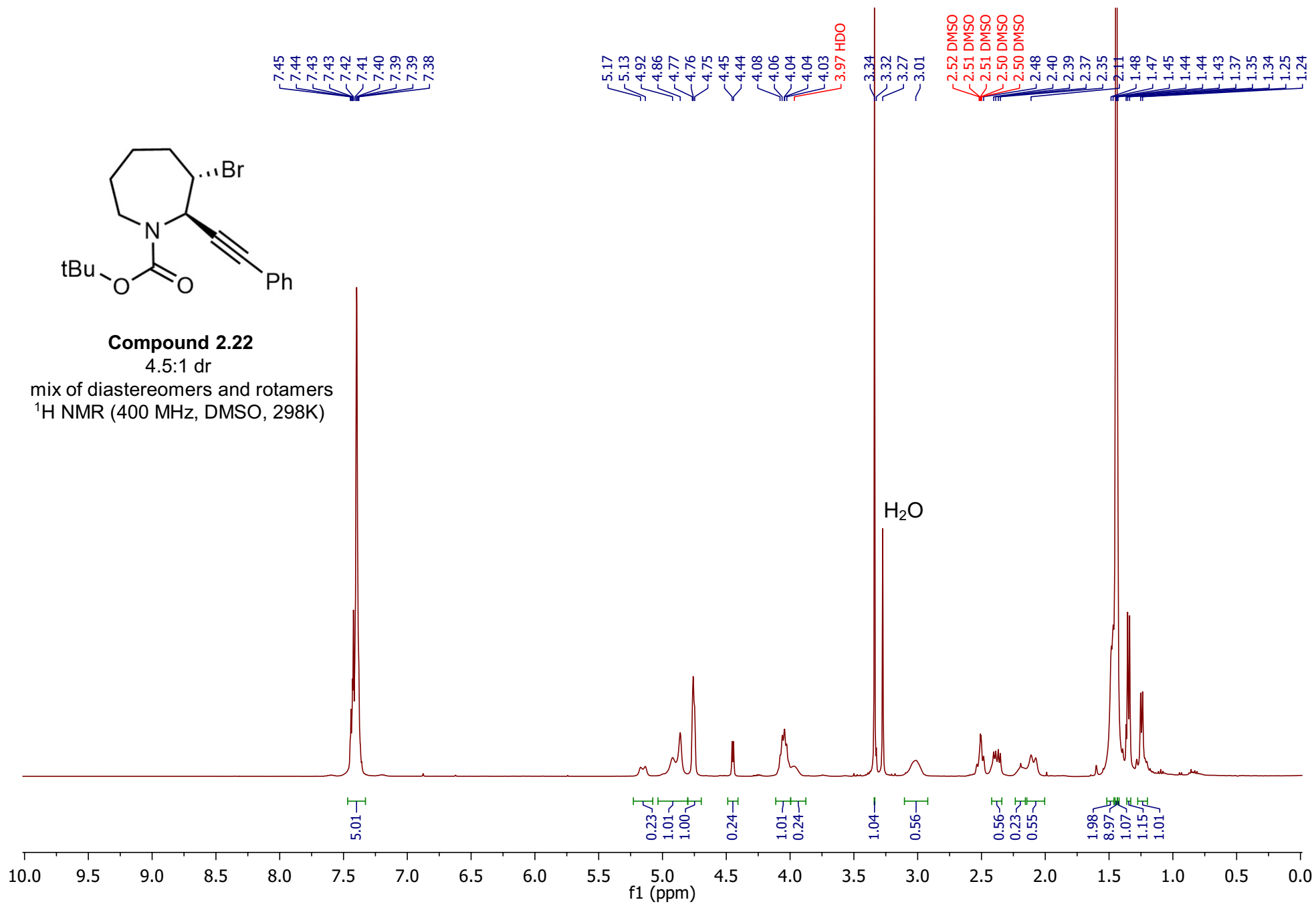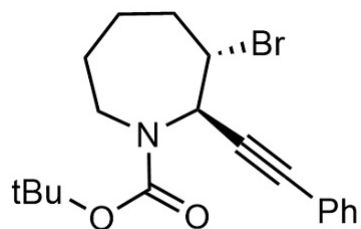
Compound 2.22
4.5:1 dr
mix of diastereomers
^{1}H NMR (400 MHz, DMSO, 350K)
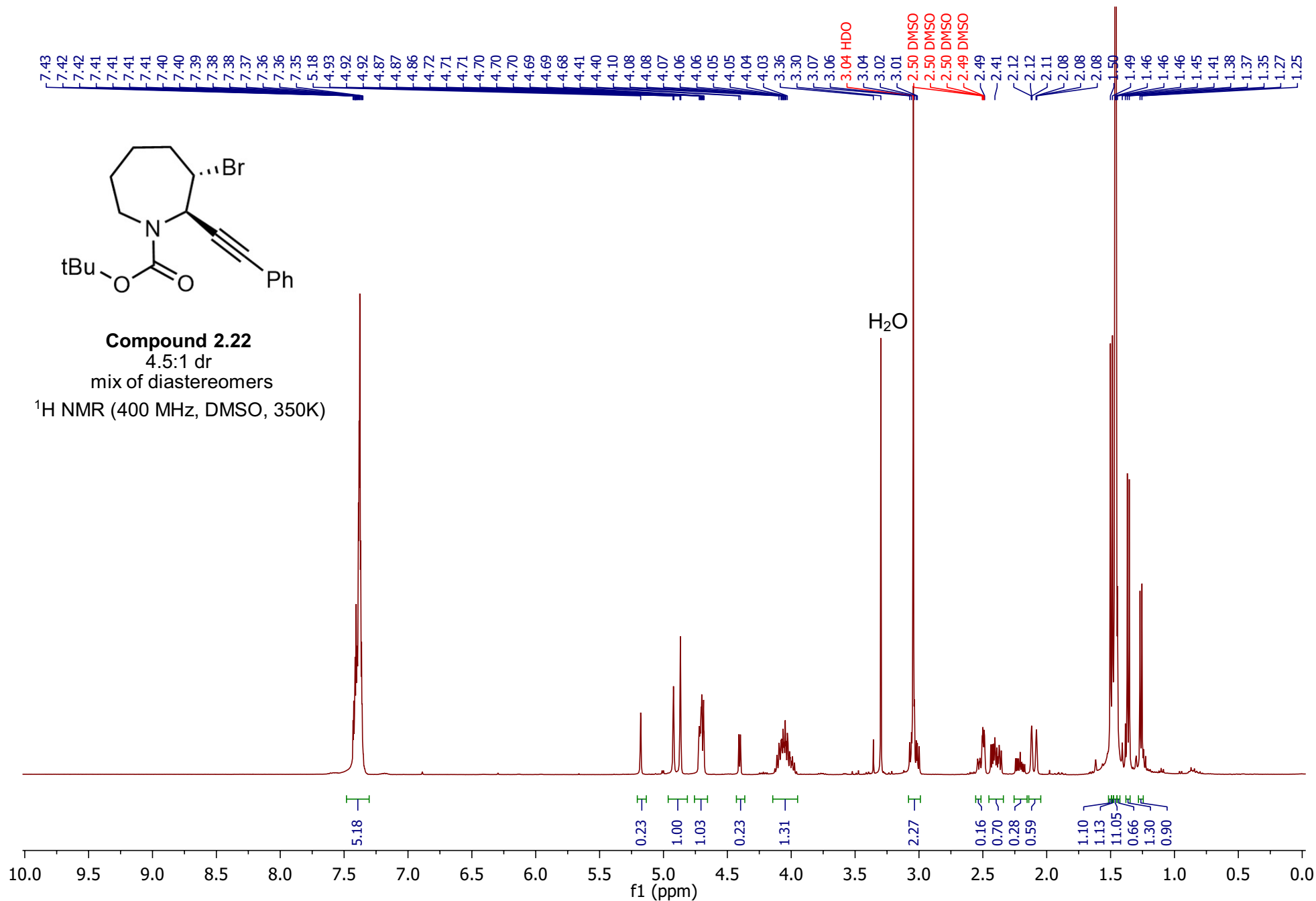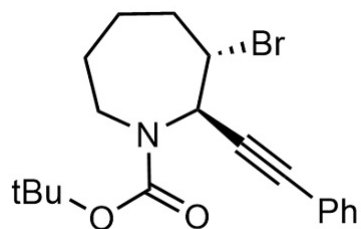
Compound 2.22
4.5:1 dr
mix of diastereomers and rotamers
^{13}C NMR (101 MHz, DMSO, 298K)

154.64, 153.76

132.03, 131.88, 129.39, 129.19, 129.15, 122.17, 122.09

87.66, 87.28, 84.21, 83.75, 80.47, 80.32

57.10, 56.74, 55.68, 54.66

44.14

35.99, 35.73, 28.41, 27.43, 27.23, 26.28
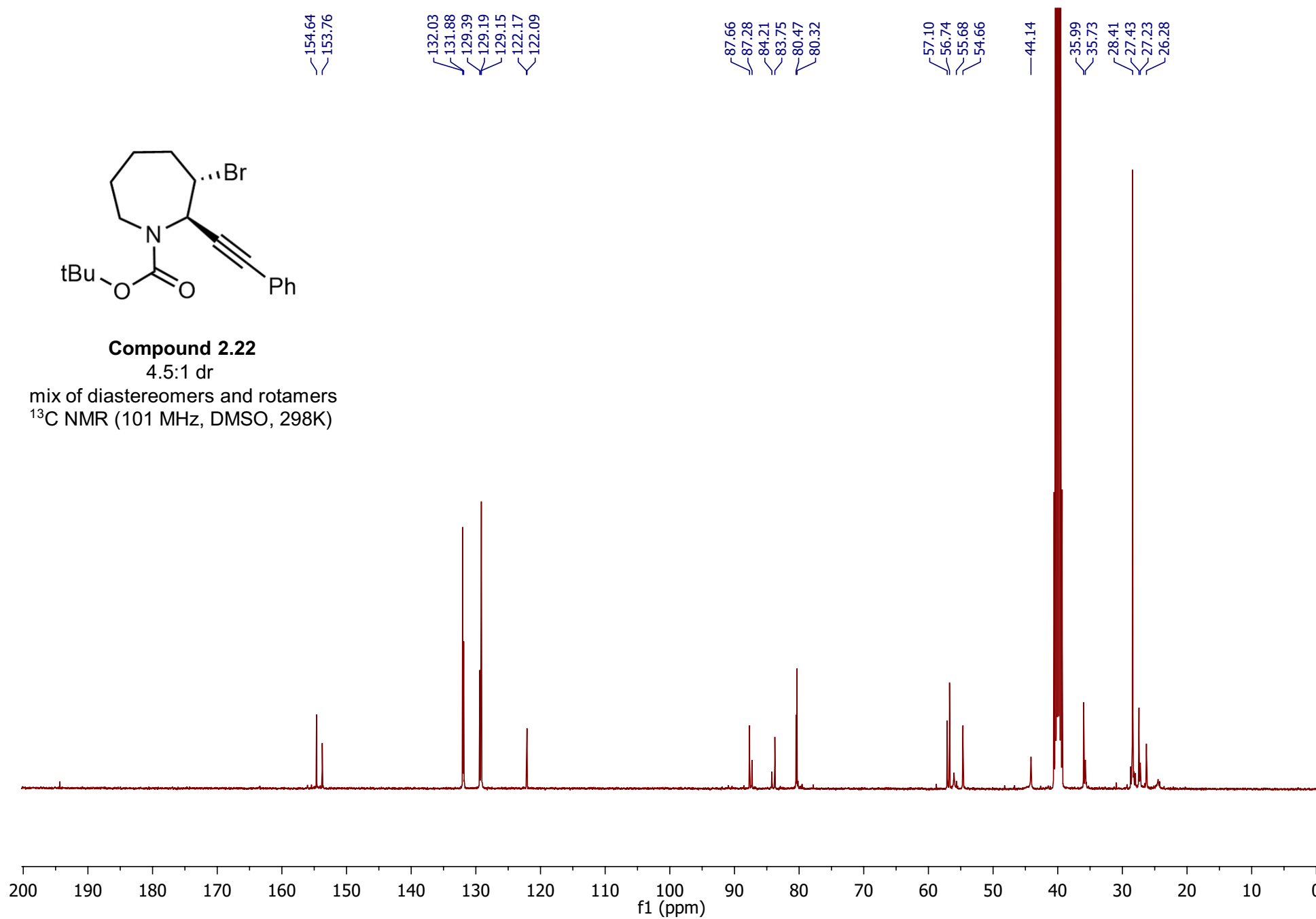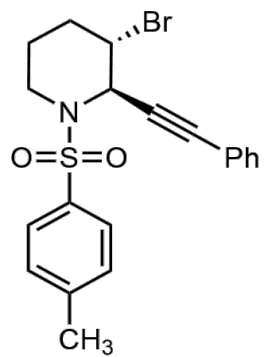
Compound 2.23
>20:1 dr
^{1}H NMR (600 MHz, CDCl$_3$)
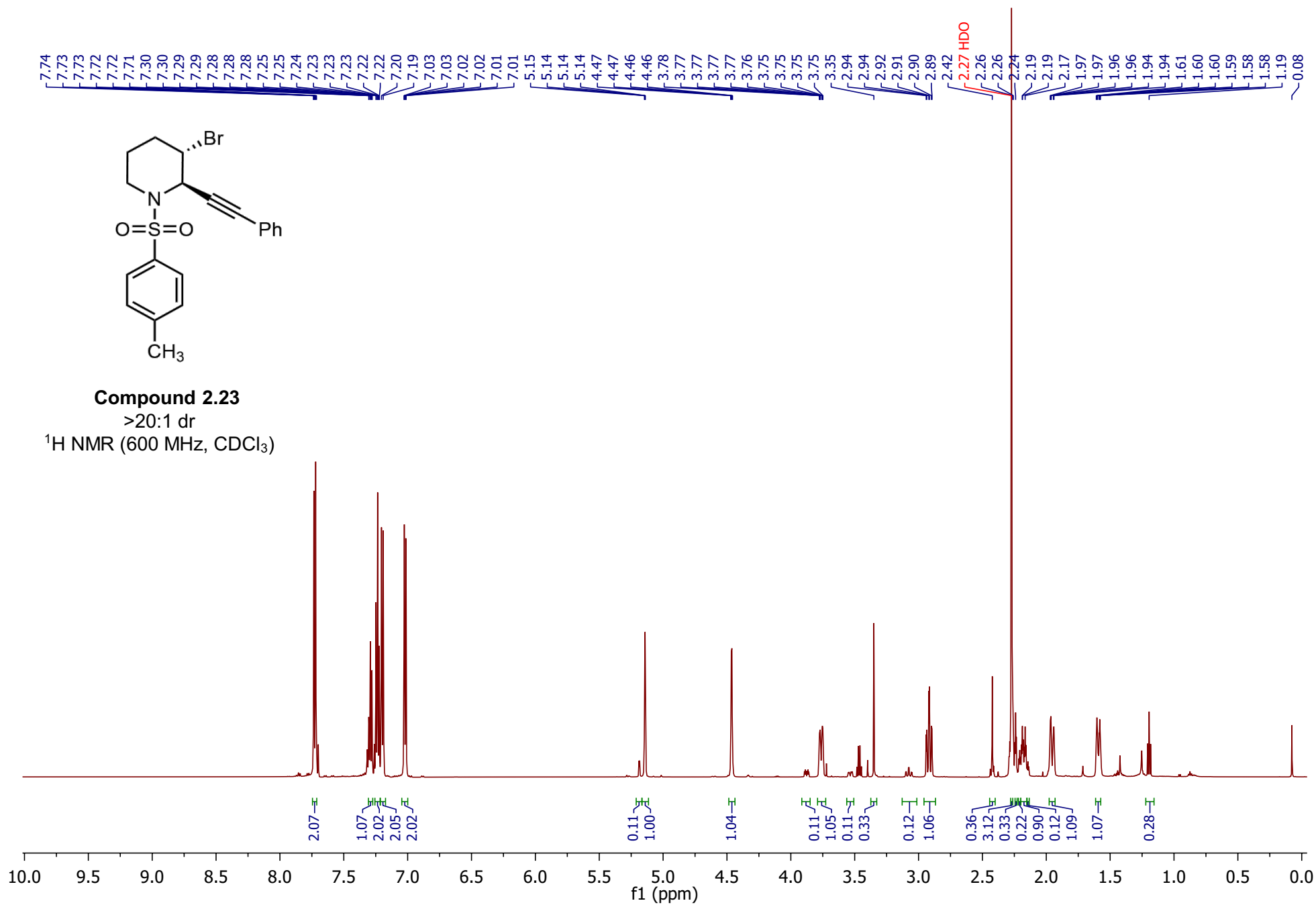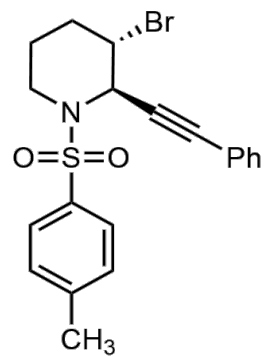
Compound 2.23
>20:1 dr
^{13}C NMR (151 MHz, CDCl$_3$)

142.72
142.50
136.61
134.05
130.45
128.88
128.35
127.79
127.14
126.90
125.82
120.40

87.65
84.77
80.74
76.32 CDCl3
76.10 CDCl3
75.89 CDCl3

64.80

55.74
51.67
48.51
48.26

40.73
37.88

28.65
28.25
26.79
25.41
20.53
20.36
19.07
14.27
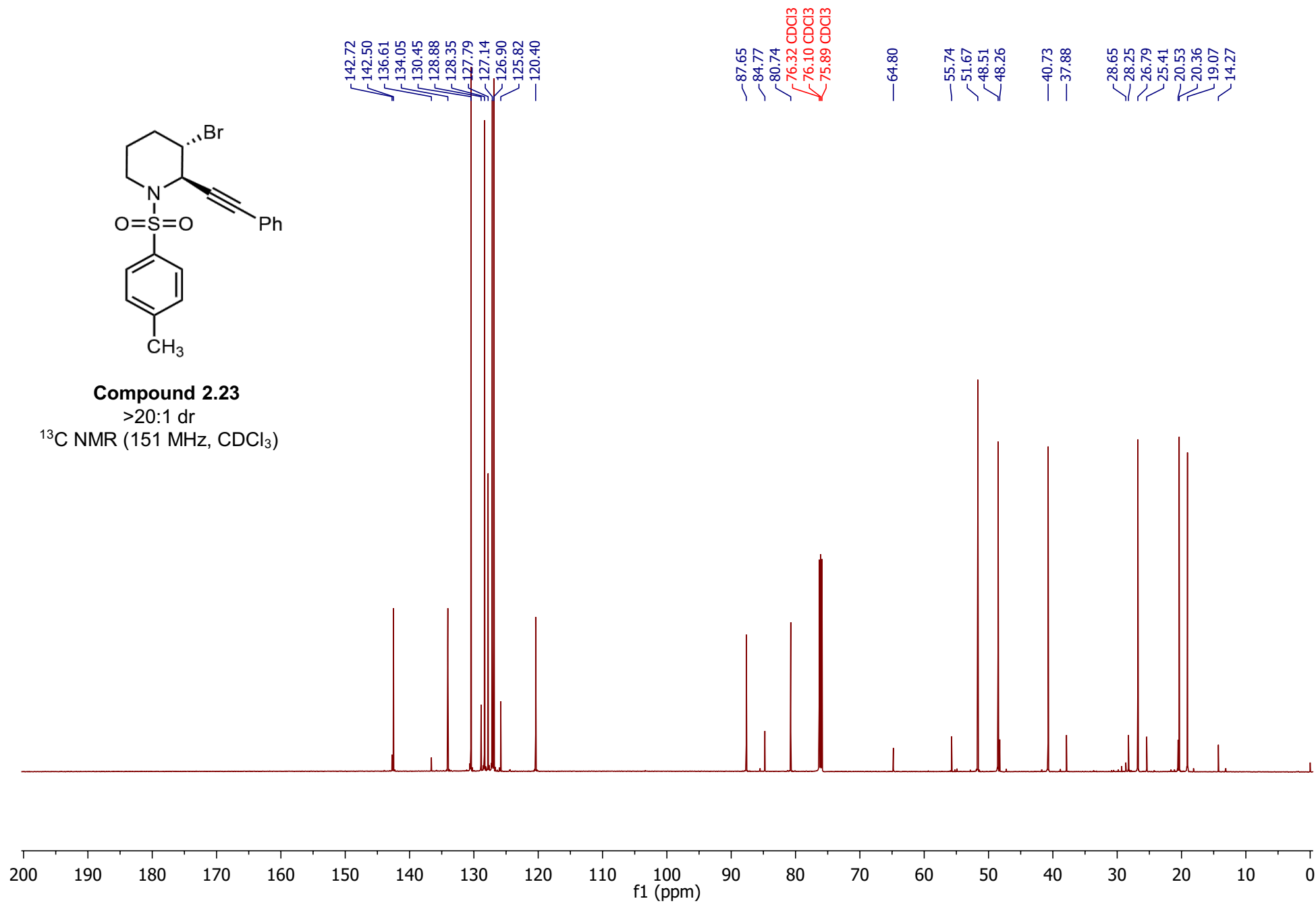
Compound 2.23-2
Vinyl Bromide
^{1}H NMR (600 MHz, CDCl$_3$)

Compound 2.23-2
Vinyl Bromide

^{13}C NMR (151 MHz, CDCl$_3$)

143.70
137.71
129.94
129.89
129.35
127.93
127.11
126.87
86.53
85.81
77.29 CDCl3
77.08 CDCl3
76.87 CDCl3
65.83
56.79
49.23
38.92
29.28
26.45
21.54
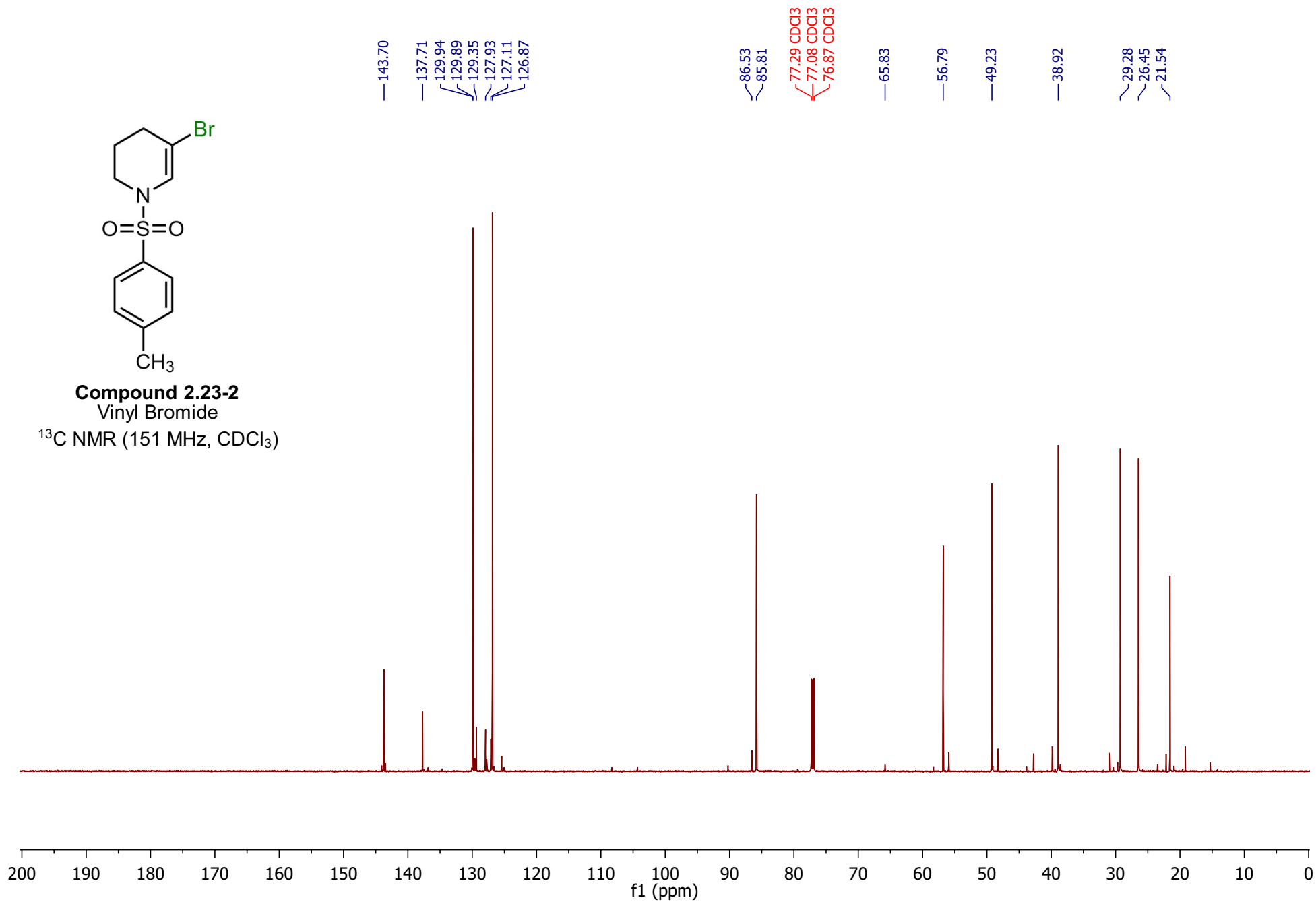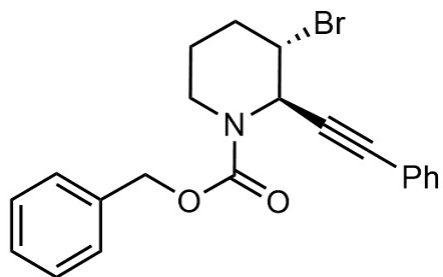
Compound 2.24
13.7:1 dr

^{1}H NMR (400 MHz, CD$_3$OD)
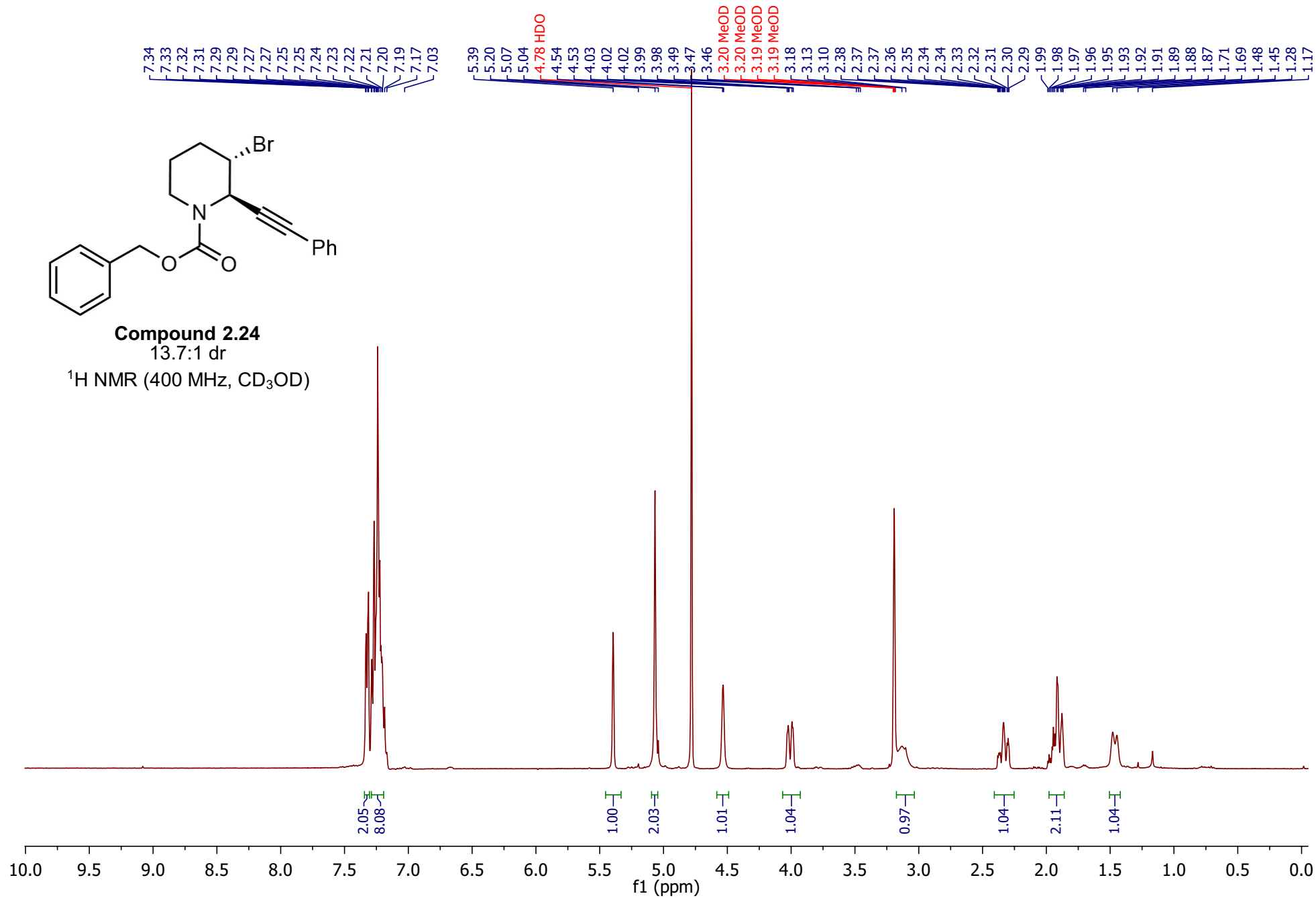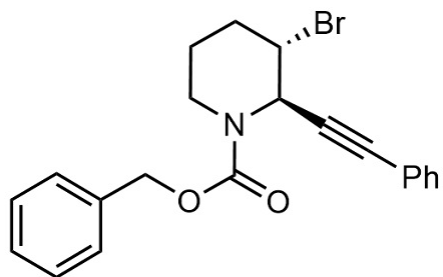
Compound 2.24
13.7:1 dr
^{13}C NMR (101 MHz, CD$_3$OD)
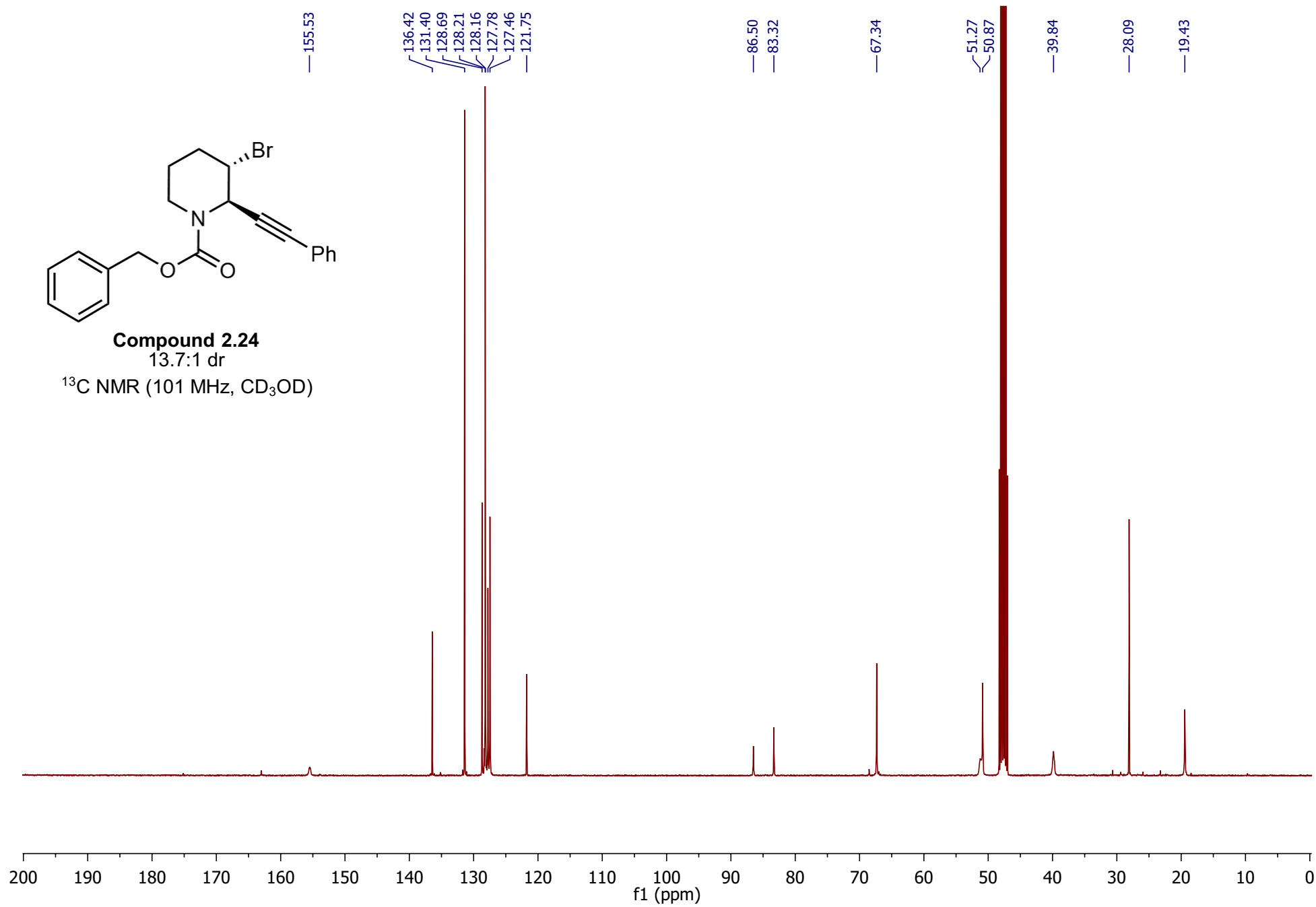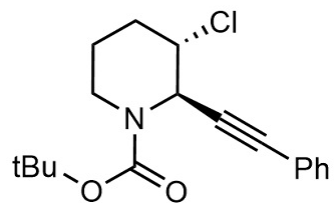
Compound 2.25
>20:1 dr
^{1}H NMR (400 MHz, CD$_3$OD)
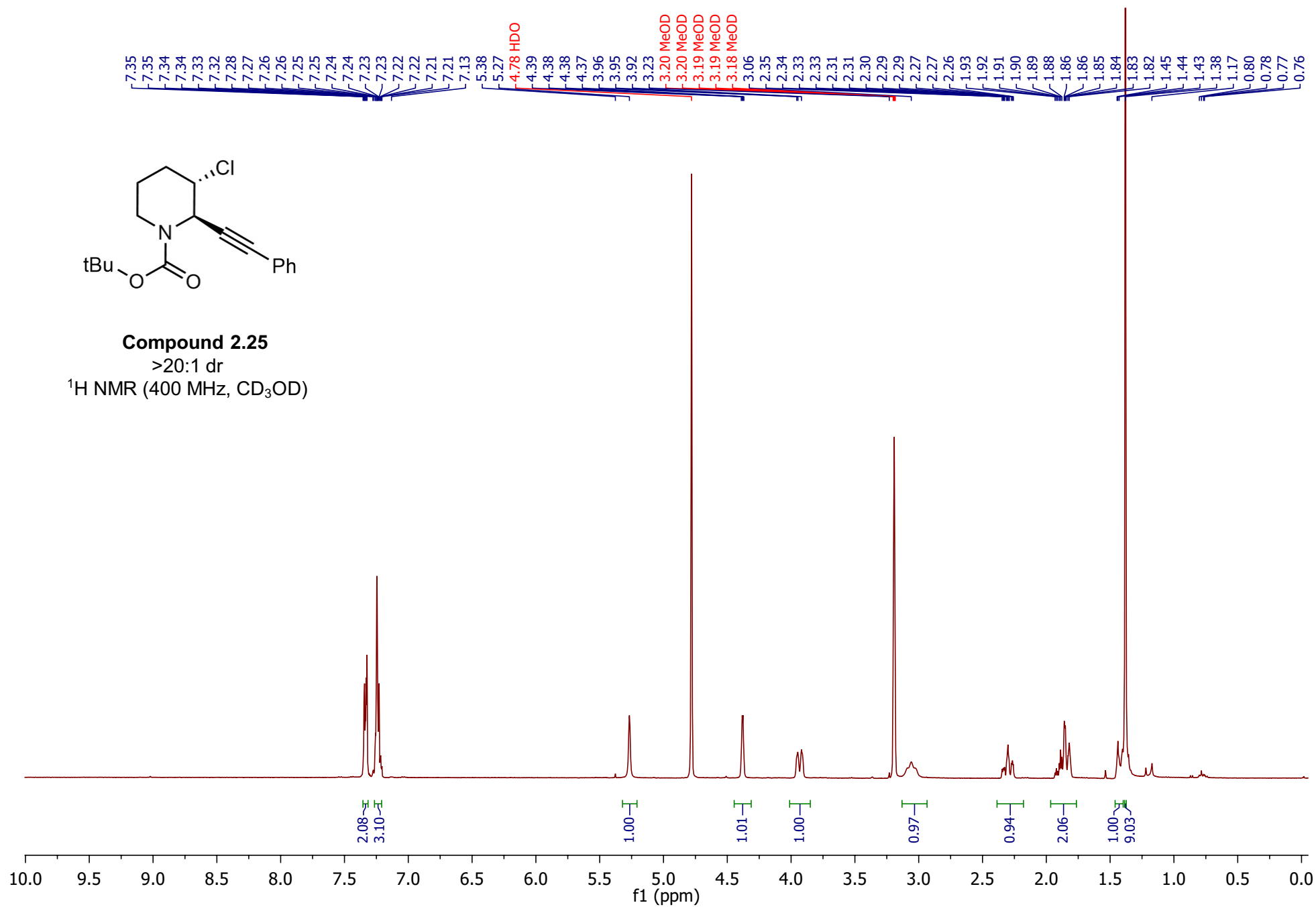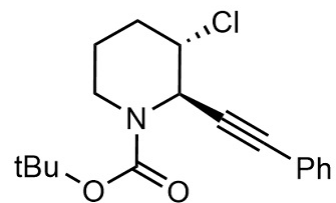
Compound 2.25
>20:1 dr
^{13}C NMR (101 MHz, CD$_3$OD)

153.36

129.74
127.04
126.62
120.23

84.67
81.90
79.12

56.89

49.67

37.90

26.00
25.63

16.99
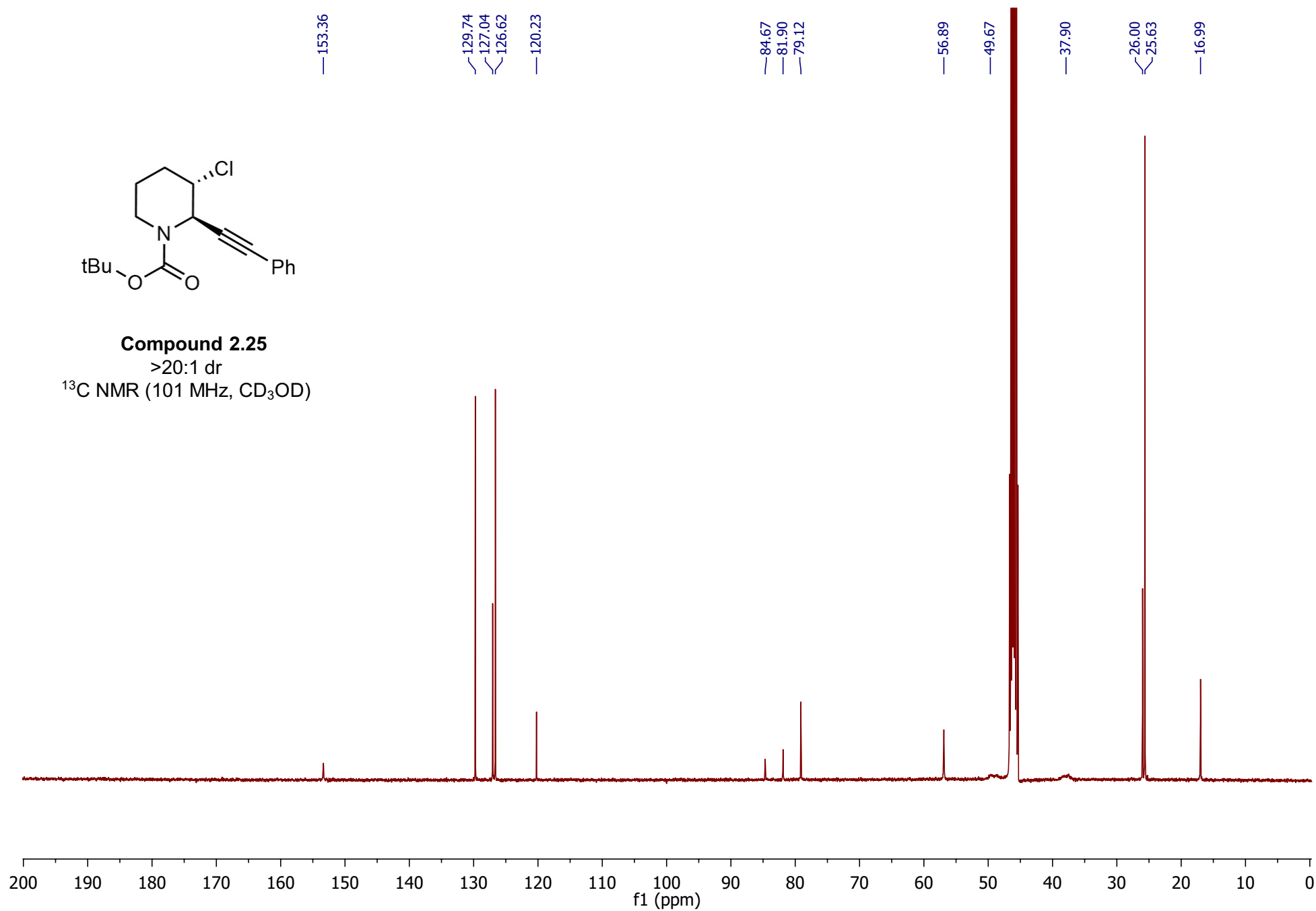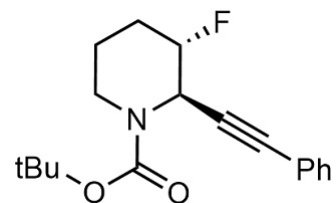
Compound 2.26
>20:1 dr
^{1}H NMR (600 MHz, CD$_3$OD)
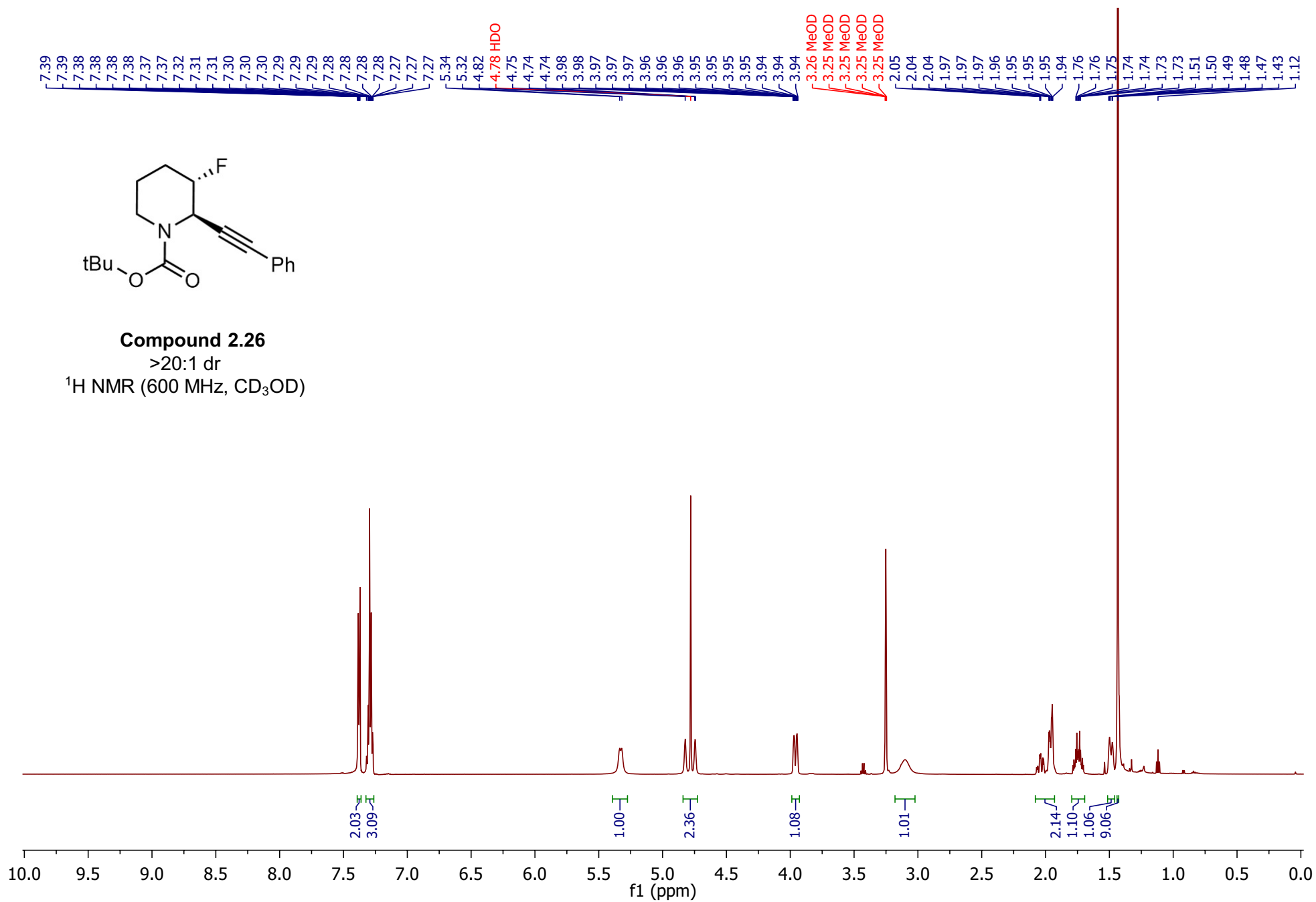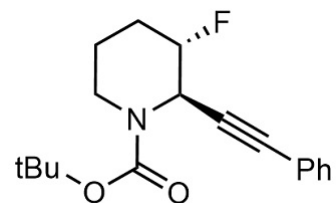
Compound 2.26
>20:1 dr
^{13}C NMR (151 MHz, CD$_3$OD)

155.11

131.32
128.53
128.16
121.96

88.30
87.11
86.15
82.51
82.40
80.54

38.99

27.21
24.96
24.82
18.84

200 190 180 170 160 150 140 130 120 110 100 90 80 70 60 50 40 30 20 10 0
f1 (ppm)
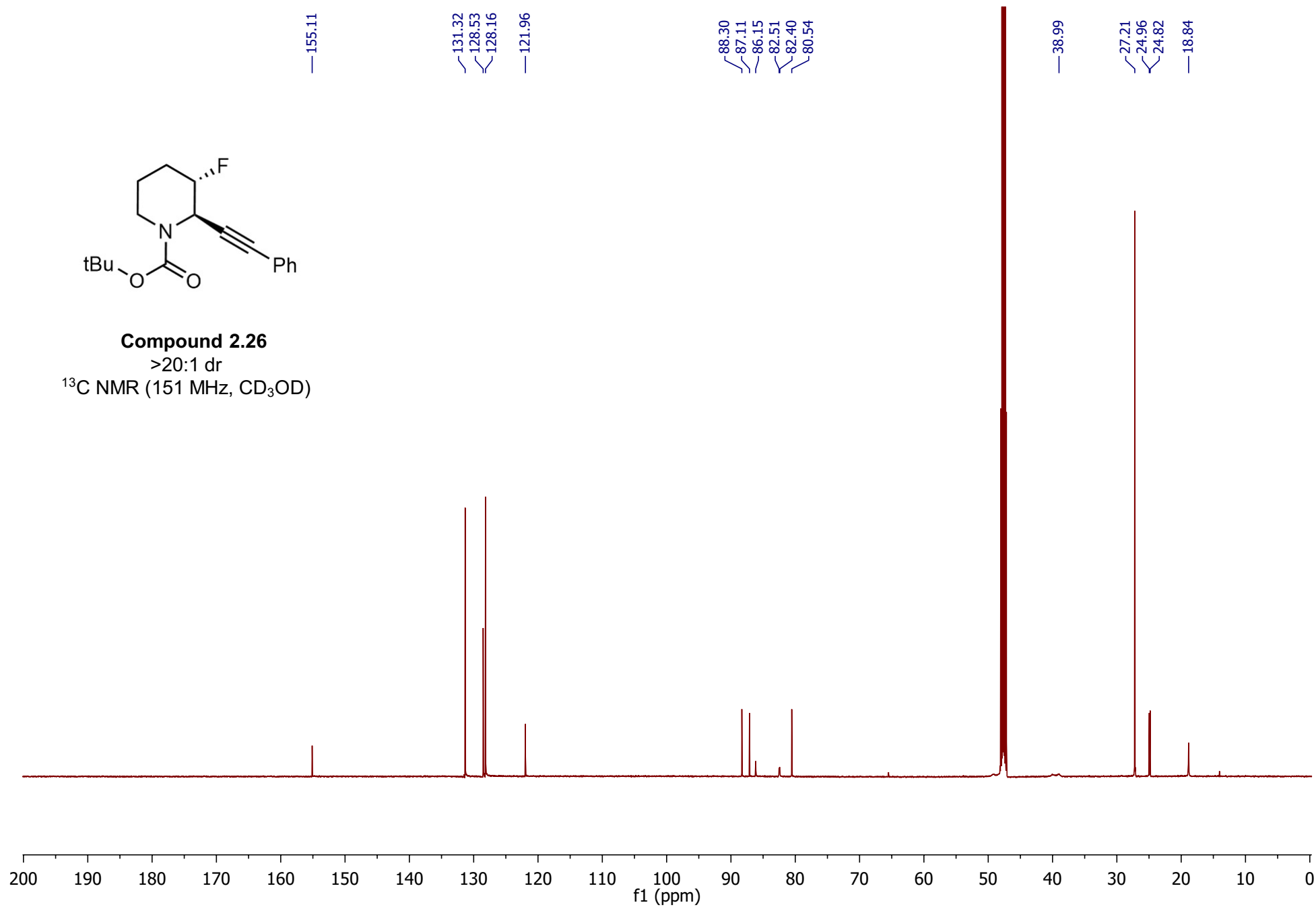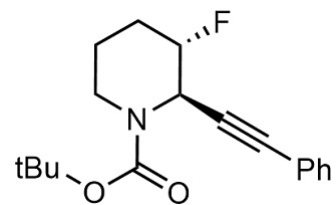
Compound 2.26
>20:1 dr
^{19}F NMR (376 MHz, CD$_3$OD)
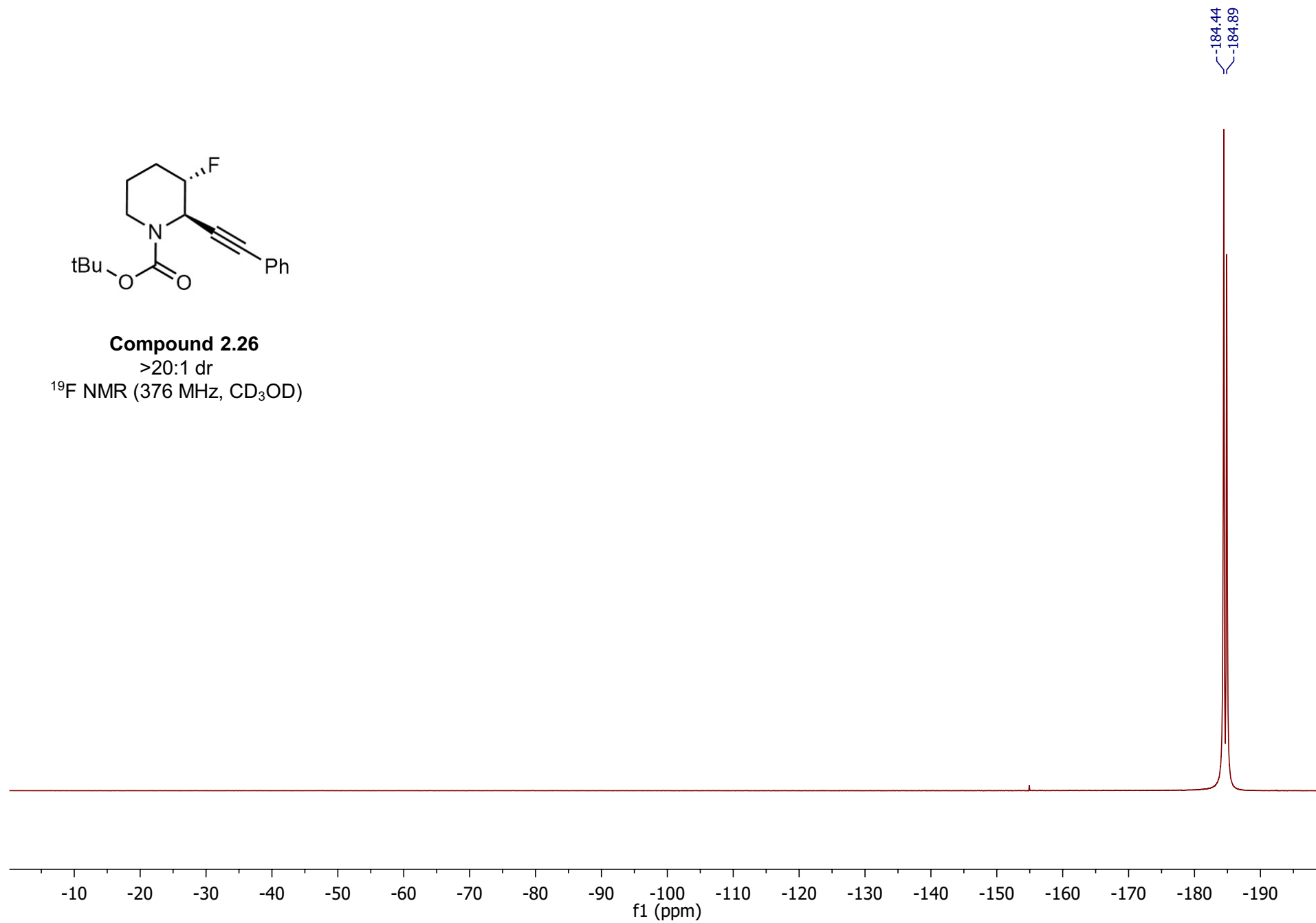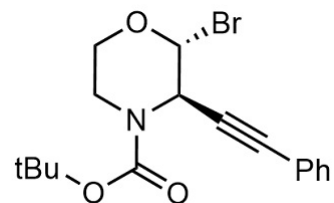
Compound 2.27
>20:1 dr
^{1}H NMR (600 MHz, CD$_3$OD)
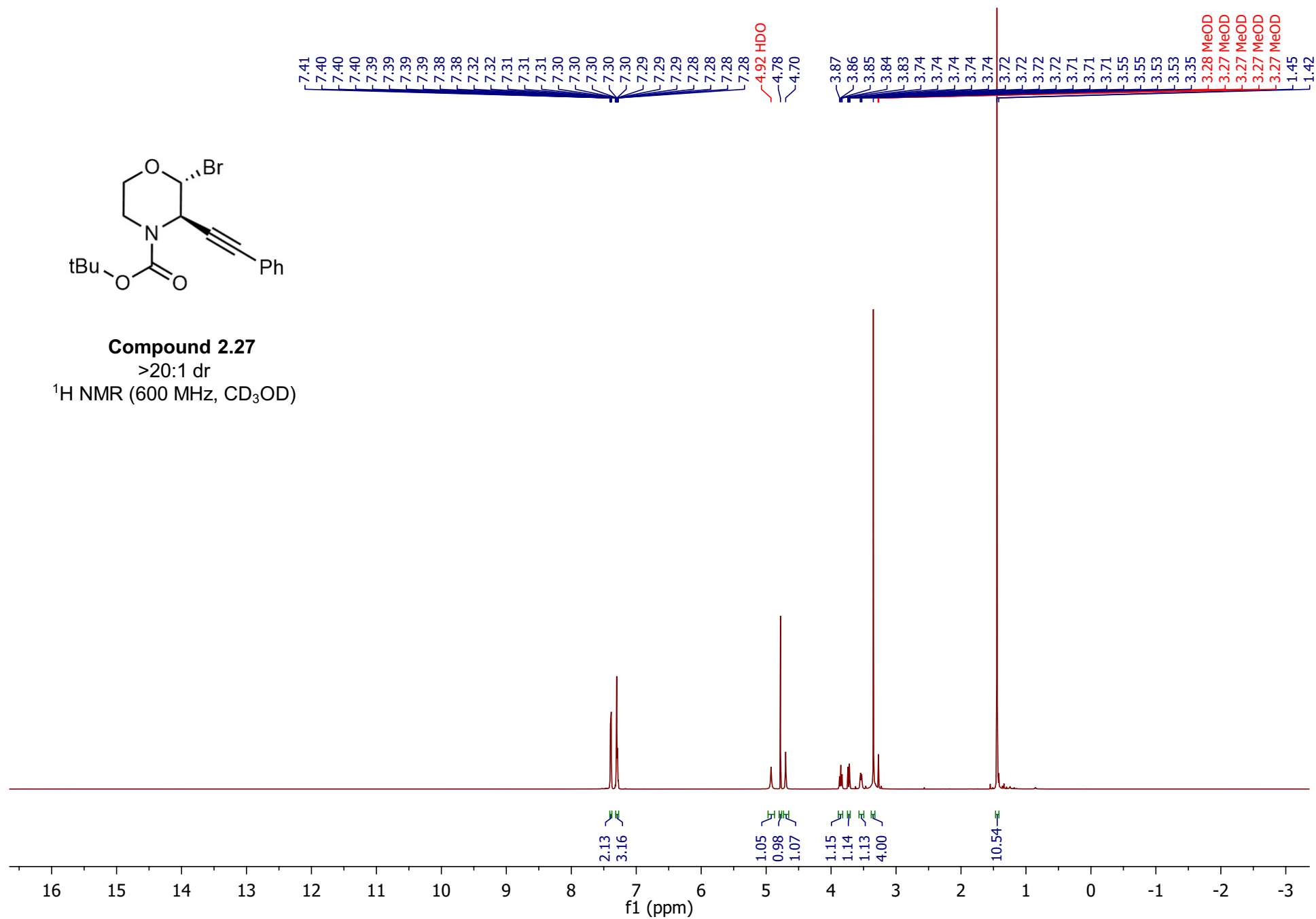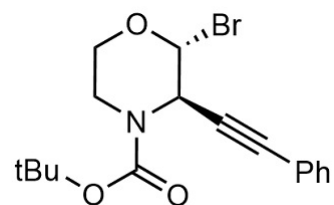
Compound 2.27
>20:1 dr
^{13}C NMR (151 MHz, CD$_3$OD)

154.98
131.38
128.35
128.12
122.28
97.66
84.42
83.68
80.73
57.85
53.65
38.72
27.21
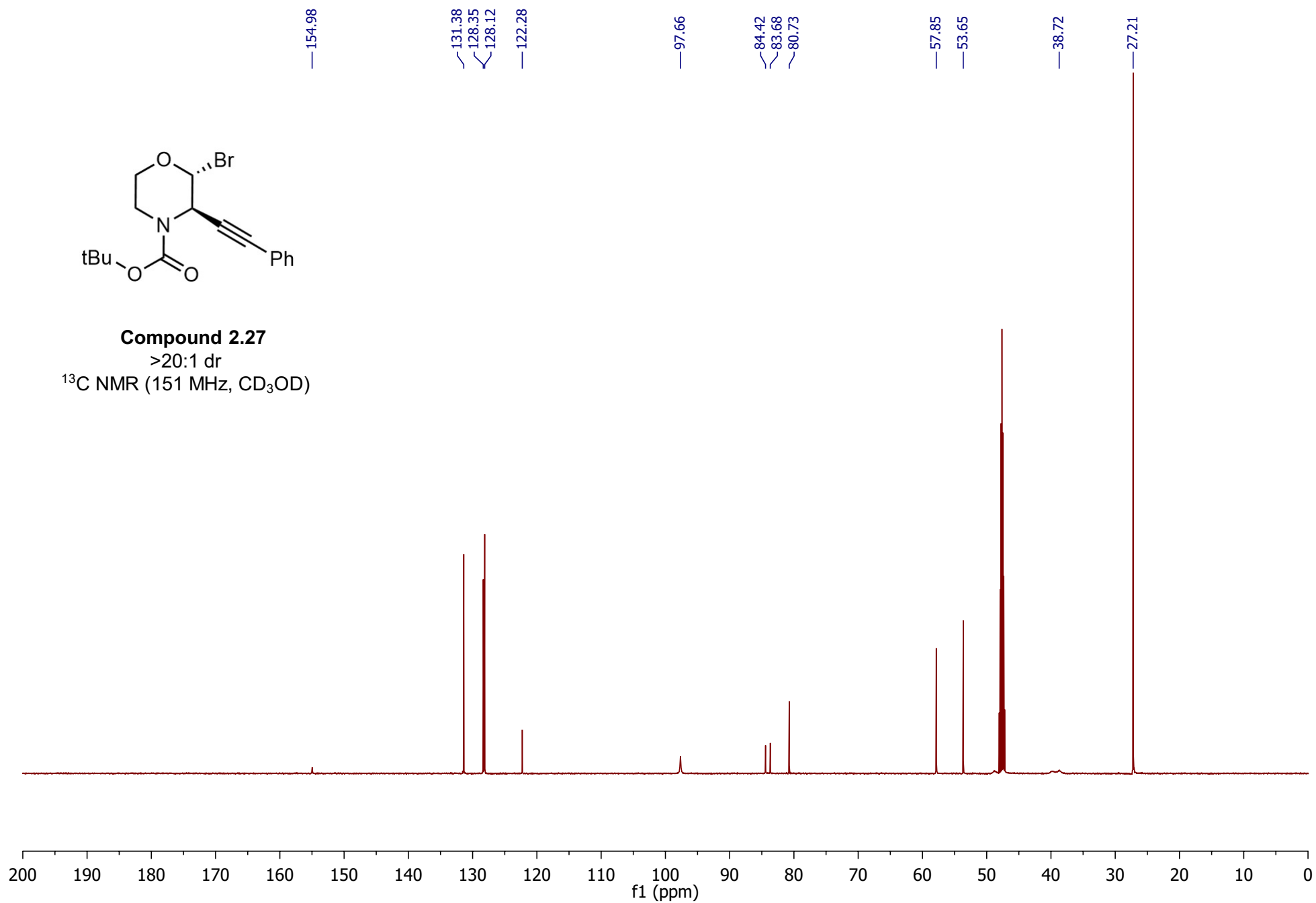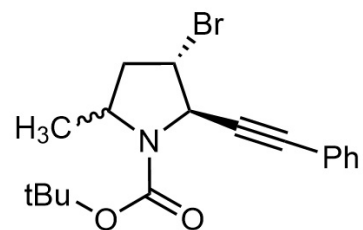
Compound 2.28
>1.2:1 dr
^{1}H NMR (400 MHz, CD$_3$OD)
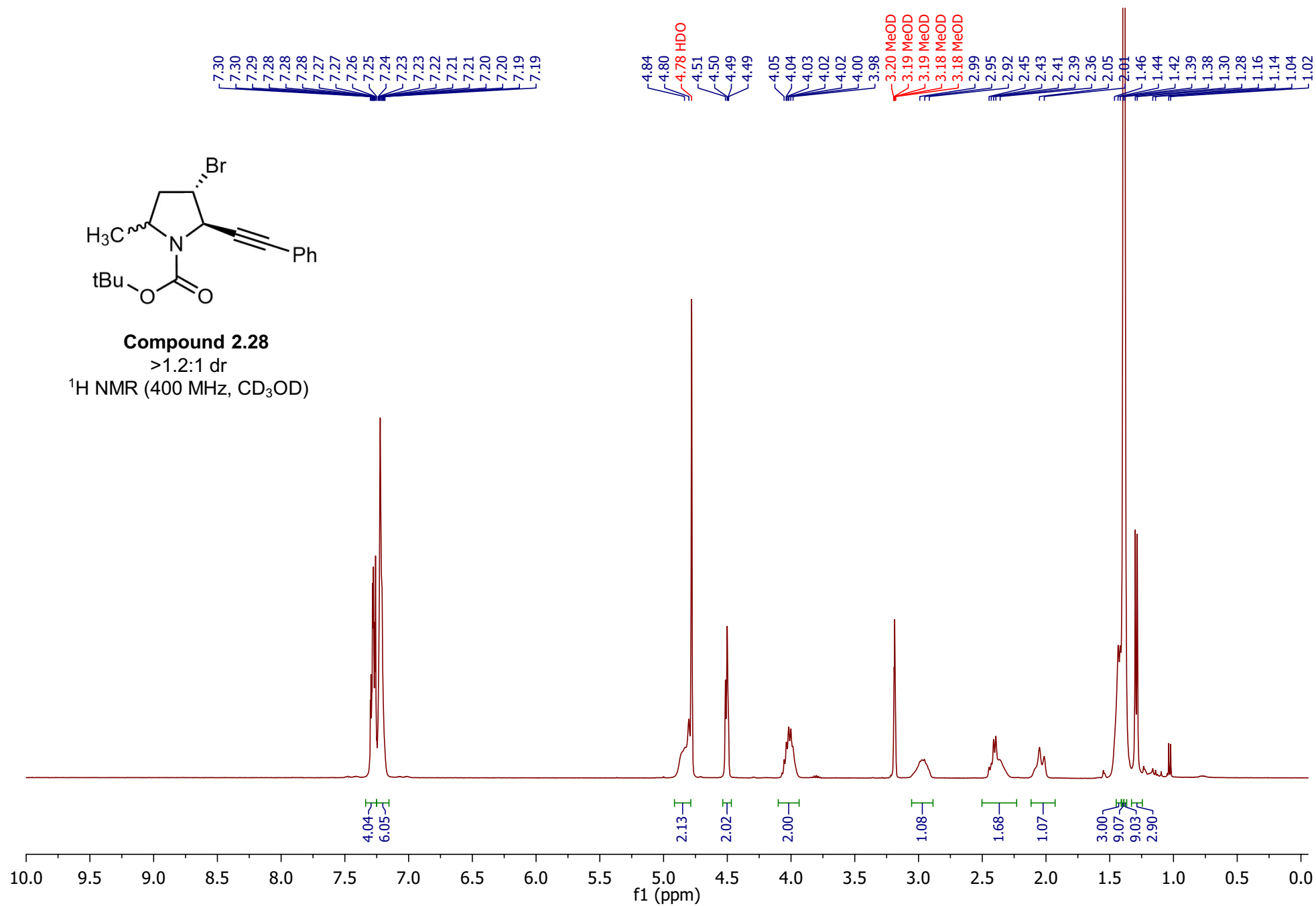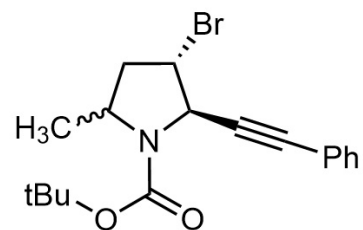
Compound 2.28
>1.2:1 dr
^{13}C NMR (101 MHz, CD$_3$OD)

153.08

129.67
126.93
126.66
126.61
120.55
120.53

84.46
84.28
83.79
82.64
82.37
79.07
78.92
78.77

58.89

51.55
49.54
48.16
47.42

39.46
38.64

25.83
25.82

19.71
18.74

200   190   180   170   160   150   140   130   120   110   100   90   80   70   60   50   40   30   20   10

f1 (ppm)
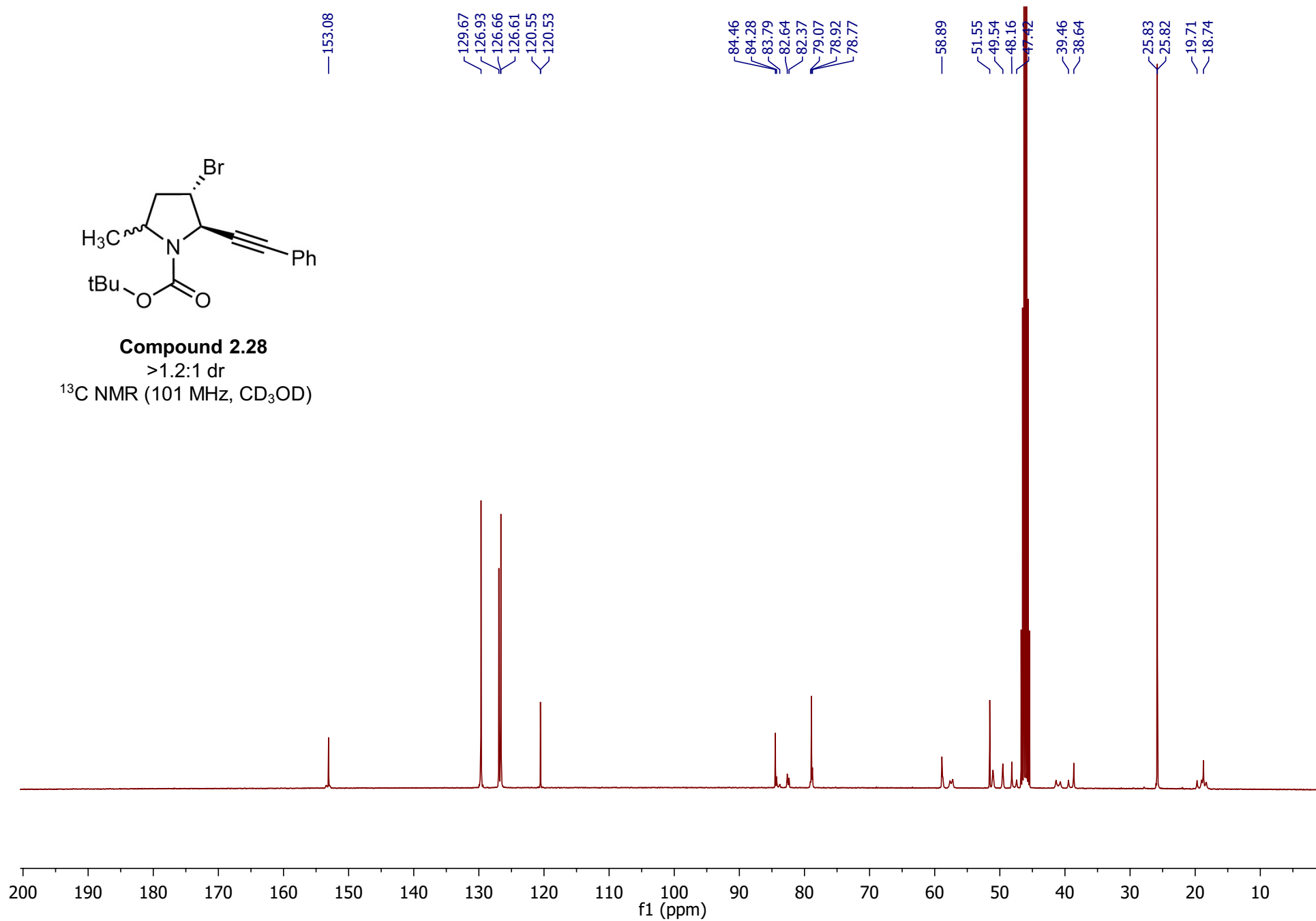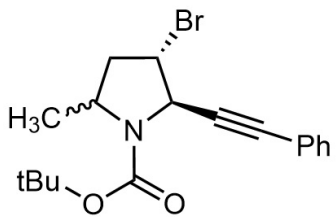
Compound 2.28
COSY, CD$_3$OD
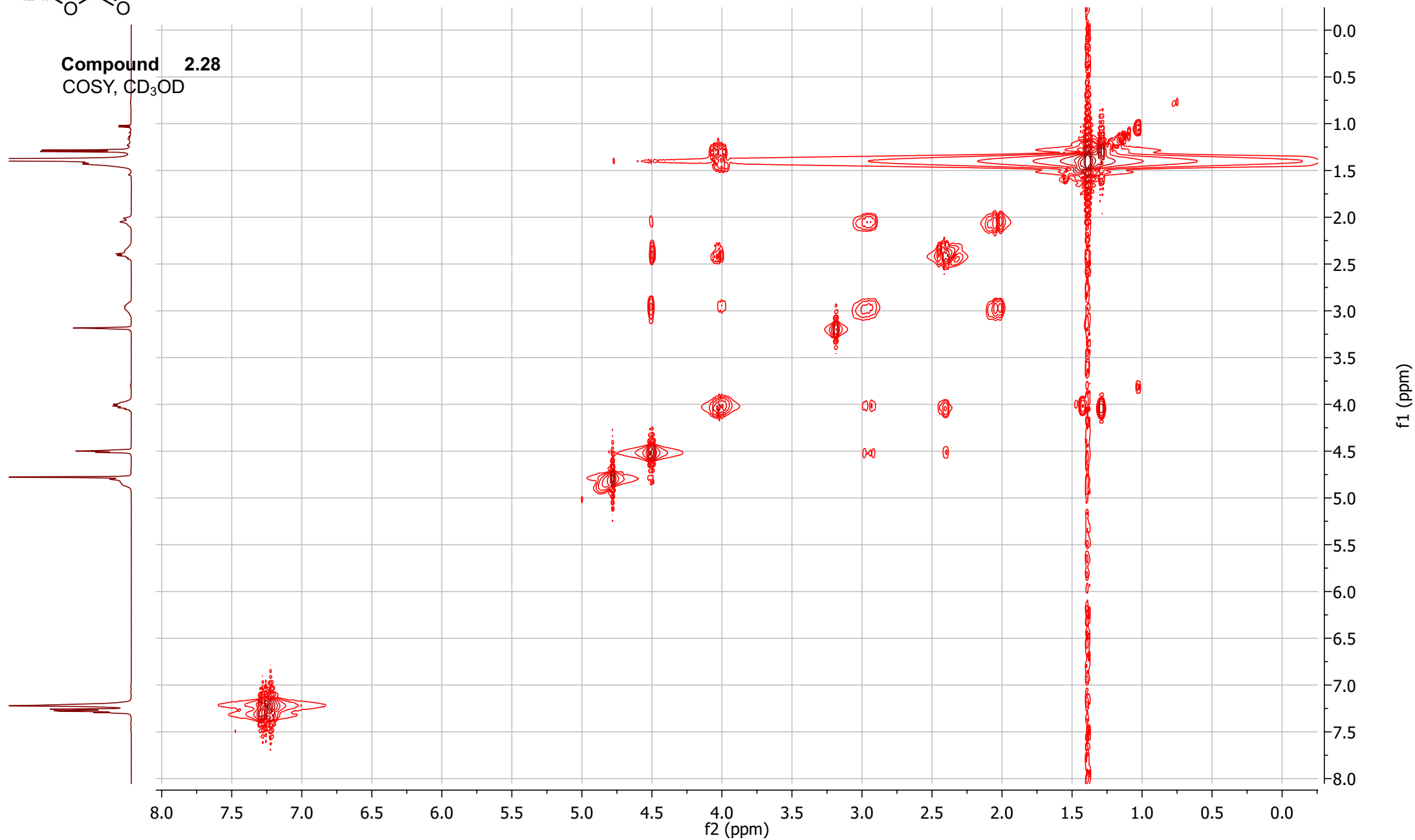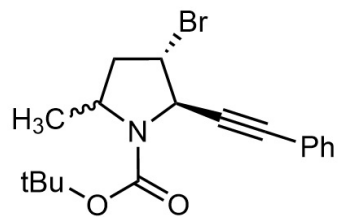
Compound 2.28
HSQC
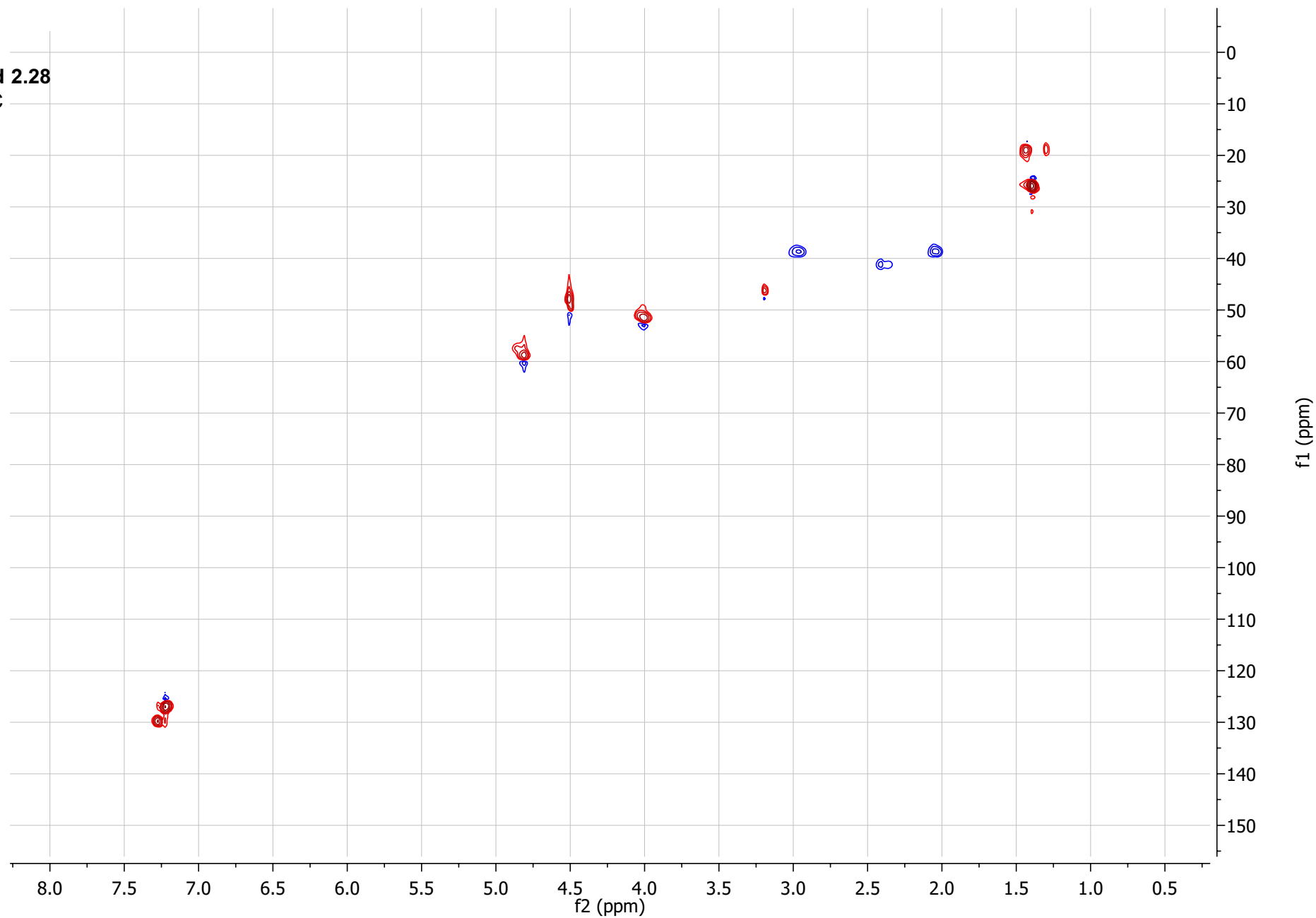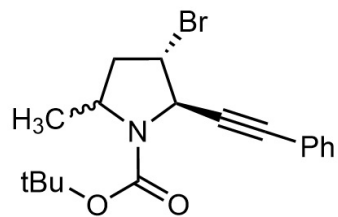
Compound 2.28
HMBC
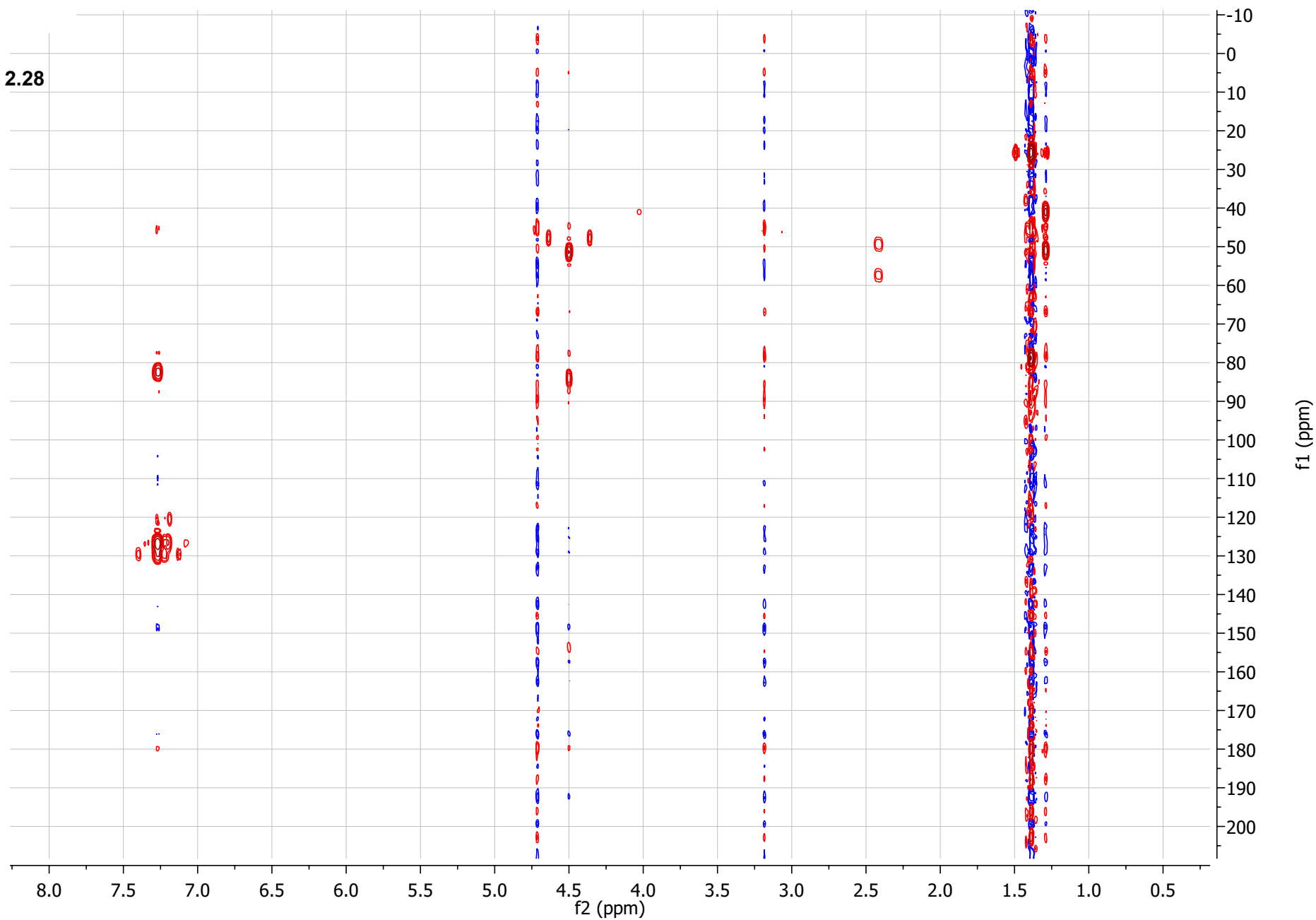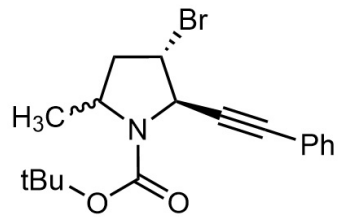
Compound 2.28

HMBC
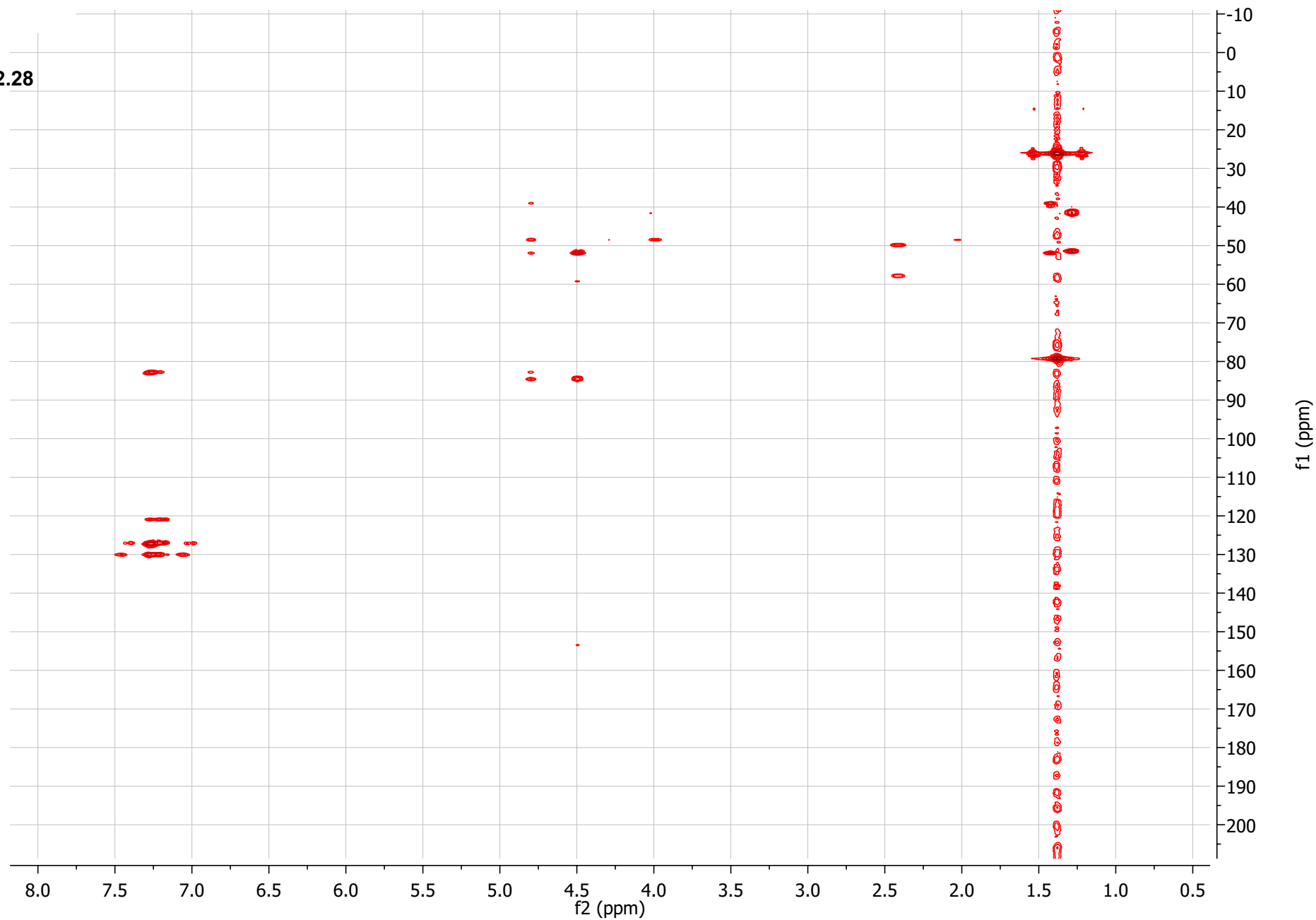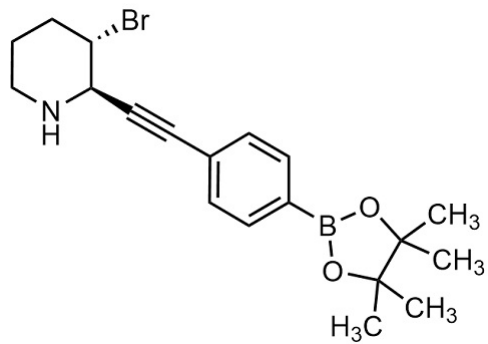
Compound 2.29
>20:1 dr
^{1}H NMR (600 MHz, CDCl$_3$)
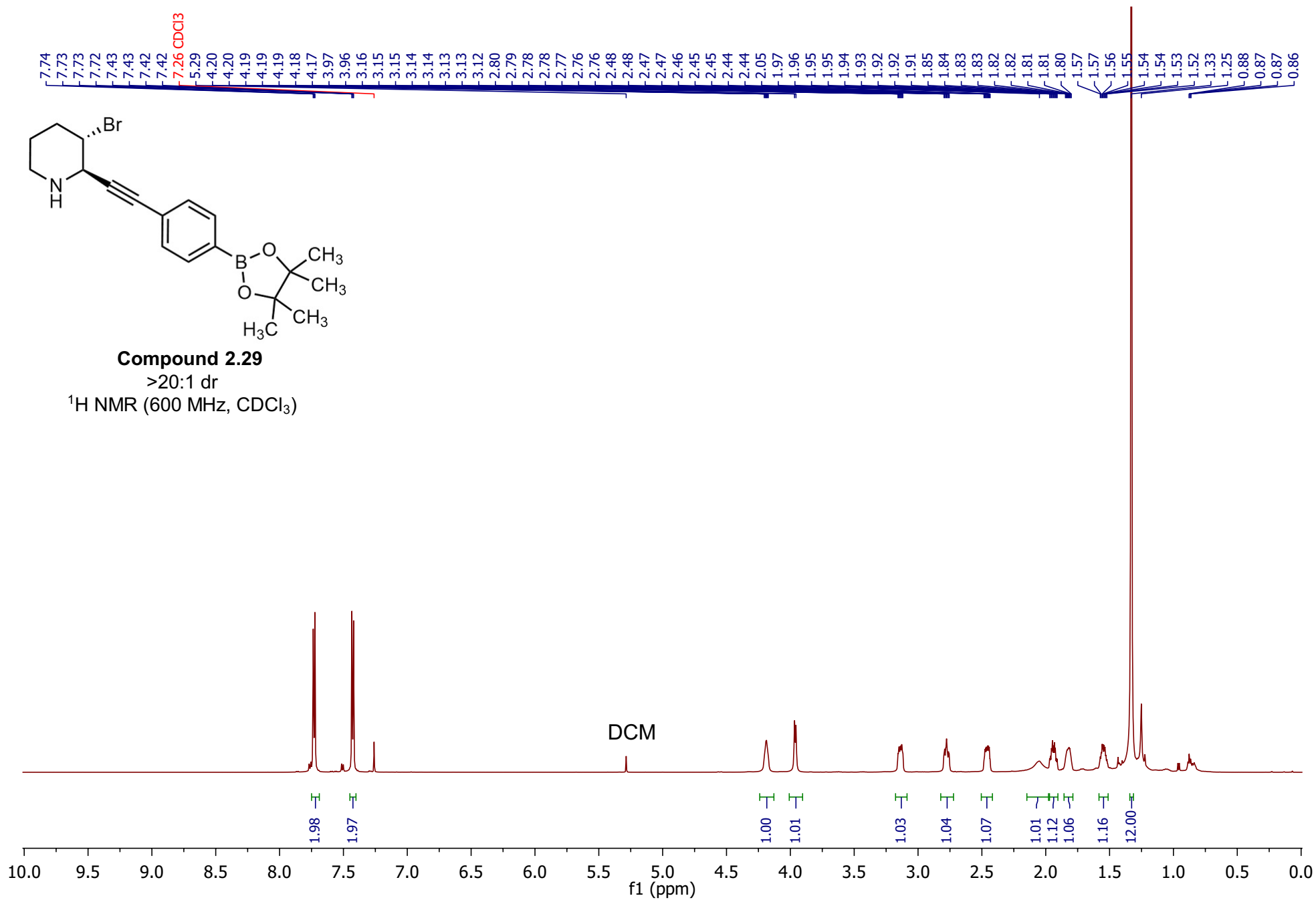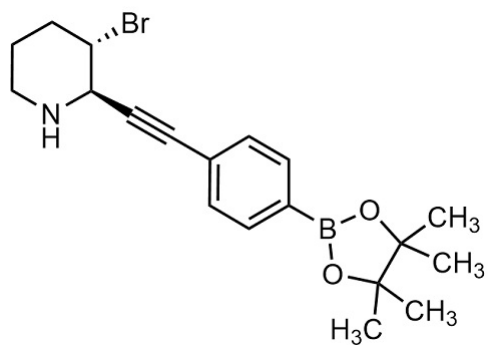
Compound 2.29
>20:1 dr
^{13}C NMR (151 MHz, CDCl$_3$)

134.51
131.60
130.91
125.29
89.13
84.93
83.95
77.26 CDCl3
77.05 CDCl3
76.84 CDCl3
55.31
53.24
43.95
33.55
25.65
24.88

f1 (ppm)

Compound 2.30
>20:1 dr
^{1}H NMR (600 MHz, CDCl$_3$)
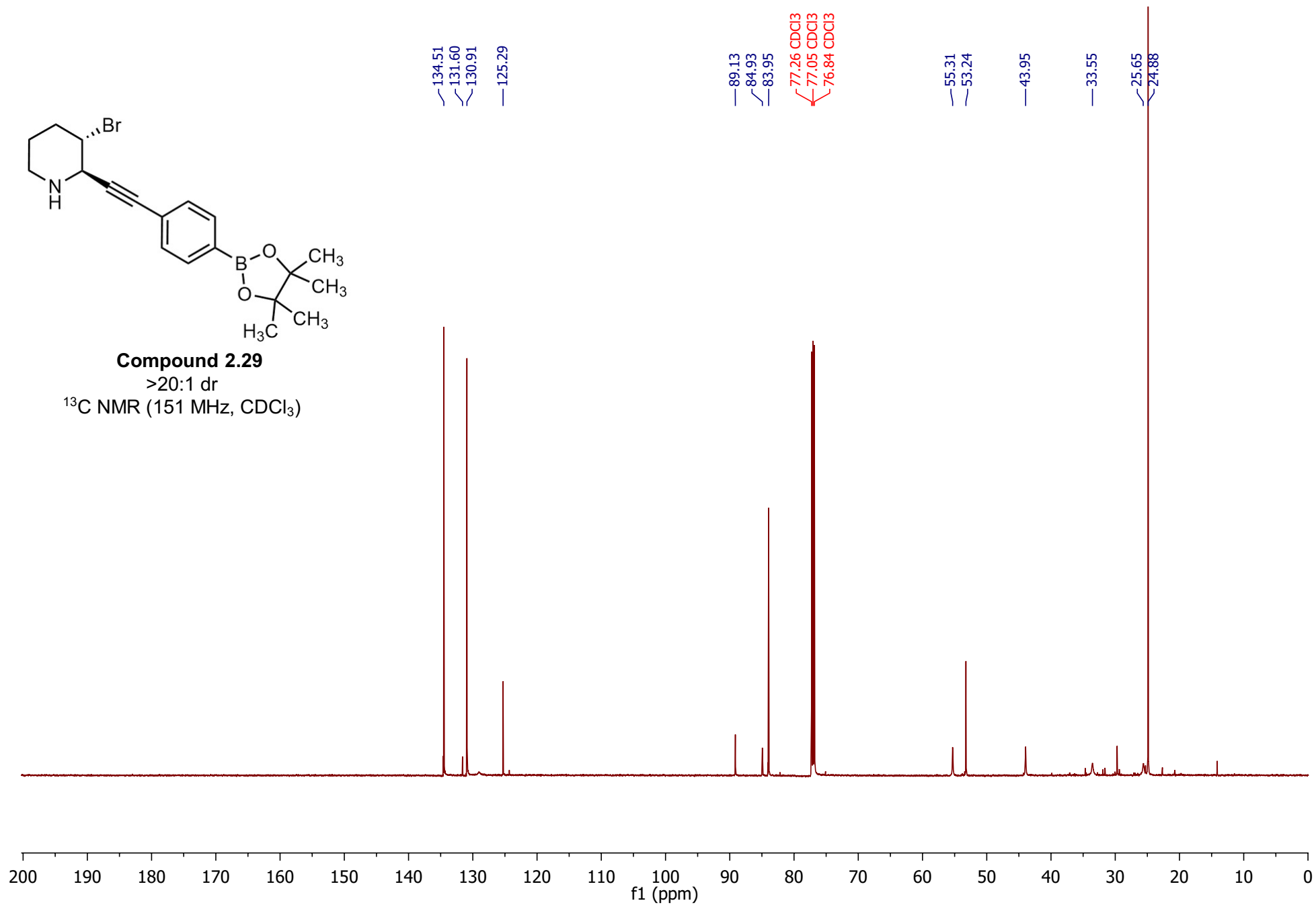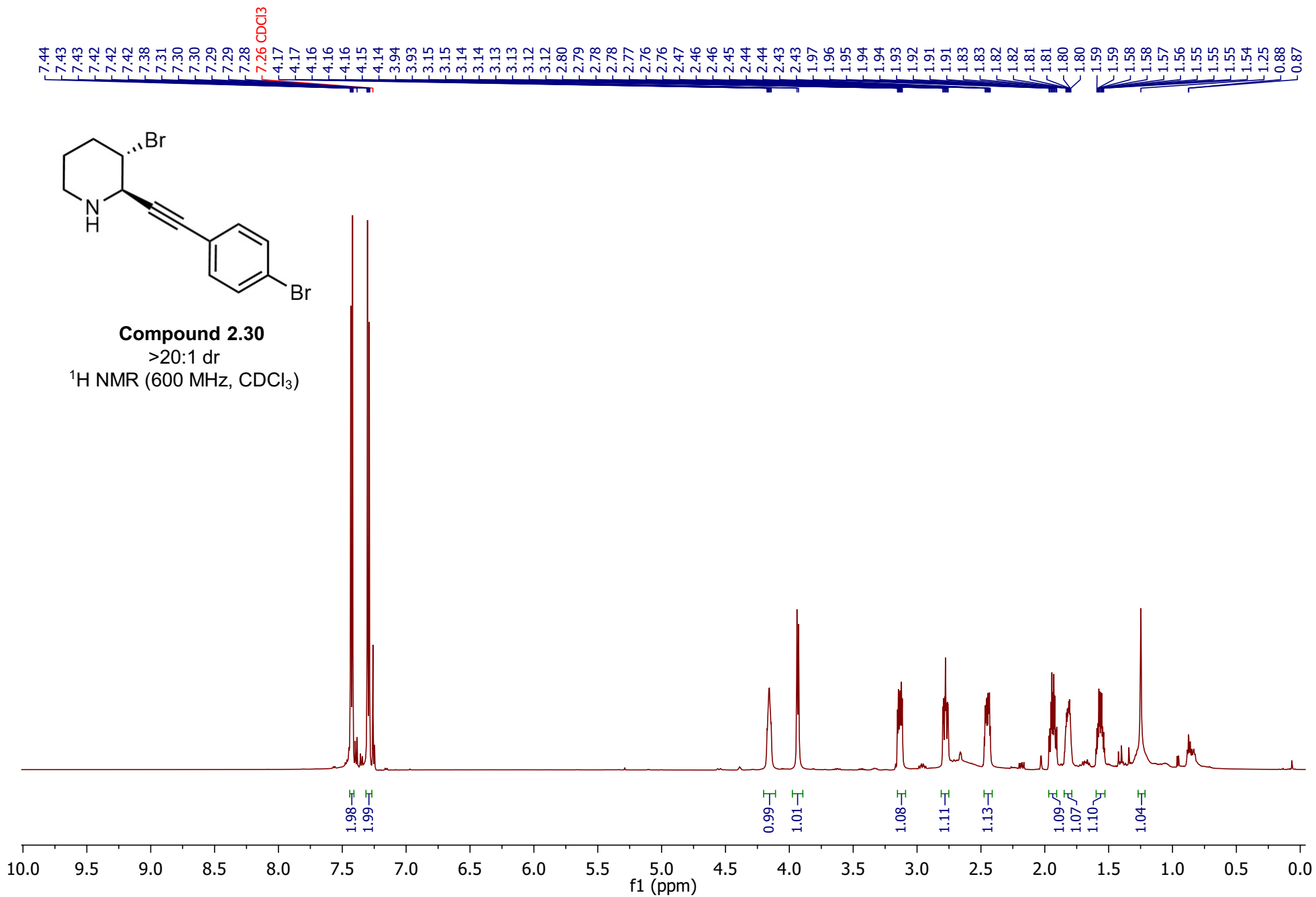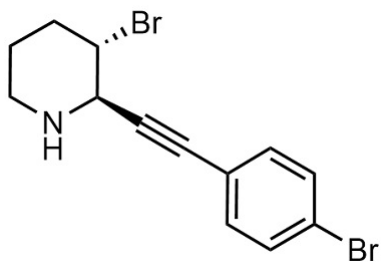
Compound 2.30
>20:1 dr
^{13}C NMR (151 MHz, CDCl$_3$)

133.21
131.54
122.70
121.50
88.83
83.84
77.26 CDCl3
77.05 CDCl3
76.84 CDCl3
55.38
52.86
44.31
33.82
25.73
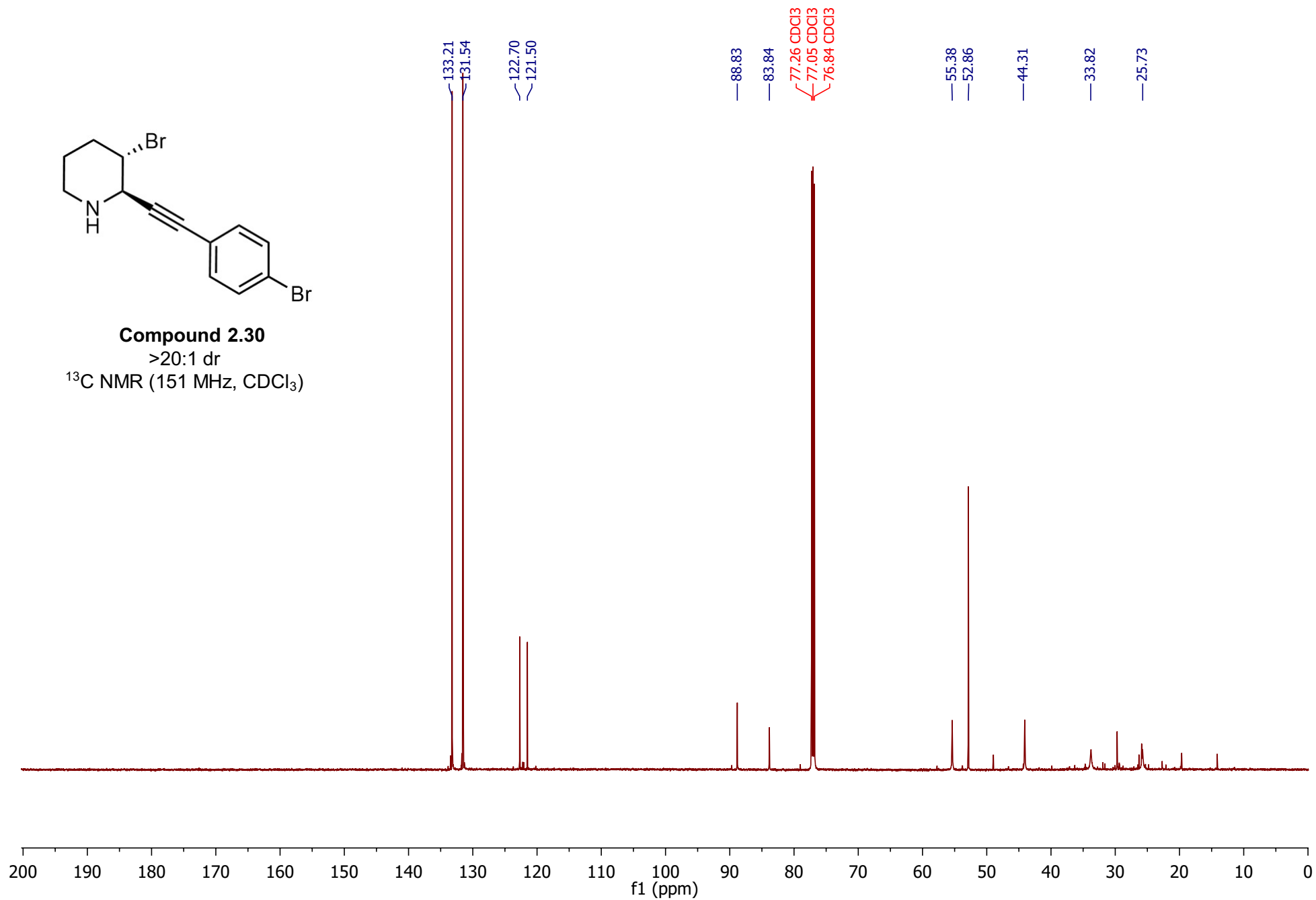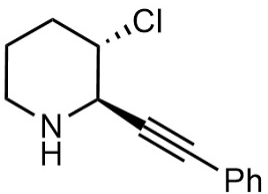
Compound 2.31
>20:1 dr
^{1}H NMR (600 MHz, CDCl$_3$)
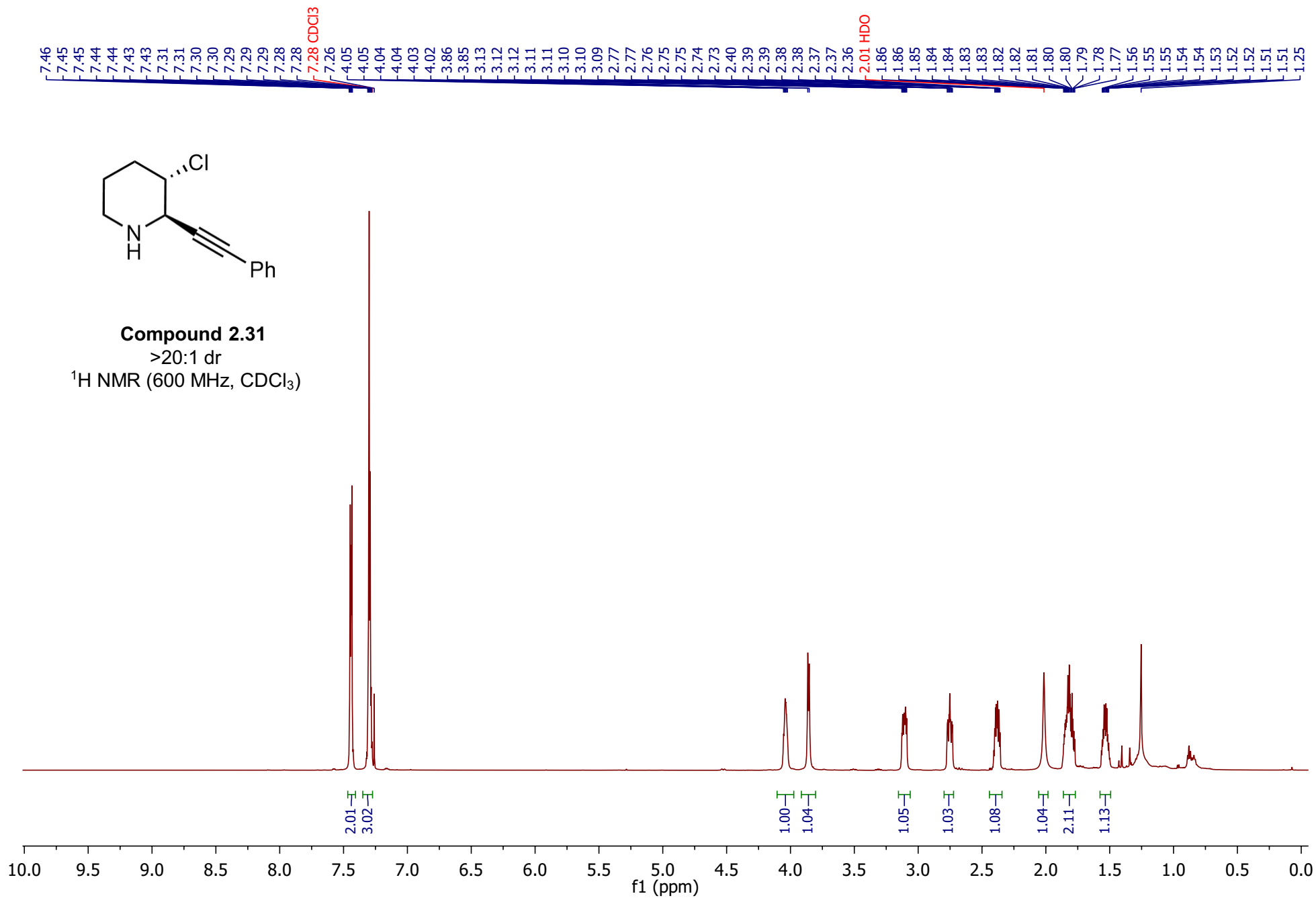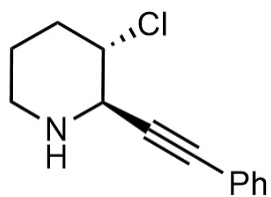
Compound 2.31
>20:1 dr
^{13}C NMR (151 MHz, CDCl$_3$)

131.78
128.37
128.25
122.65
87.57
84.78
77.28 CDCl3
77.06 CDCl3
76.85 CDCl3
60.25
55.13
43.83
32.76
24.54
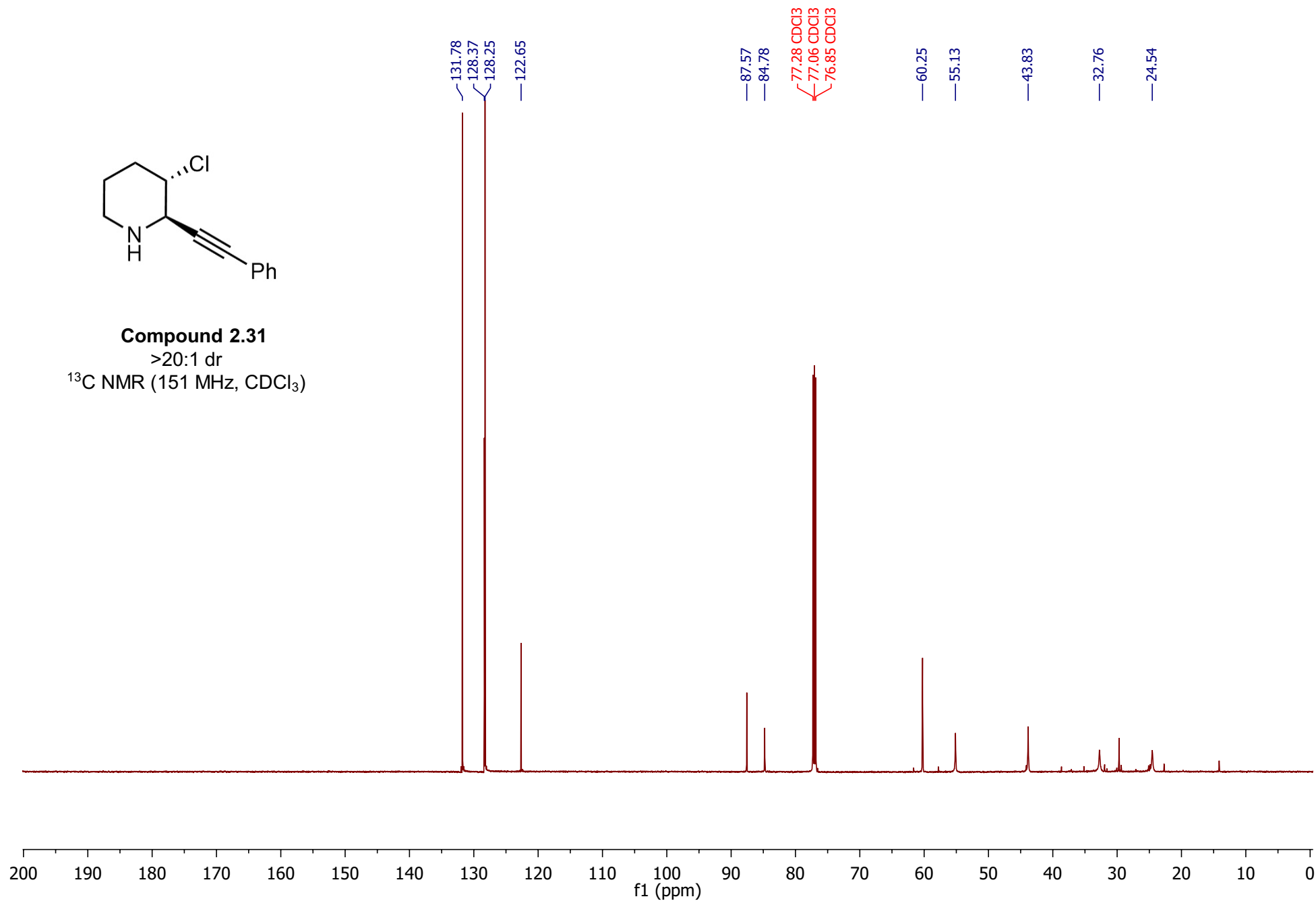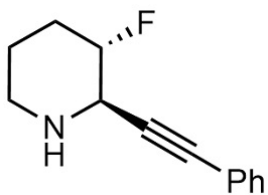
Compound 2.32
>20:1 dr
^{1}H NMR (600 MHz, CDCl$_3$)
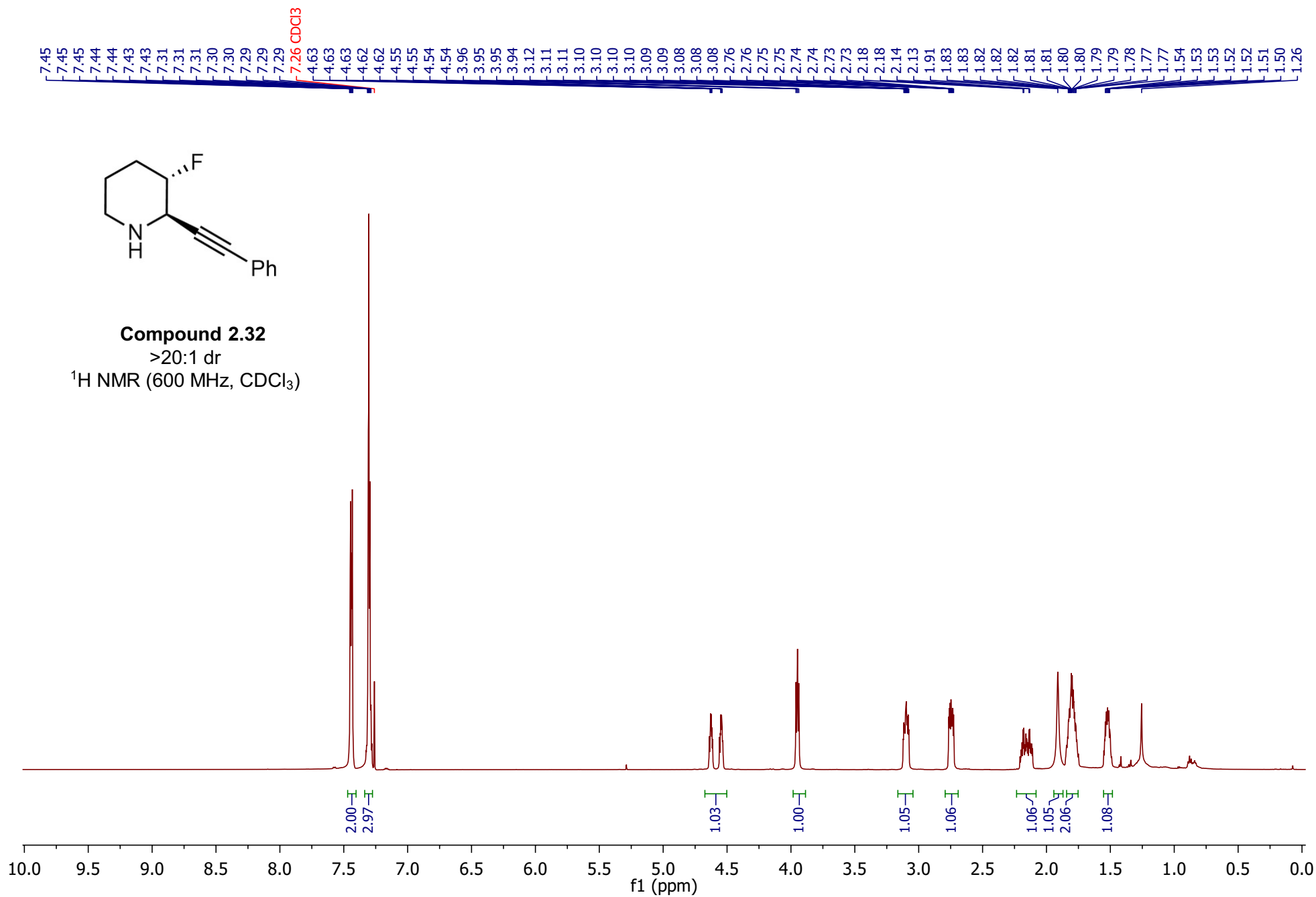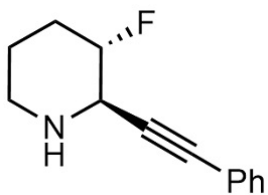
Compound 2.32
>20:1 dr
^{13}C NMR (151 MHz, CDCl$_3$)
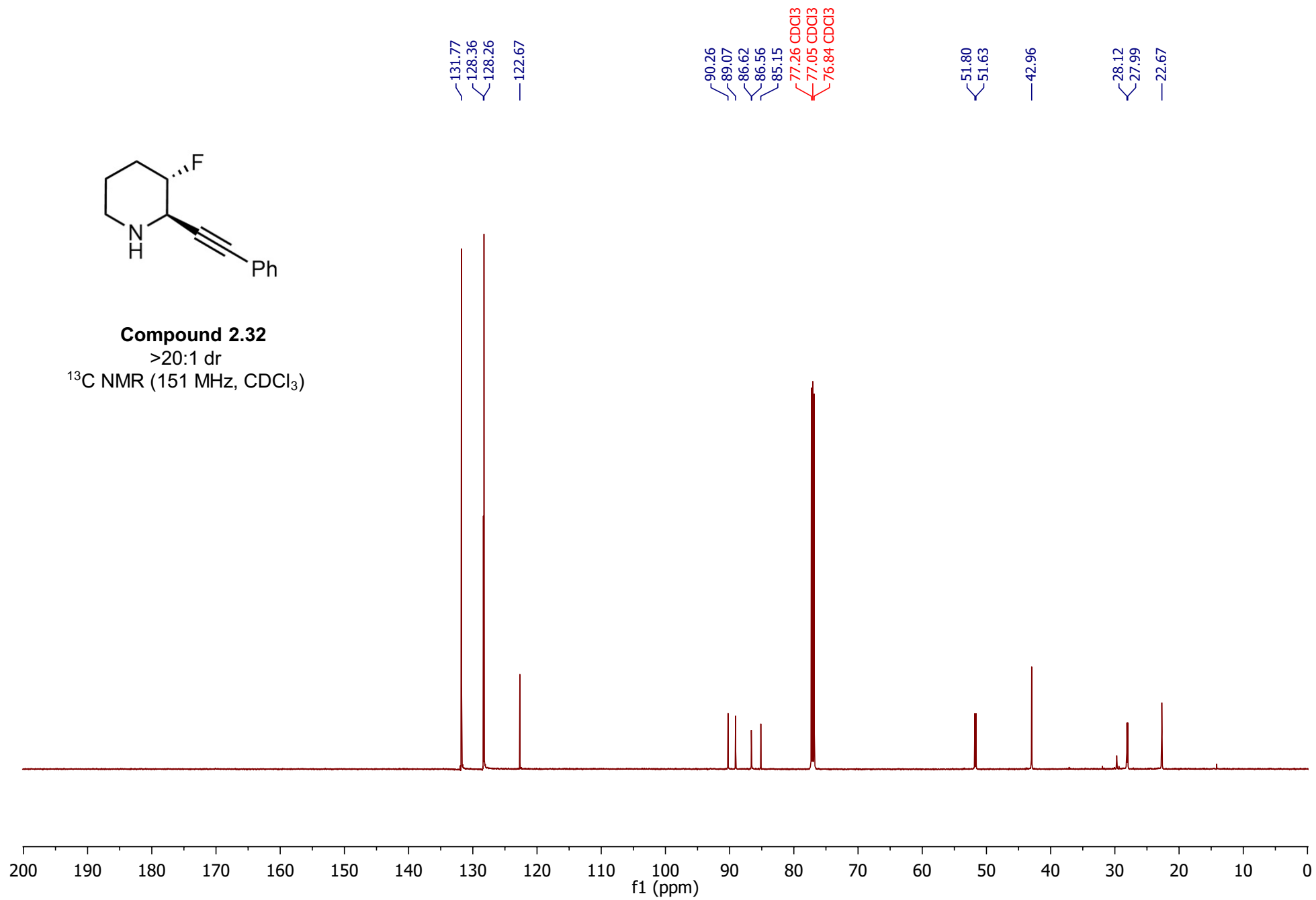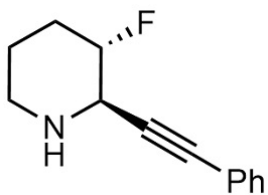
Compound 2.32
>20:1 dr
^{19}F NMR (376 MHz, CDCl$_3$)

—-179.63

Compound 2.33
1.2:1 dr
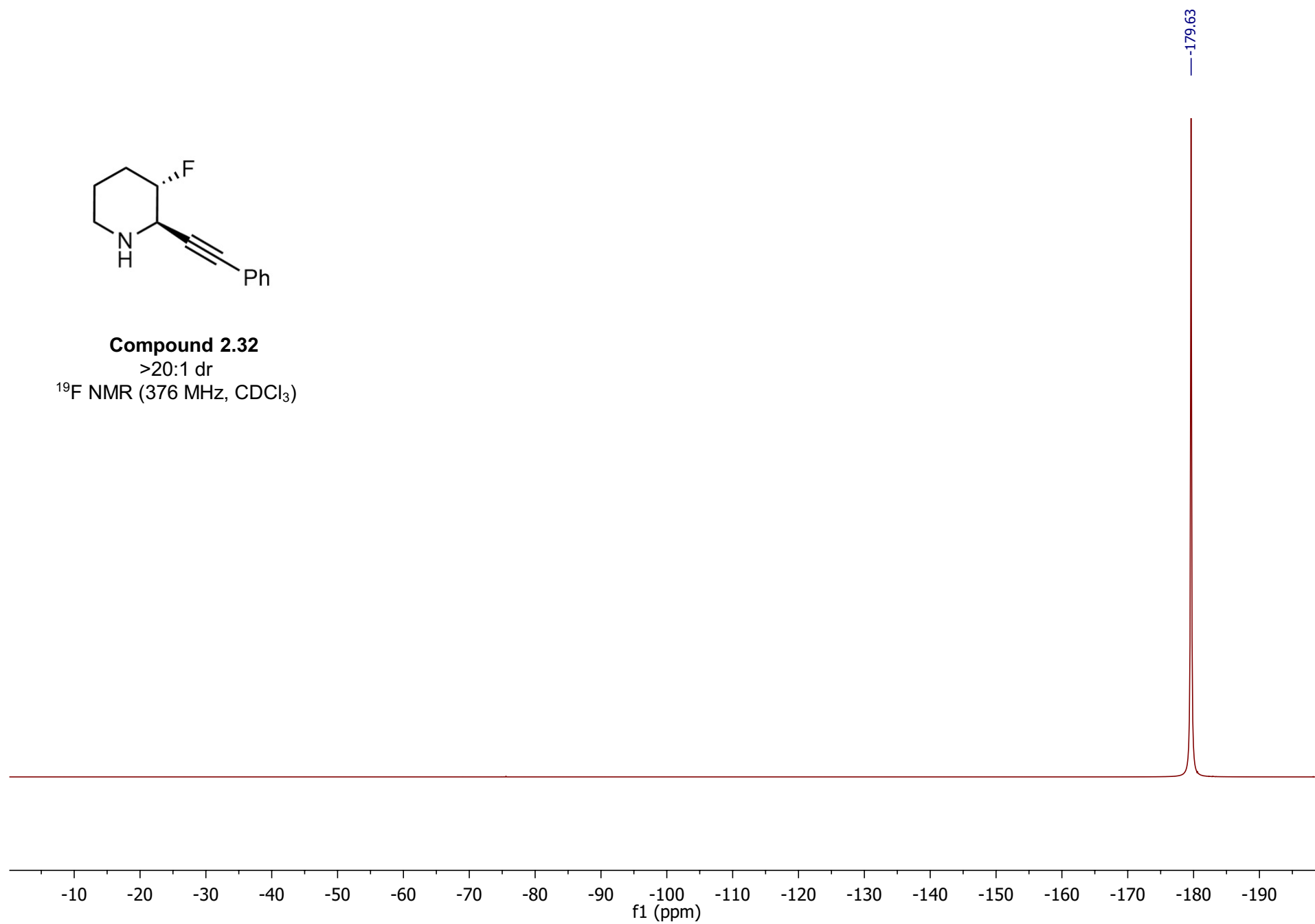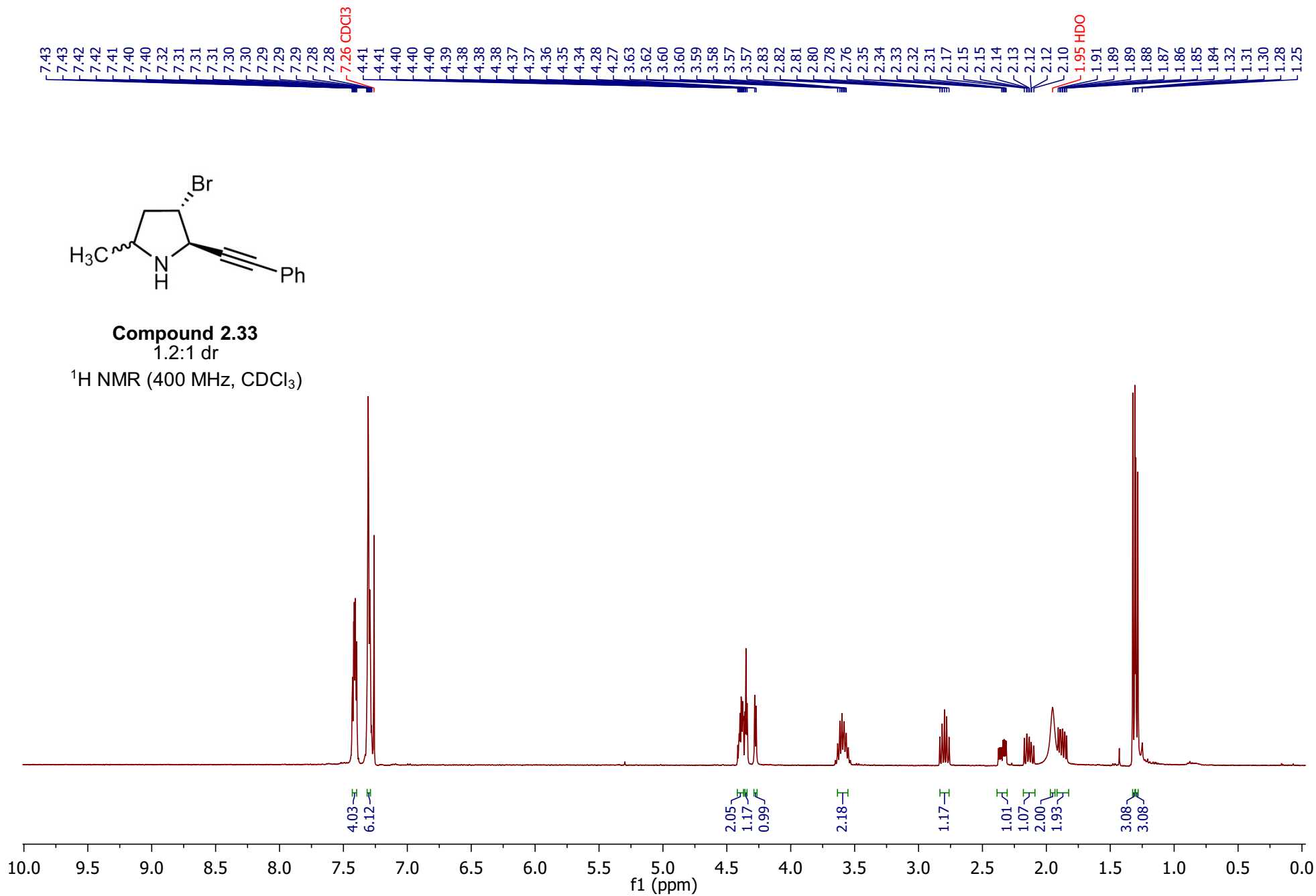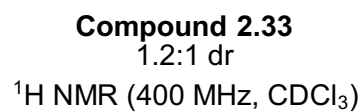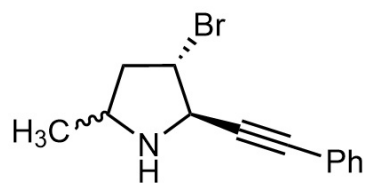
^{1}H NMR (400 MHz, CDCl$_3$)

Compound 2.33
1.2:1 dr

^{13}C NMR (101 MHz, CDCl$_3$)

131.71
131.69
128.44
128.43
128.28
122.52
122.51

87.87
87.43
84.69
84.50
77.36 CDCl3
77.04 CDCl3
76.72 CDCl3

60.26
59.84
53.75
53.31
53.08
52.83
44.48
44.07

21.97
21.49
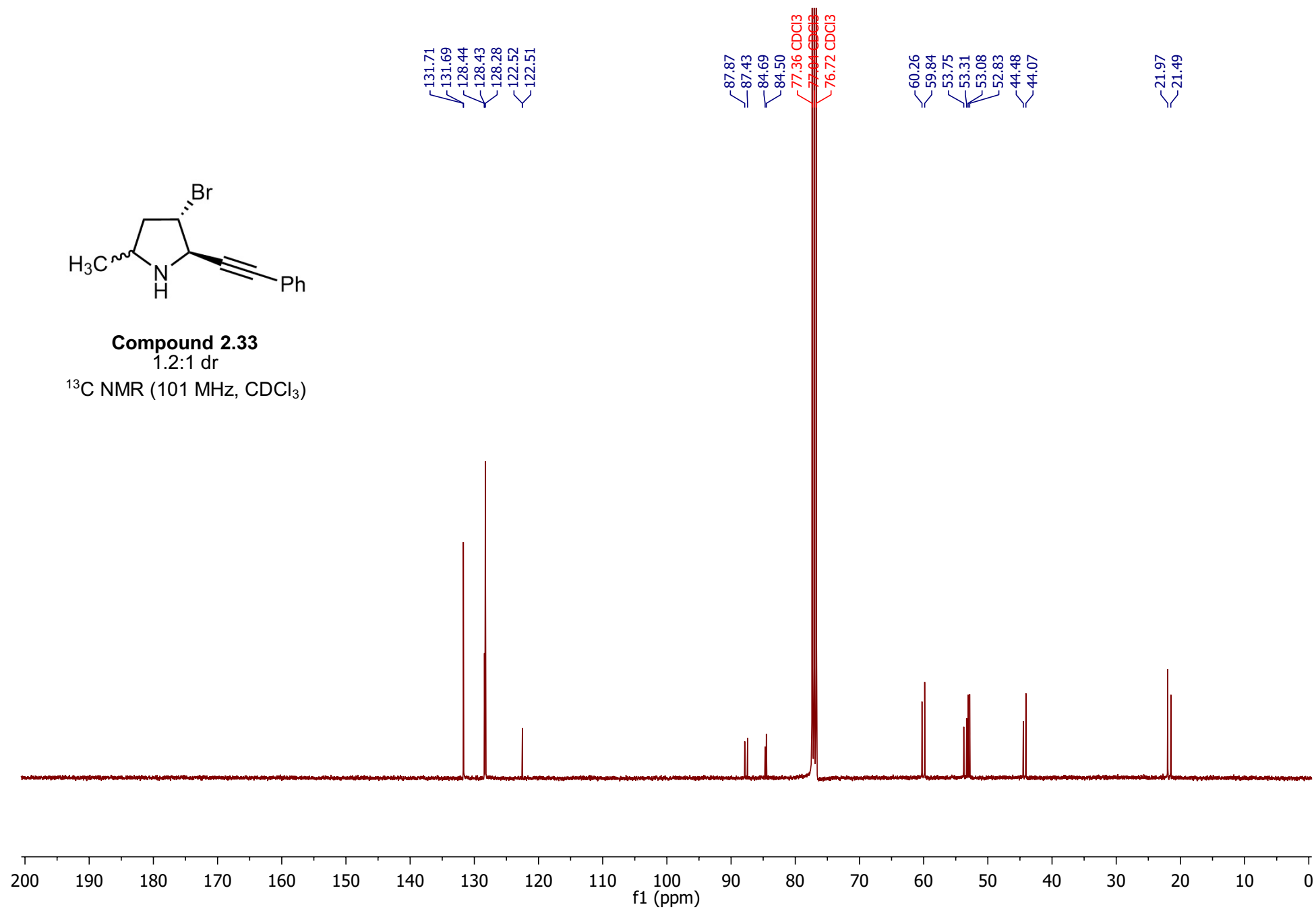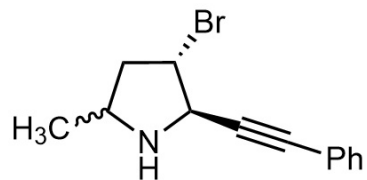
Compound 2.33
1.2:1 dr
COSY NMR
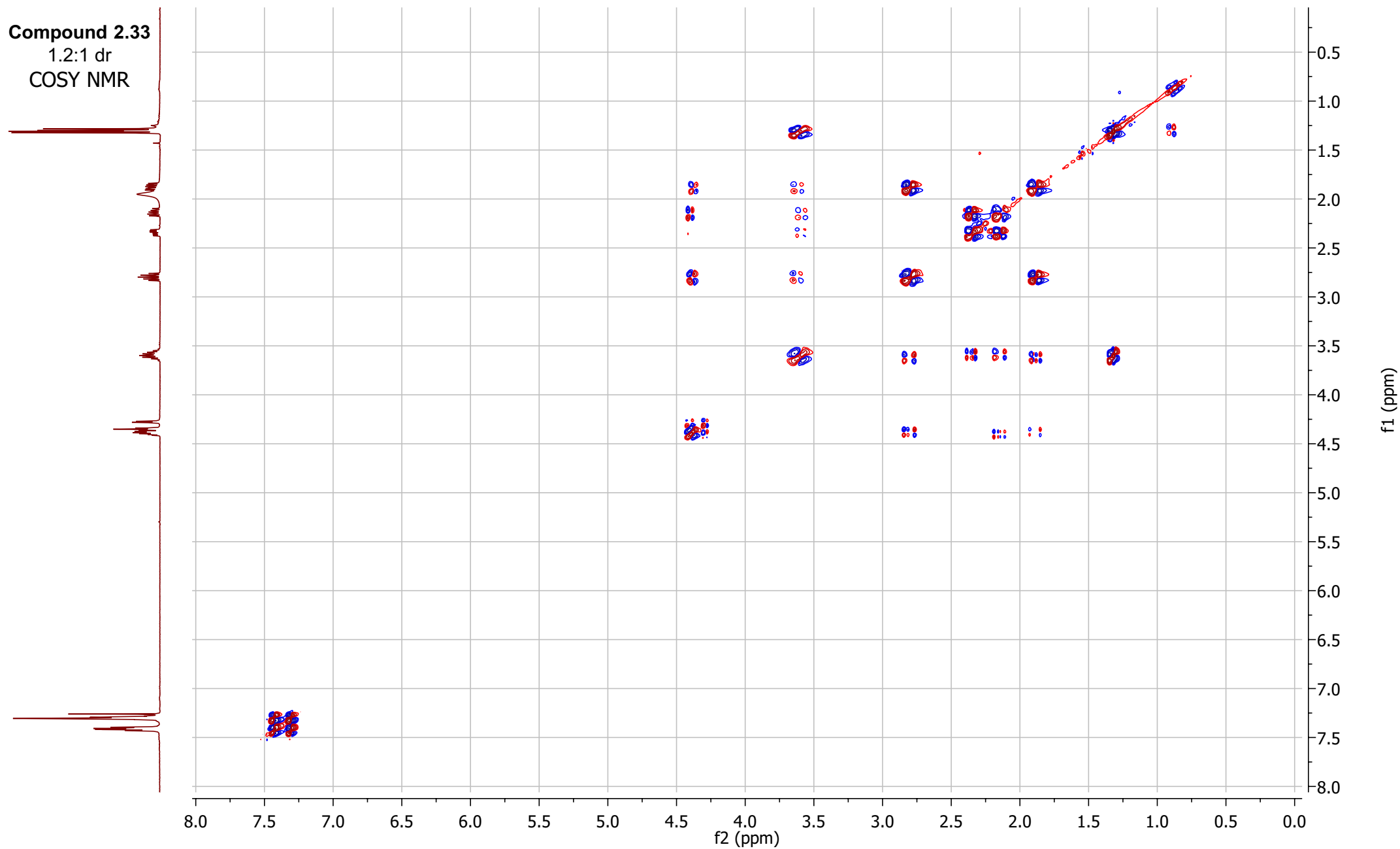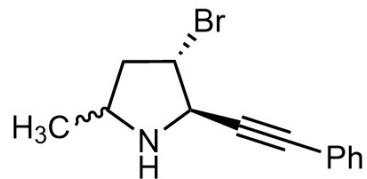
Compound 2.33
1.2:1 dr
NOESY NMR
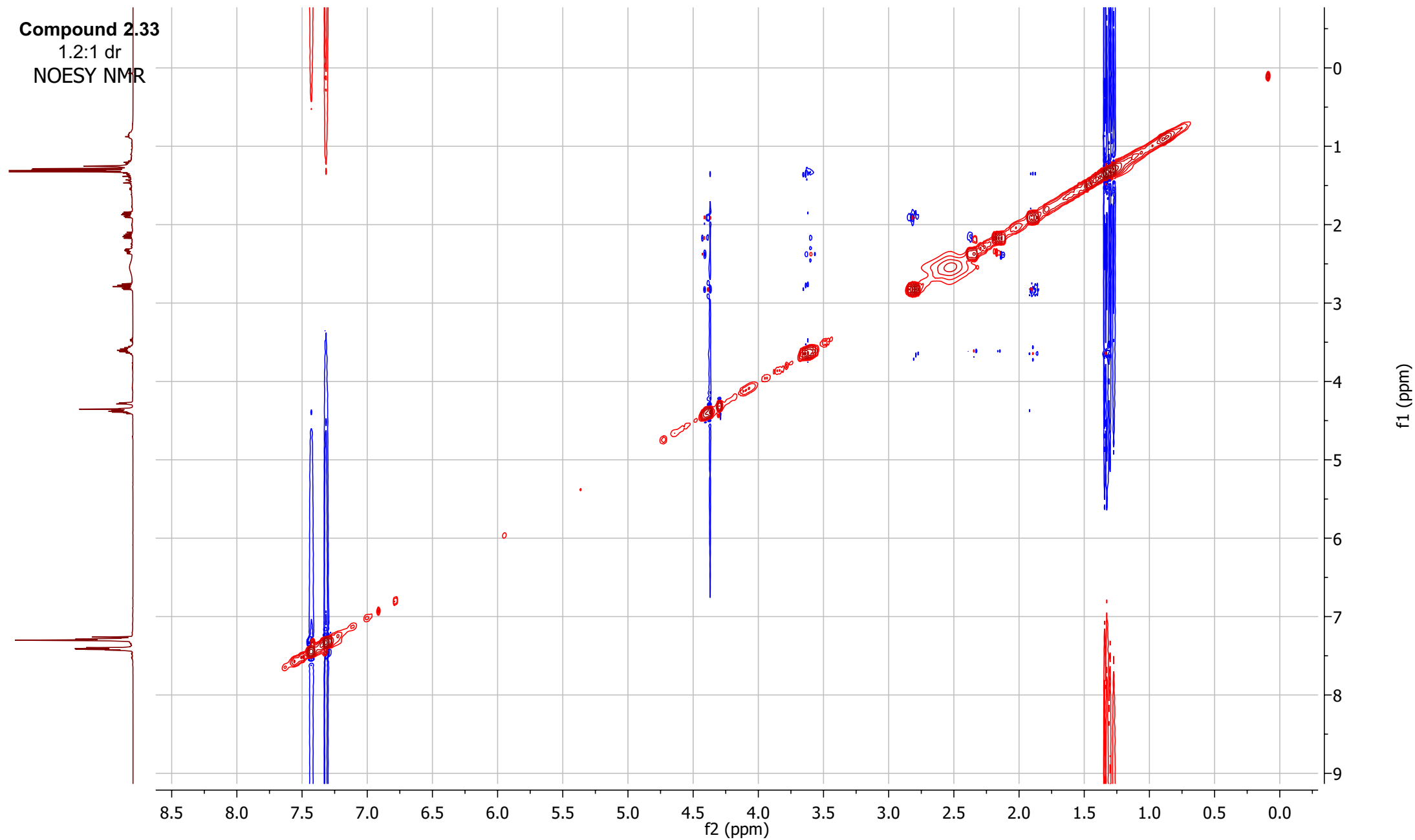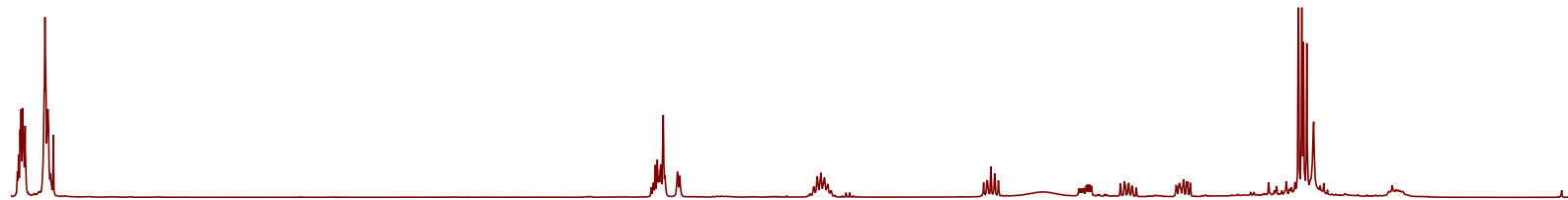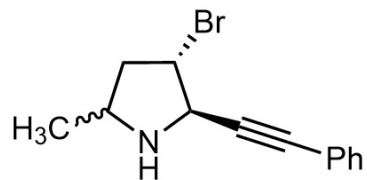
Compound 2.33
1.2:1 dr
HSQC NMR
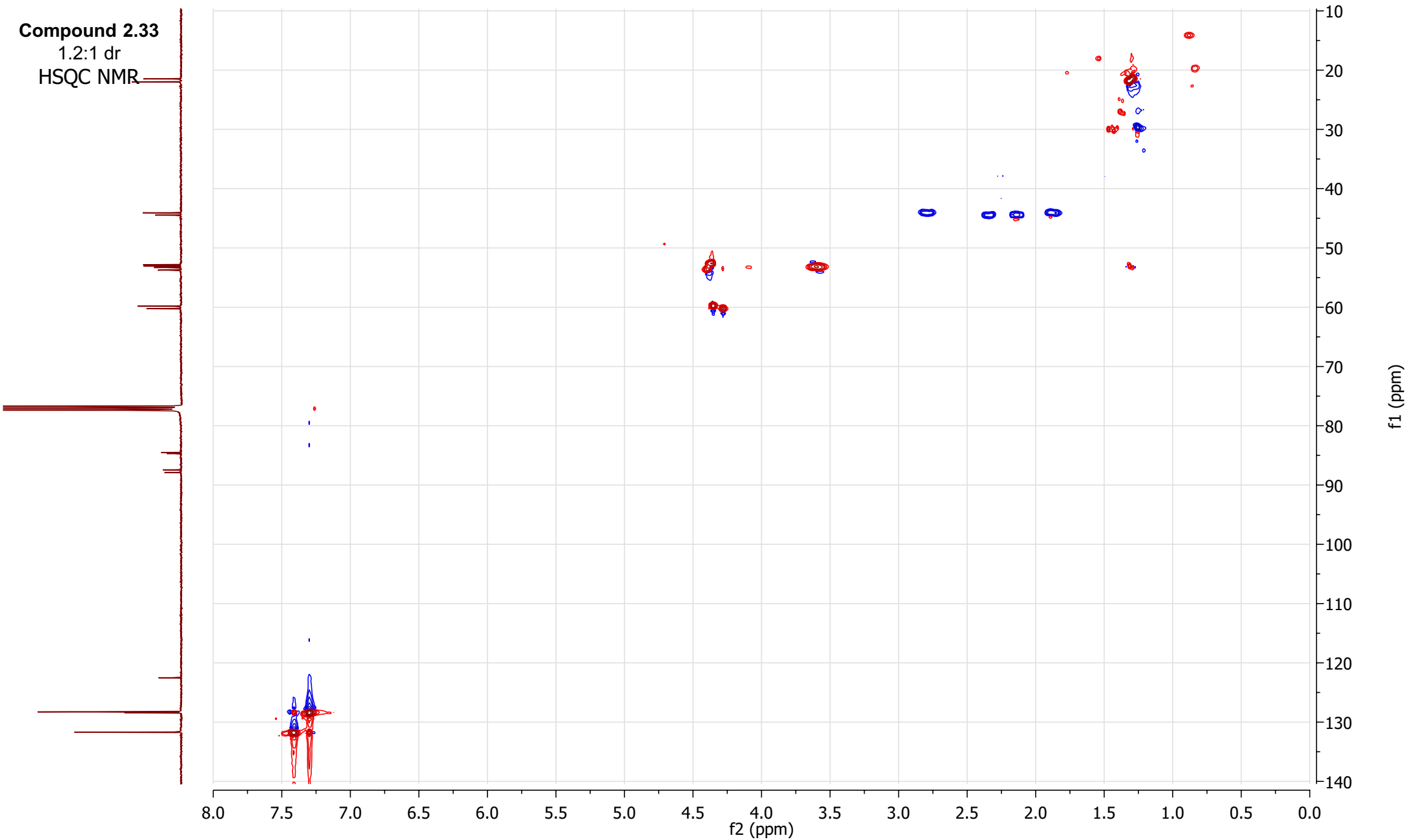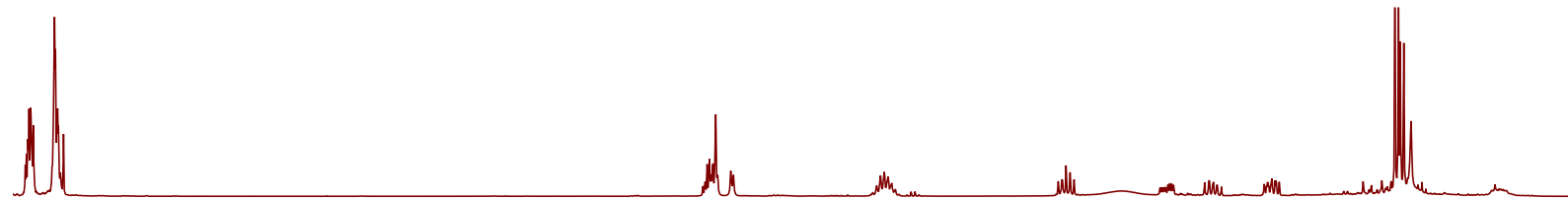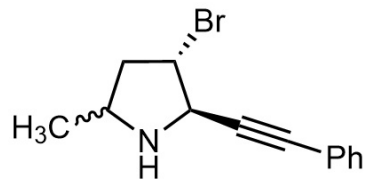
Compound 2.33
1.2:1 dr
HMBC NMR
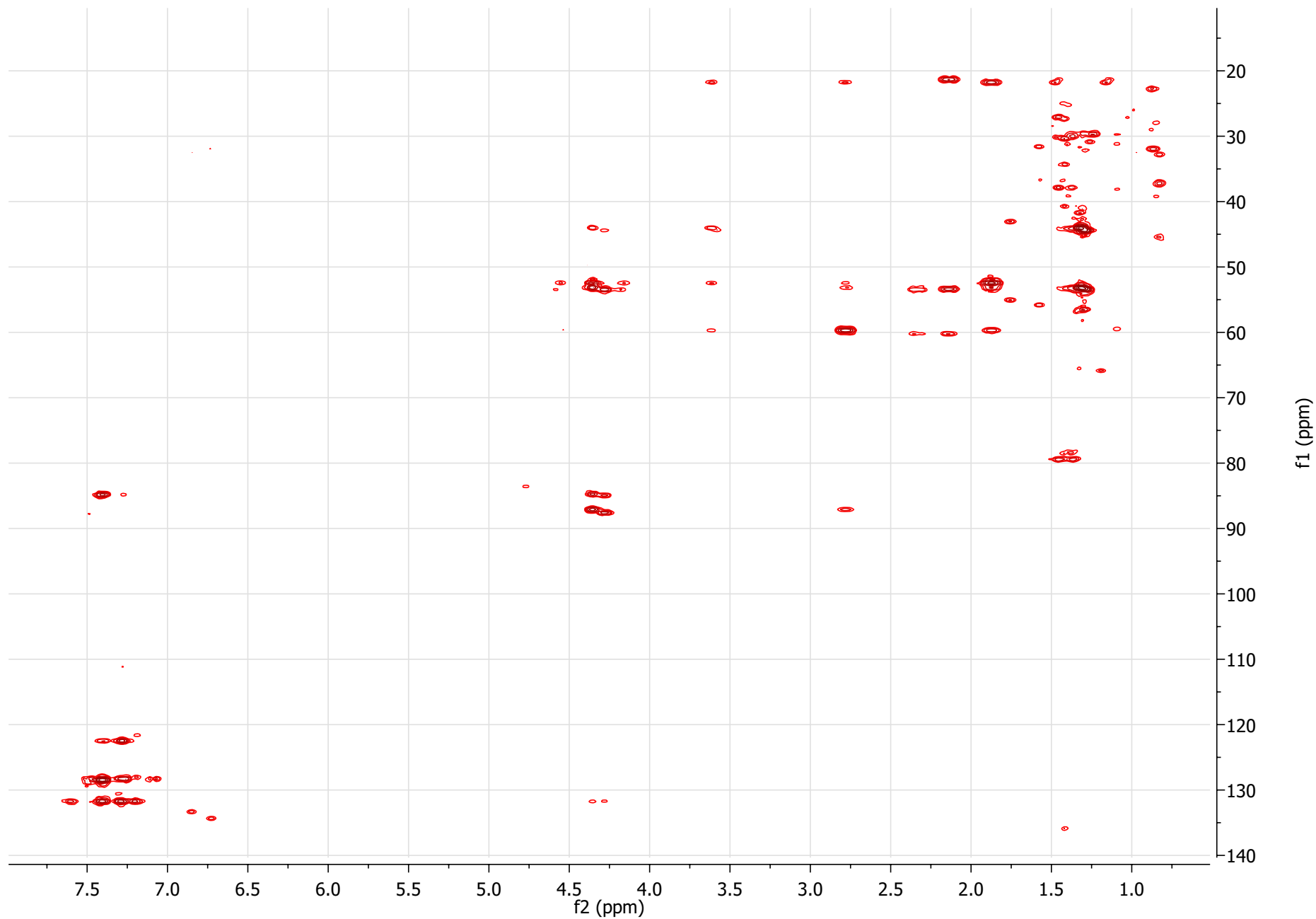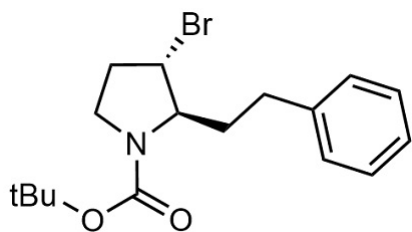
Compound 2.34
>20:1 dr, mix of rotamers
^{1}H NMR (600 MHz, CD$_3$OD)
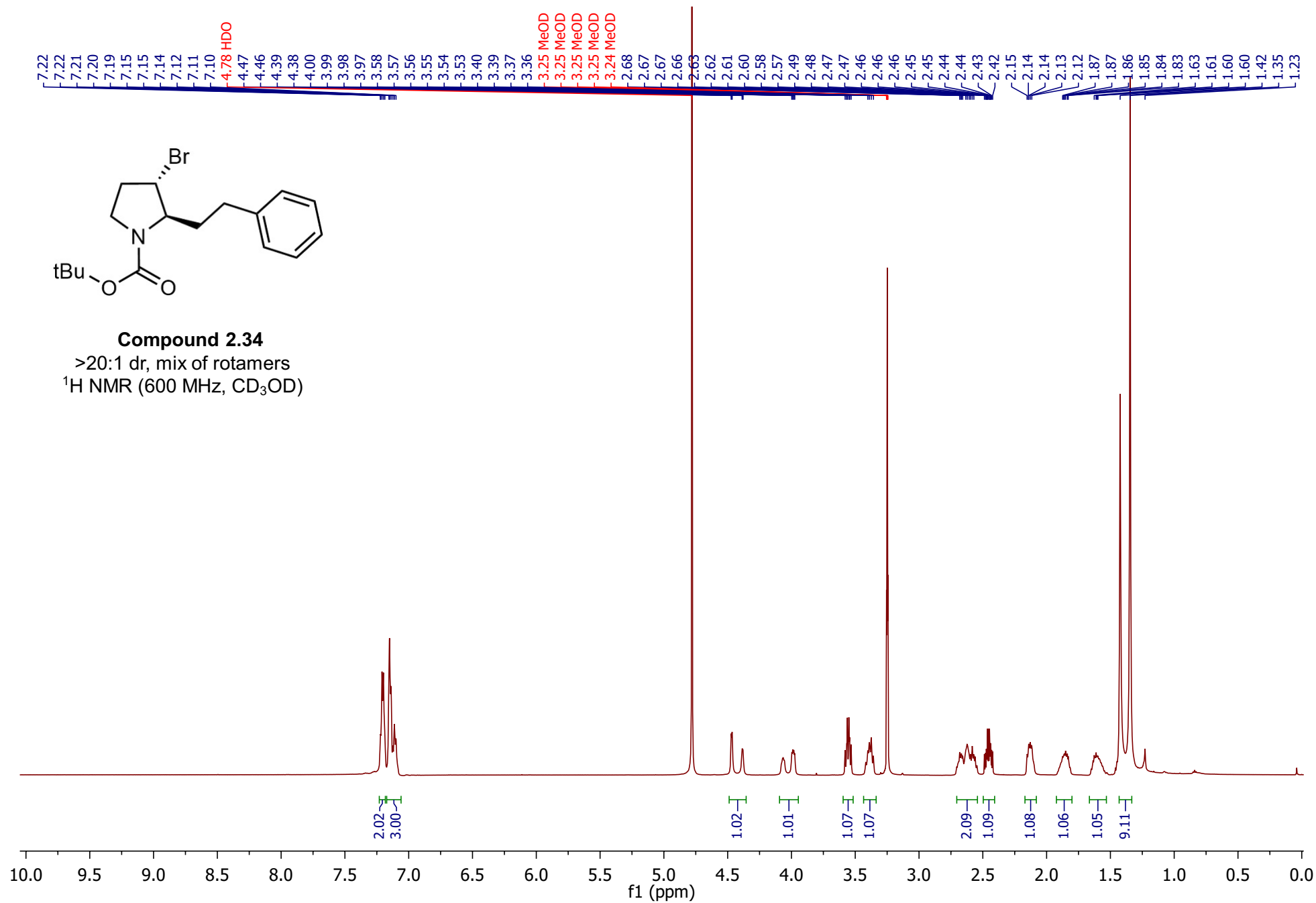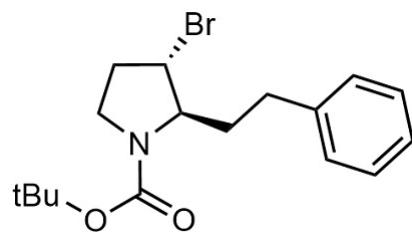
Compound 2.34
>20:1 dr, mix of rotamers
^{13}C NMR (151 MHz, CD$_3$OD)

155.11
141.30
141.01
128.13
128.09
127.97
125.71
125.61
80.00
79.75
68.07
67.85
51.79
51.33
44.01
43.57
35.82
35.66
33.45
32.66
32.36
27.33
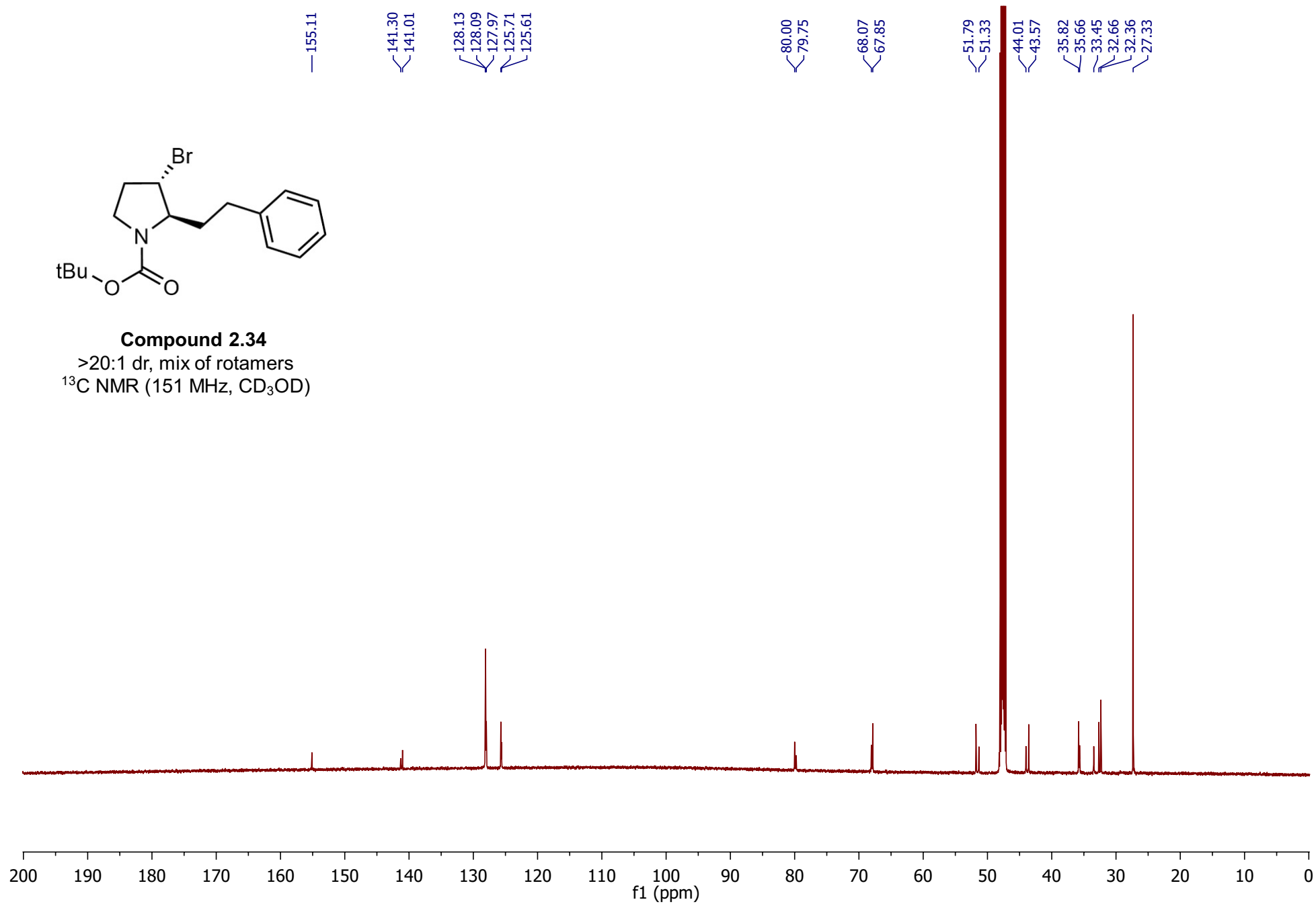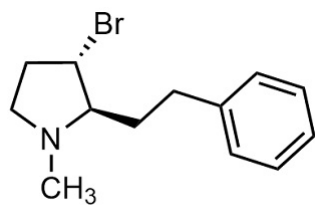
Compound 2.35
>20:1 dr
^{1}H NMR (400 MHz, CDCl$_3$)

Acetone
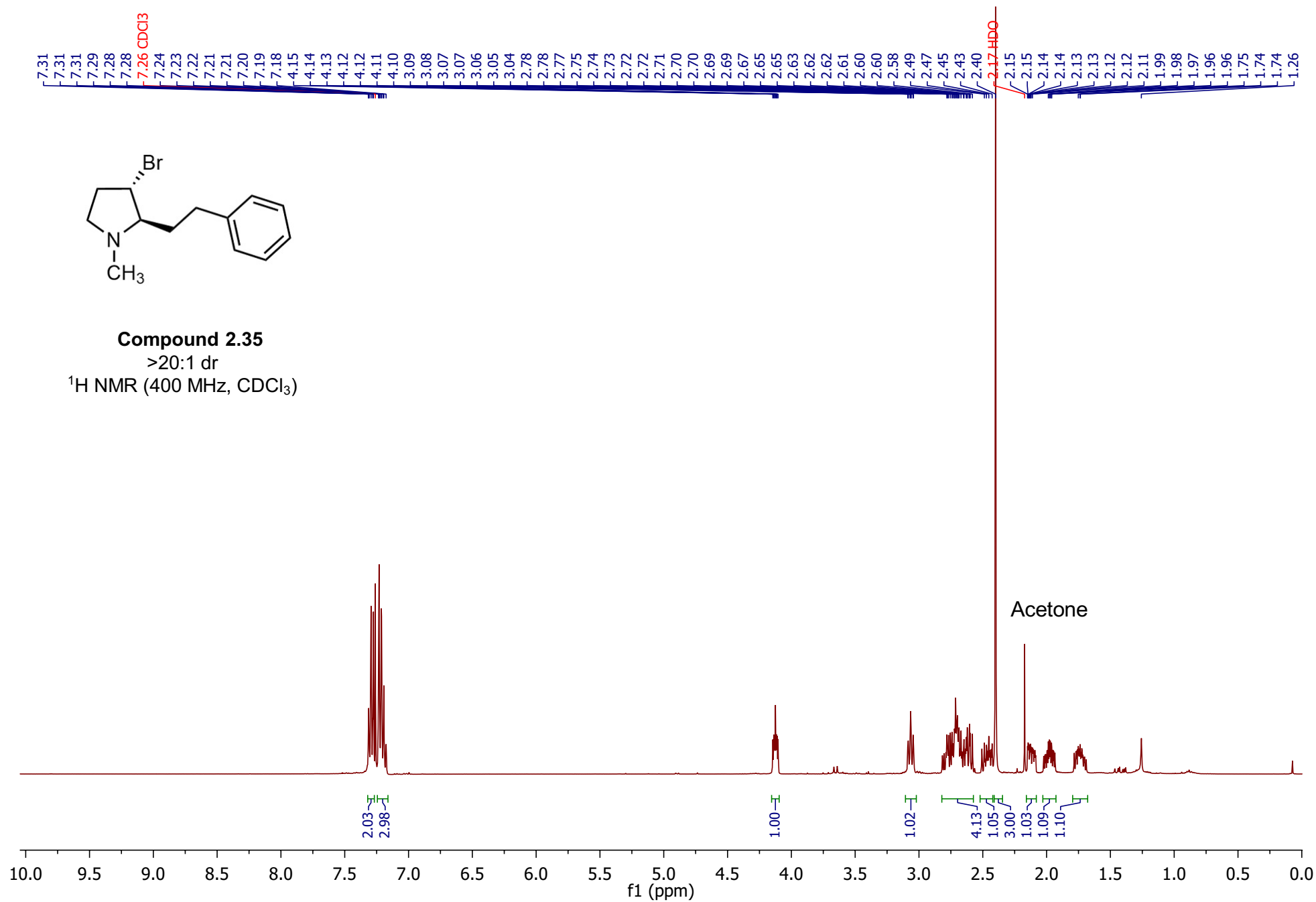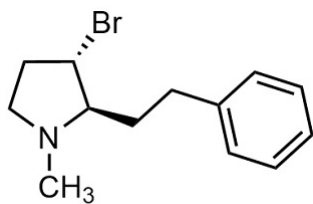
Compound 2.35
>20:1 dr
^{13}C NMR (151 MHz, CDCl$_3$)
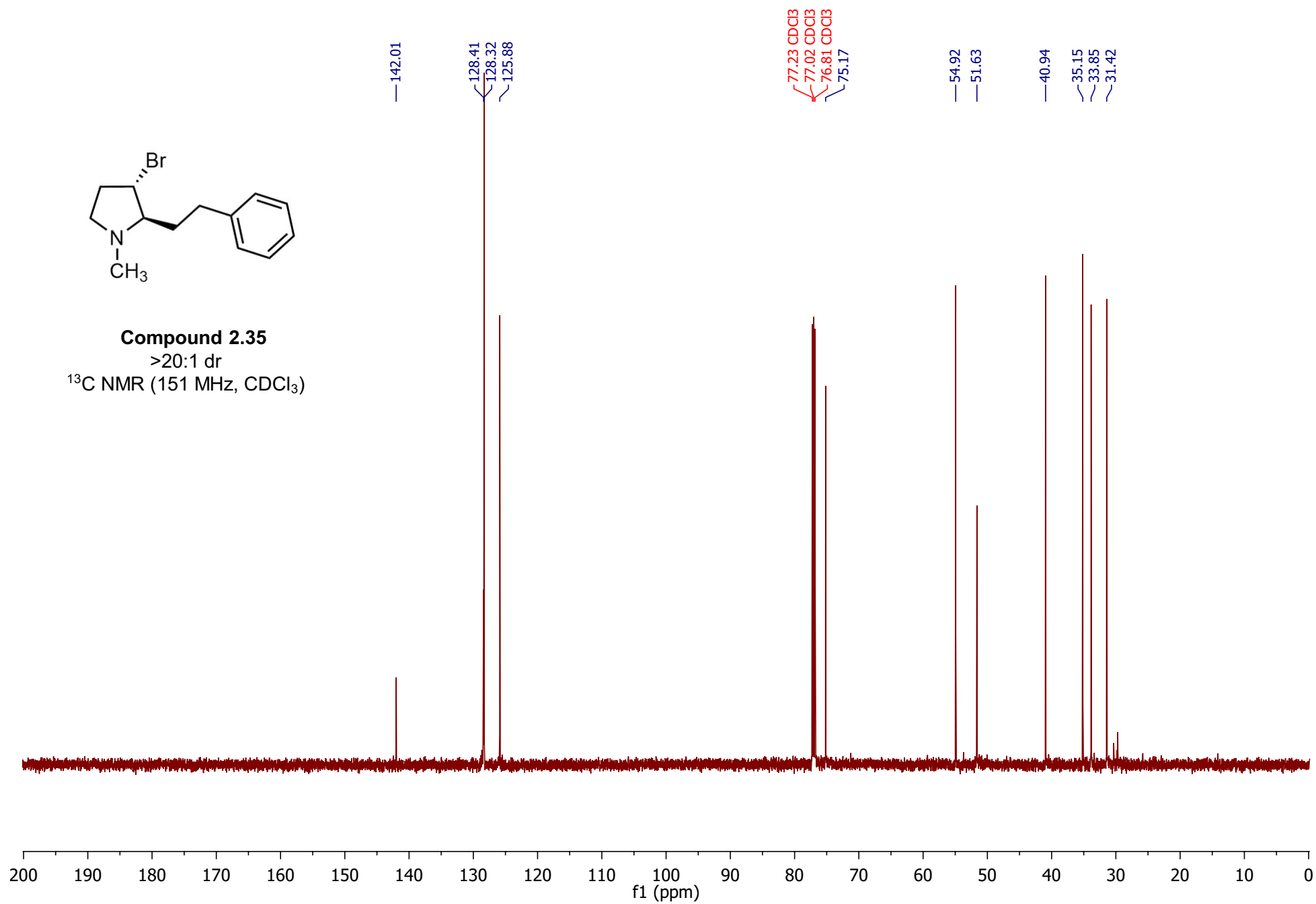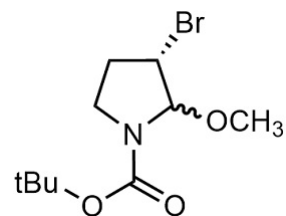
Compound 2.36
1.1:1 dr, mix of diastereomers
^{1}H (400 MHz, CDCl$_3$)
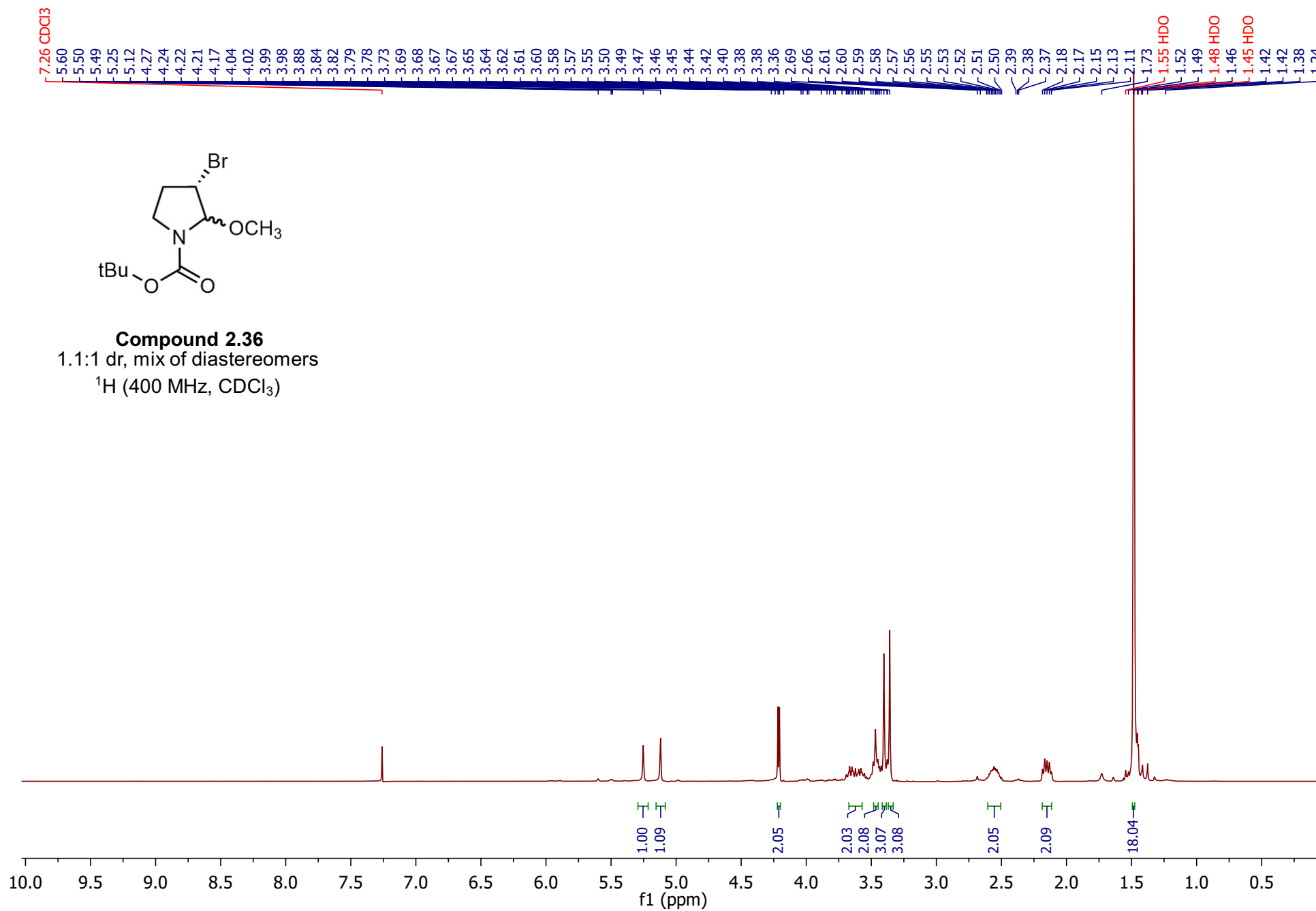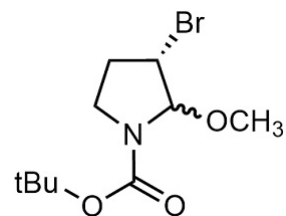
Compound 2.36
1.1:1 dr, mix of diastereomers
^{13}C (101 MHz, CDCl$_3$)
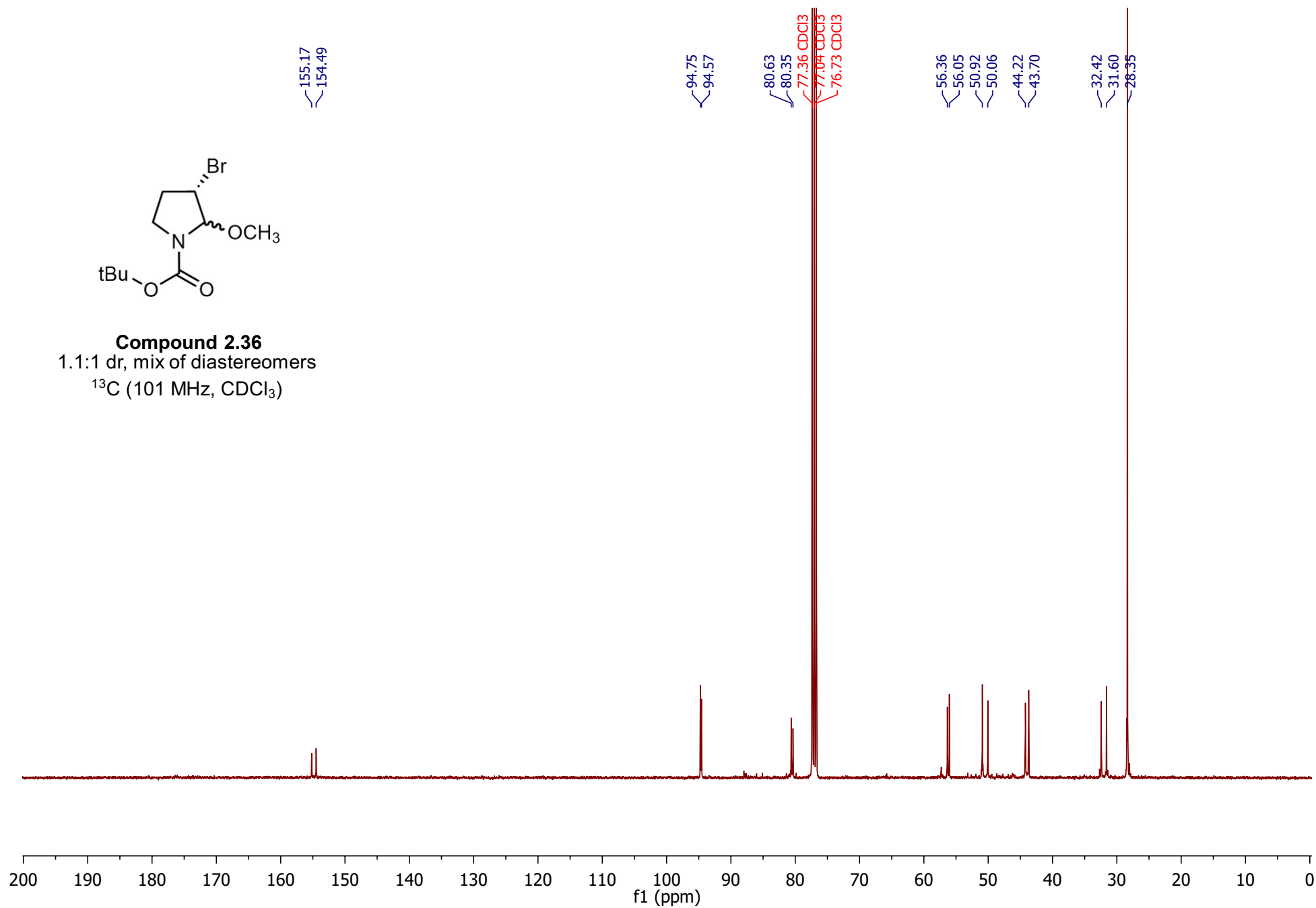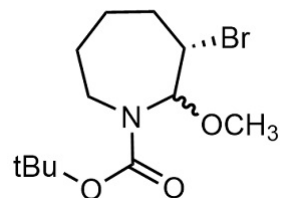
Compound 2.37

1.2:1 dr, mix of diastereomers

^{1}H NMR (400 MHz, CD$_3$OD)

155.97
154.85
92.02
91.07
80.90
80.46
54.68
54.57
54.25
54.11
41.12
40.41
35.37
35.18
28.00
27.68
27.26
27.21
26.89
26.17
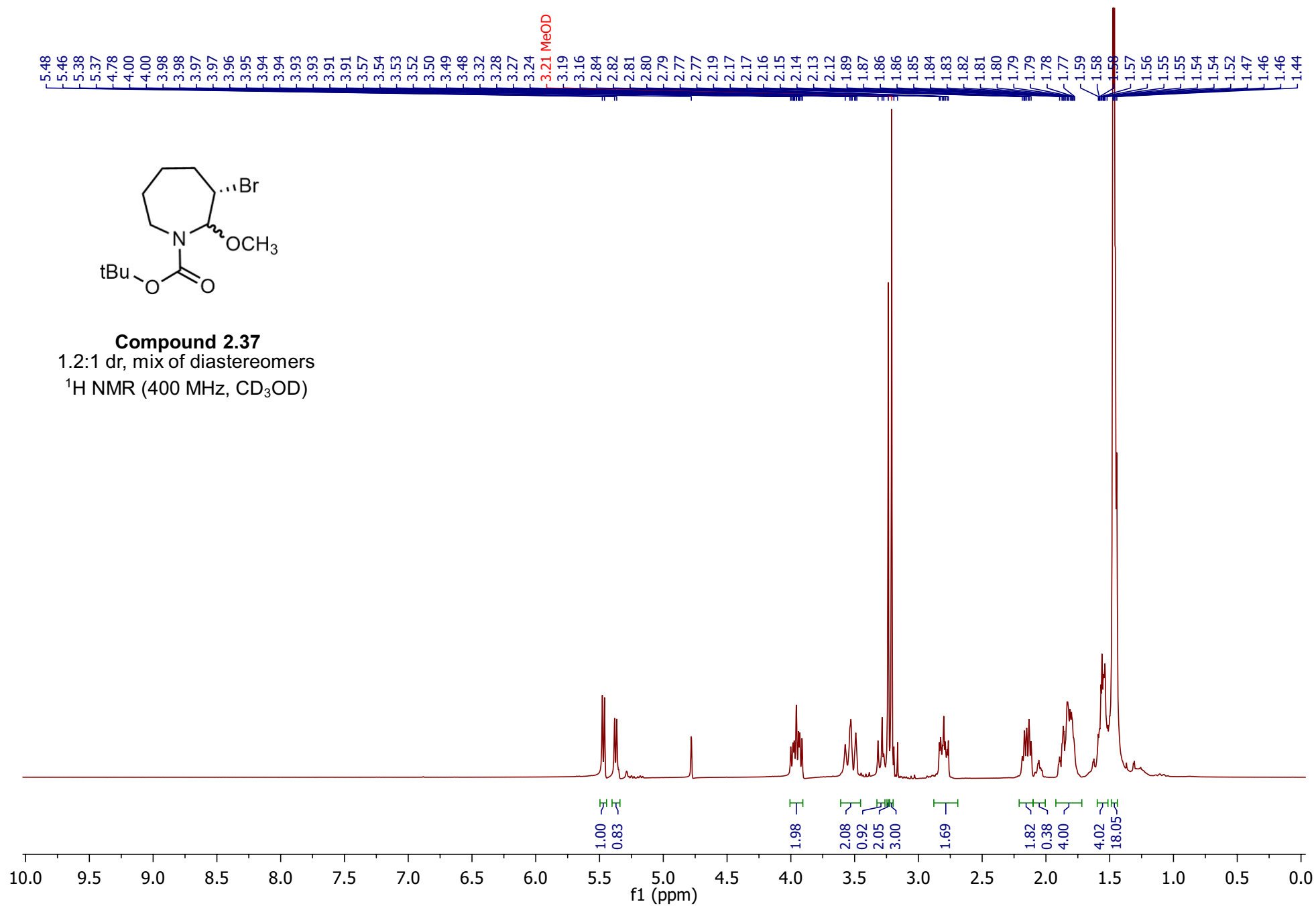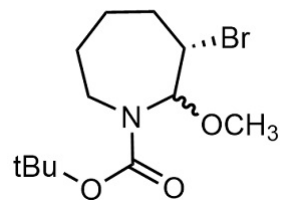
Compound 2.37
1.2:1 dr, mix of diastereomers
^{13}C NMR (101 MHz, CD$_3$OD)
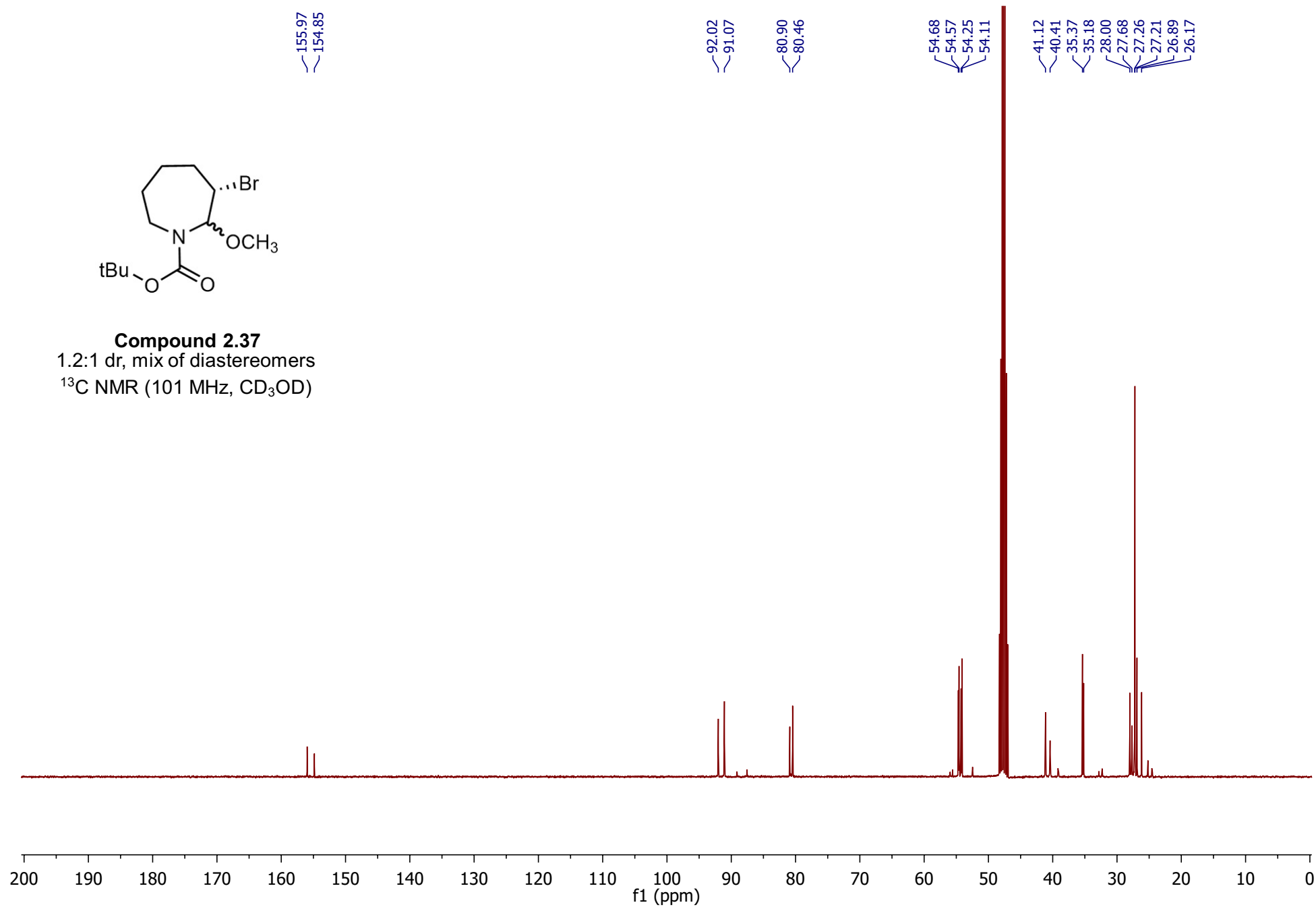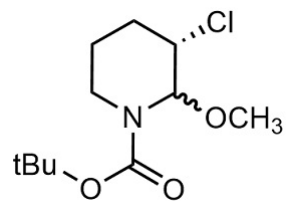
Compound 2.38
2.2:1 dr
^{1}H NMR (400 MHz, CD$_3$OD)
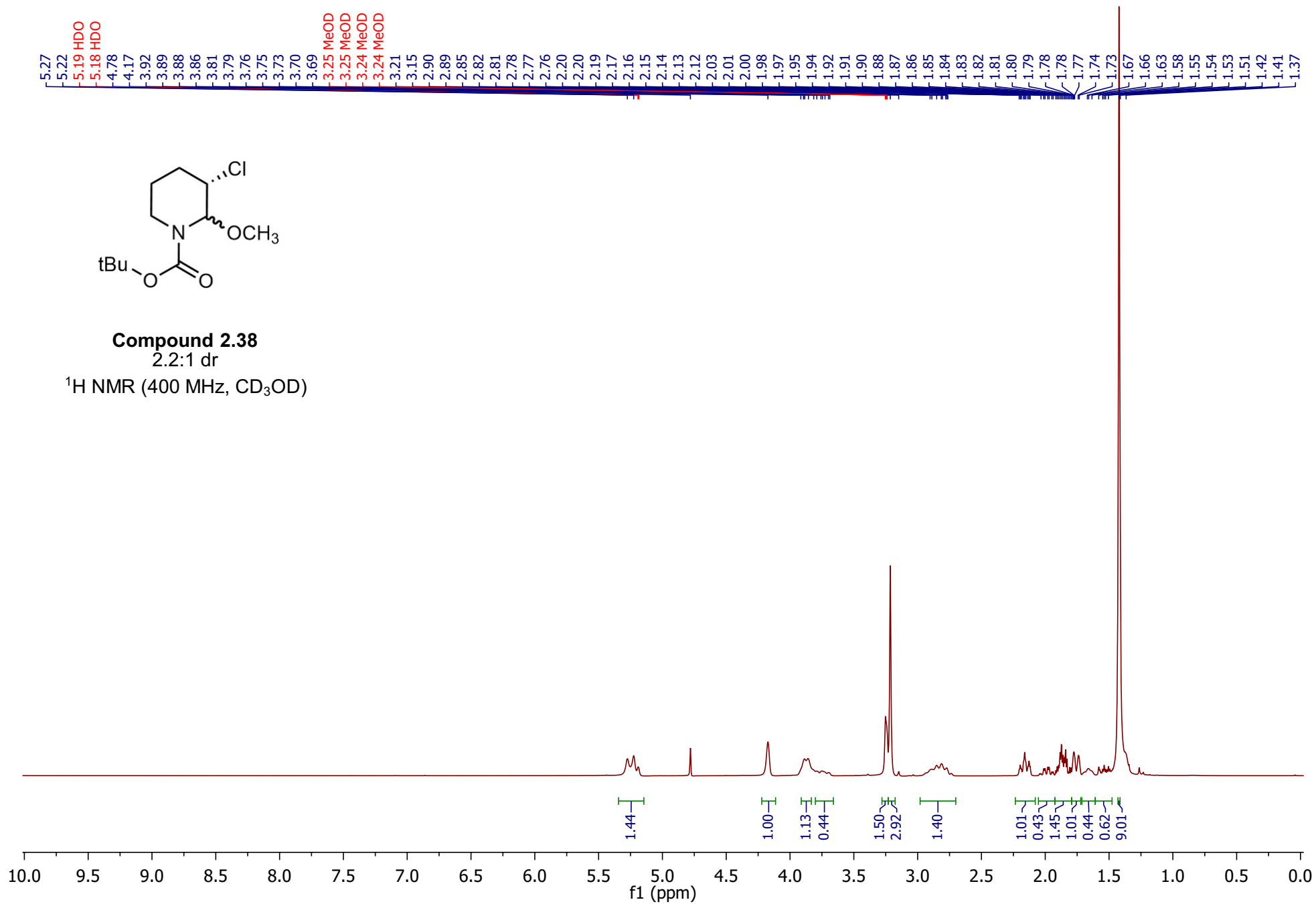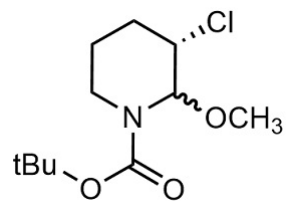
Compound 2.38
2.2:1 dr
^{13}C NMR (151 MHz, CD$_3$OD)
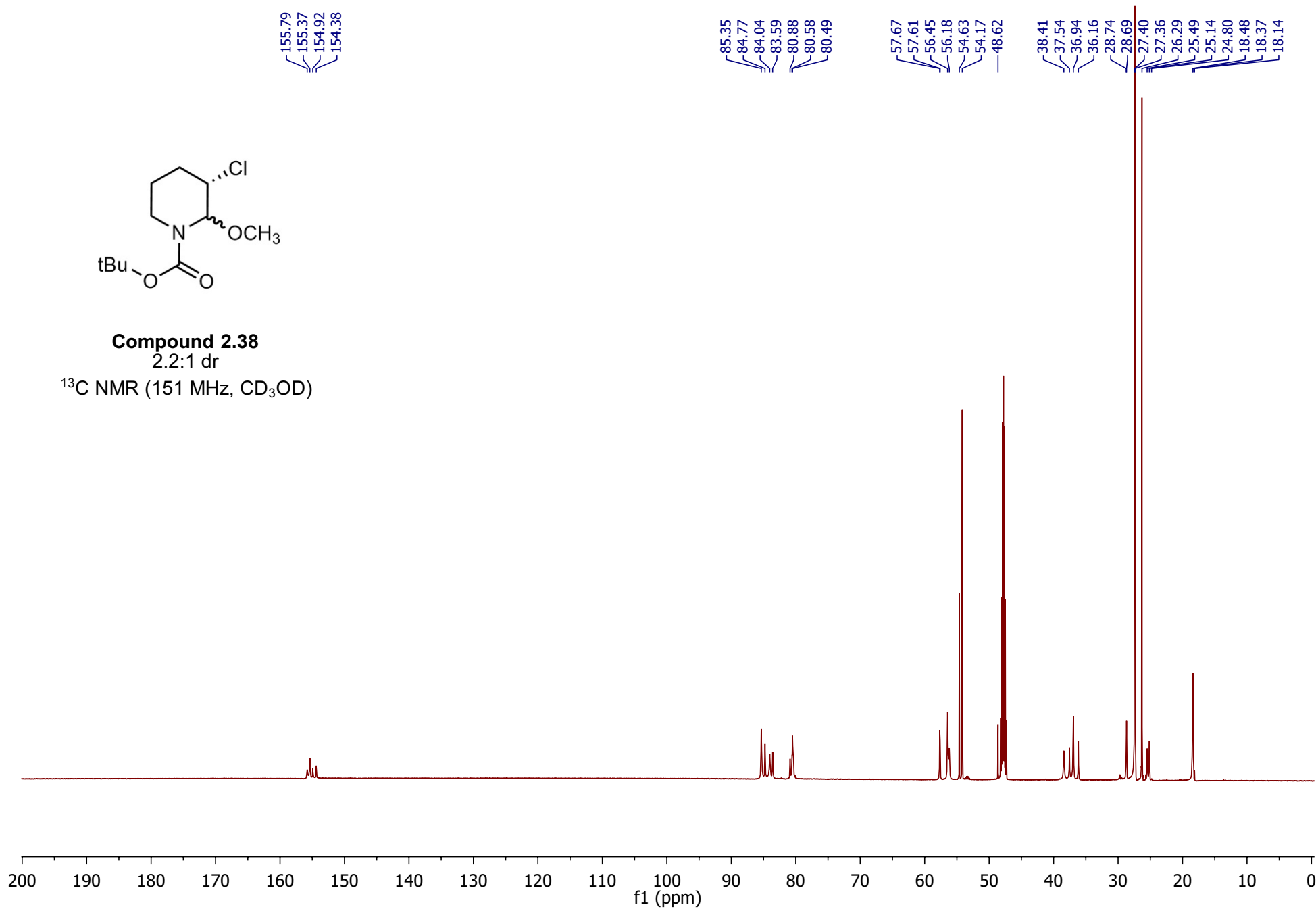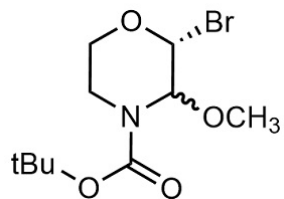
Compound 2.42
1:1 dr
mix of diastereomers and rotamers
^{1}H NMR (400 MHz, CDCl$_3$)

Compound 2.42
1:1 dr
mix of diastereomers

^{13}C NMR (101 MHz, CDCl$_3$)
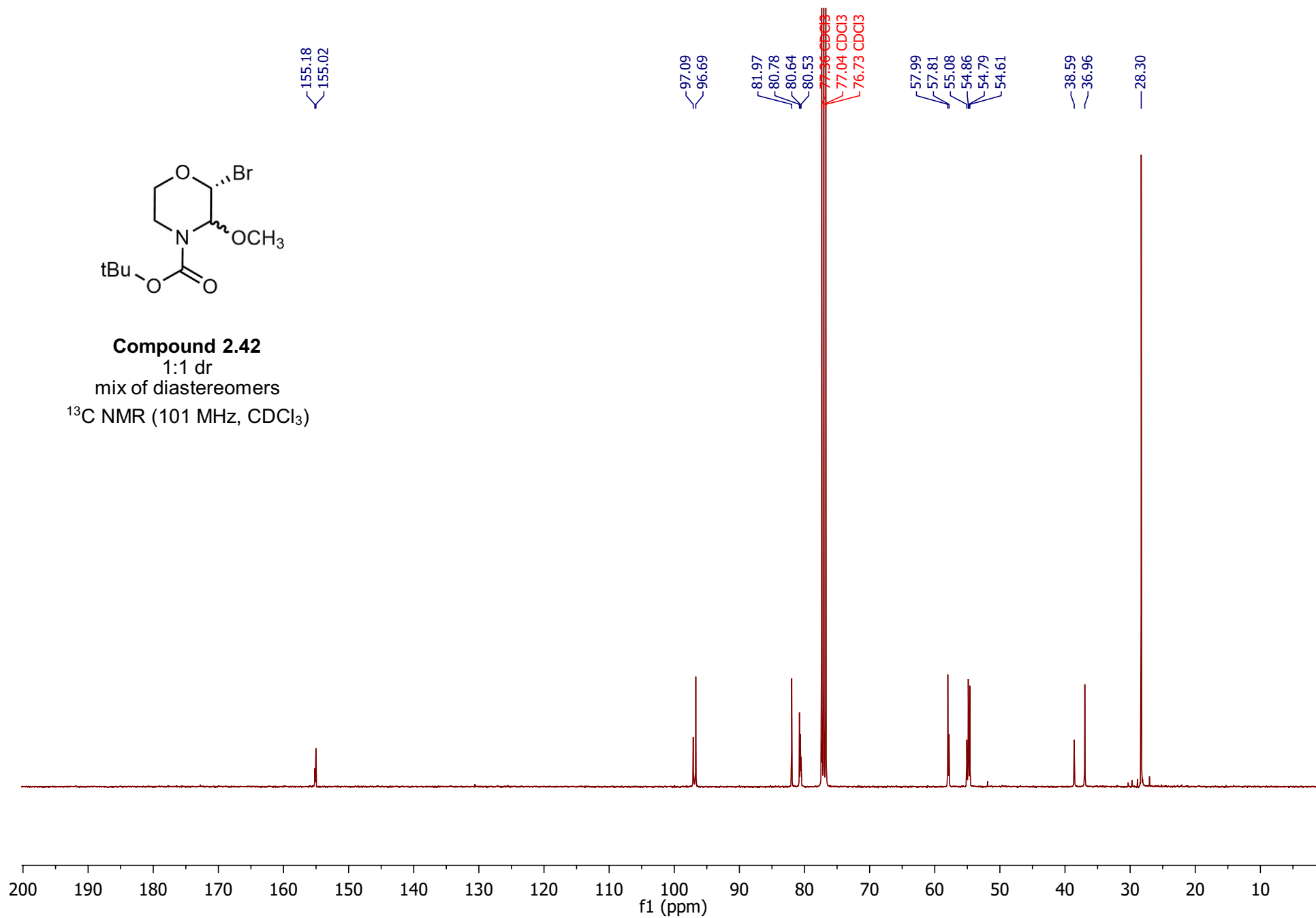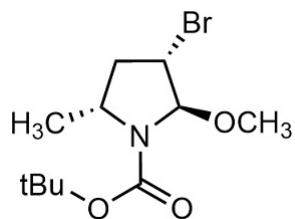
Compound 2.43
one diastereomer
^{1}H NMR (400 MHz, CD$_3$OD)
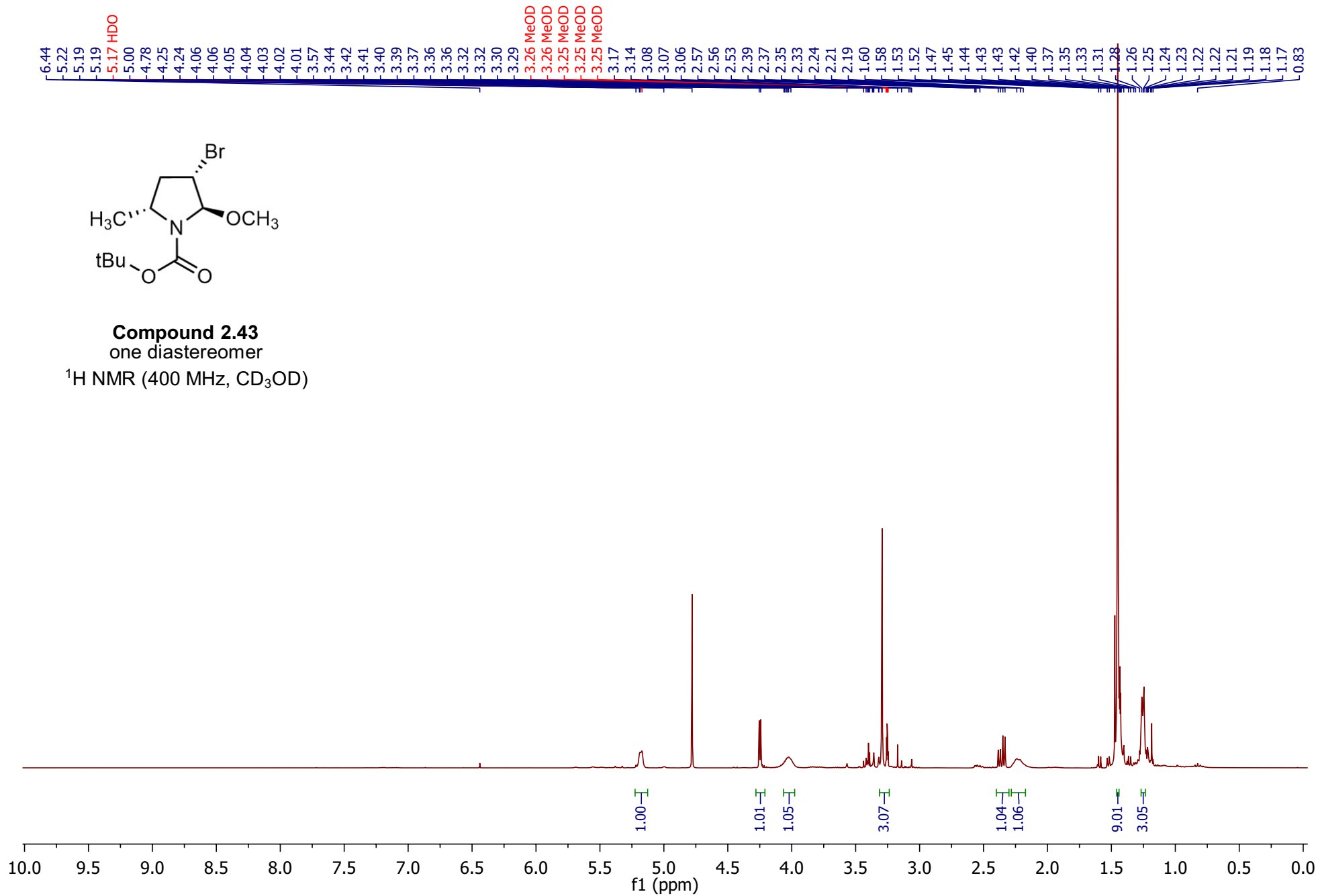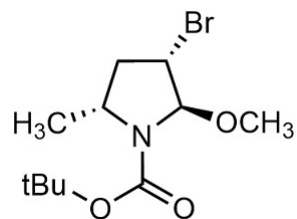
Compound 2.43
(1.2:1 dr)
^{13}C NMR (101 MHz, CD$_3$OD)
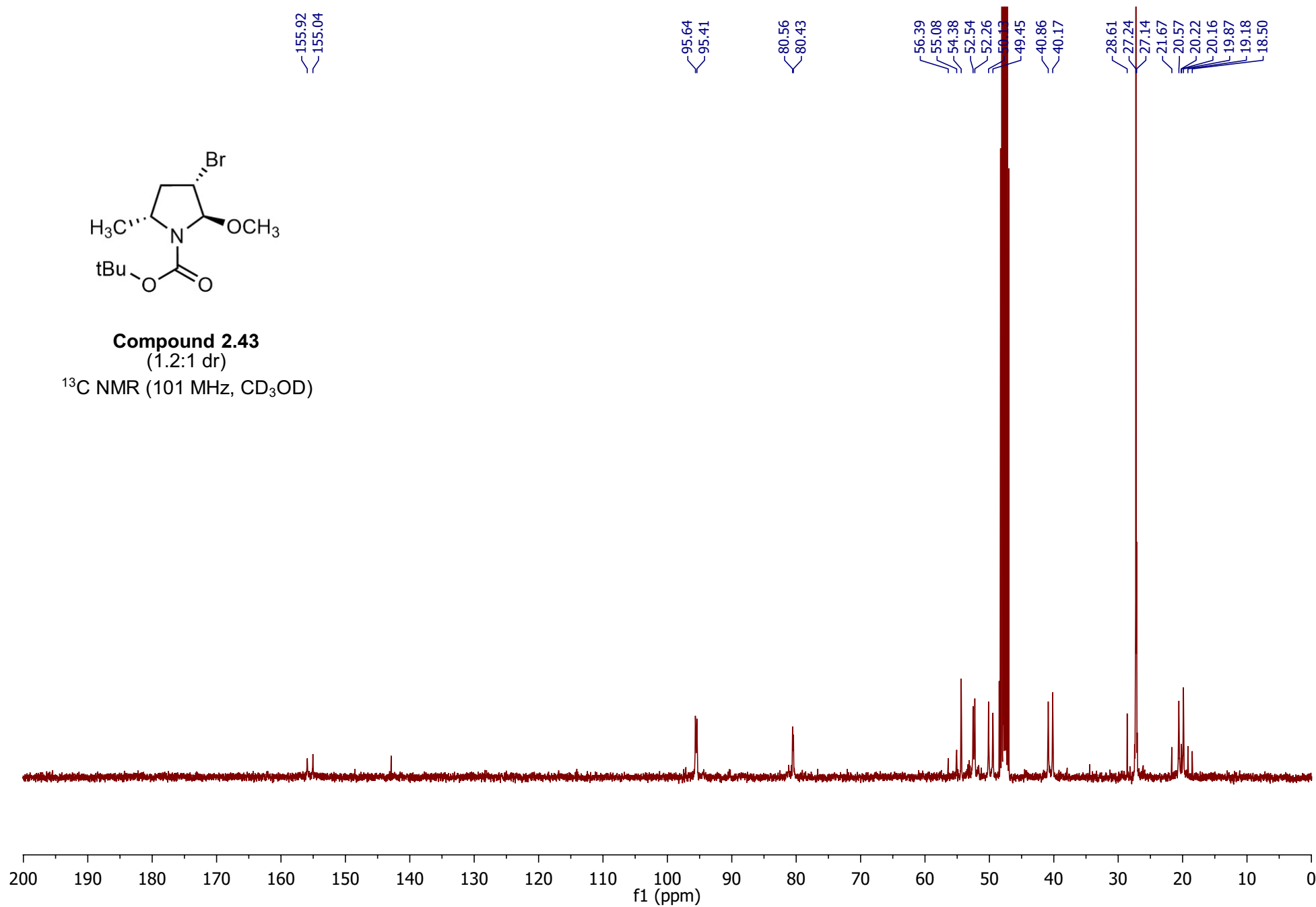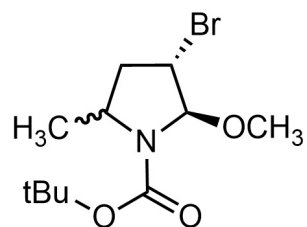
Compound 2.43
1.2:1, mix of diastereomers
^{1}H NMR (600 MHz, CD$_3$OD)
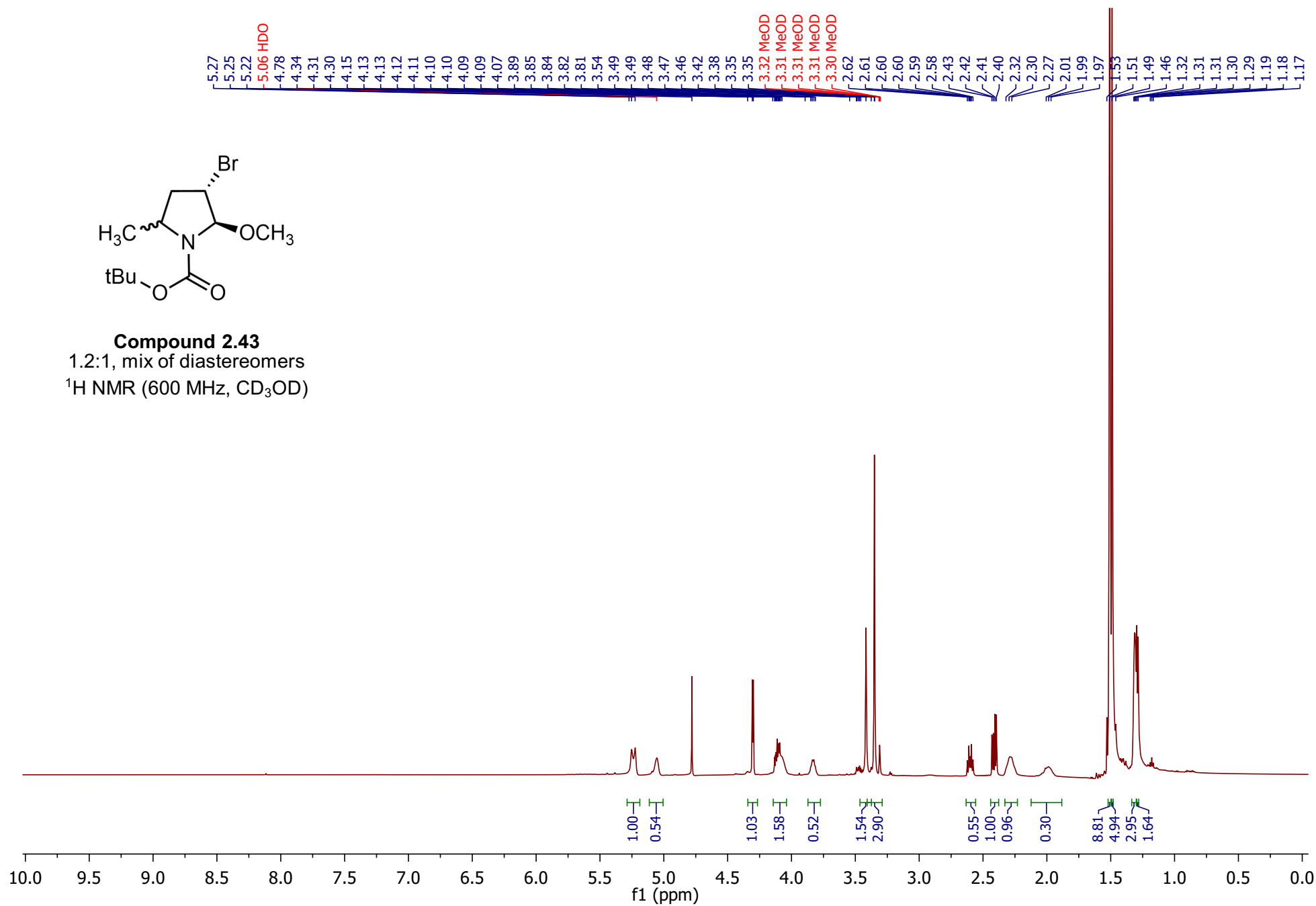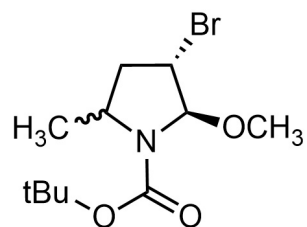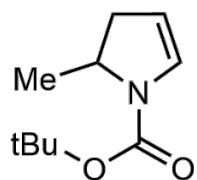
Compound 2.43
1.2:1, mix of diastereomers
^{13}C NMR (101 MHz, CD$_3$OD)

Me

tBu O O

Compound 2.45
mix of rotamers
^{1}H NMR (400 MHz, CDCl$_3$)

7.26 CDCl3

6.46
6.32

4.86
4.81
4.21
4.20
4.19
4.17
4.15
4.11
4.09
4.08
4.06

2.89
2.86
2.85
2.82
2.81
2.78
2.12
2.09
2.09
2.08
2.08
2.04
1.58
1.42 HDO
1.26
1.21
1.20
1.19
1.17
1.15

1.00
1.01
1.01
1.05
1.11
9.00
3.00

10.0   9.5   9.0   8.5   8.0   7.5   7.0   6.5   6.0   5.5   5.0   4.5   4.0   3.5   3.0   2.5   2.0   1.5   1.0   0.5   0.0
f1 (ppm)

Compound 2.45
mix of rotamers
^{13}C NMR (101 MHz, CDCl$_3$)
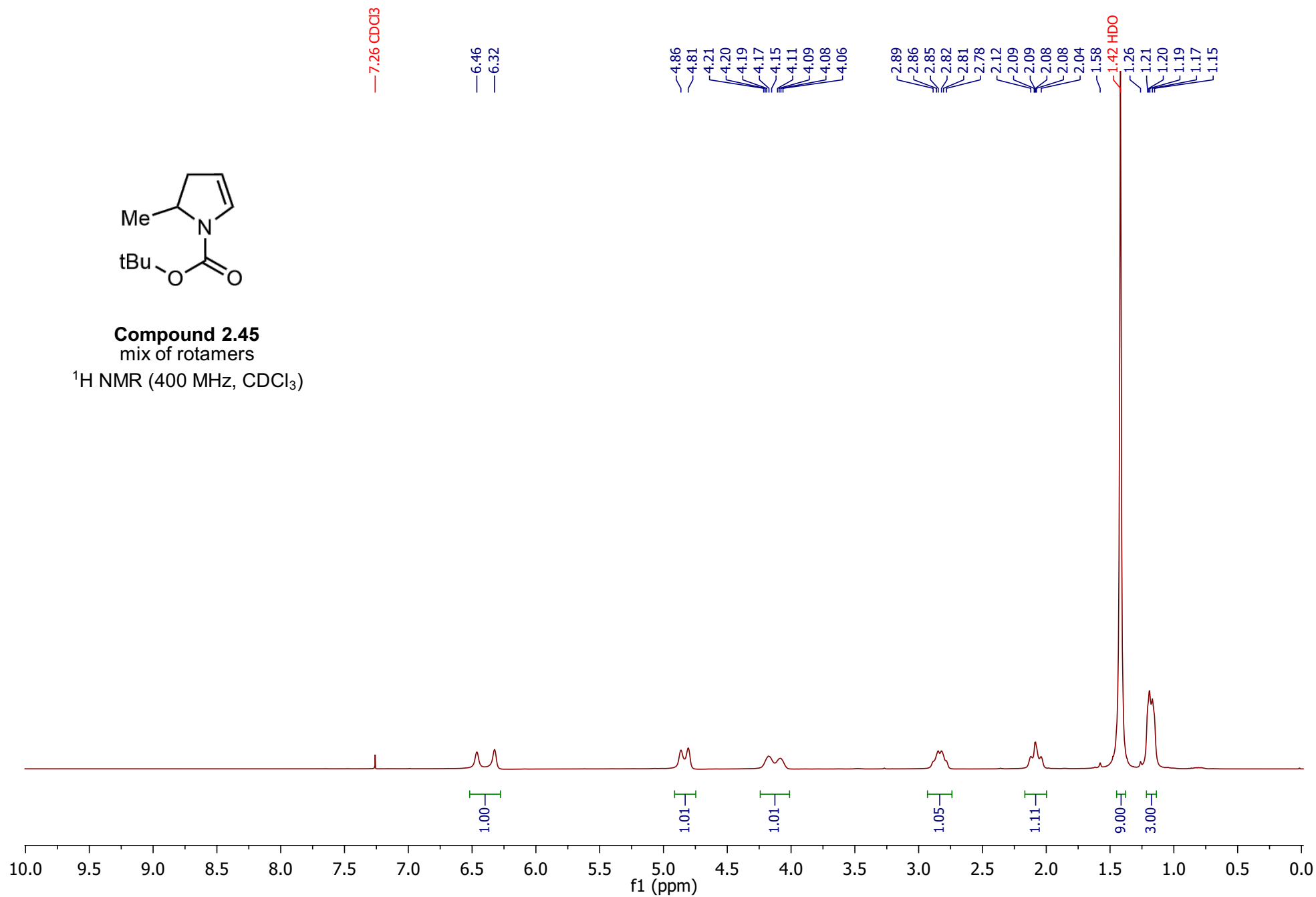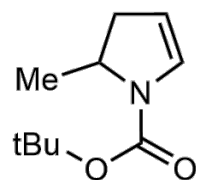
152.10
151.35
128.85
105.78
105.68
79.72
77.41 CDCl3
77.09 CDCl3
76.77 CDCl3
52.84
52.73
38.18
37.27
28.37
21.09
20.53
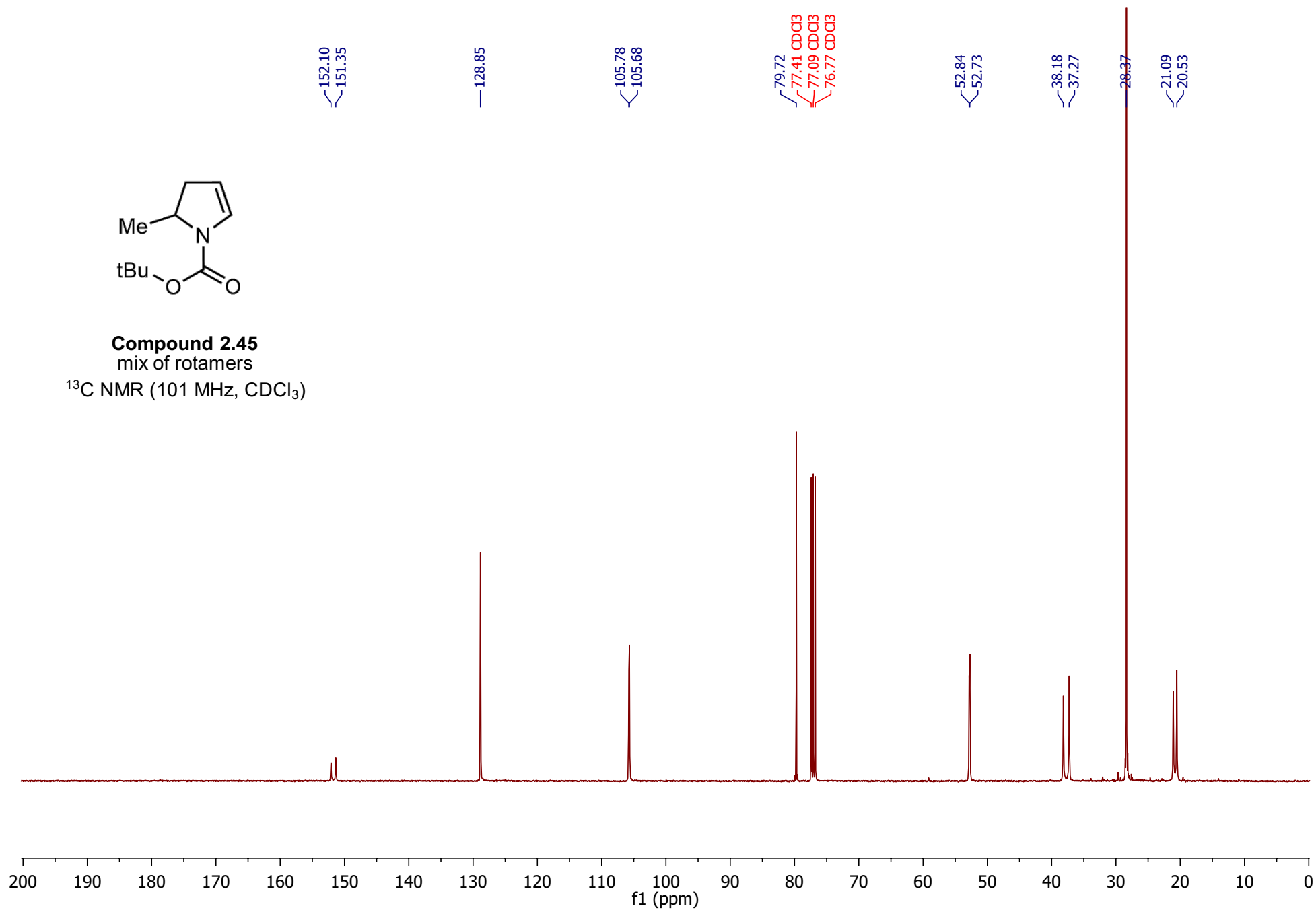
C. SPECTRAL & CHROMATOGRAPHY DATA FOR CHAPTER 3
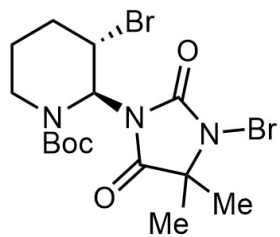
Compound 3.4
^{1}H NMR (400 MHz, CDCl$_3$)

DCM
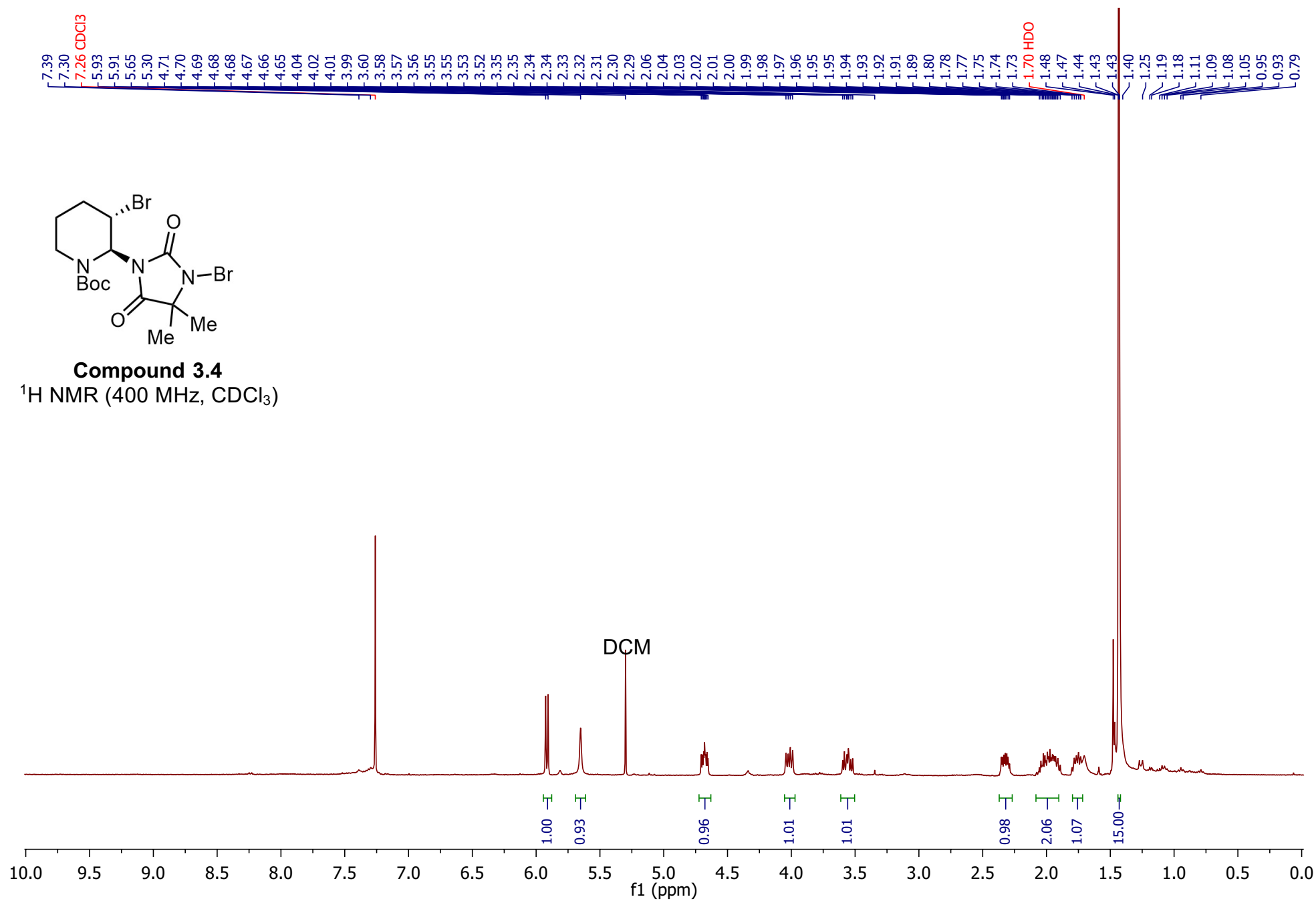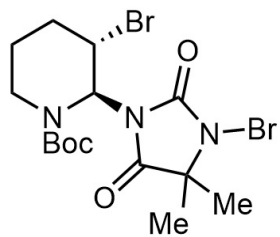
Compound 3.4
^{13}C APT NMR (101 MHz, CDCl$_3$)

176.01
155.09
154.29
81.29
77.36 CDCl3
77.04 CDCl3
76.72 CDCl3
66.44
58.47
46.36
38.61
28.81
28.34
25.15
21.31
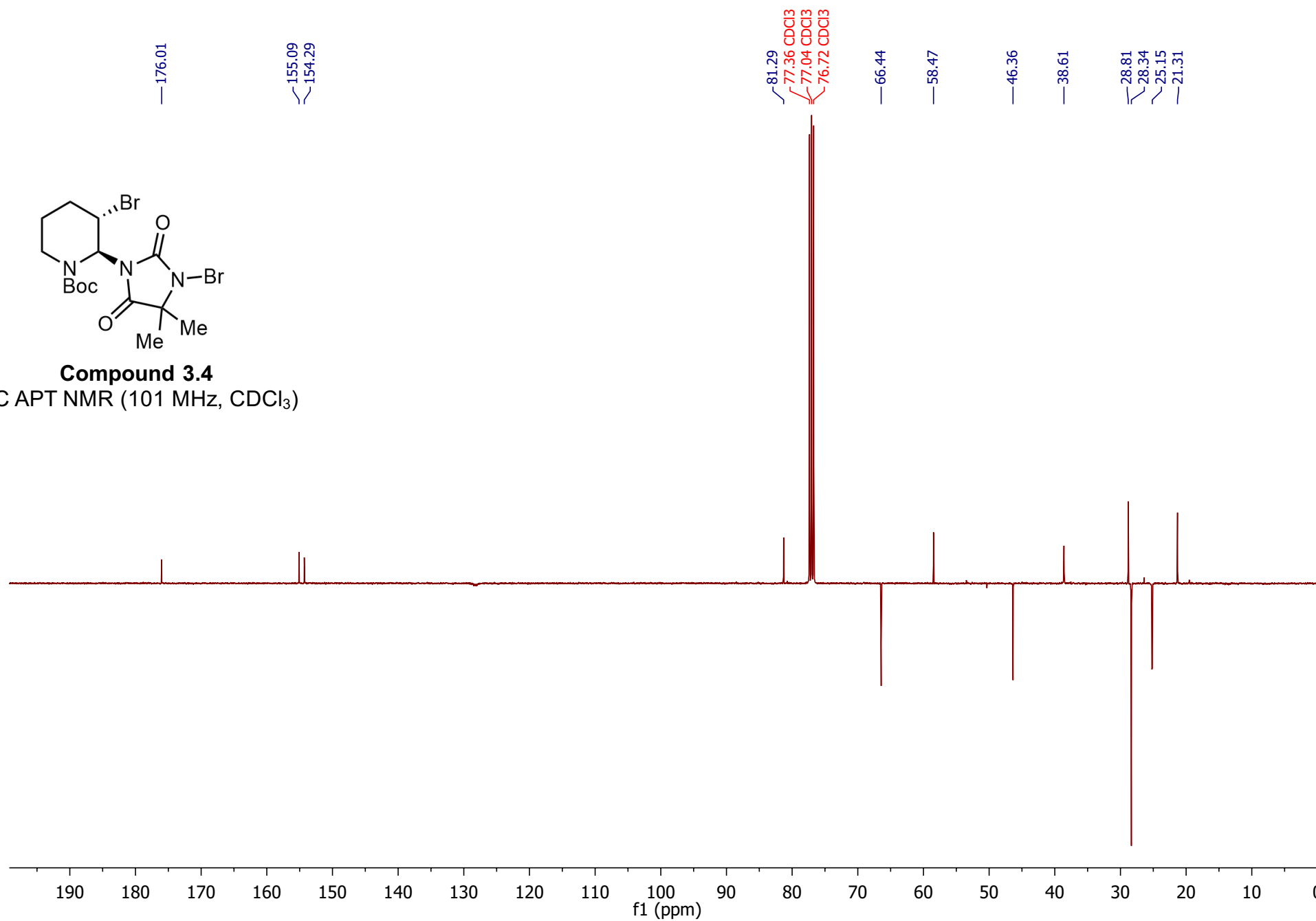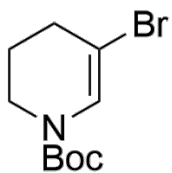
Compound 3.5
^{1}H NMR (400 MHz, CDCl$_3$)
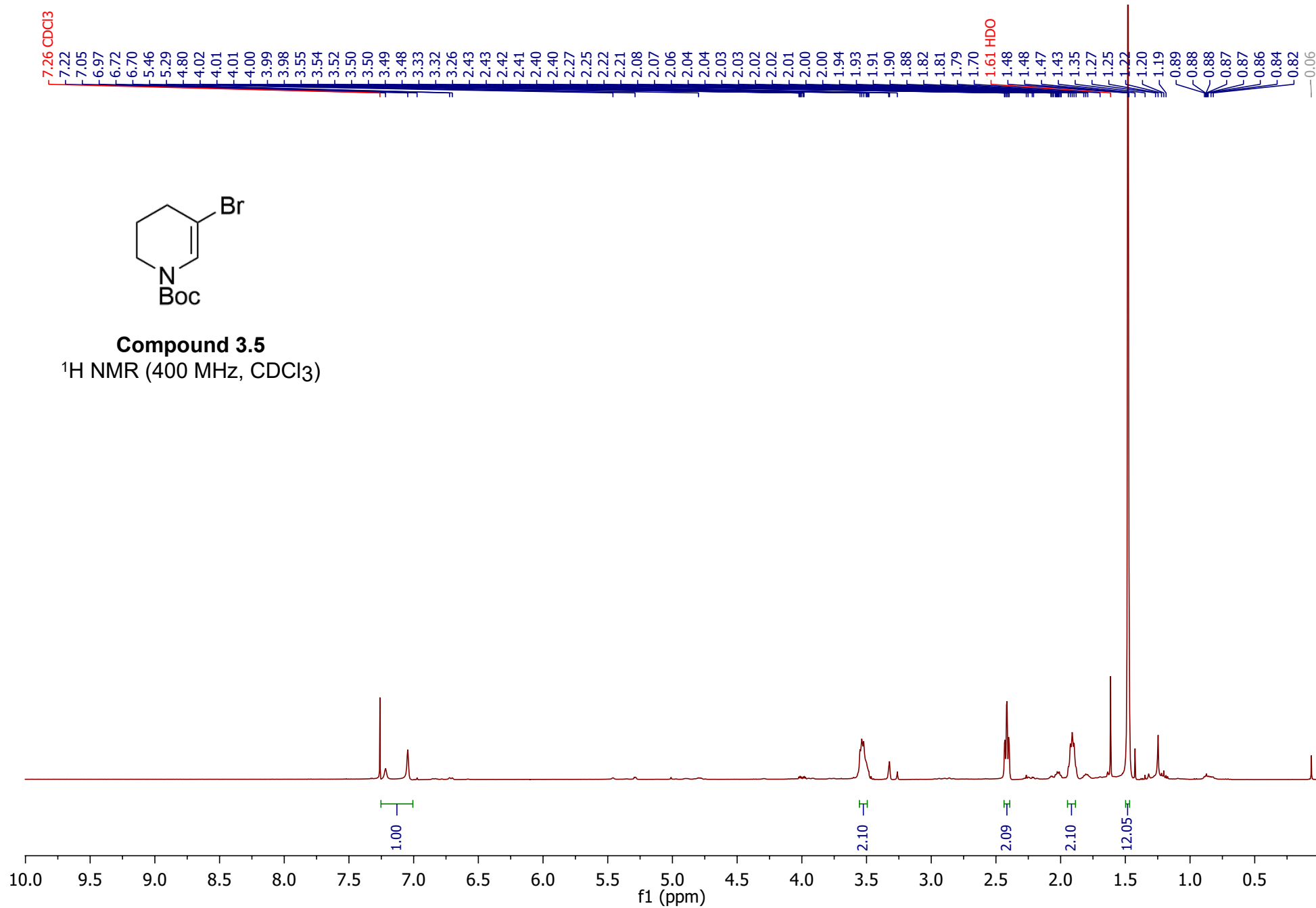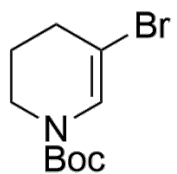
Compound 3.5
^{13}C NMR (101 MHz, CDCl$_3$)

151.91
151.41
126.48
126.21
125.52
101.71
101.16
81.41
81.17
77.35 CDCl3
77.03 CDCl3
76.72 CDCl3
41.42
40.27
31.39
31.24
30.32
29.71
28.35
28.27
22.97
22.83

f1 (ppm)
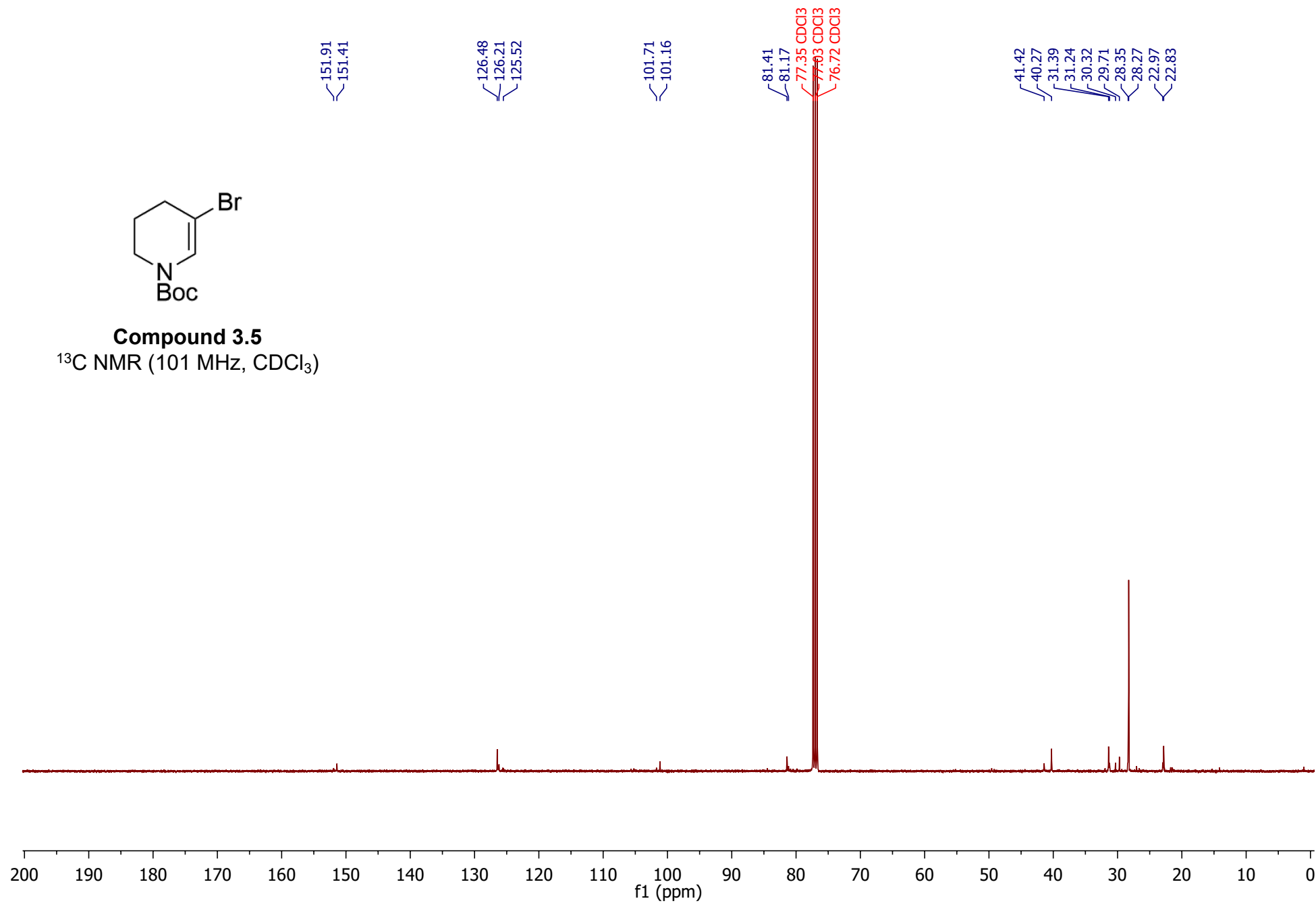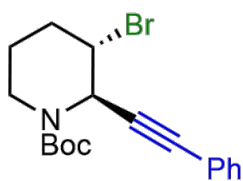
Compound 3.2, racemic

1 Det.A Ch1 / 254nm
2 Det.A Ch2 / 210nm

PeakTable

Detector A Ch1 254nm

Peak#	Ret. Time	Area	Height	Area %	Height %
1	11.783	270222	17300	50.724	56.767
2	13.326	262512	13175	49.276	43.233
Total		532734	30475	100.000	100.000

PeakTable

Detector A Ch2 210nm

Peak#	Ret. Time	Area	Height	Area %	Height %
1	11.786	183093	11797	50.870	56.968
2	13.327	176834	8912	49.130	43.032
Total		359927	20709	100.000	100.000

D. SPECTRAL & CHROMATOGRAPHY DATA FOR CHAPTER 4
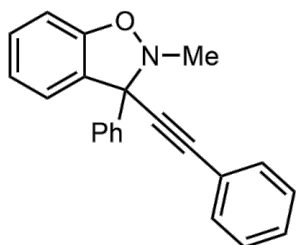
Compound 4.3
^{1}H NMR (400 MHz, CDCl$_3$)

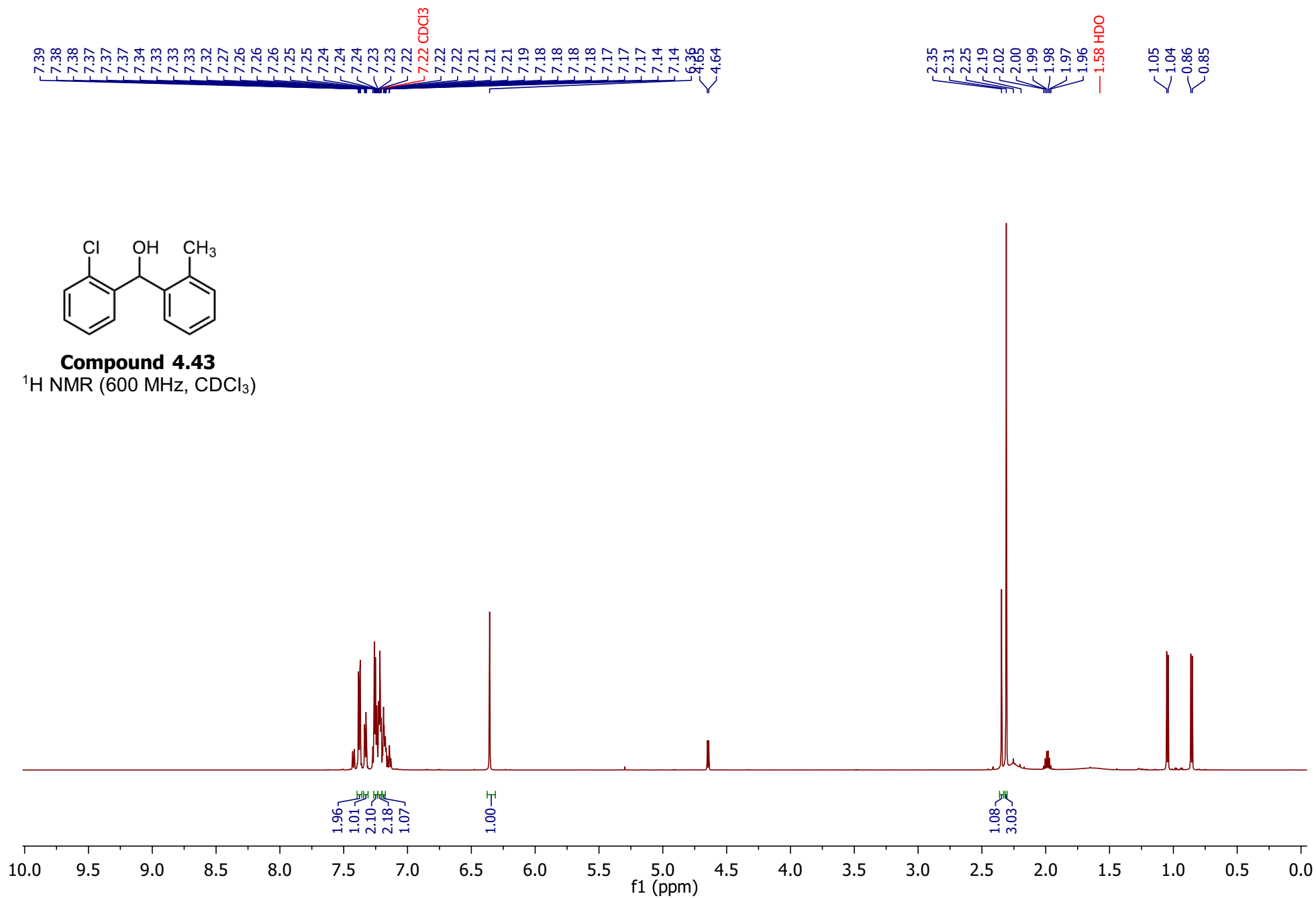H$_2$O
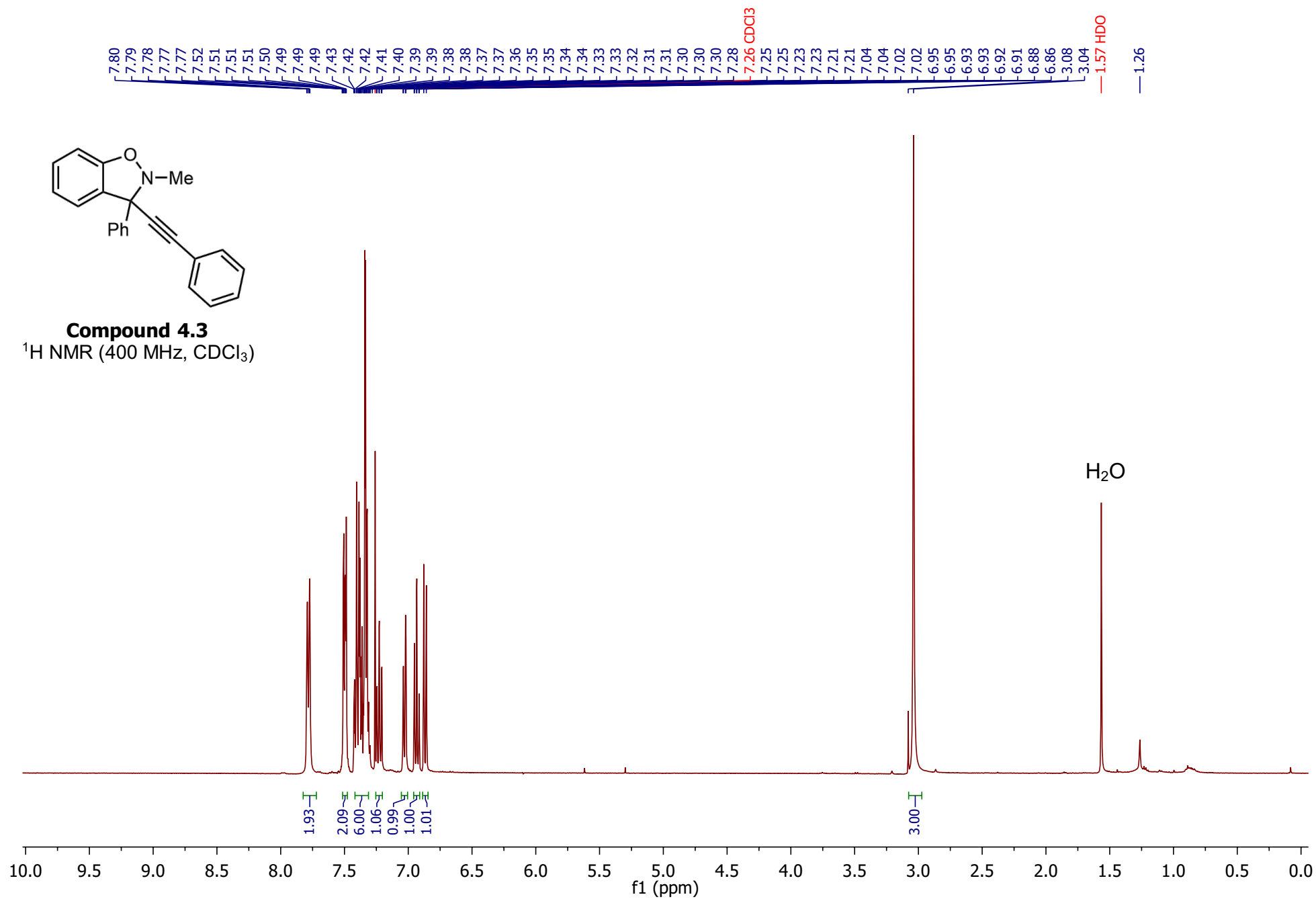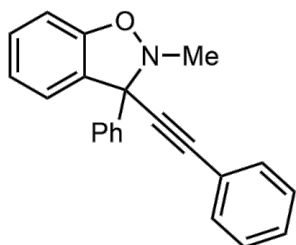
Compound 4.3
^{13}C NMR (101 MHz, CDCl$_3$)
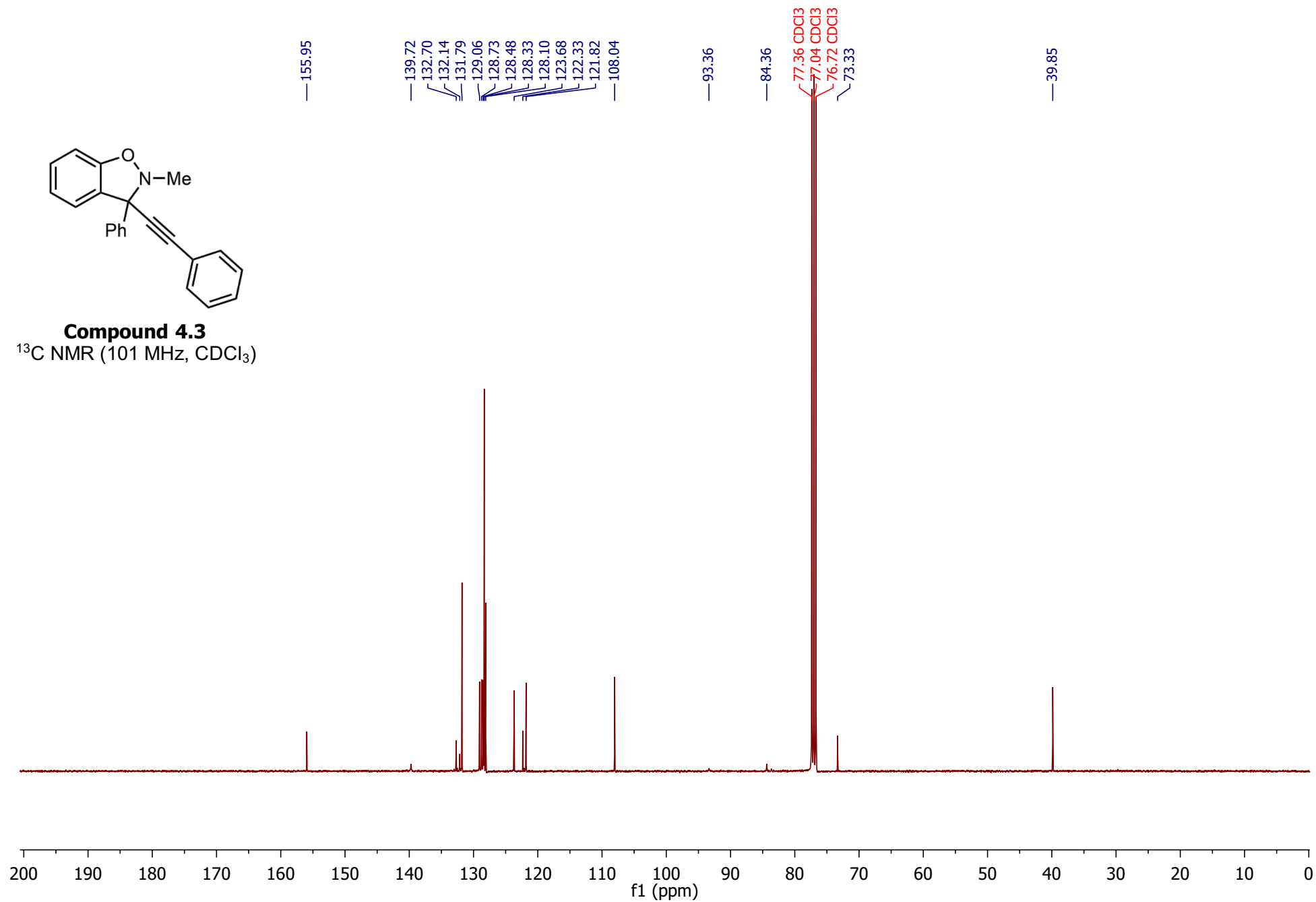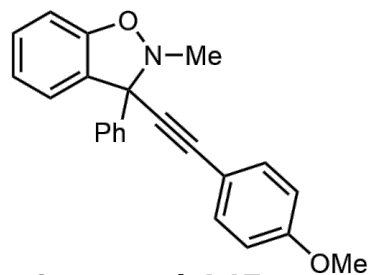
Compound 4.17
¹H NMR (400 MHz, CDCl₃)
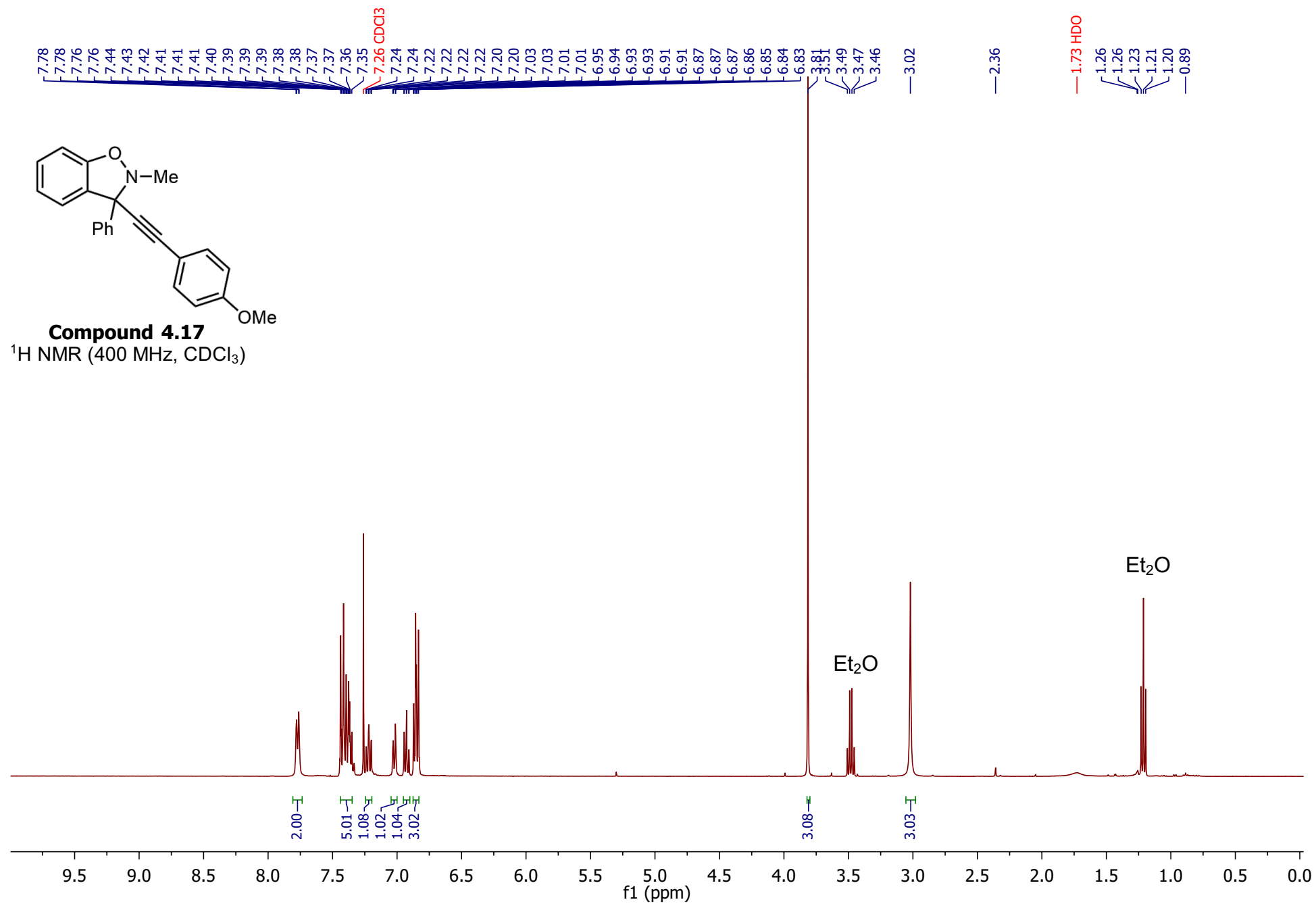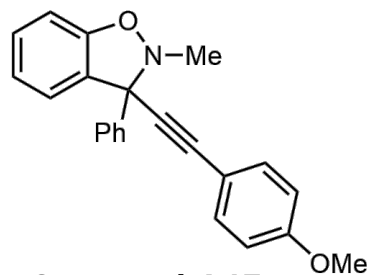
Compound 4.17
^{13}C NMR (101 MHz, CDCl$_3$)

159.89
155.92
139.92
133.27
132.83
128.98
128.42
128.29
128.11
123.68
121.79
114.40
113.91
108.03
82.91
77.35 CDCl3
76.72 CDCl3
73.40
55.34
39.86

Et$_2$O

Et$_2$O
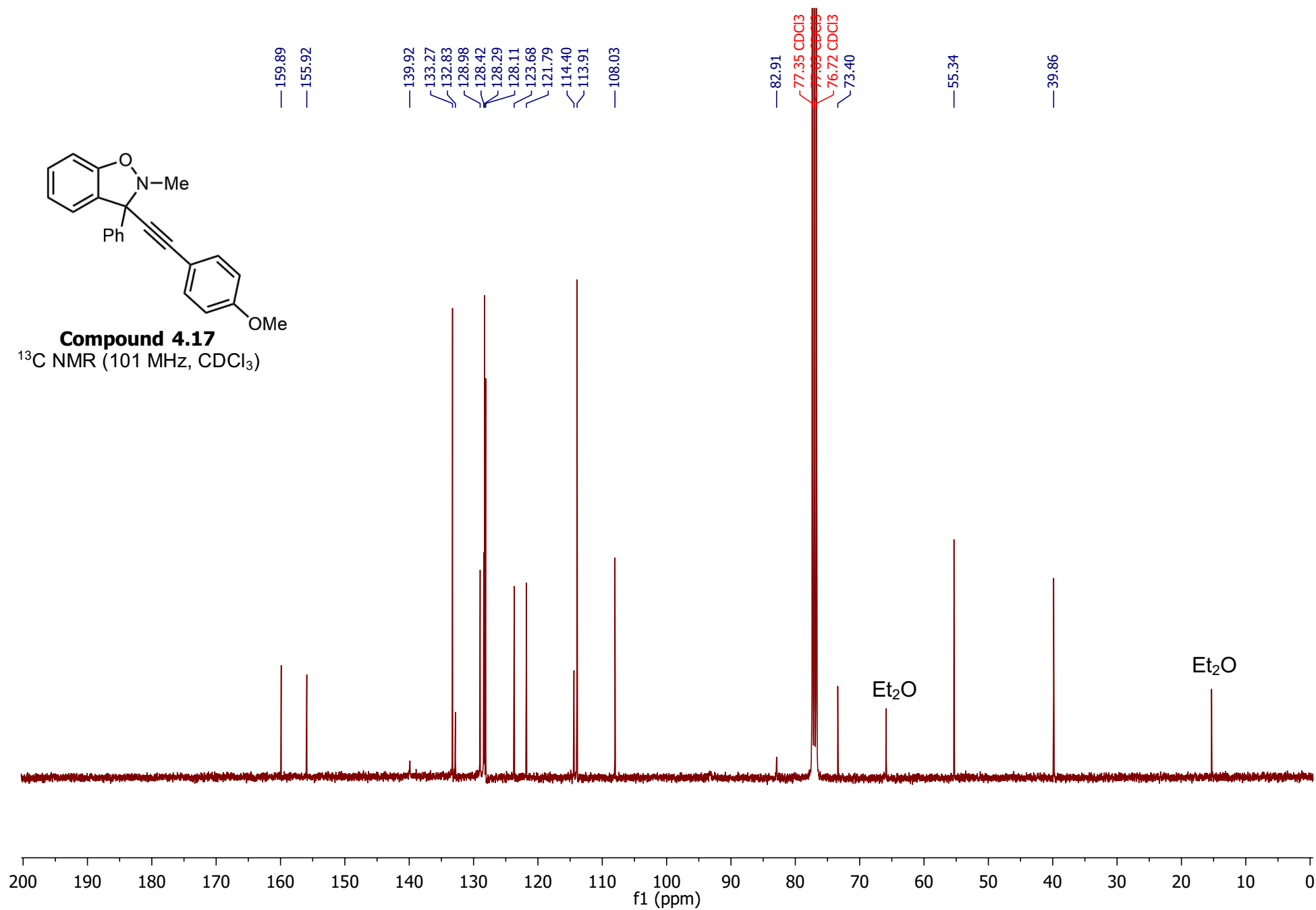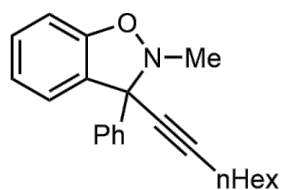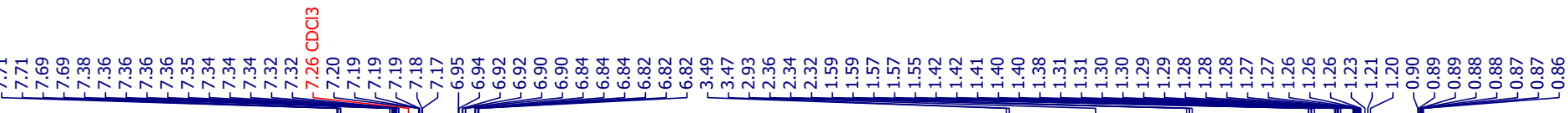
Compound 4.18
^{1}H NMR (400 MHz, CDCl$_3$)
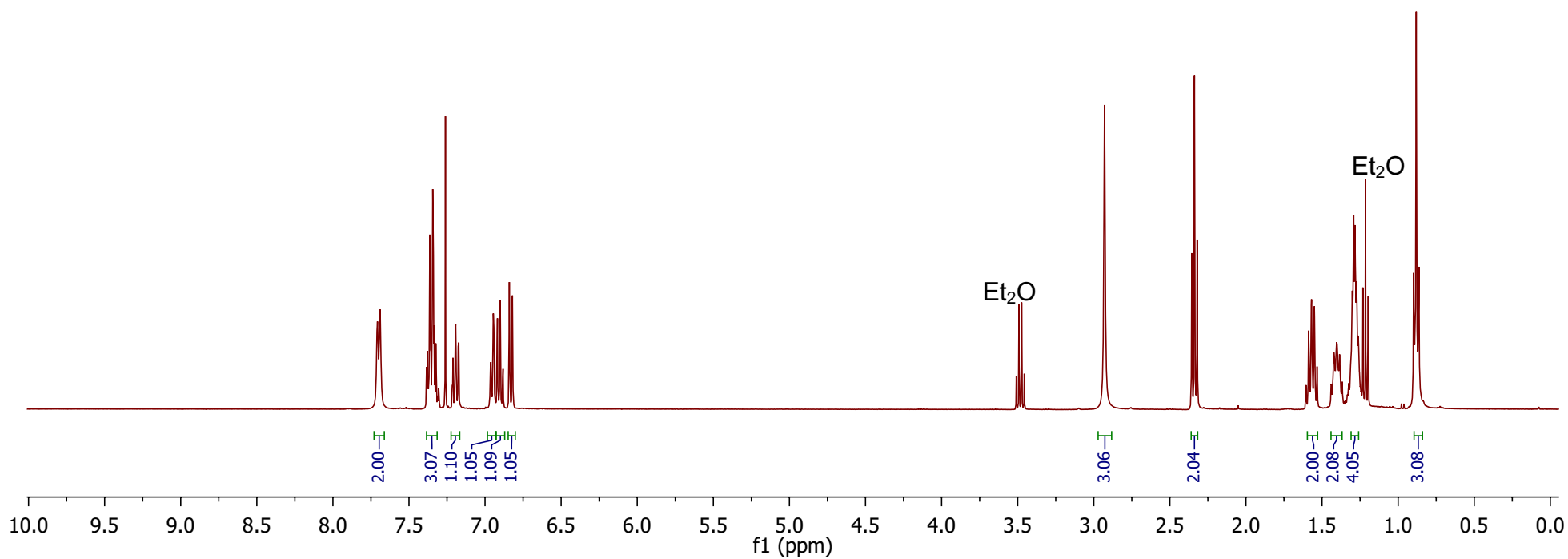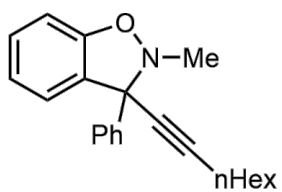
Compound 4.18
^{13}C NMR (101 MHz, CDCl$_3$)

155.80

133.38
129.05
128.78
128.23
128.15
128.08
123.49
121.67

107.94

77.35 CDCl3
77.04 CDCl3
76.72 CDCl3
73.03

39.76

31.25
28.64
28.55

22.55
19.04
14.17
14.05

Et$_2$O

Et$_2$

f1 (ppm)
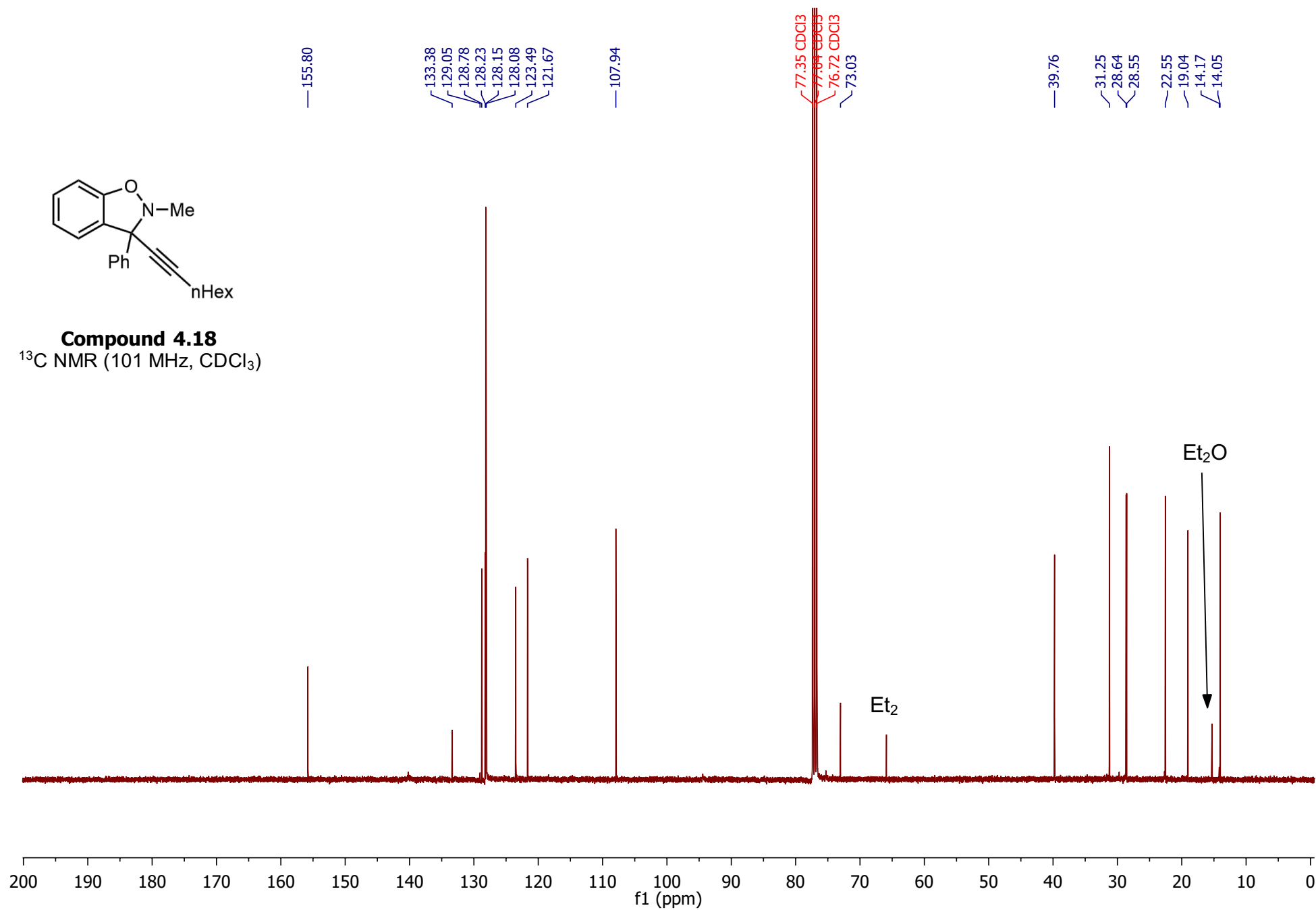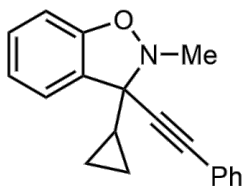
Compound 4.30
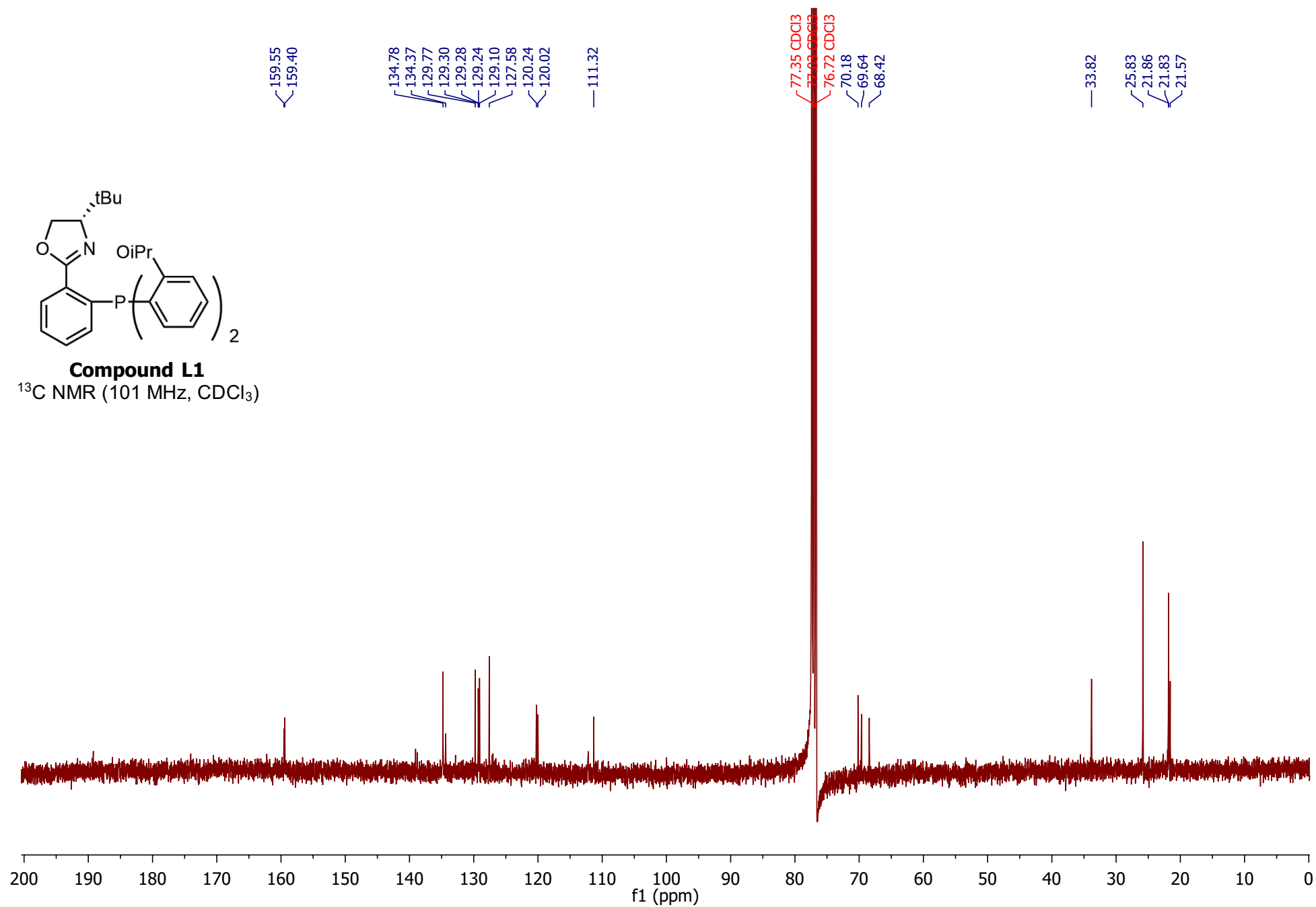^{1}H NMR (400 MHz, CDCl$_3$)
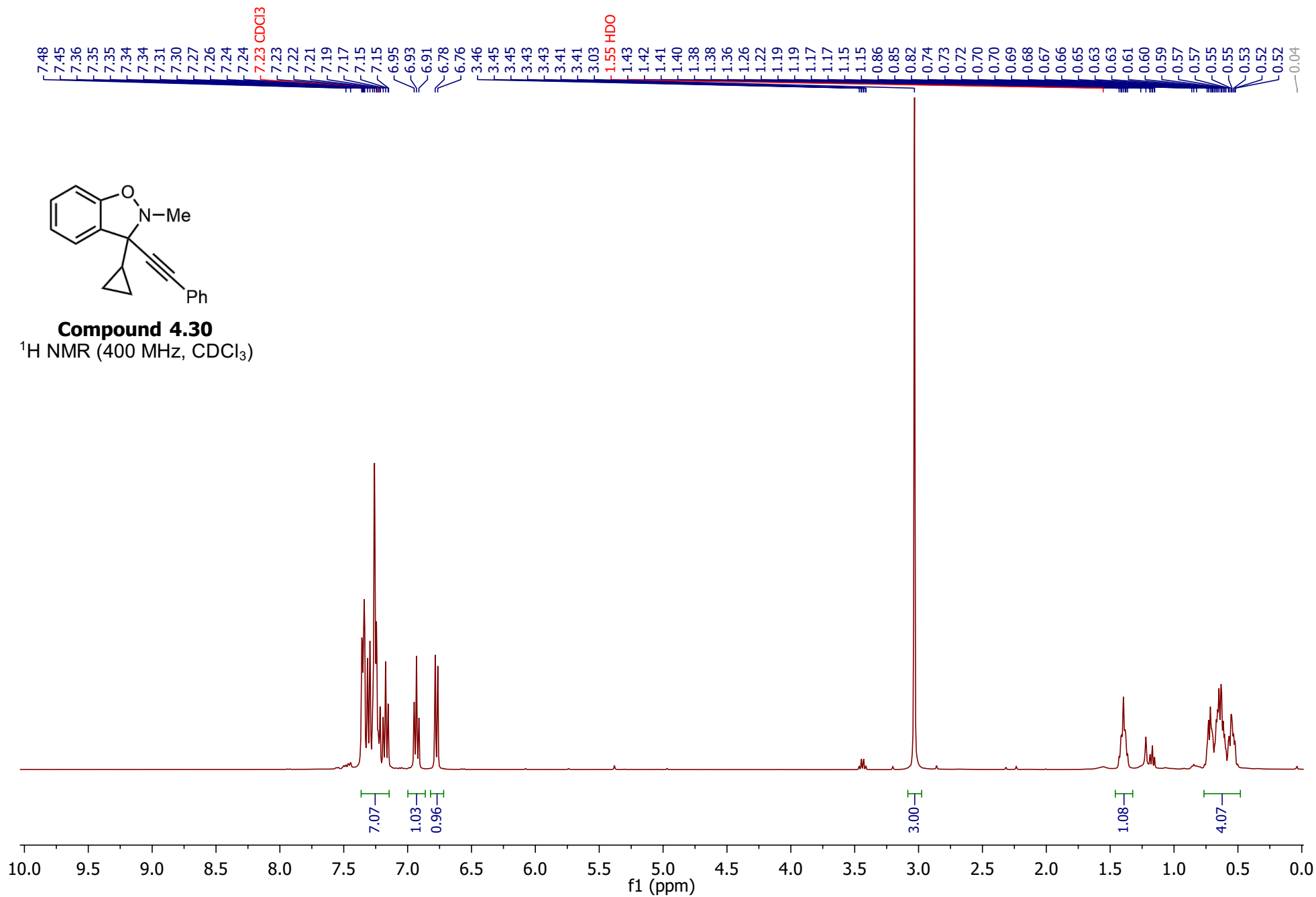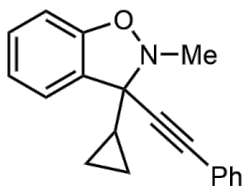
Compound 4.30
^{13}C NMR (101 MHz, CDCl$_3$)

155.64

131.76
131.56
128.93
128.60
128.25
123.15
122.18
121.48

108.18

82.51
77.32 CDCl3
77.00 CDCl3
76.68 CDCl3
71.75

65.84

41.59

17.99

0.78
0.78

200 190 180 170 160 150 140 130 120 110 100 90 80 70 60 50 40 30 20 10 0
f1 (ppm)

Compound 4.31
^{1}H NMR (400 MHz, CDCl$_3$)
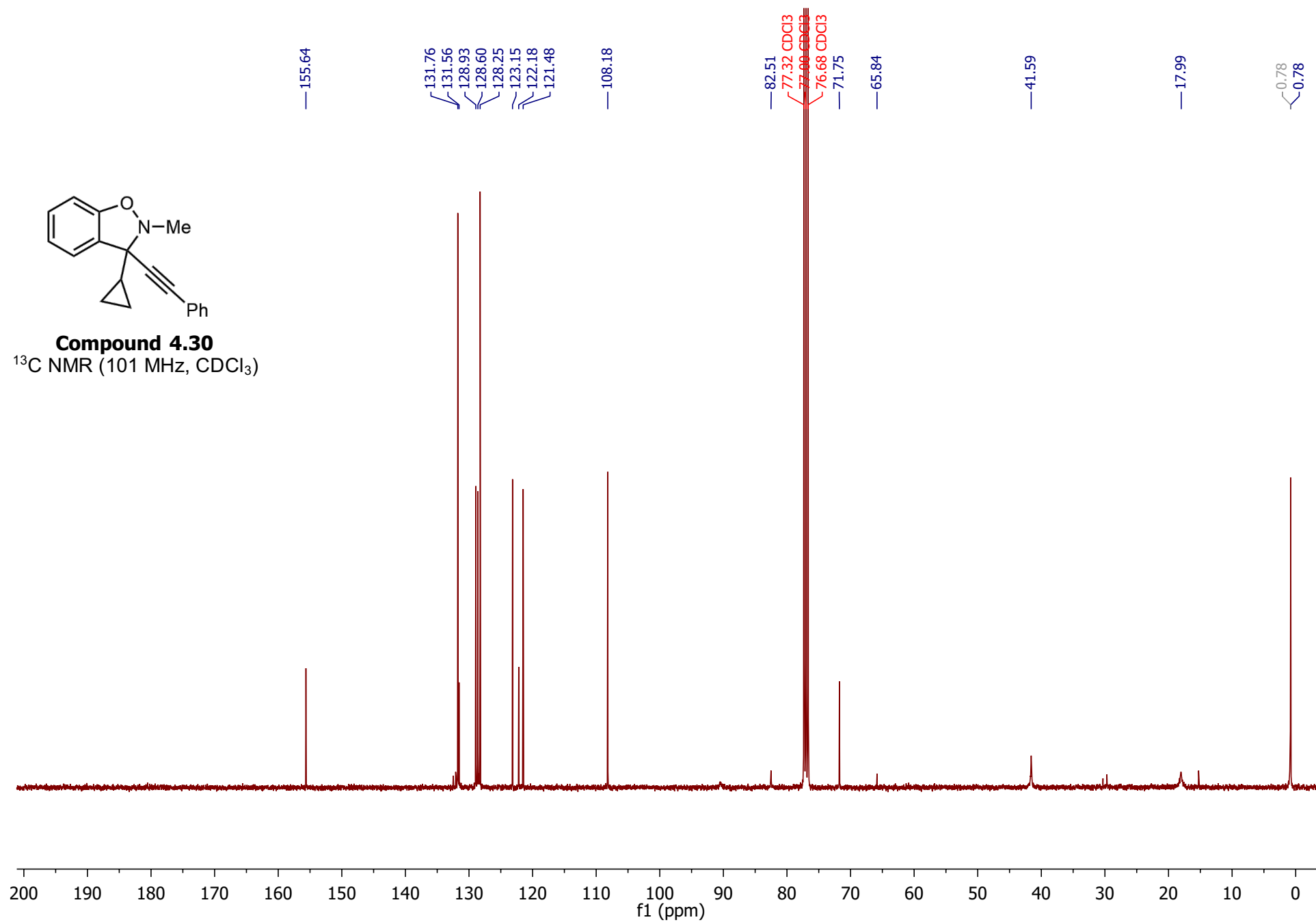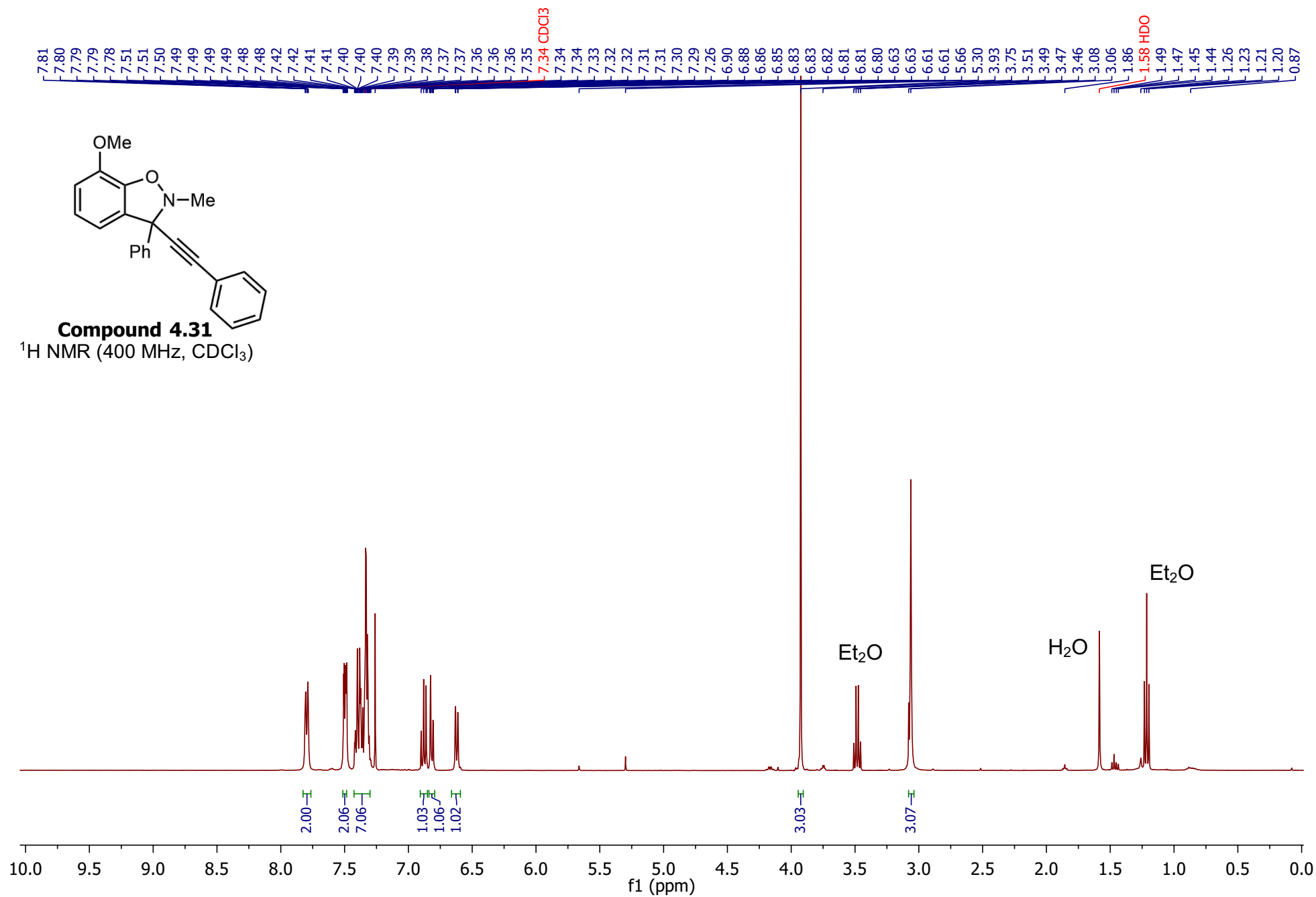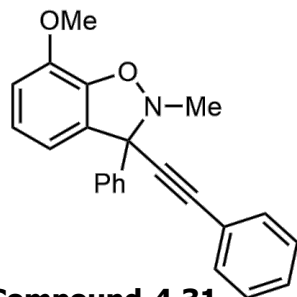
Compound 4.31
^{13}C NMR (101 MHz, CDCl$_3$)

144.75
143.20
133.83
132.14
131.79
128.81
128.71
128.50
128.32
128.30
128.16
122.51
122.35
115.59
111.99
83.66
77.37 CDCl3
77.05 CDCl3
76.73 CDCl3
73.84
56.15
39.82

Et$_2$O

Et$_2$O
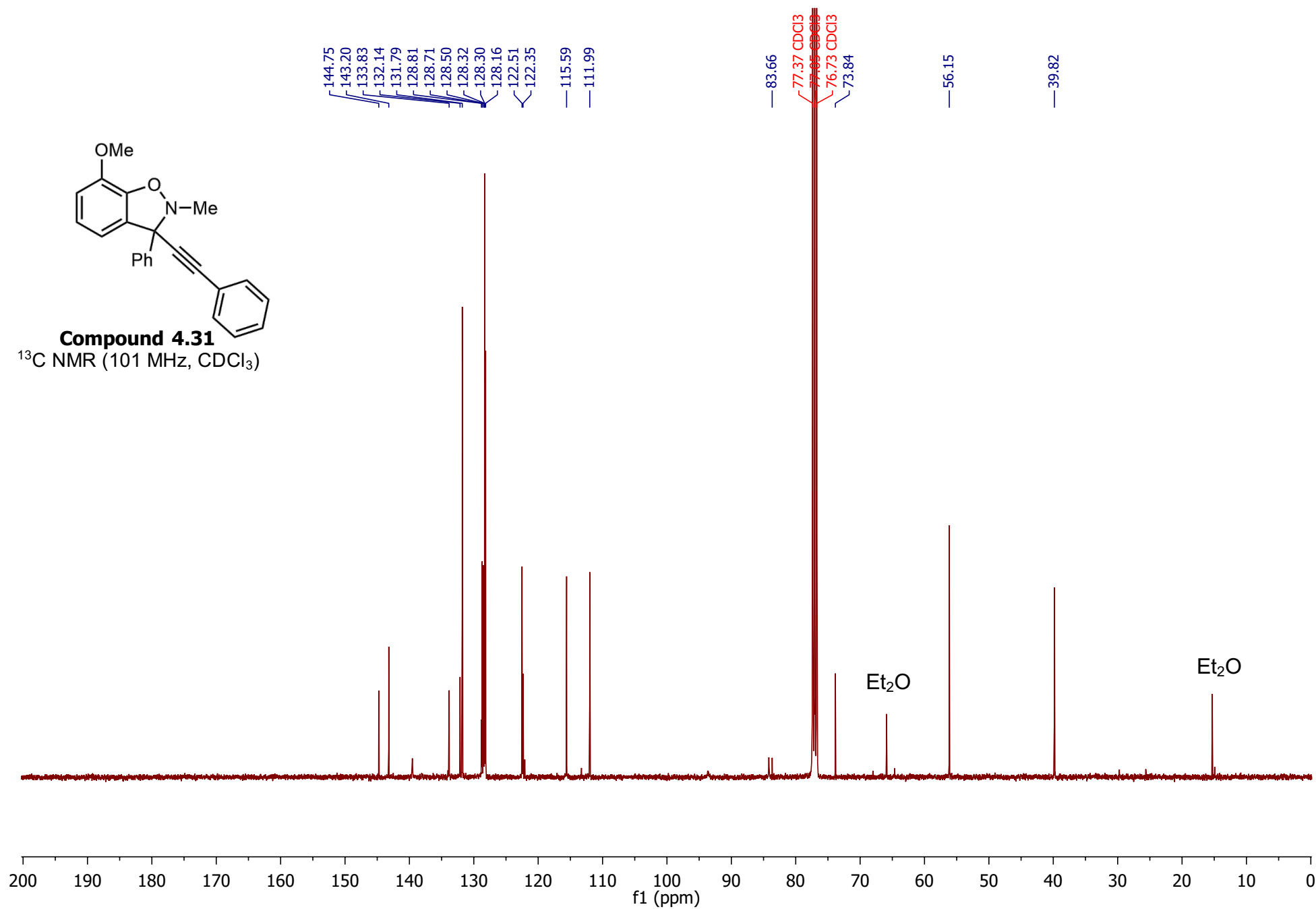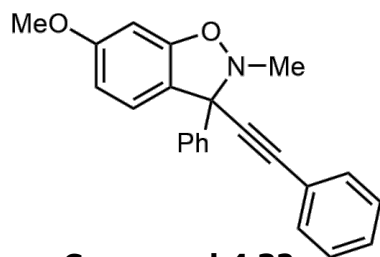
Compound 4.32
^{1}H NMR (400 MHz, CDCl$_3$)

MeO

O

N—Me

Ph
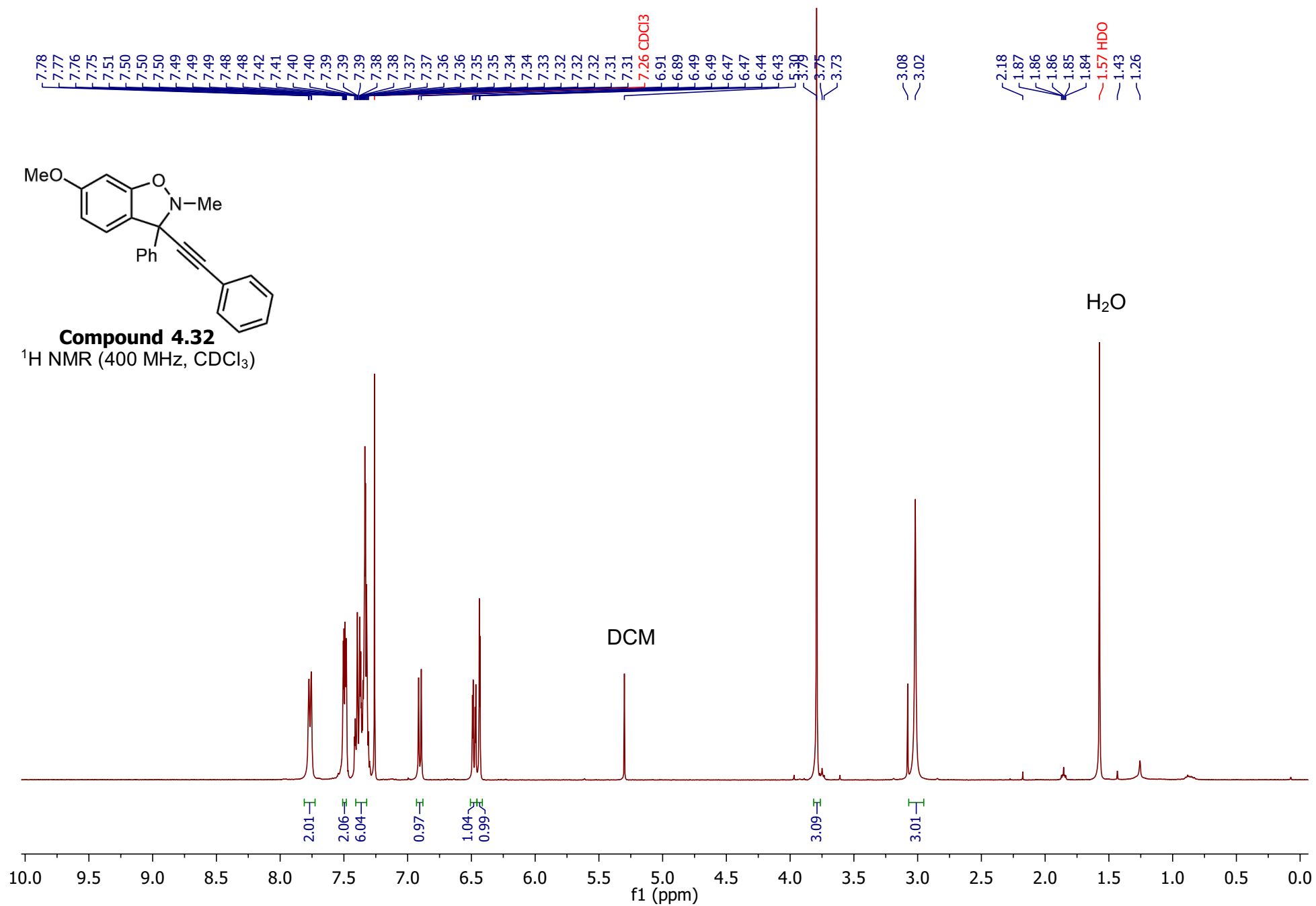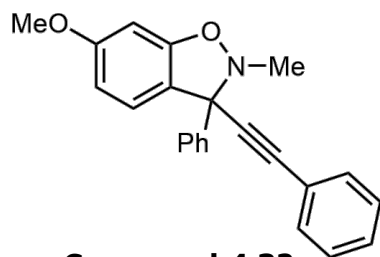
Compound 4.32
^{13}C NMR (101 MHz, CDCl$_3$)

161.00
157.20
132.51
132.13
131.77
128.81
128.67
128.43
128.32
128.04
124.96
123.93
122.40
122.07
107.66
94.33
83.66
77.36 CDCl3
76.72 CDCl3
73.10
40.00

DCM

200 190 180 170 160 150 140 130 120 110 100 90 80 70 60 50 40 30 20 10 0
f1 (ppm)

Compound 4.2
^{1}H NMR (600 MHz, DMSO-d_6)
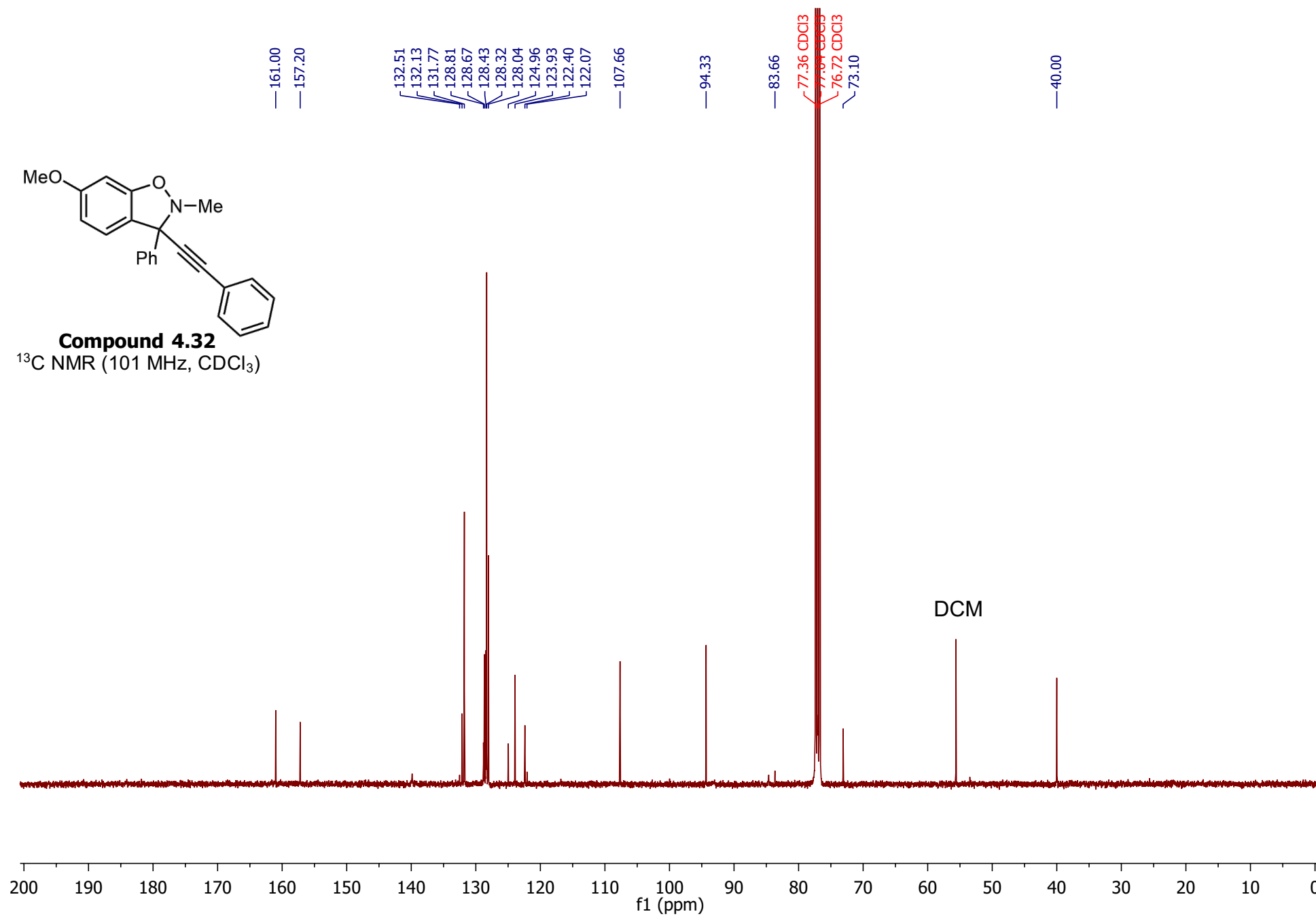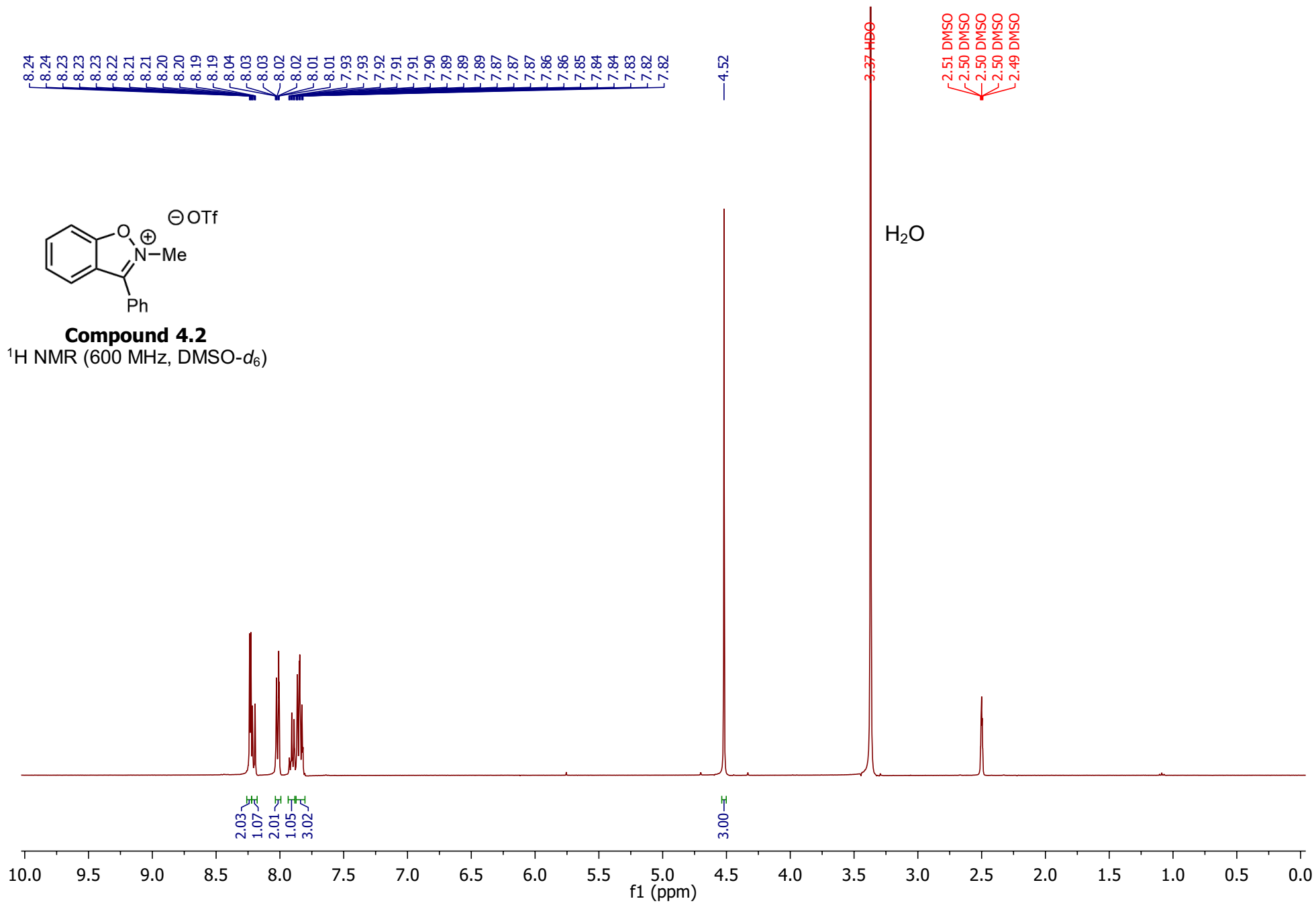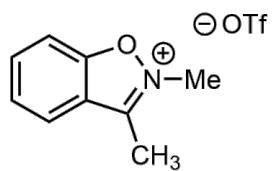
Compound 4.33
^{1}H NMR (400 MHz, DMSO-d_6)
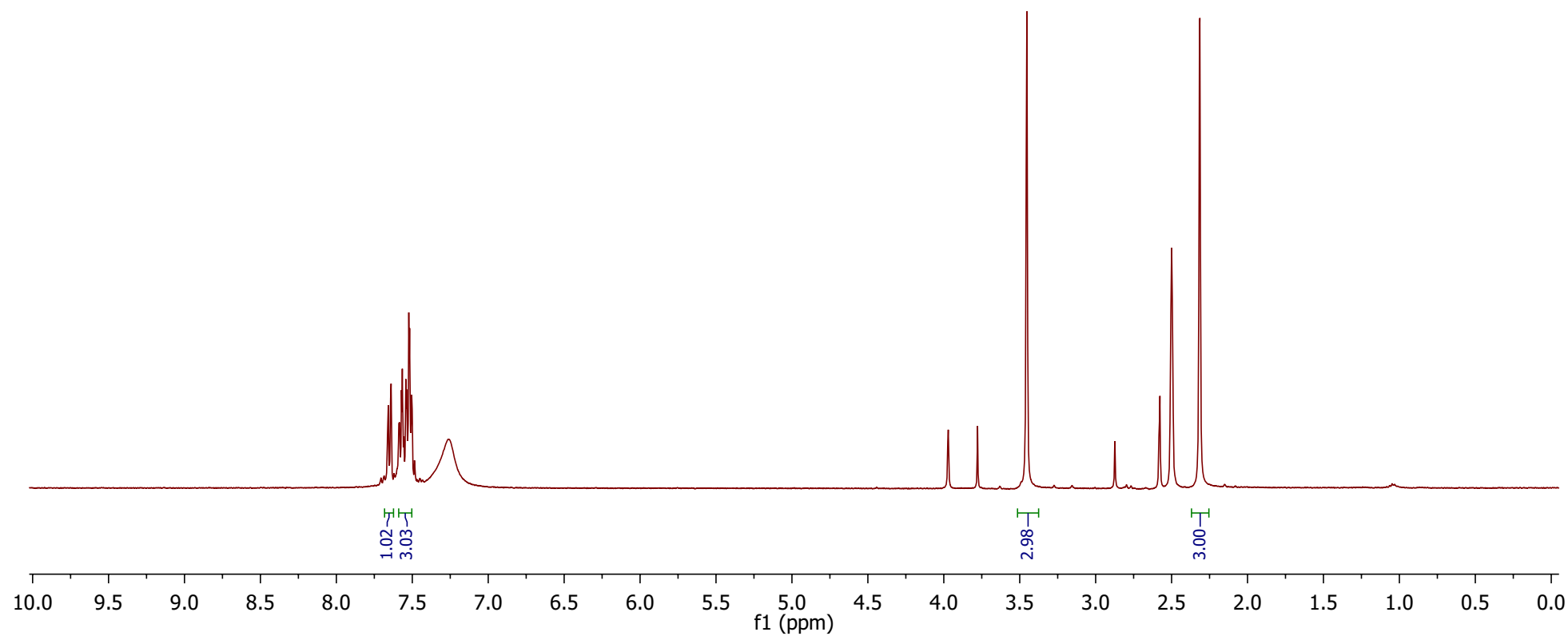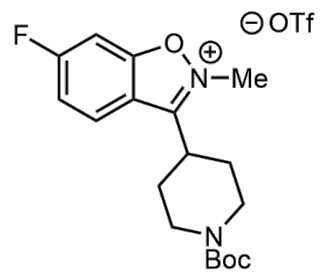
Compound 4.34
^{1}H NMR (400 MHz, DMSO-d_6)
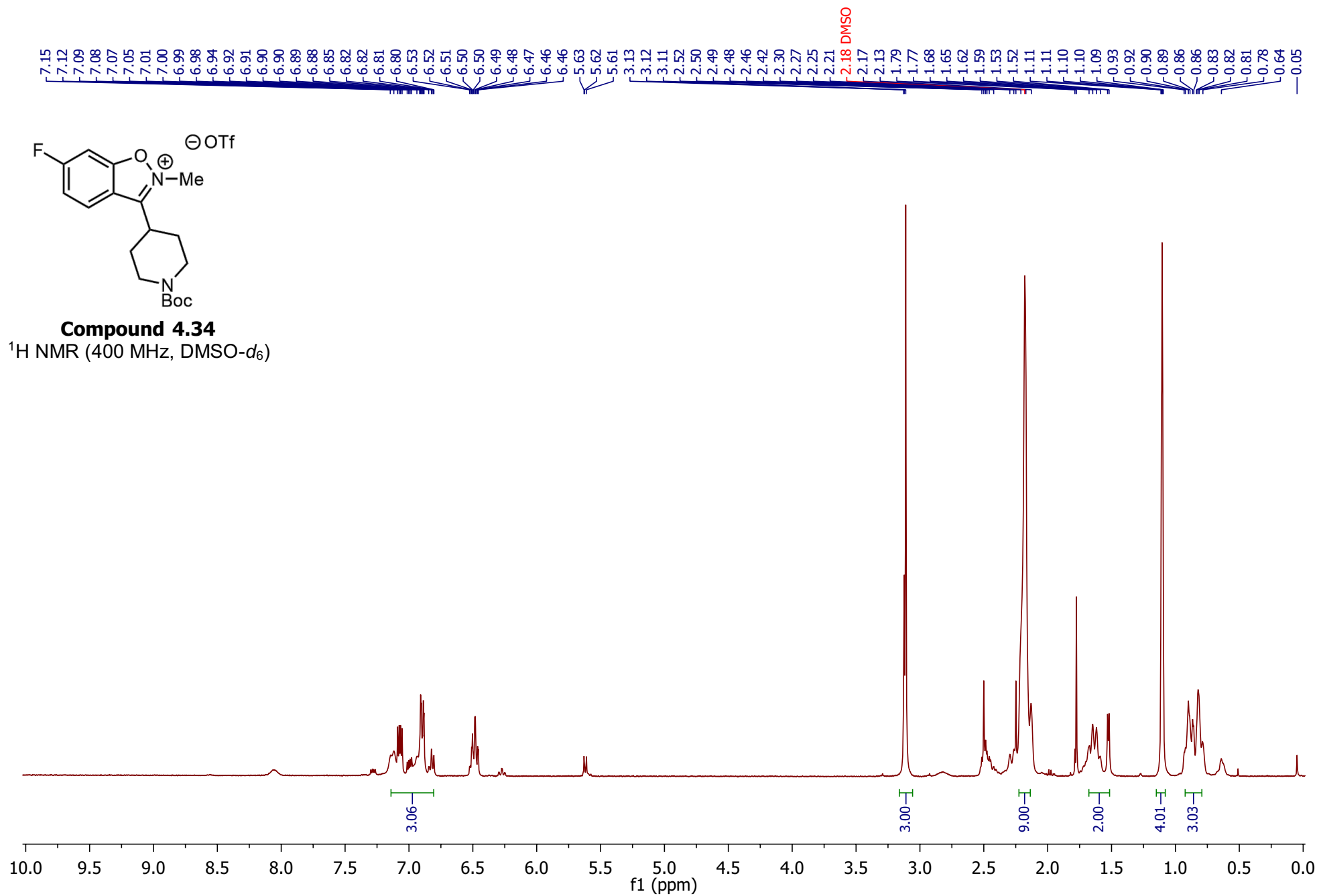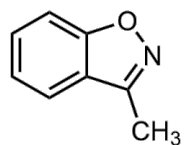
Compound 4.36
^{1}H NMR (600 MHz, CDCl$_3$)
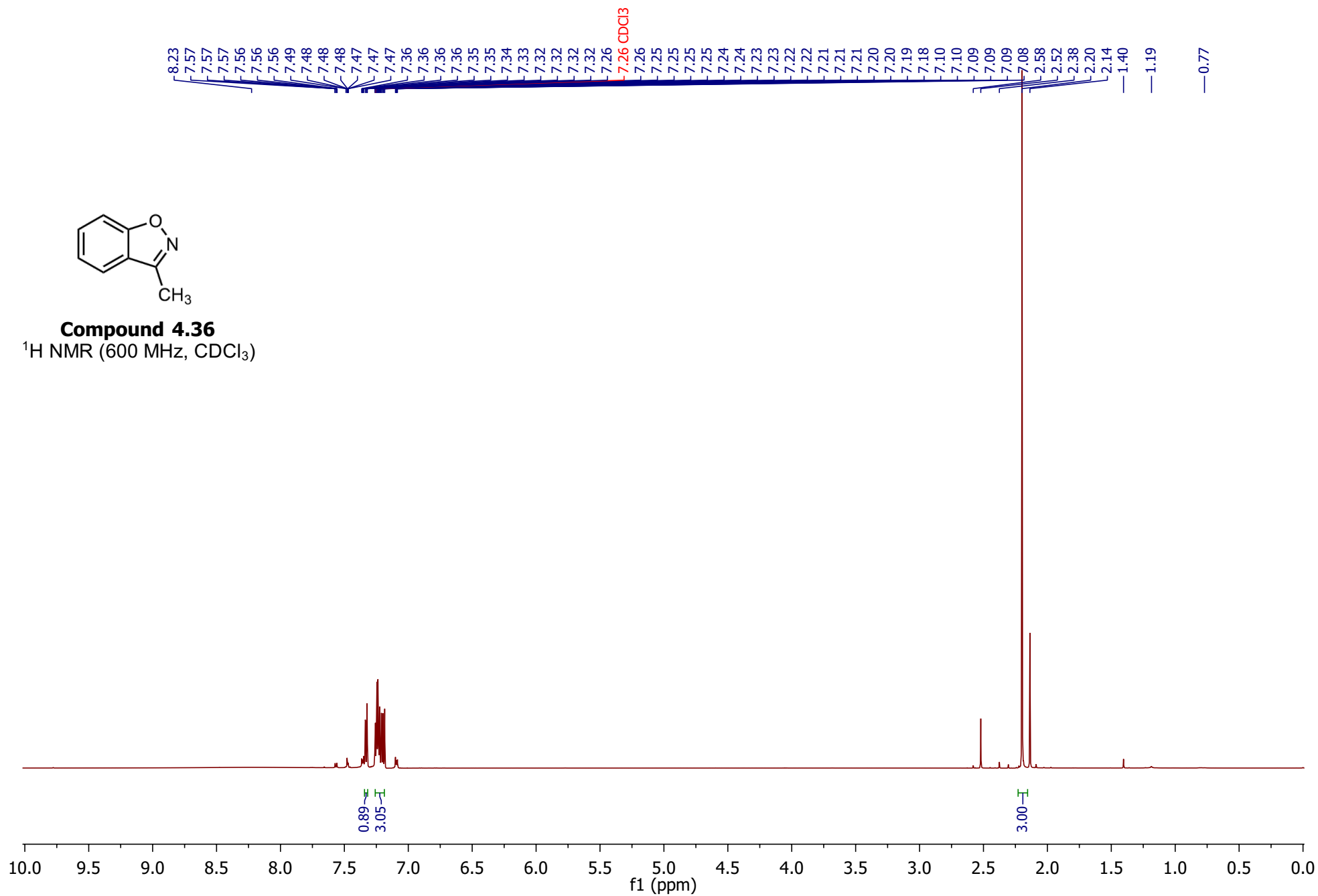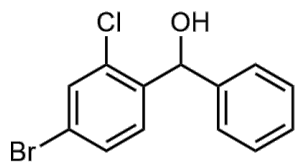
Compound 4.39
^{1}H NMR (600 MHz, CDCl$_3$)
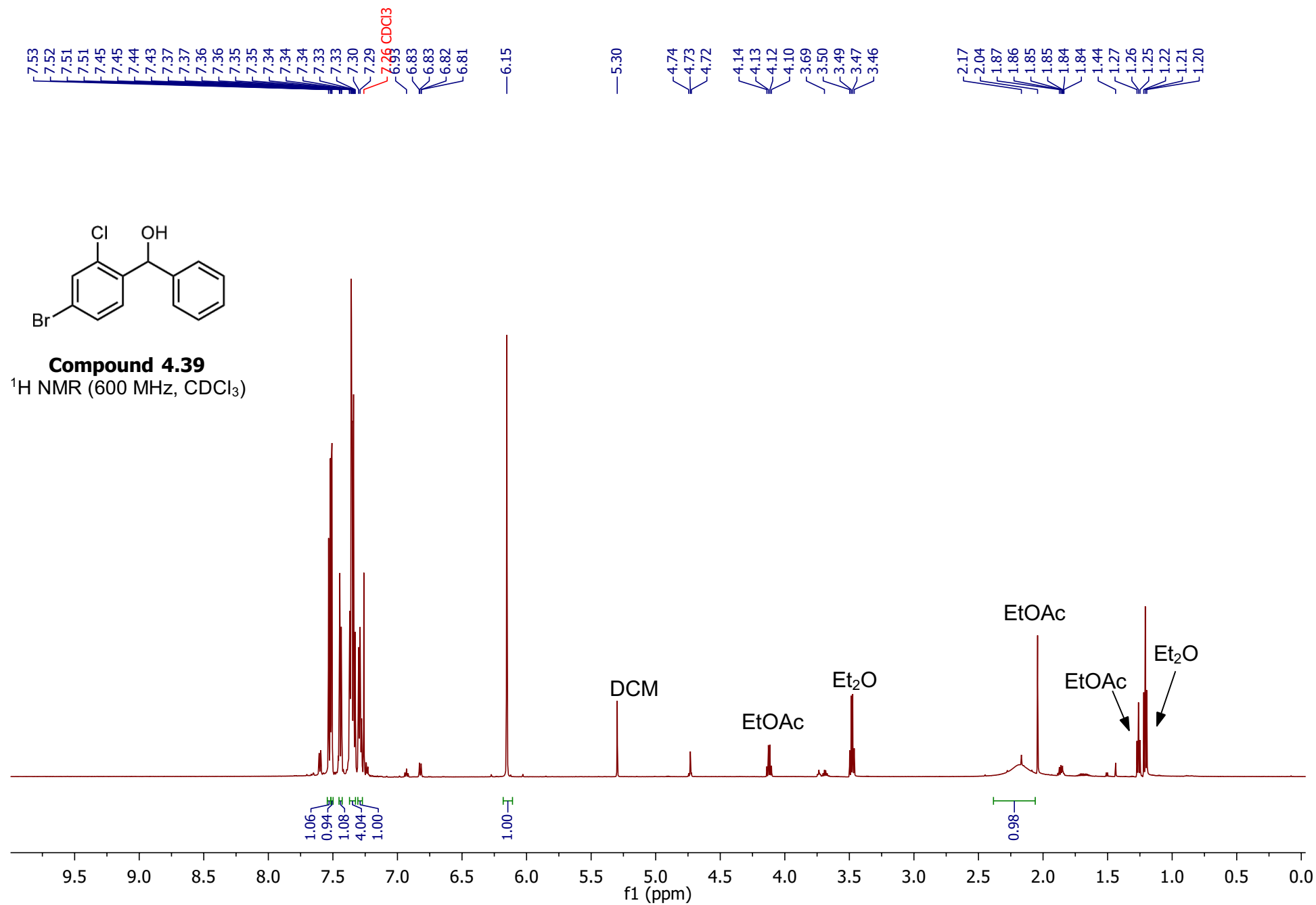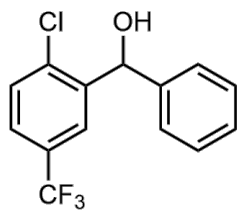
Compound 4.40
^{1}H NMR (600 MHz, CDCl$_3$)
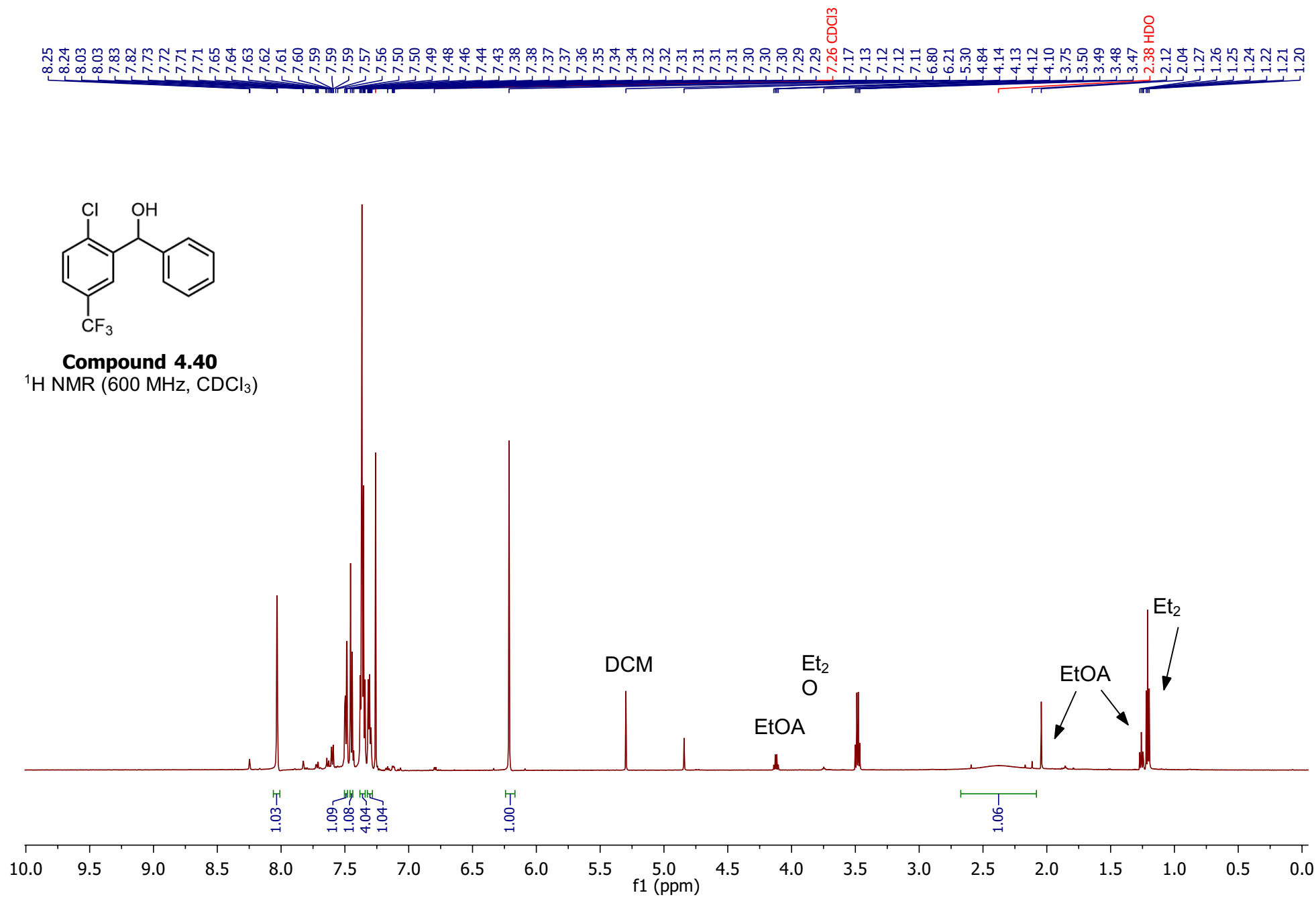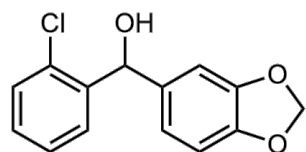
Compound 4.42
^{1}H NMR (600 MHz, CDCl$_3$)
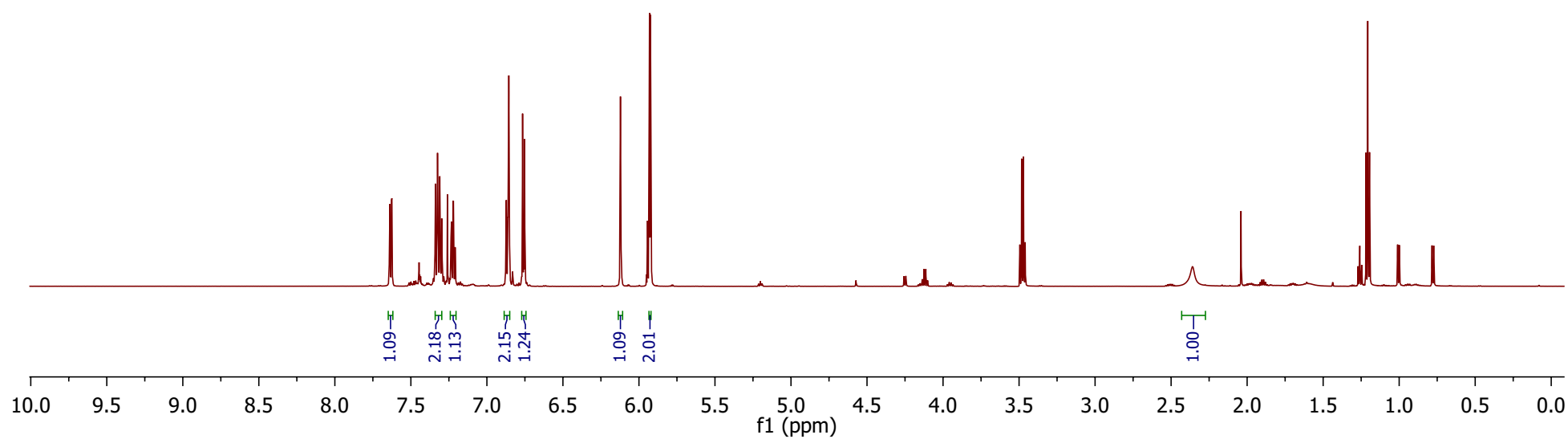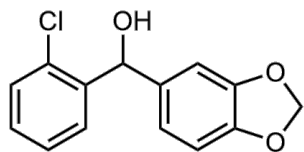
Compound 4.42
^{13}C NMR (151 MHz, CDCl$_3$)

147.76
147.13
140.98
136.30
132.38
129.58
128.74
127.75
127.10
120.62
108.14
107.55
101.07
77.24 CDCl3
77.03 CDCl3
76.82 CDCl3
72.50

f1 (ppm)
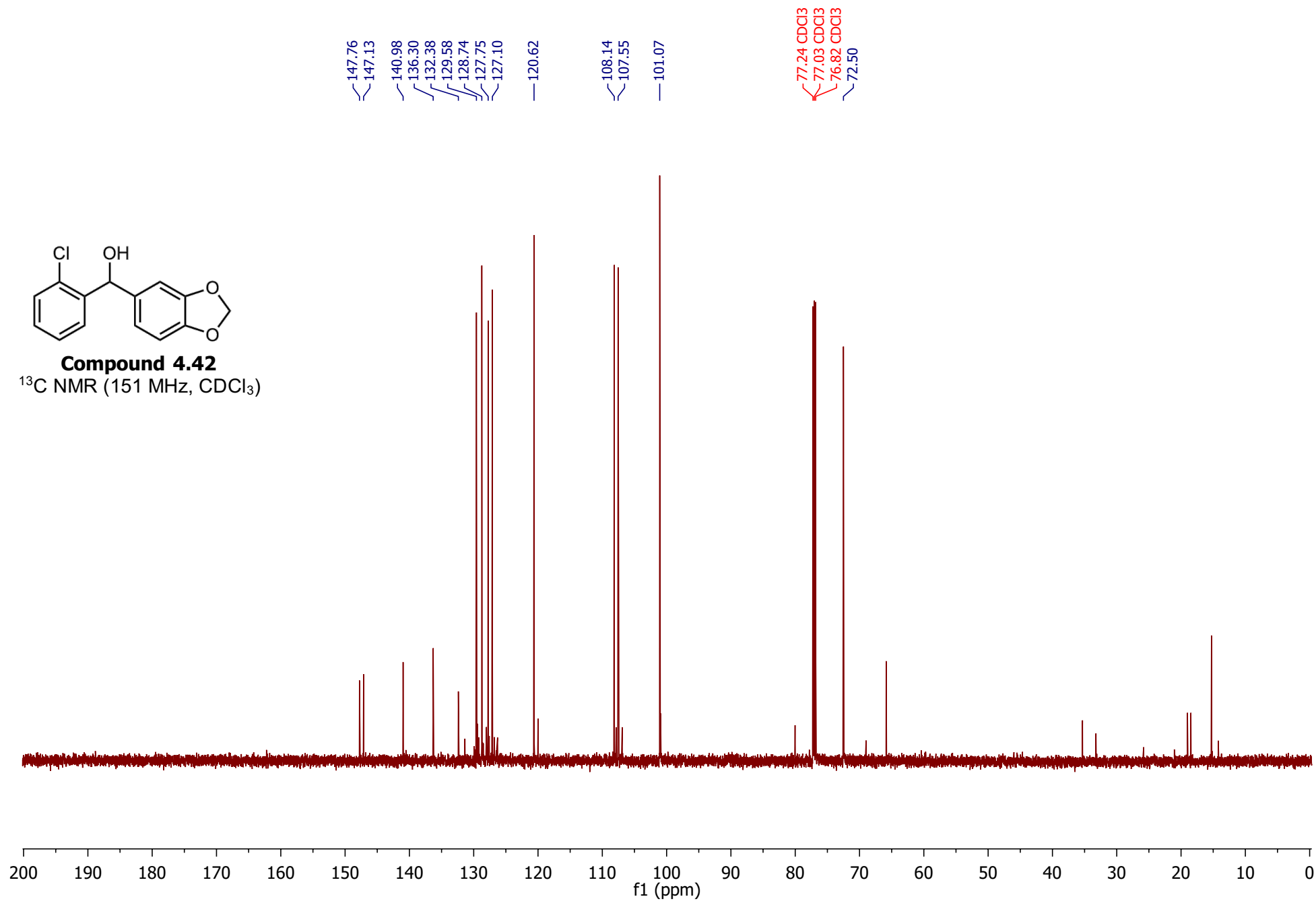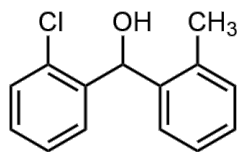
Compound 4.43
¹H NMR (600 MHz, CDCl₃)
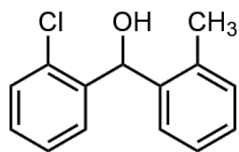
Compound 4.43
^{13}C NMR (151 MHz, CDCl$_3$)

140.31
139.93
135.93
133.24
130.51
129.57
128.90
128.55
127.80
127.01
126.33
126.11

77.24 CDCl3
77.03 CDCl3
76.82 CDCl3

69.87

19.11

200　190　180　170　160　150　140　130　120　110　100　90　80　70　60　50　40　30　20　10　0
f1 (ppm)

Compound **L1**
^{1}H NMR (400 MHz, CDCl$_3$)
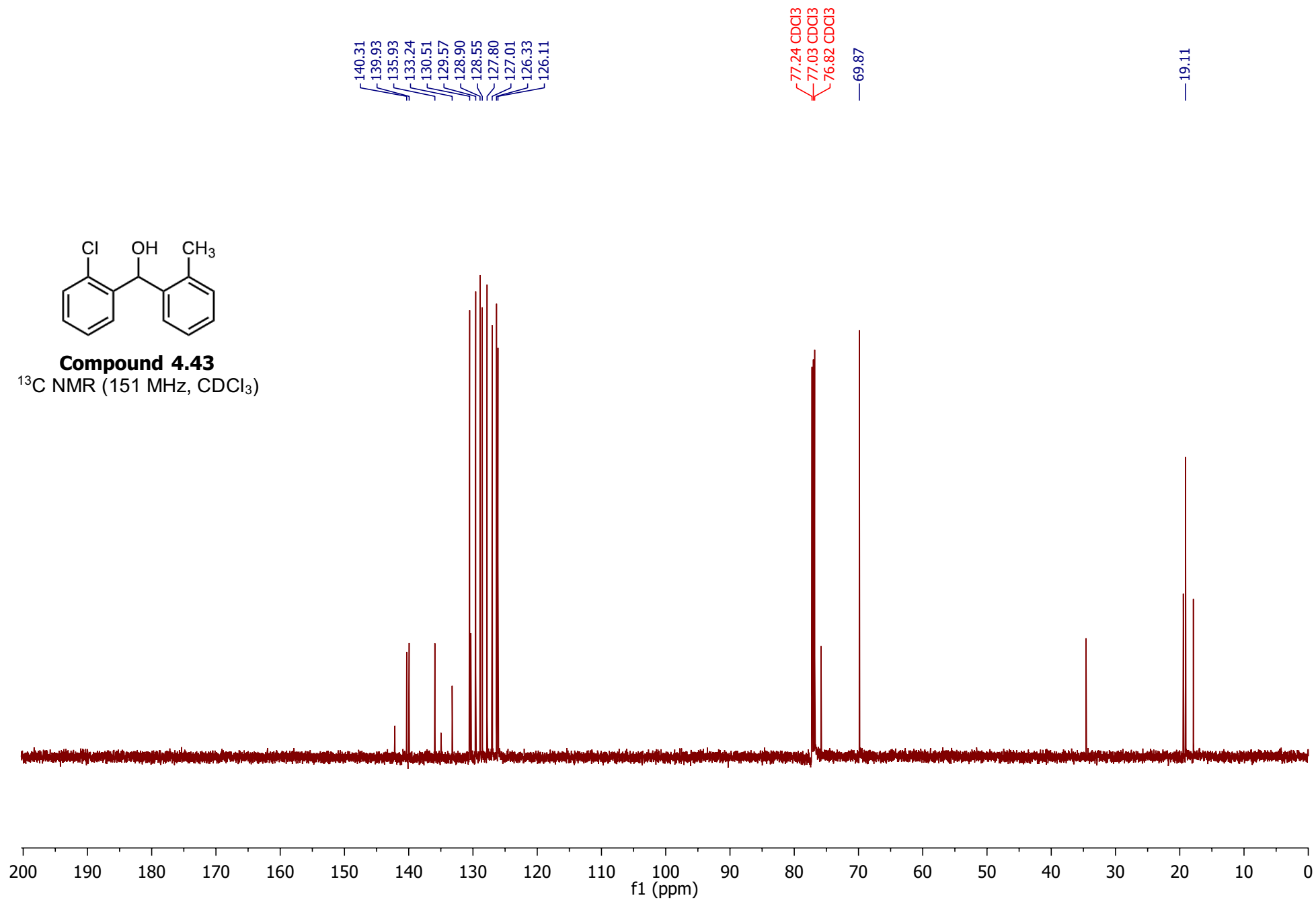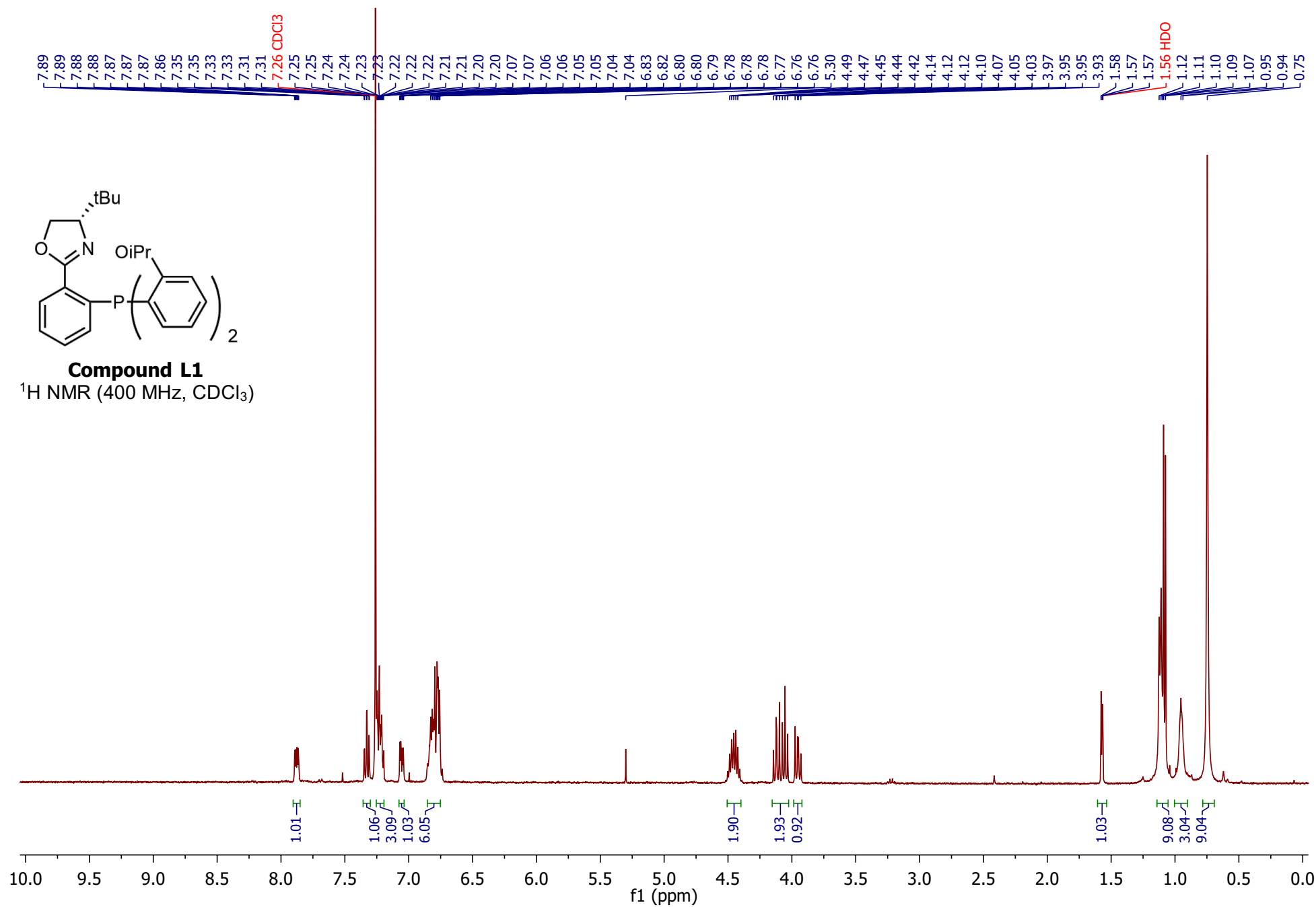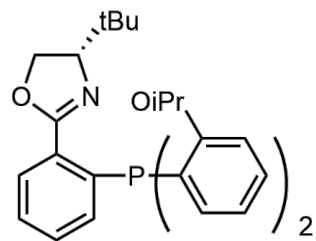
Compound L1
^{13}C NMR (101 MHz, CDCl$_3$)

159.55, 159.40, 134.78, 134.37, 129.77, 129.30, 129.28, 129.24, 129.10, 127.58, 120.24, 120.02, 111.32, 77.35 CDCl3, 76.72 CDCl3, 70.18, 69.64, 68.42, 33.82, 25.83, 21.86, 21.83, 21.57
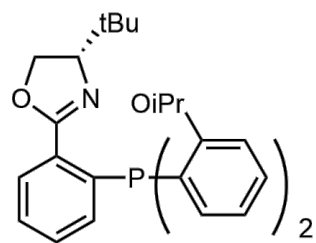
Compound L1
^{31}P NMR (162 MHz, CDCl$_3$)

−24.43

Compound 4.44
^{1}H NMR (400 MHz, CDCl$_3$)
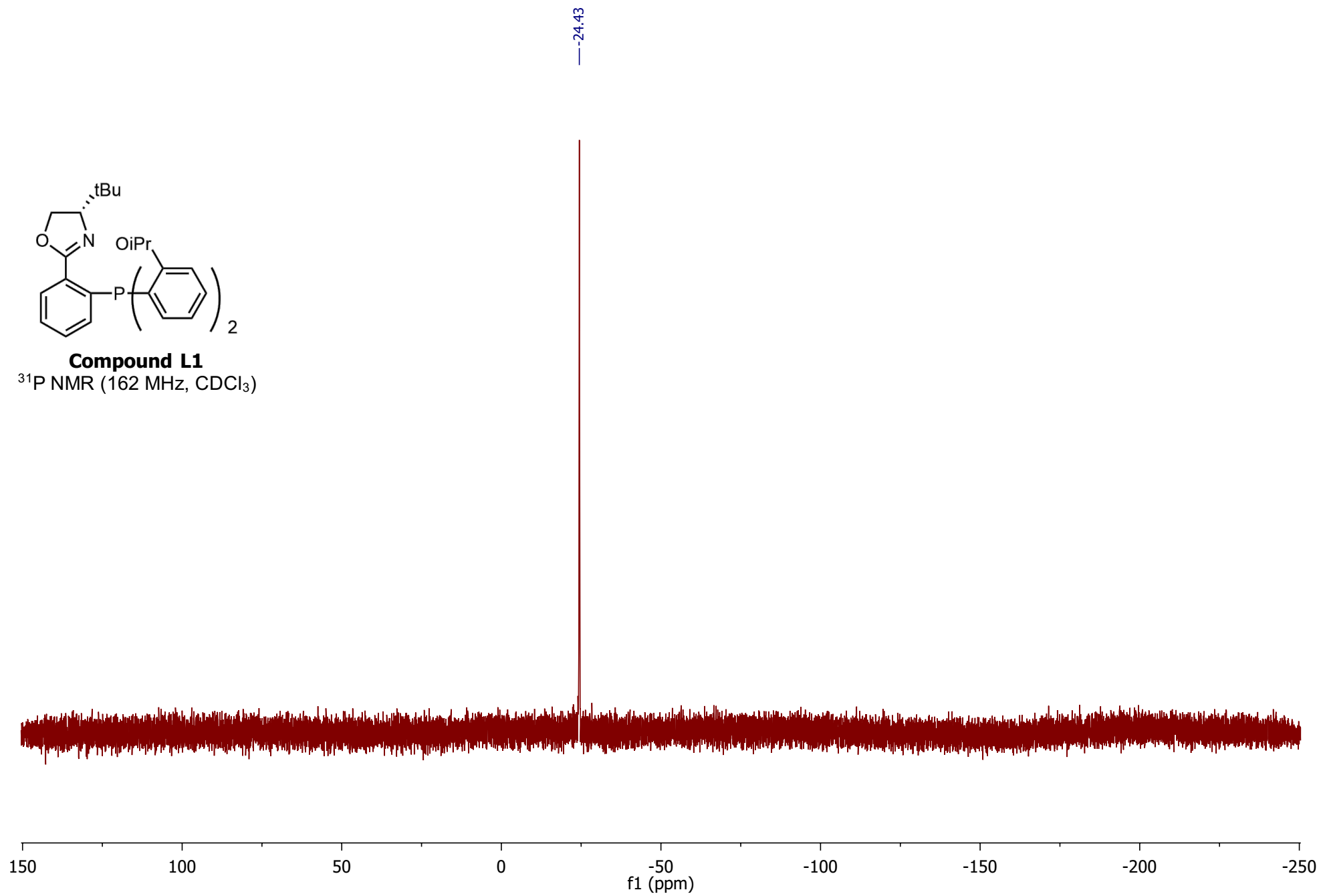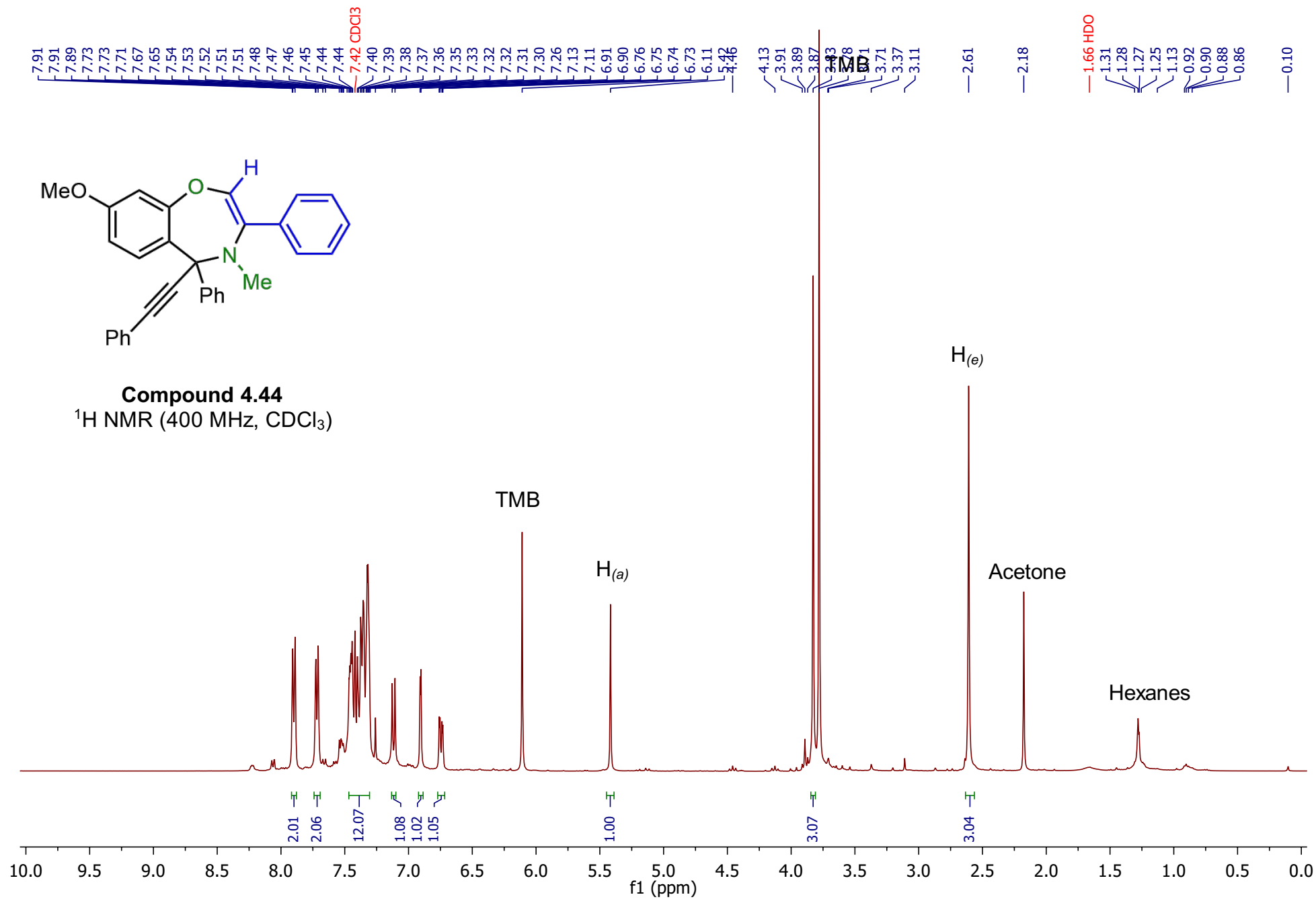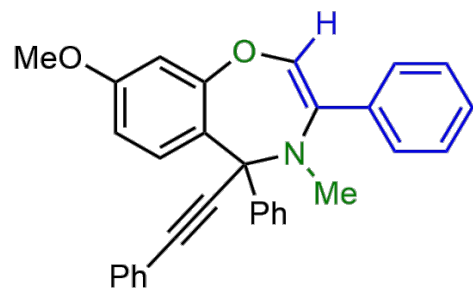
Compound 4.44
^{13}C NMR (101 MHz, CDCl$_3$)

155.85, 154.74, 149.40, 142.42, 136.15, 136.09, 131.84, 128.64, 128.61, 128.39, 128.31, 128.28, 128.04, 127.67, 125.80, 123.31, 122.89, 110.86, 110.18, 106.25, 88.17, 86.88, 67.73, 55.65, 37.54
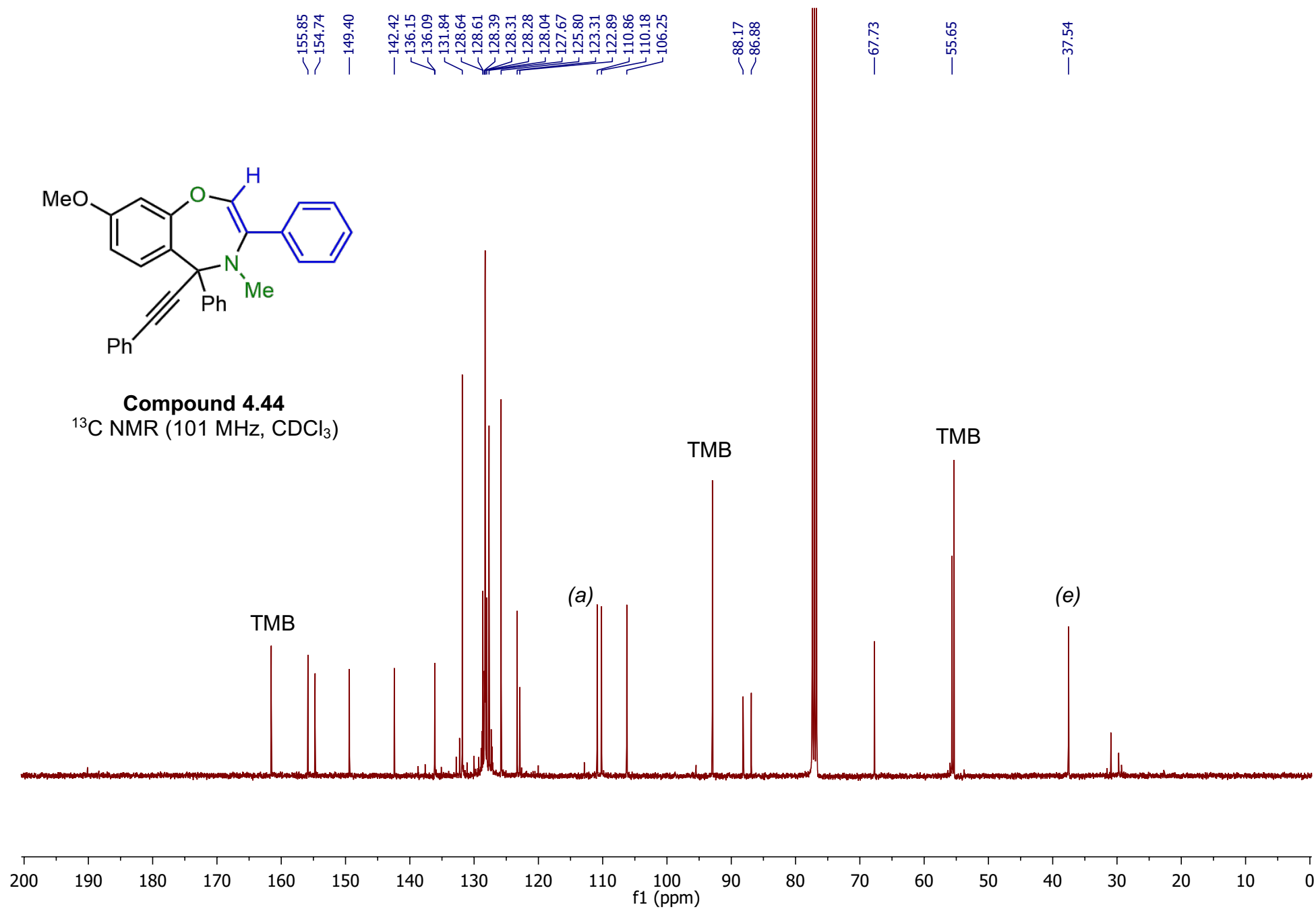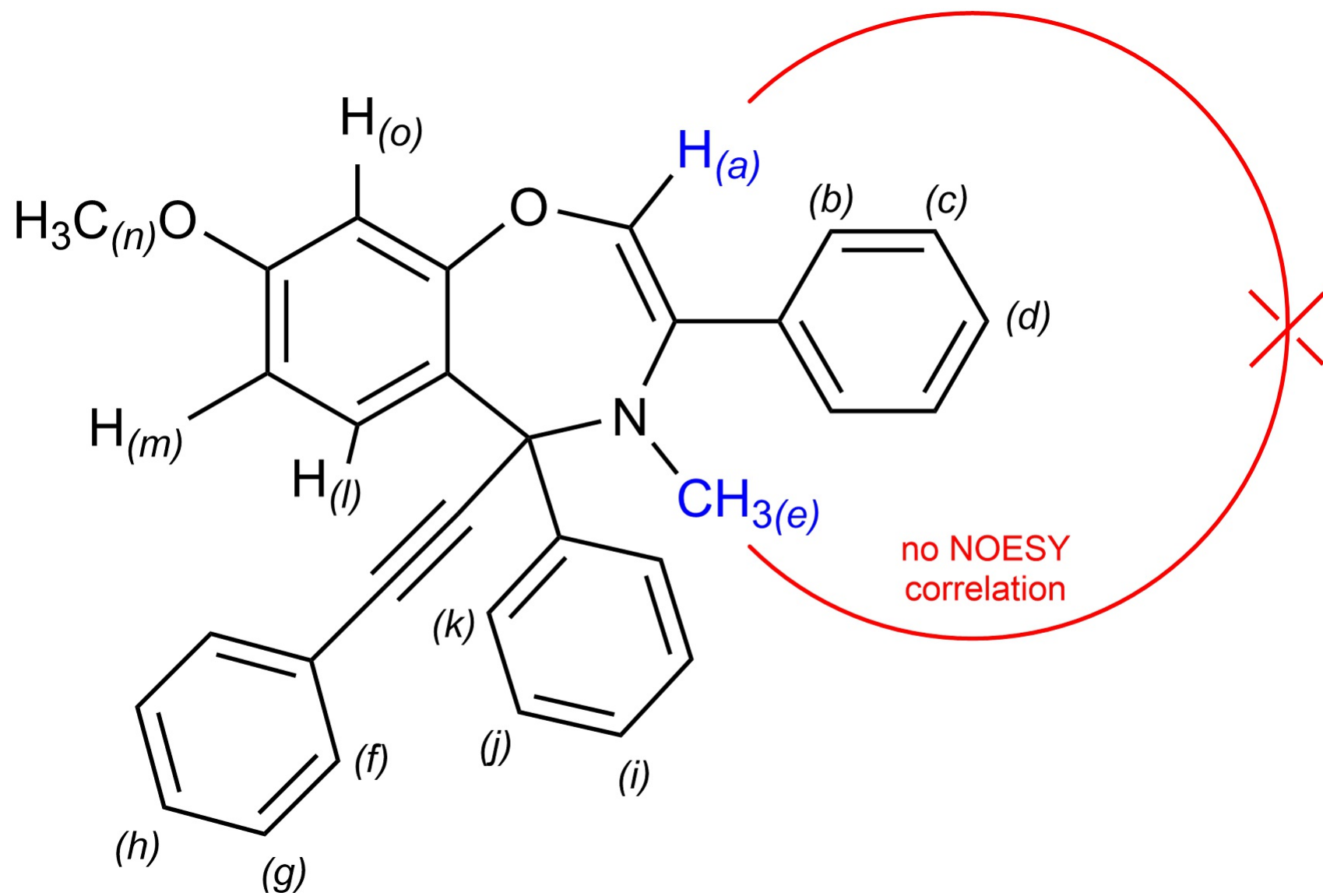
Compound 4.44
NOESY (CDCl₃)
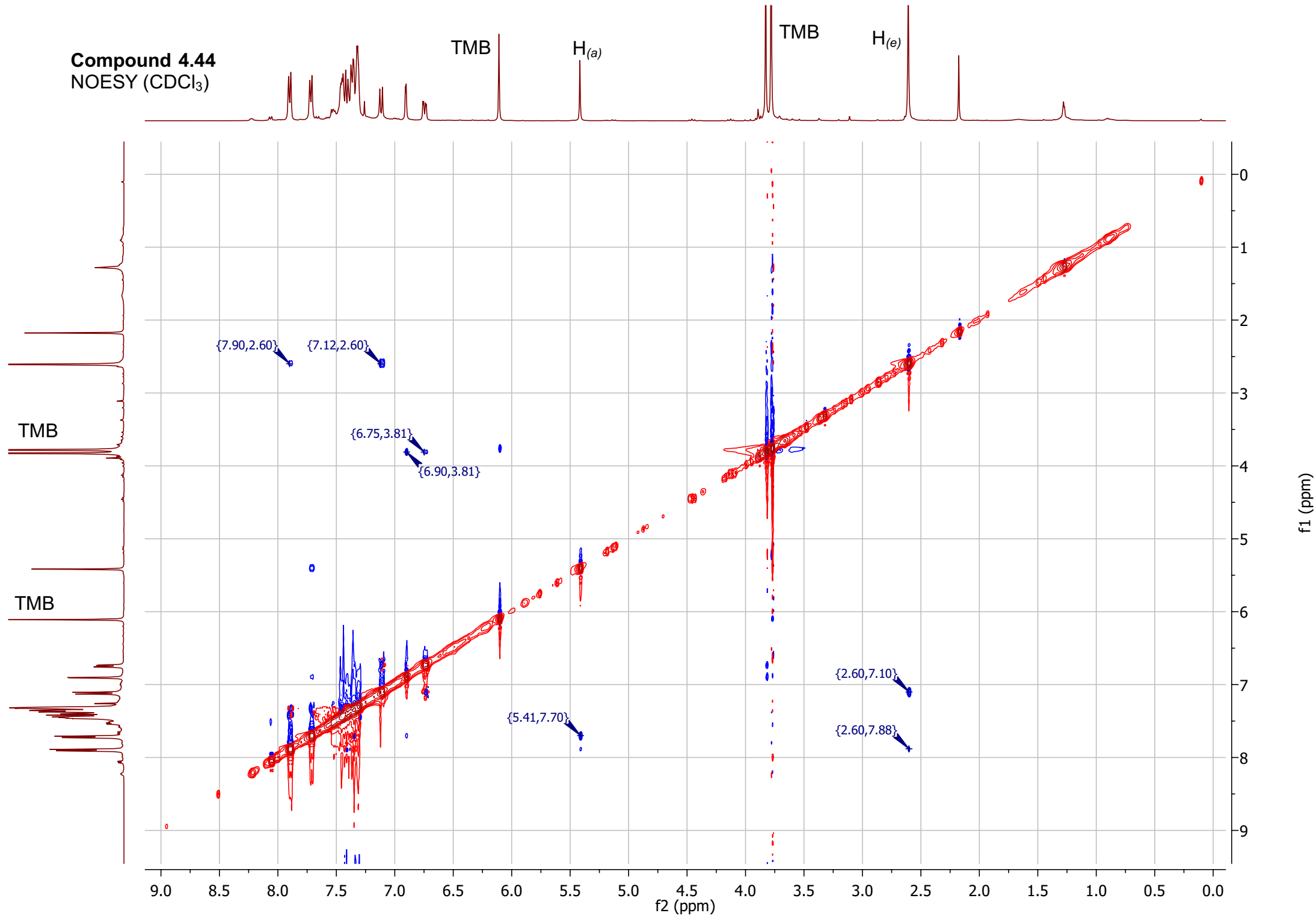
Compound 4.44
HSQC (CDCl₃)
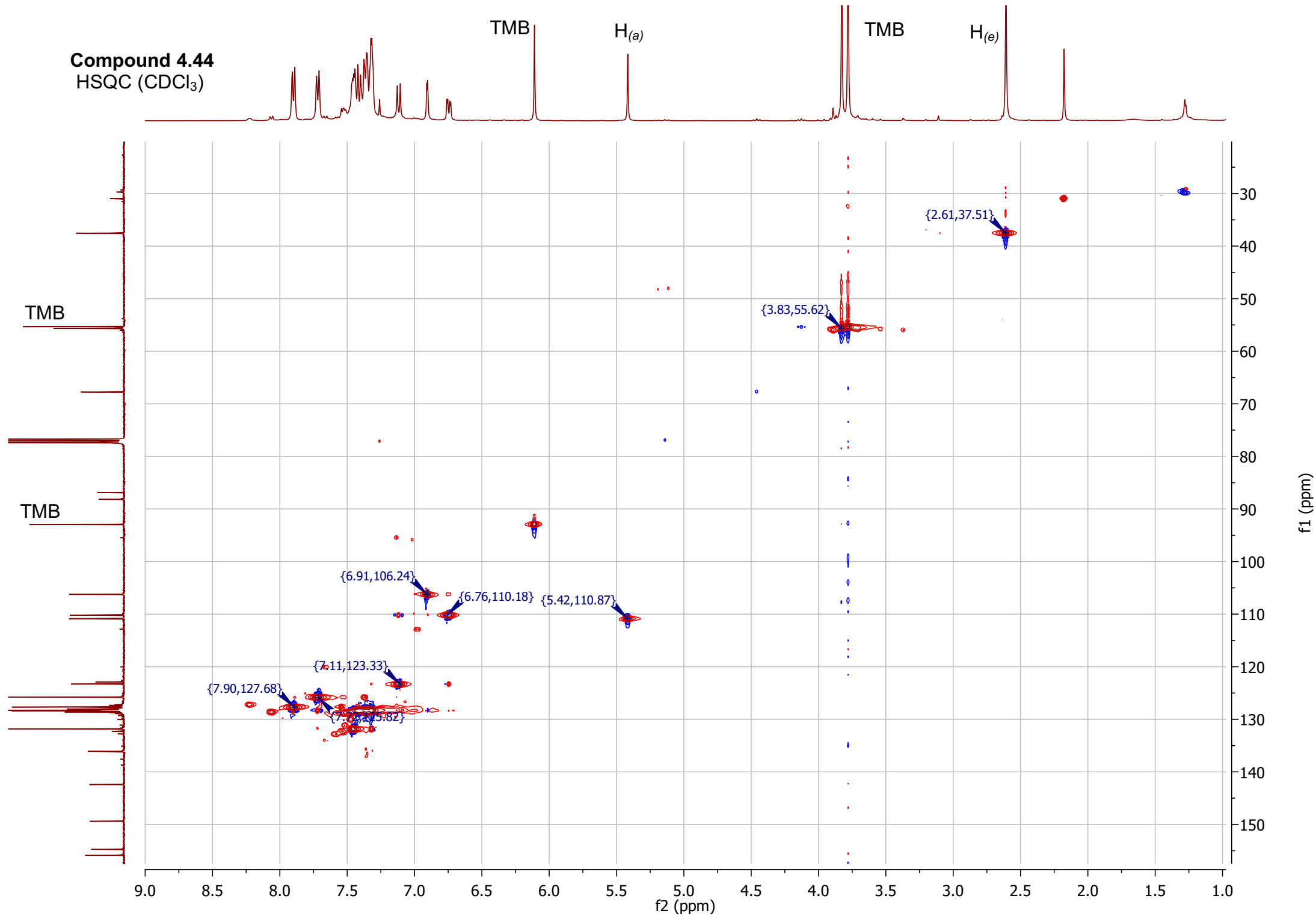
Compound 4.44
HMBC (CDCl$_3$)
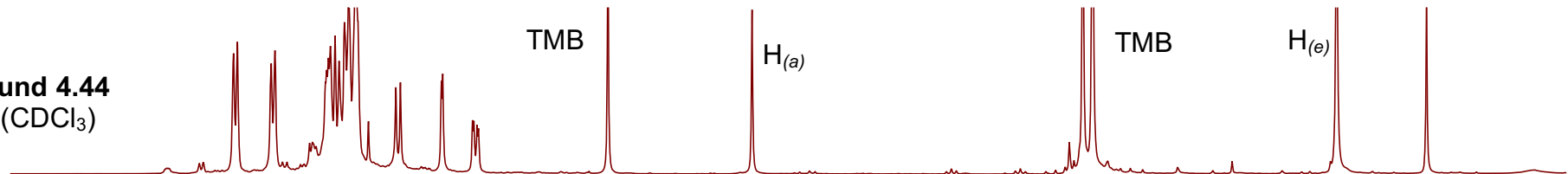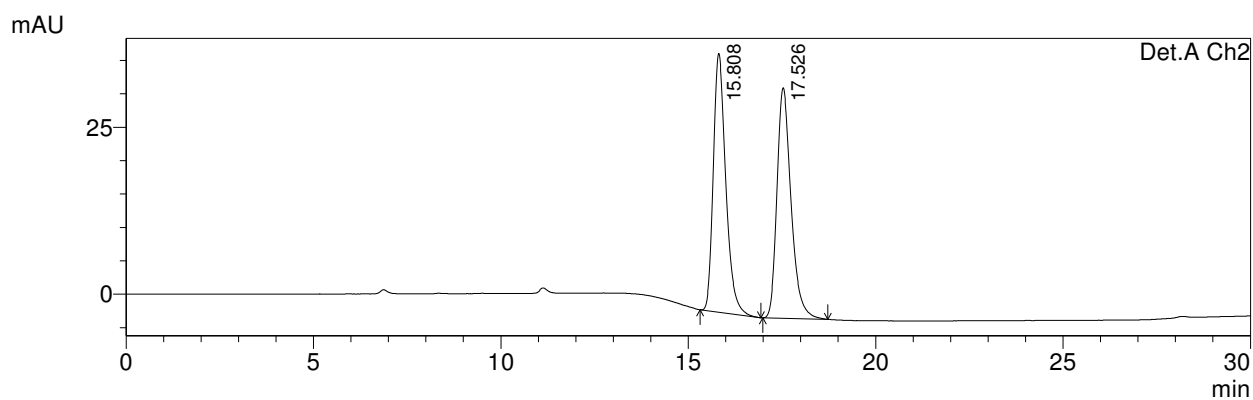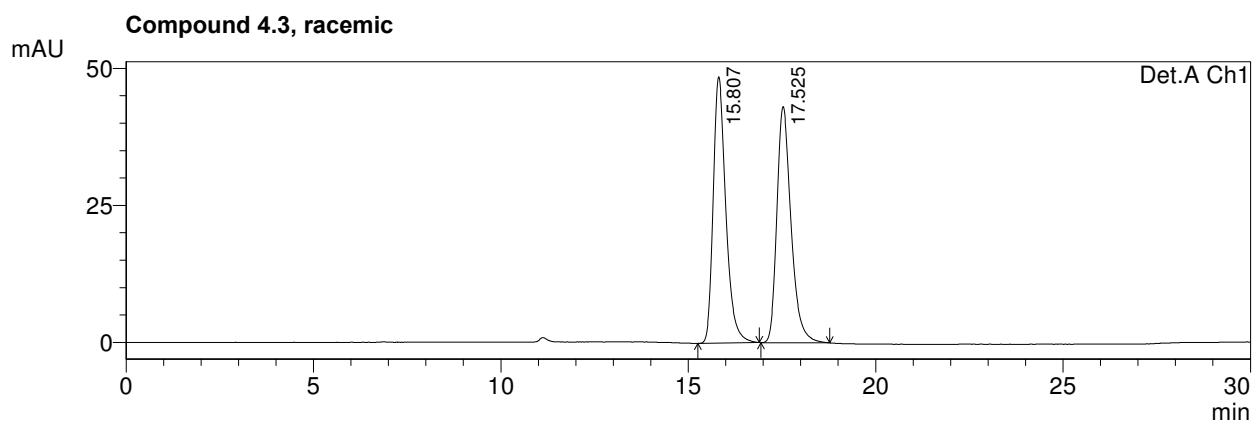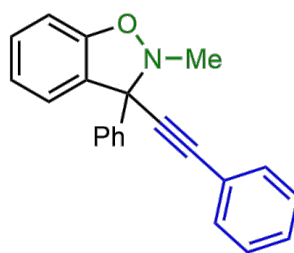
TMB H$_{(a)}$ TMB H$_{(e)}$

TMB

TMB

TMB

{7.93,67.77} {5.43,67.76} {2.62,67.76}

{5.43,86.90}

{5.43,136.14} {2.62,136.10}

{5.43,142.41}

{7.75,149.43} {5.45,149.41}

{6.95,155.87} {6.76,155.83}

{7.15,154.75} {7.15,155.85}

f1 (ppm)

f2 (ppm)

Compound 4.3, racemic

mAU

Det.A Ch1

50

15.807
17.525

25

0

0   5   10   15   20   25   30
min

mAU

Det.A Ch2

15.808
17.526

25

0

0   5   10   15   20   25   30
min

1 Det.A Ch1/254nm
2 Det.A Ch2/230nm

PeakTable

Detector A Ch1 254nm

Peak#	Ret. Time	Area	Height	Area %	Height %
1	15.807	1138362	48610	50.119	52.990
2	17.525	1132966	43124	49.881	47.010
Total		2271328	91734	100.000	100.000

PeakTable

Detector A Ch2 230nm

Peak#	Ret. Time	Area	Height	Area %	Height %
1	15.808	897222	38750	49.863	52.895
2	17.526	902153	34508	50.137	47.105
Total		1799376	73257	100.000	100.000
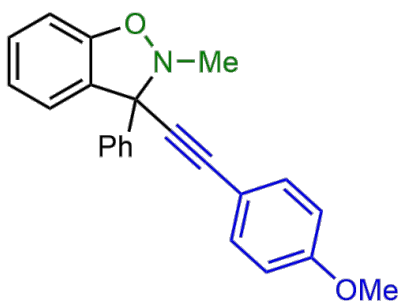
Compound 4.17, racemic
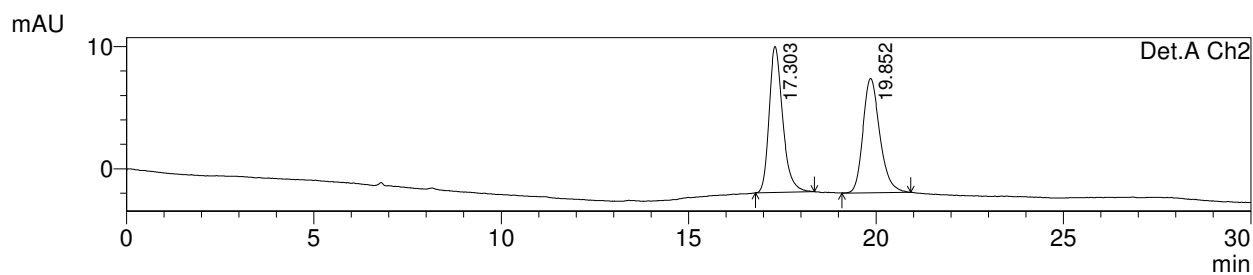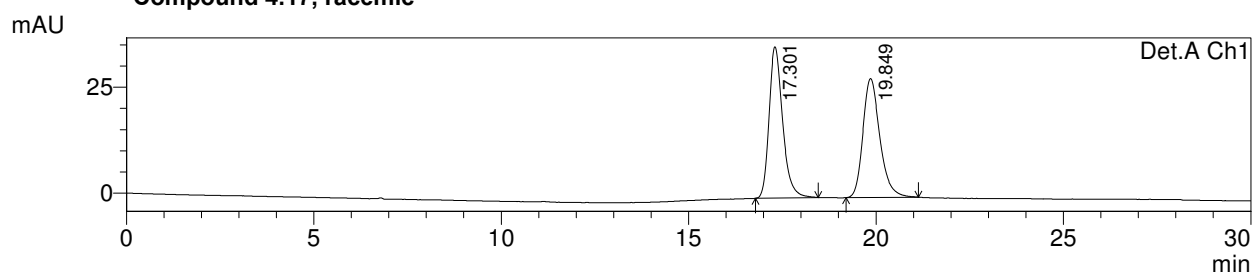
1 Det.A Ch1/254nm
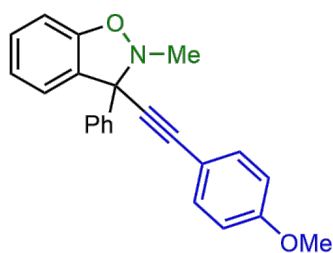2 Det.A Ch2/230nm

PeakTable

Detector A Ch1 254nm

Peak#	Ret. Time	Area	Height	Area %	Height %
1	17.301	895968	35721	50.343	55.977
2	19.849	883777	28093	49.657	44.023
Total		1779745	63814	100.000	100.000

PeakTable

Detector A Ch2 230nm

Peak#	Ret. Time	Area	Height	Area %	Height %
1	17.303	299895	11958	50.630	56.080
2	19.852	292433	9365	49.370	43.920
Total		592328	21323	100.000	100.000

Compound 4.17, racemic

1: Scan ES+
TIC
1.00e9

3.61
3.60
3.89
3.59
3.64
3.90
3.58
3.91
3.58
3.92
3.57
3.92
3.56
3.94
3.56
3.94
3.55
3.55
3.95
3.53
3.96

0.81
0.81
0.73
0.24
1.46
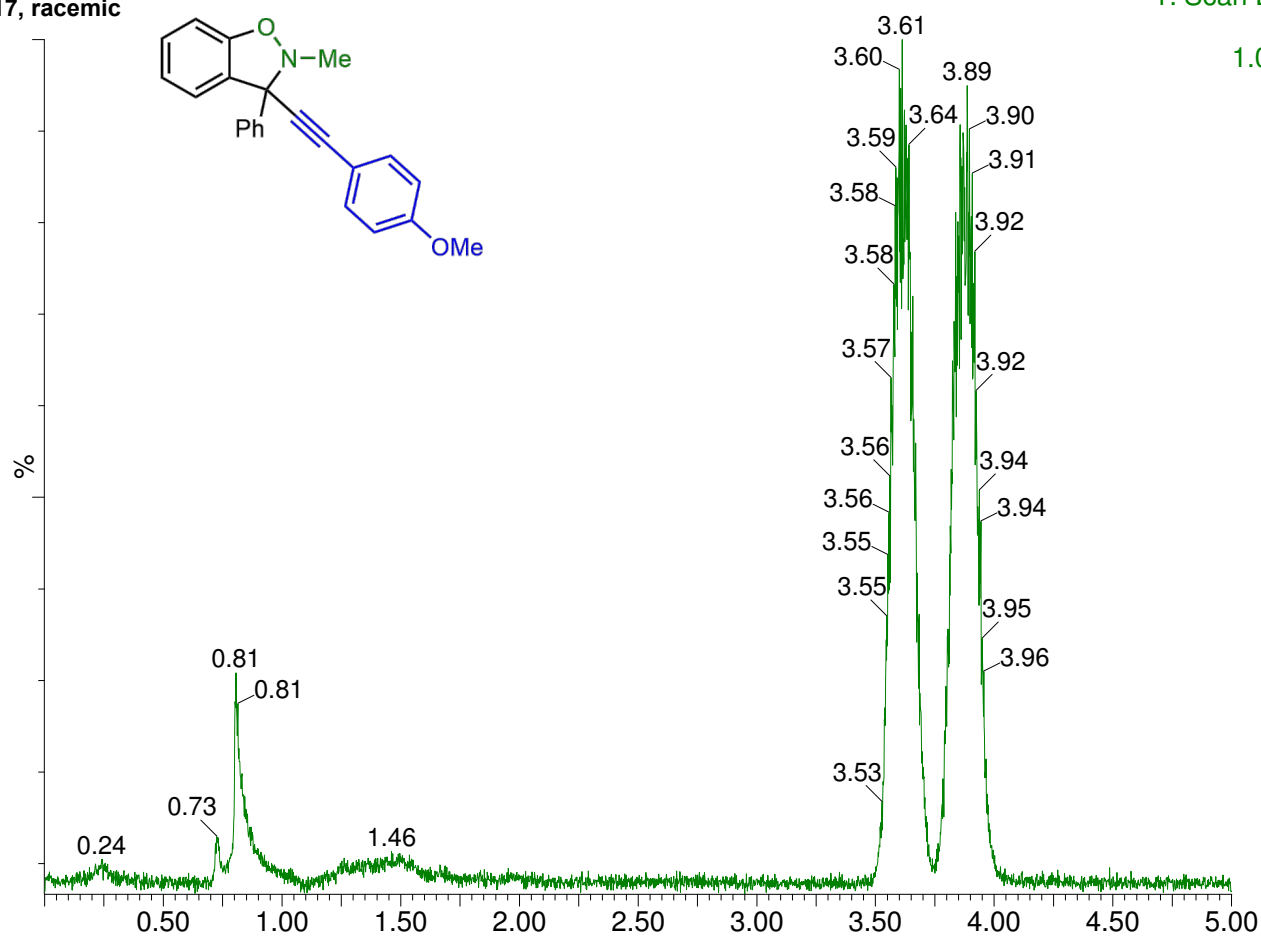
2: Diode Array
Range: 5.462
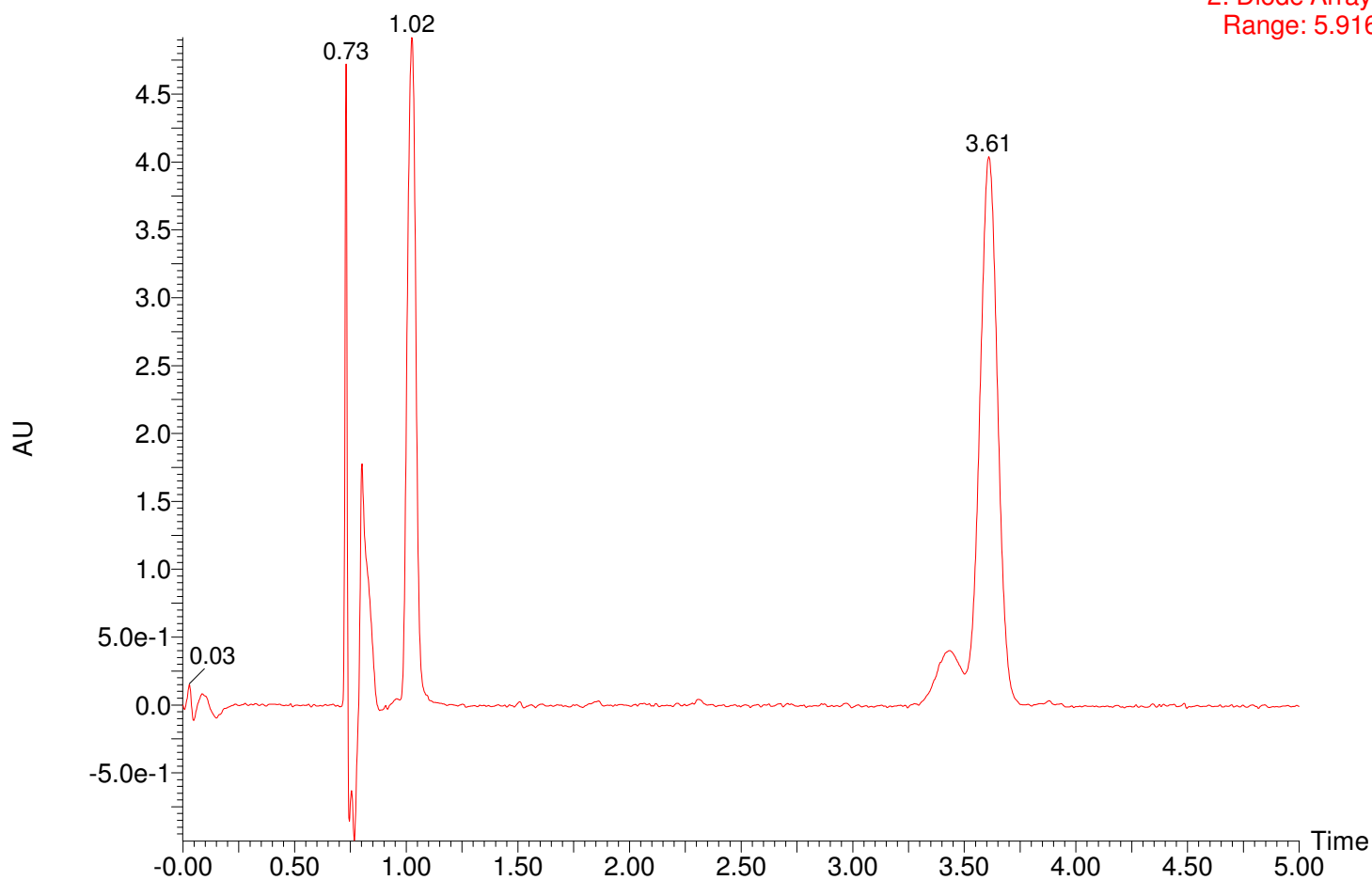
0.73
3.60
3.87
0.80
0.02
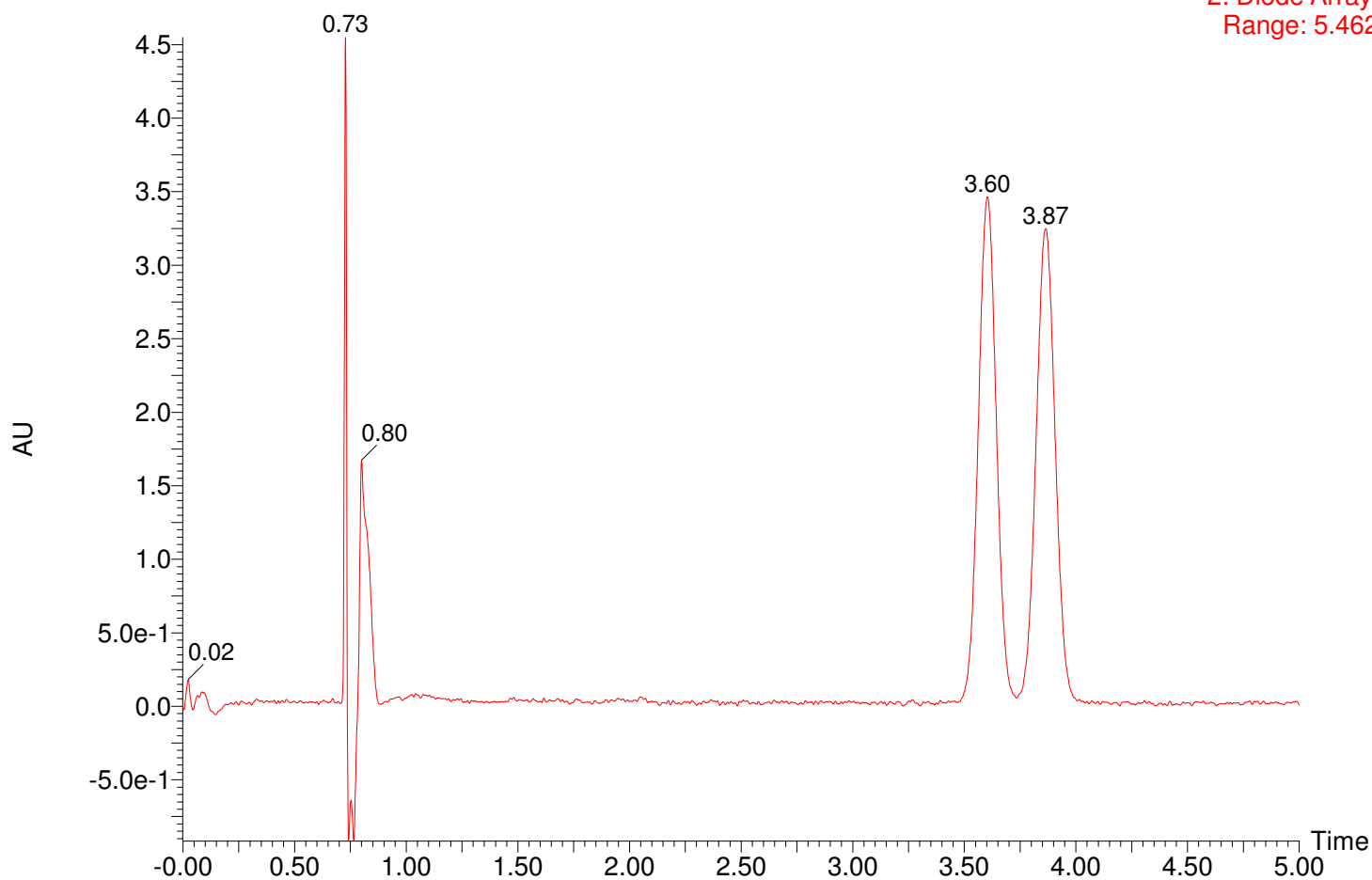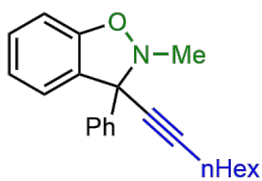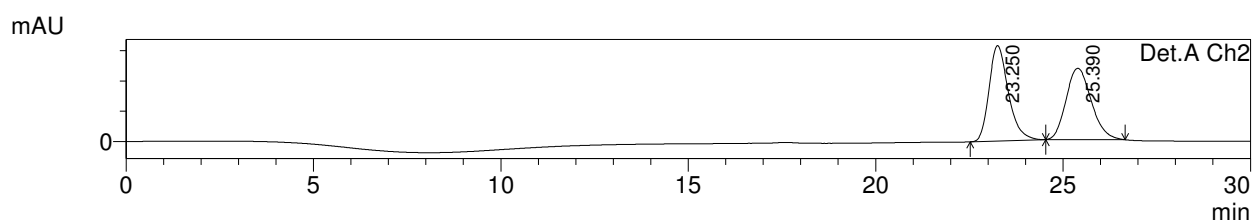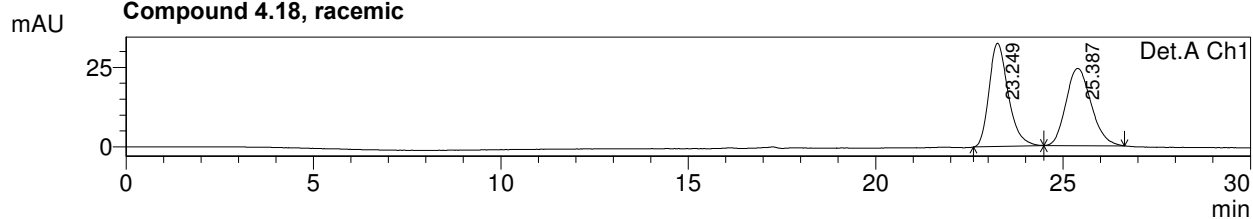
Compound 4.17, >99% ee
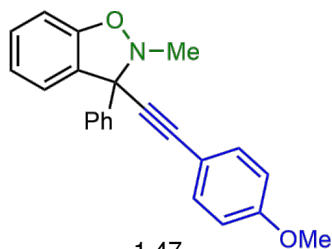
1: Scan ES+
TIC
1.51e9
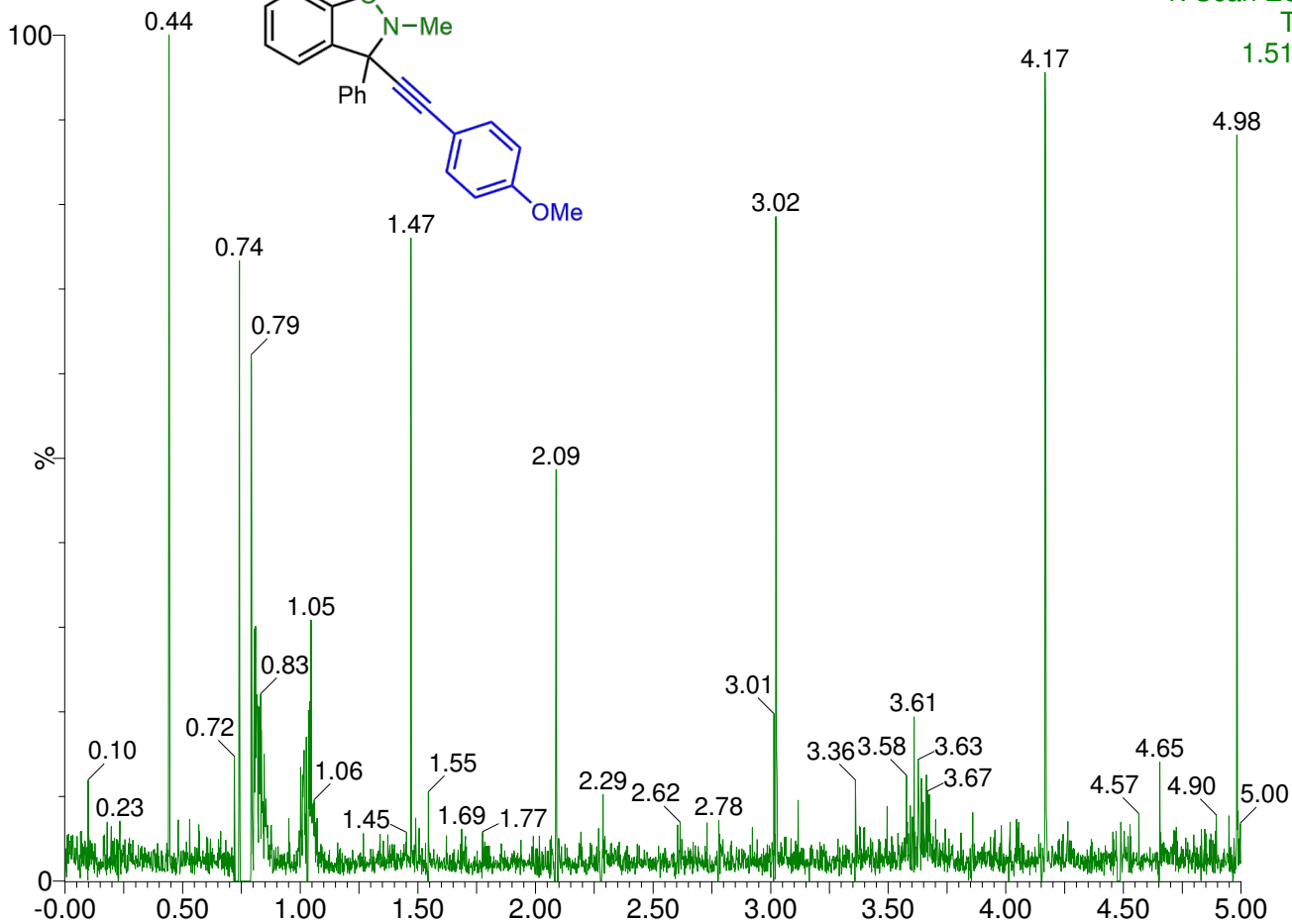
2: Diode Array
Range: 5.916

Compound 4.18, racemic

1 Det.A Ch1/254nm
2 Det.A Ch2/210nm

PeakTable

Detector A Ch1 254nm

Peak#	Ret. Time	Area	Height	Area %	Height %
1	23.249	1152922	32487	50.356	57.220
2	25.387	1136622	24289	49.644	42.780
Total		2289545	56777	100.000	100.000

Detector A Ch2 210nm

PeakTable

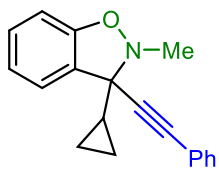| Peak#	Ret. Time	Area	Height	Area %	Height %
1	23.250	11258967	315376	50.499	57.238
2	25.390	11036649	235616	49.501	42.762
Total		22295616	550992	100.000	100.000

Compound 4.30, racemic

1: Scan ES+
TIC
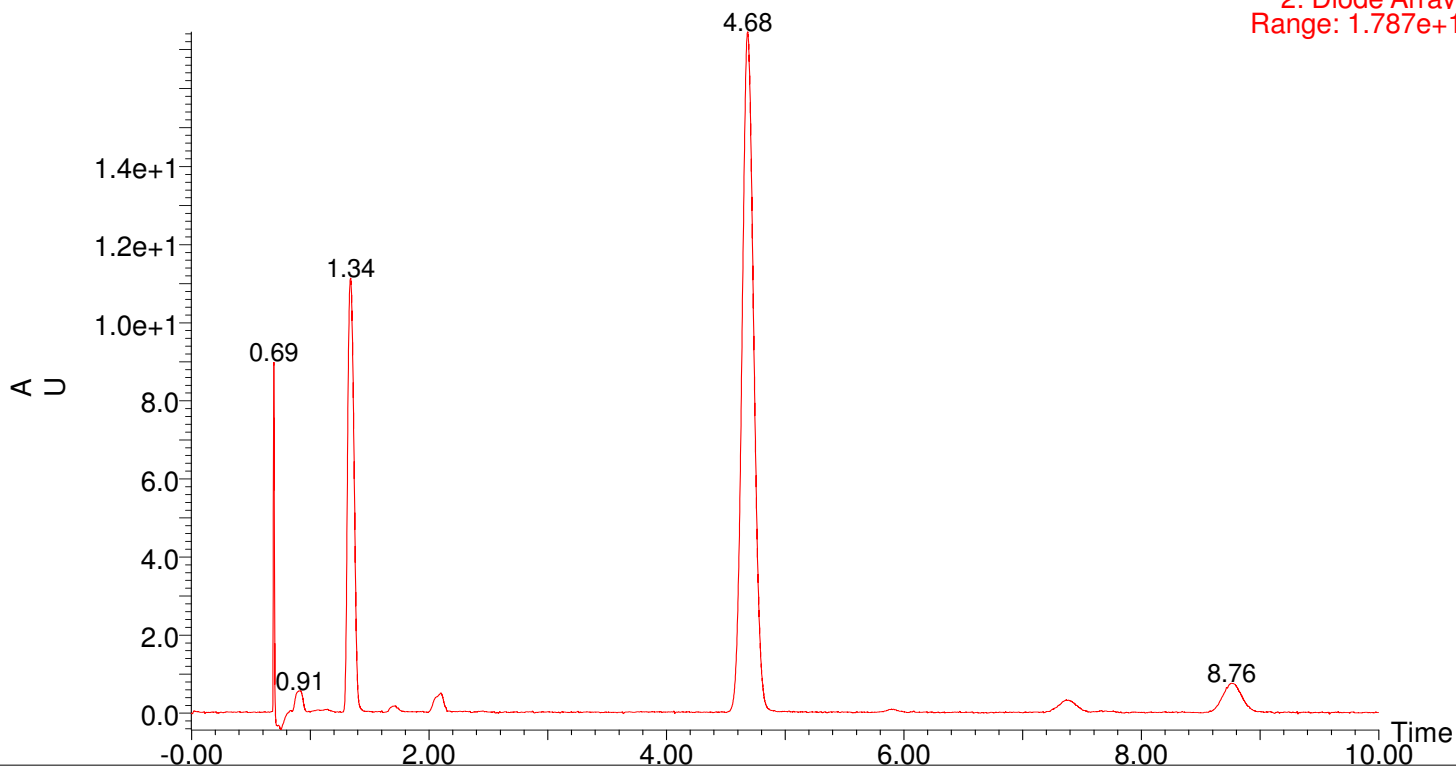6.62e8
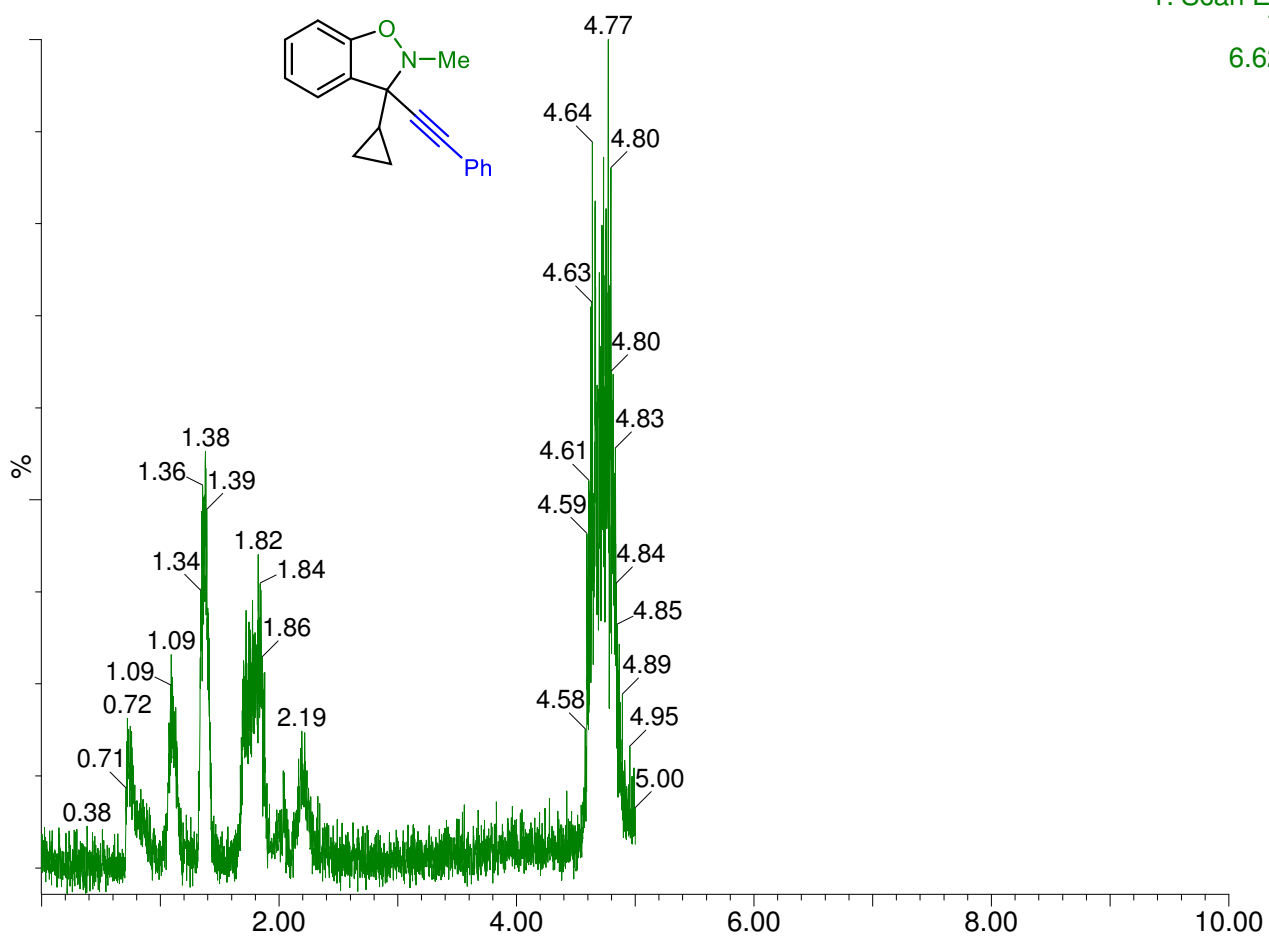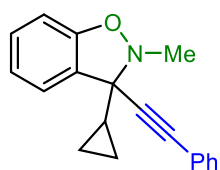
2: Diode Array
Range: 1.782e+1
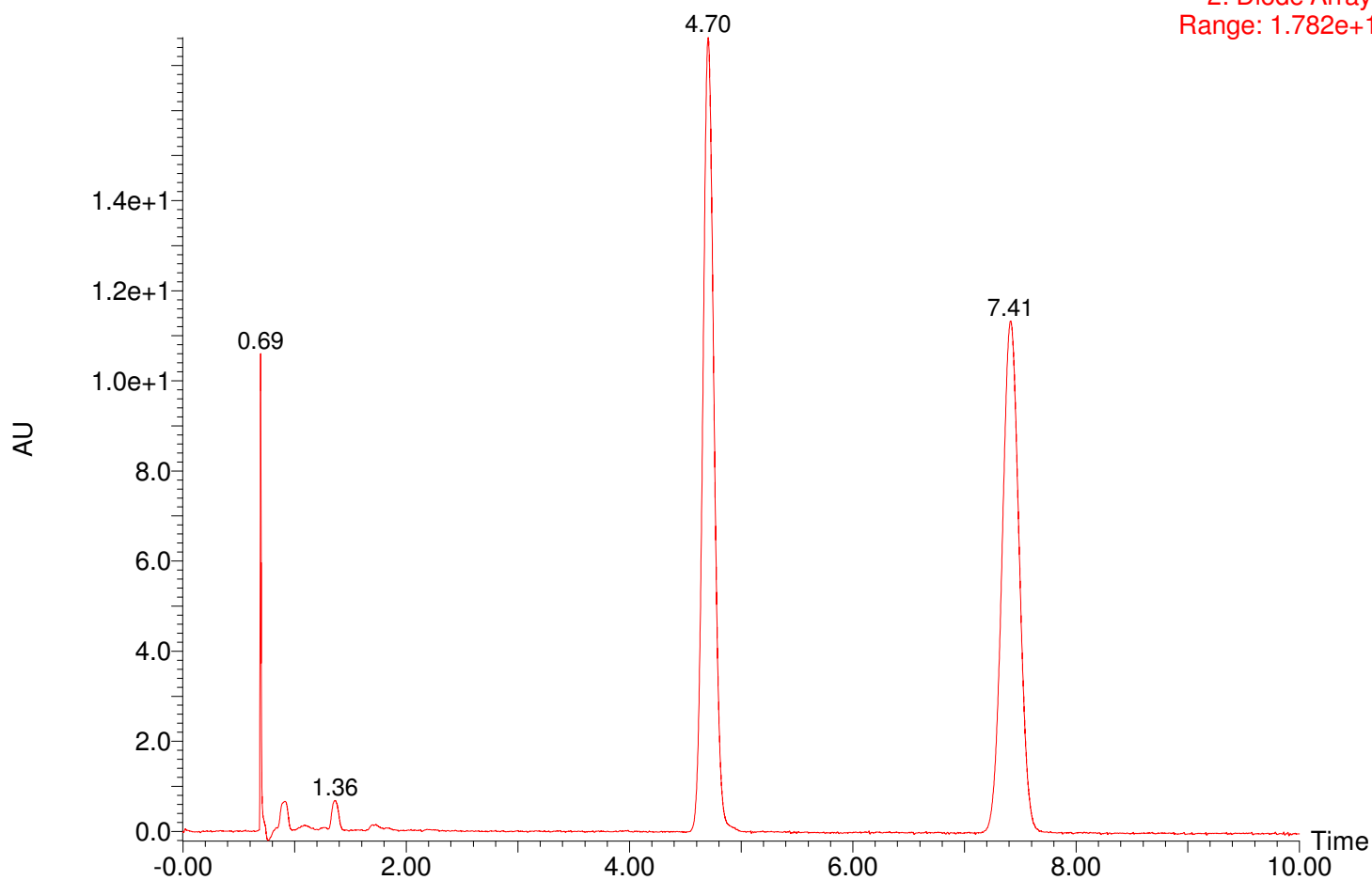
Compound 4.30, 95% ee

1: Scan ES+
TIC
7.94e8

%

0.36 0.72 0.74 1.30 1.31 1.32 1.33 1.35 1.35 1.36 1.37 1.38 1.39 1.40 1.41 2.11 4.58 4.58 4.60 4.60 4.62 4.64 4.70 4.71 4.74 4.79 4.79 4.81 4.84 4.85 7.33 7.41 7.44 8.72 8.79 8.81 8.88

2.00   4.00   6.00   8.00   10.00

2: Diode Array
Range: 1.787e+1

4.68

AU

1.4e+1
1.2e+1
1.0e+1
8.0
6.0
4.0
2.0
0.0

0.69
0.91
1.34
8.76

Time
-0.00   2.00   4.00   6.00   8.00   10.00

E. PERMISSION LETTERS